Linking Science and Technology for Global Solutions

TMS2008

137th Annual Meeting & Exhibition

March 9-13, 2008
Ernest Morial Convention Center
New Orleans, Louisiana, USA

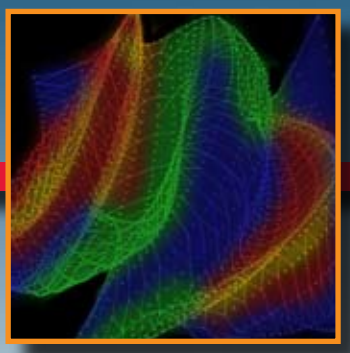

Register before February 11 at www.tms.org/annualmeeting.html

TMS2008

137th Annual Meeting & Exhibition

March 9-13, 2008
Ernest Morial Convention Center
New Orleans, Louisiana, USA

TMS 2008 is bringing top materials scientists and engineers from around the world together to address some of today's global challenges:

- Resolving technology and techno-management issues for the production of aluminum, metal castings, steel, automotive and electronic materials
- Optimizing energy utilization and addressing enviromental impacts
- Developing materials for high-performance applications
- Achieving process improvement for a variety of materials under a variety of conditions
- Preparing future materials scientists and engineers

These issues and more are presented in 56 symposia covering four major themes:

Light Metals
Extraction, Processing, Structure and Properties
Emerging Materials
Materials and Society

TMS 2008 addresses these global challenges with traditional programming presenting new developments, such as . . .

9th Global Innovations Symposium
Aluminum Reduction Technology
Bulk Metallic Glasses
Magnesium Technology 2008
Materials in Clean Power Systems III
Ultrafine Grained Materials

. . . with new partnerships represented . . .

American Physical Society and TMS present Integrated Computational Materials Engineering symposia.

The Chinese Society for Metals delegation, led by Professor Liu Yongcai, deputy secretary general, and the Indian Institute of Metals delegation, led by Dr. Sanak Mishra, vice president and chairman of the ferrous division, provide perspective in the Materials and Society symposia.

LEARN • NETWORK • ADVANCE

Linking Science and Technology for Global Solutions

. . . and new perspectives for discussion . . .

Climate Change and Greenhouse Gas Emissions
Features leaders from the world's largest aluminum companies: Alcan, Alcoa, BHP Billiton, Chalco and Hydro Aluminum

Energy Conservation in Metals Extraction and Materials Processing
Presents current and potential technology and methodologies for energy saving techniques

IOMMMS Global Materials Forum 2008: Creating the Future MS&E Professionals
Highlights approaches from China, India, Japan and the United States

Materials for Infrastructure: Building Bridges in the Global Community
Includes special guided tour for symposium attendees covering the geology of the Katrina disaster. See page 27 to learn how you can leave a lasting impression on New Orleans!

Role of Engineers in Meeting 21st Century Societal Challenges
Addresses energy, transportation, housing, health and recycling issues

Sloan Industry Centers Forum: Techno-Management Issues Related to Materials-Centric Industries
Considers aluminum, metal processing, steel, automotive, paper and wood

With 56 symposia, three short courses, six lectures, eight networking receptions, 130+ exhibitors, one free collected proceedings CD-ROM, and thousands of your colleagues from 70 countries, TMS 2008 offers you the opportunity to learn, network and advance global solutions for today's materials challenges.

Register online at www.tms.org/annualmeeting.html or see page 22.

Table of Contents

Symposia by Theme 4
Symposia Alphabetically 6
Lectures 11
Continuing Education 13
Networking Events 14
Exhibition 16
Especially for Students 18
Proceedings 20
Registration 21
Housing 23
Tours 25
Hands-On New Orleans 27

Light Metals

Alumina and Bauxite
Aluminum Alloys: Fabrication, Characterization and Applications
Aluminum Reduction Technology
Carbon Dioxide Reduction Metallurgy
Cast Shop Technology
Characterization of Minerals, Metals and Materials
Computational Thermodynamics and Kinetics
Electrode Technology
Frontiers in Process Modeling
Magnesium Technology 2008
Materials Informatics: Enabling Integration of Modeling and Experiments in Materials Science
Recycling

Related Lecture and Short Courses:

- *"Innovations in Steel Production – Animations for Aluminium Technologies?"*
- *Furnace Systems and Technology*
- *Grain Refinement of Aluminium Alloys: Theory and Practice*
- *Greenhouse Gas Emissions*

See page 12 for details.

Extraction, Processing, Structure and Properties

3-Dimensional Materials Science
9th Global Innovations Symposium: Trends in Integrated Computational Materials Engineering for Materials Processing and Manufacture
Acta Materialia Gold Medal Symposium: Recent Developments in Rare Earth Science and Technology
Advances in Roasting, Sintering, Calcining, Preheating and Drying
APS Frontiers of Computational Materials Science
Aqueous Processing
Biological Materials Science
Bulk Metallic Glasses V
Carbon Dioxide Reduction Metallurgy
Characterization of Minerals, Metals and Materials
Complex Oxide Materials: Synthesis, Properties and Applications
Computational Thermodynamics and Kinetics
Creating the ICME Cyberinfrastructure: an Interdisciplinary Technology Forum
Deformation Twinning: Formation Mechanisms and Effects on Material Plasticity – Experiments and Modeling
Emerging Interconnect and Packaging Technologies
Emerging Methods to Understand Mechanical Behavior
Energy Conservation in Metals Extraction and Materials Processing
Enhancing Materials Durability via Surface Engineering
Frontiers in Process Modeling
Hael Mughrabi Honorary Symposium: Plasticity, Failure and Fatigue in Structural Materials – from Macro to Nano
Hot and Cold Rolling Technology
Hume-Rothery Symposium: Nanoscale Phases
Materials Informatics: Enabling Integration of Modeling and Experiments in Materials Science
Materials Processing Fundamentals
Mechanical Behavior, Microstructure and Modeling of Ti and Its Alloys
Mechanics and Kinetics of Interfaces in Multicomponent Materials Systems
Minerals, Metals and Materials under Pressure
Neutron and X-Ray Studies for Probing Materials Behavior
Particle Beam-Induced Radiation Effects in Materials
Phase Stability, Phase Transformations and Reactive Phase Formation in Electronic Materials VII
Pyrometallurgy
Recent Industrial Applications of Solid-State Phase Transformations
Recycling
Refractory Metals 2008
Structural Aluminides for Elevated Temperature Applications
Ultrafine-Grained Materials: Fifth International Symposium

Related Lectures:

- *"Computational Modeling of Metals Processing: Past, Present and Future"*
- *"Smelting and Refining – Faster, Smoother, Cheaper, Safer"*
- *"High Performance Structural Metals: an Undervalued but Critical Enabling Technology"*
- *Nanoscale Metal Silicides*

See page 11 for details.

Emerging Materials

2008 Nanomaterials: Fabrication, Properties and Applications
3-Dimensional Materials Science
4th Lead-Free Solders Technology Workshop
9th Global Innovations Symposium: Trends in Integrated Computational Materials Engineering for Materials Processing and Manufacture
Acta Materialia Gold Medal Symposium: Recent Developments in Rare Earth Science and Technology
Advances in Semiconductor, Electro Optic and Radio Frequency Materials
Biological Materials Science
Bulk Metallic Glasses V
Carbon Dioxide Reduction Metallurgy
Characterization of Minerals, Metals and Materials
Complex Oxide Materials: Synthesis, Properties and Applications
Computational Thermodynamics and Kinetics
Creating the ICME Cyberinfrastructure: An Interdisciplinary Technology Forum
Emerging Interconnect and Packaging Technologies
Energy Conservation in Metals Extraction and Materials Processing
Enhancing Materials Durability via Surface Engineering
Frontiers in Process Modeling
Hael Mughrabi Honorary Symposium: Plasticity, Failure and Fatigue in Structural Materials – from Macro to Nano
Hume-Rothery Symposium: Nanoscale Phases
Materials in Clean Power Systems III: Fuel Cells, Hydrogen, and Clean Coal-Based Technologies
Materials Informatics: Enabling Integration of Modeling and Experiments in Materials Science
Mechanics and Kinetics of Interfaces in Multicomponent Materials Systems
Micro-Engineered Particulate-Based Materials
Neutron and X-Ray Studies for Probing Materials Behavior
Particle Beam-Induced Radiation Effects in Materials
Phase Stability, Phase Transformations and Reactive Phase Formation in Electronic Materials VII
Recycling
Structural Aluminides for Elevated Temperature Applications
Ultrafine-Grained Materials: Fifth International Symposium

Related Short Course:
- *Nanomechanical Characterization*

See page 13 for details.

Materials and Society

Climate Change and Greenhouse Gas Emissions
IOMMMS Global Materials Forum 2008: Creating the Future MS&E Professionals
Materials for Infrastructure: Building Bridges in the Global Community
National Materials Advisory Board Town Hall Meeting on Assessing Corrosion Education
Role of Engineers in Meeting 21st Century Societal Challenges
Sloan Industry Centers Forum: Techno-Management Issues Related to Materials-Centric Industries

About Materials and Society
Many of the programs and activities fit broadly under the umbrella of Materials and Society–from many symposia and presentations in the technical program to the community outreach that will be performed on-site. Many invited speakers will examine opportunities for the materials science and engineering community to proactively address the complex technological, professional, educational, societal, environmental, infrastructural and economic issues that challenge the sustainability of today's world. We are all challenged to improve the world as we know it for those in developing countries and to secure it for future generations.

Related Lecture and Short Course:
- *"Design for the Other 90%"*
- *Greenhouse Gas Emissions*

See page 11 for details.

Turn to the alphabetical listing of the symposia on the following pages for descriptions.

2008 Nanomaterials: Fabrication, Properties and Applications

…development, manufacture and application of functional nanomaterials

- Functional applications of nanomaterials
- Nanostructure fabrication
- Carbon nanostructures
- Quantum-dots

3-Dimensional Materials Science

…advanced characterization, modeling and microanalysis

- 3-D visualization and modeling
- 3-D microstructural evolution
- Microscopy techniques
- Microanalysis methods

4th Lead-Free Solders Technology Workshop

…TMS-Surface Mount Technology Association forum addressing critical needs

- Solder systems
- Packaging technologies
- Reliability
- Legislation

9th Global Innovations Symposium: Trends in Integrated Computational Materials Engineering for Materials Processing and Manufacture

...TMS-American Physical Society plenary discussions of advancements in materials modeling across length scales, and manufacturing impact

- Nuclear materials
- Ceramics
- Aluminum
- Nanomaterials

Acta Materialia Gold Medal Symposium: Recent Developments in Rare Earth Science and Technology

…in honor of Karl Gschneidner Jr.

- Single crystals
- Characterization and properties
- Novel applications
- Recent advancements

Advances in Roasting, Sintering, Calcining, Preheating and Drying

…state-of-the-art in processing technologies

- Iron ore
- Alumina
- Rotary kiln systems

Advances in Semiconductor, Electro Optic and Radio Frequency Materials

…development, fabrication and application of emerging technologies

- Medical device semiconductors
- Nanomaterials
- Photovoltaics

Alumina and Bauxite

…mining and refining of raw materials for aluminum production

- Alumina refinery design and development
- Alumina refinery safety and integrity
- Bauxite and digestion
- Precipitation

Aluminum Alloys: Fabrication, Characterization and Applications

…advancements in aluminum for today's marketplace

- Alloy characterization
- Alloy development
- Aluminum products and applications

Aluminum Reduction Technology

…conversion of alumina to aluminum

- Alternative processes
- Anode design and operation
- Cell fundamentals and phenomena
- Environmental and plant improvements
- Process control developments

Aluminum Reduction Symposium Organizer Martin Iffert: *"(This symposium) has a strong focus on sustainability and environmental aspects in the aluminum smelting process. This includes firsthand information about the European emission trading scheme and the influence on energy prices, smelter economy and environment."*

APS Frontiers of Computational Materials Science

…American Physical Society forum on progress in computational materials methods

Aqueous Processing

…recent progress

- Alternative leaching processes
- Precious metals
- Process-stability relationships
- New strategies and techniques

Biological Materials Science

…development of biological materials and biomaterial devices

- Biocompatibility
- Mimicking biological systems
- Bioinspired design
- Mechanical and environmental response

Bulk Metallic Glasses V

…state-of-the-art development

- Mechanical behavior
- Characterization
- Modeling
- Processing

Carbon Dioxide Reduction Metallurgy

(sponsored by TMS, American Iron and Steel Institute, and Canadian Institute of Mining, Metallurgy and Petroleum)

…state-of-the-art carbon dioxide metallurgical reduction and decreased use of carbon

- Green production of light metals
- Green production of steel
- Carbon sequestration
- Electrochemical reduction of carbon dioxide

Cast Shop Technology

…melting and metal treatment of aluminum

- Sustainability and environmental issues
- Cast house operations and melting
- Cast shop safety
- Casting, solidification and microstructures

Characterization of Minerals, Metals and Materials

…techniques for characterizing materials across a spectrum of systems and processes

- Characterization of mechanical and physical properties of materials
- Characterization of processing of materials
- Characterization of structure across length scales

Climate Change and Greenhouse Gas Emissions

…industry leaders discuss progress and challenges for the materials industries

- Alcan
- Alcoa
- BHP Billiton
- Chalco
- Hydro Aluminum

Complex Oxide Materials: Synthesis, Properties and Applications

…interdisciplinary forum bridging materials research and application

- Novel functional oxide thin films
- Nanostructures
- Oxides for energy technologies
- Ferroelectrics, multiferroics, piezoelectrics and dielectrics

Computational Thermodynamics and Kinetics

…TMS-American Physical Society symposia on fundamental modeling methods and application for materials structures

- Integrated Computational Materials Engineering (ICME)
- Microstructure properties and evolution
- Phase transformations
- Nanoscale systems

Creating the ICME Cyberinfrastructure: an Interdisciplinary Technology Forum

...TMS-American Physical Society roundtable

- State-of-the-art capabilities
- CyberDesign
- Roadmapping development needs

Deformation Twinning: Formation Mechanisms and Effects on Material Plasticity–Experiments and Modeling

…progress in fundamentals of deformation twinning

- Texture, twinning and hardening
- Constitutive modeling
- Electron microscopy
- Flow and fracture

Electrode Technology

(formerly Carbon Technology)

…anodes and cathodes used in aluminum reduction

- Sustainability and environmental issues
- Anode technology and production
- Carbon anodes
- Inert anode materials

Emerging Interconnect and Packaging Technologies

…advanced lead-free solder and packaging technologies

- Electromigration
- Microstructures and characterization
- Processing and reliability issues
- Whisker growth, design and modeling

Emerging Methods to Understand Mechanical Behavior

…advanced characterization and analytical methods

- Orientation imaging microscopy
- Texture evolution
- Nanomechanical testing
- Static, dynamic and cyclic testing

Energy Conservation in Metals Extraction and Materials Processing

…technologies to reduce energy consumption for material production

- Energy and environmental conservation
- Enhanced energy efficiency
- Alternate technologies
- Modeling, simulation and application experiences

Enhancing Materials Durability via Surface Engineering

…recent advancements in surface engineering and modification for life enhancement

- Coatings for environmental, thermal and wear resistance
- Residual stresses
- Graded and novel structures
- Modeling

Frontiers in Process Modeling

…advancing materials development

- Hot-rolling technologies
- Deformation of materials
- Primary metal production

Hael Mughrabi Honorary Symposium: Plasticity, Failure and Fatigue in Structural Materials–from Macro to Nano

…deformation and fracture mechanisms

- Single crystals
- Mathematical modeling
- Cyclic, static and dynamic loading
- Damage evolution

Help to celebrate Professor Hael Mughrabi's lifelong accomplishments at a dinner held in his honor on Monday, March 10.

See the registration form on page 22.

Hot and Cold Rolling Technology

…advanced hot- and cold-rolled products

- Texture development
- Process modeling
- Surface quality

Hume-Rothery Symposium: Nanoscale Phases

…fundamentals of structure and stability of nanoscale phase materials

- Microstructural evolution and stability
- Nano/tera scale integration
- Microscopy
- Nanowires, nanovolumes and nanocrystaliization

IOMMMS Global Materials Forum 2008: Creating the Future MS&E Professionals

…global forum with speakers representing TMS, Association for Iron & Steel Technology, Chinese Society for Metals, Indian Institute of Metals, Japan Institute of Metals, and Mining and Materials Processing Institute of Japan

- Pre-college/K-12
- Innovative university education programs
- Lifelong learning
- International cooperation
- Innovative use of technology

Magnesium Technology 2008

…all aspects of magnesium production, properties and application

- Primary production
- Alloy development
- Performance
- Global market

Materials for Infrastructure: Building Bridges in the Global Community

(sponsored by TMS, Chinese Society for Metals, and Indian Institute of Metals)

…forum devoted to infrastructure needs for the global community

- Buildings
- Public utilities
- Bridges

Materials in Clean Power Systems III: Fuel Cells, Hydrogen, and Clean Coal-Based Technologies

…in-depth coverage of advances in clean power

- Fuel cells
- Hydrogen
- Clean coal

Materials Informatics: Enabling Integration of Modeling and Experiments in Materials Science

...TMS-American Physical Society symposium advancing techniques and application of materials informatics

- Titanium alloys
- Superalloys
- Neural networks
- CyberDesign

Materials Processing Fundamentals

…design, synthesis and control of materials processes and processing

- Solidification processing
- Optimization of thermomechanical processing
- Numerical simulations
- Microstructural evolution

Mechanical Behavior, Microstructure and Modeling of Ti and Its Alloys

…progress towards predictive constitutive and damage models for titanium

- Refinement and processing
- Microstructural evolution
- Microstructure-property relationships
- Modeling and property prediction

Mechanics and Kinetics of Interfaces in Multicomponent Materials Systems

…performance-enabling interfaces across materials systems and applications

- Metal-ceramics, metal-semiconductors and metal-polymer interfaces
- Creep
- Electromigration
- Dynamic and static performance

Micro-Engineered Particulate-Based Materials

…production, characterization and utilization

- In situ nanocomposites
- Corrosion and passivation
- Aluminum
- Stainless steel

Minerals, Metals and Materials under Pressure

…interdisciplinary forum connecting theory and experiment

- Pressure-induced phase transformations
- Simulations and modeling
- High rate plasticity
- Damage and failure mechanisms

National Materials Advisory Board Town Hall Meeting on Assessing Corrosion Education

…review current status and address future needs

- Effectiveness of existing engineering curricula
- Actions to enhance corrosion-based skill and knowledge base of graduating and practicing engineers

Neutron and X-Ray Studies for Probing Materials Behavior

…progress in advanced materials characterization

- Mechanical response
- Thermal treatment
- Texture development
- Microstructural evolution

Neutron Symposium Organizer Rozaliya Barabash:
"The idea to put together two diffraction methods will demonstrate the uniqueness of both of them and mutual complementary possibilities."

Particle Beam-Induced Radiation Effects in Materials

…experimental and theoretical radiation materials science

- Damage evolution
- In situ analysis
- Radiation-induced diffusion
- Nanoscale testing

Phase Stability, Phase Transformations and Reactive Phase Formation in Electronic Materials VII

…thermodynamics and kinetics for phase stability electronic materials

- Phase evolution and stability
- Electro- and thermo-migration
- Solder interfacial reactions

Pyrometallurgy

…advanced pyrometallurgical methods

- Nonferrous pyrometallurgy
- Lead refining
- Titanium production
- Smelter improvements

Recent Industrial Applications of Solid-State Phase Transformations

…utilizing phase transformations for new products

- TRIP steels
- Friction stir welding
- Nickel-based alloys
- Magnesium

Recycling

…recycling of engineered materials today

- Light metals
- Electronic materials
- Precious metals
- Reducing environmental impact

Refractory Metals 2008

…processing and performance

- Oxidation and thin films
- Processing and mechanical deformation

Role of Engineers in Meeting 21st Century Societal Challenges

…AIME keynote session on energy, transportation, housing, health and recycling

Sloan Industry Centers Forum: Techno-Management Issues Related to Materials-Centric Industries

…in-depth coverage of business issues facing aluminum, steel, automotive, wood, paper and metal processing industries

Structural Aluminides for Elevated Temperature Applications

…fundamentals and application

- Alloy design
- Processing and fabrication
- Microstructure-property relationships
- Applications

Ultrafine-Grained Materials: Fifth International Symposium

…technological advancements in design, manufacture and application

- Severe plastic deformation
- Nanocrystalline materials
- Thermal stability
- Deformation and fracture

Women in Science Breakfast Lecture*
"Design for the Other 90%"

Monday, March 10 • 7 to 8 a.m.

Speaker: **Cynthia E. Smith**, Curator, "Design for the Other 90%" Exhibit, Smithsonian's Cooper-Hewitt, *National Design Museum*

"Design for the Other 90%" explores a growing movement among designers to develop solutions for the 5.8 billion people across the globe (90 percent of the world's total population) not traditionally served by the professional design community. Through local and global partnerships, individual designers and organizations are finding unique ways to address the lack of basic necessities faced by the poor and marginalized around the world.

**Advance registration required*

Young Leaders Tutorial Luncheon Lecture
"Computational Materials Science & Engineering: What is it and how do we Take Advantage?"

Monday, March 10 • noon to 1:30 p.m.

Speaker: **Katsuyo Thornton**, Assistant Professor, Materials Science and Engineering, *University of Michigan*
Recipient of the TMS Early Career Faculty Fellow Award

This lecture will address why experimentalists and theorists should become familiar with and utilize many of the standard materials science and engineering computational tools. An overview of the available methodologies, their applications and case studies will be presented.

Note: An optional box lunch may be purchased on the registration form.

Institute of Metals/Robert Franklin Mehl Lecture
"High Performance Structural Metals: an Undervalued but Critical Enabling Technology"

Monday, March 10 • 12:30 to 1:30 p.m.

Speaker: **James C. Williams**, Department of Materials Science and Engineering, *The Ohio State University*

This talk will describe some of the past advances in structural materials and outline some important opportunities going forward. The reality (or lack thereof) of some of the trendy topics also will be assessed and some relative value comparisons will be offered.

William Hume-Rothery Award Lecture
Nanoscale Metal Silicides

Monday, March 10 • 2 p.m.

Speaker: **L.J. Chen**, Department of Materials Science and Engineering, *National Tsing Hua University*

In this talk, an historical account of evolving roles of metal silicides in the context of integrated circuits device applications will be presented. Epitaxial growth of metal silicides on silicon and formation of amorphous interlayers in the metal/Si systems will be reviewed. In addition, synthesis and applications of metal silicide nanowires will be described, and the future outlook will be addressed.

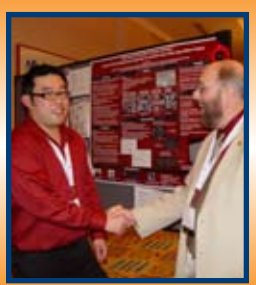

Show your support for the upcoming leaders of our profession!

Attend the TMS Technical Division Student Poster Contest.
Monday, March 10
5 to 6:30 p.m.

Leave a Lasting Impression on New Orleans

Turn to page 27 to learn how you can help the city that has welcomed the TMS Annual Meeting & Exhibition many times.

Extraction & Processing Division Luncheon Lecture*

"Computational Modeling of Metals Processing: Past, Present and Future"

Tuesday, March 11 • 12:30 to 2 p.m.

Speaker: Brian G. Thomas, Wilkins Professor, Mechanical Engineering, *University of Illinois*; Director, *Continuous Casting Consortium*

This talk will recall the early days of process modeling as well as cover recent examples, including fluid flow, heat transfer and stress analysis of processes such as continuous casting of steel. The future of computational modeling will also be contemplated.

**Advance registration required*

Extraction & Processing Division Distinguished Lecture

"Smelting and Refining–Faster, Smoother, Cheaper, Safer"

Tuesday, March 11 • 2 to 2:45 p.m.

Speaker: David G.C. Robertson, Professor, Metallurgical Engineering, *University of Missouri-Rolla*

The purpose of research and development in pyrometallurgy is to achieve at least one of the goals mentioned above (faster, smoother, cheaper, safer). This lecture will review how basic research at the university can contribute to meeting these important goals, using examples mainly from work carried out by the author and his colleagues.

Light Metals Division Luncheon Lecture*

"Innovations in Steel Production–Animations for Aluminium Technologies?"

Wednesday, March 12 • 12:30 to 2:30 p.m.

Speaker: Reiner Kopp, Professor Emeritus, *Institute of Metal Forming, RWTH Aachen University*

This lecture outlines some highlights of manufacturing new steel products and asks the question as to whether or not these innovations in steel could be animations for the development of aluminium products.

**Advance registration required*

For greater detail on any of the annual meeting lectures and speakers, visit www.tms.org/annualmeeting.html.

Grain Refinement of Aluminium Alloys: Theory and Practice

Short Course • Sunday, March 9 • 8 a.m. to 6 p.m.

Instructors
Paul Cooper, *London and Scandinavian Metallurgical Co.*
Douglas Granger, *GRAS*
Wolfgang Schneider, *Hydro Aluminium GmbH*
Peter Schumacher, *University of Leoben*
David StJohn, *Cast Metals Manufacturing*

Who Should Attend
- Professional or technical representatives in the aluminium casting industry
- University researchers

Learn About
- Fundamentals of nucleation and grain growth
- Fundamentals of grain refinement with TiB2 and TiC
- Grain refiner alloys, grain refiner tests and grain size measurement
- Influence of grain refinement on product quality
- Practice of grain refinement in DC casting and shape casting
- Influence of casting conditions on grain refinement

Greenhouse Gas Emissions

Short Course • Sunday, March 9 • 9 a.m. to 3:30 p.m.

Instructors
Halvor Kvande, *Hydro Aluminum*
Jerry Marks, *J. Marks & Associates*
Alton Tabereaux, *Consultant*

Who Should Attend
- HSE professionals
- Aluminum industry operational employees
- Others wanting to learn more about greenhouse gas emissions and their reduction

Learn About
- Environmental challenges facing the global aluminum business
- Reducing greenhouse gas emissions from aluminum smelters
- Anode effects in industrial electrolysis cells
- Action plans and activities to minimize future negative environmental impact and achieve a greener future

Nanomechanical Characterization

Tutorial • Sunday, March 9 • 1 to 5 p.m.

Instructors
Erica T. Lilleodden, *GKSS Research Center*
Brad L. Boyce, *Sandia National Laboratories*

Who Should Attend
- Scientists and engineers interested in mechanical behavior of materials at small scales, particularly nanoscale and nanostructured materials and micro and nanoscale devices
- Students, post-doctoral researchers, early career as well as senior scientists and engineers involved in academic research and industrial applications of thin films and nanomaterials subject to mechanical loads

Learn About
- Current state-of-the-art test methods
- Emerging methods
- Nanoindentation-based techniques
- MEMS-based techniques

Furnace Systems and Technology

3rd Annual Workshop • Monday Afternoon, March 10-Wednesday, March 12

Presentations from 15 companies covering:
- Basic combustion, energy savings and furnace productivity improvement
- Melting furnaces
- Burners designs
- Emissions and abatement
- Recirculating process furnaces
- Metal circulation, cleaning and dross processing
- Casting
- Refractory issues and practices
- Contract engineering
- Rotary delac/decorating systems

Get additional details about these courses and register online at www.tms.org/annualmeeting.html or see page 22.

President's Welcoming Reception

Sunday, March 9 • 6 to 8 p.m.

Seven Networking Receptions for Select Symposia

Visit www.tms.org/annualmeeting.html for details.

137th TMS and AIME Honors and Awards Presentation

With Installation of 2008 TMS President

Tuesday, March 11 • 6 p.m. Reception (Cash Bar) • 7 p.m. Dinner

Robert D. Shull
2007 TMS President

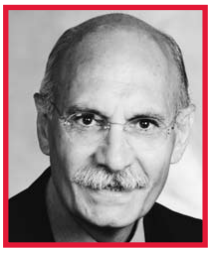

Diran Apelian
2008 TMS President

Dan Thoma
2007 AIME President

Join us as we honor those outstanding individuals who have contributed greatly to materials science and engineering through TMS and AIME. Following the awards presentation, the TMS 2007 and 2008 presidents will address the society. Order your tickets on the registration form.

About the 2008 TMS President

Diran Apelian is Howmet professor of engineering and director of the Metal Processing Institute at Worcester Polytechnic Institute, where he has worked for more than 15 years. Professor Apelian's research interests and expertise are in materials processing, and specifically, solidification and net-shape manufacturing. He is credited for pioneering work in various areas of solidification processing: molten metal processing and filtration of metals; aluminum foundry engineering; plasma deposition; and spray casting/forming. Professor Apelian has more than 400 publications to his credit and four books, which he has co-edited. He has served on, and chaired, several national materials advisory boards for the National Research Council. Professor Apelian has been an active member of TMS for more than 30 years and is the chair of the steering committee for this year's materials and society symposia.

Society Awards

TMS Fellow Class of 2008

- Tsu-Wei Chou, *University of Delaware*
- Campbell Laird, *University of Pennsylvania*
- David E. Laughlin, *Carnegie Mellon University*
- S. Lee Semiatin, *U.S. Air Force Research Laboratory*

Alexander R. Scott Distinguished Service Award
J. Wayne Jones, *University of Michigan*

Application to Practice Award
Gregory Yurek, *American Superconductor*

Bruce Chalmers Award
Alain Karma, *Northeastern University*

Champion H. Mathewson Award
Adam Badri, *Royal Dutch Shell*

Early Career Faculty Fellow
Katsuyo Thornton, *University of Michigan*

Educator Award
Robert L. Snyder, *Georgia Institute of Technology*

Institute of Metals/Robert Franklin Mehl Award
James C. Williams, *The Ohio State University*

John Bardeen Award
Pallab Bhattacharya, *University of Michigan*

Leadership Award
Bruce A. MacDonald, *National Science Foundation*

Robert Lansing Hardy Award
Ken Gall, *Georgia Institute of Technology*

TMS Foundation Shri Ram Arora Award
Sasanka Deka, *National Chemical Laboratory*

William Hume-Rothery Award
L.J. Chen, *National Tsing Hua University*

Division Awards

Electronic, Magnetic & Photonic Materials Division

Distinguished Scientist/Engineer Award
Iver Anderson, *Iowa State University*

Distinguished Service Award
Sung Kang, *IBM*

Extraction & Processing Division

Distinguished Lecturer
David G.C. Robertson, *University of Missouri-Rolla*

Distinguished Service Award
V. Ramachandran, *RAM Consultants*

Science Award
- Ortavio Fortini, *Carnegie Mellon University*
- Richard Fruehan, *Carnegie Mellon University*

Technology Award
- Alex Moyano, *Codelco-Chile*
- Carlos Caballero, *Codelco-Chile*
- Roberto Mackay, *Codelco-Chile*
- Pedro Morales, *Codelco-Chile*
- Domingo Cordero, *Codelco-IM2*
- Jonkion Font, *Codelco-IM2*

Light Metals Division

Distinguished Service Award
Barry Welch, *Welbank Consulting*

Light Metals Award
- Sebastien Leboeuf, *Alcan Inc.*
- Claude Dupuis, *Alcan Inc.*
- Bruno Maltais, *STAS*
- Marc-Andre Thibault, *STAS*
- Einar Smarason, *Alcan Iceland Ltd.*

Technology Award
Alton Tabereaux, *Technical Consultant*

Materials Processing & Manufacturing Division

Distinguished Scientist/Engineer Award
Brian Thomas, *University of Illinois*

Structural Materials Division

Distinguished Scientist/Engineer Award
S. Lee Semiatin, *U.S. Air Force Research Laboratory*

Distinguished Service Award
Marc Meyers, *University of California, San Diego*

Other Awards

2008 Acta Materialia Inc. Gold Medal Award
Karl A. Gschneidner Jr., *Iowa State University and Ames Laboratory, U.S. Department of Energy*

AIME Distinguished Service Award
Alexander R. Scott, retired, *The Minerals, Metals & Materials Society*

AIME Honorary Member
Robert H. Wagoner, *The Ohio State University*

Visit Science Avenue, Technology Avenue or Innovation Boulevard in the exhibition hall where 130+ exhibitors have the newest products and services you need to advance your work.

Exhibition Hours:
Monday, March 10 • noon to 6 p.m.
Tuesday, March 11 • 9:30 a.m. to 5:30 p.m.
Wednesday, March 12 • 9:30 a.m. to 3 p.m.

Enjoy a hosted grand opening reception on Monday, March 10, 5 to 6 p.m., and a snack break on Wednesday, March 12, 12:15 to 2 p.m., while you visit with representatives from these industries:

Light Metals Production and Processing

- Cast shop technology: combustion and furnace technology, grain refiners/hardeners, molten metal filtration and pumps, refractory and insulation products
- Industrial process control and automation, sensors
- Primary production equipment and services: carbon technology and supplies, combustion and furnace technology, HF measurement systems, industrial gases

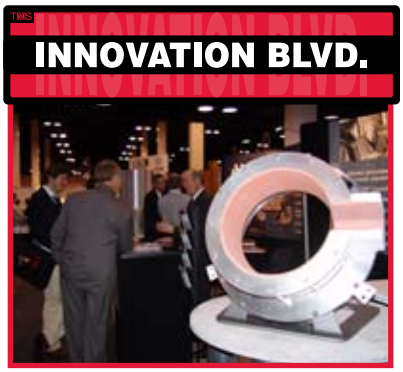

Materials Research and Development

- Characterization equipment: analysis, instrumentation, measurement, microscopy, x-ray fluorescence
- Emerging materials: biomaterials, fuel cells, nanomaterials
- Materials for R&D: alloys, rare earths, precious metals, minerals, chemicals
- Surface processes: coatings, thin films, surface modification

Products and Services for the Materials Science and Engineering Profession

- Professional services: consulting, contracting, engineering, R&D
- Publishers: journals, reference publications
- Software Vendors: design, modeling, process simulation, thermodynamics, phase diagrams
- Technology resources: collaborative programs and centers, national laboratories, nongovernmental organizations

To become an exhibitor or sponsor an event, contact:
Joe Rostan • (724) 776-9000, ext. 231, or (800) 759-4TMS • jrostan@tms.org

Our Sponsors

BP Coke..... Registration Counter
Burner Dynamics Inc.....Registration Bag Insert
Carbone Savoie..... Coffee Break
ConocoPhillips .....General Meeting
Elsevier Ltd. ..... Exhibit Hall Snack
GE Water & Process Technologies.....Lanyards
Harbison-Walker Refractories .....Event Signs, Banner and Information Booth
Hatch..... Coffee Break (Monday Morning)
Jacobs Consultancy Inc. ..... *TMS Today* Newsletter (Tuesday)
Life Cycle Engineering.....Registration Bag Insert
Mitsubishi International Company.....General Meeting
Oxbow Carbon & Minerals LLC.....General Meeting
SEC Carbon (Sumitomo).....Registration Bag Insert
Sentech Precimeter Inc......Registration Bag Insert
SGL Carbon LLC..... Coffee Break
Solios Environnement.....Registration Bags
TCP Petcoke Corporation .....General Meeting
Thermo-Calc Software Inc. .....Registration Bag Insert
Vabco .....Coffee Break (Monday Afternoon)

Exhibiting Companies	Booth No.
ABB Analytical	606
Acuity VCT	
(formerly Benchmark Automation)	232
Alcan Group	309
Aleastur	704
Almeq Norway AS	428
ALTECH SMV Ltd.	721
Aluminium International Today	TBD
Aluminium Times	TBD
Aluminum Corporation of China	222
AUMUND Foerdertechnik GmbH	722
B&P Process Equipment Systems LLC	331
BHS Marketing/Western Briquette	345
Bloom Engineering	304
Boreal Laser	136
Brochot	639
Bruker AXS	114
Buehler Ltd.	806
Burner Dynamics Inc.	110
Buss ChemTech AG	631
C.A. Picard International	233
Carl Zeiss MicroImaging	214
Carl Zeiss SMT	212
Ceradyne Inc.	100
Chongqing Runji Alloy Co Ltd.	814
CMI Novacast Inc.	113
Colt International	644
CompuTherm LLC	820
CSM Instruments	712
Cytec Industries Inc.	731
Dantherm Filtration Inc.	239
Darco Southern	104
DMC Clad Metal Division	738
EBSD Analytical Inc.	710
ECL	312
EDAX Inc.	707
Eirich Machines Inc.	211
Erico	705
FEI Company	730
FFE Minerals	223
GE Energy	322
GE Water & Process Technologies	324
Giesel Verlag GmbH-Verlag für Fachmedien	TBD
Gillespie & Powers Inc.	831
GLAMA Maschinenbau GmbH	613
GNA Alutech Inc.	724
Gouda Vuurvast	329
Graphite Engineering & Sales	209
Graphite Machining Inc.	332
Hamilton Research & Technology PVT Ltd.	832
Hauck Manufacturing Company	227
Heggset Engineering	238
Hencon BV	545
Hertwich Engineering	708
HMR Group AS	339
HRV Engineering Group	723
Hysitron	643
iCrane Systems	632
IMPEC AS	139
Industries 3R Inc.	206
Innovatherm GmbH + Co. KG	631
International Magnesium Association	TBD
Jayne Industries	101
JEOL USA Inc.	837
Jervis B. Webb Company	725
Kabert Industries	605
KB Alloys Inc.	621
KBM Affilips BV	715
KEMPE International	620
L.P. Royer Inc.	221
Laeis GmbH	631
Life Cycle Engineering	115
Light Metal Age	205
Maerz-Gautschi	600
Maruzen International Co. Ltd.	245
McAllister Mills Inc.	625
MECFOR Inc.	339
Mechatherm International Ltd.	626
Metallurg Aluminium	320
Metallurgical Society of CIM	745
Mid-Mountain Materials Inc.	213
MINTEQ International Inc.	118
Morgan AM&T/National Electrical Carbon	810
Murlin Chemical Inc.	201
N.A. Water Systems	821
Nalco Company	601
National Filter Media	739
NKM Noell Special Cranes GmbH	527
North American Manufacturing Co. Ltd.	432
Novelis	300
Olympus Micro Imaging Division	109
Opsis AB	220
Outotec Ltd.	321
Parker Hannifin	539
Pipeline Systems	127
Pyrotek Inc.	301
Resco Products	103
Rex Materials Group	533
Riedhammer GmbH	121
Rigaku	815
SELEE Corporation	501
Sente Software	231
SenTech Precimeter Inc.	805
Shenzhen Aida Aluminum Alloys Co. Ltd.	809
Shimadzu Scientific Instruments Inc.	344
SMV AS	720
Solios Environment	513
Starcyl Cylinders/MAC	203
STAS	609
Stellar Materials Inc.	700
SUAL Group	131
Taylor & Francis Group/CRC Press	819
Thermal Ceramics	507
Thermcon Ovens BV	804
ThermoCalc Software	444
Thermo Scientific Niton Analyzers	107
Thermo Scientific-Scientific Instruments	106
Thorpe Technologies Inc.	308
Urja Products PVT. Limited	713
Wagstaff Inc.	521
Zircar Ceramics Inc.	711

Students - Don't miss this opportunity!

TMS 2008 is a perfect opportunity for materials science and engineering students to learn how to prepare for a career in the materials field, make important professional contacts, and share enjoyable times outside the classroom with fellow students and professionals.

Students who are Material Advantage members may attend the technical sessions, lectures, exhibition and all student activities listed on this page for an advance registration fee of only $25. The advance registration fee for students who are not members is $50, which includes a free year of membership in the Material Advantage Student Program.

Sunday, March 9

2nd Annual Materials Bowl
Preliminary Elimination Rounds • noon
Championship Match • 8:30 to 9 p.m.

Team Registration Deadline: December 15, 2007

A total of $3,500 in prize money is awarded in this "Jeopardy"-style knowledge and trivia competition as well as the Materials Bowl Trophy! Currently, the trophy resides with the 2007 champions, Florida International University. Student chapters are invited to select a team of four chapter members to represent its school for the 2008 Materials Bowl. Eighteen teams will compete in preliminary elimination rounds, with the winners moving on to semifinal matches. The championship match will culminate at the Student Networking Mixer. View the official rules online and register your team early to be part of this exciting competition!

Orientation • 2 to 3 pm.
Find out all you need to know about student activities at TMS 2008 and meet other students with similar interests.

Career Forum • 3:30 to 5 p.m.
Representatives from key materials industries will provide personal insights on career preparation strategies, offer tips on how to develop and foster rewarding careers, and answer your questions.

Career Tips Session • 5 to 6 p.m.
Discover what human resource representatives are looking for when reviewing resumes and interviewing candidates.

Student Networking Mixer • 9 to 11 p.m.
This networking mixer provides a relaxed, casual and fun atmosphere for students, faculty members, and government and industry representatives to make connections and share experiences of professional growth.

Monday, March 10

TMS Technical Division Student Poster Contest • 5 to 6:30 p.m.
Deadline to Apply: January 10, 2008

Both undergraduate and graduate students are encouraged to participate in this dynamic and interactive event. Each of the TMS technical divisions is awarding $500 to the best undergraduate poster and $500 to the best graduate poster. A top prize of $2,500 is awarded by TMS for the "Best of Show" poster.

Ambassador Awards
Judges will select two student authors from among the poster award winners to receive the TMS Student Ambassador awards. The "ambassadors" will receive sponsorship from TMS to represent the society at a 2008 international conference. Two alternate ambassadors will also be chosen in the event the initial award winners are unable to attend the conference.

Visit www.tms.org/annualmeeting.html and click on the student page from the menu for full details about any of these student events.

Subsidize the Cost of Attending TMS 2008

Become a Student Monitor!
Deadline to Apply: December 29, 2007

Student monitors are assigned to attend technical sessions to assist as follows:
- Record the number of attendees for each paper presented in a given session.
- Report any malfunctions of audio/visual equipment to appropriate staff.
- Aid presenters with operation of room lights.

Monitors receive $40 for each one-half day session monitored. Monitor positions are filled as applications are received.

For more information about submitting an application:
- Visit www.tms.org/annualmeeting.html and click on the student page from the menu.
- Contact Cheryl Moore, technical programming assistant, at (724) 776-9000, ext. 252; (800) 759-4TMS; or cmoore@tms.org.

Apply for Travel Reimbursement!
Each Material Advantage chapter is eligible to receive $500 per calendar year in travel reimbursement for members to attend the TMS annual meeting. The travel reimbursement form must be submitted with original receipts by March 28, 2008.
Visit www.tms.org/annualmeeting.html and click on the student page from the menu for the form.

Donate a Door Prize

Student chapter members are asked to donate school logo items to the cache of items TMS will be donating for door prizes at the Student Networking Mixer. The more prizes donated, the better your chances to win! Let TMS know what you plan to bring to donate by e-mailing Bryn Stone at bstone@tms.org.

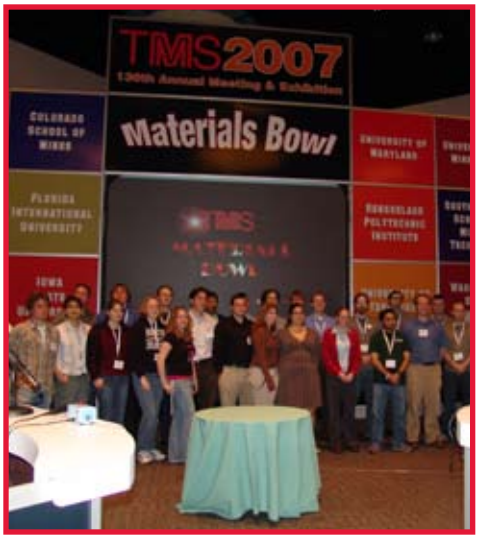

Collected Proceedings CD-ROM

To provide added value for attendees, those registering in the following categories receive a free CD-ROM containing select proceedings:

- Members
- Nonmember Authors
- Nonmembers
- TMS Senior Members
- Exhibitors Full Conference

The CD-ROM will include:

- Multiple symposia proceedings
- Keynote presentations
- Links to additional resource information
- Table of contents

Each symposium will be presented as an individual publication on the CD-ROM, with its own table of contents, standard publication reference numbers, and copyright information. Please visit www.tms.org/annualmeeting.html for a complete listing of the symposia to be included on the CD-ROM.

The CD-ROM is also available for purchase in advance on the registration form or on-site during the annual meeting. The cost per CD-ROM is $150; student price is $75.

Printed Proceedings

For those interested in purchasing printed copies of individual symposia, arrangements can be made before, during and after the annual meeting. To order in advance or after the meeting, contact:
TMS Customer Service • (724) 776-9000, ext. 256, or (800) 759-4TMS • E-mail jsmith@tms.org

Arrangements may also be made at the meeting by visiting the TMS Publications Sales area.

Register before February 11, 2008, to qualify for the advance registration rate. You save $100!

Two Ways to Register

1. Online at www.tms.org/annualmeeting.html with our secure form
2. Complete the form on the next page and mail or fax with your payment.

Your registration includes these valuable learning and networking events:

1. Technical Sessions (Monday through Thursday)
2. ICME Technology Forum* (Sunday)
3. Lead-Free Solders Technology Workshop* (Sunday)
4. Women in Science Breakfast Lecture* (Monday)
5. Young Leaders Tutorial Lecture+ (Monday)
6. Institute of Metals/Robert Franklin Mehl Lecture (Monday)
7. William Hume-Rothery Award Lecture (Monday)
8. Student Poster Contest (Monday)
9. Extraction & Processing Division Distinguished Lecture (Tuesday)
10. President's Welcoming Reception (Sunday)
11. Networking Receptions
12. Exhibition (Monday through Wednesday)
13. Hosted Grand Opening Reception in Exhibit Hall (Monday)
14. Snack Break in Exhibit Hall (Wednesday)
15. Collected Proceedings CD-ROM

*Please sign up to attend on the meeting registration form as space is limited.
+Young Leaders lecture is free. You may order lunch on the meeting registration form.

Location

All conference events, including registration, technical sessions and the exhibition, will take place at the Ernest N. Morial Convention Center; all committee meetings will be held at the Hilton New Orleans Riverside Hotel.

Advance Registrant Check-In and On-Site Registration, Hall J:

Sunday, March 9	11 a.m. to 8 p.m.
Monday, March 10	7 a.m. to 6 p.m.
Tuesday, March 11	7 a.m. to 5:30 p.m.
Wednesday, March 12	7 a.m. to 5 p.m.
Thursday, March 13	7 to 10 a.m.

Policies

Registration Policy

All attendees and meeting participants (authors, exhibitors, etc.) must register for the conference. Badges must be worn for admission to technical sessions, the exhibition and social functions.

Americans With Disabilities Act

TMS strongly supports the federal Americans with Disabilities Act (ADA) which prohibits discrimination against, and promotes public accessibility for, those with disabilities. In support of, and in compliance with, ADA, we ask those requiring specific equipment or services to contact TMS Meeting Services in advance.

Audio/Video Recording Policy

TMS reserves the right to all audio and video reproductions of presentations at TMS sponsored meetings. Recording of sessions (audio, video, still photography, etc.) intended for personal use, distribution, publication or copyright without the express written consent of TMS and the individual authors is strictly prohibited. Contact TMS Technical Programming at (724) 776-9000, ext. 212, to obtain a waiver release.

Photography Notice

By registering for the conference, all attendees acknowledge that they may be photographed by TMS personnel while at events, and that those photos may be used for promotional purposes.

Questions? Contact:

TMS Meeting Services • (724) 776-9000, ext 243, or (800) 759-4TMS

TMS2008

March 9-13, 2008 • New Orleans, LA

AM08-ADV

ADVANCE REGISTRATION FORM

Advance Registration Deadline: February 11, 2008

Payment must accompany form.
Forms received past this date will be processed at the on-site fee.

WEB **www.tms.org/AnnualMeeting.html**
Web registration requires credit card payment.

FAX **USA: (724) 776-3770**
Fax registration requires credit card payment.

MAIL **Return with payment to:** TMS Meeting Services, 184 Thorn Hill Road, Warrendale, PA 15086

1. Member of: ☐ TMS ☐ AIST ☐ SME ☐ SPE Member Number:_____
☐ Dr. ☐ Prof.
☐ Mr. ☐ Mrs. ☐ Ms. _____
Last Name First Name Middle Initial
Informal First Name to Appear on Badge:_____ Date of Birth:_____
mm / dd / yyyy
Employer/Affiliation:_____ Title:_____
Address: ☐ Business ☐ Home _____
City:_____ State/Province:_____ Zip/Postal Code:_____ Country:_____
Telephone:_____ Fax:_____
E-mail:_____

2. Registration Fees:

	Advance Fees Through 2/11/08		On-Site Fees After 2/11/08	
☐ Member	$555	M	$655	ML
☐ Nonmember Author *	$645	NMA	$745	NMAL
☐ Nonmember *	$705	NM	$805	NML
☐ Recent Graduate Member	$395	RG	$495	RGL
☐ Student Member ##	$25	STU	$50	STUL
☐ Student Nonmember ## *	$50	STUN	$100	STUNL
☐ TMS Senior Member	$395	RM	$495	RML
☐ TMS Retired Senior Member	$100	RS	$495	RSL
☐ Exhibitor Full Conference	$555	E	$555	EL
☐ Exhibit Only	$50	EO	$50	EOL

Registration TOTAL $_____

** Includes TMS membership for 2008*
Students must attach a copy of school student identification card.

3. Publications/Collected Proceedings:
Those registering at the member, nonmember author, nonmember, TMS senior member and exhibitor full conference levels will receive a free TMS 2008 collected proceedings CD-ROM.

The CD-ROM may also be purchased below. Note: CD-ROMS will not be available after the meeting. They must be picked up at the meeting; none will be shipped.

	Attendee	Student	Quantity
☐ CD-ROM	$150	$75	_____

Publications TOTAL $_____

Visit the Publications Sales area at the meeting to purchase CD-ROMs or print volumes of selected symposia proceedings. After the meeting, individual symposia proceedings volumes may be purchased online at the TMS Knowledge Resource Center, http://doc.tms.org.

4. Continuing Education:

	Advance Fees Through 2/11/08 Member	Nonmember
☐ Grain Refinement Short Course* (Sunday)	$475	$560
☐ Greenhouse Gas Emissions Short Course* (Sunday)	$475	$560
☐ Nanomechanical Characterization Tutorial (Sunday)	$100	$125

	Conference Registrants	Nonregistrants
☐ ICME Technology Forum (Sunday)	$0	$50
☐ Lead-Free Solders Technology Workshop (Sunday)	$0	$50

Continuing Education TOTAL $_____

* Includes meal

5. Furnace Systems and Technology Workshop:

	Member	Nonmember	Total
Monday 3/10/08-Wednesday 3/12/08	$200	$250	$_____

6. Social Function Tickets:

		Fee	Quantity	Total	
Mon. 3/10/08	Hael Mughrabi Honorary Dinner	$70	_____	$_____	MD
	"Women in Science" Breakfast	$0	_____	$_____	SB
Tues. 3/11/08	TMS-AIME Banquet	$70	_____	$_____	AD
	Tables of 8	$560	_____	$_____	AD8
	Table Sign to Read _____				
	Extraction & Processing Division Luncheon	$45	_____	$_____	EP
	Tables of 8	$360	_____	$_____	EP8
	Table Sign to Read _____				
Wed. 3/12/08	Light Metals Division Luncheon	$45	_____	$_____	LM
	Tables of 8	$360	_____	$_____	LM8
	Table Sign to Read _____				

Social Function TOTAL $_____

For any special dietary needs, please contact Meeting Services at (724) 776-9000, ext. 243.

7. Tutorial Luncheon Tickets:

Monday 3/10/08	Fee	Quantity	Total	
The Young Leaders Tutorial Lecture is free.				
You may purchase the optional box lunch for	$35	_____	$_____	EM

8. 2008 Membership Renewal: *For current TMS members only*

☐ Professional Member	$105	FM
☐ Recent Graduate (2006 or 2005)	$52.50	JM
☐ (ACerS/AIST/ASM/TMS) Material Advantage Student Member	$25	ST

9. Hands-On New Orleans Service Project:

	Amount	
☐ I wish to participate in the service project on Saturday, March 8.	$0	HOP
☐ I wish to contribute financially to the TMS Foundation for project costs.	$25	TFP

10. Payment Enclosed:

☐ Check, Bank Draft, Money Order

Make checks payable to TMS. Payment must be made in U.S. dollars drawn on a U.S. bank.

☐ Credit Card Expiration Date _____
Card No. _____
☐ Visa ☐ MasterCard ☐ Diners Club ☐ American Express
Cardholder Name _____
Signature _____

11. TOTAL FEES PAID $_____

Refund Policy: Written requests must be mailed to TMS, post-marked no later than February 11, 2008. A $75 processing fee is charged for all cancellations. **No refunds will be processed after February 11, 2008.**

Receive a special reduced rate by reserving your hotel before January 28, 2008.

Two ways to reserve your hotel:

1. Visit www.tms.org/annualmeeting.html and click on "Housing" from the menu.
2. Use the form on the next page.

About the Hilton New Orleans Riverside Hotel

The Hilton New Orleans Riverside Hotel is the headquarters hotel for this year's conference. It has a prime location with restaurants, shopping and entertainment close by. Located on the banks of the Mississippi River, the Hilton gives you the best New Orleans has to offer – all within easy walking distance.

Connected to the Hilton is the Riverwalk Marketplace, with more than 140 stores and a great food court. The historic French Quarter is a mere three blocks away, and the famous Aquarium of the Americas and the IMAX Theater is only one block away.

For Your Convenience

TMS has contracted a block of rooms at the Hilton New Orleans Riverside Hotel, and at an additional 15 hotels available through Travel Planners, to ensure attendees are able to obtain housing at reduced rates. Therefore, TMS has assumed a financial liability for any and all rooms in the block that are not reserved. TMS asks that you reserve your room at these hotels in order to limit financial liability for the overall success of the meeting. Thank you.

Guest Hospitality

A special guest hospitality area will be hosted each day from 7 a.m. to 9:30 a.m. in the Hilton New Orleans Riverside Hotel. TMS will sponsor a continental breakfast for the convenience of guests of meeting attendees.

Airport Shuttle

For discounted airport transportation, visit Airport Shuttle online at www.tms.org/annualmeeting.html and click on "Housing" from the menu.

TMS2008

137th Annual Meeting & Exhibition
March 9-13, 2008
Ernest Morial Convention Center, New Orleans, LA

HOUSING RESERVATION FORM

Mail or fax this housing form to:
Travel Planners Inc., 381 Park Ave. South, New York, NY 10016
FAX: (212) 779-6128 • PHONE: (800) 221-3531
In local New York City area or international, call (212) 532-1660.
(CHOOSE ONLY ONE OPTION.)

Making a reservation is easier than ever through Travel Planners' real-time Internet reservation system! Just log on to **www.tms.org/AnnualMeeting.html**, and click on "Housing Reservations." View actual availability, learn about hotel features and services, and obtain local city and sightseeing information. Most importantly, receive instant confirmation of your reservation!

Reservations must be received at Travel Planners by: Monday, January 28, 2008

Arrival Date _____ Departure Date _____

Last Name _____ First Name _____ MI _____

Company _____

Street _____ Address _____

City _____ State/County _____ Zip/Postal Code _____ Country _____

Daytime Phone _____ Fax _____

Additional Room Occupants _____

E-mail _____ (Confirmation will be sent via e-mail if address is provided.)

Nonsmoking Room Requested _____ Special Needs _____

Indicate 1st, 2nd, and 3rd hotel choice:

1. _____
2. _____
3. _____

Type of Accommodations: (check one)
☐ Single 1 person/1bed ☐ Double 2 people/1bed ☐ Twin 2 people/2 beds
☐ Triple 3 people/2 beds ☐ Quad 4 people/2 beds

If all three requested hotels are unavailable, please process this reservation according to: (check one) ☐ ROOM RATE ☐ LOCATION

HEADQUARTERS
Hilton New Orleans Riverside Hotel
$237 single/double
$287 Executive Towers single/double

Best Western St. Christopher Hotel
$139 single/double

Country Inn & Suites
$139 single/double

Courtyard by Marriott Convention Center
$179 single/double

Embassy Suites New Orleans Convention Center Hotel
$189 single/$209 double

Hampton Inn & Suites Convention Center
$169 single/double

Hilton Garden Inn New Orleans
$175 single/double

Hotel New Orleans (formerly Holiday Inn Select)
$159 single/double

Loews New Orleans Hotel
$209 single/double

Marriott New Orleans at the Convention Center
$249 single/double

Residence Inn by Marriott Downtown Convention Center
$189 single/double

SpringHill Suites by Marriott Convention Center
$179 single/double

St. James Hotel
$149 single/double

The Pelham Hotel
$139 single/double

W New Orleans
$199 single/double

Wyndham Riverfront
$199 single/double

In order to ensure that rooms are available for attendees, TMS has contracted a block of rooms at the headquarters hotel, Hilton New Orleans Riverside Hotel, along with each of the hotels listed. TMS assumes financial liability for any and all rooms that are not reserved in the blocks. Therefore, attendees are strongly encouraged to reserve rooms at the hotels listed. This will help to limit undue expenses and secure the success of TMS 2008. Thank you.

Confirmations: A confirmation is e-mailed, faxed or mailed from Travel Planners Inc. once the reservation has been secured with a deposit or credit card. The hotels do not send confirmations. If you do not receive a confirmation within seven days, please call Travel Planners Inc.

Changes/Cancellations: All changes and cancellations in hotel reservations must be made with Travel Planners Inc. until five business days prior to arrival and are subject to the individual hotel's cancellation policies. Cancellations and changes within five days of arrival MUST be made with the hotel directly. Many hotels impose fees for early departure. This rate is set by each hotel and may vary accordingly. Please reconfirm your departure date at the time of check-in.

Reservations/Deposits: All reservations are being coordinated by Travel Planners Inc. Arrangements for housing must be made through Travel Planners Inc. and NOT with the hotel directly. Reservations via Internet, phone or fax are accepted with a major credit card only. Housing forms and written requests are accepted with a major credit card or deposit of one night's room and tax payable to Travel Planners Inc. Check must be drawn in U.S. funds on a U.S. bank. No wire transfers are accepted. Deposit policies are set by each hotel and are outlined on the hotel confirmation.

Please read all hotel information prior to completing and submitting this form to Travel Planners Inc. Keep a copy of this form. Use one form per room required. Make additional copies if needed.

Deposit Payment: ☐ Check ☐ American Express ☐ MasterCard ☐ VISA ☐ Discover ☐ Diners

Account Number _____ Expiration Date _____

Cardholder Name _____ Authorized Signature _____

City and Katrina

Sunday, March 9 or Monday, March 10 • 1 to 4 p.m. • $35 per person

Explore all that makes New Orleans America's most European city. As you ride by beautiful Jackson Square, your tour guide will reconstruct the first days of the old French City. The sights and sounds of the mighty Mississippi River, St. Louis Cathedral, Cabildo and Pontalba buildings are some of the highlights of this area. You will continue past the French Market and the U.S. Mint.

Then, to New Orleans greatest challenge, the tour will proceed by the three levees that "breached" as the tour guide provides a chronology of events leading up to Hurricane Katrina and the days immediately following the disaster. You will travel through parts of the Ninth Ward and Lakeview, some of the hardest hit areas of New Orleans as well as witness the revival of the city by citizens who refuse to give up.

Next is Esplanade Avenue, the outermost boundary of the French Quarter, where you will see a stunning display of the many fine Creole homes with delicate wrought iron fences and balconies. Passing by one of the city's oldest cemeteries, you will learn about the unique above ground burial system. Across Bayou St. John is the spacious city park with its lush greenery and scenic lagoons. Located on the park's grounds is the New Orleans Museum of Art set among the overhanging oak trees and Spanish moss.

Continuing toward the lakefront, which was also affected by the hurricane, you will see Lake Pontchartrain with its lovely setting for exclusive residences, water sports, outdoor activities and many fine seafood restaurants. Following the crescent of the river to the old town of Carrollton and the route of the St. Charles streetcar, you will pass Tulane and Loyola Universities as the ancient oaks of Audubon Park come into view. The heart of uptown showcases some of the city's loveliest neighborhoods, while the Garden District is distinguished by its Greek revival architecture and splendid gardens.

Houmas House

Tuesday, March 11 • 9 a.m. to 1 p.m. • $40 per person

One of the most visited antebellum plantation homes near New Orleans is the Houmas House Plantation. With spectacular gardens, Houmas was used as the filming location for "Hush, Hush, Sweet Charlotte," starring Bette Davis.

Located in the small river community of Darrow, Houmas sits on a few acres on the Mississippi River, much smaller than the 20,000 acres that it once had. The house was built in 1840 by Col. John Smith Preston on land originally owned by the Houmas Indians.

The preservation of this home is superior, and the furnishings are period appropriate. It is lived in and entertained in, even today. Your guides, dressed in period costumes, make the history of this plantation home come alive for you!

Jean Lafitte Swamp Adventure

Wednesday, March 12 • 9:30 a.m. to 12:30 p.m. • $50 per person

Enjoy a journey by boat, Cajun style, into the heart of Louisiana's beautiful and natural swamplands. Your boat will travel deep into the swamps and meandering bayous of this exciting region. Be sure to bring your camera as you may encounter exciting and beautiful animals at any time–alligators, snakes, nesting eagles, egrets, white-tailed deer, mink and nutria. Your guide will be a native of the area who will bring history alive by recounting the exploits of pirate Jean Lafitte and his band as they plied these waters. Louisiana's mysterious waters, moss-draped bayous and the adventure of Jean Lafitte await you!

TMS2008

137th Annual Meeting & Exhibition
March 9-13, 2008
Ernest Morial Convention Center, New Orleans, LA

TOUR REGISTRATION FORM

Type or print clearly. Copy the completed form for your records.
Return this form with appropriate fee to:
MAIL: DMI-Conventions, Laura Swann, 4220 Howard Avenue, New Orleans, LA 70125
FAX: (504) 592-0529 / E-MAIL: lswann@visitnola.com / TELEPHONE: (504) 587-1604

Registration Deadline: February 27, 2008

All tour prices are in U.S. dollars and include all taxes, gratuities, entrance fees, etc. You will receive notification from DMI confirming availability of the tours you have selected. See below for refund cancellation policy.

Tour Attendee Information:

Last Name _____ First Name _____

Street _____ City _____

State/Province _____ Country _____ Postal Code _____

Home Telephone _____ Work Telephone _____

Fax _____ E-mail _____

Name of Hotel in New Orleans _____

Tours:	Hours	No. of People	Cost	Total
March 9, 2008 **City and Katrina Tour**	1 to 4 p.m.	_____x	$35	= $ _____
March 10, 2008 **City and Katrina Tour**	1 to 4 p.m.	_____x	$35	= $ _____
March 11, 2008 **Houmas House**	9 a.m. to 1 p.m.	_____x	$40	= $ _____
March 12, 2008 **Jean Lafitte Swamp Tour**	9:30 a.m. to 12:30 p.m.	_____x	$50	= $ _____
			Total (in U.S. dollars):	$ _____

Payment Information:
Credit card orders will be charged to your account upon receipt of your tour registration form.

☐VISA

☐MasterCard

Credit Card Number _____

Expiration Date _____

Name on Card _____

Signature (required) _____

REFUND/CANCELLATION POLICY
Cancellations received by February 27, 2008, will receive a refund less a $5 per tour administrative fee. Cancellations received after February 27, 2008, will not receive a refund. Should a catastrophic event occur that adversely affects the overall conference, written notice must be received by DMI Conventions for a refund subject to a $5 administration fee.
Cancellation requests must be made in writing and addressed to: DMI-Conventions, MMM308, 4220 Howard Avenue, New Orleans, LA 70125, or faxed to (504) 592-0529. Refunds will be made via check following the conference.

SOCIAL PROGRAM INFORMATION
Tickets will be distributed at the social program registration desk at the ENMCC, Hall I, for all preregistered guests. Early registration is recommended in order to guarantee your space. DMI has the right to cancel any tours if the minimum number of attendees is not met. If a tour is cancelled due to lack of minimum attendance, registrant will be notified by DMI after the registration deadline, and the registration fee refunded in full, unless an alternate choice is selected by registrant.

Hands On

Be The Change. Volunteer. | NEW ORLEANS

You Can Make a Difference in New Orleans

*Volunteer with **TMS** and "Hands On New Orleans" on Saturday, March 8, to make a direct impact on a community affected by Hurricane Katrina.*

The city of New Orleans and the surrounding Gulf Coast region continue to recover from the effects of Hurricane Katrina in 2005. TMS is partnering with Hands On New Orleans to take a team of volunteers into a community still rebuilding from the hurricane. You can help in one or more school renovation projects, such as enhancing science and math classrooms, painting science labs and classrooms, or landscaping.

Hands On New Orleans is affiliated with the national Hands On Network and specializes in developing and implementing high impact service projects. Since the hurricane, the local organization has leveraged the power of more than 4,000 visiting volunteers who gave more than 500,000 hours of service to the recovery and rebuilding of the Gulf Coast.

Saturday's Schedule

- Continental breakfast and project orientation
- Volunteers transported to project site with equipment and supplies provided
- Lunch on-site
- Evening reception

To be part of this special event, sign up on the conference registration form. Space is limited. You can also show your support by contributing $25 to the TMS Foundation to help offset the project costs.

Corporate sponsorship opportunities are also available by contacting:
Joe Rostan • (724) 776-9000, ext. 231, or (800) 759-4TMS • jrostan@tms.org

Leave a lasting impression on the city that has welcomed the TMS Annual Meeting & Exhibition many times.

All contributions to the TMS Foundation are tax deductible in the United States.
Pennsylvania residents may obtain the official registration and financial information of the TMS Foundation from the Pennsylvania Department of State by calling, toll-free within Pennsylvania, 1-800-732-0999. Registration does not imply endorsement.

Room	Sunday	Monday		Tuesday		Wednesday		Thursday
	PM	AM	PM	AM	PM	AM	PM	AM
271		Micro-Engineered Particulate-Based Materials: Session I	Micro-Engineered Particulate-Based Materials: Session II	Materials Informatics: Enabling Integration of Modeling and Experiments in Materials Science: Informatics and Materials Property Design	Materials Informatics: Enabling Integration of Modeling and Experiments in Materials Science: Informatics and Combinatorial Experiments and Materials Characterization	Materials Informatics: Enabling Integration of Modeling and Experiments in Materials Science: Informatics and Materials Theory and Modeling	Materials Informatics: Enabling Integration of Modeling and Experiments in Materials Science: Informatics and Cyberinfrastructure	
272		General Abstracts: Extraction and Processing: Session I	General Abstracts: Extraction and Processing: Session II	IOMMMS Global Materials Forum 2008: Creating the Future MS&E Professional	Materials for Infrastructure: Building Bridges in the Global Community: Session I	Materials for Infrastructure: Building Bridges in the Global Community: Session II	The Role of Engineers in Meeting 21st Century Societal Challenges -- AIME Keynote Session	
273		Ultrafine-Grained Materials: Fifth International Symposium: Modeling, Theory, and Property	Ultrafine-Grained Materials: Fifth International Symposium: Processing and Materials	Ultrafine-Grained Materials: Fifth International Symposium: Stability, Technology, and Property	Ultrafine-Grained Materials: Fifth International Symposium: Properties	Ultrafine-Grained Materials: Fifth International Symposium: Deformation Mechanisms	Ultrafine-Grained Materials: Fifth International Symposium: Structure and Evolution	
274		2008 Nanomaterials: Fabrication, Properties, and Applications: CNT	2008 Nanomaterials: Fabrication, Properties, and Applications: Nanomaterials Synthesis	2008 Nanomaterials: Fabrication, Properties, and Applications: Device	2008 Nanomaterials: Fabrication, Properties, and Applications: Application	2008 Nanomaterials: Fabrication, Properties, and Applications: Random Topics	2008 Nanomaterials: Fabrication, Properties, and Applications: Theory	
275		Emerging Interconnect and Packaging Technologies: Pb-Free Solders: Fundamental Properties, Interfacial Reactions and Phase Transformations	Emerging Interconnect and Packaging Technologies: Pb-Free and Sn-Pb Solders: Electromigation	Emerging Interconnect and Packaging Technologies: Advanced Interconnects	Emerging Interconnect and Packaging Technologies: Pb-Free Solder: Tin Whisker Formation and Mechanical Behavior	Emerging Interconnect and Packaging Technologies: Pb-Free Solders: Reliability and Microstructure Development	Emerging Interconnect and Packaging Technologies: Pb-Free Solders and Other Interconnects: Microstructure, Modeling, and Test Methods	
276		Hume-Rothery Symposium - Nanoscale Phases: Session I	Hume-Rothery Symposium - Nanoscale Phases: Session II	Hume-Rothery Symposium - Nanoscale Phases: Session III	Hume-Rothery Symposium - Nanoscale Phases: Session IV	General Abstracts: Electronic, Magnetic, and Photonic Materials Division: Session I	General Abstracts: Electronic, Magnetic, and Photonic Materials Division: Session II	
277		Complex Oxide Materials - Synthesis, Properties and Applications: ZnO Nanostructures and Thin Films	Complex Oxide Materials - Synthesis, Properties and Applications: Novel Functionality from Complex Oxide Heterointerfaces	Complex Oxide Materials - Synthesis, Properties and Applications: Functionally Cross-Coupled Heterostructures	Complex Oxide Materials - Synthesis, Properties and Applications: Epitaxial Oxides: Ferroelectric, Dielectric, and (Electro-)Magnetic Thin Films	Complex Oxide Materials - Synthesis, Properties and Applications: Scaling, Dynamics, and Switching	Complex Oxide Materials - Synthesis, Properties and Applications: Ferroelectric/ Dielectric Oxides	

Sunday	Monday		Tuesday		Wednesday		Thursday	Room
PM	AM	PM	AM	PM	AM	PM	AM	
	Advances in Semiconductor, Electro Optic and Radio Frequency Materials: Silicon-Based Optoelectronics and Microelectronics	Advances in Semiconductor, Electro Optic and Radio Frequency Materials: Compound Semiconductors and Beyond	Phase Stability, Phase Transformations, and Reactive Phase Formation in Electronic Materials VII: Session I	Phase Stability, Phase Transformations, and Reactive Phase Formation in Electronic Materials VII: Session II	Phase Stability, Phase Transformations, and Reactive Phase Formation in Electronic Materials VII: Session III	Phase Stability, Phase Transformations, and Reactive Phase Formation in Electronic Materials VII: Session IV		278
	Mechanics and Kinetics of Interfaces in Multi-Component Materials Systems: Mechanics of Adhesion, Friction and Fracture	Mechanics and Kinetics of Interfaces in Multi-Component Materials Systems: Nanoscale Structures and Simulations	Mechanics and Kinetics of Interfaces in Multi-Component Materials Systems: Mechanical Properties of Interfaces	Mechanics and Kinetics of Interfaces in Multi-Component Materials Systems: Interfacial Microstructures and Effects on Mechanical and Physical Properties	Mechanics and Kinetics of Interfaces in Multi-Component Materials Systems: Joint Session with Advances in Semiconductors, Electro Optic and Radio Frequency Materials			279
	Recent Developments in Rare Earth Science and Technology - Acta Materialia Gold Medal Symposium: Session I	Recent Developments in Rare Earth Science and Technology - Acta Materialia Gold Medal Symposium: Session II	Recycling: Electronics Recycling	Recycling: Micro-Organisms for Metal Recovery	Recycling: Light Metals	Recycling: General Sessions		280
	Advances in Roasting, Sintering, Calcining, Preheating, and Drying: Advances in Thermal Processing	9th Global Innovations Symposium: Trends in Integrated Computational Materials Engineering for Materials Processing and Manufacturing: Session I	9th Global Innovations Symposium: Trends in Integrated Computational Materials Engineering for Materials Processing and Manufacturing: Session II	Aqueous Processing - General Session: Aqueous Processing General Abstracts				281
	General Abstracts: Materials Processing and Manufacturing Division: Solidification and Casting	General Abstracts: Materials Processing and Manufacturing Division: Composition Structure Property Relationships I	General Abstracts: Materials Processing and Manufacturing Division: Composition Structure Property Relationships II	General Abstracts: Materials Processing and Manufacturing Division: Films, Coatings, and Surface Treatments	General Abstracts: Materials Processing and Manufacturing Division: Forging, Forming, and Powder Processing			282
	Materials Processing Fundamentals: Solidification and Deformation	Materials Processing Fundamentals: Process Modeling	Materials Processing Fundamentals: Powders, Composites, Coatings and Measurements	Materials Processing Fundamentals: Smelting and Refining	Pyrometallurgy - General Sessions: Pyrometallurgy			283
	Characterization of Minerals, Metals, and Materials: Emerging Characterization Techniques	Characterization of Minerals, Metals, and Materials: Characterization of Extraction and Processing	Characterization of Minerals, Metals, and Materials: Characterization of Microstructure and Properties of Materials I	Characterization of Minerals, Metals, and Materials: Characterization of Microstructure and Properties of Materials II	Characterization of Minerals, Metals, and Materials: Characterization of Microstructure and Properties of Materials III	Characterization of Minerals, Metals, and Materials: Characterization of Microstructure and Properties of Materials IV	Characterization of Minerals, Metals, and Materials: Characterization of Microstructure and Properties of Materials V	284

Room	Sunday	Monday		Tuesday		Wednesday		Thursday
	PM	AM	PM	AM	PM	AM	PM	AM
285		Emerging Methods to Understand Mechanical Behavior: Imaging Methods	Emerging Methods to Understand Mechanical Behavior: Digital Image Correlation	Emerging Methods to Understand Mechanical Behavior: Indentation and Dynamic Methods	Emerging Methods to Understand Mechanical Behavior: Subscale Methods	Emerging Methods to Understand Mechanical Behavior: Electron and Neutron Diffraction	Emerging Methods to Understand Mechanical Behavior: X-Ray Diffraction	
286		3-Dimensional Materials Science: ONR/DARPA Dynamic 3-D Digital Structure Program	3-Dimensional Materials Science: Large Datasets and Microstructure Representation I	3-Dimensional Materials Science: Large Datasets and Microstructure Representation II	3-Dimensional Materials Science: Modeling and Characterization across Length Scales I	3-Dimensional Materials Science: Modeling and Characterization across Length Scales II	3-Dimensional Materials Science: Modeling and Characterization across Length Scales III	3-Dimensional Materials Science: Modeling and Characterization across Length Scales IV
287		Recent Industrial Applications of Solid-State Phase Transformations: Superalloys and TRIP Steels/ Automotive Steels	Recent Industrial Applications of Solid-State Phase Transformations: Alloy Design, Microstructure Prediction and Control	Frontiers in Process Modeling: Metallurgical Reactors	Frontiers in Process Modeling: Casting and General Modeling	Energy Conservation in Metals Extraction and Materials Processing: Session I	Energy Conservation in Metals Extraction and Materials Processing: Session II	
288	Computational Thermodynamics and Kinetics: Poster Session	Computational Thermodynamics and Kinetics: Defect Structure I	Computational Thermodynamics and Kinetics: Defect Structure II	Computational Thermodynamics and Kinetics: Phase Field Crystal	Computational Thermodynamics and Kinetics: Functional Materials	Computational Thermodynamics and Kinetics: Phase Transformations	Computational Thermodynamics and Kinetics: Integrated Computational Materials Engineering	Computational Thermodynamics and Kinetics: Diffusion and Phase Stability
291		Magnesium Technology 2008: Magnesium Plenary Session	Magnesium Technology 2008: Wrought Alloys I	Magnesium Technology 2008: Wrought Alloys II	Magnesium Technology 2008: Wrought Alloys III	Magnesium Technology 2008: Advanced Magnesium Materials	Magnesium Technology 2008: Corrosion, Surface Finishing and Joining	
292			Magnesium Technology 2008: Primary Production	Magnesium Technology 2008: Thermodynamics and Phase Transformations	Magnesium Technology 2008: Casting	Magnesium Technology 2008: Alloy Microstructure and Properties	Magnesium Technology 2008: Creep Resistant Magnesium Alloys	
293		Aluminum Alloys: Fabrication, Characterization and Applications: Development and Applications	Aluminum Alloys: Fabrication, Characterization and Applications: Processing and Properties	Aluminum Alloys: Fabrication, Characterization and Applications: Modeling	Aluminum Alloys: Fabrication, Characterization and Applications: Alloy Characterization	Aluminum Alloys: Fabrication, Characterization and Applications: Corrosion and Protection	Aluminum Alloys: Fabrication, Characterization and Applications: Composites and Foams	
294				Carbon Dioxide Reduction Metallurgy: Mechanisms	Carbon Dioxide Reduction Metallurgy: Ferrous Industry	Carbon Dioxide Reduction Metallurgy: Electrolytic Methods		
295		Sustainability, Climate Change and Greenhouse Gas Emissions Reduction: Responsibility, Key Challenges and Opportunities for the Aluminum Industry	Cast Shop Technology: Sustainability in the Casthouse	Cast Shop Technology: Casthouse Operation	Cast Shop Technology: Melt Handling and Treatment	Cast Shop Technology: Foundry Ingots and Alloys	Cast Shop Technology: Casting Processes and Quality Analysis	Cast Shop Technology: Modelling
296			Alumina and Bauxite: HSEC	Alumina and Bauxite: Equipment	Alumina and Bauxite: Bauxite	Alumina and Bauxite: Additives	Alumina and Bauxite: Operations	Alumina and Bauxite: Precipitation/ Conclusion

Sunday	Monday		Tuesday		Wednesday		Thursday	Room
PM	AM	PM	AM	PM	AM	PM	AM	
		General Abstracts: Light Metals Division: Session I	General Abstracts: Light Metals Division: Session II	Electrode Technology Symposium (formerly Carbon Technology): Anode Manufacturing and Developments	Hot and Cold Rolling Technology: Session I	Aluminum Reduction Technology: Reduction Cell Modelling		297
		Aluminum Reduction Technology: Sustainability and Environment	Aluminum Reduction Technology: Cell Development Part I and Operations	Aluminum Reduction Technology: Process Control	Aluminum Reduction Technology: Aluminum Industry in Mid-East	Aluminum Reduction Technology: Fundamentals, Low Melting Electrolytes, New Technologies	Aluminum Reduction Technology: Cell Development Part II	298
		Electrode Technology Symposium (formerly Carbon Technology): Carbon Sustainability and Environment Aspects	Electrode Technology Symposium (formerly Carbon Technology): Anode Raw Materials and Properties	Electrode Technology Symposium (formerly Carbon Technology): Cathodes Raw Materials and Properties		Electrode Technology Symposium (formerly Carbon Technology): Cathodes Manufacturing and Developments	Electrode Technology Symposium (formerly Carbon Technology): Inert Anode	299
	Deformation Twinning: Formation Mechanisms and Effects on Material Plasticity: Experiments and Modeling: Twin Formation and Growth Mechanisms	Deformation Twinning: Formation Mechanisms and Effects on Material Plasticity: Experiments and Modeling: Twin Effects on Material Deformation I	Deformation Twinning: Formation Mechanisms and Effects on Material Plasticity: Experiments and Modeling: Twinning and Associated Defect Structures	Deformation Twinning: Formation Mechanisms and Effects on Material Plasticity: Experiments and Modeling: Twin Effects on Material Deformation II				383
	Mechanical Behavior, Microstructure, and Modeling of Ti and Its Alloys: Processing: Design, Control and Optimization	Mechanical Behavior, Microstructure, and Modeling of Ti and Its Alloys: Phase Transformation and Microstructure Development I	Mechanical Behavior, Microstructure, and Modeling of Ti and Its Alloys: Phase Transformation and Microstructure Development II	Mechanical Behavior, Microstructure, and Modeling of Ti and Its Alloys: Microstructure/ Property Correlation I	Mechanical Behavior, Microstructure, and Modeling of Ti and Its Alloys: Microstructure/ Property Correlation II	Mechanical Behavior, Microstructure, and Modeling of Ti and Its Alloys: Physical/ Mechanical Property Prediction		384
	Minerals, Metals and Materials under Pressure: New Experimental and Theoretical Techniques in High-Pressure Materials Science	Minerals, Metals and Materials under Pressure: Shock-Induced Phase Trans-formations and Microstructure	Minerals, Metals and Materials under Pressure: Electronic, Magnetic and Optical Properties of Materials under High Pressure	Minerals, Metals and Materials under Pressure: High Pressure Phase Transitions and Mechanical Properties				385

Room	Sunday	Monday		Tuesday		Wednesday		Thursday
	PM	AM	PM	AM	PM	AM	PM	AM
386		Hael Mughrabi Honorary Symposium: Plasticity, Failure and Fatigue in Structural Materials - from Macro to Nano: Dislocations: Work Hardening, Patterning, Size Effects I	Hael Mughrabi Honorary Symposium: Plasticity, Failure and Fatigue in Structural Materials - from Macro to Nano: High-emperature Mechanical Properties: Creep, Fatigue and Thermomechanical Fatigue	Hael Mughrabi Honorary Symposium: Plasticity, Failure and Fatigue in Structural Materials - from Macro to Nano: Dislocations: Work Hardening, Patterning, Size Effects II	Hael Mughrabi Honorary Symposium: Plasticity, Failure and Fatigue in Structural Materials - from Macro to Nano: Cyclic Deformation and Fatigue of Metals I	Hael Mughrabi Honorary Symposium: Plasticity, Failure and Fatigue in Structural Materials - from Macro to Nano: Mechanical Properties of Ultrafine-Grained (UFG) Metals I	Hael Mughrabi Honorary Symposium: Plasticity, Failure and Fatigue in Structural Materials - from Macro to Nano: Mechanical Properties of Ultrafine-Grained (UFG) Metals II	Hael Mughrabi Honorary Symposium: Plasticity, Failure and Fatigue in Structural Materials - from Macro to Nano: Cyclic Deformation and Fatigue of Metals II
387		General Abstracts: Structural Materials Division: Mechanical Behavior of Metals and Alloys	General Abstracts: Structural Materials Division: Mechanical Behavior of Materials	General Abstracts: Structural Materials Division: Structure/Property Relations	General Abstracts: Structural Materials Division: Novel Issues in Materials Processing	General Abstracts: Structural Materials Division: Microstructure/ Property Relations in Steel I	General Abstracts: Structural Materials Division: Microstructure/ Property Relations in Steel II	
388		Enhancing Materials Durability via Surface Engineering: Residual Stress Effects on Durability	Enhancing Materials Durability via Surface Engineering: Steel and Other Alloys Surface Durability	Enhancing Materials Durability via Surface Engineering: Superalloy Surface Durability	Enhancing Materials Durability via Surface Engineering: Novel Surface Durability Approaches National Academies Corrosion Education Study Commuity Town Hall Meeting	Refractory Metals 2008: Processing	Refractory Metals 2008: Characterization	Refractory Metals 2008: Properties of Refractory Metals
389		Particle Beam-Induced Radiation Effects in Materials: Metals I	Particle Beam-Induced Radiation Effects in Materials: Metals II	Particle Beam-Induced Radiation Effects in Materials: RIS and Multilayers	Particle Beam-Induced Radiation Effects in Materials: Ceramics and Nuclear Fuel Materials	Particle Beam-Induced Radiation Effects in Materials: Carbides, Semiconductors and Other Non-Metals	Particle Beam-Induced Radiation Effects in Materials: Nanostructures	
390		Biological Materials Science: Mechanical Behavior of Biological Materials I	Biological Materials Science: Implant Biomaterials I	Biological Materials Science: Bioinspired Design and Processing	Biological Materials Science: Scaffold Biomaterials	Biological Materials Science: Functional Biomaterials	Biological Materials Science: Mechanical Behavior of Biological Materials II	Biological Materials Science: Implant Biomaterials II
391		Neutron and X-Ray Studies for Probing Materials Behavior: Resolving Local Structure	Neutron and X-Ray Studies for Probing Materials Behavior: Diffraction at Small Dimensions	Neutron and X-Ray Studies for Probing Materials Behavior: Phase Transitions and Beyond	Neutron and X-Ray Studies for Probing Materials Behavior: Recrystallization	Neutron and X-Ray Studies for Probing Materials Behavior: Stresses/Strains and Structure	Neutron and X-Ray Studies for Probing Materials Behavior: Scattering and Understanding of Materials Properties	
392		Materials in Clean Power Systems III: Fuel Cells, Hydrogen-, and Clean Coal-Based Technologies: Plenary Session	Materials in Clean Power Systems III: Fuel Cells, Hydrogen-, and Clean Coal-Based Technologies: Gas Separation and CO_2 Capture	Materials in Clean Power Systems III: Fuel Cells, Hydrogen-, and Clean Coal-Based Technologies: Solid Oxide Fuel Cells: Metallic Interconnects	Materials in Clean Power Systems III: Fuel Cells, Hydrogen-, and Clean Coal-Based Technologies: Metallic Interconnects in SOFCs: Oxidation, Protection Coatings	Materials in Clean Power Systems III: Fuel Cells, Hydrogen-, and Clean Coal-Based Technologies: Metallic Interconnects and Sealing in SOFCs	Materials in Clean Power Systems III: Fuel Cells, Hydrogen-, and Clean Coal-Based Technologies: PEM Fuel Cells and Solar Technologies	Materials in Clean Power Systems III: Fuel Cells, Hydrogen-, and Clean Coal-Based Technologies: Hydrogen Technologies

Sunday	Monday		Tuesday		Wednesday		Thursday	Room
PM	AM	PM	AM	PM	AM	PM	AM	
	Bulk Metallic Glasses V: Structures and Mechanical Properties I	Bulk Metallic Glasses V: Structures and Mechanical Properties II	Bulk Metallic Glasses V: Structures and Modeling I	Bulk Metallic Glasses V: Structures and Mechanical Properties III	Bulk Metallic Glasses V: Glass Forming Ability and Alloy Development	Bulk Metallic Glasses V: Structures and Modeling II	Bulk Metallic Glasses V: Processing and Properties	393
	Structural Aluminides for Elevated Temperature Applications: Applications	Structural Aluminides for Elevated Temperature Applications: Mechanical Behavior	Structural Aluminides for Elevated Temperature Applications: FE and Other Alumindes	Structural Aluminides for Elevated Temperature Applications: Processing and Microstructure Control	Structural Aluminides for Elevated Temperature Applications: Phase and Microstructure Evolution	Structural Aluminides for Elevated Temperature Applications: New Class of Gamma Alloys - & - Poster Session	Structural Aluminides for Elevated Temperature Applications: Environmental Effects and Protection	394
		Sloan Industry Centers Forum: Techno-Management Issues Related to Materials-Centric Industries: Session I	Sloan Industry Centers Forum: Techno-Management Issues Related to Materials-Centric Industries: Session II					397
	Frontiers of Computational Materials Science: Session I							APS, Hall A
Poster Sessions: 2008 Nanomaterials: Fabrication, Properties, and Applications Computational Thermodynamics and Kinetics General Poster Session Hael Mughrabi Honorary Symposium: Plasticity, Failure and Fatigue in Structural Materials - from Macro to Nano Ultrafine-Grained Materials: Fifth International Symposium								Hall I 2

2008 Nanomaterials: Fabrication, Properties, and Applications: Application ... 274 ... Tues PM ... 207
2008 Nanomaterials: Fabrication, Properties, and Applications: CNT ... 274 ... Mon AM ... 59
2008 Nanomaterials: Fabrication, Properties, and Applications: Device ... 274 ... Tues AM ... 152
2008 Nanomaterials: Fabrication, Properties, and Applications: Nanomaterials Synthesis ... 274 ... Mon PM ... 101
2008 Nanomaterials: Fabrication, Properties, and Applications: Poster Session ... Hall I 2 ... Sun PM ... 39
2008 Nanomaterials: Fabrication, Properties, and Applications: Random Topics ... 274 ... Wed AM ... 260
2008 Nanomaterials: Fabrication, Properties, and Applications: Theory ... 274 ... Wed PM ... 308
3-Dimensional Materials Science: Large Datasets and Microstructure Representation I ... 286 ... Mon PM ... 102
3-Dimensional Materials Science: Large Datasets and Microstructure Representation II ... 286 ... Tues AM ... 153
3-Dimensional Materials Science: Modeling and Characterization across Length Scales I ... 286 ... Tues PM ... 209
3-Dimensional Materials Science: Modeling and Characterization across Length Scales II ... 286 ... Wed AM ... 262
3-Dimensional Materials Science: Modeling and Characterization across Length Scales III ... 286 ... Wed PM ... 309
3-Dimensional Materials Science: Modeling and Characterization across Length Scales IV ... 286 ... Thurs AM ... 355
3-Dimensional Materials Science: ONR/DARPA Dynamic 3-D Digital Structure Program ... 286 ... Mon AM ... 60
9th Global Innovations Symposium: Trends in Integrated Computational Materials Engineering for Materials Processing and Manufacturing: Session I ... 281 ... Mon PM ... 104
9th Global Innovations Symposium: Trends in Integrated Computational Materials Engineering for Materials Processing and Manufacturing: Session II ... 281 ... Tues AM ... 155
Advances in Roasting, Sintering, Calcining, Preheating, and Drying: Advances in Thermal Processing ... 281 ... Mon AM ... 62
Advances in Semiconductor, Electro Optic and Radio Frequency Materials: Compound Semiconductors and Beyond ... 278 ... Mon PM ... 104
Advances in Semiconductor, Electro Optic and Radio Frequency Materials: Joint Session with Mechanics and Kinetics of Interfaces in Multi-Component Materials Systems ... 279 ... Wed AM ... 296
Advances in Semiconductor, Electro Optic and Radio Frequency Materials: Silicon-Based Optoelectronics and Microelectronics ... 278 ... Mon AM ... 63
Alumina and Bauxite: Additives ... 296 ... Wed AM ... 263
Alumina and Bauxite: Bauxite ... 296 ... Tues PM ... 210
Alumina and Bauxite: Equipment ... 296 ... Tues AM ... 156
Alumina and Bauxite: HSEC ... 296 ... Mon PM ... 106
Alumina and Bauxite: Operations ... 296 ... Wed PM ... 311
Alumina and Bauxite: Precipitation/Conclusion ... 296 ... Thurs AM ... 356
Aluminum Alloys: Fabrication, Characterization and Applications: Alloy Characterization ... 293 ... Tues PM ... 211
Aluminum Alloys: Fabrication, Characterization and Applications: Composites and Foams ... 293 ... Wed PM ... 312
Aluminum Alloys: Fabrication, Characterization and Applications: Corrosion and Protection ... 293 ... Wed AM ... 264
Aluminum Alloys: Fabrication, Characterization and Applications: Development and Applications ... 293 ... Mon AM ... 64
Aluminum Alloys: Fabrication, Characterization and Applications: Modeling ... 293 ... Tues AM ... 157
Aluminum Alloys: Fabrication, Characterization and Applications: Processing and Properties ... 293 ... Mon PM ... 107
Aluminum Reduction Technology: Aluminum Industry in Mid-East ... 298/299 ... Wed AM ... 266
Aluminum Reduction Technology: Cell Development Part I and Operations ... 298 ... Tues AM ... 159
Aluminum Reduction Technology: Cell Development Part II ... 298 ... Thurs AM ... 357
Aluminum Reduction Technology: Fundamentals, Low Melting Electrolytes, New Technologies ... 298 ... Wed PM ... 313
Aluminum Reduction Technology: Process Control ... 298 ... Tues PM ... 213
Aluminum Reduction Technology: Reduction Cell Modelling ... 297 ... Wed PM ... 315
Aluminum Reduction Technology: Sustainability and Environment ... 298 ... Mon PM ... 108
Aqueous Processing - General Session: Aqueous Processing General Abstracts ... 281 ... Tues PM ... 214
Biological Materials Science: Bioinspired Design and Processing ... 390 ... Tues AM ... 160
Biological Materials Science: Functional Biomaterials ... 390 ... Wed AM ... 267
Biological Materials Science: Implant Biomaterials I ... 390 ... Mon PM ... 110
Biological Materials Science: Implant Biomaterials II ... 390 ... Thurs AM ... 358
Biological Materials Science: Mechanical Behavior of Biological Materials I ... 390 ... Mon AM ... 66
Biological Materials Science: Mechanical Behavior of Biological Materials II ... 390 ... Wed PM ... 316
Biological Materials Science: Scaffold Biomaterials ... 390 ... Tues PM ... 215
Bulk Metallic Glasses V: Glass Forming Ability and Alloy Development ... 393 ... Wed AM ... 268
Bulk Metallic Glasses V: Processing and Properties ... 393 ... Thurs AM ... 359
Bulk Metallic Glasses V: Structures and Mechanical Properties I ... 393 ... Mon AM ... 67
Bulk Metallic Glasses V: Structures and Mechanical Properties II ... 393 ... Mon PM ... 110
Bulk Metallic Glasses V: Structures and Mechanical Properties III ... 393 ... Tues PM ... 216
Bulk Metallic Glasses V: Structures and Modeling I ... 393 ... Tues AM ... 161
Bulk Metallic Glasses V: Structures and Modeling II ... 393 ... Wed PM ... 317
Carbon Dioxide Reduction Metallurgy: Electrolytic Methods ... 294 ... Wed AM ... 270
Carbon Dioxide Reduction Metallurgy: Ferrous Industry ... 294 ... Tues PM ... 219
Carbon Dioxide Reduction Metallurgy: Mechanisms ... 294 ... Tues AM ... 163
Cast Shop Technology: Casthouse Operation ... 295 ... Tues AM ... 164
Cast Shop Technology: Casting Processes and Quality Analysis ... 295 ... Wed PM ... 319
Cast Shop Technology: Foundry Ingots and Alloys ... 295 ... Wed AM ... 271
Cast Shop Technology: Melt Handling and Treatment ... 295 ... Tues PM ... 220
Cast Shop Technology: Modelling ... 295 ... Thurs AM ... 361
Cast Shop Technology: Sustainability in the Casthouse ... 295 ... Mon PM ... 112
Characterization of Minerals, Metals, and Materials: Characterization of Extraction and Processing ... 284 ... Mon PM ... 113

Characterization of Minerals, Metals, and Materials: Characterization of Microstructure and Properties of Materials I ..... 284 ..... Tues AM 166
Characterization of Minerals, Metals, and Materials: Characterization of Microstructure and Properties of Materials II ..... 284 ..... Tues PM 221
Characterization of Minerals, Metals, and Materials: Characterization of Microstructure and Properties of Materials III ..... 284 ..... Wed AM 272
Characterization of Minerals, Metals, and Materials: Characterization of Microstructure and Properties of Materials IV ..... 284 ..... Wed PM 321
Characterization of Minerals, Metals, and Materials: Characterization of Microstructure and Properties of Materials V ..... 284 ..... Thurs AM 362
Characterization of Minerals, Metals, and Materials: Emerging Characterization Techniques ..... 284 ..... Mon AM 69
Complex Oxide Materials - Synthesis, Properties and Applications: Epitaxial Oxides: Ferroelectric, Dielectric, and (Electro-)Magnetic Thin Films ..... 277 ..... Tues PM 222
Complex Oxide Materials - Synthesis, Properties and Applications: Ferroelectric/Dielectric Oxides ..... 277 ..... Wed PM 322
Complex Oxide Materials - Synthesis, Properties and Applications: Functionally Cross-Coupled Heterostructures ..... 277 ..... Tues AM 167
Complex Oxide Materials - Synthesis, Properties and Applications: Novel Functionality from Complex Oxide Heterointerfaces ..... 277 ..... Mon PM 114
Complex Oxide Materials - Synthesis, Properties and Applications: Scaling, Dynamics, and Switching ..... 277 ..... Wed AM 274
Complex Oxide Materials - Synthesis, Properties and Applications: ZnO Nanostructures and Thin Films ..... 277 ..... Mon AM 70
Computational Thermodynamics and Kinetics: Defect Structure I ..... 288 ..... Mon AM 71
Computational Thermodynamics and Kinetics: Defect Structure II ..... 288 ..... Mon PM 116
Computational Thermodynamics and Kinetics: Diffusion and Phase Stability ..... 288 ..... Thurs AM 364
Computational Thermodynamics and Kinetics: Functional Materials ..... 288 ..... Tues PM 223
Computational Thermodynamics and Kinetics: Integrated Computational Materials Engineering ..... 288 ..... Wed PM 323
Computational Thermodynamics and Kinetics: Phase Field Crystal ..... 288 ..... Tues AM 168
Computational Thermodynamics and Kinetics: Phase Transformations ..... 288 ..... Wed AM 275
Computational Thermodynamics and Kinetics: Poster Session ..... Hall I 2 ..... Sun PM 42
Deformation Twinning: Formation Mechanisms and Effects on Material Plasticity: Experiments and Modeling: Twin Effects on Material Deformation I ..... 383 ..... Mon PM 117
Deformation Twinning: Formation Mechanisms and Effects on Material Plasticity: Experiments and Modeling: Twin Effects on Material Deformation II ..... 383 ..... Tues PM 225
Deformation Twinning: Formation Mechanisms and Effects on Material Plasticity: Experiments and Modeling: Twin Formation and Growth Mechanisms ..... 383 ..... Mon AM 73
Deformation Twinning: Formation Mechanisms and Effects on Material Plasticity: Experiments and Modeling: Twinning and Associated Defect Structures ..... 383 ..... Tues AM 169
Electrode Technology Symposium (formerly Carbon Technology): Anode Manufacturing and Developments ..... 297 ..... Tues PM 225
Electrode Technology Symposium (formerly Carbon Technology): Anode Raw Materials and Properties ..... 299 ..... Tues AM 171
Electrode Technology Symposium (formerly Carbon Technology): Carbon Sustainability and Environment Aspects ..... 299 ..... Mon PM 119
Electrode Technology Symposium (formerly Carbon Technology): Cathodes Manufacturing and Developments ..... 299 ..... Wed PM 325
Electrode Technology Symposium (formerly Carbon Technology): Cathodes Raw Materials and Properties ..... 299 ..... Tues PM 226
Electrode Technology Symposium (formerly Carbon Technology): Inert Anode ..... 299 ..... Thurs AM 365
Emerging Interconnect and Packaging Technologies: Advanced Interconnects ..... 275 ..... Tues AM 172
Emerging Interconnect and Packaging Technologies: Pb-Free and Sn-Pb Solders: Electromigation ..... 275 ..... Mon PM 119
Emerging Interconnect and Packaging Technologies: Pb-Free Solder: Tin Whisker Formation and Mechanical Behavior ..... 275 ..... Tues PM 228
Emerging Interconnect and Packaging Technologies: Pb-Free Solders and Other Interconnects: Microstructure, Modeling, and Test Methods ..... 275 ..... Wed PM 326
Emerging Interconnect and Packaging Technologies: Pb-Free Solders: Fundamental Properties, Interfacial Reactions and Phase Transformations ..... 275 ..... Mon AM 74
Emerging Interconnect and Packaging Technologies: Pb-Free Solders: Reliability and Microstructure Development ..... 275 ..... Wed AM 277
Emerging Methods to Understand Mechanical Behavior: Digital Image Correlation ..... 285 ..... Mon PM 121
Emerging Methods to Understand Mechanical Behavior: Electron and Neutron Diffraction ..... 285 ..... Wed AM 278
Emerging Methods to Understand Mechanical Behavior: Imaging Methods ..... 285 ..... Mon AM 75
Emerging Methods to Understand Mechanical Behavior: Indentation and Dynamic Methods ..... 285 ..... Tues AM 173
Emerging Methods to Understand Mechanical Behavior: Subscale Methods ..... 285 ..... Tues PM 229
Emerging Methods to Understand Mechanical Behavior: X-Ray Diffraction ..... 285 ..... Wed PM 328
Energy Conservation in Metals Extraction and Materials Processing: Session I ..... 287 ..... Wed AM 279
Energy Conservation in Metals Extraction and Materials Processing: Session II ..... 287 ..... Wed PM 329
Enhancing Materials Durability via Surface Engineering: Novel Surface Durability Approaches ..... 388 ..... Tues PM 231
Enhancing Materials Durability via Surface Engineering: Residual Stress Effects on Durability ..... 388 ..... Mon AM 77
Enhancing Materials Durability via Surface Engineering: Steel and Other Alloys Surface Durability ..... 388 ..... Mon PM 122
Enhancing Materials Durability via Surface Engineering: Superalloy Surface Durability ..... 388 ..... Tues AM 175
Frontiers in Process Modeling: Casting and General Modeling ..... 287 ..... Tues PM 232
Frontiers in Process Modeling: Metallurgical Reactors ..... 287 ..... Tues AM 177

Frontiers of Computational Materials Science ..... APS, Hall A ..... Mon AM 78
General Abstracts: Electronic, Magnetic, and Photonic Materials Division: Session I ..... 276 ..... Wed AM 280
General Abstracts: Electronic, Magnetic, and Photonic Materials Division: Session II ..... 276 ..... Wed PM 331
General Abstracts: Extraction and Processing: Session I ..... 272 ..... Mon AM 78
General Abstracts: Extraction and Processing: Session II ..... 272 ..... Mon PM 124
General Abstracts: Light Metals Division: Session I ..... 297 ..... Mon PM 125
General Abstracts: Light Metals Division: Session II ..... 297 ..... Tues AM 178
General Abstracts: Materials Processing and Manufacturing Division: Composition Structure Property Relationships I ..... 282 ..... Mon PM 126
General Abstracts: Materials Processing and Manufacturing Division: Composition Structure Property Relationships II ..... 282 ..... Tues AM 179
General Abstracts: Materials Processing and Manufacturing Division: Films, Coatings, and Surface Treatments ..... 282 ..... Tues PM 233
General Abstracts: Materials Processing and Manufacturing Division: Forging, Forming, and Powder Processing ..... 282 ..... Wed AM 282
General Abstracts: Materials Processing and Manufacturing Division: Solidification and Casting ..... 282 ..... Mon AM 79
General Abstracts: Structural Materials Division: Mechanical Behavior of Materials ..... 387 ..... Mon PM 128
General Abstracts: Structural Materials Division: Mechanical Behavior of Metals and Alloys ..... 387 ..... Mon AM 81
General Abstracts: Structural Materials Division: Microstructure/Property Relations in Steel I ..... 387 ..... Wed AM 283
General Abstracts: Structural Materials Division: Microstructure/Property Relations of Steels II ..... 387 ..... Wed PM 332
General Abstracts: Structural Materials Division: Novel Issues in Materials Processing ..... 387 ..... Tues PM 234
General Abstracts: Structural Materials Division: Structure/Property Relations ..... 387 ..... Tues AM 180
General Poster Session ..... Hall I 2 ..... Sun PM 44
Hael Mughrabi Honorary Symposium: Plasticity, Failure and Fatigue in Structural Materials - from Macro to Nano: Cyclic Deformation and Fatigue of Metals I ..... 386 ..... Tues PM 236
Hael Mughrabi Honorary Symposium: Plasticity, Failure and Fatigue in Structural Materials - from Macro to Nano: Cyclic Deformation and Fatigue of Metals II ..... 386 ..... Thurs AM 333
Hael Mughrabi Honorary Symposium: Plasticity, Failure and Fatigue in Structural Materials - from Macro to Nano: Dislocations: Work Hardening, Patterning, Size Effects I ..... 386 ..... Mon AM 82
Hael Mughrabi Honorary Symposium: Plasticity, Failure and Fatigue in Structural Materials - from Macro to Nano: Dislocations: Work Hardening, Patterning, Size Effects II ..... 386 ..... Tues AM 182
Hael Mughrabi Honorary Symposium: Plasticity, Failure and Fatigue in Structural Materials - from Macro to Nano: High-Temperature Mechanical Properties: Creep, Fatigue and Thermomechanical Fatigue ..... 386 ..... Mon PM 129
Hael Mughrabi Honorary Symposium: Plasticity, Failure and Fatigue in Structural Materials - from Macro to Nano: Mechanical Properties of Ultrafine-Grained (UFG) Metals I ..... 386 ..... Wed AM 285
Hael Mughrabi Honorary Symposium: Plasticity, Failure and Fatigue in Structural Materials - from Macro to Nano: Mechanical Properties of Ultrafine-Grained (UFG) Metals II ..... 386 ..... Wed PM 367
Hael Mughrabi Honorary Symposium: Plasticity, Failure and Fatigue in Structural Materials - from Macro to Nano: Poster Session ..... Hall I 2 ..... Sun PM 49
Hot and Cold Rolling Technology: Session I ..... 297 ..... Wed AM 287
Hume-Rothery Symposium - Nanoscale Phases: Session I ..... 276 ..... Mon AM 84
Hume-Rothery Symposium - Nanoscale Phases: Session II ..... 276 ..... Mon PM 131
Hume-Rothery Symposium - Nanoscale Phases: Session III ..... 276 ..... Tues AM 184
Hume-Rothery Symposium - Nanoscale Phases: Session IV ..... 276 ..... Tues PM 237
IOMMMS Global Materials Forum 2008: Creating the Future MS&E Professional ..... 272 ..... Tues AM 185
Magnesium Technology 2008: Advanced Magnesium Materials ..... 291 ..... Wed AM 288
Magnesium Technology 2008: Alloy Microstructure and Properties ..... 292 ..... Wed AM 289
Magnesium Technology 2008: Casting ..... 292 ..... Tues PM 238
Magnesium Technology 2008: Corrosion, Surface Finishing and Joining ..... 291 ..... Wed PM 335
Magnesium Technology 2008: Creep Resistant Magnesium Alloys ..... 292 ..... Wed PM 336
Magnesium Technology 2008: Magnesium Plenary Session ..... 291/292 ..... Mon AM 85
Magnesium Technology 2008: Primary Production ..... 292 ..... Mon PM 132
Magnesium Technology 2008: Thermodynamics and Phase Transformations ..... 292 ..... Tues AM 186
Magnesium Technology 2008: Wrought Alloys I ..... 291 ..... Mon PM 133
Magnesium Technology 2008: Wrought Alloys II ..... 291 ..... Tues AM 188
Magnesium Technology 2008: Wrought Alloys III ..... 291 ..... Tues PM 240
Materials for Infrastructure: Building Bridges in the Global Community: Session I ..... 272 ..... Tues PM 242
Materials for Infrastructure: Building Bridges in the Global Community: Session II ..... 272 ..... Wed AM 291
Materials in Clean Power Systems III: Fuel Cells, Hydrogen-, and Clean Coal-Based Technologies: Gas Separation and CO_2 Capture ..... 392 ..... Mon PM 135
Materials in Clean Power Systems III: Fuel Cells, Hydrogen-, and Clean Coal-Based Technologies: Hydrogen Technologies ..... 392 ..... Thurs AM 368
Materials in Clean Power Systems III: Fuel Cells, Hydrogen-, and Clean Coal-Based Technologies: Metallic Interconnects and Sealing in SOFCs ..... 392 ..... Wed AM 292
Materials in Clean Power Systems III: Fuel Cells, Hydrogen-, and Clean Coal-Based Technologies: Metallic Interconnects in SOFCs: Oxidation, Protection Coatings ..... 392 ..... Tues PM 243
Materials in Clean Power Systems III: Fuel Cells, Hydrogen-, and Clean Coal-Based Technologies: PEM Fuel Cells and Solar Technologies ..... 392 ..... Wed PM 338

Materials in Clean Power Systems III: Fuel Cells, Hydrogen-, and Clean Coal-Based Technologies: Plenary Session ..... 392 ..... Mon AM 86
Materials in Clean Power Systems III: Fuel Cells, Hydrogen-, and Clean Coal-Based Technologies: Solid Oxide Fuel Cells: Metallic Interconnects ..... 392 ..... Tues AM 189
Materials Informatics: Enabling Integration of Modeling and Experiments in Materials Science: Informatics and Cyberinfrastructure ..... 271 ..... Wed PM 339
Materials Informatics: Enabling Integration of Modeling and Experiments in Materials Science: Informatics and Combinatorial Experiments and Materials Characterization ..... 271 ..... Tues PM 244
Materials Informatics: Enabling Integration of Modeling and Experiments in Materials Science: Informatics and Materials Property Design ..... 271 ..... Tues AM 191
Materials Informatics: Enabling Integration of Modeling and Experiments in Materials Science: Informatics and Materials Theory and Modeling ..... 271 ..... Wed AM 293
Materials Processing Fundamentals: Powders, Composites, Coatings and Measurements ..... 283 ..... Tues AM 192
Materials Processing Fundamentals: Process Modeling ..... 283 ..... Mon PM 136
Materials Processing Fundamentals: Smelting and Refining ..... 283 ..... Tues PM 245
Materials Processing Fundamentals: Solidification and Deformation ..... 283 ..... Mon AM 86
Mechanical Behavior, Microstructure, and Modeling of Ti and Its Alloys: Microstructure/Property Correlation I ..... 384 ..... Tues PM 246
Mechanical Behavior, Microstructure, and Modeling of Ti and Its Alloys: Microstructure/Property Correlation II ..... 384 ..... Wed AM 294
Mechanical Behavior, Microstructure, and Modeling of Ti and Its Alloys: Phase Transformation and Microstructure Development I ..... 384 ..... Mon PM 138
Mechanical Behavior, Microstructure, and Modeling of Ti and Its Alloys: Phase Transformation and Microstructure Development II ..... 384 ..... Tues AM 193
Mechanical Behavior, Microstructure, and Modeling of Ti and Its Alloys: Physical/Mechanical Property Prediction ..... 384 ..... Wed PM 340
Mechanical Behavior, Microstructure, and Modeling of Ti and Its Alloys: Processing: Design, Control and Optimization ..... 384 ..... Mon AM 88
Mechanics and Kinetics of Interfaces in Multi-Component Materials Systems: Interfacial Microstructures and Effects on Mechanical and Physical Properties ..... 279 ..... Tues PM 247
Mechanics and Kinetics of Interfaces in Multi-Component Materials Systems: Joint Session with Advances in Semiconductors, Electro Optic and Radio Frequency Materials ..... 279 ..... Wed AM 296
Mechanics and Kinetics of Interfaces in Multi-Component Materials Systems: Mechanical Properties of Interfaces ..... 279 ..... Tues AM 194
Mechanics and Kinetics of Interfaces in Multi-Component Materials Systems: Mechanics of Adhesion, Friction and Fracture ..... 279 ..... Mon AM 89
Mechanics and Kinetics of Interfaces in Multi-Component Materials Systems: Nanoscale Structures and Simulations ..... 279 ..... Mon PM 139
Micro-Engineered Particulate-Based Materials: Session I ..... 271 ..... Mon AM 90
Micro-Engineered Particulate-Based Materials: Session II ..... 271 ..... Mon PM 140
Minerals, Metals and Materials under Pressure: Electronic, Magnetic and Optical Properties of Materials under High Pressure ..... 385 ..... Tues AM 196
Minerals, Metals and Materials under Pressure: High Pressure Phase Transitions and Mechanical Properties ..... 385 ..... Tues PM 249
Minerals, Metals and Materials under Pressure: New Experimental and Theoretical Techniques in High-Pressure Materials Science ..... 385 ..... Mon AM 91
Minerals, Metals and Materials under Pressure: Shock-Induced Phase Transformations and Microstructure ..... 385 ..... Mon PM 140
National Academies Corrosion Education Study Community Town Hall Meeting ..... 388 ..... Tues PM 232
Neutron and X-Ray Studies for Probing Materials Behavior: Diffraction at Small Dimensions ..... 391 ..... Mon PM 141
Neutron and X-Ray Studies for Probing Materials Behavior: Phase Transitions and Beyond ..... 391 ..... Tues AM 197
Neutron and X-Ray Studies for Probing Materials Behavior: Recrystallization ..... 391 ..... Tues PM 250
Neutron and X-Ray Studies for Probing Materials Behavior: Resolving Local Structure ..... 391 ..... Mon AM 92
Neutron and X-Ray Studies for Probing Materials Behavior: Scattering and Understanding of Materials Properties ..... 391 ..... Wed PM 341
Neutron and X-Ray Studies for Probing Materials Behavior: Stresses/Strains and Structure ..... 391 ..... Wed AM 297
Particle Beam-Induced Radiation Effects in Materials: Carbides, Semiconductors and Other Non-Metals ..... 389 ..... Wed AM 299
Particle Beam-Induced Radiation Effects in Materials: Ceramics and Nuclear Fuel Materials ..... 389 ..... Tues PM 251
Particle Beam-Induced Radiation Effects in Materials: Metals I ..... 389 ..... Mon AM 94
Particle Beam-Induced Radiation Effects in Materials: Metals II ..... 389 ..... Mon PM 143
Particle Beam-Induced Radiation Effects in Materials: Nanostructures ..... 389 ..... Wed PM 342
Particle Beam-Induced Radiation Effects in Materials: RIS and Multilayers ..... 389 ..... Tues AM 198
Phase Stability, Phase Transformations, and Reactive Phase Formation in Electronic Materials VII: Session I ..... 278 ..... Tues AM 199
Phase Stability, Phase Transformations, and Reactive Phase Formation in Electronic Materials VII: Session II ..... 278 ..... Tues PM 253
Phase Stability, Phase Transformations, and Reactive Phase Formation in Electronic Materials VII: Session III ..... 278 ..... Wed AM 300
Phase Stability, Phase Transformations, and Reactive Phase Formation in Electronic Materials VII: Session IV ..... 278 ..... Wed PM 343
Pyrometallurgy - General Sessions: Pyrometallurgy ..... 283 ..... Wed AM 301

Recent Developments in Rare Earth Science and Technology - Acta Materialia Gold Medal Symposium: Session I ..... 280 ..... Mon AM 95
Recent Developments in Rare Earth Science and Technology - Acta Materialia Gold Medal Symposium: Session II ..... 280 ..... Mon PM 144
Recent Industrial Applications of Solid-State Phase Transformations: Alloy Design, Microstructure Prediction and Control ..... 287 ..... Mon PM 145
Recent Industrial Applications of Solid-State Phase Transformations: Superalloys and TRIP Steels/Automotive Steels ..... 287 ..... Mon AM 96
Recycling: Electronics Recycling ..... 280 ..... Tues AM 201
Recycling: General Sessions ..... 280 ..... Wed PM 345
Recycling: Light Metals ..... 280 ..... Wed AM 302
Recycling: Micro-Organisms for Metal Recovery ..... 280 ..... Tues PM 255
Refractory Metals 2008: Characterization ..... 388 ..... Wed PM 346
Refractory Metals 2008: Processing ..... 388 ..... Wed AM 303
Refractory Metals 2008: Properties of Refractory Metals ..... 388 ..... Thurs AM 369
Sloan Industry Centers Forum: Techno-Management Issues Related to Materials-Centric Industries: Session I ..... 397 ..... Mon PM 147
Sloan Industry Centers Forum: Techno-Management Issues Related to Materials-Centric Industries: Session II ..... 397 ..... Tues AM 202
Structural Aluminides for Elevated Temperature Applications: Applications ..... 394 ..... Mon AM 97
Structural Aluminides for Elevated Temperature Applications: Environmental Effects and Protection ..... 394 ..... Thurs AM 370
Structural Aluminides for Elevated Temperature Applications: FE and Other Alumindes ..... 394 ..... Tues AM 203
Structural Aluminides for Elevated Temperature Applications: Mechanical Behavior ..... 394 ..... Mon PM 148
Structural Aluminides for Elevated Temperature Applications: New Class of Gamma Alloys ..... 394 ..... Wed PM 347
Structural Aluminides for Elevated Temperature Applications: Phase and Microstructure Evolution ..... 394 ..... Wed AM 304
Structural Aluminides for Elevated Temperature Applications: Poster Session ..... 394 ..... Wed PM 349
Structural Aluminides for Elevated Temperature Applications: Processing and Microstructure Control ..... 394 ..... Tues PM 255
Sustainability, Climate Change and Greenhouse Gas Emissions Reduction: Responsibility, Key Challenges and Opportunities for the Aluminum Industry ..... 295/296 ..... Mon AM 99
The Role of Engineers in Meeting 21st Century Societal Challenges -- AIME Keynote Session ..... 272 ..... Wed PM 351
Ultrafine-Grained Materials: Fifth International Symposium: Deformation Mechanisms ..... 273 ..... Wed AM 306
Ultrafine-Grained Materials: Fifth International Symposium: Modeling, Theory, and Property ..... 273 ..... Mon AM 99
Ultrafine-Grained Materials: Fifth International Symposium: Poster Session ..... Hall I 2 ..... Sun PM 50
Ultrafine-Grained Materials: Fifth International Symposium: Processing and Materials ..... 273 ..... Mon PM 149
Ultrafine-Grained Materials: Fifth International Symposium: Properties ..... 273 ..... Tues PM 257
Ultrafine-Grained Materials: Fifth International Symposium: Stability, Technology, and Property ..... 273 ..... Tues AM 205
Ultrafine-Grained Materials: Fifth International Symposium: Structure and Evolution ..... 273 ..... Wed PM 352

2008 Nanomaterials: Fabrication, Properties, and Applications: CNT

Sponsored by: The Minerals, Metals and Materials Society, TMS Electronic, Magnetic, and Photonic Materials Division, TMS: Nanomaterials Committee
Program Organizers: Seong Jin Koh, University of Texas; Wonbong Choi, Florida International University; Donna Senft, US Air Force; Ganapathiraman Ramanath, Rensselaer Polytechnic Institute; Seung Kang, Qualcomm Inc

Monday AM Room: 274
March 10, 2008 Location: Ernest Morial Convention Center

Session Chair: To Be Announced

8:30 AM Invited
Carbon Nanotubes - Related Technologies and Engineering Concepts: *Pulickel Ajayan*[1]; [1]Rice University

Carbon nanotube has an important place in nanotechnology. From nanoelectronics to high strength composites, these structures have shown promise and there is a large effort world-wide in research and development of these materials. Several start ups and newly initiated activities at large companies on nanotubes bear testimony to the importance of this material in the technologies to come. The focus in our laboratory over the last decade has been on the engineering of these materials through directed assembly and different approaches in synthesis and processing. The talk will present concepts that lead to the engineering of individual nanostructures as well as assembled architectures that might be used in applications, such as nanoelectronics and sensors, membranes, composites, thermal management and energy related products. The overall scope for this material and our approach in the near term emerging technologies will be briefly discussed.

9:00 AM
Controlled Single-Walled Carbon Nanotubes Growth for High Performance Electronic Devices: *Jun Huang*[1]; Wonbong Choi[1]; [1]Florida International University

Single-walled carbon nanotubes (SWNTs) have been proposed as the building blocks for future nanoelectronics due to their exceptional electronic and mechanical properties. However, the SWNT devices have often been fabricated by using individual nanotubes, positioned randomly on the substrate. For large scale applications, it is highly desired to control the SWNTs growth direction so that large arrays of nanotube devices can be fabricated in a reproducible way. We have demonstrated the aligned growth of SWNTs by varying different parameters, such as electric field, gas flow and substrate. In this presentation, we will discuss the effect of these parameters on the directional growth of SWNTs. The devices fabricated using these aligned SWNTs demonstrate high $I_{on/off}$ ratio, high mobility and no hysteresis effect. It is suggested that the aligned nanotubes can be used for large scale fabrication of SWNT devices for future integrated nanotube electronics.

9:15 AM
Mechanical Properties of Metal-Carbon Nanotube Composites: *Guangping Zheng*[1]; [1]University of Hong Kong

Carbon nanotubes (CNTs) are promising in the producing of strong and light composite materials because of their unique mechanical properties such as exceptional elastic modulus, ultrahigh mechanical strength and large ultimate tensile strain. Although CNT-polymer and CNT-ceramic composites have been successfully fabricated and their mechanical properties have been extensively investigated in the past decade, the CNT-metal composites are still in their infancy. In this study, Multi-walled (MW) CNT metal-matrix composite is synthesized by electrodeposition. X-ray diffraction, transmission electron microscopy and Raman spectroscopy characterizations of the specimens show that MWCNTs are successfully embedded in the cobalt-nickel alloy matrix. The content of MWCNTs can be as large as 5 wt %. The hardness of the composite is larger than that of cobalt. In order to have a better understanding of the mechanical properties of CNT-metal matrix composite, we investigate the metal-CNT interaction using atomistic simulation.

9:30 AM Invited
The Evolution of Helical Forms in Nanotube and Nanofiber Growth: Thermodynamic Model and Experiment: *Prabhakar Bandaru*[1]; Apparao Rao[2]; [1]University of California, San Diego; [2]Clemson University

The synthesis of helical morphologies of nanotubes and nanofibers, through Chemical Vapor Deposition (CVD), has been widely reported and can be made practical for a wide variety of applications, e.g., nanoscale mechanical springs and electrical inductors. Coiled structures are also scientifically interesting in that helices abound in nature, e.g., DNA, proteins etc. and a connection is being made at the nanoscale between carbon based inorganic and organic structures. I will first briefly review the models, in vogue, for the growth of helical forms and point out their shortcomings. Second, a thermodynamic model, based on exclusion volume principles, common in chemical and biological systems, will be introduced to explain coiling. Third, specific predictions will be made for the rational synthesis of nano-coils/-helices. Finally, experimental results conforming to the above model, on the role of Indium catalyst particles and local temperature in influencing the coil pitch in nanotubes/fibers, will be presented.

10:00 AM
Deposition of Ultrathin Polymer Films on CNTs for Enhanced Dispersion and Interfacial Bonding by Plasma Polymerization in CNT-Alumina Composites: *Donglu Shi*[1]; Yan Guo[1]; Hoon Sung Cho[1]; Jie Lian[2]; Yi Song[1]; Jandro Abot[1]; Bed Poudel[3]; Zhifeng Ren[3]; Rod Ewing[2]; [1]University of Cincinnati; [2]University of Michigan; [3]Boston College

Effects of nanoparticle/nanotube surface plasma coating on interfacial behaviors in single wall nanotubes (CNTs)-Al_2O_3 nanocomposites was studied by using high resolution transmission electron microscopy (HRTEM) and mechanical testing. A unique plasma polymerization method was used to coat the alumina nanoparticles and CNTs, which were precursors for the composites. The CNTs-Al_2O_3 nanocomposites were processed by both ambient pressure and hot press sintering. The HRTEM results showed ultrathin pyrrole films (~ 3 nm) on the surfaces of CNTs and Al_2O_3 nanoparticles. A distinctive stress-strain curve difference related to the structural interfaces and plasma coating was observed from the composites. The mechanism on the mechanical property enchancement due to nanoparticle surface plasma coating is discussed.

10:15 AM
Epoxidation of Carbon Nanotubes through Controlled Organic Acid Treatment: *Shiren Wang*[1]; [1]Texas Technological University

Carbon nanotube (CNT) is the strongest fiber so far and has been regarded the most promising reinforcement for next generation multifunctional high-performance composites. However, the current fabrication challenges have seriously restricted these potential applications. In this research, we epoxidized carbon nanotubes with controlled organic acid treatment. Scanning Electron Microscope characterization indicated that dispersion of functionalized CNTs in the epoxy resin has been remarkably improved. It is also found that functionalized CNTs were well embedded in the polymer resin, suggesting improved interface bonding. With only 1wt% loading, epoxidized CNTs/Epoxy composites demonstrated a 50% increase in the Young's modulus, 32% improvement in the tensile strength while un-modified CNTs composites showed worse strength. Epoxy group can be converted into different kinds of functionalities through a ring-opening reaction. Therefore, epoxidation of CNTs significantly enriched the chemistry and facilitated their applications. This investigation provides a solid foundation for the further industrial application of CNTs.

10:30 AM
Fabrication and Mechanical Properties of Carbon Nanotube/Metal Nanocomposites Processed: *Kyung Tae Kim*[1]; Seung Il Cha[2]; Yong Jin Jeong[3]; Thomas Gemming[1]; Juergen Eckert[1]; Soon Hyung Hong[3]; [1]IFW Dresden; [2]NIMS; [3]KAIST

The recent application of nanotechnologies to structural materials is a promising way to produce new strong materials that exceed current limitations. Grain size refinement is considered as one of the most effective strengthening method of materials. At the same time, the addition of carbon nanotubes (CNTs) in a material is known more effective than conventional reinforcements. Here, CNT/Co nanocomposites were fabricated by reinforcing the CNTs in nanocrystalline Co matrix using modified molecular level mixing process. The CNT/Co pearl-necklace-structured nanopowders, consisting of Co nanoparticles penetrated by

CNTs, were fabricated and then consolidated into CNT/Co nanocomposites using spark plasma sintering. The CNT/Co nanocomposite showed outstanding yield strength of 1.5 GPa, which is comparable to those of ceramics. This indicates that the synergistic strengthening mechanism of homogeneously dispersed CNTs in nanocrystalline metal matrix could extend the limitation of mechanical properties of materials.

10:45 AM Break

11:00 AM Invited
Solution-Processed Transparent and (Semi) Conducting Single Walled Carbon Nanotube Thin Films: *Manish Chhowalla*[1]; [1]Rutgers University

Low-density random networks of SWNTs have received significant attention for applications such as transparent electrodes for solar cells and active layers in field-effect transistors. We will briefly review the optoelectronic properties of individual carbon SWNTs and networks. Secondly, we will show how the degree of bundling of SWNTs suspended in water can be determined as a function of the sedimentation time by monitoring their optical transmittance at different depth levels of the vessel. We discuss how the formation and aggregation of 1-200 nm-diameter nanotube bundles in suspension typically occurs on time scales of 0-20 hours and can be understood in the framework of the Mie theory of light scattering. Finally, morphology, optical properties and the electronic performance of solution-processed SWNT networks will be correlated to the type and age of the starting suspensions by means of spectroscopic ellipsometry and Raman spectroscopy combined with electrical transport measurements.

11:30 AM
Mechanical Properties of Well-Aligned Multi-Walled Carbon Nanotube Mats: *Christian Deck*[1]; Jason Flowers[1]; Brandon Reynante[1]; Chi-nung Ni[1]; Prabhakar Bandaru[1]; Kenneth Vecchio[1]; [1]University of California

Carbon nanotubes (CNTs) have been of interest in many fields, due to their exceptional mechanical properties and geometry. In this work, the mechanical properties of well-aligned CNT mats were investigated using two distinct methods. A stage was designed to allow in-situ scanning electron microscopy observation of compression, tension, and shear testing of CNT mats. Force measurements were taken and the elastic modulus of the CNT mats was measured. The flexural rigidity (the product EI) is also important in predicting mechanical response, and an optical method for measuring the flexural rigidity of CNT mats was developed. The deflection of CNTs was observed by introducing fluid flow over CNT mats; this deflection was correlated with measurements of transmitted laser intensity, where intensity drops were observed with increased velocity due to CNT bending. The fluid drag force was simulated, and the experimental and simulation results were used to determine the CNT flexural rigidity.

11:45 AM
Multi-Scale Tribology of Plasma Sprayed Carbon Nanotube Reinforced Aluminum Oxide Nanocomposite Coating: *Kantesh Balani*[1]; Sandip Harimkar[2]; Narendra Dahotre[2]; Arvind Agarwal[1]; [1]Florida International University; [2]University of Tennessee

Our previous studies have revealed that carbon nanotube (CNT) reinforced plasma sprayed Al_2O_3 coating results in improved fracture toughness. In the present study, tribological properties of these coatings have been evaluated at multi-length scale. Owing to disparity of wear and friction at nanosurface contact and loss of material as a bulk, multi-scale tribological study becomes critical in bridging of the wear phenomenon. Pin-on-disc technique is utilized to calculate wear rate of the plasma sprayed coatings at a macro scale, whereas nanoscratch technique is adopted to describe the wear phenomenon at a nano scale. Role of CNT addition and dispersion has shown intriguing results in establishing the material loss of plasma sprayed nanocomposites. Scanning electron microscopy (SEM) has evinced pinning of wear debris by CNTs resulting in the reduced material loss.

12:00 PM Invited
Atomic and Molecular Nanostructures: From Assembly to Function: *Klaus Kern*[1]; [1]Max-Planck-Institut für Festkörperforschung

A promising route toward the realization of functional nanosystems is the exploitation of nature's inherent drive to generate complexity. The transcription of the corresponding organization principles to artificial compounds and environments comprises intriguing perspectives. We emphasize the conductance of self-organized growth processes at well-defined surfaces. The atomistic insight gained into the underlying mechanisms and interactions is used to control the formation of low-dimensional atomic and molecular architectures. This know-how opens up new avenues in engineering nanomaterials of well-defined shape, composition and functionality to be harnessed for future technological applications.

12:30 PM
Redox Synthesis of MnOx-CNT Composites for Supercapacitor Applications: Xianbo Jin[1]; Shengwen Zhang[1]; Wuzong Zhou[2]; *George Chen*[1]; [1]University of Nottingham; [2]University of St. Andrews

Direct reaction between solid carbon (graphite) and permanganate ion in aqueous solutions was first demonstrated recently by this group to be capable of coating the solid carbon with a thin layer of MnOx which exhibited highly satisfactory capacitive behaviour with high stability in cycle life tests. This presentation describes experimental findings in our extension of the previous work by replacing the graphite with carbon nanotubes (CNTs). By variation of the reaction conditions, it has been found through XRD, SEM and TEM that the reaction products can be composites of carbon nanotubes coated individually with MnOx with carbon/manganese ratio being controllable according to the redox reaction. The MnOx deposition mechanism has been proposed, based on experimental evidence, to include two steps: direct carbon-MnO4- reaction and the micro-electrochemical cell. The products are shown to be of ideal materials for supercapacitor applications with the electrode specific capacitance reaching beyond 5 F/cm2.

12:45 PM
Studying on the Ce/Zr Oxide Coating on Carbon Nano-Tubes: *Zhi Guo Dong*[1]; Yao Guangchun[1]; [1]Northeastern University

Carbon nano-tube is a promising reinforcing material for its unique mechanical and physical properties, but the wetting property of metal-matrix and carbon nano-tube is poor. So, in this paper, a continuous Ce/Zr oxide layer was prepared on to the surface of carbon nano-tube to improve the wetting property with Al-matrix then improve the interfacial strength. As to carbon nano-tube, it is difficult to gain continuous Ce/Zr oxide layer because of lame proportion of longitudinal axis length and its diameter, weak reaction capacity, lame curvature of surface, small diameter. So, a series of way of optimization (oxidization, sensitization and activation) were used to increase the activated sites of carbon nano-tube before coating. The result of TEM, XPS, XRD showed that a continuous Ce/Zr oxide layer was successfully prepared onto the nanotube, which indicated a foreground of composite material of carbon nano-tube.

3-Dimensional Materials Science: ONR/DARPA Dynamic 3-D Digital Structure Program

Sponsored by: The Minerals, Metals and Materials Society, TMS Structural Materials Division, TMS: Advanced Characterization, Testing, and Simulation Committee
Program Organizers: Michael Uchic, US Air Force; Eric Taleff, University of Texas; Alexis Lewis, Naval Research Laboratory; Jeff Simmons, US Air Force; Marc DeGraef, Carnegie Mellon University

Monday AM — Room: 286
March 10, 2008 — Location: Ernest Morial Convention Center

Session Chairs: Julie Christodoulou, Office of Naval Research; Alexis Lewis, Naval Research Laboratory

---

8:30 AM Invited
Dynamic 3-D Digital Structure: *Julie Christodoulou*[1]; [1]Office of Naval Research

Launched in the spring of 2005, the Dynamic 3-D Digital Structure program is an ONR-DARPA jointly funded initiative that aims to establish a robust protocol for developing and extracting data, creating quantitative representation of salient materials features, and developing and linking modeling tools to enable a ten-fold increase in the efficiency by which materials science is developed and communicated. Within the program, we are developing both experimental and computational tools, recognizing the effectiveness of using physics-based and

statistical models to guide more rigorous experimentation. Three teams led by the Ohio State University, QuesTek LLC, and the Naval Research Laboratory are engaged in this effort. Their objectives and recent accomplishments will be introduced in this talk.

8:55 AM Invited
The Direct 3-Dimensional Characterization and Digitization of Complex Microstructures in Ti-Based Alloys across Length Scales: *Peter Collins*[1]; Robert Williams[1]; Hamish Fraser[1]; [1]Ohio State University

There have been significant efforts at developing models relating composition, microstructure, and properties in a variety of Ti-based alloys. Until recently, the microstructural information has been estimated from two-dimensional images, resulting in descriptions of the average features determined using classical stereological methods. However, given the recent advent of direct three-dimensional characterization methods, it is possible to characterize the microstructural features without the a priori assumptions associated with stereology. This talk will focus on four novel techniques for the direct three-dimensional characterization of complex microstructures in Ti-based alloys for a range of length scales, from meso-scale (e.g., grain size), through micro-scale (e.g., α-lath thickness) and nano-scale features (e.g., secondary a in Ti-based alloys) to distributions of atomic species in ultra-fine clusters (e.g., athermal ω). These results will be related to those obtained using classical stereological approaches to show that many aspects of the microstructures cannot be accurately obtained using two-dimensional approaches.

9:20 AM Invited
Crystal Plasticity Models with Multi-Time Scaling for Cyclic Deformation of Polycrystalline Metals: *Somnath Ghosh*[1]; Deepu Joseph[1]; Pritam Chakraborty[1]; [1]Ohio State University

The recent years have seen a paradigm shift towards the use of detailed micromechanical models to understand damage mechanisms leading to fatigue failure. Crystal plasticity theories with explicit grain structures are effective in predicting localized cyclic plastic strains. The recent years have seen significant efforts in modeling cyclic plasticity and fatigue with considerations of microstructural stress-strain evolution. Modeling cyclic deformation using conventional time increments can be an exorbitant task for crystal plasticity computations. Most simulations performed with 3D crystal plasticity are in the range of 100 cycles and the results are subsequently extrapolated for fatigue predictions. In modeling fatigue, it is however desirable to conduct simulations for a significantly high number of cycles to reach local states of damage initiation and growth. Conventional methods of time integration using semi discretization present numerous challenges due to the variation in time scales ranging from the scale of the entire process to the time resolution required by the damage evolution and crack propagation. A method of solution of crystal plasticity equations is developed in this paper using multiple time scaling that involves compression and rarefaction of time scales. The method enables large time scale homogenization in relatively benign periods of deformation, to very fine time scale simulations in temporal regions needing high resolution, e.g. with evolving localization. The multi time scaling formulation for polycrystalline materials is based on asymptotic expansion based homogenization method in the time domain. The comparison with the single time scale reference solution shows excellent accuracy while the efficiency gained through time compression can be enormous.

9:45 AM Invited
Dynamics of 3D Microstructures: *Erik Lauridsen*[1]; [1]Riso National Laboratory

This talk will present highlights of studies of the dynamics of 3D microstructures conducted as part of the collaborative D-3D network funded by ONR/DARPA. Using non-destructive synchrotron X-ray based techniques such as 3D X-ray diffraction (3DXRD) microscopy and micro-tomography the microstructural evolution of selected titanium alloys have been monitored with a spatial resolution of a few micrometers. Results from studies of precipitation kinetics and grain growth in titanium alloys will be presented and the coupling of such evolving 3D experimental data with modeling efforts will be discussed.

10:10 AM Break

10:30 AM Invited
Morphological and Crystallographic 3D Reconstruction of β-Grains in Ti-21S: *David Rowenhorst*[1]; Alexis Lewis[1]; George Spanos[1]; [1]Naval Research Laboratory

A large serial sectioning experiment was performed using 200 sections in Ti-21S, a β-stabilized Ti alloy, resulting in a three dimensional (3D) data set containing over 1000 grains. In addition to the morphological information, EBSD was used to determine the crystallographic orientation of each grain, which allows for the analysis of the grain boundary texture, nearest neighbor relationships, and exact morphological measurements of the structure such as grain sizes and interface curvature. The experimental results will be compared to grain growth theory and simulations.

10:55 AM Invited
Simulating Grain Growth in Three Dimensions: I. McKenna[1]; M. Gururajan[1]; M. Na[2]; Y. Wang[2]; *Peter Voorhees*[1]; [1]Northwestern University; [2]Ohio State University

There have been tremendous advances in the ability to collect experimental data on the three-dimensional microstructure of a multigrain material. To follow the evolution of a system of grains that have been measured experimentally, we have developed a single-order-parameter model that accounts for all five degrees of freedom that determine the grain boundary energy and a multiorder parameter model for grain growth. To insure that the computations using the multiorder parameter model are in the boundary-curvature-driven limit, we examine the dependence of grain growth kinetics on the boundary thickness. The single-order-parameter model for grain growth employs quarternions to account for the dependence of the grain boundary energy on the misorientation, a tensorial gradient energy coefficent to account for the change in grain boundary energy with boundary normal, and a singular diffusivity for the order parameter. A comparison of the multiorder and single order parameter models will be presented.

11:20 AM Invited
Atom-Probe Tomographic Characterization of Multicomponent Fe-Cu Based Steels: *David Seidman*[1]; [1]Northwestern University

Atom-probe tomography (APT) is employed to characterize on a sub-nano scale multicomponent Fe-Cu based precipitation strengthening steels being developed for various applications. The three-dimensional (3D) characterization of the micro- and nano-structures is determined, for different thermal processing conditions, as a function of aging time. APT permits us to obtain a complete inventory of the different alloying elements of an area that approaches 200 x 200 nm2 and a depth that can exceed one micrometer: copper-rich and metal carbide precipitates at disparate number densities are also studied. In parallel with the 3D characterization we are studying different mechanical properties: microhardness, yield strength, ultimate tensile strength, plasticity at failure, Charpy V-notch values, and blast resistance. All this information is used to determine the optimum thermal aging treatments that yield the desired values of the key mechanical properties. This research is supported by the Office of Naval Research, Dr. Julie Christodoulou, grant officer.

11:45 AM Invited
Computational Modeling of Ductile Failure of Steel: Direct Numerical Simulation and a Multi-Scale Micromorphic Constitutive Damage Model: *Brian Moran*[1]; Wing Liu[1]; Gregory Olson[1]; [1]Northwestern University

We discuss recent advances in computational analysis of failure mechanisms in high strength steel (McVeigh et al., JMPS, 2007; Vernerey et al., JOM, 2006). Computational issues regarding modeling of the geometry, distribution and material behavior of the dispersed phases present in the microstructure of steel are described. The investigation of the failure mechanisms using computational cell model methodology in two and three dimension is then presented with an emphasis on microvoid-induced shear failure occurring at the scale of sub-micron grain-refining carbide precipitates. The failure of a 3D particle cluster extracted from tomographic analysis of an engineering alloy is simulated. A recently developed multi-scale micromorphic constitutive model (Vernerey et al., JMPS, 2007, submitted) which accounts for failure mechanisms at multiple scales is also discussed. Comparisons between the model and direct numerical simulation of microstructural failure are presented.

Advances in Roasting, Sintering, Calcining, Preheating, and Drying: Advances in Thermal Processing

Sponsored by: The Minerals, Metals and Materials Society, TMS Extraction and Processing Division, TMS: Pyrometallurgy Committee
Program Organizers: Jerome Downey, Montana Tech of the University of Montana; Guy Fredrickson, Idaho National Laboratory

Monday AM Room: 281
March 10, 2008 Location: Ernest Morial Convention Center

Session Chairs: Jerome Downey, Montana Tech of the University of Montana; Guy Fredrickson, Idaho National Laboratory

8:30 AM Introductory Comments

8:35 AM
Pre-Cast Trifoil Heat Exchangers for Rotary Kiln Systems: *Joel Filius*[1]; [1]LWB Refractories

LWB Refractories has developed and patented the design and installation of Internal Heat exchanger systems for rotary kilns. Installations to date total nearly 40 individual systems, installed primarily in Rotary Lime Kilns. These systems vary in installed length and orientation to maximize the thermal transfer of heat from the gas stream to the material burden. Internal Heat exchangers have demonstrated benefits of lowering fuel consumption through improved thermal transfer to the load, increasing production potentials and lowering inlet gas temperatures. This paper will explore the current benefits of these systems, with the direction towards application in Waelz or Calcining systems of the Zinc recovery systems. LWB's patent covers the production of 3, 4 and 5 leg internal systems.

9:05 AM
Investigation on Preparing Strontium Carbonate from Celestite Concentrate by Agglomeration-Reduction Roasting Process: *Mudan Liu*[1]; Jiang Tao[1]; Guanghui Li[1]; [1]Central South University

An agglomeration-reduction roasting process leading to the preparation of SrCO3 from celestite flotation concentrate was studied. A laboratory pelletization mill was used (18 to 20 min balling time) to produced 9% moisture green pellets with a high drop strength. Lignin xanthate binder improved the pellet formation and the pelletizing rate by enhancing the hydrophilicity of the concentrate particle surfaces. Under the optimal roasting conditions (i.e., between 30 and 50 min) at 1100 to 1150°C, 82 to 83% of the pelletized celestite (SrSO4) was converted to strontium oxide when anthracite was used as reductant. This result was 10% higher than that attained by roasting celestite lumps under the same conditions. High-purity strontium carbonate (greater than 97% SrCO3 containing less than 0.3% CaCO3) was obtained by leaching, purifying, and carbonating the roasted pellets.

9:35 AM
The Simulation and Application of Spray Dryer Tower in Alumina Rotary Kiln Sintering: *Hongliang Zhang*[1]; Jie Lie[1]; Xiangtao Chen[1]; [1]Central South University

The paper presents a new technology for alumina rotary kiln sintering, namely the spray dryer sintering. The process flow of the technology was as following: the raw slurries were ejected into the dryer tower, where they were heated and dehydrated by exhaust gases from the end of rotary kiln, and then they were transformed into dry solid particles, which were finally fed into rotary kiln. A 3-dimensional numerical model of the spray dryer tower was built using the CFD package Fluent. The distributions of the temperature, velocity, particles tracks and drying speed were analyzed. Industrial applications show that this technology can reduce the construction cost of rotary kiln, the energy consumption, and it is valuable for alumina plant.

10:05 AM Break

10:35 AM
Development and Application of Optimal Model for Iron Ore Sintering Process Parameters: *Dai fei Liu*[1]; Xiao hui Fan[1]; Hong ming Long[1]; [1]Central South University

Input and output network optimization models were separately developed by analyzing the relationships between the iron ore mixing scheme, process parameters, yield, and quality indexes. Because the neural network modeling results favored the input network model, optimal process parameters were calculated using the input network model in conjunction with neural network and genetic algorithms. The model's effectiveness and practicability were demonstrated by a reduction in the sintering process energy consumption and improved sinter yield and quality.

11:05 AM
Induration Mechanism of Oxidized Pellets Prepared by Magnetite Concentrate and Hematite Concentrate Mixture: *Mudan Liu*[1]; Guanghui Li[1]; Tao Jiang[1]; [1]Central South University

This investigation provides a theoretical basis for the establishing and optimizing the calcination of oxidized pellets prepared from a magnetite and hematite mixture. Strength formation mechanisms of Fe2O3 pellets were studied. Pellets were prepared by preheating and calcining mixtures of magnetite and hematite. The results indicate that the crystallite connection of Fe2O3, in hypo-hematite formed during the preheating process, is the main contributor to pellet strength. The strength of the Fe2O3 matrix in the hypo-hematite produced by oxidizing magnetite exceeded that of original hematite (from hematite concentrate). When calcined below 1250°C, pellet strength is mainly provided by the development of Fe2O3 crystals between hypo-hematite grains. When calcined above 1280°C, the Fe2O3 recrystallization in original hematite was well-developed, the grains within pellets were fully connected, and a strength approaching the theoretical maximum was obtained.

11:35 AM
A New Multi-Region Double Thresholds Segmentation and Its Application in Alumina Rotary Kiln Flame Image: *Hongliang Zhang*[1]; Jie Li[1]; [1]Central South University

Careful flame characteristics control is very important in the calcination stage of the alumina production process. This paper describes a multi-region double threshold segmentation algorithm, which is based on the kiln's "fire region" and the "material region." The algorithm iteratively calculates the corresponding region thresholds and segments the flame image with the two thresholds. In experimental evaluations, the flame image was initially sampled with a charge coupled device from an alumina rotary kiln, and then the single threshold, fuzzy c-means, and multi-region double threshold methods were applied to segment the flame image. The results indicated that multi-region double threshold method more rapidly achieved approximately the same result as fuzzy c-means method, and that both methods produced better results than the single threshold method. The research is of great significance for the flame pattern recognition and for the intelligent control of the rotary kiln.

Advances in Semiconductor, Electro Optic and Radio Frequency Materials: Silicon-Based Optoelectronics and Microelectronics

Sponsored by: The Minerals, Metals and Materials Society, TMS Electronic, Magnetic, and Photonic Materials Division, TMS: Thin Films and Interfaces Committee
Program Organizers: Nuggehalli Ravindra, New Jersey Institute of Technology; Narsingh Singh, Northrop Grumman Corporation ES; Choong-un Kim, University of Texas - Arlington; Yanfa Yan, National Renewable Energy Laboratory; Bhushan Sopori, National Renewable Energy Laboratory; Greg Krumdick, Argonne National Laboratory

Monday AM Room: 278
March 10, 2008 Location: Ernest Morial Convention Center

Session Chairs: Narsingh Singh, Northrop Grumman Corporation ES; Choong-un Kim, University of Texas

8:30 AM Introductory Comments

8:40 AM Invited
Present Status of Silicon Photovoltaics: *Bhushan Sopori*[1]; [1]National Renewable Energy Laboratory

Manufacturing and sales of photovoltaic (PV) cells and modules have been growing at rates exceeding 30% for the last several years. In 2006, PV production exceeded 2 GW and it is expected to surpass 3 GW in 2007. Silicon continues to be the dominant technology with > 90% market share. The position of Si-PV has been strengthened by many technological advances that have led to efficiencies > 16% and 20% for low-cost solar cells and for single-crystal, high-efficiency devices in commercial production. These advances include: improved as-grown material quality; cell processing techniques that include light trapping, impurity gettering, and hydrogen passivation; automation that has enabled high throughput; and newer diagnostics methods. The brisk growth in the market has resulted in a shortage of poly silicon feedstock. However, its impact has only been minor because the PV industry reacted fast to invest into new poly plants, some of which will cater solely to the PV industry. New approaches are needed to increase cell/module efficiencies, develop energy-efficient processing techniques, develop low-cost sources of feedstock, and minimize encapsulation costs. R&D efforts need to be extended into module technology to lower the module costs. This paper will review recent technical advances in Si-PV technology, discuss technical bottlenecks that limit efficiency of current solar cells, and describe potential approaches to overcome them.

9:10 AM Invited
Silicon Integrated Microplasma Optoelectronics: *Anthony Fiory*[1]; Martin Lepselter[2]; Nuggehalli Ravindra[1]; [1]New Jersey Institute of Technology; [2]BTL Fellows Inc.

Microplasma devices are considered for illumination sources in silicon-based opto-microelectronics, owing to their high brightness and efficiency. A pressurized microplasma triode can optically pump microlasers on silicon chips for all-optic integrated systems. The plasma discharge optical pump comprises a microcavity plasma triode device that is fabricated with precision microbridge technology. Plasma elements utilize silicon hollow cathodes with regeneration chemistry for inhibiting erosion and enhancing operating lifetime. This technology enables fabrication of a massively parallel all-optical buss with microplasma microlasers (10^{13} bits/scm^2 at 1 W/cm^2 power dissipation). Miniature plasma displays can be implemented entirely in a silicon chip using microplasma illuminators. High system reliability derives from broad experience with the technology components of gas microplasma display devices, air bridges, silicon microelectronics and plasma display panels. Moreover, laser sources are built in silicon using materials and processing techniques that are integrable with optoelectronics in standard CMOS.

9:40 AM Invited
Characterization of Silicon Doped with Rare-Earth Metals: *Sufian Abedrabbo*[1]; Asmaa Haddad[1]; Qais Mahammed[1]; Anthony Fiory[2]; Nuggehalli Ravindra[2]; [1]University of Jordan; [2]New Jersey Institute of Technology

While silicon is intrinsically an inefficient light emitter, there is considerable interest in improving its optical emission efficiency through materials modification, owing to the inherent advantages of integrating silicon photonics with VLSI technology. In this work, rare-earth metals impurity centers in silicon are investigated. Erbium is co-evaporated with silicon on silicon substrates along with other proper dopants to yield improved emission efficiency. The processed samples are investigated optically by photoluminescence and structurally by Rutherford backscattering.

10:10 AM
Formation of a Ni-FUSI/HfO_2 Gate Stacks by a Novel Integration Process: *Shiang Yu Tan*[1]; [1]Chinese Culture University

The low resistivity nickel fully silicided (FUSI) gate have received increasing attention over the past several years due to the simply integration scheme for implementation and ease of passivation of the underlying gate dielectric for sub-65 nm/45 nm CMOS devices. In order to obtain a thermally stable Ni-FUSI gate electrode, we developed a unique integration process to achieve NiSi phase stabilize at temperature 900°C and delay the agglomeration of NiSi. For the first time, we established an effective way to identify the phase transformations by some nondestructive techniques such as X-ray diffraction, sheet resistance measurement and AFM analysis. The correlations between its electrical and morphological changes during Ni-Si phase transformation were presented.

10:35 AM Break

10:45 AM Invited
Production of High Purity Silicon with Physical Metallurgical Method: Liang Pang[1]; *Huimin Lu*[1]; [1]Beijing University of Aeronautics and Astronautics

A physical metallurgical method has been used to purify industrial raw silicon to high pure silicon from 99.95% to 99.9999% purity. At present, polysilicon with 99.9999% purity has been used to solar battery. The traditional method of produce polysilicon is SIEMENS method. Current high-purity polysilicon technology is a combined technique of metallurgy and directional solidification method. The industrial raw silicon is crushed to 250μm firstly, and then acid dipping and placing processed silicon into a special refining furnace to purify with vacuum environment. The next step is directional solidification. Super high-purity polysilicon in excess of 99.9999% is produced.

11:15 AM
Mechanisms of Front Contact Formation in Si Solar Cells: *Vishal Mehta*[1]; Bhushan Sopori[2]; Nuggehalli Ravindra[3]; [1]National Renewable Energy Laboratory, New Jersey Institute of Technology; [2]National Renewable Energy Laboratory; [3]New Jersey Institute of Technology

In commercial Si solar cell fabrication, the front and backside contacts are formed simultaneously in a one-step process. Because the front contact is formed on a rather shallow junction, its control is very critical. The front contact is typically screen-printed using a Ag-based ink and fired at about 800°C. The Ag-based ink also contains other constituents such as solvent metal(s), glass frit, and an organic binder, all of which help to achieve the desired properties of the contact. The reactions that occur during firing are quite complex. They include: (i) interaction of the solvent metal to lower the eutectic point of Si-Ag, (ii) fusion of various Ag particles to produce a laterally conducting bus, and (iii) formation of a Si-Ag alloy at the interface. To achieve the desired characteristics of the junction, one must understand various reactions and control them to minimize shunting and series resistance and to achieve high performance of the cell. We have studied contact formation in multicrystalline Si solar cells. Solar cells were screen-printed and fired under different processing conditions in a static optical furnace, and their solar cell parameters were measured. We measured other characteristics, such as Si-Ag contact fraction, sheet rho of the bus bar, and shunt resistance of the contact. Likewise, we also evaluated physical parameters of the front contact to investigate various aspects of contact formation. This paper will present results of our studies.

11:40 AM

Effect of Process-Induced Damage during SiN:H Deposition on the Surface Recombination of Silicon: Chuan Li[1]; *Bhushan Sopori*[2]; Rene Rivero[3]; Nuggehalli Ravindra[3]; [1]National Renewable Energy Laboratory and New Jersey Institute of Technology; [2]National Renewable Energy Laboratory; [3]New Jersey Institute of Technology

Hydrogenated silicon nitride (SiN:H) is used in solar cell fabrication to provide bulk and surface passivation. However, SiN:H deposition is also known to produce a damaged region beneath the Si surface. Such surface damage can increase the effective surface recombination velocity (SRV) by introducing an extended region of interface state densities (Dit) in the space-charge region (SCR). Although the firing process can heal some of the surface damage, experimental results show that extended damage remains after annealing. To fully understand the effect of surface damage on surface recombination, we developed a model for calculating SRV of a wafer, which incorporates carrier recombination due to the distribution of Dit in the SCR. This paper describes the proposed model and discusses the results of calculations that relate SRV to the distribution of the damage. We will also describe the verification of the model from SRV measurements of unfired and fired samples, using lifetime data from the quasi-steady-state photoconductance decay technique.

12:05 PM

Edge Passivation in Small-Area N-P Junction Devices: Modeling and Experiments: *Jesse Appel*[1]; Bhushan Sopori[2]; Nuggehalli Ravindra[3]; [1]National Renewable Energy Laboratory, New Jersey Institute of Technology; [2]National Renewable Energy Laboratory; [3]New Jersey Institute of Technology

A small-area mesa diode array, fabricated by chemical etching, is a very valuable technique for detailed characterization of photovoltaic substrates. These devices can be probed with an automatic prober to provide local solar cell parameters such as open-circuit voltage, short-circuit current, and fill factor, and other materials-related parameters such as resistivity, defect density, and minority-carrier diffusion length. Fabricating mesa diode arrays requires passivation of the diode edges, which occurs intrinsically during mesa etching with the Sopori etch by generating a H-saturated suboxide on the etched surface. However, the quality of the passivation is strongly controlled by the cleanliness of the fabrication process. This paper describes a computer model developed to study the influence of edge passivation on the measured cell parameters of the local device(s). We have developed a FE model, which includes generation-recombination at the diode edges. This model takes into account the charge accumulation at the suboxide layer and the loss of carriers that flow into the edge region as a function of the diode voltage. We discuss theoretical results of the model and describe its experimental verification.

Aluminum Alloys: Fabrication, Characterization and Applications: Development and Applications

Sponsored by: The Minerals, Metals and Materials Society, TMS Light Metals Division, TMS: Aluminum Committee
Program Organizers: Subodh Das, Secat Inc; Weimin Yin, Secat Inc

Monday AM Room: 293
March 10, 2008 Location: Ernest Morial Convention Center

Session Chairs: Subodh Das, Secat Inc; Weimin Yin, Secat Inc; Zhong Li, Aleris International Inc

8:30 AM

Composition and Process Optimization of AA 5083 Aluminum Sheet for Quick Plastic Forming: *Ravi Verma*[1]; Paul Krajewski[1]; [1]General Motors Corporation

Sheet manufacturing data collected on approximately 175 coils of superplastic grade 5083 aluminum alloy was analyzed. Key alloy composition and processing variables affecting superplastic elongation of the 5083 sheet were identified. Of these variables, manganese and chromium contents of the alloy, and ingot homogenization time had the most effect on the sheet superplastic elongation, which improved with increasing manganese and chromium contents and longer homogenization time. Significant improvement in material performance was achieved by implementing recommendations based on this study.

8:50 AM

An Aluminum Alloy Development Study to Investigate the Potential to Improve the Formability of the Alloys for Automotive Application: *Kerry Border*[1]; Yansheng Liu[2]; Shridas Ningileri[2]; [1]Toyota Technical Center; [2]Secat Inc

Developing new aluminum alloys with formability comparable to steel will enable the existing tooling systems for steel to be used with minor modifications. The current investigation focuses on this topic and starts out by evaluating the current alloys and the effects of various alloying elements on the material characteristics. Several aluminum alloys are suggested as potential choices for development. Feasibility of various processes ranging from direct chill cast to strip casting as well as spray forming are discussed. Every step of the process starting from ingot casting through rolling process and heat treatment ending at stamping is reviewed based on potential costs. The paper also looks at certain technologies that can be applied at the fabrication shops to improve the materials ease of forming. The investigation also looks at the future prospects of aluminum alloy usage in automotive applications.

9:10 AM

Effects of Scandium and Thermal History on the Structure and Properties of Spray Formed Aluminum 7055 Alloys: *Junyeon Hwang*[1]; John Whetten[2]; T.J. Eden[3]; A. Robinson[3]; W. Sharpe[4]; Michael Kaufman[5]; [1]University of North Texas; [2]University of Idaho; [3]Pennsylvania State University; [4]U.S. Army Research Laboratory; [5]Colorado School of Mines

7xxx series Al-Zn-Mg-(Cu) alloys are widely used in aerospace applications due to their excellent mechanical properties. In this study, the effects of small additions of scandium and the influence of conventional and novel, interrupted heat treatments on the precipitation hardening response of a spray-formed 7055 alloys have been investigated using microhardness, analytical electron microscopy and three-dimensional atom probe tomography. Specifically, single, two-step and multiple-step aging treatments were performed in order to gain insight into the influence of Sc and thermal history on the kinetics of the precipitation hardening response. It will be shown that the initial hardening rate of the alloy containing Sc at low aging temperatures is considerably higher than the Sc-free material. The results will be discussed with an emphasis on elucidating both the mechanism of the increased rate of hardening in the microstructural evolution as a function of the novel aging treatments.

9:30 AM

Development of Al-30%B4C Metal Matrix Composites for Neutron Absorber Material: *X.-Grant Chen*[1]; Robert Hark[1]; [1]Alcan Inc.

In recent years, aluminum boron carbide particulate-reinforced composites have been increasingly used as an excellent neutron absorber material in the nuclear industry. Alcan has developed a unique liquid mixing process to manufacture these metal matrix composites. The fabrication of durable and usable components with higher B4C content composites (up to 30%) is challenging in several aspects ranging from mixing, casting, extruding and rolling. In this paper, the results of development of Al-30%B4C metal matrix composites from raw material via semi-finished to finished products are presented. The casting processes as well as downstream processes (extrusion and rolling) are described. The micro-structural characteristics of Al-30%B4C composites at as-cast and deformed conditions are investigated. The mechanical properties of extruded and rolled components at different conditions are examined. Finally, the perspective of potential application and commercial production of these materials is outlined.

9:50 AM

Enabling Environmentally-Informed Materials Selection Decisions: Robustness of Early Stage Life-Cycle Assessment: *Anna Allen*[1]; Subodh Das[2]; Frank Field[1]; Jeremy Gregory[1]; Randolph Kirchain[1]; [1]Massachusetts Institute of Technology; [2]Secat, Inc

This paper explores the robustness of materials selection decisions when using various life-cycle assessment methods. Improving the environmental performance of vehicles is a topic of growing concern met by today's designer. One approach to this goal is through vehicle mass reduction, enabled through the implementation of a growing array of material candidates. While LCA methods

are available to provide quantitative input into this selection decision, LCA applications are evolving and distinct. Specifically, this paper surveys the major analytical variations of LCA implementations and explores the implications of one major variant when applied to an automotive materials selection case study involving aluminum. This case study examines analytical variations in treatment of recycling by exploring allocation methods that affect product end-of-life. Preliminary results indicate that the choice of analytical method can have real impacts on individual metrics and there are sets of analytical variation over which strategic results are strongly affected.

10:10 AM

Impact of Mass Decompounding on Assessing the Value of Lightweighting: *Catarina Bjelkengren*[1]; Theresa Lee[2]; Richard Roth[1]; Randolph Kirchain[1]; [1]Massachusetts Institute of Technology; [2]General Motors

There is an increasing realization about the need for fuel efficient vehicles. An effective way to accomplish this is through mass reduction. Although primary mass reduction is often associated with additional costs, a decision to lightweight may, depending on when in the development process the decision is taken, result in secondary mass savings such that the value of lightweighting is increased. In this study, we develop a methodology to use regression analysis and vehicle development data to estimate the potential for secondary mass savings at different times in the development process. Subsequently, we employ performance data to estimate the value of the compounded savings in terms of fuel economy and acceleration improvements. Lastly, we utilize market data to estimate how much the improved performance is worth to the consumer. A case study of aluminum automotive closures will be adopted to assess the compounded value of lightweighting using the above methodology.

10:30 AM Break

10:40 AM

A Review of the Warpage Behavior of Aluminum Alloys: *E. Lee*[1]; Omar Es-Said[2]; [1]Naval Air System Command; [2]Loyola Marymount University

Extruded I sections of 7075-T6 aluminum were machined into four different sections shapes. Samples were solution treated and quenched in either a 30% polyalkylene Glycol solution or water. Points on the distorted samples were recorded before and after the solution treatment; the difference between the measurements indicated the extent of warpage. Structural components machined from aluminum forgings can exhibit distortion and poor dimensional quality due to residual stresses formed primarily during heat treatment. The purpose of this investigation was to characterize the influence of compressive strain on the mechanical properties achieved after subsequent aging treatment in aluminum alloy 7050 both by experiment and modeling.

11:00 AM

Ageing of Al-Zn-Mg-Cu Alloys with Minor Sc Additions: *Oleg Senkov*[1]; Marat Shaghiev[1]; Svetlana Senkova[1]; [1]UES Inc.

The effect of Sc additions on precipitation strengthening in an Al-Zn-Mg-Cu alloy was studied after natural and artificial aging. Microhardness, room temperature tensile properties, and microstructure of the alloy were determined after different steps of aging as a function of the Sc content and the strengthening mechanisms were discussed. Minor additions of Sc increase the strength of cast and solution heat treated Al-Zn-Mg-Cu alloys due to precipitation of fine coherent Al3(Sc,Zr) particles. Sc has no effect on the natural aging, which is controlled by formation and growth of GP I zones. However, the Sc additions accelerate the aging process at 120°C and 150°C within a period of time of formation and growth of GP II zones and η' precipitates. At longer aging times at 120°C and 150°C, the aging response of the Sc-containing alloys slows down due to faster coarsening of the η' precipitates and their transformation into η particles.

11:20 AM

Characterizing Microstructural Alterations upon Retrogression and Reaging (RRA) Treatment in Al-Li-Cu-Mg Alloys: *Karuna Ghosh*[1]; K. Das[1]; U. Chatterjee[1]; [1]Indian Institute of Technology - Kharagpur

Al-Li-Cu-Mg alloys of peak aged T8 tempers were subjected to retrogression and reaging (RRA) treatment. XRD, DSC, TEM techniques and electrochemical polarization studies have been used to evaluate the microstructural features of the T8, retrogressed, and RRA T77 tempers. Tensile testing studies have also been carried out to determine the mechanical properties of the alloy tempers. Retrogression treatment has caused dissolution of matrix strengthening d' (Al3Li) precipitates into solution resulting in decrease of strength, but, reaging the retrogressed state to peak aged temper resulted in regaining the initial T8 temper strength - attributed to the reprecipitation of the d' phase in the matrix. The investigation of microstructural features (such as the size, volume fraction and the distribution of d' (Al3Li), d (AlLi), T1 (Al2CuLi), S' (Al2CuMg) phases etc.) of the RRA tempers reveal that the microstructures of the T77 tempers approach to that of the over aged T7 tempers.

11:40 AM

Effects of Heat Treating Aluminum Alloy 6061 in 8 T and 20 T Magnetic Fields: *Samuel Adedokun*[1]; Akin Fashanu[2]; Bayo Ogunmola[2]; [1]Florida Agricultural and Mechanical University-Florida State University, College of Engineering; [2]University of Lagos, Nigeria

Aluminum alloy 6061 has been used extensively for structural and other applications. Its properties is modified by various heat treatments ranging from solution heat treatment to aging processes. In this work, aluminum alloy 6061 of about 13 mm thickness was solution heat treated at 560C for 2 hours, then quenched in water at room temperature. The quenched piece was then cold rolled to aboout 2 mm thickness, that is about 85% severe deformation. Pieces were cut from the deformed aluminum alloy and heat treated at various periods of time at different temperatures in 8 T superconducting magnet and 20 T hybrid magnet. Texture measurements were carried using an x-ray diifractometer. It has been found that heat treatment in the 8 T magnetic field enhanced recovery and suppress recrystallization, whereas the 20 T field enhanced recrystallization.

11:55 AM

The Correlation between Deformation Conditions and Peripheral Coarse Grain Structure in Extrusion of AA7020 Aluminum Alloy: *Ali Reza Eivani*[1]; Hany Ahmed[1]; Jie Zhou[2]; Jureg Duszczyk[2]; [1]Netherlands Institute for Metals Research; [2]Delft University of Technology

In this investigation, a special heat treatment which resembled the actual conditions in the peripheral parts of an extrudate was applied after hot compression. The effects of deformation conditions and the subsequent heat treatment on the formation of coarse grain structure in the AA7020 aluminum alloy were investigated. The microstructure of the samples at two different cooling conditions, namely: (i) water quench and (ii) after the special heat treatment process, were studied in terms of the fraction recrystallized, average grain size and homogeneity. It was found that with increasing deformation temperature or decreasing strain rate, the recrystallized grain size increased. It was also observed that a homogeneous microstructure could be achieved by increasing strain rate. The coarse recrystallized grain structure was attributed to high temperature rather than strain rate.

12:10 PM

An Investigation of the Hot Deformation Behavior of AA7020 and AA7475 Aluminum Alloys: *Hany Ahmed*[1]; Ali Eivani[1]; Jie Zhou[2]; Jurek Duszczyk[2]; [1]Netherlands Institute for Metals Research; [2]Delft University of Technology

An extensive set of experiments, using a Gleeble 3500 thermo-mechanical simulator, was performed to investigate the hot deformation and subsequent recrystallization behavior of industrially significant AA7020 and AA7475 aluminum alloys during hot compression. A wide variety of deformation conditions along with different post-deformation heat treatments were employed in this investigation. The relationship between the deformation conditions and the resulting flow stresses, fraction recrystallized and the post-deformation heat treatments of both alloys was investigated. It was found that AA7475 has higher strength and a relatively higher fraction recrystallized compared to AA7020. It was also observed that steady state flow stress can only be achieved at higher temperatures in AA7020 whereas it is attained at all temperature range for AA7475, which may be attributed to the difference in their recrystallization behavior and in turn to the difference in their zirconium content and zinc to magnesium ratio.

12:30 PM

Development of Al-Si-P Master Alloy and Its Application in Al-Si and Al-Mg-Si Alloys: *Liu Xiangfa*[1]; [1]Shandong University

A new type master alloy rich in phosphorus - Al-Si-P master alloy has been developed by melt reacting method. The master alloy contains pre-formed AlP particles, most of them enveloped in Si phases, this improves their distribution

remarkably. The new copper-free master alloy containing a high concentration of phosphorus (4-5 wt.%) is effective to refine primary Si particles for near eutectic and hypereutectic Al-Si alloys at lower temperature, addition rates, short contract times and without any composition contamination. Now the master alloy is widely applied in a lot of piston manufacturers and die cast factories. In addition, the master alloy can also be used in Al-12.67%Mg-10.33%Si alloy for the refinement and modification of Mg_2Si. The refinement mechanisms are also be researched for primary Si and Mg_2Si.

Biological Materials Science: Mechanical Behavior of Biological Materials I

Sponsored by: The Minerals, Metals and Materials Society, TMS Structural Materials Division, TMS: Biomaterials Committee, TMS/ASM: Mechanical Behavior of Materials Committee

Program Organizers: Ryan Roeder, University of Notre Dame; Robert Ritchie, University of California; Mehmet Sarikaya, University of Washington; Lim Chwee Teck, National University of Singapore; Eduard Arzt, Max Planck Institute; Marc Meyers, University of California, San Diego

Monday AM Room: 390
March 10, 2008 Location: Ernest Morial Convention Center

Session Chair: Ryan Roeder, University of Notre Dame

8:30 AM Keynote
How Really Tough is Human Cortical Bone?: *Robert Ritchie*[1]; Kurt Koester[1]; Joel Ager[1]; [1]University of California

Human bone is more difficult to break than split. However, appropriate fracture-toughness measurements to break bone (in transverse directions) are rare. Most measurements focus on crack-initiation, whereas bone principally derives its toughness during crack-growth; moreover, the few crack-growth measurements are for longitudinal "splitting" orientations. Here we use nonlinear-elastic fracture mechanics to determine R-curves for both orientations in human cortical bone, using in-situ testing within an environmental SEM to simultaneously examine the salient damage/toughening mechanisms. We find that stress-intensities up to 5MPam$^{1/2}$ are required to propagate large cracks along the bone long axis, whereas to propagate a crack only 500 microns in transverse directions requires stress-intensities some five times higher. Such toughnesses are far larger than previously thought, yet represent a truer depiction of conditions to break bone. Mechanistically, behavior results from microcracking at osteon/interstitial interfaces, which promotes gross crack deflections for transverse cracking and crack bridging for longitudinal orientations.

9:10 AM Invited
Post-Yield Energy Dissipation and Bone Quality: *Xiaodu Wang*[1]; [1]University of Texas at San Antonio

A number of factors across multiple length scales may contribute to the toughness of bone, thus hindering a complete mechanistic explanation for bone fragility. Bone possesses a highly hierarchical structure, consisting of water, mineral, and collagen phases and showing a rather complex response to the mechanical loading. While previous research has investigated bone fracture mechanics, fatigue behavior, and load-induced damage accumulations, little is known about the progressive changes in the post-yield behavior of bone with increasing deformation (strain) levels. In this study, we investigated the progressive post-yield behavior of bone using a novel diagnostic loading scheme, so as to gain more information on the underlying mechanism of post-yield energy dissipation in bone. It was observed that two distinct modes exist in the post-yield behavior of bone and the major portion of energy dissipation is realized through an initial acute microdamage accumulation, followed by a mechanism dominated by a viscoplastic deformation.

9:40 AM
Bone Fracture Mechanisms under Dynamic Loading: *Robb Kulin*[1]; Jiang Fengchun[1]; Kenneth Vecchio[1]; [1]University of California San Diego

Fracture of cortical bone in clinical situations for both human and animal subjects happens primarily under impact loading as experienced in crashes, falls or violence. However, despite this a full understanding of the fracture mechanisms occurring under dynamic loading is lacking. Mechanical testing was therefore performed under dynamic and quasi-static loading conditions on equine femoral and third-metacarpal bones subjected to bending and compression loading conditions. Bending tests were performed using a four-point geometry on single and double notched samples. The double-notched samples facilitated an in-depth study of the fracture paths followed under both loading scenarios, and these were analyzed using confocal and electron microscopy techniques. Both bending and compression specimens were studied under loading parallel and transverse to the long axis of the bone in wet conditions, and represented horses ages 6 months to 28 years in order to study the age effects on dynamic response as well.

10:00 AM
Structure and Mechanical Properties of American Elk Antlers: *Po-Yu Chen*[1]; Andrew Stokes[1]; Joanna McKittrick[1]; [1]University of California

We have examined structure and mechanical properties of the American elk antlers from the Cervidae family. Antlers are designed to be resilient, tough and able to sustain large bending loads, making them superior structural materials. Antlers have a similar structure to human bone apart from the higher collagen content and lesser degree of mineralization. Antlers were tested in bending to failure in both wet and dry state. The work of fracture and fracture toughness values were determined. The mechanical properties were highly anisotropic and correlated with the orientation of collagen fibers. Tensile and compressive tests were conducted in longitudinal and transverse directions. Compressive tests were further performed on interior cancellous and exterior compact bone. Correlation of mechanical properties with fracture surfaces was discussed along with fracture mechanism. Comparisons between antler and bone were made. This research is supported by the National Science Foundation Grant DMR 0510138.

10:20 AM Break

10:30 AM Invited
Biomechanical Design Lessons for Engineered Materials: *Mehmet Sarikaya*[1]; Martha Somerman[1]; Hanson Fong[1]; [1]University of Washington

Hard tissue formation is controlled by proteins leading to complex and highly functional, hierarchical architectures. The inorganics include calcium carbonate polymorphs ($CaCO_3$) in mollusk shells and echinoderm spines/tests, silica-based (SiO_2) skeletal units of single-celled organisms, e.g., radiolarian, and spicules of sponges, magnetic (Fe_3O_4) nanoparticles in magnetotactic bateria, and hydroxyapatite in bone and dental tissues of mammalians. Proteins control nucleation, growth, and structural organization of inorganics and provide molecular scaffolds. In addition, proteins and other fundamental biomolecules, such as polysaccharides, form the soft component of hard tissues that are complex nano- and micro-composites. Here, we will describe nanostructure-nanomechanical function relationships of several biological composites, including: i. Nacre, "mother-of-pearl," ii. Enamel and cementum of teeth, and iii. Spicules of sponges and draw design lessons for practical materials. Guidelines will be drawn for potentially cell-free tissue engineering in medicine and peptide-assisted inorganic structures in practical nanotechnology. Supported by NSF-MRSEC, BioMat, and NIDCR Programs.

11:00 AM
Modeling Collective Effects in Nacre: *Mark Jhon*[1]; Daryl Chrzan[1]; [1]University of California, Berkeley and Lawrence Berkeley National Laboratory

Nacre is a hierarchically structured material with toughness greater than expected from the rule of mixtures. It consists of brittle aragonite platelets layered with a ductile organic phase. The inherent discreteness of this brick-and-mortar structure creates challenges for traditional continuum modeling techniques. Most existing models focus on identification of the dominant small scale structure and its impact on the deformation process. These studies, however, are incomplete in that they do not account for the large scale deformation patterns observed in nacre: deformation is not highly localized, but rather is spread over large volumes involving many platelets. Towards this end, a simplified spring-block model for the mechanical behavior of nacre, similar to the Burridge-Knopoff model for earthquakes, is introduced and analyzed via Monte Carlo simulations. This work was supported by the U.S. Department of Energy under Contract No. DE-AC02-05CH11231.

11:20 AM
Characterization of Sandwich Structures in Avian Materials: *Sara Bodde*[1]; Yasuaki Seki[1]; Marc Meyers[1]; [1]University of California

Avian bills and feather rachises have been investigated as examples of sandwich structures in nature. Tensile strength at varied humidity and temperature conditions has been determined for the keratinous exterior of beaks and feathers rachises. The beak of toucan and hornbill is described as a keratinous shell (rhamphotheca) enclosing a closed-cell foam comprised of bony trabeculae as edges and lipid membranes as faces. The rhamphotheca of toucan and hornbill beaks have been imaged by electron microscopy. By TEM, filaments ranging in diameter from 7 nm to 12 nm were observed. The fiber-reinforcement may be correlated to anisotropic behavior observed in hornbill rhamphotheca. Foam geometry was characterized by SEM and computed tomography. Feather rachis consists of a keratinous sheath enclosing a honeycomb structure. The cells of the honeycomb, approximately 30 mm in diameter, are closed by surfaces comprised of fibers as observed by SEM and confocal microscopy techniques.

11:40 AM
Bioinspired Design of Dental Multilayers: Experiments and Models: *Nima Rahbar*[1]; Xinrui Niu[2]; Stephen Farias[2]; Wole Soboyejo[2]; [1]Princeton University, Department of Civil and Environmental Engineering; [2]Princeton University, Department of Mechanical and Aerospace Engineering

This paper explores the bioinspired design of dental multilayers within a combined computational/theoretical and experimental framework. Inspired by interfacial stress reductions associated with the almost linear gradation in moduli across the micron-scale dento-enamel junction (DEJ), this study explores the effects of graded architecture on the stress distributions and crack driving forces in model multilayered structures that are relevant to dental restorations. These are shown to result in: reduced maximum principal stresses; significant improvements in the critical crack lengths; a 30% increase in the critical loads to pop-in, and significant improvements in the number of fatigue cycles to failure over a wide range of clinically-relevant loading rates. The implications of the results are then discussed for the design of durable dental multilayers.

12:00 PM
3D Computer Graphic Modeling of Avian Beaks: *Yasuaki Seki*[1]; Sara Bodde[1]; Falko Kuester[1]; Marc Meyers[1]; [1]University of California

The internal structure of the beaks of selected species of Toucan and Hornbill has been investigated. The beak is a sandwich composite with an exterior consisting of staggered keratin tiles and a core consisting of a closed-cell foam. The edges of the closed-cell foam are bony trabeculae while the faces are lipid. Computed Tomography (CT) was employed for characterizing macrostructure of the network of osteal-trabeculae comprising the interior of the Toco Toucan and Wreathed hornbill bills. From CT image data, the internal foam structure was reconstructed by computer graphic imaging techniques. Visualization Tool Kit (VTK) was used to deal with CT images. Two different techniques, volume (Raycasting) and geometric rendering (Marching cube) techniques, were applied to visualize beak interior structure. The geometric rendering extracts the isosurface and creates the polygonal mesh. Delaunay tessellation was used for creating a finite element model.

Bulk Metallic Glasses V: Structures and Mechanical Properties I

Sponsored by: The Minerals, Metals and Materials Society, TMS Structural Materials Division, TMS/ASM: Mechanical Behavior of Materials Committee
Program Organizers: Peter K. Liaw, University of Tennessee; Wenhui Jiang, University of Tennessee; Guojiang Fan, University of Tennessee; Hahn Choo, University of Tennessee; Yanfei Gao, University of Tennessee

Monday AM — Room: 393
March 10, 2008 — Location: Ernest Morial Convention Center

Session Chairs: Peter K. Liaw, University of Tennessee; William Johnson, California Institute of Technology

8:30 AM Keynote
The Nature of Randomness in Metallic Glasses: *William Johnson*[1]; Marios Demetriou[1]; [1]California Institute of Technology, Keck Laboratory of Engineering

Variations in physical behavior among known metallic glasses and glass forming liquids can be broadly related to the liquid fragility as defined by Angell's parameter, m. In this talk, it is proposed that fragility is related to the degree of randomness in the properties Potential Energy Landscape (PEL) of the liquid. A simple 1-dim model PEL is proposed which consists of a finite sum of N sine waves of unit amplitude and random phase, and having a random distribution of wave-vectors, Q. Each sine wave represents a degree of freedom of a cluster of N/3 atoms within the liquid or glass. Randomness is characterized by the variance, σQ^2, of the Q distribution compared with average squared wave-vector $\langle Q^2 \rangle$, and by the number terms in the sum (number of degrees of freedom). A dimensionless parameter, $\chi = \sigma_Q^2/\langle Q \rangle^2$ is introduced which characterizes landscape fragility. The thermodynamic and kinetic properties of this model can be computed. The relationship of this model to real BMG's and their landscapes is discussed. Results for the model are compared with experimental results on strong and fragile metallic glasses. The simple model reveals the microscopic origin of the properties of metallic glasses and liquids and shows that fragile liquids/glasses are characterized by a more disordered landscape compared with strong liquids.

9:00 AM Invited
Anelastic Deformation in an Al-Rich Metallic Glass: The Effect of Preexisting Shear Bands: *Michael Atzmon*[1]; Koteswararao Rajulapati[1]; Dongchan Jang[1]; Adam Ganuza[1]; [1]University of Michigan

In order to characterize the dependence of anelastic strain relaxation on the state of a metallic glass, macroscopic and microscopic bending experiments have been conducted in Al86.8Ni3.7Y9.5. Cold rolling and/or annealing below the glass-transition temperature were used prior to bending in order to modify the state of the glass. At room temperature, time-dependent deformation is predominantly anelastic, whereas at higher temperatures, permanent deformation is also observed. The time constants for anelastic relaxation range from seconds to hundreds of hours. While relaxation anneals prior to bending do not result in significant changes in the subsequent response to bending, both cold rolling and subsequent annealing lead to significant changes. Trends in the dependence of anelastic deformation behavior on the extent of cold rolling will be discussed. Measurements of the time-dependent behavior of individual shear bands will be described. This work was supported by the National Science Foundation, Grant DMR-0605911.

9:20 AM Invited
Characterization and Control of Shear Band Propagation in Metallic Glasses: *Katharine Flores*[1]; Y. Jean[2]; Glenn Daehn[1]; [1]Ohio State University; [2]University of Missouri - Kansas City

Bulk metallic glasses exhibit impressive mechanical properties and processing capabilities that make them attractive for structural applications. However, the formation and rapid propagation of shear bands present significant challenges for sub-T_g processing and structural applications. We discuss ongoing investigations of the glass structure and its evolution with deformation as well as potential processing techniques to enhance the utilization of metallic glasses. Positron

annihilation spectroscopy results for several glasses reveal that the open volume in the glass may be divided into three distinct size ranges and is redistributed after shear band propagation, with the sizes decreasing and concentration of large sites increasing with total strain. Because shear band propagation in tension typically leads to catastrophic failure, techniques for distributing flow under tensile conditions are of interest. A high velocity ring expansion experiment successfully generated numerous shear bands in the bulk metallic glass ring, resulting in approximately 3% plastic strain at failure.

9:40 AM Invited

Mechanical Properties and Electronic Structure of Fe-Based Structural Amorphous Metals: *Gary Shiflet*[1]; S. Poon[1]; [1]University of Virginia

The design and characterization of Fe-based structural amorphous metals (SAM) to obtain good plasticity and toughness while retaining the high fracture strength near 4 GPa and good glass forming ability is central to current work at the University of Virginia. This talk will focus on the synthesis, mechanical properties, and basic knowledge of Fe-SAM. The Fe-SAM undergoes a ductile-to-brittle transition. This ductile-to-brittle transition is suggested to correlate with the change of local atomic short-range order or bonding configurations. The local atomic electronic structures of Fe-Mo-C-B metallic glasses are investigated using electron energy loss spectroscopy (EELS). Working towards reducing the shear modulus, the variations of compressive plasticity and elastic properties with compositions are investigated, and the deformation and fracture features are examined. The present investigation underlines the role of local order and interatomic interactions in the elastic moduli and Poisson's ratio, and hence the ductility. Research sponsored by DARPA/ONR.

10:00 AM Invited

Probing the Nanoscale Strength Distribution in Metallic Glasses: *Corinne Packard*[1]; Christopher Schuh[1]; [1]Massachusetts Institute of Technology

The relationship between metallic glass structure and the process of deformation through shear banding has not yet been established. Using nanoindentation, we investigate plasticity in metallic glasses by characterizing the first shear band event under a local mechanical contact. We observe that the first shear band event is stochastic, and show that the strength distribution arises from local variations in the glass structure. By intentionally altering the glass structure through annealing, we observe subtle but consistent changes to the shape of the distribution. In addition, cyclic loading in the elastic range results in apparent strengthening, suggesting a mechanism of structural evolution during nominally elastic deformation. Implications of these results on the macroscopic properties of metallic glasses are discussed, as are potential connections to the modeling and simulation community.

10:20 AM Invited

Two-Glassy Phase Bulk Metallic Glass with Remarkable Plasticity: X. Du[1]; *Jacob Huang*[1]; K. Hsieh[2]; J. Jang[3]; P. Liaw[4]; [1]National Sun Yat Sen University; [2]National Sun Yat Sen Univ; [3]I-Shou University; [4]University of Tennessee

By using the computational thermodynamic approach, the potential compositions of Zr-Cu-Ni-Al alloy system exhibiting the two-liquid miscibility phase equilibrium in the liquid temperature region have been identified. The resulting Zr base bulk metallic glasses exhibit a microstructure of two micro-scaled glassy phases mixed uniformly, i.e., the hard phases within some nanocrystals (Zr_2Ni) surrounded by the soft phases. The Zr base glasses possess a high compressive strength (~1.9 GPa), continuous "work hardening" and remarkable macroscopic plastic strain (~20%) before instable deformation at room temperature. The gain of mechanical properties is attributed to the unique deformation mode with microscale multistep shear bands originating from shear-induced breakage and coalescence of hard phases which have experienced nanocrystallization process under compression loading. This novel phenomenon provides a mechanism for strain hardening to offset the natural strain softening of the glass matrix and to assist delocalization of the plastic flow.

10:40 AM Break

10:45 AM Invited

Engineering Capabilities of Highly Porous Metallic Glass Foam: *Marios Demetriou*[1]; William Johnson[1]; Robert Conner[2]; Nikolaj Wolfson[3]; Aaron Wiest[1]; [1]California Institute of Technology; [2]California State University, Northridge; [3]University of Southern California

Owing to their remarkably high plastic yield strengths, amorphous metals are thought to be attractive base materials for ultra strong foams. In addition, due to their ability to be processed thermoplastically above the glass transition, these materials are considered promising for high porosity foaming. In this presentation, a foam synthesis route will be introduced by which metallic glass foams with porosities as high as 92% are produced. The foams are capable of effectively inheriting the high plastic yield strength and low modulus of the parent amorphous metal under static as well as dynamic loading, and are able to deform plastically to full densification absorbing high amounts of energy. Potential applications for the foam will be discussed, and its engineering capabilities as an energy-absorbing cellular structure or a property-matched bone scaffold will be explored.

11:05 AM Invited

Influence of Free Volume on the Ductile-to-Brittle Transition in Rapidly Solidified Mg-Based Glasses: *Jorg Loffler*[1]; Dirk I. Uhlenhaut[1]; Florian H. Dalla Torre[1]; Alberto Castellero[1]; [1]ETH Zurich

Rapidly quenched Mg–Cu–Y glasses show ductility upon bending for a limited time at room temperature but then embrittle within a short time. This time-dependent embrittlement can be associated with a structural relaxation, which lowers the enthalpic content and increases the elastic constants of the metallic glass, as measured via acoustic excitation. Since the shear modulus increases faster than the Young's modulus, the Poisson ratio is found to decrease as the alloy ages and the ductile-to-brittle transition is observed at a critical value of 0.32. Using results obtained from synchrotron x-ray diffraction and positron annihilation experiments, we can relate this embrittlement to the amount and extent of free volume, which alters during room-temperature aging and also changes the Poisson ratio of the glass. Here we discuss the interrelation between the mechanical properties and the defect structure in the Mg-based glass.

11:25 AM Invited

Plasto-Hydrodynamic Deformation of Brittle Bulk Metallic Glass at Room Temperature: *Fuqian Yang*[1]; John Nychka[1]; Gongyao Wang[2]; Wenhui Jiang[2]; Brett G. Compton[1]; Peter K. Liaw[2]; [1]University of Kentucky; [2]University of Tennessee

The deformation of materials can be altered by the application of particular stress states. In this contribution we present results which offer a new approach to achieve high degrees of plastic deformation without catastrophic failure in brittle bulk metallic glasses (up to 36% plastic strain). The large strains are observed in uniaxial compression at room temperature with aid of a plastic layer at the fixed ends of the specimen. The result is of particular interest because the plastic deformation occurs in the presence of complex shear band formation on all surfaces without fracture or in situ crystallization. Implications of these findings suggest possible new strategies for deformation processing of bulk metallic glasses.

11:45 AM

Thermal and Elastic Response of Cu-Based Bulk Metallic Glasses to Cyclic Elastic Deformation: *Rainer Hebert*[1]; Arif Mubarok[1]; [1]University of Connecticut

It is well know that metallic glasses reveal structural relaxation or ageing when heated to temperatures near the glass transition or below. Little is known, however, about the effect of cyclic elastic deformation at room temperature on atomic rearrangements and the thermal behavior of the glasses during subsequent annealing. Suction-cast amorphous Cu-Zr and Cu-Ti-Hf rods were tested in compression-compression testing with strain amplitudes of 0.1%-0.3%, strain rates of about ten to the minus four and compression cycles ranging from 200 to 20,000. The thermal analysis reveals a decrease by approximately 80% of the enthalpy of crystallization for an amorphous Cu50Zr50 rod without a shift in the crystallization onset temperature and a decrease in the strength of the glass-transition signal. The results indicate that sustained elastic deformation can have a significant impact on the crystallization behavior or Cu-based metallic glasses.

12:00 PM

Deformation of an Annealed Zr41Ti14Cu12.5Ni10Be22.5 Bulk Metal Glass under Vickers Indenter: *Haowen Xie*[1]; Jianguo Lin[1]; Yuncang Li[1]; Peter Hodgson[1]; Cui'e Wen[1]; [1]Deakin University

Zr41Ti14Cu12.5Ni10Be22.5 bulk metal glass (BMG) was annealed near the glass transition temperature, and the structure relaxation occurred. Vickers indentation was conducted on the annealed sample. The development of the shear band patterns was studied by using a bonded interface technique. The results indicated that the plastic deformation in the annealed sample was accommodated by the semicircular (primary) and radial (secondary) shear bands. Compared with the as-cast sample, the annealed sample exhibits the different distribution and patterns of shear bands due to the altered elastic-plasticity. The inter-band spacing of the semicircular shear bands at the variant angles was strongly dependent on the distribution of the stresses. The size of the deformation zone was measured, and the values are compared with the predictions by some theoretical models.

12:15 PM Invited

Effect of Coexistence of Alike Elements on Improving Glass-Forming Ability of Alloys: *Tao Zhang*[1]; [1]Beijing University of Aeronautics and Astronautics

The effect of unlike component elements on GFA of alloys have been studied extensively and it is generally recognized that the main constituent elements of the alloys with high glass-forming ability (GFA) usually have large difference in atomic size and large negative heat of mixing among them. In the present work, we developed a series of rare-earth metal-based alloys with superior glass-forming ability (GFA) by using the approach of coexistence of alike elements in the alloys. Especially a La-Ce-Al-Co-Cu bulk metallic glass (BMG) with a diameter up to 32 mm can be synthesized by copper-mold casting, for which the GFA is significantly higher than that for ternary Ln-Al-TM alloys (Ln = La/Ce; TM = Co/Cu). This indicates that the coexistence of alike elements (elements with similar atomic size and chemical properties) has significant effect on GFA of alloys, which can also be observed in Zr-Al-(Ni-Cu), Cu-(Zr-Ti) and Pd-(Cu-Ni)-P glassy alloy systems, etc. Mechanism of coexistence of alike elements on improving GFA of alloys is also discussed. The Authors would like to acknowledge the financial supports from National Nature Science Foundation of China (No. 50631010), PCSIRT (IRT0512) and the Cultivation Fund of the Key Scientific and Technical Innovation Project, Ministry of Education of China (No. 705006).

12:35 PM

Relationship between Shear Displacement and Shear Band Spacing in Bulk Metallic Glasses: *Hongwen Zhang*[1]; Ghatu Subhash[2]; Spandan Maiti[1]; Gerald Bourne[2]; [1]Michigan Technological University; [2]University of Florida

Bonded-interface technique is used to investigate the relationship between the shear band spacing and shear displacement in bulk metallic glasses. The vertical surfaces of the split-specimens were engraved with a set of lines at regular intervals (100 microns) and then bonded together for indentation test on the top surface along the interface. As the induced shear bands cut across the grid pattern, the resulting shear displacement along each shear band can be measured by the offset (displacement) of the different segments of an original straight line. It was revealed that widely spaced shear bands accommodate larger shear displacement and vice versa. To rationalize these observations, a thermo-micromechanical model that takes into account momentum diffusion mechanism at the core of shear band, free volume theory and heat diffusion analysis was developed. The model verifies that widely spaced shear bands indeed accommodate larger shear displacement.

12:50 PM

Stress-Induced Phase Transformation during In-Situ Compression Test of a Glass-Forming CuZr Alloy: *Feng Jiang*[1]; Yandong Wang[2]; Yang Ren[3]; James Morris[1]; Peter Liaw[1]; Hahn Choo[1]; [1]University of Tennessee; [2]Northeastern University of China; [3]Argonne National Laboratory

The in-situ compression test was applied on a glass-forming CuZr alloy, simultaneously, synchrotron X-ray is used to study the structure change. The results show that phase transformation occurs during in-situ compression test. The phase of martensite- (with the space group of P21/m) transforms to martensite α (with the space group of Cm) through twin mechanism.

Characterization of Minerals, Metals, and Materials: Emerging Characterization Techniques

Sponsored by: The Minerals, Metals and Materials Society, TMS Extraction and Processing Division, TMS: Materials Characterization Committee
Program Organizers: Jian Li, Natural Resources Canada; Toru Okabe, University of Tokyo; Ann Hagni, Intellection Corporation

Monday AM — Room: 284
March 10, 2008 — Location: Ernest Morial Convention Center

Session Chairs: Jian Li, Natural Resources Canada; Donato Firrao, Politecnico di Torino

8:30 AM

Understanding the Effects of High Speed Orientation Mapping: *Matthew Nowell*[1]; Stuart Wright[1]; John Carpenter[1]; [1]EDAX-TSL

The automated analysis of Electron Backscatter Diffraction (EBSD) patterns for orientation mapping has become an accepted microstructure characterization tool. Data acquisition speeds have increased by over two orders magnitude over the past decade. These increases are enabled primarily by digital CCD cameras capable of output frame rates greater than analog video rates. One feature of these cameras is the ability to group together adjacent pixels in a processes referred to as binning. This process reduces the pixel resolution of the output image and allows faster output frame rates. As CCD frame rates and binning options increase, understanding the effects of image resolution on EBSD pattern analysis is key to optimizing the quality of the orientation mapping data. In this work, the effects of camera resolution, coupled with band detection parameters, is examined. Indexing success rates and angular accuracy as a function of acquisition speed and camera resolution will be discussed.

8:50 AM

The Research Applications of Photoemission Electron Microscopy: *Mingdong Cai*[1]; J. Thomas Dickinson[2]; Wayne Hess[3]; [1]University of Houston; [2]Washington State University; [3]Pacific Northwest National Laboratory

Photoelectron emission microscopy (PEEM) is a developing technique that images electrons emitted from conductor and semiconductor surfaces under UV, X-ray, or laser irradiation. Low energy PEEM can reveal surface morphology on a 10 nm scale and is sensitive material properties such as phase, adsorbed molecules, surface electronic structure, and other physical properties that affect work function and hence the photoelectron yield. We have used PEEM to study phase transformation in shape memory alloys, diffusion of Cu in Cu/Ru bilayers and laser-induced oxygen vacancy creation on TiO_2. In this talk, we will focus on using PEEM to study thermally-induced martensitic phase transformations in polycrystalline CuZnAl and thin-film NiTiCu shape memory alloys. In situ real-time PEEM images provide information on the spatial distribution of these phases and the evolution of the surface microstructure during transformation.

9:10 AM

Phase Identification and Quantification Utilizing QEMSCAN® Technology: *Ann Hagni*[1]; [1]Intellection Corporation

Phase identification techniques such as optical microscopy (reflected light and transmitted light microscopy), X-ray diffraction (XRD), cathodoluminescence microscopy (CLM), and X-ray photoelectron spectroscopy (XPS) have been utilized by materials scientists for many years. Quantification of phases has generally been limited to Rietveld XRD and XPS. Elemental mapping and high magnification imaging of specific areas have been conducted by scanning electron microscopy (SEM), energy dispersive spectroscopy (EDS), and back-scattered electron imaging (BSI). An additional phase identification and quantification technique complements these older techniques. QEMSCAN® employs custom built SEM with EDS, BSI, and sophisticated software to identify and quantify inorganic phases, determine particle surface areas, particle shapes, phase associations, and statistics of phases. Automation of QEMSCAN® allows for analyses of large areas in an unattended mode of naturally occurring and synthetic raw materials, processed materials, and waste products. An overview of QEMSCAN® applications and techniques will be presented.

9:30 AM
Thermoreflection Measurement of Thermal Conductivity of Glassy Polymeric Carbon Bombarded with MeV Proton: *Bangke Zheng*[1]; Z. Xiao[2]; B. Chhay[1]; A. Sharma[3]; D. Ila[1]; [1]Alabama A&M University, Center for Irradiation of Materials; [2]Alabama A&M University, Electrical Engineering School; [3]Alabama A&M University, Department of Physics

Thermoreflection is a suitable method for measurements of thermal conductivity of thin electrically conductive glassy polymeric carbon samples, which can not be measured by using 3ω method. A layer of reflective metal film such as aluminum is deposited on the sample. When an Nd: YAG pulsed laser (with a pulse width of 5 ns, and a power of 1 mJ) radiates on the metal film, there is an increase in the reflection of probing laser (a diode laser) beam that is reflected by the surface of metal layer, the reflection of probing laser decays gradually. By measuring the decay time of reflection, which is related to thermal conductivity, the thermal conductivity of GPC with various MeV proton bombardment fluences can be obtained.

9:50 AM Break

10:10 AM
Application of Double Knudsen Cell Mass Spectrometry to Measurement on Thermodynamic Properties of Oxides: *Takashi Nagai*[1]; Masao Miyake[2]; Hisao Kimura[1]; Masafumi Maeda[1]; [1]University of Tokyo; [2]University of Illinois

Thermodynamic knowledge on alloys and oxides forms a scientific foundation for the development of new technologies for refining steel and alloys, and also for the development of new materials with required physicochemical properties. Double Knudsen cell mass spectrometry was developed as a method to measure thermodynamic properties of metals and alloys. This method was not often used to measure thermodynamic measurement on oxide and oxide system, since oxygen potential in measuring system can not be controlled easily, though control of oxygen potential in measuring system in thermodynamic measurement on oxide and oxide system is important. In this research, double Knudsen cell mass spectrometry equipment which has a system injecting gas, such as mixed gas carbon monoxide and carbon dioxide, into Knudsen cell to control oxygen potential was developed. And thermodynamic properties of calcium phosphates were investigated.

10:30 AM
Evaluation of the Influence of Median Rank Expression Selection and Location Factor over Weibull Modulus in Brittle Materials Characterization: *Eduardo de Carvalho*[1]; Sergio Monteiro[1]; [1]Universidade Estadual do Norte Fluminense

This work dealt with the influence of the location parameter and several expressions that may be used to define probability rank, over Weibull Modulus estimates for a sample analysis. A sample containing 71 red-ceramic specimens was used together with Probability Plot method to estimate distribution parameters. Sub-lots extracted from this major lot were created to evaluate sample size impact over factor estimations. For this lot a 15% difference was found for Weibull Modulus value when different rank expressions were used. The Location Parameter different fro zero hypothesis drastically altered Weibull Modulus and Scale Parameter values and made necessary the introduction of other analytical elements to allow for a final valid conclusion.

10:50 AM
Electrostatic Levitation: An Emerging Materials Characterization Technique: *Jan Rogers*[1]; Robert Hyers[2]; [1]NASA/Marshall Space Flight Center; [2]University of Massachusetts

Electrostatic levitation (ESL) uses electrostatic fields to position samples between electrodes during processing and characterization studies. Because the samples float between the electrodes during studies, they are free from any contact with a container or test apparatus. This provides a high purity environment for the study of high-temperature (up to 3400°C), reactive materials, as well as access to deeply undercooled melts and metastable states. ESL can be used to process a wide variety of materials including metals, alloys, ceramics, glasses and semiconductors. Apparatus and techniques have been developed to use this technique to provide data for phase diagram determination, creep resistance, emissivity, specific heat, density/thermal expansion, viscosity, surface tension and triggered nucleation of melts. Scientific topics investigated using ESL include phase selection and the formation of quasicrystals and bulk metallic glasses. Results from selected ESL-based characterization studies performed at NASA's Marshall Space Flight Center will be presented.

11:10 AM
Microstructure Evolution and Deformation in Low Solvus High Refractory (LSHR) Ni-Base Superalloy: *Vikas Sinha*[1]; Patrick Martin[2]; Donna Ballard[2]; M. Scott[1]; [1]UES Inc; [2]US Air Force Research Laboratory

Low Solvus High Refractory (LSHR) is a high strength Ni-base superalloy, which has been patented by NASA-Glenn Research Center. Although developed primarily for disk applications, LSHR may be attractive for other applications in the sheet product form. In the current work, the microstructure evolution of LSHR at different times and temperatures (in the vicinity of the gamma prime solvus) has been examined. The microstructures have been characterized via Scanning Electron Microscopy (SEM) and Electron BackScattered Diffraction-Orientation Imaging Microscopy (EBSD-OIM) techniques. The compressive flow behavior at temperatures in both the sub-solvus and super-solvus regimes has been determined. The microstructural modifications resulting from the compression tests have also been examined. The results of the current work will be discussed in the context of hot rolling LSHR sheets.

Complex Oxide Materials - Synthesis, Properties and Applications: ZnO Nanostructures and Thin Films

Sponsored by: The Minerals, Metals and Materials Society, TMS Electronic, Magnetic, and Photonic Materials Division
Program Organizers: Zhiming Wang, University of Arkansas; Ho Nyung Lee, Oak Ridge National Laboratory

Monday AM
March 10, 2008
Room: 277
Location: Ernest Morial Convention Center

Session Chair: To Be Announced

8:30 AM Invited
Polar-Surface Induced Novel Growth Structures of ZnO Nanobelts: *Zhong Lin (Z.L.) Wang*[1]; [1]Georgia Tech

The two important characteristics of the wurtzite structure are the non-central symmetry and the polar surfaces. The structure of ZnO, for example, can be described as a number of alternating planes composed of tetrahedrally coordinated O2- and Zn2+ ions, stacked alternatively along the c-axis. The oppositely charged ions produce positively charged (0001)-Zn and negatively charged (000-1)-O polar surfaces, resulting in a normal dipole moment and spontaneous polarization along the c-axis. This polar surface gives rise a few interesting growth features. In this presentation, we will focus on the polar surface induced formation of nanospring, nanoring and nanohelix. [1]X.Y. Kong and Z.L. Wang, Nano Letters, 2 (2003) 1625. [2]X.Y. Kong, Y. Ding, R.S. Yang, Z.L. Wang, Science, 303 (2004) 1348. [3]P.X. Gao, Y. Ding, W.J. Mai, W.L. Hughes, C.S. Lao and Z.L. Wang, Science, 309 (2005) 1700. [4]http://www.nanoscience.gatech.edu/zlwang/.

9:00 AM Invited
Catalyst-Free Selective Growth of ZnO Nanorods on Si Substrates: *Gyu-Chul Yi*[1]; [1]Pohang University of Science and Technology

Position-controlled vertical arrays of semiconductor nanorods offer the ideal geometry for use as functional components in nanoscale integrated electronics and optoelectronics. Recently, a few well-controlled semiconductor nanorods have been prepared by either metal catalyst-assisted or catalyst-free methods. For metal catalyst-assisted methods, the selective growth of nanorods can be easily obtained by controlling metal catalyst sites. Meanwhile, for catalyst-free growth, the critical factors leading to the catalyst-free, selective growth of nanorods have yet to be established. Furthermore, there has been only a few reports on the selective growth of semiconductor nanorods on Si substrates although Si is the most important substrate for many device applications. Here I will present two different methods to grow ZnO nanorods at specific positions on Si substrates without using any metal catalyst: wet chemical solution growth and metal-organic chemical vapor deposition.

9:30 AM Invited
Controlled Growth ZnO Nanostructures by Thermal Evaporation: *Zhengwei Pan*[1]; [1]University of Georgia

ZnO exhibits rich morphologies at the nanoscale, which are very sensitive to the growth techniques and growth conditions. In this talk, we show our effort on controlled growth of ZnO nanostructures with different morphologies by a thermal evaporation-based technique. The morphologies include nanorods, nanowires, nanobelts, combs and styluses. The growth mechanism will be discussed briefly. [1]Pan, Z.W., Dai, Z.R. and Wang, Z.L. Science 291, 1947-1949 (2001). [2]Pan, Z.W. Mahurin, S.M., Dai, S. and Lowndes, D.H. Nano Letters 5, 723-727 (2005). [3]Pan, Z.W., Rouleau, C.M., Dai, S. and Lowndes, H.L. Angew. Chem. Int. Ed. 44, 274 (2005).

10:00 AM Break

10:30 AM Invited
Atomically Controlled Heteroepitaxy of ZnO Enabling UV Emitting and Quantum Hall Devices: *Atsushi Tsukazaki*[1]; Akira Ohtomo[1]; Masashi Kawasaki[1]; [1]Tohoku University, IMR

ZnO has been recognized as one of the key materials in Oxide Electronics enabling UV emitter, thin film transistor, self-organized nanostructures, spintronics, and so on. We have been focusing our effort for a decade on making ZnO epitaxy as perfect as possible. One of the breakthroughs was the development of high temperature annealed ZnO or $Mg_xZn_{1-x}O$ buffer layer (HITAB) formed on lattice-matched $ScAlMgO_4$ substrate. During the regrowth of ZnO on such an atomically-smooth buffer layer, intensity oscillation of reflection high-energy electron diffraction persists and the point defect concentration can be minimized. Based on that technology level, we could demonstrate blue light-emitting pn junction diode and quantum Hall effect in high-mobility two-dimensional electron gases at abrupt heterointerfaces between ZnO and $Mg_xZn_{1-x}O$.

11:00 AM
Nanostructures in Thin Films of ZnO: *Harish Bahadur*[1]; A. Srivastava[1]; Rashmi[1]; Sudhir Chandra[1]; [1]National Physical Laboratory

Structure property co-relationship of thin films of ZnO grown by sol-gel spin process using zinc acetate and RF magnetron sputtering method has been studied. The films were crystalline in nature. The crystallite size for the film grown by using zinc acetate varied with the type of growth techniques and lay in the range of 15-145 in the c-axis direction of the growth. TEM exhibited that the film with uniform microstructure consisted of distribution of nanosized grains of the order of 5 nm. Selected area electron diffraction patterns have shown the presence of different rings corresponding to different planes of hexagonal ZnO crystal structure. The RF sputtered films have shown the formation of nanorods of ZnO which were found to have uniform distribution of crystallites of the size ~10 nm. Photoluminescence measurements also showed the quantum confinement of ZnO crystallites. The results would find application in nanoelectronic piezoelectric sensors.

11:20 AM
Effect of Defect Generation on Structural, Electrical and Optical Properties of ZnO Thin Films by Using Ar-Implantation: *Sang Yeol Lee*[1]; Jung Kun Lee[2]; M. Nastasi[2]; [1]Korean Institute of Standards and Technology; [2]Los Alamos National Laboratory

In order to investigate the effect of defects on the structural, electrical and optical properties of ZnO thin films, we have performed Ar ion implantation on ZnO thin films grown by pulsed laser deposition and sputtering. The variation of structural property has been observed before and after rapid thermal annealing on Ar implanted ZnO thin films. Ar implantation has been adopted to generate defects intentionally since Ar could not be doped into ZnO and the effect of defect on ZnO could be observed. We have changed the dose of Ar ions, the growth temperature of ZnO thin films and the deposition methods and compared the variation of structural, electrical and optical properties of ZnO thin films caused by the generation of defects due to Ar implantation.

Computational Thermodynamics and Kinetics: Defect Structure I

Sponsored by: The Minerals, Metals and Materials Society, TMS Electronic, Magnetic, and Photonic Materials Division, TMS Materials Processing and Manufacturing Division, ASM Materials Science Critical Technology Sector, TMS: Chemistry and Physics of Materials Committee, TMS/ASM: Computational Materials Science and Engineering Committee, TMS/ASM: Phase Transformations Committee
Program Organizers: Yunzhi Wang, Ohio State University; Long-Qing Chen, Pennsylvania State University; Jeffrey Hoyt, McMaster University; Yu Wang, Virginia Tech

Monday AM Room: 288
March 10, 2008 Location: Ernest Morial Convention Center

Session Chairs: Meijie Tang, Lawrence Livermore National Laboratory; Yunzhi Wang, Ohio State University

8:30 AM Invited
Dynamic Complexity and Nanostructure Formation Due to Particle Irradiation: *Chung Woo*[1]; [1]Hong Kong Polytechnic University

The evolution of irradiation damage accumulation is conventionally described by coupled rate equations, analogous to the description of diffusion-controlled chemical processes, the dynamic complexity of which is well known. However, to maintain the manageability of the calculation, a simplifying mean-field approximation is usually adopted. It has now been realized that important features of complex systems such as dynamic instabilities and bifurcations together with the accompanying phase-change-like behavior of the system may have been neglected. In this paper, ordering due to alignment of the microstructure along the crystallographic directions under irradiation is studied as an effect produced by one-dimensionally migrating self-interstitials on the post-bifurcation evolution of the system.

8:55 AM Invited
Quantitative Phase Field Model for Diffusion-Controlled Microstructural Evolutions in the Solid State: *Pascal Bellon*[1]; Arnoldo Badillo[1]; Robert Averback[1]; [1]University of Illinois

Current phase field (PF) models for diffusion-controlled evolutions in the solid state are based on phenomenological kinetic equations. The lack of absolute time and space scale raises problems when applying PF models to alloys subjected to irradiation by energetic particles, since this external forcing introduces new length scales and time scales. We propose here a derivation of the phase field equations, by coarse graining in space and time a microscopic model. For a binary alloy with pairwise atomic interactions, in the framework of the cluster variation method, we derive the kinetic equation describing the evolution of its composition field. This derivation makes it possible to take into account important irradiation effects, namely the production and elimination of point defects and the forced chemical mixing. Examples of application of the model are given for spinodal decomposition in three dimensions, both in the absence and in the presence of irradiation.

9:20 AM Invited
Time-Evolution of Short-Range and Long-Range Ordering in Ni_4Mo Alloys during Isothermal Annealing and under Irradiation Studied by Monte Carlo Simulation: *Syo Matsumura*[1]; Satoshi Hata[1]; Tatsurou Takahashi[1]; Christian Abromeit[2]; [1]Kyushu University; [2]Hahn-Meitner-Institut, Berlin

The authors will give an overview of their achievements in study of time-evolution of short-range ordering (SRO) and long-range order (LRO) of $D1_a$ type in Ni_4Mo alloys by means of Monte Carlo (MC) simulation. First, semi-quantitative high resolution TEM and MC simulation show that the SRO state consists of mixture of subunit cell clusters of $D1_a$, $D0_{22}$ and Pt_2Mo structures in the atomistic level of microstructure. The second part of the talk will mention the kinetics of disordering from $D1_a$-type LRO to SRO under particle irradiation. One can easily distinguish the disordering kinetics of LRO and the time-evolution of SRO in the MC simulations, owing to the characteristic feature that the two states show intensity maxima at different positions in the Fourier space.

The disordering behavior is discussed as a function of size of disordered zones due to particle collisions.

9:45 AM

Modeling the Effect of Particle Size Distribution on Platinum Surface Area Loss in PEMFC Cathodes: *Dane Morgan*[1]; Edward Holby[1]; Yang Shao-Horn[2]; Wenchao Sheng[2]; [1]University of Wisconsin; [2]Massachusetts Institute of Technology

The long-term durability of platinum catalysts in Proton Exchange Membrane Fuel Cell (PEMFC) cathodes is an important issue in achieving the Department of Energy's 5000 hour PEMFC lifetime goal. Fuel cell efficiency is decreased as electrochemically active surface area (ECASA) of platinum is lost. A kinetic model has been used to explore the influence of particle size distribution on the loss of ECASA under both constant potential holds and cycled potentials for carbon supported Pt catalysts. It is shown that the thermodynamics of the nanoscale particles strongly impacts the Pt loss. It is found that the mean diameter and functional form of the initial particle size distribution are important considerations in the long-term loss of ECASA in PEMFCs. Also, it is confirmed that changes in the particle size distribution upon heat treatment help to explain the improved durability associated with heat-treating catalysts.

10:00 AM

First Principles Study of Point Defects in Uranium Dioxide and Cerium Dioxide: *Ying Chen*[1]; Misako Iwasawa[2]; Yasunori Kaneta[1]; Toshiharu Ohnuma[2]; Hua-Yun Geng[1]; Motoyasu Kinoshita[2]; [1]University of Tokyo; [2]Central Research Institute of Electric Power Industry

UO_2 is a widely used fuel in nuclear power generation, under its high burn-up, a characteristic fine grain structure is found to be formed. CeO_2 is used as simulation materials of UO_2 in the accelerator experiments due to their similar structural and thermodynamic properties. To get understanding on the fundamental properties and essential difference of these two substances, so as to clarify the origin of formation of the characteristic defective structure, the comprehensive first-principles calculations for two systems containing various types of point defects have been performed using the PAW-GGA+U. The electronic structure, the atomic displacement, and the defect formation energies are evaluated under lattice relaxation, the size effect of supercells on these properties is also investigated. Based on the results of electronic structures, the concentration of various types of point defects are further estimated in the framework of the point defects model.

10:15 AM Break

10:35 AM Invited

From Dislocation Dynamics to Continuum Modelling of Plastic Deformation in Ni-Base Superalloys: Aurelien Vattre[1]; Arjen Roos[1]; *Benoit Devincre*[2]; [1]ONERA; [2]Centre National de la Recherche Scientifique

Understanding the plastic properties of alloys containing metallic precipitates of sub-micrometric size, such as Ni-based superalloys, is a difficult task. It has been emphasized many times that the plastic deformation of single crystalline superalloys depends in a complex manner on orientation. Three-dimensional simulations of dislocation dynamics dedicated to Ni-based superalloys have been developed, in which the boundary value problem is rigorously resolved through a coupled approach involving a FE and a DD code. These simulations aim at understanding the relation between the nature and number of activated slip systems and the macroscopic stress-strain behavior. In addition, they deliver a quantitative description of the microstructural mechanisms at the origin of strain localization in slip bands. The model results are found consistent with experimental observations and provide guidelines for the development of physically justified crystal plasticity models.

11:00 AM Invited

3D Dislocation Dynamics Simulations of the Deformation Behavior of Micrometer-Sized Crystals of FCC Ni and Superalloys: *Satish Rao*[1]; Dennis Dimiduk[2]; Triplicane Parthasarathy[1]; Meijie Tang[3]; Michael Uchic[2]; Christopher Woodward[2]; [1]UES Inc.; [2]Air Force Research Laboratory/MLLM; [3]Lawrence Livermore National Laboratory

We use large scale 3-dimensional dislocation simulations to study the deformation behavior of micron sized FCC single crystals as well as superalloys with initial dislocation source densities varying from 7x1011/m2 to 1013/m2 and specimen column diagonal sizes ranging from 0.5 to 20 micron. Mechanisms that are responsible for strengthening are identified through the use of dislocation dynamics (DD) simulations. The simulations reveal two size-sensitive hardening processes that are sufficient to produce the dimensional scaling of the flow stress and similar flow behavior observed experimentally. One mechanism, surface-mediated source-truncation hardening, is especially potent in micrometer-scale volumes and is attributed to the stress required to operate single-ended sources in such small micrometer volumes. Other mechanisms, termed 'exhaustion hardening', attributed to junction and debris formation, is a direct result of the paucity of mobile dislocations present in small crystals and the high stresses achieved during micro-plasic flow.

11:25 AM

Large Scale Dislocation Dynamics Simulations of Single Crystal Ta: A Realization of the Multi-Scale Modeling Strategy: *Meijie Tang*[1]; Tom Arsenlis[1]; M. Rhee[1]; G. Hommes[1]; Vasily Bulatov[1]; Liming Yang[1]; D. Orlikowski[1]; R. Becker[1]; [1]Lawrence Livermore National Laboratory

Over the years, we try to develop computational tools to carry out multi-scale modeling of mechanical properties of body-center-cubic single crystals in order to develop physics based predictive capabilities for materials mechanical behavior under a wide range of pressure/temperature/strain rate conditions. We have finally carried out the strategy by linking the data obtained at different length scales from the atomistic to the microscale, and to macroscale. This talk will present the multi-scale modeling work with a focus on the role of large scale dislocation dynamics (DD) simulations of single crystal Ta. Will discuss the inputs on dislocation mobilities obtained from first principle based atomistic simulations to the dislocation dynamics simulations, and to analyze the mechanical response obtained from the large scale DD simulations and the development of strength models based on the DD results for continuum level modeling of macroscopic behavior. The work is performed under the auspices of the U. S. Department of Energy by the University of California, Lawrence Livermore National Laboratory under Contract No. W-7405-Eng-48.

11:40 AM

Application of Fourier-Spectral Moving Mesh Method to Phase-Field Model of Dislocations: *Weiming Feng*[1]; Peng Yu[1]; Shenyang Hu[2]; Zi-Kui Liu[1]; Qiang Du[1]; Long-Qing Chen[1]; [1]Pennsylvania State University; [2]Los Alamos National Laboratory

We recently developed a new adaptive Fourier-spectral semi-implicit method (AFSIM) for domain and phase coarsening described by Allen-Cahn and Cahn-Hilliard equations. It combines the adaptive moving mesh method with the semi-implicit Fourier spectral algorithm. In this presentation, we report our recent progress in applying AFSIM to phase-field model of a multi-dislocation system with anisotropic elasticity. Accuracy and efficiency are analyzed by comparing with existing numerical algorithms. Numerical examples are presented for both two and three space dimensions.

11:55 AM

Investigation of Misfit Dislocation at Fe/Mo Interface: *Nirand Pisutha-Arnond*[1]; Bo Yang[2]; Mark Asta[2]; Katsuyo Thornton[1]; [1]University of Michigan; [2]University of California at Davis

We present a dislocation model based on Peierls-Nabarro's formulation to study dislocation structure during the epitaxial growth of Fe on Mo(110). The continuum model calculates the elastic field originating from the misfit dislocation array and network within a film of finite thickness. We use the stacking fault energy of the Fe/Mo system from an *ab initio* calculation as an input to the model. The interfacial energy stemming from the misfit dislocation is calculated using this model. The predicted dislocation structure within the thin film is compared to experimental observations, while the predictions for thick films and islands are compared to an experimental estimation of the dislocated interface in the Fe/Mo(110) system.

12:10 PM

Phase Field Modeling of the Electrochemical Interface: *Jonathan Guyer*[1]; David Saylor[2]; James Warren[1]; William Boettinger[1]; Geoffrey McFadden[1]; [1]National Institute of Standards and Technology; [2]Food and Drug Administration

We previously developed a phase field model of the electrochemical interface [Phys. Rev. E 69, 021603 & 021604 (2004)] and demonstrated that a simple

set of assumptions gives rise to a rich set of behaviors. However, the need to resolve both the small charge separation distances (the Debye length) and large differences in concentrations placed severe limits on the time steps that could be taken. We have recently applied a variety of numerical techniques to this problem, including moving meshes and different discretizations, that have resulted in simulating larger domains, in higher dimensions, than previously achievable, while retaining the essential physics of the electrochemical interface. We have been able to increase the maximum stable time step by several orders of magnitude. We will present the approaches we have taken to make this problem tractable, as well as the results of simulations for a variety of applications.

Deformation Twinning: Formation Mechanisms and Effects on Material Plasticity: Experiments and Modeling: Twin Formation and Growth Mechanisms

Sponsored by: The Minerals, Metals and Materials Society, TMS Structural Materials Division, TMS/ASM: Mechanical Behavior of Materials Committee
Program Organizers: George Gray, Los Alamos National Laboratory; Subhash Mahajan, Arizona State University; Ellen Cerreta, Los Alamos National Laboratory

Monday AM Room: 383
March 10, 2008 Location: Ernest Morial Convention Center

Session Chair: Subhash Mahajan, Arizona State University

8:30 AM Introductory Comments

8:40 AM Invited
Properties of Twinning Dislocations in the HCP Metals Revealed by Computer Simulation: *David Bacon*[1]; Hassan Khater[1]; Anna Serra[2]; Yuri Osetskiy[3]; [1]University of Liverpool; [2]Politechnic University of Catalunya; [3]Oak Ridge National Laboratory

Deformation twin boundary motion occurs by stress-activation of sources of twinning disconnections, which are interfacial defects with step and dislocation character. The present work on the HCP metals uses topological theory to identify possible interfacial defects and atomic-scale computer simulation to study their properties. Motion of disconnections in otherwise planar boundaries and the influence of other interfacial defects on their mobility have been studied. The operation of a continuous source of disconnections has been demonstrated. A method to simulate the motion of twin boundaries over large distance has been developed and used to investigate the interaction of a moving {10-12} twin boundary with self-interstitial or vacancy clusters in α-zirconium. This has shown that the applied stress for boundary motion is raised by interaction with defect clusters, and moving boundaries can act as sinks or recombination centres for defects, thereby providing a means for removing defects from regions of radiation damage.

9:10 AM
Twinning as a Monatomic Phase Transformation: *John Gilman*[1]; [1]University of California

Twinning is a particularly simple phase transformation because no change in chemical potential is involved; only a change in mechanical potential. Also, twinning is intrinsically athermal so changes in electronic structure determine its rate. Direct measurements have shown that twin interfaces can move at velocities up to, and possibly exceeding, elastic shear wave velocities in solids. Past estimates of the energies of twin nuclei have been excessive. A new estimate is pesented. The onset of twinning is abrupt because it results from electron tunneling and the tunneling probability increases rapidly over a narrow range of applied stresses. The basic tunneling process is athermal but the rate is affected by temperature because the barrier to tunneling decreases with increasing temperature. The velocity of sound limits the rate because atoms as well as electrons must move in the process. Therefore, the tunneling attempt frequency is determined by atomic vibration frequencies.

9:30 AM
On the Formation and Evolution of Microtwins during Creep Deformation in Ni-Base Superalloys: *Raymond Unocic*[1]; Libor Kovarik[1]; Peter Sarosi[1]; Chen Shen[1]; Yunzhi Wang[1]; Michael Mills[1]; [1]Ohio State University

During high temperature creep deformation, microtwinning is a principle mode of deformation depending upon microstructure (γ' size, distribution, morphology, and γ channel width spacing), temperature and stress. In this TEM-based deformation mechanism study, the aim was to identify microtwin nucleation sources and track their evolution into fully developed microtwins as a function of increasing plastic deformation. Creep specimens were interrupted at different levels of plastic deformation. In the early stages of creep, deformation is highly localized around MC and $M_{23}C_6$ type carbides, which act as a dislocation source of a/2<110> matrix dislocations. Due microstructural effects and low matrix stacking fault energies, the dislocations readily dissociate into Shockley partial dislocations. The detailed process by which these partials cooperatively shear both γ and γ' phases during the course of deformation will be discussed. The salient microstructural features that lead to the microtwinning mechanism will also be addressed.

9:50 AM
The Role of Interstitials on Slow Twin Growth in Alpha and Beta Titanium Alloys: *Paul Oberson*[1]; Sreeramamurthy Ankem[1]; [1]University of Maryland

Recent models for some of the twins in HCP and BCC materials show that the octahedral sites where interstitials reside are not conserved at the twin-matrix interface. If interstitial atoms such as oxygen in titanium are present, then these interstitial atoms must move away from the interface so that twin growth can proceed. Recent observations in regard to the low temperature creep of alpha and beta titanium alloys show that the twins grow very slowly due to the time factor involved in diffusion of oxygen atoms away from the twin-matrix interface. The activation energies measured from the twin growth were compared to that of oxygen diffusion in alpha and beta titanium alloys at room temperature and were found to be in good agreement. The details of the twin-growth and other details of the investigation will be presented. This work is supported by NSF under Grant Number 0513751.

10:10 AM
True Twin Formation in Gamma TiAl by <211]/(111) Pseudo-Twin Shear: *Dongsheng Xu*[1]; Hao Wang[1]; Rui Yang[1]; Patrick Veyssière[2]; [1]Chinese Academy of Sciences, Institute of Metal Research; [2]Laboratoire d'Etude des Microstructures, Centre National de la Recherche Scientifique-ONERA

A mechanism for true-twin growth resulting from the shearing of gamma TiAl along a <211] pseudo-twinning direction on a {111} plane was identified by extensive atomistic simulations. Twinned and perfect L10 lattices were shear-deformed under different hydrostatic pressures. It was found that under zero pressure or hydrostatic tension, true twins can grow by a dislocation-mediated mechanism even when the shear direction does not favor the deformation twinning. A twin thickens by one layer by a process involving five partial dislocations gliding on two adjacent atomic planes, with a total Burgers vector of 2/3[211]. The strain thus provided, which is four times larger than that associated with a conventional twin or pseudotwin, is more effective in accommodating severe mechanical conditions. The dislocation substructure and critical conditions for this process to occur were studied using molecular dynamics and 'generalized' gamma surfaces were introduced to analyze the new twin growth process.

10:30 AM Break

11:00 AM Invited
The Double Cross-Slip Mechanism of Deformation Twinning: *Pirouz Pirouz*[1]; [1]Case Western Reserve University

This talk reviews a twinning mechanism based on the different mobility of partial dislocations constituting a screw dislocation and the cross-slip of the latter. In most materials, the different mobility of partials arises from their different core structures. Thus, in compound semiconductors, a screw dislocation dissociates into two 30° partials each having a different atomic species at its core. A simple extension of the Frank-Read source, taking the different mobilities of partials into account, then accounts for twinning at low temperatures and high strain rates. On the other hand, the climb dissociation of screw dislocations and the operation of the same mechanism explains basal twinning in sapphire. A number of experiments in semiconductors and in sapphire in support of this

mechanism will be presented and the model will be compared with the classical pole mechanism proposed nearly half a century ago.

11:30 AM
Influence of Shockwave Obliquity on Deformation Twin Formation: *George Gray*[1]; Ellen Cerreta[1]; Robert Hixson[1]; Larry Hull[1]; [1]Los Alamos National Laboratory

Shock-loading of a material in contact with a high explosive(HE) experiences a complex loading path which evolves in both space and time. Energetic loading subjects a material to a "Taylor wave" (triangular wave) loading profile that as a function of obliquity experiences an evolving balance of hydrostatic and deviatoric stresses. While much has been learned over the past five decades concerning the propensity of deformation twinning in samples shock-loaded using "square-topped" profiles as a function of peak stress, achieved via flyer plate loading, considerably less quantitative information concerning direct in-contact HE-driven and sweeping detonation-wave loading on twinning propensity in materials is known. The influence of shock prestraining on various metals shock loaded via direct energetic loading on deformation twin formation was studied. Twinning propensity is shown to increase with increasing shock obliquity consistent with the increasing deviatoric shear stresses and decreasing peak shock stress with increasing shock obliquity.

11:50 AM
An Electron Microscope Study of Mechanical Twinning in Gamma-Based Titanium Aluminides: *Fritz Appel*[1]; [1]GKSS Research Centre

Modern gamma-based titanium aluminide alloys are multiphase assemblies with complex constitution microstructure. Mechanical twinning in these alloys has been investigated by conventional and high-resolution electron microscopy. The major areas of the study are: twin nucleation and growth, effects of solid solution and precipitation hardening and the association of twinning and fracture. Particular emphasis is paid on the stress-induced transformation of the B_2 and orthorhombic phases, which are significant constituents in these alloys. These two phases are apparently unstable under mechanical distortion and transform into gamma phase by distinct shuffle operations. Thus, the product structure is not crystallographically identical to the matrix and the mechanism may be described as pseudo-twinning. Since such structures have been frequently observed in deformed and fatigued samples, it might be expected that this stress-induced transformation serves as a toughening mechanism.

12:10 PM
Formation Mechanism of Deformation Twinning in High-Nitrogen Austenitic Stainless Steel: *Tae-Ho Lee*[1]; Chang-Seok Oh[1]; Sung-Joon Kim[1]; [1]Korea Institute of Materials Science

Formation mechanism of deformation twinning in high-nitrogen austenitic stainless steel was discussed based on the characteristics of dislocation configuration using dynamical two-beam theory. Deformation twinning showed strong orientation dependence: (i) primary and conjugate twinning system cooperated in <111>; (ii) only one twinning system was activated in <110>; (iii) no deformation twinning was observed in <100> orientation, respectively. At the early stage of deformation, fault pairs composed of stacking fault planes and bounding partials heterogeneously nucleated, and grew into overlapping stacking faults, resulting in the formation of deformation twinning. The dynamical two-beam analyses showed that the twinning partials were confirmed to be a Shockley dislocation with Burgers vector 1/6[1-21] and no other dislocation components such as Frank or stair-rod are found. The formation mechanism of deformation twinning could be accounted for by the three-layer twin model, and is discussed in comparison with other models.

Emerging Interconnect and Packaging Technologies: Pb-Free Solders: Fundamental Properties, Interfacial Reactions and Phase Transformations

Sponsored by: The Minerals, Metals and Materials Society, TMS Electronic, Magnetic, and Photonic Materials Division, TMS: Electronic Packaging and Interconnection Materials Committee
Program Organizers: Carol Handwerker, Purdue University; Srinivas Chada, Medtronic; Fay Hua, Intel Corporation; Kejun Zeng, Texas Instruments, Inc.

Monday AM — Room: 275
March 10, 2008 — Location: Ernest Morial Convention Center

Session Chairs: Carol Handwerker, Purdue University; Darrel Frear, Freescale Semiconductor

8:30 AM Introductory Comments

8:35 AM Invited
Materials Characterizations of Sn-In Based Solders: *Fay Hua*[1]; Yi He[1]; Jim Maveety[1]; Rajat Agarwal[1]; Carl Deppisch[1]; [1]Intel Corporation

Sn-Ag-Cu based solders have a number of limitations, such as a high melting point, being relatively stiff, etc. New alternative Pb-free solders are needed to meet both FLI (1st level, flip chip) and SLI (2nd level, BGA) applications. The requirements for the new solders are as follows: 1> highly deformable to absorb the thermo-mechanical strain caused by CTE mismatch of package and PCB materials during temperature cycling. 2> highly fatigue resistant to serve as electrical pass for products during operation under high stress. 3> Pb-free is a given requirement due to world wide ROHS requirements; 4> highly electro-migration resistant to avoid premature failure during operation at high current and temperature applications. In order to meet the requirements, detailed characterization on 2 to 15 wt.% of SnIn alloys were conducted. Very-small ~120°C peak observed in some of the high Sn SnIn solders from in DSC analysis likely due to macro segregation during solidification in current package assembly. Lab shear, creep and isothermal fatigue tests were also conducted for various SnIn solders. The mechanical behavior was optimized with smaller 3rd element doping. Lab scale solder joints electron migration was evaluated. The data shows superb current carrying capability of the SnIn based solder joints. SEM, EDX and other analytical tools were used in the evaluation. The paper summarizes all the material characterization of the materials series.

9:05 AM
A Novel Low-Temperature Solder Based on Intermetallic-Compound Phases with Superior High-Homologous Temperature Reliability: *Daewoong Suh*[1]; Chi-won Hwang[1]; Minoru Ueshima[2]; Jun Sugimoto[2]; [1]Intel Corporation; [2]Senju Metal Industry Company

A novel low-temperature solder which consists entirely of two phases of intermetallic compounds is recently developed in an attempt to develop a highly reliable low-temperature solder for 125C reflow. The materials design, key properties and package-level reliability performance are presented in this article. The new solder can be reflowed at 125C and yet maintains high-temperature mechanical properties and reliability at homologous temperatures exceeding 0.9. Specifically, the new solder has creep resistance and high-temperature retention capability exceeding those of conventional low-temperature solders, and its strength even exceeds that of Sn-4%Ag-0.5%Cu (SAC405) at the same homologous temperatures. Accordingly, reliable temperature cycling performances up to 1000 cycles are demonstrated at the peak temperature corresponding to the homologous temperature exceeding 0.9. The new solder also exhibits ductility exceeding conventional solders at room-temperature, delivering drop reliability superior to SAC405.

9:20 AM
Oxidation Resistant Rare Earth-Containing Pb-Free Solders: *Martha Dudek*[1]; Nikhilesh Chawla[1]; [1]Arizona State University

Small additions of the Rare-Earth (RE) La to Sn-Ag-Cu alloys have been shown to significantly increase ductility, without significant loss in strength. Since most REs are prone to oxidation, this can severely affect the mechanical

performance of the solder. In this work, we have investigated the effect of the addition of Ce, La, and Y rare-earths on the oxidation behavior and shear strength of a Sn-3.9Ag-0.7Cu alloy. The degree of oxidation and oxidation mechanisms were studied by conducting experiments in air at 60°C, 95°C, and 130°C. The Ce-containing solders showed the highest oxidation resistance, approaching that of conventional Sn-Ag-Cu. Microstructure characterization of as-processed and reflowed samples was conducted to determine the influence of RE-containing phases on the mechanical properties and oxidation resistance. The oxidation mechanisms and their influence on mechanical performance will be discussed.

9:35 AM
Reaction Phases in the Sn/Ni-V Couples: *Chih-chi Chen*[1]; Sinn-wen Chen[1]; Chih-horng Chang[1]; [1]National Tsing Hua University

Ni-V alloys are barrier materials in flip chip technology and Sn is the primary constituent of Pb-free solders. The interfacial reactions in the Sn/Ni-V are different from those in the Sn/Ni couples. A ternary T phase layer is formed at the early stage of the Sn/Ni-7wt.%V reaction couple at 200°C. After 48 hours reaction, a Ni_3Sn_4 phase layer is formed between Sn and T phase, the reaction path is Ni-V/T/Ni_3Sn_4/Sn. Periodic layers, Ni-V/T/Ni_3Sn_4/T/Ni_3Sn_4/Sn, are found in the couples after 72 hours reaction. The ternary T phase is examined by using transmission electron microscopy (TEM), grazing incident x-ray diffraction (GIXD) and electron probe microanalysis (EPMA). T phase composition varies with vanadium content which indicates T phase is with some amorphous characteristics. By TEM and GIXD analysis, T phase also shows some crystalline characteristics and it consists of fine grains. T phase is an amorphous phase with some ultra-fine crystalline grains.

9:50 AM Break

10:10 AM Invited
Sn/Co Interfacial Reactions: Chao-hong Wang[1]; *Sinn-wen Chen*[1]; [1]National Tsing Hua University

Interfacial reactions in the Sn/Co couples have been examined. The reaction temperature ranges from 150°C to 250°C and $CoSn_3$ phase is the dominant reaction phases. The growth rates of the reaction phases are very fast, and the layer thickness increases with linearly with the reaction time in the initial stage of the reaction. A very unique cruciform pattern is formed in the Sn/Co couple reacted at 200°C. The reaction phase layers are thick and uniform along the edges of the Co substrate, and there are no reaction phases at the corners. For the Sn/Co couple reacted at 180°C, a metastable $CoSn_4$ phase is formed at the corner in addition to the $CoSn_3$phase formed along the edge of the Co substrate. The cruciform pattern of the reaction $CoSn_3$ phase layer is formed either by cracking or transformation to the CoSn4 phase at the corners where stresses are most intensified.

10:40 AM
High Impact Strength Tin-Copper Based Lead-Free Solder Bump Alloys: *Keith Sweatman*[1]; Tetsuro Nishimura[1]; Shoichi Suenaga[1]; [1]Nihon Superior Company, Ltd.

The advantages of the higher ductility of the Sn-Cu eutectic as a bumping alloy has previously been acknowledged but its use as a solder was initially limited its non-eutectic behaviour. With the success of an addition of Ni at a very specific level in promoting eutectic behaviour apparent in the very widespread use of a proprietary alloy in wave soldering consideration has been given to its application in BGA. In this paper we report the results of testing the impact strength of Sn-Cu-Ni BGA spheres soldered to ENIG and Cu/OSP substrates with pendulum hammer speeds of 10, 1000 and 4000mm/s. At the highest pendulum speed the energy to fracture Sn-Cu-Ni joint was consistently and significantly higher than that of similar Sn-Ag-Cu alloy spheres soldered to the same substrates. Study of the fracture surfaces confirmed the more ductile character of the failure in the Sn-Cu-Ni joints.

10:55 AM
The Effects of Minor Fe, Co, and Ni Additions to Lead-Free Solders on the Thickness of Cu_3Sn at the Interface: *Yi-Wun Wang*[1]; C. Robert Kao[1]; [1]National Taiwan University

The transition to lead-free solders in the microelectronics industry presents many reliability challenges. Examples include package compatibility, creep, and Kirkendall voids. It is widely accepted that the formation of the Kirkendall voids is related to the growth of Cu_3Sn. The objective of this study is to investigate the effects of minor Fe, Co, and Ni additions on the soldering and aging reactions between lead-free solders and Cu. The experimental results show that the presence of minor elements can in fact reduce the growth rate of Cu_3Sn but increase the formation of Cu_6Sn_5. We find Kirkendall voids in the reaction between Sn2.5Ag-xNi (x=0~0.1wt.%) and electroplated Cu at 160°C. However, we didn't find voids in the reaction between Sn2.5Ag0.8Cu-xNi (x=0~0.1wt.%) and electroplated Cu. We consider that the Cu concentrations in the solders and the types of Cu substrate are two factors influencing Kirkendall voids formation.

11:10 AM
Wetting Kinetics of Eutectic Lead and Lead-Free Solders: Spreading over Cu Surface: *Hui Zhao*[1]; Dinesh Reddy Nalagatla[1]; Dusan Sekulic[1]; [1]University of Kentucky

The main objective of this paper is to contribute to fundamental understanding of physical mechanisms of the kinetics of the triple line movement for solder systems over Copper substrates. This effort is devoted to a phenomenological and quantitative investigation of spreading of three representative, commonly considered lead-free solder systems, i.e., Sn, eutectic Sn-Ag, and an eutectic Sn-Cu, vs. an eutectic Pb - Sn solder over Cu substrates. Wetting kinetics was studied using a real time in situ monitoring of the triple line movement, facilitated by a hot-stage microscopy system under a controlled atmosphere. A significantly different kinetics of lead vs. lead-free solders is documented. In case of the eutectic lead solder, three characteristic spreading stages were identified. Spreading of lead-free solders features two stages with a sharp change of the spreading rate. SEM and EDX analysis of the re-solidified solder surface within the halo region is discussed.

11:25 AM
Surface Tension and Oxide Film Studies of Lead-Free Solders: *Kym Watling*[1]; Kazuhiro Nogita[1]; Arne Dahle[1]; [1]University of Queensland

The relative surface tensions of a range of lead-free solders were determined on pyrex and copper substrates using the sessile drop method. Studies were performed under controlled atmospheres including air and protective gases. The formation of thin protective films was seen for some alloys, while bulk oxides showing interference colors were observed for others under the same atmosphere and temperature conditions. X-ray Photoelectron Spectroscopy was used to determine the chemical nature of the surface oxides and the thickness of thin protective films. The thickness of bulk films was studied using a spectral reflectance technique. Significant differences in the oxide film characteristics were observed between the different solders and for different atmospheres.

Emerging Methods to Understand Mechanical Behavior: Imaging Methods

Sponsored by: The Minerals, Metals and Materials Society, TMS Structural Materials Division, TMS Materials Processing and Manufacturing Division, TMS: Advanced Characterization, Testing, and Simulation Committee, TMS/ASM: Mechanical Behavior of Materials Committee, TMS: Nanomechanical Materials Behavior Committee
Program Organizers: Brad Boyce, Sandia National Laboratories; Mark Bourke, Los Alamos National Laboratory; Xiaodong Li, University of South Carolina; Erica Lilleodden, Forschungszentrum

Monday AM — Room: 285
March 10, 2008 — Location: Ernest Morial Convention Center

Session Chair: Brad Boyce, Sandia National Laboratories

8:30 AM Invited
Elasticity and Large Strain Plasticity of Semiconductor Nanowires and Nanobelts: *Zhong Lin (Z.L.) Wang*[1]; Xiaodong Han[2]; Ze Zhang[2]; [1]Georgia Tech; [2]Beijing University of Technology

Covalence bonded materials are usually high strength and high hardness but with low temperature brittleness. However, lowering the dimension of the materials may result in dramatic change in their mechanical properties. In this talk, we will present mechanical characterization of individual oxide nanobelts

by AFM and Si and SiC nanowires by in situ nano-mechanical deformation in TEM. As for SiC nanowires (NWs), we demonstrated unusually large-strain plasticity of ceramics SiC nanowires (NWs) at temperatures close to room temperature that was directly observed. The continuous plasticity of the SiC NWs is accompanied by a process of increased dislocation density at early stage, followed by an obvious lattice distortion, and finally reaches an entire structure amorphization at the most strained region of the NW. These unusual phenomena for the SiC NWs are fundamental important for understanding the nano-scale fracture and strain induced band structure variation for high temperature semiconductors.

9:00 AM
***In Situ* Compression of Nanoparticles**: Julia Nowak[1]; William Mook[1]; *Joysurya Basu*[2]; William Gerberich[1]; C. Carter[2]; [1]University of Minnesota; [2]University of Connecticut

The mechanical properties of nanoparticles are difficult to characterize because of the length scales which are inherently involved. With traditional nanoindentation methods, the crystallographic orientation of the particle usually cannot be determined, and it is impossible to definitively ascertain the presence of defects prior to deformation. These issues can be circumvented by compressing the nanoparticles in the transmission electron microscope (TEM), which is particularly sensitive to crystal structure. Previous studies on nanoparticles have shown length scale effects on particle flow stress, modulus and fracture toughness. This work uses a specially designed sample holder to compress individual nanoparticles *in situ*. The particles are compressed between a sapphire substrate and a diamond tip while quantitative load-displacement data is simultaneously acquired. By compressing the particles inside the TEM it is possible to observe the deformation events directly as they occur and correlate them to the particle's mechanical response.

9:20 AM
Nanomechanical Testing of Gum Metal: *Elizabeth Withey*[1]; Miao Jin[1]; Jia Ye[2]; Andrew Minor[2]; Shigeru Kuramoto[3]; Daryl Chrzan[1]; John Morris[1]; [1]University of California; [2]Lawrence Berkeley National Laboratory, National Center for Electron Microscopy; [3]Toyota Central Research and Development Laboratories, Inc.

"Gum Metal" describes a newly developed set of alloys with nominal composition Ti-24(Nb+V+Ta)-(Zr,Hf)-O. In the cold-worked condition these alloys have exceptional elastic elongation and high strength; the available evidence suggests that they do not yield until the applied stress approaches the ideal strength of the alloy, and then deform by mechanisms that do not involve conventional crystal dislocations. To clarify the mechanisms involved, in situ nanoindentation and microcompression experiments were performed in a TEM on electron transparent windows and pillars fabricated with a focused-ion beam. Results from these tests on solution-treated and cold-worked specimens were compared with TEM observations after ex situ nanoindentation, which revealed unusual patterns in the pits of the indents.

9:40 AM
In Situ Nanotension and Nanocompression Tests of Metallic Glasses in a TEM: *Evan Ma*[1]; [1]Johns Hopkins University

For metallic glasses (MGs), the initial evolution of plastic strains in both time and space has not been resolved, because of strain localization in ~10 nm shear bands that propagates rapidly to failure. We discuss in situ tests, in tension and compression, of Zr-based and Cu-Zr-Al MGs in a TEM, employing samples with dimensions of the order of 100 nanometers. The tensile experiments were a collaboration with H. Guo and M.L. Sui at SYNL (H. Guo et al., Nature Mater. 2007), and the nanocompression was a joint project with Z.W. Shan of Hysitron/LBNL (Z.W. Shan et al., submitted, 2007). These tests show uniform deformation and extensive necking or slow shear displacement rate, i.e. deformation modes similar to their crystalline counterparts. The sample size effects revealed in these nanoscale in situ tests have implications for understanding the mechanical behavior of amorphous metals and their applications in thin films and micro-devices.

10:00 AM
In Situ TEM Nanoindentation of a 50nm Particle: Observed Deformation Mechanisms and Theoretical Analysis: *Chris Carlton*[1]; Oleg Lourie[2]; Paulo Ferreira[1]; [1]University of Texas at Austin; [2]Nanofactory Instruments

Indentation of nanostructured materials is a very rapidly growing area of investigation. Many nanoindentation experiments have been performed on nanostructured materials to determine the fundamental effects of length scale constraints on their mechanical behavior. An in-situ deformation experiment was performed on a single crystal nanoparticle with a diameter of approximately 50nm. Evidence of dislocation nucleation and motion was observed during in-situ TEM nanoindentation, but upon unloading dislocations were no longer visible. The experiment provides insight into how nanomaterials behave under deformation. Because observed dislocations intersected the particle's surface, both the dislocation loop and image force only assumptions made by previous models explaining dislocation behavior are inadequate for addressing the situation observed. Additionally, dislocations are not seen to nucleate from Frank-Read sources, contrary to what is commonly assumed in models for nanoindentation. A new analytical model for explaining dislocation instability is introduced, and application of this model is considered.

10:20 AM Break

10:35 AM Invited
3D Resolved in Situ Studies of Grain Dynamics and Plastic Strain: *Henning Poulsen*[1]; [1]Risø National Laboratory

The status of two hard x-ray characterization techniques will be presented along with examples of applications: 1) 3DXRD microscopy is a diffraction method based on imaging/reconstruction principles. It enables fast and comprehensive characterization of the individual grains within thick specimens. 3D orientation maps can be acquired with a spatial resolution of currently ~ 5 µm, while diffracting units of size 20 nm can be observed. 3DXRD microscopy for the first time enables dynamic studies of the individual grains in polycrystals. Focus will be on recent extensions of the methodology to deformed specimens. 2) A universal method for 3D plastic strain characterisation has been developed based on displacement of markers and the use of x-ray tomography. The combination with FEM analysis will be illustrated.

11:05 AM Invited
Direct Observation and Measurement of Fundamental Deformation Mechanisms at the Nanoscale: *Oden Warren*[1]; Zhiwei Shan[1]; S.A. Syed Asif[1]; Andrew Minor[2]; [1]Hysitron, Inc.; [2]Lawrence Berkeley National Laboratory, National Center for Electron Microscopy

Nanoindentation has advanced sufficiently to become a routine technique, and is most commonly used to determine elastic modulus and hardness of small volumes of materials. However, there also is considerable interest in using nanoindentation to understand how material deformation proceeds at the nanoscale. But unfortunately, the often observed discontinuities in nanoindentation force-displacement curves do not represent unique fingerprints for specific deformation mechanisms. In order to directly observe and measure fundamental deformation mechanisms at the nanoscale, we have placed the nanoindentation technique into the transmission electron microscope (TEM). We have used this fully quantitative in situ TEM technique to correlate specific features of the nanoindentation force-displacement curve to the corresponding microstructure evolution, and to examine the response of individual nanostructures to compression or bending. Some in situ TEM results support conventional wisdoms whereas others do not, and it is the latter that will be the primary focus of this presentation.

11:35 AM
Design and Fabrication of In Situ Micro-Device to Study Mechanical Properties of One Dimensional Nanoscale Building Blocks: Y. Ganesan[1]; Y. Lu[1]; A. Minor[2]; *Jun Lou*[1]; [1]Rice University; [2]Lawrence Berkeley National Laboratory

This paper presents a simple micro-device that allows in situ quantitative mechanical characterization of one-dimensional nanoscale building blocks, such as metallic nanowires and carbon nanotubes, in scanning electron microscope (SEM) chamber equipped with a nanomanipulator, or transmission electron microscope (TEM) chamber equipped with a quantitative nanoindenter. The unique design of this device makes it possible to convert compression

from nanoindentation to uni-axial tension at the sample stages. Fabrication of the micro-device is successfully demonstrated using established micro-fabrication processes. Finite element analysis (FEA) is employed to model the device behavior under mechanical loading and compared with experiments. Finally, initial results from testing Ni nanowires and CNT bundles will also be discussed.

11:55 AM

Multistage Fatigue Model for an Extruded AZ31 Mg Alloy: *Yibin Xue*[1]; Marcos Lugo[1]; Mark Horstemeyer[1]; Jim Newman[1]; [1]Mississippi State University

Microstructure-fatigue properties relation is developed based on multiscale fatigue experiments and micromechanical simulations. The large inclusion particles at or near the surface are identified as the fatigue damage incubation sites. The shape and composition of the inclusion particles, as well as the bonding strength between the particle and alloy matrix, affects the fatigue incubation life as observed in micromechanical simulations in conjunction with the modified microscale Coffin-Manson law. The microstructurally and physically small crack growths were observed using in-situ SEM fatigue testing setup. The crack growth rate was directly quantified as a function of applied stress amplitude with a weight function of applied stress ratio. The fatigue long crack growth was modeled combining a generalized Paris law with the application of a strip-yield model at the crack tip. Finally, the multistage fatigue model was implemented to evaluate the fatigue life of a simple component in an automobile Mg-front end application.

12:15 PM

Application of Moiré Interferometry to Whole Field Strain Measurement in Thin Film Specimens: *Arash Tajik*[1]; Hamid Jahed[1]; [1]University of Waterloo

This paper presents the results of the application of Moiré interferometry to strain field measurements in thin films. For strain field measurements, gratings are milled directly on the film using Focused Ion Beam (FIB). The effect of FIB process parameters and the grating geometry on the mechanical property of the film, as well as on the quality and noise level of the Moiré interferogram is studied. Phase stepping and continuous wavelet ridge detection are used to enhance the sensitivity of the technique to 10nm displacements. This technique is potentially a versatile tool for investigation of the static and dynamic behavior of thin films. Tensile testing and the related results on free standing Aluminum thin films are also presented.

Enhancing Materials Durability via Surface Engineering: Residual Stress Effects on Durability

Sponsored by: The Minerals, Metals and Materials Society, TMS Structural Materials Division, TMS/ASM: Corrosion and Environmental Effects Committee, TMS: High Temperature Alloys Committee

Program Organizers: David Mourer, GE Aircraft Engines; Andrew Rosenberger, US Air Force; Michael Shepard, Air Force Resaearch Laboratory/MLLMN; Bruce Pint, Oak Ridge National Laboratory; Brian Gleeson, Iowa State University

Monday AM — Room: 388
March 10, 2008 — Location: Ernest Morial Convention Center

Session Chair: Michael Shepard, Air Force Research Laboratory

8:30 AM

Advanced Residual Stress Inducing Surface Treatments: *Mike Shepard*[1]; [1]Air Force Research Laboratory, Materials and Manufacturing Directorate

With the advent of processes capable of introducing deep, high magnitude residual compression into arbitrary geometries the use of engineered residual stresses has gained increased attention. Several processes, including laser shock processing (LSP) and low plasticity burnishing (LPB), have evolved and are entering common usage in fatigue critical applications. The chief characteristics and applications of these processes will be reviewed. The evolving suite of techniques used to successfully engineer stress distributions will also be described.

8:50 AM

Effects of Laser Shock Peening on the Microstructure and Residual Stress Distributions in Ti-6Al-4V Alloy: *Yixiang Zhao*[1]; Seetha Mannava[1]; Vijay Vasudevan[1]; [1]University of Cincinnati

Laser shock peening (LSP) is a novel surface process that generates deep compressive residual stresses and microstructural changes and thereby dramatically improves fatigue strength of critical metal aircraft engine parts. The present study was undertaken to develop a basic understanding of the effects of LSP parameters on the residual stress distributions and microstructural changes in Ti-6Al-4V. Coupons of the alloy with and without a sacrificial/ablative layer were LSP-treated using the LSP system at GE and LSP Technologies, Inc. Depth-resolved characterization of the macro residual strains and stresses and was achieved using high-energy synchrotron x-ray diffraction. The near-surface and through-the-depth changes in strain, texture and microstructure were studied using EBSD/OIM and by TEM of thin foils fabricated from specific locations using the FIB method. Local property changes were examined using microhardness. The results showing the relationship between LSP processing parameters, microstructure, residual stress distributions and hardness are presented and discussed.

9:15 AM Invited

Bulk Residual Stress Measurements to Support Durability Enhancement: *Michael Hill*[1]; Adrian DeWald[1]; [1]Hill Engineering, LLC

Residual stress measurement is a key technology for engineering of durability enhancement through surface treatment. The contour method is a new way to measure bulk residual stress fields in components that provides data useful for forecasting fatigue life. Relying on simple assumptions and straightforward experimental procedures, the method provides the two-dimensional spatial distribution of residual stress normal to a plane of interest within the component. When the method is applied at sections with high failure risk, the residual stress field determined may be used directly with standard methods for predicting fatigue crack initiation and growth. The paper provides a summary of the experimental details of the contour method and residual stress distributions measured in example surface treated components. The paper further provides a few case studies demonstrating the use of measured residual stress distributions in correlating the fatigue performance of surface treated coupons.

9:40 AM Break

9:50 AM

Modeling of Mechanical Surface Treatments: *Adrian DeWald*[1]; [1]Hill Engineering, LLC

This presentation provides an overview of the methodology and a summary of capabilities for a model that predicts the effects of residual stress inducing surface treatments on foreign object damage (FOD) tolerance. The proposed model gives an efficient means for predicting the residual stresses (compressive and tensile) in complex 3D parts, which is useful for design calculations. In addition, the model is capable of predicting the effects of changes in the processing parameters and treatment zone, which provides an efficient means to iterate the process. Ultimately, the model is intended for use as a tool to help organizations adopt residual stress treatments with lower risk, lower cost, and reduced time to market.

10:15 AM

Fatigue Design Diagram (FDD) Code to Design Compressive Residual Stresses to Improve Performance of Damage-Limited Components and Structures: *Narayanan Jayaraman*[1]; Paul Prevey[2]; Ravi Ravindranath[3]; Michael Shepard[4]; [1]Lambda Technologies; [2]Lambda Research; [3]NAVAIR; [4]Air Force Research Laboratory

The Fatigue Design Diagram (FDD) is mainly used to design residual stresses to mitigate different damage conditions. It is also designed to take credit for beneficial residual stresses in components to achieve a required or optimal fatigue performance. The FDD code has been developed to interact with commercial finite element analysis (FEA) codes to determine the required residual stress distribution in a component or structure. Design features include determination of minimum, maximum and optimum residual stress distribution for fixed mean stress condition and fixed stress-ratio (R = Smin/Smax) condition. Other analytical features like prediction of fatigue life in the presence of known residual stress distributions will also be discussed. In this paper, the progress

made to date on the use of the FDD Code will be described. The paper will demonstrate the coupling of the FDD code with other standard commercial analytical tools with specific examples.

10:40 AM

Incorporating Residual Stress in Probabilistic Life Prediction of an α+β Titanium Alloy: *Sushant Jha*[1]; Reji John[2]; James Larsen[2]; [1]Universal Technology Corporation; [2]US Air Force Research Laboratory

The effect of surface residual stress (RS) on the fatigue lifetime variability of Ti-6Al-2Sn-4Zr-6Mo was studied at 260°C. The RS profiles induced by low stress grinding (LSG) and shot peening (SP) were considered. Particular focus was on relating the crack initiation mechanisms under these surface conditions to the mean vs. the life-limiting behavior. Deterministic and probabilistic life-prediction analyses, that incorporated the relaxation (upon exposure to temperature and cyclic loading) and variability in the RS profile, were developed. While SP provided a benefit in terms of the mean lifetime response when compared to the RS free condition, the lower-tail behavior was not significantly affected. The LSG treatment provided a greater benefit, both in the mean as well as the life-limiting behavior. These effects were related to the incidence of surface-crack-initiation mechanisms that occurred at a much smaller size scale under the LSG condition than the SP treated surface.

11:05 AM Break

11:15 AM

Relaxation of Shot-Peened Residual Stresses in a Nickel-Base Superalloy: *Dennis Buchanan*[1]; Reji John[2]; Robert Brockman[1]; [1]University of Dayton Research Institute; [2]US Air Force

Creep tests on shot-peened nickel-base superalloy specimens, subject to applied stresses near yield, have been performed at 650°C on IN100 to characterize the residual stress relaxation behavior. Retained residual stress depth profiles show that yielding during the initial loading produces the largest change in the residual stress profile. For sustained loads above yield, a continual relaxation of residual stresses occurs with increasing exposure time. However, for stresses below yield the retained residual stress profiles are similar to specimens subject to thermal exposure alone. Baseline virgin samples subject to room temperature plastic deformation and tested under elevated temperature creep conditions display a creep rate dependency on prior plastic strain. These prestrain experiments simulate the deformation experienced by the material during shot-peening and form the basis of a coupled creep-plasticity constitutive model. The model successfully predicts the retained residual stress profiles of shot-peened IN100 specimens subject to elevated temperature loading histories.

11:40 AM Invited

Materials Development and Process Modeling for Engineered Surfaces – An Integrated Approach for Gas Turbine Engine Component Design: *Ann Bolcavage*[1]; Kang Lee[1]; Kong Ma[1]; [1]Rolls-Royce Corporation

Modern gas turbine engines are required to provide increasing amounts of thrust and withstand severe environmental conditions. Resulting operational factors such as higher temperatures and loading for a given mission can be detrimental to the service life of the engine, and their effects are often manifested in the degradation or alteration of the component surface properties. To address these challenges to optimum performance, materials development and process modeling are increasingly coordinated during component definition and design. The benefits of an integrated approach include reduced part-to-part variability, increased component capability via the tailoring of surface-specific materials and mechanical properties, and better prediction of the effects of harsh environments on serviceable life. Examples include diffusion coating alloy optimization for oxidation resistance and peening process development and modeling.

Frontiers of Computational Materials Science

Sponsored by: The Minerals, Metals and Materials Society, American Physical Society, TMS Electronic, Magnetic, and Photonic Materials Division, TMS Materials Processing and Manufacturing Division, ASM Materials Science Critical Technology Sector, TMS: Chemistry and Physics of Materials Committee, TMS/ASM: Computational Materials Science and Engineering Committee, TMS: Global Innovations Committee, TMS: Nanomechanical Materials Behavior Committee, TMS/ASM: Phase Transformations Committee, TMS: Powder Materials Committee, TMS: Process Technology and Modeling Committee, TMS: Shaping and Forming Committee, TMS: Solidification Committee, TMS: Surface Engineering Committee
Program Organizers: Mark Asta, University of California; Giulia Galli, University of California, Davis

Monday AM — Room: APS Room, Hall A
March 10, 2008 — Location: Ernest Morial Convention Center

Session Chair: To Be Announced

Program to be announced.

General Abstracts: Extraction and Processing: Session I

Sponsored by: The Minerals, Metals and Materials Society, TMS Extraction and Processing Division, TMS: Aqueous Processing Committee, TMS: Materials Characterization Committee, TMS: Process Technology and Modeling Committee, TMS: Pyrometallurgy Committee, TMS: Recycling and Environmental Technologies Committee
Program Organizers: Boyd Davis, Queens University; Michael Free, University of Utah

Monday AM — Room: 272
March 10, 2008 — Location: Ernest Morial Convention Center

Session Chair: Boyd Davis, Queens University

8:30 AM

Study on AC Impedance Equivalent Circuit and Experimental Condition for Solution and Melts Electrical Conductivity Measurement by CVCC Technique: *Xianwei Hu*[1]; Zhaowen Wang[1]; Guimin Lu[1]; Jianzhong Cui[1]; Zhongning Shi[1]; Xiaozhou Cao[1]; Xingliang Zhao[1]; [1]Northeastern University

Continuously varying cell constant(CVCC) technique is an advanced method for measuring the electrical conductivity of solution and melts. AC impedance spectroscopy of CVCC experimental conductivity cell system analyzed, and viewpoint error of former researchers was pointed out. So the AC impedance rational condition for electrical conductivity measurement by CVCC technique was determined. It was thought that the AC impedance course of the circuit researched was controlled by both of electrochemical polarization and concentration polarization. Warburg diffusion character was represented for AC impedance diffusion course of solution, meanwhile, melts' concentration polarization impedance was assumed to be Gerischer impedance. When electrical conductivity was calculated by CVCC equation, the best option of the circuit resistance was the sum of solution/melts resistance and electrode and line resistance gained by fitting the equivalent circuit. If fitting error was considered, the circuit high frequency resistance was also a good option.

8:55 AM

Improvements on the Process of Gold-Antimony Concentrate Smelting in China: Liu Weifeng[1]; Yang Tianzu[1]; *Dou Aichun*[1]; Liu Yong[1]; Chen Fangbin[1]; [1]Central South University

On the basis of the brief introduction of the gold-antimony concentrate smelting process in China, the problems of some procedure in the original process were analyzed and the corresponding improvements were introduced in this paper, such as the treatment of antimony matte, the refinement of gold-silver alloys, the concentrating gold from gold-antimony alloys, the treatment of As-enriched slag, the pre-treatment of gold concentrate with high arsenic. The

roasting method that was used to treat the antimony matte was transfered to the ore dressing method. The solvent extraction was used to refine the gold alloys instead of the electrolytic method. The technology of selective chlorination leaching under controlling potential was applied to concentrate gold from the gold-antimony alloys and gold-lead alloys instead of the electrolysis method. As-enriched slag was recovered by the second reducing smelting method substituting for the method of compound of sodium arsenite. The pre-treatment roasting method was used for removing arsenic in gold concentrate with high arsenic.

9:20 AM

A Comparative Analysis of the Main Metallurgical and Mechanical Properties of Self-Reducing Pellets and Briquettes: *Jose Noldin*[1]; Jose D'Abreu[2]; Nivea Pimentel[3]; [1]Tecno-Logos S/A; [2]Catholic University - PUC-Rio; [3]Aços Villares

The Tecnored process is a new ironmaking technology based on the use of cold bonded self-reducing agglomerates both in the form of pellets and/or briquettes as the primary feedstock. The main characteristic of self-reducing agglomerates is the extremely fast reaction rates achieved due to the proximity of the reactants, their small size and inert gases free environment; almost complete reduction can be achieved within reaction times ranging from 5 to 10 minutes for temperatures between 1273K and 1423K. This paper discusses the main metallurgical and mechanical properties of both cold bonded self-reducing pellets and briquettes containing different types of raw materials, including mining and steelmaking resides.

9:45 AM Break

10:05 AM

Reduction Behavior of Lignite and Coke Fine Containing Composite Pellets: *Aliye Arabaci*[1]; Ercin Ersundu[2]; Süheyla Aydin[2]; [1]Istanbul University; [2]Istanbul Technical University

In the present investigation, an attempt has been made to study the reduction behaviour of composite pellets consisting of iron oxide fines and coke or lignite fines as reducing agents. The reduction experiments were carried out under isothermal conditions and constant flow rate of nitrogen gas in the temperature range of 900-1100°C. The variables investigated were the reduction temperature, Cfix/Fe_3O_4 ratio, reduction time and reductant type. In the experiments carried out at a temperature of 1100°C, for 40 min. and on the condition that Cfix/Fe_3O_4 ratio is 0.2, in which lignite and coke fines were used as reductant, degree of reduction was obtained as 91% and 86%, respectively. The highest degree of reduction was obtained by using lignite as reductant.

10:30 AM

Meeting the New Challenge in Smelter Gas Handling: *Erik Dupon*[1]; Rick Oliana[1]; Travis Turco[1]; Peter Klut[1]; [1]Danieli-Corus BV

New and stricter environmental and health regulations and specifications force Smelter operators to improve on their gaseous and particulate emissions from the potroom. A techno-economical overview is provided of available technologies to reduce emissions to the environment and health hazards inside the potroom. Special attention is given to reduction of emissions by the application of new technology developments such as GTC upgrading and boosted suction. Recent examples of application of these new technologies will be provided.

10:55 AM

Conceptual Design Criteria for Metallurgical Waste Heat Boilers and Electro Static Precipitators Downstream of Smelting- and Converting-Furnaces and Fluid Bed Reactors: *Kurt Westerlund*[1]; Jan Deisenroth[2]; Uwe Bock[2]; [1]Kamwest Oy; [2]Alstom Energy Recovery GmbH

The article deals with conceptual design originating from the reactors themselves; Gas temperature, Gas analyses, splashes, Dust carry over and exothermic dust gas reactions along the cooling path in the Waste heat boiler. Results and interpretations of Gas flow simulation and reactions are discussed. The article also deals with dust smelting, softening temperatures and arrangement of cooling surfaces in the Waste heat boiler; cooling walls, screens, bundles and cleaning methods of these. The advantages and limitations in applying thermal siphons for cooling to avoid water leakages into the reactors are also outlined. Temperature operating windows for Waste heat boiler cooling surfaces are presented. Furthermore the article outlines the precipitation efficiency of different dusts at their optimal precipitation temperatures.

11:20 AM

Scrubbing: Development of a Technical Audit System for Process, Operation and Maintenance: *Mario Dion*[1]; Michel Meyer[1]; [1]Alcan International Ltd

Following the acquisition of Pechiney by Alcan, audit systems and expertise from both companies had to be integrated to take into account different equipment and practices. As part of this global approach, a team of experts was set up and created an audit system on gas scrubbing, covering four subjects: process, operation, maintenance and management, and based on the knowledge and best practices of both companies. This tool promotes the use of these Best Practices and gives a holistic picture of the status of a gas or fume treatment center, as well as a detailed action plan to improve the system performance. The new Alcan scrubbing audit system has been successfully tested through internal and external technology licensing projects.

General Abstracts: Materials Processing and Manufacturing Division: Solidification and Casting

Sponsored by: The Minerals, Metals and Materials Society, TMS Materials Processing and Manufacturing Division, TMS/ASM: Computational Materials Science and Engineering Committee, TMS: Global Innovations Committee, TMS: Nanomechanical Materials Behavior Committee, TMS/ASM: Phase Transformations Committee, TMS: Powder Materials Committee, TMS: Process Technology and Modeling Committee, TMS: Shaping and Forming Committee, TMS: Solidification Committee, TMS: Surface Engineering Committee
Program Organizers: Ralph Napolitano, Iowa State University; Neville Moody, Sandia National Laboratories

Monday AM — Room: 282
March 10, 2008 — Location: Ernest Morial Convention Center

Session Chairs: Mark Jolly, University of Birmingham; Benjamin Hamilton, Miami University

8:30 AM

Austenite Grain Refining of As-Cast Bloom Surface by Reduction of Oscillation Mark Depth: *Yasuhide Ohba*[1]; Shin-ichi Kitade[1]; Ichiro Takasu[1]; [1]Sanyo Special Steel Company, Ltd.

Austenite grain refining in the surface layer of as-cast bloom is effective for the reduction of surface cracks in steel production. This study was carried out to clarify the influence of cooling rate on the as-cast austenite grain size and its growth mechanism. The austenite grains at the bloom surface were refined under the oscillation conditions of higher frequency and shorter stroke. The average cooling rates were estimated to be 6-16K/s in austenite phase temperature. It was found that the austenite grain growth direction did not vary even when characteristics of oscillation mark changed. The austenite grain size below the surface layer was also determined by that of bloom surface.

8:50 AM

Quality Assessment of Casting Filling Method: Carl Reilly[1]; *Mark Jolly*[1]; [1]University of Birmingham

Cast component reliability is dependent on the quality of the casting process. This can be characterised by fluid flow characteristics within the running system. Prevention of free surface turbulence and oxide entrainment is critical to the mechanical integrity of the component. Past research highlighted that return waves were a major cause of free surface entrainment. These can be reduced by developing a quiescent flow regime. Using Flow 3D, the Froude number was extracted to allow the quantitative assessment of sumps at the end of the runner. The results showed the addition of a sump at the end of the running system can reduce the Froude number but increase the persistence and is therefore

detrimental to the cast component. Additionally, in-gate design is of utmost importance in controlling the back pressure and thus the persistence of the back wave which has a direct effect of the level of oxide entrainment.

9:10 AM
Phase Field Simulation of Irregular Eutectic Solidification: *Ruijie Zhang*[1]; Mei Li[1]; John Allison[1]; [1]Ford Motor Company

The phase-field models have been originally developed for solidification of two phase system and then extended to multiphase system. In real multiphase alloy systems, facet phase often appears in the solidification process, such as Si in Al-Si alloy, Mg_2Si in Al-Mg-Si alloy. These facet phases are usually the highly anisotropic stoichiometric intermetallic compounds and solidify as a eutectic phase in solidification process. Their size, distribution and volume fraction are key factors which greatly affect the materials mechanical performance. So simulation of the growth of such phase will be very important for the alloy design and materials performance prediction. In this paper, the multiphase phase field model was extended to describe the solidification of irregular eutectic alloy. The strong anisotropy in interfacial energy and phase field mobility were considered. As an example, the simulation of irregular eutectic growth in Al-Si alloy was executed.

9:30 AM
Effect of Al Contents on Hot Crack Formation of the High-Manganese Steel: *Hyukjin An*[1]; Yang-Mo Koo[1]; [1]Pohang University of Science and Technology

The cracking condition near melting temperature during continuous casting of the high-manganese steel have been studied. During solidification, the peritectic solidification has been known to cause harm effects to the hot crack formation. The effects of Al contents on brittle temperature range for hot crack formation are analyzed by differential scanning calorimetry(DSC). To calculate the brittle temperature range, micro-segregation model and proper solidification model are used. To determine the proper Al contents for continuous casting, peritectic reaction range and brittle temperature range are calculated from heat flow graph during solidification with vary Al and Mn contents.

9:50 AM
A Numerical Scheme for Solving Microsegregation for Solidifying Metallic Alloys: *Salah Uddin*[1]; Mainul Hasan[1]; [1]McGill University

In this study, the microsegregation problem, which arises during solidification of an alloy, was analyzed for three different geometrical shapes namely, rectangular, cylindrical and spherical dendrite arms and for several pertinent parameters. A previously proposed numerical method for solidification/melting problems was extended in this study to deal with solute diffusion in both solid and liquid regions. An algorithm is proposed to solve the strongly coupled model transport equations. The algorithm is based on the control volume finite-difference scheme with an appropriately transformed gird system. In order to verify the accuracy of the present method with regard to tracking the solid/liquid interfaces in the microsegregation problem, the well-known analytical solution of the Stefan problem was used. A good agreement between the model predictions and the analytical solution was found. The developed computational procedure was also found to be stable for a wide range of values of the parameters.

10:10 AM Break

10:20 AM
Microstructural Characterization of Laser-Consolidated (LC) SS420 Stainless Steel: *Jianyin Chen*[1]; Lijue Xue[1]; [1]National Research Council Canada

Laser consolidation (LC) is a novel process that produces a net shape functional part layer by layer directly from a CAD model by using a laser beam to melt the injected powder and re-solidifying it on the substrate or previous layer. As an alternative to the conventional machining process, this computer-aided manufacturing (CAM) process can build complete parts or features on an existing part by adding instead of removing material. Due to the rapid solidification associated with this process, LC materials always show exceptionally fine dendritic microstructure, resulting in significantly improved mechanical properties as compared to the respective cast materials. In this paper, LC SS420 stainless steel was investigated. After various post-heat-treatments, the microhardness and residual stresses of the LC SS420 were measured. Their microstructure was examined by optical microscopy, SEM/EDS and XRD. The implication of the post-heat-treatment on the microstructure and mechanical properties of LC SS420 was also discussed.

10:40 AM
Process Optimization in Laser Processing of Ceramics: *Anoop Samant*[1]; Narendra Dahotre[1]; [1]University of Tennessee

An integrated modeling technique based on modular approach is considered for the laser processing of the material. Heat transfer phenomenon during laser processing of alumina ceramic was modeled using COMSOL software. The macroscopic melt depth predicted using the software was enhanced by the Carman-Kozeny equations to analyze the effect of recoil pressure. Predicted residual stresses determined the range of laser fluence which doesn't cause failure of components. Taguchi method for the design of experiments identified a combination of process and materials parameters that will optimize any desirable material property. The estimated melt depths were substantially close to the measured values. For the laser processing conditions under study, the components did not fail in compression and in tension, majority of the stresses being compressive. Taguchi analysis gave a set of processing parameters that could optimize the grain size and porosity.

11:00 AM
Advances in NDT Techniques for Friction Stir Welding Joints of AA2024: *Telmo Santos*[1]; Pedro Vilaça[1]; Luis Reis[1]; Luísa Quintino[1]; Manuel Freitas[1]; [1]Instituto Superior Técnico

Industrial applications of solid state welding technology have undergone a significant development with the advent of Friction Stir Welding (FSW). Although the good quality of FSW joints some defects may arise which are difficult or even impossible to detect with conventional NDT techniques. This work addresses an innovative NDT Eddy currents probe that was developed and tested for quality assessment of FSW joints of aeronautic aluminium alloy AA2024-T351. The influence of defects with different locations and morphology in joint mechanical efficiency are investigated under static and fatigue loads. The application potential of the new NDT Eddy currents probe in detecting the different defects is evaluated and compared with other NDT techniques. The results show a strong dependence between FSW parameters and defects formation and the feasibility in using the new NDT Eddy currents probe mainly concerning the detection of root defects which have a critical role in mechanical joint efficiency.

11:20 AM
A Thermal Model of Friction Stir Welding Applied to Aluminum 7136-T76511 Extrusions: *Benjamin Hamilton*[1]; Stanislaw Dymek[2]; Marek Blicharski[2]; Isabella Kalemba[2]; [1]Miami University; [2]AGH University of Science and Technology

A thermal model of friction stir welding is developed that utilizes an energy-based scaling factor to account for tool slip. The proposed slip factor is derived from an observed, empirical relationship between the ratio of the maximum welding temperature to the solidus temperature and energy per unit length of weld. The thermal model successfully predicts the maximum welding temperatures over a range of energy levels and supports the concept that the relationship between the temperature ratio and energy level is characteristic to aluminum alloys with similar thermal emissivities. The thermal model is applied to aluminum 7136-T76511 extrusions that were joined through friction stir welding at six different RPM and evaluated for residual properties. Residual mechanical properties of the alloy correlated with the energy per length of weld, i.e. the highest joint efficiency was achieved at the highest welding temperature.

11:40 AM
Purification of Cadmium from 4N (99.99%) to 6N (99.9999%) Level by Selective Vaporization Technique under Vacuum: *Gouni Rajkiran*[1]; Rizwan Abdul Rahman Rashid[1]; Siva Jyoth Reddy[1]; Prasad Goud[1]; [1]Mahatma Gandhi Institute of Technology

High purity (6N) cadmium is obtained through multiple vacuum distillation using 4N pure Cd as input material. The metal is purified by vapor phase condensation of cadmium on to a graphite collector. During the experiment, the process of selective vaporization of cadmium is carried out in a stainless steel retort under vacuum. The sample preparation procedure for chemical analysis using Inductively Coupled Plasma Optical Emission Spectrometry (ICP-OES) is studied and the results are explained with respect to their vapor pressures. The

vacuum and its effect on vapor pressure have also been observed. The detailed analysis of input as well as purified Cd was carried out by ICP-OES for 29 major elements. The final analysis shows the impurity content reduction from 190 to 1.8 ppm (6N) upon three consecutive vacuum distillations. The studies showed that the major impurities separated from the distilled cadmium are Zn, Cu, Ag, Sb, Pb, Bi, etc.

12:00 PM
Effect of Ultrasonic Vibration on Solidification Structure of TCS Stainless Steel: Jianping Liang[1]; Lixin Wang[1]; Changjiang Song[1]; Lihua Liu[1]; Fengmei Sun[1]; *Qijie Zhai*[1]; [1]Shanghai University

The effect of ultrasonic vibration on solidification structure of TCS steel was investigated in this present work. Ultrasonic power was injected into molten alloy along the horizontal direction. Experimental results show that when the ultrasonic vibration is imposed on the melt, the chill zone is extended, columnar crystals zone become narrow and dense and equiaxed crystal zone also is refined. Though ultrasonic attenuates very rapidly, the effect of refinement does not decrease markedly. Base on the experimental and theoretical deduction, it is confirmed that ultrasonic energy make the crystal accreting on the wall of mould desquamated, and the acoustic streaming make the desquamated crystal flowed into the liquid zone of cast. Desquamation of nucleus and acoustic streaming play an important role in metal structure refinement.

General Abstracts: Structural Materials Division: Mechanical Behavior of Metals and Alloys

Sponsored by: The Minerals, Metals and Materials Society, TMS Structural Materials Division, TMS: Advanced Characterization, Testing, and Simulation Committee, TMS: Alloy Phases Committee, TMS: Biomaterials Committee, TMS: Chemistry and Physics of Materials Committee, TMS/ASM: Composite Materials Committee, TMS/ASM: Corrosion and Environmental Effects Committee, TMS: High Temperature Alloys Committee, TMS/ASM: Mechanical Behavior of Materials Committee, TMS/ASM: Nuclear Materials Committee, TMS: Product Metallurgy and Applications Committee, TMS: Refractory Metals Committee, TMS: Superconducting and Magnetic Materials Committee, TMS: Titanium Committee
Program Organizer: Ellen Cerreta, Los Alamos National Laboratory

Monday AM — Room: 387
March 10, 2008 — Location: Ernest Morial Convention Center

Session Chairs: Fang Cao, Los Alamos National Laboratory; Marian Kennedy, Clemson University

8:30 AM
A Comparative Study of the Tensile Response of Pure Mo and a Mo-Si-B Solid Solution Alloy: *Padam Jain*[1]; S. Kumar[1]; [1]Brown University

The Mo-Si-B solid solution matrix in multiphase Mo-Si-B alloys is thought to dominate low-temperature toughness and high-temperature creep resistance. Thus, it is important to understand the mechanical behavior of the solid solution phase in isolation. Uniaxial tension tests were performed on an extruded Mo-Si-B solid solution alloy between 400ºC and 1200ºC and nominal strain rates of 10^{-4} s^{-1} and 10^{-6} s^{-1}. Dynamic Strain Aging (DSA) was observed in two different temperature and strain rate regimes. Tests were conducted on pure Mo in the recrystallized condition for comparison to isolate the possible role of B and Si on DSA in the solid solution alloy. In addition, constant load tensile creep tests were performed on the ternary solid solution alloy at 1000ºC and 1200ºC to evaluate the steady-state creep behavior. The deformed/fractured specimens were characterized to understand the underlying mechanisms. These observations will be presented and discussed.

8:50 AM
A Delta-Function Model for Three-Dimensional Axisymmetric Crystals: *Ping Du*[1]; Harris Wong[1]; [1]Louisiana State University

A surface energy polar plot contains two possible singularities: the cusps that give facets on an equilibrium crystal, and the circular arcs connecting the cusps that can lead to missing orientations. The common approach of specifying the surface energy usually cannot handle both singularities simultaneously. We model the surface stiffness to avoid missing orientations. Furthermore, a facet is represented by the Dirac delta function with the weight of the delta function equal to the width of the facet. Thus, both singularities are treated precisely. This approach has been shown to work for two-dimensional symmetric[1] and axially symmetric[2] crystals. Here, we extend the delta-function model to three dimensions by modeling three-dimensional axisymmetric crystals. [1]Xin, T. and H. Wong "A δ-function model of facets," Surface Science 487, L529-L533 (2001). [2]Du, P. and H. Wong "A delta-function model for axially symmetric crystals," Scripta Materialia 55, 1171-1174 (2006).

9:10 AM
Anisotropic Elastic/Plastic Model for Description of High Purity Alpha Titanium: *M.E. Nixon*[1]; Oana Cazacu[2]; R.A. Lebensohn[3]; [1]Air Force Research Laboratory and University of Florida; [2]University of Florida/REEF; [3]Los Alamos National Laboratory

Accurate modeling of anisotropic hexagonal closed packed (hcp) polycrystals such alpha-titanium requires the description of the interplay between slip and twinning and its effects on texture evolution and hardening response. In this paper, an anisotropic model that captures the influence of evolving texture on the plastic response of hcp metals is proposed. Yielding is described using a new criterion which captures simultaneously anisotropy and compression-tension asymmetry associated with deformation twinning. The anisotropy coefficients as well as the size of the elastic domain are evolving with the plastic strain. Application of the model to the simulation of the three-dimensional deformation of high-purity alpha-titanium beams subjected to four-point bend tests along different directions is presented. Comparison between predicted and measured macroscopic strain fields and beam sections shows that the proposed model describes very well twinning and its role on evolving the material anisotropy.

9:30 AM
Blocking and Self-Locking of Superdislocations in Intermetallics: *Bella Greenberg*[1]; M. Ivanov[1]; [1]Russian Academy of Sciences

Superdislocations are carriers of plastic deformation in intermetallics. A large translation vector, different types of stacking faults and antiphase boundaries determine the diversity of dislocation configurations, both glissile and blocked ones. A significant point is that blocked superdislocations, which are formed due to re-splitting of glissile superdislocations or rearrangement of the superpartial dislocation core, have the lowest energy. A new concept about the possibility of thermally activated blocking of superdislocations in the absence of external stresses (self-locking) was proposed. A sufficiently general thermally activated process, which causes the extension of a dislocation in a preferred direction and constitutes a necessary step in dislocation transformations leading to blocking, was revealed. By its nature, this process represents the flip of a dislocation from a shallow valley to a deep valley of the potential relief. Reasons for the multivalley relief and the presence of preferred directions vary for dislocations of different types in different materials. Consecutive stages of this rearrangement of an initial dislocation with the direction approaching a preferred one: the formation of a double kink and its subsequent reorientation in a preferred direction. The driving force of the process was calculated and conditions for its realization in the cases of perfect, superpartial and partial dislocations were formulated. An experimental proof of the proposed concept was obtained: self-locking of dislocations, which were induced by preliminary deformation, was detected in Ni3(Al, Nb) and TiAl during no-load heating.

9:50 AM
Crack Growth across Grain Boundaries in Zinc Bicrystals: Experiments and Modeling: *Dhiraj Catoor*[1]; Sharvan Kumar[1]; [1]Brown University

Crack growth in polycrystalline materials prone to crystallographic cleavage is examined by studying fracture of bicrystals of zinc. Here, we will discuss the interaction of a crack with a grain boundary and its transmission across the boundary. In-situ fracture experiments were conducted using bicrystals, with the first grain oriented for mode I basal cleavage; the basal plane in the second grain is "twist-misoriented" w.r.t to the first. Three-dimensional finite element analysis incorporating crystal plasticity to account for anisotropy and cohesive zones to provide for crack growth is used to complement the experimental observations. Crack arrest, nucleation of secondary cracks, and extensive twinning and slip are observed in the vicinity of the grain boundary for misorientations of 10º

and 20º; for larger misorientations, the crack could not be transmitted across the boundary.

10:10 AM
Crack Growth on the Basal Planes in Zinc Single Crystals: Experiments and Modeling: *Dhiraj Catoor*[1]; Sharvan Kumar[1]; [1]Brown University

Although basal cleavage in zinc single crystals has been extensively studied, less is known on controlled crack growth, the nature of crack tip plasticity and its effects on crack propagation. To this end we have conducted in situ fracture tests on single crystal zinc specimens oriented for mode I fracture along the (0001) plane and along the <11-20> and <1-100> directions. Microstructural events such as twinning and slip that mediate crack propagation were recorded in real time along with the load-displacement curves. Basal slip, though unfavorable, was found to dominate crack tip plasticity; {10-12} <10-11> twinning was additionally noted. A 3-D finite element model incorporating crystal plasticity and a cohesive zone formulation to account for fracture has been developed to describe the crack growth process and assess stresses and strains in the vicinity of the crack tip; the results are in good agreement with experimental observations.

10:30 AM Break

10:50 AM
Deformation Behavior of Mg Single- and Bi-Crystals: *Badirujjaman Syed*[1]; Sharvan Kumar[1]; [1]Brown University

Single and bicrystals of pure Mg have been grown using the vertical Bridgman technique. Room-temperature compression and tension tests were conducted by loading chemically polished single crystal specimens along the [0001] and [10-11] directions in-situ under the optical microscope. Surface deformation markings were continuously recorded and observed slip and twinning systems were identified and were correlated with the resulting stress-strain curves. Higher temperature ex-situ tests were performed by loading along these orientations at multiple strain rates, and the deformation behavior was catalogued in tension and in compression to determine the effect of temperature and strain rate on the flow curves as well as operating deformation mechanisms. Isothermal constant load tests are being conducted on bicrystals of Mg in the temperature range 300C-450C to obtain an appreciation for the grain boundary sliding characteristics. These results will be presented and their implication for polycrystalline deformation at high temperatures will be discussed.

11:10 AM
Modeling of Grain Size Distribution Effect on Mechanical Properties of Ti Alloys: *Qizhen Li*[1]; [1]University of Nevada, Reno

Due to their outstanding properties including high specific strength and light weight, Ti alloys are broadly used in aerospace industry. Since materials failures will cause the huge disasters environmentally and financially to the human world, a clear understanding of the relation between microstructure and mechanical properties is needed in materials selection and structural design. Extensive research was done to understand how the average grain size affects the mechanical behaviors of materials. This work will focus on studying the effect of grain size distributions with a fixed average grain size, since grain size fluctuation is a common phenomenon in the crystalline materials. Finite element modeling is applied to investigate the grain size distribution effect, and the results can guide the microstructure design to realize certain required property.

11:30 AM
Grain Size and Strain Rate Dependency of Flow Stress in FCC Metals: *Khaled Al-Fadhalah*[1]; [1]Kuwait University

The effects of grain size and boundary structure on the flow stress of FCC metals were examined as a function of strain rate (less than 10^{-1}). Annealed samples of pure copper and aluminum were tested in tension at room temperature for grain size ranging from 5 μm to 50 μm. The resultant microstructure consists of grains with large population of annealing twin boundaries. By varying the strain rate, the dependency of flow stress on grain size and twin boundaries are modeled using polycrystal plasticity. Microstructure development during plastic deformation such as dislocation accumulation, and dislocation interaction at twin boundaries was accounted for in the model using the density of mobile and immobile dislocations. Computing both dislocation densities allows better simulation of the flow stress, showing good agreement with the experimental results.

11:50 AM
Effect of the γ/γ' Lattice Mismatch on the Creep Behaviour at 760°C of New Generation Single Crystal Superalloys: *Pierre Caron*[1]; Frédéric Diologent[2]; [1]ONERA; [2]Ecole Polytechnique Federale de Lausanne

We have analysed the creep behaviour at 760°C and 840 MPa of two new generation single crystal nickel-based superalloys. Both alloys exhibit similar amounts and sizes of γ' precipitates, but different values of γ/γ' lattice mismatch. The high lattice mismatch alloy exhibits a small primary creep strain and a long creep life, while a large extent of primary creep and a reduced creep life are obtained for the low lattice mismatch alloy. Transmission electron microscopy on the creep strained materials revealed different dislocation microstructures. Elevated coherency stresses due to the high lattice mismatch promote spreading of the matrix dislocations between the precipitates, resulting in homogeneous deformation and strong strain hardening. Moreover, decorrelation of matrix dislocations in two well-separated Shockley partials signs their low mobility. Shearing of the γ/γ' microstructure by heterogeneous <112>{111} slip in the alloy with a moderate lattice mismatch explains the high primary creep strain.

12:10 PM
High Temperature Oxidation of Alloy 617 in He-CO-CO_2 and He-H_2-H_2O Environments: *Deepak Kumar*[1]; Gary Was[1]; [1]University of Michigan

The helium coolant in the very high temperature gas cooled reactor (VHTR) contains CO, CO_2, H_2, H_2O and CH_4 as reactive impurities. Based on the oxidation and carburization potentials of the impurities, binary gas mixtures in helium have been selected to investigate the corrosion behavior of alloy 617; CO-CO_2, H_2-H_2O. Exposure experiments up to 750 hours were conducted in He-CO-CO_2 and He-H_2-H_2O environments at 900°C at similar oxidation potentials given by the CO/CO_2 and H_2/H_2O ratios. The nature and rate of gas/metal interactions occurring at the surface were determined by analyzing the gas mixtures at both the inlet and outlet of the reaction zone using a gas chromatograph and moisture analyzer. The microstructure stability and the surface scale on the exposed samples were analyzed using SEM. The oxidation behavior in the two different environments will be compared based on the TEM, XRD and EDX results.

Hael Mughrabi Honorary Symposium: Plasticity, Failure and Fatigue in Structural Materials - from Macro to Nano: Dislocations: Work Hardening, Patterning, Size Effects I

Sponsored by: The Minerals, Metals and Materials Society, TMS Structural Materials Division, TMS Materials Processing and Manufacturing Division, TMS: High Temperature Alloys Committee, TMS/ASM: Mechanical Behavior of Materials Committee, TMS: Nanomechanical Materials Behavior Committee
Program Organizers: K. Jimmy Hsia, University of Illinois, Urbana-Champaign; Mathias Göken, Universitaet Erlangen-Nuernberg; Tresa Pollock, University of Michigan - Ann Arbor; Pedro Dolabella Portella, Federal Institute for Materials Research and Testing; Neville Moody, Sandia National Laboratories

Monday AM — Room: 386
March 10, 2008 — Location: Ernest Morial Convention Center

Session Chairs: K. Jimmy Hsia, University of Illinois, Urbana-Champaign; Mathias Göken, University Erlangen-Nürnberg

8:30 AM Introductory Comments

8:40 AM Keynote
Fatigue of Nanostructured Metals and Alloys: *Subra Suresh*[1]; Ming Dao[1]; [1]Massachusetts Institute of Technology

Nanoscale grain refinement is known to have a profound effect on the strength, hardening, rate sensitivity, ductility, toughness and tribological response. However, the resistance of fully nanocrystalline metals and alloys to cyclic deformation and fatigue crack initiation and growth is relatively poorly understood because of the paucity of experimental information. In this presentation, available experimental results, mechanistic models as well as information on the effects of structure and composition on cyclic strain hardening characteristics, stress-controlled fatigue, strain-controlled fatigue and fatigue

crack growth are examined for nanocrystalline and ultra-fine-grained metals and alloys. Effects of grain refinement on the resistance to contact fatigue are also discussed on the basis of experimental results available for nanocrystalline materials subjected to repeated indentation and frictional sliding contact fatigue. The results reveal competing effects of grain refinement on flaw nucleation and growth, and offer useful structural design guidelines for the surface and interior of fatigue-critical components.

9:10 AM Keynote
The Modeling of Plasticity: How Can Dislocation Dynamics Simulations Help?: *Ladislas Kubin*[1]; Benoit Devincre[1]; Thierry Hoc[2]; [1]Centre National de la Recherche Scientifique-ONERA; [2]Ecole Centrale Paris

A major weakness of dislocation-based plasticity models resides in their inability to integrate the full complexity of the microscopic behavior at the scale of a single crystal or of the grain of a polycrystal. A few examples illustrate how dislocation dynamics simulations can help in establishing predictive models at the scale of a representative volume element, which can further serve as constitutive formulations in crystal plasticity codes. The first topic deals with the Hall-Petch relation in ultra-fine grained polycrystals and a critical comparison between simulated behavior and existing models. The second topic discusses experimentally known aspects of deformation stages in face-centered cubic crystals that have never been modeled like stage I mechanisms, the transition between stage I and stage II, the orientation dependence of stage II, multislip deformation and the orientation dependence of dynamic recovery. Current limitations of these approaches are discussed.

9:40 AM Invited
Dislocation Microstructure, Strain Localisation and Crack Initiation in Fatigue Studied by 3D Discrete Dislocation Simulations: *Marc Fivel*[1]; Christian Robertson[2]; Christophe Depres[3]; Chan Sun Shin[4]; [1]SIMaP-GPM2; [2]Commissariat à l'Énergie Atomique/SRMA; [3]Laboratoire Systémes et Matériaux pour la Mecatronique; [4]Korea Atomic Energy Research Institute

First, 3D discrete dislocation simulations are performed in order to analyse the cyclic plasticity that occurs in surface grains of AISI 316L stainless steel. Simulations performed under various loading and boundary conditions show the crucial role played by cross-slip in the formation of the dislocation microstructure. As the cycling proceeds, slip bands exhibiting well organised dislocation arrangements progressively substitute to dislocation tangles. Calculations of the plastic steps printed on the free surface during the cycling give access to the surface relief which is found to be made of extrusion and intrusion profiles. Analyses of stress and distortion energy concentrations inside the slip bands reveals that a crack would most probably initiate at the surface when multipoles, driven by interfacial dislocations, will reach the surface. Finally, the fatigue behaviour of precipitate hardened materials is investigated and compared to the case of AISI 316L.

10:00 AM Invited
How Large are the Strains at Intersections of Slip Bands and What is Their Geometry?: *Peter Neumann*[1]; [1]Max-Planck Institute for Iron Research

In slip bands, shear strains beyond 100% are quite common. The superposition of such large strains cannot be carried out linearly. In order to obtain correct results, either the displacement vectors have to be added or the non-linear terms in the strain tensors have to be taken into account exactly. The former leads to a differential equation, which can be solved easily, the latter leads to a non-linear matrix formula. The results are identical for both methods and show that extremely large strains can occur. It is shown in computer animations that drastic rearrangements of material or material separation can occur.

10:20 AM Break

10:30 AM Invited
Characterization of Lattice Defects by X-Ray Diffraction: *Tamas Ungar*[1]; [1]Eotvos University

Plasticity, failure and fatigue in structural materials is in closest correlation with lattice defects, especially long-range internal stresses, dislocations, subgrain size and planar defects. X-ray line broadening is an alternative method to electron microscopy for characterizing the density and character of lattice defects. (i) Long-range internal stresses are revealed by characteristically asymmetric line broadening. (ii) Dislocation densities and Burgers vector analysis are provided by the dislocation model of strain anisotropy. (iii) Subgrain size and size-distribution are given by the order independent part of line profiles. (iv) The frequency of stacking faults and twin boundaries is determined by specific line shifts and broadening. The four listed defect types can be separated since they follow different hkl dependences with limited correlations.

10:50 AM Invited
Professor Mughrabi's Strain Hardening Models as Applied to Transition Metals and Alloys: *David Davidson*[1]; [1]Southwest Research Institute

Models based on dislocation interactions during tensile straining of fcc metals developed by Prof. Mughrabi in the 1980's have been found to be useful in describing the strain hardening behavior of straining single crystals in the series Nb-Mo-Re, which are bcc. Parameters used in these models must, therefore, be interpreted somewhat differently between the two systems, which will be the subject of this presentation.

11:10 AM Invited
Bulk Dislocation Microstructures Probed with Sub-Micrometer Spatial Resolution Using Synchrotron X-Rays: *Lyle Levine*[1]; Bennett Larson[2]; Jonathan Tischler[2]; Michael Kassner[3]; Peter Geantil[3]; Wenjun Liu[4]; [1]National Institute of Standards and Technology; [2]Oak Ridge National Laboratory; [3]University of Southern California; [4]Argonne National Laboratory

The existence and magnitude of long range elastic strains (and thus stresses) in dislocation cell interiors and walls in deformed metals have been the subject of extensive investigation for more than 20 years. Although numerous volume-averaged measurements have been used to infer their existence, direct measurements were not possible before the recent development of intense submicron X-ray beams. We have used submicron X-ray beams to directly measure the axial elastic strains within individual dislocation cells in copper single crystals deformed in both tension and compression. These spatially resolved measurements found large elastic strains that are consistent with Mughrabi's composite model. Moreover, the strains were found to exhibit large cell-to-cell variations. More recent experiments have studied the distributions of elastic strains within individual dislocation cell walls and looked at elastic strains within extended contiguous sample volumes containing numerous dislocation cells.

11:30 AM
Atomistic Simulations of Grain Boundary Dislocation Nucleation: *Mark Tschopp*[1]; David McDowell[2]; [1]Air Force Research Laboratories/Universal Technology Corporation; [2]Georgia Institute of Technology

The objective of this research is to use atomistic simulations to investigate dislocation nucleation from asymmetric tilt grain boundaries in FCC copper and aluminum. The use of a 3D periodic bicrystal configuration enables the investigation of how the boundary degrees of freedom impact both boundary structure and dislocation nucleation from these boundaries. Simulation results show that dislocation nucleation from asymmetric tilt grain boundaries requires understanding of the structure and faceting of these boundaries. Deformation simulations under uniaxial tension and compression show entirely different nucleation mechanisms, i.e., nucleation of full dislocations in copper from the grain boundary under compression. The role of the grain boundary as a dislocation source is discussed in terms of a perfect source/sink model. Last, the resolved stress normal to the slip plane on which the dislocation nucleates plays an integral role in dislocation nucleation for single crystals and interfaces.

11:45 AM
Statistical Refinement of Mughrabi's Composite Model: *Wolfgang Pantleon*[1]; Tamas Ungár[2]; [1]Technical University of Denmard, Risoe National Laboratory; [2]Eötvös University Budapest

For explaining yielding under stress reversal, the composite model was introduced by Häel Mughrabi distinguishing two phases of different strength: dislocation-rich walls and dislocation-depleted cell interiors. The asymmetry of radial x-ray diffraction profiles has been rationalized successfully by the composite model as superposition of two sub-profiles mutually shifted by internal stresses and broadened by the local dislocation content. The later has prompted criticism as the local dislocation density between the walls observed by transmission electron microscopy is much less than expected from profile analysis. Recent investigations by high angular resolution three-dimensional x-ray diffraction revealed nearly dislocation-free regions in deformed metals.

These dislocation-free regions experience quite different backward elastic strains and cause distinct sharp profiles at different radial positions. Consequently, the sub-profile associated with cell interiors is not broadened by the local dislocation content, but by shifts of several individual sharp profiles. A statistical refinement of the composite model is presented.

12:00 PM

On the Relevance of the Schmid's Factor to Analyse Cyclic Slip Activity and Crack Initiation in Polycrystals: *Patrick Villechaise*[1]; José Mendez[1]; [1]Ecole Nationale Supérique De Mécanique Et D´Aérotechnique/Centre National de la Recherche Scientifique

In metallic polycrystalline materials one of the most common fatigue crack initiation process involves localization of cyclic plasticity in slip bands. In this field, crystallographic orientation constitutes one of the main local characteristics to be considered. It determines some essential parameters in a mechanical point of view like the Schmid's factor and geometrical configuration of slip bands emergence at the free surface. The progress of electron back scattering diffraction technique permits now to investigate the influence of the crystallographic orientation taking into account a great number of grains. A quasi statistical approach of texture configuration that favour fatigue damage can be then developed. We propose to come back on the relevance or non relevance of the Schmid's factor to describe the local microstructure that favour slip activity and crack initiation. This will be illustrated from results obtained on a 316L stainless steel and on a Ti64 titanium alloy.

12:15 PM

Detection of Incipient Fatigue Damage with Scanning SQUID Microscopy: *John Morris*[1]; Tae-Kyu Lee[2]; John Clarke[1]; [1]University of California, Berkeley; [2]Cisco Systems

The fatigue process can be detected and monitored in the earliest stages of high-cycle fatigue, by the increase in dislocation density and hardness, and in the final stages, through the direct observation of initiated cracks. But there are no probative, non-destructive techniques to follow incipient fatigue through the critical intermediate stage between dislocation saturation and prior to crack nucleation. In this study, we report initial success using SQUID microscopy for this purpose. The remanence fields of fatigued ferritic steel specimens were mapped using a high-resolution scanning magnetic microscope based on a high transition temperature Superconducting Quantum Interference Device (SQUID). The results of scans of fatigued specimens of ferritic steel show the development of local peaks in remanent magnetization prior to the development of visible fatigue cracking. Their spatial localization not only identifies incipient fatigue failure, but also identifies the specific locations where cracks will appear.

12:30 PM

Orientation Distributions in Plastically Deformed Copper Single Crystals: *Andras Borbely*[1]; Claire Mauirce[2]; René Fillit[2]; Julian H. Driver[2]; [1]Max-Planck Institut für Eisenforschung; [2]Ecole des Mines de Saint Etienne

Local misorientation distributions developed in copper single-crystals deformed in tension and plane strain-compression were investigated experimentally by X-ray rocking curve (RC) analysis and by backscattered electron diffraction (EBSD). Based on the results obtained on the same samples with the two techniques, the applicability limit of the EBSD method for a statistical interpretation of orientation data was explored. It is shown that in spite of the very small penetration depth of the electrons into copper (of about 10-15 nm), large EBSD scans can provide a statistically-satisfactory characterization of deformation induced dislocation structures. Consequences of the limitations in angular resolution of the EBSD, but also the advantages of EBSD over the X-ray RC analysis are presented. A newly developed imaging method is made known, together with its successful application to the analysis of "geometrically necessary" and "incidental" dislocation boundaries developed during deformation of the investigated copper single crystals.

Hume-Rothery Symposium - Nanoscale Phases: Session I

Sponsored by: The Minerals, Metals and Materials Society, TMS Electronic, Magnetic, and Photonic Materials Division, TMS: Alloy Phases Committee
Program Organizers: Sinn-wen Chen, National Tsing Hua University; David Cockayne, University of Oxford; Seiji Isoda, Kyoto University; Robert Nemanich, Arizona State University; K.-N. Tu, University of California, Los Angeles

Monday AM — Room: 276
March 10, 2008 — Location: Ernest Morial Convention Center

Session Chairs: King-Ning Tu, University of California, Los Angeles; Robert Nemanich, Arizona State University

8:30 AM Introductory Comments

8:35 AM Keynote

Nanoscale Metal Silicides: *L. J. Chen*[1]; [1]National Tsing Hua University

Metal silicides have been introduced into microelectronics devices in late 1970s as gates, contacts and interconnects. In the 1980s, almost all transition metal silicides were found to grow epitaxially on silicon to some extent. In the 1990s, amorphous interlayers of a few nm in thickness were observed to occur in all refractory metal/Si and a number of rare-earth metal and platinum group metal and crystalline silicon systems. As the integrated circuits (IC) industry moves into the nano era, scaling down the metal silicide contacts and gates have become an important issue. A large number of epitaxial and free-standing silicide nanowires were grown.In this talk, a historical account of evolving roles of metal silicides will be presented. Epitaxial growth of silicides on silicon and formation of amorphous interlayers in the metal/Si systems will be reviewed. Synthesis and applications of silicide nanowires will be described. Future outlook will be addressed.

9:25 AM Invited

In Situ Studies of Reactions in Metal Silicides and Metal Oxides: *Robert Sinclair*[1]; [1]Stanford University

In future integrated circuit devices, metal silicides and oxides are becoming increasingly important. However any reactions which occur during processing can adversely influence the designed properties. This article reviews the study of this behavior for some metal-silicon systems (e.g. Ni-Si,Ti-Si) and some metal oxides (e.g, Ta oxide, Hf-Si-O). The processes range from silicidation and metal mediated crystallization in the former, to crystallization and spinodal decomposition in the latter. In situ TEM has proved to be very profitable for such investigations.

9:50 AM Invited

Nucleation and Growth Kinetics of Semiconductor Nanowires: *Frances Ross*[1]; [1]IBM Research

The exciting applications of semiconductor nanowires are best realised through a detailed understanding of the crystal growth processes that take place during wire formation. For this it is important to quantify both the nucleation of wires from their catalyst particles and their subsequent steady-state growth. We have therefore examined both processes using time-resolved environmental microscopy, growing Si and Ge wires from Au catalysts in situ in a TEM. We firstly discuss a simple model for nucleation which explains the time at which nuclei appear and their immediate growth rate. For nanowire heterostructures, we show how nucleation determines the morphology at the heterojunction. Subsequently, the dependence of growth rate on conditions allows us to determine the rate limiting step, while direct observations of the catalyst structure show unexpected features of growth, such as the existence of a liquid phase far below the eutectic temperature that is stabilised by growth-driven supersaturation.

10:15 AM Break

10:30 AM Invited
Silicide Formation: Bulk vs. Thin Films vs. Nanowires: *King-Ning Tu*[1]; Kuo-Chang Lu[1]; Yi-Chia Chou[1]; [1]University of California, Los Angeles

Owing to the applications of thin film silicide as contacts and gates in microelectronic Si devices, the interfacial reaction between metal film and silicon have been studied systematically. Single silicide phase formation in the thin film reactions has been found and has been explained by a competing growth model combining diffusion-controlled and interfacial-reaction-controlled processes. In comparison, a diffusion-controlled growth of multiple silicide phases is obeyed in bulk diffusion couples of metal and Si. Recently, in the point contact reaction between a nano metal wire and a nano Si wire, a supply-controlled growth of nano silicide is found. In this talk, a comparison among the three kinds of reactions; diffusion-controlled, interfacial-reaction-controlled, and supply-controlled growth will be given.

10:55 AM Invited
Transition Metal Silicide Nanowires: *Song Jin*[1]; [1]University of Wisconsin-Madison

We report general synthetic approaches to transition silicide nanowires (NWs), their properties and applications in nanoelectronics, nanophotonics, spintronics, and thermoelectric energy conversion. We utilize chemical vapor deposition (CVD) of metal carbonyl-silyl single source organometallic precursors without any catalyst seeds on silicon substrates covered with a thin (1-2 nm) layer of silicon oxide to produce FeSi and CoSi NWs. We have also developed a complementary method of chemical vapor transport (CVT) to prepare NWs of silicides for which analogous precursors can not be readily made, such as $CrSi_2$, Ni_2Si and Ni_3Si. We discovered a new and general nanowire growth mechanism that is different from the typical vapor-liquid-solid NW growth and critically depends on the oxide thickness. The nanophase formation rules and nanophases of some Nowotny Chimney Ladder phases will be discussed. The physical properties of these silicide NWs were investigated using electrical transport, thermal transport, X-ray spectroscopy, and magnetometry.

11:20 AM Invited
A Global Perspective of New Paradigm and Challenges of Semiconductor Industry in the Nano/Tera Scale Integration Era: *Chih-Yuan Lu*[1]; [1]Macronix International Company, Ltd.

After more than fifty years rapid evolution of semiconductor devices from ZSI to GSI, the linewidth scaled down to nanimeter and thus the transistor integration up to multi-giga bit scale, this scaling power totally changed the human daily life in the world. First we will review the roadmap and discuss the possibility of continuous scaling from technological point of view, and how could keep its pace by close cooperation among academia, consortium, and industrial labs. In addition to technology evolution, the investment scale and economics of semiconductor industry has dramatically changed due to its minimum barrier for the R&D resources threshold level and manufacturing critical mass. We will illustrate these facts by reviewing historical data and possible future roadmap, and some visionary scenarios will be suggested.

Magnesium Technology 2008: Magnesium Plenary Session

Sponsored by: The Minerals, Metals and Materials Society, TMS Light Metals Division, TMS: Magnesium Committee
Program Organizers: Mihriban Pekguleryuz, McGill University; Neale Neelameggham, US Magnesium LLC; Randy Beals, Chrysler LLC; Eric Nyberg, Pacific Northwest National Laboratory

Monday AM — Room: 291/292
March 10, 2008 — Location: Ernest Morial Convention Center

Session Chair: Mark Verbrugge, General Motors Research and Development

8:30 AM Introductory Comments
Automotive Programs in Materials Engineering: Mihriban Pekguleryuz[1]; [1]McGill University

8:45 AM
Integrated Computational Materials Engineering (ICME) for Magnesium: An International Pilot Project: *John Allison*[1]; Baicheng Liu[2]; Kevin Boyle[3]; Randy Beals[4]; Louis Hector, Jr.[5]; [1]Ford Motor Company; [2]Tsinghua University; [3]CANMET Materials Technology Laboratory; [4]Chrysler Corporation; [5]General Motor Corporation

Integrated Computational Materials Engineering (ICME), a new paradigm within the materials profession, offers a means to unify analysis of manufacturing, design and materials into a holistic system. A central component of ICME is the development and utilization of advanced material models which capture our quantitative knowledge of processing-structure-property relationships in a form which can be used by the broader engineering community. This talk will provide an overview of a recently initiated international collaborative project to develop an ICME infrastructure for magnesium for use in automotive body applications. The work will be conducted at leading universities, national labs and industrial research facilities in the US, China and Canada. This project is sponsored by the U.S. Department of Energy, the U.S. Automotive Materials Partnership (USAMP), Chinese Ministry of Science and Technology (China) and Natural Resources Canada (Canada).

9:15 AM
Magnesium Front End Research and Development: A Canada-China-USA Collaborative Program: *Alan Luo*[1]; Eric Nyberg[2]; Kumar Sadayappan[3]; Wenfang Shi[4]; [1]General Motors Corporation; [2]Pacific Northwest National Laboratory; [3]Canmet Materials Technology Laboratory; [4]China Magnesium Center

The Magnesium Front End Research & Development (MFERD) Program is a jointly sponsored effort by the United Sates Department of Energy, the United Sates Automotive Materials Partnership (USAMP), the Chinese Ministry of Science and Technology and the Natural Resources Canada to demonstrate the technical and economic feasibility of a magnesium intensive automotive body structure. The MFERD program started in early 2007 by initiating R&D in the following areas: crashworthiness, NVH, fatigue and durability, corrosion and surface finishing, extrusion and forming, sheet and forming, high-integrity body casting, as well as joining and assembly. In addition, the MFERD program is also connected to the Integrated Computational Materials Engineering (ICME) program that will investigate the processing/structure/properties relations for various magnesium alloys and manufacturing processes.

9:45 AM
The Chrysler Magnesium Alloy Development Program: *Randy Beals*[1]; [1]Chrysler LLC

The Chrysler Magnesium Alloy Development (CMAD) program used a Design of Experiments (DOE) approach to create several new high pressure die cast creep resistant magnesium alloys. The goal of this approach was to find the optimum combination of the following alloy characteristics; good corrosion resistance, good castability, creep resistance, high strength and elongation that can be produced at a reasonable cost. A dynamic computer program was developed in order to control the DOE of various chemical compositions (ratio

of elements, etc.) during the high pressure die casting of the specimens. A total of seven alloy groups were produced and investigated (series 0 to 6) that had differing amounts of following alloying elements; Al, Zn, RE, Sr, Ca and Sn. Data will be presented comparing the cost effective performance of these materials to other commercially available magnesium and aluminum alloys.

10:15 AM
Performance of Creep-Resistant Magnesium Alloys in Dynamometer and Component Testing of the USAMP Magnesium-Intensive V6 Engine: *Bob Powell*[1]; William Miller[1]; Larry Ouimet[1]; Joy Hines[2]; John Allison[2]; Randy Beals[3]; Robert McCune[4]; Lawrence Kopka[3]; Peter Ried[5]; [1]General Motors Corporation; [2]Ford Motor Company; [3]DaimlerChrysler; [4]Robert C. McCune and Associates LLC; [5]Ried and Associates LLC

In 2007 the US Automotive Materials Partnership- and US Department of Energy-supported Magnesium Powertrain Cast Components project team completed all support aspects of this six year project and began engine dynamometer and component testing the V6 engine with its four Mg components (cylinder block, oil pan, front engine cover, and rear seal carrier). A full array of dynamometer testing was conducted, including hot scuff, cold scuff, global durability, high speed durability, thermal cycle and deep thermal shock. The purpose of these tests was to validate the predictions of the engine design and to identify any critical areas for further work in bringing the mass reduction potential of Mg into major powertrain applications. Engine test results to date, lessons learned, and other project accomplishments will be presented.

10:35 AM Panel Discussion

Materials in Clean Power Systems III: Fuel Cells, Hydrogen-, and Clean Coal-Based Technologies: Plenary Session

Sponsored by: The Minerals, Metals and Materials Society, TMS Structural Materials Division, TMS/ASM: Corrosion and Environmental Effects Committee
Program Organizers: Zhenguo "Gary" Yang, Pacific Northwest National Laboratory; Michael Brady, Oak Ridge National Laboratory; K. Scott Weil, Pacific Northwest National Laboratory; Xingbo Liu, West Virginia University; Ayyakkannu Manivannan, National Energy Technology Laboratory

Monday AM Room: 392
March 10, 2008 Location: Ernest Morial Convention Center

Session Chair: Ayyakkannu Manivannan, National Energy Technology Laboratory

8:30 AM Introductory Comments

8:40 AM Keynote
DOE Perspectives of Materials for Advanced Power Systems: *Robert Romanosky*[1]; [1]National Energy Technology Laboratory
Abstract not available.

9:25 AM Keynote
"Near Zero" Emissions Solid Oxide Fuel Cell (SOFC) Power Generation Systems for Operation on Hydrocarbon and Coal Derived Fuels: Technology Review: *Prabhakar Singh*[1]; Nguyen Minh[1]; [1]Pacific Northwest National Laboratory

Intermediate to high temperature (600-1000°C) operation and novel electrode processes in solid oxide fuel cells (SOFC) enable efficient utilization of hydrocarbons and coal derived fuels. SOFC's also show tolerance to higher levels of fuel impurities (compared to low temperature fuel cells), utilizes a much simpler balance of plant and offer the potential to develop "near zero emissions" power systems architecture. This presentation will review recent advances in SOFC technology including materials of construction, electrode processes, and long term degradation. Cell and stack designs will be reviewed with emphasis on structural analysis and thermal management. Systems requirements for stationary, mobile and portable applications will be presented. Key challenges will be examined and discussed and current research trends will be presented.

10:10 AM Invited
CO_2-Selective Membranes for Hydrogen Purification and CO_2 Capture: He Bai[1]; *W.S. Winston Ho*[1]; [1]Ohio State University

This talk covers carbon dioxide-selective membranes for applications in hydrogen purification for fuel cells and in carbon dioxide capture for the greenhouse gas sequestration. We have synthesized new membranes for the removal of carbon dioxide from hydrogen-containing synthesis gas by incorporating amino groups into polymer networks. The membranes are selective to carbon dioxide preferentially versus hydrogen since the acid gas permeates through the amine-containing membranes via the facilitated transport mechanism due to its reversible reaction with the amine. The membranes synthesized have shown high carbon dioxide permeability and selectivity vs. hydrogen or carbon monoxide. This type of membranes has the potential for hydrogen purification for environmentally friendly fuel cells, including the use of the membrane in the membrane reactor configuration to enhance water gas shift (WGS) reaction. Results from WGS membrane reactor experiments have shown carbon monoxide conversion/reduction to 10 ppm as well as significant hydrogen enhancement via carbon dioxide removal. The data have been in good agreement with modeling prediction. The carbon dioxide captured on the permeate side had a dry concentration of greater than 98% by using steam as the sweep gas. Hydrogen sulfide has much higher reaction rate with the amine than carbon dioxide as the former reacts with the amine via proton transfer and the latter reacts with the amine via carbamate formation primarily. Thus, hydrogen sulfide can permeate through the membrane much faster than carbon dioxide. Our initial membrane data have shown hydrogen sulfide with about 3 times permeability of carbon dioxide. In addition, our initial experiments with a limited membrane area have shown a nearly complete removal of hydrogen sulfide from 50 ppm in the synthesis gas feed to about 10 ppb in the hydrogen product, which is good for fuel cell applications.

Materials Processing Fundamentals: Solidification and Deformation

Sponsored by: The Minerals, Metals and Materials Society, TMS Extraction and Processing Division, TMS: Process Technology and Modeling Committee
Program Organizer: Prince Anyalebechi, Grand Valley State University

Monday AM Room: 283
March 10, 2008 Location: Ernest Morial Convention Center

Session Chair: Prince Anyalebechi, Grand Valley State University

8:30 AM
Bicrystalline Silicon Growth in Si-Al: Principles of Morphological Selection: *Ralph Napolitano*[1]; [1]Iowa State University

Low velocity gradient-zone growth from Si-Al melts gives rise to a primary structure consisting of very large bicrystalline domains, with each comprised of a 210/310 twin pair sharing a common <001> axis aligned in the growth direction. Strong morphological selection of this primary structure is investigated with respect to (i) mechanisms of lateral propagation for the array, (ii) high mobility coherent twin configurations within the primary cores, and (iii) diffusion-based selection principles. Based on detailed morphological and compositional measurements and high resolution TEM analysis, the observed morphology is attributed to a hybrid primary/coupled growth mode, where the persistent defect structure at the front is the critical feature, affording a substantial kinetic advantage for strong selection. The diffusional component of this mode selection is investigated using a phase field approach, accounting for high anisotropy. Scaling rules for selection are compared with the more common diffusion-based selection observed in nonfaceted dendritic growth.

8:50 AM

Rapid Freeze Prototyping of Investment Cast Thin-Wall Metal Matrix Composites I – Pattern Build and Molding Parameters: *Von Richards*[1]; Edward Druschitz[1]; Sriram Isanaka[1]; Ming Leu[1]; Matt Cavins[1]; Tim Hill[1]; [1]University of Missouri

Rapid Freeze Prototyping (RFP) is a novel solid freeform fabrication technology that creates parts by depositing water droplets and freezing them rapidly to form layers. An investigation into the smallest thickness that can be achieved by the RFP process was conducted. The factors that could significantly affect the thickness of the part built by this process including substrate temperature, volumetric feed rate, table velocity, nozzle frequency, nozzle standoff distance, and head pressure were considered. A shell building technique for use with the RFP system has been developed. Thin wall ice patterns have been invested using production shell building techniques and an alcohol-based slurry. The finished shells were quantitatively evaluated by inspecting their total shell thickness, mold cavity dimensional reproducibility and shell strength.

9:10 AM

Solidification Cracking of Allvac 718Plus: *Joel Andersson*[1]; Göran Sjöberg[1]; Anssi Brederholm[2]; Hannu Hänninen[2]; [1]Volvo Aero Corporation; [2]Helsinki University of Technology

Weldability is a broad term used to explain how a material behaves when it is welded. There is an increasing demand for weldable superalloys since fabricated components or several castings are joined together to add up to the final component. Allvac 718Plus is a newly developed superalloy and has a high potential in terms of fabricated structures. Transvarestraint testing has been employed when testing the weldability or susceptibility to solidification cracking.

9:30 AM

Thermal Study and Metallographic Characterization of Zn-20%Al and Zn-20%Al-10%Si-3%Cu Alloys Directionally Solidified: Alicia Ares[1]; Sergio Gueijman[1]; *Carlos Schvezov*[1]; [1]CONICET/University de Misiones

The present investigation was undertaken to investigate the directional solidification of Zn-20%Al and Zn-20%Al-10%Si-3%Cu alloys under different conditions of heat transfer at the metal/mould interface. The type of structure obtained in both cases is analyzed and related to the solidification thermal parameters such as cooling rate, growth rate, thermal gradient and recalescence which were determined from the temperature versus time curves. These parameters were correlated with the structure-like length of columnar grains and size of equiaxed grains. The metallographic analyses were done performing quantitative metallography and composition analysis of the different alloying elements along the cast samples were done by SEM (Scanning Electron Microscopy) and EDXA (Energy Dispersive X-Ray Analysis). Correlations between properties, structures and compositions were found.

9:50 AM

Effect of Cross-Hatched Mold Surface Topography on Shell Morphology in the Solidification of an Aluminum Alloy: *Prince Anyalebechi*[1]; [1]Grand Valley State University

The effects of a mold surface topography consisting of cross-hatched grooves and casting speed on the morphology of solidifying shells of an aluminum alloy 3003 have been characterized by a series of immersion tests. The cross-hatched grooves were 0.232 mm deep with wavelength or spacing between 1 mm and 15 mm. The shells solidified at casting speed of less than 10 mm/s on a 1 mm spaced cross-hatched grooved mold surface were fairly uniform with little or no localized variations in thickness. However, the propensity for non-uniform shell growth morphology was exacerbated by increase in casting speed, melt superheat, and the wavelength of the cross-hatched grooves. This is provisionally attributed to the effects of the casting conditions and the cross-hatched grooves on interfacial heat transfer and wetting of the mold surface by the molten metal.

10:10 AM Break

10:20 AM

Effects of Silicon, Iron, and Chromium on the Response of Aluminum Alloy 3004 Ingots to Homogenization: *Prince Anyalebechi*[1]; [1]Grand Valley State University

The effects of Si (0.19-0.52 wt.%), Fe (0.20 wt.%-0.44 wt.%), and Cr (0-0.10 wt.%) on the response of ingots of aluminum alloy 3004, solidified at different rates (0.10 K/s to 30 K/s), to homogenization heat treatment have been investigated. Response to homogenization was determined by quantifying the following microstructural parameters: (i) amount of Mn retained in solid solution; (ii) types, relative amounts, sizes, size distributions, shapes, and chemical compositions of second phases; (iii) extent of the alpha-transformation reaction; (iv) interparticle spacing; (v) dispersoid formation; and (vii) alleviation of dendritic microsegregation. Of the three alloying elements investigated, Si had the greatest effect on the response of aluminum alloy 3004 to the homogenization heat treatment. Increase in Si content, fineness of cast microstructure, and homogenization temperature facilitated alpha-transformation reaction, dissolution of Mg2Si, loss of Mn supersaturation, and formation of All2(Fe,Mn)3Si and Mg_2Si dispersoids.

10:40 AM

Effect of Interfaces on Melting and Solidification Behavior of Lead, Bismuth and Tin Embedded in Icosahedral Quasicrystalline Phase: *Alok Singh*[1]; AnPang Tsai[2]; [1]National Institute for Materials Science; [2]Tohoku University

Novel interfaces were created by embedding lead, bismuth or tin nano-particles in an Al-Cu-Fe matrix. By heat treatment, three states of matrix phase were obtained, altering the nature of interfaces. Interface structures were studied by TEM and melting and solidification behavior was studied by differential scanning calorimetry (DSC). Each of the embedded elements showed a different melting and solidification behavior. Lead shows a lowering of melting temperature in quasicrystalline matrix and no clear solidification peak. Bismuth shows superheating in quasicrystalline matrix but a significant lowering of temperature in the microcrystalline matrix. Tin shows no change of melting temperature in either matrix, and clear solidification peaks in both. Through a crystallographic analysis and a study of the interfaces, it is shown that melting and solidification of heavily dependent of the crystallographic match between the two phases and consequently the interface structure.

11:00 AM

Effect of Oxygen Content on Type of Inclusion Precipitated during Unidirectional Solidification of Steel: Huigai Li[1]; *Shaobo Zheng*[1]; Liwei Wang[1]; Qijie Zhai[1]; [1]Shanghai University

The fine titanium oxide inclusions precipitated during solidification are favorable for intragranular ferrite nucleation. The oxygen content before solidification affects the type and size of inclusions. The type of the precipitated inclusions in Mn and Ti alloyed steel was studied by means of thermodynamic calculation and experiment in this paper. The micro-segregation of Mn, Ti and O during solidification was considered in the calculation. The unidirectional solidification apparatus was employed in the experiment to ensure that the alloy elements diffused along the solidification direction. The results showed that, the inclusions are mainly Ti_2O_3 when the oxygen content is in 10ppm; they are Ti_2O_3 and $MnTiO_3$ when it is in 20ppm and $MnTiO_3$ in 30ppm. With the increase of the oxygen content, the size of the inclusions increases.

11:20 AM

Influence of Chemical Composition on Bake Hardening Effect for Hot Rolled Multiphase Steels: *Heinz Palkowski*[1]; Mehdi Asadi[1]; Goran Kugler[1]; [1]Technical University of Clausthal

Recent trends in the automotive industry lead to increasing interest in advanced high strength steels (AHSS). Beside good ductility and high strength, those steels have a high bake hardening effect (BH), giving additional contribution to the strength of structural parts, subjected to the paint baking process. For hot rolled AHSS, namely dual phase and martensitic steels, the effect of process conditions on mechanical properties had been investigated by the authors. However, the study of the influence of chemical composition on BH ability of the AHSS is not been investigated sufficiently and published in literature. In the current research, samples of different chemical compositions within the characteristic interval for industrial production had been studied under different pro-load conditions, simulating the thermo-mechanical production process. The samples were then

subjected to BH process. Tensile tests were performed to study the varying chemical composition on the BH effect.

11:40 AM

Microstructure and Texture Evolution of Pure Gold in Intense Torsion Straining: *Jong Soo Cho*[1]; Jeong Tak Moon[1]; Seok-Hoon Gang[2]; Kyu-Hwan Oh[2]; [1]MKE; [2]Seoul National University

The microstructure development of pure gold wire (99.99 wt.%) deformed at low temperature (usually less than 0.4 Tm) in intense torsion straining was studied here. Gold rod(100mm dia.) deformed by torsion straining was drawn through dies to 25um dia. Samples of pure gold wire were characterized by FIB (Focused Ion Beam), EBSD (Electron Back Scattered Diffractometer), and mechanical properties of samples were measured by tensile tester. The effect of grain size, mechanical properties and strain rate was also investigated, compared with non-torsion process. The torsion process of gold rod increased considerably mechanical properties, and It also were examined and discussed that substantial grain refinement, texture evolved from initial (100) fiber to (111) fiber in the center part especially, an large amount of low angle grain boundary.

Mechanical Behavior, Microstructure, and Modeling of Ti and Its Alloys: Processing: Design, Control and Optimization

Sponsored by: The Minerals, Metals and Materials Society, TMS Structural Materials Division, TMS: Titanium Committee
Program Organizers: Ellen Cerreta, Los Alamos National Laboratory; Vasisht Venkatesh, TIMET; Daniel Evans, US Air Force

Monday AM Room: 384
March 10, 2008 Location: Ernest Morial Convention Center

Session Chair: Vasisht Venkatesh, TIMET

8:30 AM Introductory Comments

8:40 AM Keynote

Models for Mill Processing of Alpha/Beta Titanium Alloys: *S. Semiatin*[1]; Perikles Nicolaou[2]; Ayman Salem[3]; Michael Glavicic[2]; [1]Air Force Research Laboratory; [2]UES, Inc.; [3]Universal Technology Corporation

Models for the mill processing of alpha/beta titanium alloys will be reviewed. Attention will be focused on coarsening, spheroidization, and cavitation during the breakdown of colony microstructures and on texture evolution during plate rolling. The mechanisms and kinetics of the coarsening of lamellar microstructures, which impacts the ease of spheroidization, will be summarized. An approximate diffusion analysis is used to model this coarsening process. Second, models to treat the growth and shrinkage of cavities formed during multi-step hot working sequences involving strain-path changes will be presented. The cavitation phenomena have been interpreted in the context of concurrent dynamic spheroidization. Last, the effect of hot working variables (preheat temperature, reheating/cooling practice) on the evolution of deformation and transformation alpha-phase textures during plate rolling will be discussed. The effect on texture of strain partitioning between the alpha and beta phases during rolling and preferential alpha-variant selection during cooldown will be highlighted.

9:20 AM

Design of High Formable and Strong Titanium Alloys through Plasticity Induced Transformation: *Suresh Neelakantan*[1]; Pedro E.J. Rivera-Díaz-del-Castillo[1]; Sybrand van der Zwaag[1]; [1]Delft University of Technology

Preliminary works show the existence of Plasticity induced Transformation in metastable β-Titanium alloys (PiTTi), similar to TRIP steels. Extensive studies have been carried out to understand the defining parameters of PiTTi effect in β-metastable Ti-10V-2Fe-3Al (wt.%) and β-Cez alloys. Mechanical testing results show that the microstructures, which depend on heat treatment temperature and time, have a significant effect on the PiTTi properties. Optimizing PiTTi effect would aid in achieving improved strength-ductility relation in existing Ti-alloys or new alloy sets. A model was developed to estimate the M_s temperature (a critical optimizing parameter for PiTTi) of Ti-base systems incorporating Fe, Al, V, Nb, Mo, Cr, Zr and Sn. The chemical inhomogeneities in β phase are employed to predict its ability to transform into martensite. The model is based on a modified version of Ghosh and Olson theory for martensite nucleation, [*Acta. Met. Vol. 42, pp. 3361, 1994*].

9:40 AM

Fabrication Method of SCS-6/Ti-6-4 Titanium Alloy Matrix Composite: *Chitoshi Masuda*[1]; [1]Waseda University

The new fabrication method was proposed in order to obtain the homogenous fiber arrangement and the fabrication method and the microstructure and interfacial reaction layer were examined. The bulk composite was foil/sheet/foil method and hot press method at 900°C revealed that the SCS-6 fibers have been arranged homogenously and the fiber spacing was about 100mm. The interfacial reaction layer was also observed and the layer thickness was about 0.6mm and the grain size was about 10 micro-m. On the other hands, the same foil/sheet/foil was consolidated by Spark Plasma Sintering method at various temperatures and the composite were good consolidated from 700 to 900°C. As the interfacial reaction layers were also observed, the layer thickness was thinner than those for hot press method. Tensile strength was examined and the effect of hot press and SPS methods on the tensile strength was discussed.

10:00 AM

Innovative Direct Powder Rolling Process for Producing Titanium and Titanium Alloy Flat Products from Hydrogenated Titanium Powder: *Jane Adams*[1]; Volodymyr Duz[2]; Vladimir Moxson[2]; [1]Army Research Laboratory; [2]ADMA Products Inc

Titanium alloys exhibit attractive mechanical properties, good corrosion resistance and low density, but they are expensive. This paper is related to use of low cost direct powder rolling (DPR) processes to produce titanium and titanium alloy flat products (plates, sheets, foils) from hydrogenated Titanium powder. A blended elemental (BE) approach is used in this study in which hydrogenated titanium powder produced by a modified Kroll process is alloyed with a master alloy to achieve the required chemistry. Direct roll-compacting to form flat products of near final thickness and subsequent vacuum sintering produces near full density Titanium alloys with optimized microstructures and properties equivalent to those of the ingot metallurgy. This article reviews the general DPR process, microstructures, properties and ability to produce the Titanium alloy flat product in a cost-effective manner. Heat treatments performed on sintered alloys demonstrated that it is possible to achieve refined microstructures with the resulting improved combination of mechanical properties.

10:20 AM Break

10:40 AM Invited

Novel Heat-Treatments for the Production of Refined Microstructures in α/β Ti Alloys: Jonathan Orsborn[1]; Peter Collins[1]; Michael Loretto[2]; *Hamish Fraser*[1]; [1]Ohio State University; [2]University of Birmingham

High strength α/β Ti alloys often involve sub-solvus thermo-mechanical processing to effect a duplex, equaixed alpha/transformed beta, microstructure. There are, however, significant advantages to be accrued from effecting such high strengths in alloys with a microstructure consisting either of Widmanstätten alpha plates in either the colony or basketweave forms. The coarseness of the microstructural features and the significant volume fraction of allotriomorphic alpha phase precipitated along prior beta grain boundaries limit the strength that can be achieved in these alloys with these microstructures when conventionally processed, i.e., solution heat-treatment in the beta phase field followed by cooling to room temperature followed by a sub-solvus annealing/aging treatment. This paper describes a new heat-treatment process that produces a refined distribution of Widmanstätten alpha plates with minimal grain boundary alpha phase which results in very high strengths (e.g., yield strengths ~1200MPa) in alloys such as Ti-6-4 and Ti-6-2-2-2-2.

11:10 AM
Interaction between NiTi SMA and Graphite Mold in Unidirectional Solidification Process: *Chonghe Li*[1]; Ming Zhu[1]; Leyou Wang[2]; Xiemin Mao[1]; [1]Shanghai University; [2]General Research Institute for Nonferous Metals Beijing

One unidirectional solidification equipment based on Bridgman method with high temperature gradient was designed, and used to fabricate NiTi single crystal SMA (shape memory alloy) together with a selective growing zigzag-shaped crystallizer and a steady growth container that were made of electro graphite. The results show that this special shape crystallizer can enhance that only one crystal/(or 2-3 grain) survived at the exit of the selective growing crystallizer. Although the carbon dissolves into the melt and reacts with molten Ti to form TiC duo to the long time contact between the liquid melt and graphite container at 1450°C, this TiC particles can not become the nucleus of new grain, thus almost have no influence on the further direction solidification growth of crystal grain at the exit of the selective growing crystallizer.

11:30 AM
Oxygen Diffusion Dramatically Improves Tribological Characteristics for Titanium by Enabling Anti-Wear Surface Boundary Film Formation: *Jun Qu*[1]; Peter Blau[1]; Jane Howe[1]; Larry Walker[1]; [1]Oak Ridge National Laboratory

Titanium alloys have poor wear-resistance and cannot be efficiently lubricated because of their incompatibility with common anti-wear lubricant additives, such as zinc-dialkyl-dithiophosphate (ZDDP). This paper describes a surface engineering process, oxygen diffusion (OD), which has demonstrated great potential for improving the tribological characteristics of titanium by increasing surface hardness (from 3.7 to 12-14 GPa (HK)) and enabling tribochemical tractions with ZDDP to form an anti-wear boundary film. The OD treated Ti-6Al-4V demonstrated a 70% friction reduction and a remarkable six orders of magnitude wear reduction compared to untreated Ti-6Al-4V in an engine oil-lubricated, piston ring-on-flat bench test. The composition of the anti-wear boundary film was analyzed and the mechanisms of the tribochemical tractions between an oxygen-diffused titanium surface and ZDDP are discussed. Relative to more sophisticated surface treatment methods, oxygen diffusion offers much lower cost, few geometric restrictions, and no spallation of the treated layer.

11:50 AM
Processing of Ti Alloys by ECAE: Process Scale-up, FEM Simulation and Experimental Validation: *Shankar Sastry*[1]; Gian Colombo[1]; [1]Washington University

Equal channel angular extrusion (ECAE) is a processing method during which large amounts of plastic strain are induced in a material through simple shear deformation. This is done by forcing the material through a die consisting of two channels of equal cross-sectional area that intersect Current studies on ECAE processing have used billets in the size range of 0.5 inches to 1 inch. Promising results for grain refinement and property improvement for billets of this size have been reported, but these small size billets have limited industrial use. In order for industry to take advantage of the beneficial aspects of ECAE, the billet sizes must be increased for them to be suitable for subsequent working and fabrication of structural components. In the present investigation, the feasibility of scaling up the ECAE process for producing 2.0 in diameter Ti-6Al-4V billets was demonstrated. FEM simulation and experimental results will be presented.

12:10 PM
Viscosity of Slags for High Titanium Ferroalloy by Vacuum Refining: *Lina Jiao*[1]; Ting'an Zhang[1]; Jianming Yao[1]; Jianming Yao[1]; [1]Northeastern University

Viscosity of CaO-Al_2O_3-CaF_2-TiO_2 and CaO-Al2O_3-CaF_2-SiO_2 quaternary system was researched by internal-rotating cylinder method for their use as refining slag to remove oxygen and inclusions in crude high titanium ferroalloy produced by aluminothermy reduction process. It was showed that the viscosity of CaO-Al_2O_3-CaF_2-TiO_2 and CaO-Al_2O_3-CaF_2-SiO_2 system was below 0.4 Pa•S, when the temperature is up to 1520°C and 1495°C, respectively. Viscosity of the two systems both decreased with the increasing content CaF_2 content at a constant basicity. XRD results has showed that the major phases of molten CaO-Al_2O_3-CaF_2-TiO_2 were 3CaO•Al_2O_3, 12 CaO•7Al_2O_3, $Ca_{12}Al_{14}O_{32}F_2$, $Ca_3(AlO_3)2$ and $CaTiO_3$ and the major phases of the melted slags were $Ca_{12}Al_{14}O_{32}F_2$, Ca_2SiO_4, $Ca_2SiO_2F_2$, $Ca_3Al_2(SiO_4)3$, 5CaO•3Al_2O_3 and $Al_2(SiO_4)O$.

Mechanics and Kinetics of Interfaces in Multi-Component Materials Systems: Mechanics of Adhesion, Friction and Fracture

Sponsored by: The Minerals, Metals and Materials Society, TMS Electronic, Magnetic, and Photonic Materials Division, TMS Structural Materials Division, TMS/ASM: Composite Materials Committee, TMS: Thin Films and Interfaces Committee
Program Organizers: Bhaskar Majumdar, New Mexico Tech; Rishi Raj, University of Colorado, Boulder; Indranath Dutta, US Naval Postgraduate School; Ravindra Nuggehalli, New Jersey Institute of Technology; Darrel Frear, Freescale Semiconductor

Monday AM — Room: 279
March 10, 2008 — Location: Ernest Morial Convention Center

Session Chairs: Indranath Dutta, US Naval Postgraduate School; John Lewandowski, Case Western Reserve University

8:30 AM Keynote
Adhesion of Interfaces in Hierarchical Layered Structures for Emerging Technologies: *Reinhold Dauskardt*[1]; [1]Stanford University

Understanding the mechanics and kinetics of debonding of interfaces in layered structures remains a crucial challenge for the integrity and reliability of layered structures in a wide range of technology areas including microelectronic devices and high-performance metal laminates. The layered structures are frequently engineered over a range of length scales, producing a hierarchical structure with selected compositions and structures at length scales ranging form the atomic to macroscale dimensions. We review understanding of the mechanics and kinetic aspects of adhesion and time dependent delamination in blanket and patterned layered structures representative of some of the above technologies. Particular attention is given to micromechanical characterization of properties under complex loading and chemically active environmental conditions. The effects of interface parameters and thin-film composition and porosity will also be considered including novel strategies to strengthen and toughen nanostructured materials. Implications for device reliability and integration of new materials are considered.

9:10 AM
Adhesion of Rough Curved Surfaces and Applications in Nanotribology: Bing Ye[1]; *Bhaskar Majumdar*[1]; Somuri Prasad[2]; [1]New Mexico Tech; [2]Sandia National Laboratory

Adhesion of surfaces, as influenced by topology and texture, is central to the understanding and manipulation of phenomena at the micron and nanometer length scales, including biological and micro-electro-mechanical systems. Here, we analyze the general adhesion of initially rough curved surfaces and show that the pressure distribution over the region of contact does not contain any singularity, unlike the case of JKR singularity for smooth curved surfaces. Most significantly, we show a simple universal form for the adhesive pull-off load, which decreases with elastic modulus, increases with initial effective curvature, and is nearly inversely proportional to the surface roughness. The results suggest methods by which adhesion/de-adhesion could be actively manipulated, and may actually be exploited by insects and geckos for adhesion and locomotion. Applications of the results in nano-contact and adhesion at interfaces will be presented.

9:35 AM
Sliding at Metal–Ceramic Interfaces at Elevated Temperatures: *Rishi Raj*[1]; [1]University of Colorado

Measurement of sliding viscosity at metal–ceramic interfaces, measured by the periodic cracking method will be presented. Two unexpected results deriving from two systems, copper–silica and aluminum–spinel, are: i) the activation energy for sliding is significantly lower than for grain boundary diffusion in the polycrystalline metals, and ii) the sliding behavior is always linear viscous, that is, the power law creep seen in polycrystals is absent. These results suggest that dislocation creep may not play a significant role in accommodating sliding at such interfaces. Possible reasons for this interpretation will be discussed.

10:00 AM Break

10:15 AM Invited
On the Role of Interfacial Layers and Shear Accommodation in the Frictional Behavior of Solid Lubricants: *Somuri Prasad*[1]; Thomas Scharf[2]; [1]Sandia National Laboratories; [2]University of North Texas

Friction coefficient is generally regarded as independent of applied load, as predicted by Amontons' law of friction. However, in many instances involving contact with polymeric materials, or whenever a liquid or solid lubricating film is used to mitigate friction, load dependency on the coefficient of friction (COF) has been observed. For the case where the contact is purely elastic, the data fit the general trend that the COF is proportional to the inverse of the mean Hertzian contact stress, COF = $(S_o/P)+\alpha$, where S_o is the interfacial shear strength of the lubricating layer separating the surfaces. Numerous examples from literature involving lamellar solids (e.g., graphite, MoS_2, WS_2), diamond and diamond-like carbon, and polymers (e.g., PTFE) that exhibit non-Amontonian friction behavior are analyzed. The role of environmental reactions and tribochemistry influencing shear accommodation of friction-induced interfacial layers will be presented with examples from our recent work on diamond-like nanocomposite coatings.

10:45 AM Invited
Interface Effects on Fracture and Fatigue of Laminated Aluminum Composites: *John Lewandowski*[1]; H. Hassan[1]; [1]Case Western Reserve University

The effects of interface changes on the fracture and fatigue behavior of Laminated Aluminum Composites will be presented. Laminates were prepared via diffusion bonding or adhesive bonding with various aluminum alloys and DRA composites to systematically vary the interfacial strength. These laminated aluminum composites were tested in the crack divider and crack arrestor orientations under both quasi-static and fatigue crack growth conditions. The significant effects of changes in interfacial character and layer thickness on the toughness and fatigue crack growth behavior of these systems will be demonstrated and compared to non-laminated materials of similar chemistry.

11:15 AM Invited
Grain Boundary Fracture Initiation Parameter for Creep of a Co Based Superalloy: *Thomas Bieler*[1]; Sara Longanbach[1]; Carl Boehlert[1]; [1]Michigan State University

Surface deformation of grain boundary engineered Udimet alloy 188 was examined in a scanning electron microscope during in-situ creep at 760°C and 220MPa. Grain boundary cracking was followed using surface imaging and EBSD mapping. Careful observation was needed to distinguish cracks from ledges that developed from grain boundary sliding. EBSD pattern quality (image quality) maps were inadequate to positively identify crack locations. Cracking occurred preferentially along general high-angle grain boundaries and less than 15% of the cracks were found on low angle grain boundaries and coincident site lattice boundaries. A fracture initiation parameter analysis was performed to identify the role of slip system interactions at the grain boundaries and their impact on crack nucleation. This analysis was successful in separating the population of intact random grain boundaries from cracked random grain boundaries at lower levels of strain, but not after crack coalescence dominated the grain boundary fracture process.

Micro-Engineered Particulate-Based Materials: Session I

Sponsored by: The Minerals, Metals and Materials Society, TMS Materials Processing and Manufacturing Division, TMS: Powder Materials Committee
Program Organizers: Khaled Morsi, San Diego State University; Iver Anderson, Iowa State University

Monday AM Room: 271
March 10, 2008 Location: Ernest Morial Convention Center

Session Chairs: Iver Anderson, Iowa State University; Khaled Morsi, San Diego State University

8:30 AM
Phase Transformations in Reactive Gas Atomized Stainless Steel Powders That Promote an Oxide Dispersion Strengthened Microstructure: *Joel Rieken*[1]; Iver Anderson[2]; M. Kramer[2]; D. Shechtman[1]; M. Besser[2]; [1]Iowa State University; [2]Ames Laboratory

A novel processing technique employing gas atomization reaction synthesis (GARS) has been used to produce stainless steel powders that are encapsulated with a thin chromium oxide shell. This paper will investigate the reactions involved with transformation from as-atomized Fe-(12.5-15.0)Cr-(0.3-1.0)Y powders (wt.%) to a consolidated isotropic oxide dispersion strengthened microstructure. A series of heat treatment studies were conducted in an effort to understand and control the oxygen exchange reaction occurring between chromium oxide and yttrium at elevated temperatures. Scanning electron microscopy and transmission electron microscopy were used to evaluate post heat treatment microstructures. Phase transformations associated with volume fraction changes were tracked using x-ray diffraction analysis. Initial high temperature tensile strength analysis was performed to assess the effectiveness of the resulting heat treatment procedure. Support from the DOE-FE (ARM program) through Ames Laboratory contract no. DE-AC02-07CH11358 is gratefully acknowledged.

8:55 AM
Tailored Oxide Films on Precursor Powders for Isotropic ODS Ferritic Stainless Steels: *Iver Anderson*[1]; Joel Rieken[1]; [1]Iowa State University

Innovation is needed to exploit the benefits of a new type of precursor alloy powder for simplified processing of oxide dispersion strengthened (ODS) stainless steels. While the heat treatment of consolidated forms of such Fe-Cr-Y powder is under extensive study, the options for liquid state, mushy state, or solid state oxidation processes also are being explored to tune the starting balance of Cr and Y oxides associated with the powders. Because of the competition for oxidation between Cr and Y that is designed into the Fe-Cr-Y system, detailed characterization by SEM, XPS, and AES is needed to understand the oxide phase development on the powders. This is critical to the quest for an ideal state where the ODS microstructure consists only of nano-metric dispersoids without remnants of the oxide supply phase due to a completed exchange reaction. Supported by USDOE-FE-ARM Program through Ames Laboratory contract no. DE-AC02-07CH11358.

9:20 AM
Analytical Electron Microscopy of Mechanically Alloyed 12YWT and 14YWT Nano-Structured Ferritic Alloys for Structure-Property-Processing Correlations: *James Bentley*[1]; David Hoelzer[1]; Larry Walker[1]; [1]Oak Ridge National Laboratory

The contributions of analytical (transmission) electron microscopy (AEM) to understanding structure-property-processing correlations in nano-structured ferritic alloys that include prototypical 12YWT (12%Cr) and ORNL-developed 14YWT (Fe-14.2%Cr-1.95%W-0.22%Ti-0.25%Y_2O_3) will be described. Beyond conventional AEM methods (e.g. for grain-size measurements and x-ray microanalysis of second-phase particles), energy-filtered transmission electron microscopy (EFTEM) methods have been emphasized for reliably revealing the oxide nano-clusters (typically with diameters less than 4 nm and concentrations exceeding 10^{23} m^{-3}) that are responsible for the exceptional mechanical properties of these materials. Material processing steps include mechanical alloying of base-alloy and yttria powders followed by extrusion. Supplemented by electron

probe microanalysis (EPMA) measurements, correlations of AEM results with ball-milling parameters and extrusion temperatures identified undesirable processing conditions and aided the selection of more optimum protocols. AEM characterization of tensile- and creep-tested specimens allowed an assessment of the nano-cluster contribution to yield strength and revealed the remarkable high-temperature stability of the nanoclusters.

9:45 AM
Characterization of Al-TiC Composites Produced via Mechanical Alloying: *Elif Can Özgün*[1]; Mustafa Lütfi Öveçoglu[1]; [1]Istanbul Technical University

The microstuctural and mechanical evolution of TiC reinforced aluminium metal matrix composites in three different weight fractions were investigated. The TiC particles were dispersed in aluminium matrix using powder metallurgy technique via mechanical alloying (MA) using five different MA times for every weight fraction. The powders were consolidated and sintered under argon atmosphere. Both mechanical alloyed powders and sintered samples were characterized using optical microscope, XRD, SEM with EDS unit, BET and hardness tests. After sintering at 630°C, needle like intermetallic phases were observed.

10:10 AM Break

10:30 AM
In Situ Aluminum Based Nanocomposites Produced by Friction Stir Processing: *I. S. Lee*[1]; S. H. Lee[1]; C. F. Chen[1]; P. W. Kao[1]; [1]National Sun Yat-Sen University

In this study, friction stir processing (FSP) is applied to produce aluminum based nanocomposites from powder mixtures of Al-10at%Fe and Al-2mol%Fe_2O_3. Billet of powder mixtures was prepared by the use of conventional press and sinter route. It was then subjected to multiple passages of FSP. This technique has combined the hot working nature of FSP and the exothermic reaction between Al and Fe or Al and Fe_2O_3. The composites produced were fully dense with high strength. Transmission electron microscopy (TEM) showed that the second phase particles (~100 nm in size) were distributed uniformly, and the grain size of aluminum matrix was ~1 µm. The particles were identified as $Al_{13}Fe_4$ in Al-Fe, and $Al_{13}Fe_4$ and Al_2O_3 in Al-Fe_2O_3. The fine structure of these composites can be attributed to the severe deformation in FSP. The mechanical properties of these nanocomposites were evaluated by using microhardness, tensile and compressive tests.

10:55 AM
Research of Electrodeposited RE-Ni-Fe-P-PTFE Composite Coating: *Jinhui Li*[1]; Xinhai Li[1]; [1]Central South University

Composite coating is a very important part in new materials because it has special excellent physical and chemical properties. PTFE(ploye traflur ethylen) is a special particle with some excellent propertities. Experiment of electrodeposited RE-Ni-Fe-P-PTFE composite coating is proceeded and the effect of surfactant, PTFE, and the ion of rare earth on the coating's content of PTFE were researched. The results shows that the optimum process parameters are that the conc. of rare earth La is 3g/L, the conc. of PTFE solution is 50ml/L, temperature is 55°C, current density is 10 ampere per square decimeter. And that the coefficient of friction of the coating is decreased, and the lubricating property is improved.

11:20 AM
Properties of Silver-Doped Titania Antibacterial Powder Coating with Alumina: *Wei Shunwen*[1]; [1]Centeral South University

The life of silver doping antibacterial powder was related to the release rate of silver ion from powder in water. In order to improve the life of silver-doped titania antibacterial material, the composite antibacterial powder was prepared by coating silver-doped titania core with a layer of alumina. Analysis results shown that the shape of particle was spherical with a diameter of about 200-600nm, and the coating γ-Al_2O_3 film was observed at the surface of the silver-doped titania particle and the thickness of the alumina shell was approximately 30-40nm. The Ag+ release rate of the composite powder was decreased with increasing annealed temperature. A direct deposition of alumina onto the surface of silver-doping titania particles was proved to control the release of silver ion effectively, it suggested that coating process was help to lengthen the life of the materials.

Minerals, Metals and Materials under Pressure: New Experimental and Theoretical Techniques in High-Pressure Materials Science

Sponsored by: The Minerals, Metals and Materials Society, TMS Structural Materials Division, TMS: Chemistry and Physics of Materials Committee
Program Organizers: Richard Hennig, Cornell University; Dallas Trinkle, University of Illinois; Ellen Cerreta, Los Alamos National Laboratory

Monday AM — Room: 385
March 10, 2008 — Location: Ernest Morial Convention Center

Session Chairs: Ellen Cerreta, Los Alamos National Laboratory; Eric Brown, Los Alamos National Laboratory

8:30 AM Introductory Comments

8:35 AM Invited
Atomistic and Mesoscale Modeling of the Response of Molecular Crystals to Dynamical Loading: *Alejandro Strachan*[1]; [1]Purdue University

We use large scale molecular dynamics (MD) with an accurate, first principles-based interatomic potential to characterize the atomic level mechanisms that govern inelastic deformation of the molecular crystal α-HMX under dynamical loading along the [100] direction. We find that for weak shocks plastic deformation is governed by dislocations with Burgers vector b= and b= . As the shock strength is increased we observe a gradual transformation to a regime governed by shear bands characterized individual molecular events that cluster in thick bands and do not show a well defined crystallographic slip. I will also describe a new approach for coarse-grain simulations that leads to a thermodynamically accurate description of materials. The new method, denoted dynamics with implicit degrees of freedom (DID), shows excellent agreement with all-atom MD simulations when parameterized with using classical statistics but also enables the incorporation of quantum thermal effects that are critical in molecular materials.

9:05 AM
High Rate Plasticity under Pressure Using an Oblique-Impact Isentropic-Compression Experiment: *Jeffrey Florando*[1]; David Lassila[1]; Grant Bazan[1]; Tong Jiao[2]; Stephen Grunschel[2]; Rodney Clifton[2]; [1]Lawrence Livermore National Laboratory; [2]Brown University

An experimental technique has been developed to study the strength of materials under conditions of moderate pressures and high strain rates. The technique is similar to the traditional pressure-shear experiments except that window interferometry is used to measure both the normal and transverse particle velocities at the sample-window interface. Additionally, the sample is impacted with a graded density impactor, which imposes a near isentropic compression ramp wave and controls the strain rate to between 10^4–10^6. Both simulation and experimental results on copper samples with a sapphire window will be presented to show the utility of the technique to measure the strength properties under dynamic loading conditions.

9:25 AM Break

9:40 AM Invited
Quantum-Based Atomistic Simulation of Metals at Extreme Conditions: *John Moriarty*[1]; [1]Lawrence Livermore National Laboratory

First-principles generalized pseudopotential theory (GPT) provides a fundamental basis for bridging the quantum-atomistic gap from density-functional quantum mechanics to large scale atomistic simulation in metals and alloys. In directionally-bonded bcc transition metals, advanced generation *model* GPT or MGPT potentials based on canonical *d* bands have been developed for Ta, Mo and V and successfully applied to a wide range of thermodynamic and mechanical properties at both ambient and extreme conditions of pressure and temperature, including multiphase equation of state; phase transitions, melting and solidification; thermoelasticity; and the atomistic simulation of point defects, dislocations and grain boundaries needed for the multiscale modeling of plasticity and strength. Recent algorithm improvements have also allowed an MGPT implementation beyond canonical bands to achieve increased accuracy,

extension to *f*-electron actinide metals, and high computational speed. A further advance in progress is the development of temperature-dependent MGPT potentials that subsume important electron-thermal contributions to high-temperature properties. This work was performed under the auspices of the U.S. Department of Energy by the University of California Lawrence Livermore National Laboratory under contract No. W-7405-Eng-48.

10:10 AM
First-Principles Phonon Approach to the Equation-of-States of Al, Cu, Ta, Pt, and Au: *Yi Wang*[1]; Zi-Kui Liu[1]; Long-Qing Chen[1]; [1]Pennsylvania State University

The main objective of this work is to make the equation-of-state standard for the diamond-anvil-cell experiment. Calculated 300-K isotherms and Hugoniots at pressures up to shock-wave melting points for the five reference metals Al, Cu, Ta, Pt, and Au are reported using the first-principles phonon approach. With these data, shock-reduced 300 K isotherms are derived for these metals by subtracting the calculated thermal volume expansion from the experimental shock-wave data.

10:30 AM Break

10:45 AM
Acoustic Properties of Fluoropolymers at High Pressure: *Dana Dattelbaum*[1]; Muhtar Ahart[2]; Russell Hemley[2]; [1]Los Alamos National Laboratory; [2]Geophysical Laboratory

Fluoropolymers are a class of polymers that are used extensively in engineering applications because of their favorable properties that include chemical inertness, thermal stability, low coefficients of friction, and high densities. For the first time, the acoustic properties of a series of semi-crystalline fluoropolymers have been measured from ambient pressure to >12 GPa using Brillouin spectroscopy. From the measured acoustic properties, elastic constants, moduli, and Poisson's ratios were calculated as a function of pressure. P-V isotherms were also constructed, and fit to a range of empirical/semi-empirical isothermal equation-of-state (EOS) forms. From this analysis, the isothermal bulk modulus and its pressure derivative were obtained for the polymers interrogated, and the static results were compared to available shock wave compression data. The Brillouin data also show sensitivity to crystalline phase transitions and non-linear compressibility at low pressures.

11:05 AM
Plasticity, Spall Damage and Microstructure Interactions in Shock Loaded Copper Multicrystals: *Pedro Peralta*[1]; Shima Hashemian[1]; Stephan DiGiacomo[1]; Heber D'Armas[2]; Shengnian Luo[3]; Eric Loomis[3]; Dennis Paisley[3]; Robert Dickerson[3]; Darrin Byler[3]; Ken McClellan[3]; [1]Arizona State University; [2]Universidad Simon Bolivar; [3]Los Alamos National Laboratory

Correlations among plasticity, damage and local microstructure were investigated in copper via impact tests conducted with laser-driven plates at low pressures (3-6 GPa). The copper samples had a large grain size as compared to the thickness, which was either 200 or 1000 μm, to isolate the effects of microstructure on the local response. Velocity interferometry was used to measure the bulk response of the free-surface velocity of the samples to monitor traditional spall tensile failure. Electron Backscattering Diffraction (EBSD) was used to relate crystallography to plasticity and to the presence of porosity around defects. A transition between transgranular and intergranular damage was observed as the grain sized was reduced from 230 μm to 150 μm in thin samples, whereas both modes were observed in thick specimens (450 μm grain size). Potential sites for preferred damage nucleation were identified in terms of their crystallography via statistical sampling in serial sectioned specimens.

Neutron and X-Ray Studies for Probing Materials Behavior: Resolving Local Structure

Sponsored by: National Science Foundation, The Minerals, Metals and Materials Society, TMS Structural Materials Division, TMS: Advanced Characterization, Testing, and Simulation Committee
Program Organizers: Rozaliya Barabash, Oak Ridge National Laboratory; Yandong Wang, Northeastern University; Peter K. Liaw, University of Tennessee

Monday AM — Room: 391
March 10, 2008 — Location: Ernest Morial Convention Center

Session Chairs: Rozaliya Barabash, Oak Ridge National Laboratory; Judy Pang, Oak Ridge National Laboratory

8:30 AM Keynote
Spatially-Resolved Polychromatic Neutron and X-Ray Microdiffraction: *Gene Ice*[1]; [1]Oak Ridge National Laboratory

Polychromatic microdiffraction is an emerging materials-characterization tool made practical by powerful x-ray and neutron sources, and by advanced optics and software. With polychromatic techniques, local crystalline properties including phase, texture (orientation), elastic strain and defect density can be mapped with good spatial resolution in 3 dimensions. The evolving ability to nondestructively map local crystal structure in three dimensions, addresses long-standing issues of inhomogeneous grain-growth, deformation, fracture, and elastic strain. Applications impact virtually all materials including electronic, solar, and LED materials, nanomaterials, structural materials and joining materials In addition the ability to focus small beams on small samples dramatically increases signal-to-noise and greatly reduces the cost of extreme environmental chambers required for high-pressure, high temperature, high magnetic field or corrosive environments. These techniques efficiently use source brilliance and minimize the required sample volume, which is essential for hard-to-make materials, irreplaceable materials, and for radioactive, toxic or otherwise dangerous materials.

9:05 AM Invited
Structural Characterization by Three Dimensional X-Ray Diffraction Microscopy: *Wenjun Liu*[1]; Gene Ice[2]; Bennett Larson[2]; Jonathan Tischler[2]; Paul Zschack[1]; [1]Argonne National Laboratory; [2]Oak Ridge National Laboratory

The principle research activities in the beamline 34-ID-E at the Advanced Photon Source involve development of exciting new micro/nano-diffraction techniques for characterization and microscopy in support of material sciences and condensed matter physics. With high-brilliance, third generation synchrotron X-ray source, advanced focusing mirrors, and the newly developed depth profiling techniques, spatially resolved diffraction measurements can be made in all three dimensions with submicron resolution. Properties that can be measured include local crystallographic orientations, orientation gradients and strains. This capability enables detailed studies of fundamental deformation processes, basic grain-growth behavior, and meoscale structures. The performance of the beamline facility and future development plan are discussed.

9:30 AM
X-Ray Microbeam Probing the Inhomogeneous GNDs Distribution near the Boundary of a Ni Bicrystal: *Rozaliya Barabash*[1]; J. Pang[1]; G. Ice[1]; Tetsuya Ohashi[2]; [1]Oak Ridge National Laboratory; [2]Kitami Institute of Technology

In this study we report on inhomogeneous plastic deformation in a natural Ni bicrystal after uniaxial pulling. A focused, polychromatic synchrotron X-ray microbeam together with orientation imaging microscopy, scanning electron microscopy, and finite element simulations were used to characterize the physics of geometrically necessary dislocation formation and their collective behavior during plastic deformation. The local crystallographic orientation of subgrain volumes were characterized to determined the plastic response during deformation. Finite element simulations were used to understand the influence of grain orientation and the initial structural inhomogeneities on the evolution of geometrically necessary dislocations arrangement and distribution. Strain in both grains increases in the vicinity of the coherent boundary.

9:50 AM Invited

Studying Complex Materials Using Submicron-Resolution Laue X-Ray Microdiffraction: *John Budai*[1]; W. Liu[2]; J.Z. Tischler[1]; D.D. Sarma[3]; G. Shenoy[2]; B.C. Larson[1]; G.E. Ice[1]; S.-W. Cheong[4]; [1]Oak Ridge National Laboratory; [2]Argonne National Laboratory; [3]Indian Institute of Science; [4]Rutgers University

We have developed a polychromatic, scanning synchrotron microbeam capability with 3D submicron spatial resolution. White-beam Laue diffraction patterns are analyzed with automated software, yielding real-space maps of the local crystal structure, lattice orientation, and strain tensor. Polychromatic scanning x-ray microdiffraction has been used to investigate a variety of complex materials, and this talk will illustrate with examples from 1D, 2D and 3D systems. 1D nanostructures mounted on TEM grids make convenient samples, and we have mapped the crystal perfection along individual 200nm ZnO nanorods. In 2D studies of thin films, microdiffraction studies revealed atomic-level mechanisms for local crystallographic tilting in epitaxial oxide buffer layers for superconducting applications. In 3D, structural investigations have included nondestructive studies of thermal grain growth in polycrystalline aluminum and local eutectic phase separation in complex manganite crystals. Support by DOE-BES, DMS&E at ORNL; UT-Battelle; UNI-XOR by ORNL and APS by DOE-BES.

10:15 AM Break

10:20 AM Invited

A Synchrotron X-Ray Diffraction Method for Measuring the Micromechanical Response of Multiphase Alloys: *Matthew Miller*[1]; Jun Park[1]; Alexander Kazimirov[1]; Martin Mataya[2]; [1]Cornell University; [2]Colorado School of Mines

Diffraction is a powerful tool for understanding deformation partitioning with a multiphase alloy. This talk describes a powder diffraction method developed to measure lattice strain pole figures during in-situ loading. The pole figures are used to calculate the distribution of crystal stresses over orientation space. The inversion method for reduction of the pole figure data is motivated by quantitative texture analysis. Issues that are particular to multiphase experiments include peak overlap and detection of extreme ranges of x-ray intensity. Results from experiments conducted at the Cornell High Energy Synchrotron Source (CHESS) on a number of alloys including iron/copper, aluminum/beryllium and titanium are presented.

10:45 AM Invited

In-Situ Observations of Subgrain Dynamics by High Energy X-Ray Diffraction: *Wolfgang Pantleon*[1]; Christian Wejdemann[1]; Ulrich Lienert[2]; Bo Jakobsen[1]; Henning Poulsen[1]; [1]Risoe National Laboratory; [2]APS Argonne National Laboratory

By means of high angular resolution three-dimensional X-ray diffraction, individual subgrains can be identified within a single grain in the bulk of a polycrystalline, macroscopic specimen. Each broadened Bragg reflection constitutes of individual sharp peaks superimposed on a broad cloud of enhanced intensity. The sharpness of the peaks in all directions of reciprocal space and their integrated intensity allows their identification with almost dislocation-free subgrains. In this manner, the evolution of the dislocation structure can be monitored during in-situ loading: Intermittent subgrain dynamics is observed during in-situ tension with individual subgrains emerging and disappearing in the course of deformation, indicating a rather volatile dislocation structure. On the other hand, no significant changes are observed in the subgrain structure during stress relaxation or unloading; the individual subgrains survive, but redistribute their internal stresses. During strain path changes, dissolution and re-building of the entire subgrain structure is observed.

11:10 AM Invited

X-Ray Imaging of Phonon Interaction with Dislocations: *Emil Zolotoyabko*[1]; [1]Technion-Israel Institute of Technology

Unique characteristics of synchrotron radiation are used for ultra-fast time-resolved measurements of structural dynamics in crystals. For example, by exploiting the pulsed structure of synchrotron radiation combined with the stroboscopic mode of data acquisition, the periodic processes with frequencies up to a few GHz can be probed with temporal resolution down to 50 ps. By using this technique we studied high-frequency dislocation dynamics in brittle crystals induced by interaction with acoustic waves (phonons). Stroboscopic topographs taken from acoustically excited $LiNbO_3$ crystals exhibited well-resolved individual acoustic wave fronts as well as their distortions due to dynamic deformation fields related to vibrating dislocation segments. The dislocation dynamics is characterized by very high velocities (in significant parts of the speed of Rayleigh waves) and extremely low viscosity coefficients, 2-3 orders of magnitude lower than measured in ductile materials. Such low viscosity in dislocation motion can be hardly probed by the established characterization techniques.

11:35 AM Invited

Local Dislocation Properties and Diffraction Methods: *Patrick Veyssiere*[1]; [1]LEM, Centre National de la Recherche Scientifique-ONERA

The aim of this contribution is chiefly to review transmission electron microcopy (TEM) methods used to establish local dislocation properties and their relation with the plastic behaviour of materials. Several TEM operation modes are reviewed with their potential and limitations critically assessed. Special emphasis is placed on the so-called weak beam method whose unique capability to provide information not only on the core of dislocations but also on the organization of these, are demonstrated from studies on metallic systems. It will be shown that weak-beam observations can help uncover local dislcoation mechanisms controlling plasticity. An attempt will be made to place TEM, X-ray (or neutrons) into perspective will be made.

12:00 PM

Slip System - Dependent Calculations of Dislocation Density and Dislocation-Wall Spacing from In-Situ Neutron Measurements: *E-Wen Huang*[1]; Rozaliya Barabash[2]; Bjørn Clausen[3]; Yandong Wang[4]; Yang Ren[5]; Peter Liaw[1]; Hahn Choo[1]; [1]University of Tennessee; [2]Oak Ridge National Laboratory; [3]Los Alamos National Laboratory; [4]Northeastern University; [5]Argonne National Laboratory

Monotonic-tensile experiments were conducted to observe diffraction-profile evolutions at room temperature. The pseudo-Voigt function had been applied to distinguish the diffractions from Gaussian to Lorentzian distributions. The randomly-distributed dislocations and non-uniform dislocation walls diffracted neutrons in Gaussian and Lorentzian distributions, respectively. The calculations of the distributions accompanying with the contrast factor determine the dislocation density and the dislocation-wall spacing as a function of the strains. As a result, the slip system -dependent calculated dislocation density and dislocation-wall spacing of the annealed HASTELLOY® C-22HSTM nickel-based superalloy were examined by the in-situ neutron-diffraction experiment. The stress evolutions as a function of strains are compared with the evolution of the dislocation density and the dislocation walls spacing in light of the activation from different slip systems during the monotonic-tension experiments.

12:15 PM

Neutron and X-Ray Microbeam Diffraction Studies around a Fatigue Crack after Overload: *Sooyeol Lee*[1]; Rozaliya Barabash[2]; Jin-Seok Chung[3]; Yinan Sun[1]; Hahn Choo[1]; Peter Liaw[1]; Donald Brown[4]; Gene Ice[2]; [1]University of Tennessee; [2]Oak Ridge National Laboratory; [3]Soongsil University; [4]Los Alamos National Laboratory

Fatigue-crack-growth experiments were performed on a compact-tension specimen of a Type 316 LN austenitic stainless steel. A single overload was applied during fatigue tests and a retardation period was observed, showing a temporary decrease in crack growth rates. Neutron diffraction and X-ray microdiffraction techniques were used to study crack-tip deformation behaviors in millimeter and submicrometer spatial resolutions, respectively. From neutron diffraction, elastic lattice strain profiles and dislocation densities were measured as a function of the distance from crack tip. Futhermore, Laue diffraction patterns obtained from polychromatic X-ray microdiffraction at different locations near the crack tip showed alternating regions with high and low dislocation densities. Authors acknowledge the financial supports from the National Science Foundation, the International Materials Institutes Program (DMR-0231320). The research is sponsored in part by the Division of Materials Sciences and Engineering Office of Basic Energy Sciences, U.S. Department of Energy, under Contract DE-AC05-00OR22725 with UT-Battelle, LLC.

Particle Beam-Induced Radiation Effects in Materials: Metals I

Sponsored by: The Minerals, Metals and Materials Society, American Nuclear Society, TMS Structural Materials Division, TMS/ASM: Nuclear Materials Committee
Program Organizers: Gary Was, University of Michigan; Stuart Maloy, Los Alamos National Laboratory; Christina Trautmann, Gesellschaft fur Schwerionenforschung; Maximo Victoria, Lawrence Livermore National Laboratory

Monday AM Room: 389
March 10, 2008 Location: Ernest Morial Convention Center

Session Chairs: David Jenkins, CSIRO; Stuart Maloy, Los Alamos National Laboratory

8:30 AM
Materials Research at the Paul Scherrer Institute for Developing High Power Spallation Targets: Yong Dai[1]; Friedrich Groeschel[1]; *Werner Wagner*[1]; [1]Paul Scherrer Institut

For the R&D of high power spallation targets, one of key issues is the understanding of behaviors of structural materials in severe irradiation environments in spallation targets. At PSI, several experiments have been conducted in the targets of the Swiss spallation source (SINQ) for studying radiation damage effects induced by high energy protons and spallation neutrons. Meanwhile, experiments have been performed to investigate liquid lead-bismuth (LBE) corrosion and embrittlement effects on the T91 steel under irradiation of 72 MeV protons. In this presentation, an overview will be given to show the main outcome of these experiments and the inspection of spent SINQ targets as well, which will cover the mechanical properties and microstructure of structural materials such as T91, SS316L, Zircaloy-2, and $AlMg_3$ irradiated to doses ever obtained from irradiations in spallation environment, and the behaviors of T91 irradiated with 72 MeV protons in contact with flowing LBE.

9:10 AM
Novel Characterization Methods for Ti-6Al-4V Implanted with High Energy Ions: *Kale Stephenson*[1]; Kip Findley[1]; Michael Carroll[1]; Vaithiyalingam Shutthanandan[2]; [1]Washington State University; [2]Environmental Molecular Sciences Laboratory; Pacific Northwest National Laboratory

Titanium alloys are valuable in structural and biomedical applications because of their high strength-to-weight ratio and biocompatability. With the demand for titanium alloys in these critical areas, it is important to develop surface treatments that can improve fatigue, wear, and corrosion resistance. Ti-6Al-4V was implanted with nitrogen, gold, and aluminum ions with energies of 1-5 MeV. Nanoindentation experiments were conducted to determine the surface hardness and modulus gradient for each of the implantation conditions; additionally, electron backscatter diffraction (EBSD) was used to assess the extent of lattice damage as a function of distance from the implanted surface in each condition. These results were correlated to Rutherford Backscatter Spectrometry measurements of the implantation depths and TRIM calculations of ion projected ranges and displacement events. The specimens implanted with aluminum ions were heat treated to determine if Ti-Al intermetallics could be produced with the experimental dose rates and their subsequent surface hardness.

9:30 AM
A Description of Stress Driven Bubble Growth and Gas Release of Helium Implanted Tungsten: *Shahram Sharafat*[1]; Akiyuki Takahashi[2]; Koji Nagasawa[2]; Nasr Ghoniem[1]; [1]University of California Los Angeles; [2]Tokyo University of Science

Low energy (< 100 keV) helium implantation of tungsten has been shown to result in the formation of unusual surface pore morphologies, following annealing over a large temperature range. We developed and employed a space-dependent Kinetic Rate Theory code to model spatial distributions of defect concentrations as well as stable helium-bubble nuclei and a Kinetic Monte Carlo simulation code to model helium bubble migration and coalescence. In this work, we describe bubble growth and gas release during annealing of implanted helium including the influence of stress fields. First, the spatial profile of stable bubble nuclei and defect concentrations are calculated. Next, effects of matrix strain caused by pressurized bubbles are included. The influence of near-surface stress fields on bubble migration is also modeled. Surface pore densities and size distributions are compared with experimental results and the role of stress fields on bubble and surface-pore evolution is compared with stress-free simulations.

9:50 AM
High Temperature Surface Effects of He+ Implantation in ICF Fusion First Wall Materials: *Samuel Zenobia*[1]; Gerald Kulcinski[1]; [1]University of Wisconsin, Madison

The first wall armor of Inertial Confinement Fusion (ICF) reactor chambers must withstand high temperatures and significant radiation damage from ICF target debris and neutrons. The resilience of multiple materials to one component of the target debris has been investigated using energetic (20-40 keV) helium ions generated in the UW Inertial Electrostatic Confinement (IEC) device. Studied materials include: single-crystalline, polycrystalline, and powder metallurgy prepared tungsten, tungsten coated TaC and HfC "foams," tungsten-rhenium alloy, CVD SiC, carbon-carbon velvet (CCV), and tungsten coated CCV. Steady-state irradiation temperatures ranged from 750–1250°C with helium fluences between $5x10^{17}$–$1x10^{20}$ He^+/cm^2. The crystalline, rhenium alloyed, carbide foam, and powder metallurgical tungsten specimens each experienced pore formation after irradiation. Flaking and pore formation occurred on CVD SiC samples after He+ implantation. Individual fibers of CCV specimens sustained erosion and corrugation, in addition to roughening and rupturing of tungsten coatings after He+ implantation.

10:10 AM Break

10:30 AM
Displacement Rate Effects in Nucleation Processes: *Kenneth Russell*[1]; [1]Massachusetts Institute of Technology

Nucleation in solids depends crucially on the concentrations and mobilities of point defects, in particular vacancies, self-interstitials, and impurity interstitials. These defects provide solute mobility and may also act as nucleus components. Changes in displacement rate give changes in defect concentrations that are reflected in the kinetics of nucleation. This paper analyzes the effects of displacement rate on the nucleation rates of the voids that give rise to swelling and the Cu-rich precipitates that contribute to pressure vessel embrittlement. The resulting equations are intended to be of use in designing radiation resistant materials.

10:50 AM
Amorphization at Grain Boundaries in Zr-Ti-Ni-Cu Alloys by 300 MeV Kr Ions: *Gerhard Schumacher*[1]; Stefan Mechler[2]; Siegfried Klaumünzer[1]; Nelia Wanderka[1]; Michael Macht[1]; Christian Abromeit[1]; [1]Hahn-Meitner-Institut Berlin; [2]Harvard University

Structural changes in quasicrystalline Zr64.5Ti11.4Ni13.8Cu10.3 alloy (V4-0) during room temperature irradiation with 300 MeV Kr ions were studied ex-situ by means of XRD and TEM. XRD measurements revealed a continuously decreasing amount of the volume fraction V(qc) of the quasicrystalline phase up to a fluence of about 1•E15 Kr/cm2. Above this fluence V(qc) levelled off approaching a value of about 25% compared to the initial value. TEM investigation showed that the regions near the grain boundaries had transformed to the amorphous state while the cores of the quasicrystals remained stable. The influence of the nuclear and electronic energy loss on amorphization of the highly defective grain boundaries is discussed. The interior of the quasicrystals may serve as nuclei for subsequent crystallization which promotes the stability of the grain interior.

11:10 AM
Enhanced Catalytic Structures by Beam Irradiation: *Claudiu Muntele*[1]; Liviu Popa-Simil[2]; [1]Center for Irradiated Metals-Alabama Agricultural and Mechanical University; [2]LAVM LLC.

The thin layer deposition of catalytic layers offers low porosity, high density and adhesion, while making a fluffy deposition in controlled atmosphere the porosity and surface is becoming good but mechanical properties are weakened. The usage of acompact deposition with beam based treatment using implantation in order to create volume controlled structure by generating wide range of defects-dislocations. The dislocations-voids inside make surface very rough allowing the catalytic process to cover the entire surface and get volume. Tests have been

made for the reactivity modifications of Pa, Pt and Ni thin layers. Relationship between the thickness on silicon wafer support of the catalyst deposition and absorbed micro-dose is traced as function of chemical reactive composition. The experiment shows the capability of the ion beam processing of the catalyst layers to create a more suitable structure for catalytic depositions that to mitigate the high reactivity and good adhesion resulting in an extended life product.

11:30 AM

Swelling Measurements Using an Ion Beam Accelerator and Nanoscale Measurements: *Peter Hosemann*[1]; Stuart Maloy[1]; Richard Greco[1]; [1]Los Alamos National Laboratory

Radiation induced swelling can be a major concern for designing systems operating in a radiation environment. Swelling experiments on materials are in general very time consuming and costly material tests. Accelerator experiments on the other hand in combination with nanoscale techniques such as atomic force microscopy, micro machining, interferometry and nano indentation allow one to perform fast and relatively inexpensive experiments where radiation induced swelling can be studied in great detail. This study shows results of a study where µm scale structures are created in tungsten and tantalum and their size and shape accurately measured before exposing them to irradiation. Next, a He+ beam was used to create the radiation induced swelling. Post analysis of the structures was done using atomic force microscopy. The shape and size change of the structures allows accurate measurement of void swelling and can be compared to swelling from fission reactor irradiations.

Recent Developments in Rare Earth Science and Technology - Acta Materialia Gold Medal Symposium: Session I

Sponsored by: The Minerals, Metals and Materials Society, TMS Electronic, Magnetic, and Photonic Materials Division, TMS: Superconducting and Magnetic Materials Committee

Program Organizers: Vitalij Pecharsky, Iowa State University; Ashutosh Tiwari, University of Utah; James Morris, Oak Ridge National Laboratory

Monday AM — Room: 280
March 10, 2008 — Location: Ernest Morial Convention Center

Session Chairs: Thaddeus Massalski, Carnegie Mellon University; Vitalij Pecharsky, Iowa State University

8:30 AM Opening Remarks: Recognition of *Karl Gschneidner, Jr*, the Acta Materialia Gold Medal Award recipient.

8:45 AM Keynote

The Magnetocaloric Effect, Magnetic Refrigeration and Ductile Intermetallic Compounds: *Karl Gschneidner, Jr*[1]; [1]Iowa State University

The magnetocaloric effect (MCE) is the ability of a magnetic material, particularly near its Curie temperature, to heat up when a magnetic field is applied (magnetization) and to cool when the field is removed (demagnetization). A number of new materials, especially $Gd_5(Si_{1-x}Ge_x)_4$, have outstanding MCE properties, significantly better than the well known standard, Gd metal. The giant MCE effect observed in the $Gd_5(Si_{1-x}Ge_x)_4$ alloys for $x \geq 0.5$ is due to a coupled magnetostructural transformation. The coupled transformation also accounts for several other interesting phenomena – giant magnetoresistance; colossal magnetostriction; spontaneous generation of voltage; unusual training, dynamical and thermal phenomena; acoustic emissions; and a novel glass-like kinetically retarded state. Extension of the work on the MCE has led to the near commercialization of magnetic refrigeration as a viable cooling technology, and to the discovery of ductile RM (R = rare earth, T = transition metal) B2 cesium chloride-type intermetallic compounds.

9:15 AM Invited

Strongly Correlated Electron Phenomena in Filled Skutterudite Compounds: *M. Brian Maple*[1]; [1]University of California, San Diego

The filled skutterudite compounds MT_4X_{12} (M = alkali metal, alkaline earth, lanthanide, actinide; T = Fe, Ru, Os; X = P, As, Sb) display a wide variety of strongly correlated electron phenomena and are candidates for thermoelectric applications. The strongly correlated electron phenomena include conventional BCS superconductivity, unconventional superconductivity, magnetic order, quadrupolar order, valence fluctuation behavior, heavy fermion behavior, non–Fermi liquid behavior, and hybridization gap insulator behavior. When M is a lanthanide or actinide atom, the localized f–states hybridize with the ligand–states of the surrounding pnictogen atoms that form atomic "cages" within which the M atoms reside. The ground states are determined by a delicate interplay between the hybridization of the f– and ligand–states, crystalline electric field splitting of the f–electron energy levels, magnetic and quadrupolar interactions, and electron band structure. Examples of the strongly correlated electron phenomena found in filled skutterudite compounds are reviewed in this talk.

9:45 AM Invited

Progress in Understanding the High Ductility of Rare Earth B2 (CsCl-type) Intermetallics: *Alan Russell*[1]; Karl Gschneidner, Jr[1]; S. Biner[1]; L. Chumbley[1]; Sujing Xie[1]; Andrew Becker[1]; Qian Chen[1]; Andrew Frerichs[1]; Scott Williams[1]; [1]Iowa State University

In recent years, several rare earth intermetallic compounds with the B2 (CsCl-type) structure have been reported to exhibit high tensile ductility and high KIC fracture toughness at room temperature; these materials retain considerable ductility even at 77K. These are noteworthy findings because most intermetallics possess poor room temperature ductility and low fracture toughness unless one or more special "contrivances" are applied (e.g., doping with small additions of interstitial elements, off-stoichiometric compositions, testing in ultra-dry atmospheres, etc.). This presentation will summarize recent findings on rare earth B2 intermetallics' active slip systems; their strain rate sensitivities and yield strength maxima at elevated temperatures; the search for possible twinning and stress-induced phase transformations; ab initio calculations on their defect energies and the anisotropy of dislocation line tension; the potential applications of these materials; and the possibilities that their study may suggest ductilizing strategies for other intermetallic compounds.

10:10 AM

Magnesium Rare Earth B2 Intermetallics: Brittle Behaviors in a Family of Ductility: *James Wollmershauser*[1]; Sean Agnew[1]; [1]University of Virginia

Intermetallics with B2 (CsCl) structure, comprised of a rare earth metal and a late transition metal have recently been shown to be a new family of ductile compounds. The present study was initiated to determine if rare earth metal – magnesium compounds would exhibit a similar effect. However, polycrystalline MgCe and MgNd are revealed to exhibited brittle transgranular cleavage fracture. SEM-based stereology plus electron backscatter diffraction (EBSD), has been used to determine the cleavage plane present. All of the intermetallics presently under investigation are line compounds MgY, MgCe, MgNd, and MgDy possess the B2 structure, verified by x-ray diffraction. It is hoped that by further defining the qualifications for ductility in B2 intermetallics, more complete theories can be realized and their applications can be expanded.

10:20 AM

A Comparative Neutron Diffraction Study of B2 Intermetallics: *James Wollmershauser*[1]; Sean Agnew[1]; [1]University of Virginia

Intermetallic alloys with fully-ordered B2 (CsCl) structures were examined by in-situ neutron diffraction. The alloys under investigation (NiAl, CoZr, AgCe, and CuZn) exhibit a wide range of ductility. It is important to note that, depending upon the operative dislocation slip modes, many materials with the B2 structure fail to satisfy the Taylor criterion requiring 5 independent slip systems and, therefore, should not be ductile. Of the selected alloys, only the brass is known to satisfy the Taylor criterion, and should arguably be the only ductile alloy in the study. Indeed, NiAl is known to exhibit brittle behavior at room temperature. However, CoZr and some rare-earth containing compounds similar to AgCe, have recently been shown to sustain approximately 20% room temperature elongation. The experiments are designed to determine if the internal strain and Bragg peak intensity evolutions of the B2 compounds correlate with distinctions in their propensities to exhibit appreciable ductility.

10:25 AM Break

10:40 AM Invited
X-Ray Magnetic Circular Dichroism (XMCD) for Rare Earth Magnets: Toward Quantitative Analysis: *Bruce Harmon*[1]; [1]Iowa State University

In 1992 and 1993 sum rules for x-ray magnetic circular dichroism (XMCD) were derived, and have since been employed with great benefit for studies involving magnetic materials containing 3d-transition elements. The great utility of these sum rules applied to XMCD spectra stems from their ability to extract element and orbital specific information (spin and orbital magnetic moments) for highly complex alloys and compounds. Unfortunately these sum rules break down when applied to rare earth elements. Since rare earths are often constituents for the best permanent magnets, there is strong motivation to develop XMCD into a quantitative analytical tool for analysis. This talk will focus on the physics of rare earth magnetism and the odyssey of unraveling the intricacies of why the XMCD spectra disobey the sum rules. Emphasis will be on recent examples of first principles electronic structure calculations in concert with precise experiments on rare earth containing magnetic materials.

11:10 AM Invited
Research on 5f Electron Systems: Surprises at the End of the Periodic Table: *Gerard Lander*[1]; [1]European Commission, JRC, Institute for Transuranium Elements

Experiments on the transuranium elements are difficult, time consuming, require special facilities, and deal with material that is actually changing during the experiment. Despite this, new effects can be found in this little explored part of the periodic table that are relevant to some of the important questions in condensed-matter physics. Although the heavier actinide elements show behavior reminiscent of their 4*f* analogs, the lighter actinide elements (U, Np, Pu) are quite different. Recent experiments, mainly involving the application of pressure, have shown how these two different aspects are connected. This talk will make comparisons between the physics of the 4f and 5f systems and will focus mainly on the elements but include also some discussion on the recently discovered 18 K superconductor, $PuCoGa_5$.

11:40 AM Invited
Optimization of Ionic Conductivity in Doped Ceria: *Borje Johansson*[1]; [1]Royal Institute of Technology and Uppsala University

Oxides with the cubic fluorite structure, e.g., ceria (CeO2), are known to be good solid electrolytes when they are doped with cations of lower valence than the host cations. The high ionic conductivity of doped ceria makes it an attractive electrolyte for solid oxide fuel cells, whose prospects as an environmentally friendly power source are very promising. In these electrolytes, the current is carried by oxygen ions that are transported by oxygen vacancies, present to compensate for the lower charge of the dopant cations. Ionic conductivity in ceria is closely related to oxygen-vacancy formation and migration properties. A clear physical picture of the connection between the choice of a dopant and the improvement of ionic conductivity in ceria is still lacking. Here we present a quantum-mechanical first-principles study of the influence of different trivalent impurities on these properties. Our results reveal a remarkable correspondence between vacancy properties at the atomic level and the macroscopic ionic conductivity. The key parameters comprise migration barriers for bulk diffusion and vacancy-dopant interactions, represented by association (binding) energies of vacancy-dopant clusters. The interactions can be divided into repulsive elastic and attractive electronic parts. In the optimal electrolyte, these parts should balance. This finding offers a simple and clear way to narrow the search for superior dopants and combinations of dopants. The ideal dopant should have an effective atomic number between 61 (Pm) and 62 (Sm), and we elaborate that combinations of Nd/Sm and Pr/Gd show enhanced ionic conductivity, as compared with that for each element separately.[1] [1]D. Andersson et al. PNAS | March 7, 2006 | vol. 103 | no. 10 | 3518-3521.

12:10 PM Invited
Electrochemical Single Crystal Growth by Electrolyzing Rare Earth Ion Conducting Solids: *Nobuhito Imanaka*[1]; [1]Osaka University

In general, for the single crystal growth, the starting materials should be heated above the melting temperature of the target compounds by the conventional procedures such as Czochralski, Verneuil methods. Accordingly, the operating temperature is high if the compounds are refractory oxides. In this presentation, however, single crystals of the high refractory rare earth oxides such as Sc2O3, Y2O3 were grown by dc electrolyzing the Ln2(MoO4)3 solid electrolytes at elevated temperatures. Here, solid electrolytes (Ion conducting solids) are the solid materials that only single ion species can conduct in solids. In addition, single crystals of the intermediate oxide phases of TbnO2n-2m were also successfully grown for the first time by the electrolysis.

Recent Industrial Applications of Solid-State Phase Transformations: Superalloys and TRIP Steels/ Automotive Steels

Sponsored by: The Minerals, Metals and Materials Society, TMS Materials Processing and Manufacturing Division, TMS/ASM: Phase Transformations Committee
Program Organizer: Milo Kral, University of Canterbury

Monday AM Room: 287
March 10, 2008 Location: Ernest Morial Convention Center

Session Chair: Milo Kral, University of Canterbury

8:30 AM Introductory Comments

8:35 AM Keynote
Is Phase Transformation Research Still Important?: Morris Fine[1]; *Sungho Jin*[2]; [1]Northwestern University; [2]University of California at San Diego

Does further research on solid-state phase transformations have a high probability of being scientifically important and industrially useful at this time? This Symposium's answer is a strong yes! The large number of presentations in this Symposium's program is proof to that answer. All processes for making materials (sintering, mechanical working, thermal treatment, microstructural manipulations, self-assembly, etc) are basically accomplished by phase transformations. Degradation of materials (corrosion, mechanical failure, overaging of the microstructure, etc) occurs by phase transformations. Nanotechnology is becoming a subject of great interest to the scientific and industrial community these days. Achieving desired structures down to the sub-nano scale often depends on phase transformations and their control. Examples of recent important developments will be given for a variety of materials such as biological materials, electronic materials and magnetic materials.

9:25 AM Invited
Precipitation Simulation of Nickel Alloys: *Fan Zhang*[1]; Kaisheng Wu[1]; Y. Chang[2]; [1]CompuTherm LLC; [2]University of Wisconsin

The mechanical properties of a material depend on its microstructure which is determined by the alloy chemistry and processing conditions. To achieve desired microstructure and mechanical properties, alloy chemistry and processing parameters need to be carefully selected and optimized. This optimization process, normally accomplished by a slow and labor-intensive series of experiments, is significantly sped up due to the modeling efforts currently being undertaken. In this presentation, we will present efforts in the modeling of U720 alloy, which includes both thermodynamic calculation and kinetic simulation. Thermodynamic calculation is based on the Calphad approach, while kinetic simulation of γ' precipitation is based on the mean-field approximation. This modeling tool allows the simulation of the amount of γ' precipitate, its average size and size distribution change with heat treatment conditions for U720 alloy. It can also be applied to other nickel alloys and integrated with other models.

9:50 AM Invited
Development of Microstructure Modeling Tools for Industrial Applications Using Phase Field Approach: Ning Ma[1]; Billie Wang[1]; *Yunzhi Wang*[1]; [1]Ohio State University

Phase transformations in solid state are usually dominated by long-range elastic interactions among different defects and produce extremely complicated microstructures with strong spatial correlation and anisotropy. The traditional constitutive models representing microstructural features by their average values may not be sufficient to quantitatively define the microstructure. In this presentation we review our recent efforts in developing quantitative microstructure modeling tools for industrial applications using the phase field approach that has proven to be able to handle realistic microstructural

patterns. In particular we show the synergy of coupling phase field simulations to experimental characterization in developing fundamental understanding of the mechanisms that govern microstructural evolution during solid state phase transformations, upon which fast-acting models could be formulated for direct industrial applications. Critical issues related to modeling nucleation and interaction among different extended defects will be addressed. Examples of applications will be given for Ni-base superalloys and alpha/beta Ti alloys.

10:15 AM
Prediction of Microstructure Evolution of Ni-Base Superalloy Bond Coats: *Carelyn Campbell*[1]; [1]National Institute of Standards and Technology

The high temperature performance of many superalloys depends on a thermal barrier coating (TBC). A bond coat is placed between the superalloy and the TBC to act as a diffusion barrier and to accommodate large difference in thermal expansion between the TBC and the superalloy. Understanding the microstructure evolution at the substrate/bond coat interface is a critical step to predicting the life of the TBC system. Diffusion simulations, using multicomponent thermodynamics and diffusion mobilities, predict the microstructure evolution of various Ni-base superalloys and bond coat compositions. The Ni-base superalloy consists of a γ (fcc) matrix with γ' ($L1_2$) and various carbide precipitates. The bond coat compositions considered are either single phase B2 (ordered BCC) or a B2 matrix with γ' precipitates. 1-D diffusion simulations that predict the composition and phase fraction profiles to optimize the bond coat composition are presented and discussed.

10:40 AM Break

10:50 AM Invited
Transformation Behaviors of Intercritically Annealed and As-Hot Rolled TRIP Steels: *John Jonas*[1]; Youliang He[2]; [1]McGill University; [2]Cornell University

TRIP steels can be prepared by intercritical annealing followed by transformation into bainite or else employed directly after hot rolling and transformation. The textures formed by following these two contrasting processing routes are presented and compared. Another aspect of importance is whether hot rolling is carried out above or below the Tnr or recrystallization-stop temperature. In the former case, the austenite microstructure is equiaxed prior to transformation, whereas in the latter case, it is flattened or "pancaked". This aspect of hot rolling also affects the transformation texture. The austenite texture components responsible for the principal features of the as-hot rolled bainite textures are described. In a similar manner, the ferrite texture components responsible for the principal features of the intercritically processed material are also presented. The role of variant selection in accentuating some of the features of the final textures is also considered.

11:15 AM Invited
Orientation Relationships and Variant Selection during Phase Transformations in Ultra High Performance Steels: *Stephane Godet*[1]; Arnaud Pétein[2]; Pascal Jacques[2]; [1]Universite Libre de Bruxelles; [2]Université Catholique de Louvain

In recent years, TRIP steels have drawn the attention of many researchers, mainly because of their exceptional mechanical properties that render them very attractive to the automotive industry. Their large ductilities and high work-hardening rates originate from the dynamic transformation of austenite in martensite (TRansformation Induced Plasticity). Specimens were deformed at various temperatures. The orientation relationships holding during the different phase transformations (i.e. the transformation of austenite into bainte and epsilon or alpha' martensite) were characterised using high-resolution orientation imaging and EBSD techniques. The results are presented in the fundamental zones of Rodrigues-Frank space corresponding to the different phase transformations under consideration (cubic to cubic or cubic to hexagonal transformations). Rodrigues-Frank space enables a straightforward comparison with the various orientation relationships proposed in the literature. The variant selection taking place during these transformations is also analysed.

11:40 AM Invited
Recent Development in Transformation Hardening Steel Sheets for Automobile: *Hiroshi Takechi*[1]; [1]Fukuoka Institute of Technology

For reducing fuel consumption and CO_2 emission, weight saving of car should be promoted by using high strength steel sheets (HSS). Many kinds of HSS have been developed, in which transformation hardening HSS such as DP (Dual Phase) steel and TRIP(TRansformation Induced Plasticity) steel are highly evaluated on the relationship among strength, formability and energy absorption during car crashing.Metallurgical features of the transformation hardening HSS are presented as well as a new mechanism for controlling deep drawability of TRIP steel by transformed components. Another recent technology called hot stamping is compared with the application of transformation hardening HSS to produce stronger automobile parts.

12:05 PM Invited
Strategy and Application of Bar Steels Development for Future Automotive Components: *Hyounsoo Park*[1]; [1]Hyundai Motors

A major trend of automotive components development has been practically focused on maximizing the fatigue strength while minimizing the production cost. To achieve this goal, a combined approach should be considered both in alloy design and process optimization. Microalloy steels, mainly for the application of engine and chassis components, have been widely used to eliminate additional uenching-tempering heat treatment after forging process. Traditional ferritic-pearlitic microalloy steels have been widely used for crankshafts and connecting rods. Due to the needs for higher endurance limit for heavy-duty engine performance, needs for higher strength steels has been raised while fulfilling affordable machinability and cost saving. This paper will introduce recent development in next generation microalloy steels for the essential parts of engines and chassis. Regarding development of the transmission gear and shaft steels, a new approach has been carried out to achieve both high strength and cost saving. Vacuum carburizing at higher temperature exhibits the best results. This treatment should be accompanied by special alloy design application for the best results. In this presentation, details of new application and development of innovative alloys along with the controlled forging, state of art carburizing process.

Structural Aluminides for Elevated Temperature Applications: Applications

Sponsored by: The Minerals, Metals and Materials Society, TMS Structural Materials Division, TMS: High Temperature Alloys Committee, TMS/ASM: Mechanical Behavior of Materials Committee
Program Organizers: Young-Won Kim, UES Inc; David Morris, Centro Nacional de Investigaciones Metalurgicas, CSIC; Rui Yang, Chinese Academy of Sciences; Christoph Leyens, Technical University of Brandenburg at Cottbus

Monday AM — Room: 394
March 10, 2008 — Location: Ernest Morial Convention Center

Session Chairs: Dennis Dimiduk, US Air Force; Wilfried Smarsly, MTU Aero Engines GmbH

8:30 AM Opening Remarks

8:40 AM Invited
Gamma TiAl Applications at GE Aviation: *Michael Weimer*[1]; Thomas Kelly[1]; [1]GE Aviation

Overview of the implementation status of GE alloy 48Al-2Nb-2Cr applications in aircraft engines. This will be an update of the presentation made in Bamberg in May of 2006.

9:10 AM
Refractory Crucible Melting and Related Mechanical Properties of Nb-Containing TiAl Alloys: *Antonin Dlouhy*[1]; Katerina Docekalova[1]; Ivo Dlouhy[1]; Ladislav Zemcik[2]; [1]Academy of Sciences; [2]Brno University of Technology

Aiming at a cheaper processing technology, the present study focuses on a vacuum induction melting and related mechanical properties of Nb-containing

TiAl intermetallic cast parts. The attention is mainly given to a cost-effective melting process in which a primary alloy ingot is re-melted in a ceramic crucible and cast into a ceramic shell mould. Besides standard Al2O3 coated crucibles, a new type of crucible (based on Y2O3) is considered. Depending on the refractory type and the coating strategy, there is a potential for chemical reactions between the molten intermetallic and the crucible wall. Results suggest that the wall attack can be considerably limited by either using the Y2O3 (with no SiO2-type binder) or by a suitable wall coating. Mechanical properties of the Nb-containing alloys were investigated before and after remelting in the refractory crucibles. Results show that a limited impairment of alloy strength may occur due to remelting.

9:30 AM

The Development of a Tranquil Tilt Pouring Process for Casting Titanium Aluminides: *Richard Harding*[1]; Michael Wickins[1]; Hong Wang[2]; Georgi Djambazov[2]; Koulis Pericleous[2]; [1]University of Birmingham; [2]University of Greenwich

Reactive alloys such as gamma TiAl are commonly melted in water-cooled crucibles using processes such as Induction Skull Melting (ISM). The limited superheat is compensated for by rapid mold filling, but the resulting surface turbulence readily entrains gas bubbles which often persist as defects in the solidified casting. The present research has developed a novel quiescent casting process for TiAl which combines clean melting in an ISM with the well-established Durville tilt casting method. The potential of this process has been explored using a combination of practical trials and a novel computer model of mold filling, heat transfer and solidification. This paper will describe the equipment used to evaluate the feasibility of this process, and show examples of its use to produce TiAl turbine blades up to 300 mm long. Numerical results will be included which highlight the importance of rotation control, vent location and superheat retention on defect elimination.

9:50 AM

Refractories as Mould Face Coatings for Investment Casting TiAl-Based Alloys: *Qing Jia*[1]; Yuyou Cui[1]; Rui Yang[1]; [1]Institute of Metal Research CAS

Interfacial reactions between Ti-46Al (at.%) casting and ceramic shell mould made of ZrO_2 and Al_2O_3 were compared using a range of techniques. On the surface of the TiAl casting, a reaction layer as thick as 230μm was found in the case of the zirconia mould, whereas there was no visible reaction layer for the alumina mould. Electron probe microanalysis indicated that elements of the two kinds of shell moulds diffused into the alloy melt during casting but to different extents. Metallographic analysis, microhardness measurements and composition analysis showed that alumina was stable and suitable for use as shell moulds when casting TiAl based alloys. In the case of zirconia however Al_2Zr formed at the dendrite boundaries of gamma TiAl constituting the reaction layer. It is concluded that zirconia-based face coat, while suitable for casting titanium alloys, is not suitable for casting TiAl although the latter is generally regarded less reactive.

10:10 AM Break

10:20 AM Invited

Current Status of Mass Production of Gamma Titanium Aluminide Alloy Turbine Rotors in Turbochargers and Future Challenges: *Toshiharu Noda*[1]; [1]Daido Steel Company, Ltd.

Gamma titanium aluminide alloys have a great potential for use in aircraft engine and automobile engine components. Since we demonstrated the potential of gamma titanium aluminide as a turbocharger turbine wheel in 1987, a great effort has been paid in order to put the gamma titanium aluminide turbine wheel to practical use. Through successful development of a gamma titanium aluminide alloy and of processes of casting and joining between the turbine wheel and an alloy steel shaft, we got into mass production of titanium aluminide turbine rotors of turbochargers for passenger car application in 2003. Current automobile companies compete fiercely to develop more fuel-efficient car in order to reduce CO_2 emission. Turbocharger is focused on as one of the key technologies to downsize engines. In this paper, current status of mass production of cast gamma titanium aluminide turbine rotors in turbochargers is discussed along with future challenges.

10:50 AM

Development of the Cost-Affordable TiAl Alloy Based Turbo-Charger Rotor: *Si Young Sung*[1]; Myoung Gyun Kim[2]; Sang Ho Noh[1]; Beom Suck Han[1]; Young Jig Kim[3]; [1]Korea Automotive Technology Institute (KATECH); [2]RIST/ New Metallic Materials Research Team; [3]Sungkyunkwan University

A turbo-charger rotor has been focused on the increment of both the power efficiency and the fuel reduction in an automotive internal combustion engine. However, the "turbo-lag" which delays the steady state operation of turbo-charger under 2,000 rpm is a fatal disadvantage. The simplest way to improve the performance of them is to substitute the lightweight materials the turbine wheel for steels and Ni-based superalloys. TiAl alloys could be a substantial alternative since they have the combination of high specific strength, excellent mechanical properties, and heat resistance. In our study, as a feasible approach for the economic net-shape forming of TiAl turbocharger, the alpha-case formation, fluidity, alloy design for the improvement of oxidation resistance, and welding. The results of the investment casting of TiAl alloys confirm that the casting route can be an effective approach for the economic net-shape forming of TiAl alloys.

11:10 AM

Properties of Cast Al-Rich Ti-Al Alloys: *Michael Paninski*[1]; Anne Drevermann[1]; Georg Schmitz[1]; Martin Palm[2]; Frank Stein[2]; Nico Engberding[2]; Martin Heilmaier[3]; Holger Saage[3]; Klemens Kelm[4]; Stephan Irsen[4]; [1]ACCESS Materials and Processes; [2]Max-Planck-Institut für Eisenforschung GmbH; [3]Otto-von-Guericke-Universität Magdeburg; [4]Caesar Research Center

Gamma TiAl alloys with a lamellar TiAl + Ti3Al microstructure are on their way into industrial application but oxidation at operating temperatures exceeding 900°C still poses a problem. Titanium alloy systems with an increased aluminum content are expected to reveal a higher oxidation resistance and provide a significant additional weight reduction up to 20 percent. Casting processes like ISM (Induction Skull Melting), Investment Casting and Bridgman Solidification will be presented. Furthermore the temperature dependant mechanical properties and a characterization of the microstructure by combined TEM imaging techniques of Al-rich TiAl + Al2Ti alloys will be discussed, as well as the influence of alloy modifications with Nb and Cr.

11:30 AM

The Solidification Feature of TiAl Alloy with Different Boron Addition: *Kui Liu*[1]; Bo Chen[1]; Yingche Ma[1]; Ming Gao[1]; Weidong Wang[1]; Yiyi Li[1]; [1]Institute of Metal Research

The behavior during solidification process of Ti45Al8Nb with different boron addition from 0.2at% to 0.7 at.%B has been studied by high temperature heating the sample at L+beta phase zone and quickly quenched it to preserve the solidified feature method. Optical microscope and SEM analysis show B addition really affected Ti45Al8Nb initial solidified temperature but not effect on the final solidified temperature. Boride has begun precipitating in the liquid phase at more boron addition, but low content it just appeared at low temperature, in L+beta phase zone. Solidified structure of Ti45Al8Nb with different boron content gives the results that big beta grain formed at low boron addition, and small beta grain in the high boron alloy. Beta grain refinement by added certain amount of boron in Ti45Al8Nb alloy in this study on its solidification process may be benefited to clarify boron refining mechanism to TiAl alloys.

11:50 AM

Development of a Cost-Effective Recycling Process for Titanium Aluminides: *Bernd Friedrich*[1]; Jan Reitz[1]; Claus Lochbichler[1]; [1]IME Process Metallurgy and Metals Recycling

An innovative recycling concept for scraps from intermetallic titanium alloys has been developed and successfully proved at laboratory and semi-pilot scale at the IME. It is based on vacuum induction melting (VIM) for melt-down and homogenization of the scraps, using ceramic crucibles and thus accepting a significant oxygen pick up at first-hand. Subsequently VIM and electroslag remelting (ESR) are used for deoxidization. In a last step vacuum arc remelting (VAR) is applied for final refining and consolidation. The process allows the treatment of various scrap types (flexibility) and for correcting the initial melt composition. Careful investigations on the origin of non-metallic inclusions (NMI) have been conducted particularly with regard their subsequent removal in VAR, along with other impurities from the desoxidation step. With 95% of TiAl

being scrapped along present processing routes, this recycling process promises substantial cost-reduction.

Sustainability, Climate Change and Greenhouse Gas Emissions Reduction: Responsibility, Key Challenges and Opportunities for the Aluminum Industry

Sponsored by: The Minerals, Metals and Materials Society, TMS Light Metals Division
Program Organizer: Halvor Kvande, Hydro Aluminium AS

Monday, 8:30 AM Room: 295/296
March 10, 2008 Location: Ernest Morial Convention Center

Session Chair: Halvor Kvande, Hydro Aluminium

Presentations by the world's leading aluminum companies, including:

***Dick Evans,* Rio Tinto Alcan**

***Bernt Reitan,* Alcoa Inc**

***Eivind Reiten,* Norsk Hydro**

Chalco (tentative)

United Company Rusal (tentative)

Program will conclude with a panel discussion by the presenters. There will be an opportunity for the audience to ask questions of the panelists.

Ultrafine-Grained Materials: Fifth International Symposium: Modeling, Theory, and Property

Sponsored by: The Minerals, Metals and Materials Society, TMS Structural Materials Division, TMS Materials Processing and Manufacturing Division, TMS: Shaping and Forming Committee, TMS: Nanomechanical Materials Behavior Committee
Program Organizers: Yuri Estrin, Monash University and CSIRO Melbourne; Terence Langdon, University of Southern California; Terry Lowe, Los Alamos National Laboratory; Xiaozhou Liao, University of Sydney; Zhiwei Shan, Hysitron Inc; Ruslan Valiev, UFA State Aviation Technical University; Yuntian Zhu, North Carolina State University

Monday AM Room: 273
March 10, 2008 Location: Ernest Morial Convention Center

Session Chairs: Yuri Estrin, Monash University; Vesselin Yamakov, National Institute of Aerospace; Florian Dalla Torre, Swiss Federal Institute of Technology; Suveen Mathaudhu, US Army Research Laboratory

8:30 AM Introductory Comments

8:35 AM Invited
On the Role of Diffusion Creep in the Deformation of Nanocrystalline Materials: Paul Millett[1]; Tapan Desai[1]; *Dieter Wolf*[1]; [1]Idaho National Laboratory

We have previously demonstrated by means of molecular-dynamics simulation that for the very smallest grain sizes, nanocrystalline silicon and nanocrystalline fcc metals deform via grain-boundary diffusion creep, provided the applied stress is low enough to avoid microcracking and dislocation nucleation from the grain boundaries. Here we review recent MD simulations that show that in the absence of grain growth both, a nanocrystalline model bcc metal (Mo) and a model metal oxide (UO2) also deform via diffusion creep. However, in the case of Mo both grain-boundary and lattice diffusion are observed to contribute to the creep rate; i.e., the deformation mechanism involves a combination of Coble and Nabarro-Herring creep. Moreover, in the case of UO2 chemical diffusion of both ionic species through the grain boundaries represents the rate-controlling process that governs the intricate interplay between grain-boundary sliding and grain-boundary diffusion during the Coble creep.

8:55 AM
Multiscale Modeling of Fracture in Ultrafine Grained Aluminum: Constitutive Relation for Interface Debonding: *Vesselin Yamakov*[1]; Erik Saether[2]; Dawn Phillips[3]; Edward Glaessgen[2]; [1]National Institute of Aerospace; [2]NASA/Langley Research Center; [3]Lockheed Martin Space Operations

Intergranular fracture is a dominant mode of failure in ultrafine grained materials. In the presented study, the atomistic mechanisms of grain-boundary debonding during intergranular fracture in aluminum are modeled using a coupled molecular dynamics – finite element simulation. Through a developed statistical procedure, a series of constitutive traction-displacement relationships characterizing the load transfer across a growing edge crack at different loading conditions are extracted from atomistic simulations and then recast in a form suitable for inclusion within continuum finite element models. A cohesive zone model, which incorporates the atomistic aspects of the elasto-plastic processes at the crack tip is created. The sensitivity of the extracted cohesive zone models on the conditions of the simulation, system size and temperature, is discussed for the example of a high-angle S99 symmetric tilt grain boundary in aluminum. The study is a step towards relating atomistically derived decohesion laws to macroscopic predictions of fracture.

9:10 AM
Atomistic Simulations of Diffusional Creep in Nanocrystalline BCC Molybdenum: *Paul Millett*[1]; Vesselin Yamakov[2]; Tapan Desai[1]; Dieter Wolf[1]; [1]Idaho National Laboratory; [2]National Institute of Aerospace

As grain sizes are reduced to ultra-fine and nanocrystalline dimensions, the role of diffusional creep as a dominant deformation mechanism becomes important. In this work, molecular dynamics (MD) simulations are used to study diffusion-accomodated creep deformation in nanocrystalline molybdenum, a body-centered cubic metal commonly used as structural cladding. The microstructures are subjected to constant-stress loading at levels below the dislocation nucleation threshold and at high temperatures (i.e., T > 0.75Tmelt) thereby ensuring that the overall deformation is indeed attributable to atomic diffusion. Remarkably, the results show that both GB diffusion in the form of Coble creep and lattice diffusion in the form of Nabarro-Herring creep contribute to the overall deformation. Visual analysis confirms that the GB's serve as sources for lattice vacancies that form within the GB's and subsequently emit into the grain interiors thus enabling lattice diffusion.

9:25 AM
Molecular Dynamics Simulations of Dislocation Nucleation from Special and General Grain Boundaries in Fcc Metal Bicrystals: Yvonne Ritter[1]; *Alexander Stukowski*[1]; Karsten Albe[1]; [1]Technische Universitat Darmstadt

Plastic deformation of nanostructured metals is determined by an intricate interplay between dislocation motion and grain boundary (GB) processes. Although it is well established that grain boundaries in nanocrystalline materials serve as sources for dislocations, the fundamental mechanisms of dislocation nucleation are still not understood. In this contribution we investigate detail mechanisms of dislocation nucleation from grain boundaries of elemental fcc metals by molecular dynamics simulations. Rather than simulating the deformation of nanocrystalline microstructures, we are studying well defined bicrystal geometries. Special tilt and twist GBs as well as general GBs are considered under various loading conditions and the influence of materials parameters, loading and grain boundary structure are discussed.

9:40 AM
Intrinsic Microstrain in Nanocrystalline Metals: *Jürgen Markmann*[1]; Vesselin Yamakov[2]; Alexander Stukowski[3]; Karsten Albe[3]; Jörg Weissmüller[4]; [1]Universität des Saarlandes; [2]National Institute of Aerospace; [3]Technische Universität Darmstadt; [4]Forschungszentrum Karlsruhe in der Helmholtz-Gemeinschaft

Determination of the grain size and microstrain by x-ray diffraction is an important characterisation technique when investigating nanocrystalline materials. Interestingly, the observed microstrain in nanocrystalline metals exceeds the one measured in even heavily deformed conventional materials. To investigate this, defect-free nanocrystalline 3-dimensional microstructures containing between 16 and 1024 grains were thermally relaxed at 300 K by molecular dynamics simulation. X-ray diffractograms were calculated and the x-ray peak broadening was analysed to determine the average grain size and

microstrain. The evaluated grain size is in excellent agreement with the grain size of the starting microstructure. Nevertheless there is a large amount of microstrain in the relaxed samples. The lack of extrinsic sources for microstrain in these "samples" supports an intrinsic nature of microstrain in nanocrystalline metals. Investigation of atomic stress levels were used to localise the microstrain and to determine the underlying mechanism of its occurence.

9:55 AM Invited

Modeling Microstructure and Mechanical Properties of Polycrystalline Materials that Deform by Multiple Slip and Twinning Modes under Severe Plastic Deformation: *Irene Beyerlein*[1]; [1]Los Alamos National Laboratory

This talk will present recent results from our theoretical and experimental program focused on texture and substructure evolution and plastic deformation after severe plastic deformation. In our previous work, we developed a multi-scale model for equal channel angular extrusion including the macroscale extrusion [Mat. Sci. Engng. 380 (2004) 171], polycrystal deformation, and individual crystal hardening [Int. J. Plast. 23 (2007) 640]. For materials that deform by one slip mode, such as Cu and Al, the model could reasonably predict texture evolution and mechanical behavior in subsequent reloading of the processed material [J. Mat. Sci. 42 (2007) 1733]. The mechanisms leading to important features, such as anisotropy, work softening, and tension-compression asymmetry, could be studied. Using the same basic framework, we extend our application to materials that deform by multiple slip and twinning modes. In this case, the model must accurately find their relative contributions and treat appropriately their interactions.

10:15 AM Break

10:30 AM Invited

On the Derivation of the Cottrell-Stokes Law for Very Small Grain Size Metals: *Yannick Champion*[1]; [1]Centre National de la Recherche Scientifique

In large grain sized ductile metals, multiplication and interactions between mobile dislocations leads to an inverse dependence between the activation volume and the stress; this behaviour is known as the Cottrell-Stokes law. When the grain size is refined to fine grain and nanoscale domains, a linear dependence is observed up to a non-dependence of the activation volume with stress at low strain rate and/or high temperature. This behaviour was observed on nanostructured copper with grain size of 90 nm. Activation volume was measured by jump test and stress relaxation technique from RT to 120°C. Derivation of the Cottrell-Stokes law is proposed for small grain size metals starting with the Orowan relation and taking into account the contribution of grain-boundaries in the mechanism of plasticity.

10:50 AM

Role of Microstructural Inhomogeneity on Stress Concentration during Grain-Boundary-Controlled Creep Deformation in Polycrystals: Lucian Zigoneanu[1]; Jijun Lao[1]; *Dorel Moldovan*[1]; [1]Louisiana State University

Grain boundary diffusion and grain boundary sliding are widely accepted as the main plastic deformation mechanisms in fine-grained polycrystalline metals and ceramics at high homologous temperatures. Mesoscopic simulations are used to elucidate the effects of grain size distribution and of heterogeneity in grain boundary diffusivity and grain- boundary sliding resistance on creep deformation and stress concentration in polycrystals. Considering two-dimensional model microstructures we investigate the stress distribution around various topological and grain boundary inhomogeneity (i.e., distributions in grain boundary diffusivities and sliding resistances) at the onset of creep and during the steady state regime. Our simulations indicate that at higher strains the mechanism of grain boundary migration plays a critical role in mediating various topological transformations crucial for maintaining the equiaxed character of the microstructure.

11:05 AM

Finite Element Modeling and Experimental Validation of Equal Channel Angular Pressing: *Venkata Nagasekhar Anumalasetty*[1]; Tick-Hon Yip[2]; [1]University of Queensland; [2]Nanyang Technological University

Equal channel angular pressing (ECAP) is the most promising severe plastic deformation (SPD) for fabrication of bulk nanostructured materials, compaction of powders nearer to theoretical density, and property enhancement of tubular materials. In current study, single pass ECAP finite element modeling was carried by using tool angles of 90 and 10 deg by considering the strain hardening behavior of pure copper. In order to validate the FEM results, pure copper is subjected to single pass ECAP at room temperature. Hardness measurements were carried in the flow plane of single pass ECAP copper. The effective strain variations are compared with the flow plane hardness measurements. Experimental and simulated load-stroke curves and peak load calculations are also compared. The results showed that FEA strain homogeneity has good conformity with hardness measurements, and peak load calculations.

11:20 AM

Effect of Strain on "Hardening by Annealing and Softening by Deformation" Phenomena in Ultra-Fine Grained Aluminum: *Daisuke Terada*[1]; Hironobu Houda[1]; Nobuhiro Tsuji[1]; [1]Osaka University

Ultra-fine grained (UFG) metals fabricated by severe plastic deformation (SPD) sometimes exhibit peculiar mechanical properties. For example, it was reported that the strength increased by an annealing and decreased by deformation in UFG aluminum, which was totally opposite to the behaviors of conventional coarse grained materials. In this study, an effect of SPD strain on the peculiar phenomena was investigated. The UFG aluminum was fabricated by various cycles of the accumulative roll-bonding (ARB) process with lubrication. The specimen ARB processed by 10 cycles certainly showed the "hardening by annealing and softening by deformation" phenomena. On the other hand, the 6-cycle specimen did not showed the phenomena, but was softened by annealing and hardened by deformation normally. The results will be discussed on the basis of microstructural differences.

11:35 AM

The Effect of the ECAP Induced Microstructure on Tensile Properties of an Al6082 Alloy: *Ilchat Sabirov*[1]; Yuri Estrin[2]; Matthew Barnett[1]; Ilana Timokhina[2]; Peter Hodgson[1]; [1]Deakin University; [2]Monash University

Aluminium alloy 6082 was subjected to 8 passes of equal channel angular pressing (Route B_c) at 100°C, which resulted in an ultra-fine grained (UFG) microstructure with an average grain size in the range of 0.2-0.4 μm. A pronounced effect of this extreme grain refinement on the strain rate sensitivity of the flow stress and the uniform tensile elongation was found. The classical Hart criterion of tensile necking fails to explain the observed enhanced ductility of the UFG material in the low strain rate regime. The mechanisms underlying plastic deformation of the UFG alloy were studied in detail by SEM and AFM analysis. The higher-than-expected uniform elongation is discussed in terms of the active deformation mechanisms.

11:50 AM

Grain Growth in Nanocrystalline Materials: Effect of Non-Linear Interface Kinetics: *Moneesh Upmanyu*[1]; Paul Martin[1]; Anthony Rollett[2]; [1]Colorado School of Mines; [2]Carnegie-Mellon University

Grain growth in polycrystalline materials is based on a linear gradient approximation for the underlying interface migration (IM) rates, wherein the migration fluxes at the interfaces vary linearly with the driving force. Recent experimental studies have shown that coarsening of nanocrystalline interface microstructures is unexpectedly stable compared to conventional parabolic coarsening kinetics. Here, we show that during early stage coarsening of these microstructures, IM rates can develop a non-linear dependence on the driving force, the mean interface curvature. We derive the modified mean field law for coarsening kinetics. Molecular dynamics simulations of individual grain boundaries reveal a sub-linear curvature dependence of IM rates, suggesting an intrinsic origin for the slow coarsening kinetics observed in ultra-fine grained metals.

12:05 PM

Rate Dependent Characteristics of Pure Magnesium and ZK60 Alloy: *Shailendra Joshi*[1]; Bin Li[1]; Evan Ma[1]; Kaliat Ramesh[1]; Toshiji Mukai[2]; [1]Johns Hopkins University; [2]National Institute for Materials Science

In the quest for light weight structural materials, nanostructured magnesium (Mg) and its alloys have generated tremendous interest as the potential candidates for strong structural components. Whereas the microstructural underpinnings of the mechanical behavior for both coarse-grained (CG) pure and alloyed Mg (e.g. ZK60) are reasonably well explored, the impact of ultrafine grain size on the mechanical properties remains elusive especially due to the strong influence of the texture. In this work, our goal is to articulate this relationship and

understand the pertinent deformation mechanisms. We perform strain controlled experiments on pure Mg and ZK60 over a wide range of strain rates (10-4 -10+4 s-1) under compression. The corresponding microstructural characterization of the deformed microstructures as a function of the imposed strains provides insight in to the deformation mechanisms in the CG and fine-grained Mg alloys and its relation with the observed mechanical response.

2008 Nanomaterials: Fabrication, Properties, and Applications: Nanomaterials Synthesis

Sponsored by: The Minerals, Metals and Materials Society, TMS Electronic, Magnetic, and Photonic Materials Division, TMS: Nanomaterials Committee
Program Organizers: Seong Jin Koh, University of Texas; Wonbong Choi, Florida International University; Donna Senft, US Air Force; Ganapathiraman Ramanath, Rensselaer Polytechnic Institute; Seung Kang, Qualcomm Inc

Monday PM Room: 274
March 10, 2008 Location: Ernest Morial Convention Center

Session Chair: To Be Announced

2:00 PM Invited
Nanoprobes and Applications Based on Carbon Nanotubes: *Sungho Jin*[1]; [1]University of California

The key component of the AFM is the probe tip, the size and properties of which determine the resolution and reliability of nanoscale imaging. We have fabricated an extremely sharp probe based on carbon nanocone structure directly grown on an AFM cantilever at a predetermined tilt angle by orientation-controlled DC plasma CVD process. The high-aspect-ratio yet thermal-vibration-resistant geometry, together with excellent mechanical strength of the carbon nanocone AFM probes offer many advantages for nanoscale imaging in nanotech and biotech applications. We have also fabricated MFM probes for analysis of magnetic nanostructures, and special AFM probes with extremely low modulus, about three orders of magnitude reduced, for imaging of soft matters, living cells or delicate components. Stresses and Si cantilever beam bending introduced during CVD growth of carbon nanotubes, and techniques to prevent such undesirable geometry changes are also discussed.

2:30 PM
Nanotechnology in Early Disease Detection and Diagnostics: *Matt Trau*[1]; [1]Uinversity of Queensland

Diagnostics that detect diseases such as cancer at an early stage, when the disease is most responsive to contemporary therapies, provide the greatest social and economic benefits to society. This has been demonstrated in early disease detection programs such as the PAP smear cervical cancer test and colonoscopy for colon cancer. Unfortunately, current diagnostic protocols typically depend on a complicated variety of tests based on a wide range of different, and often expensive, technological platforms. Each different platform requires significant investment in single-use equipment and training. Despite this investment, results can be ambiguous and require multiple, different tests to produce a confirmed result for a single pathogen. Nanotechnology offers the promise of miniaturized, inexpensive, flexible and robust "plug-and-play" molecular reading systems which can be effectively deployed in the field. In this talk we will present several platforms which our Centre is currently developing for such applications.

2:45 PM
Quantum-Dot-Activated Luminescent Carbon Nanotubes via a Nano Scale Surface Functionalization for *In Vivo* Imaging: *Donglu Shi*[1]; Yan Guo[1]; Zhongyun Dong[1]; Jie Lian[1]; Wei Wang[1]; Guokui Liu[2]; Lumin Wang[3]; Rodney Ewing[2]; [1]University of Cincinnati; [2]Argonne National Laboratory; [3]University of Michigan

A critical challenge for biomarking, based on luminescent materials, has been the development of nano structures with highly visible or characteristic near infrared emissions for precise imaging, combined with nanoscale cavities for drug storage and delivery. The design of such materials requires complex nanostructures that have both the intense emissions and appropriate storage geometries. We report here a scheme for the use of novel nanostructures designed to satisfy both of these important requirements. Hypodermal and *in vivo* organic imaging from quantum dot conjugated carbon nanotubes has been realized in mice for the first time. The coupling of quantum dots on carbon nanotubes was materialized based on a novel plasma nanotube surface polymerization. The quantum dot activated carbon nanotubes exhibited intense visible light emissions in both fluorescent spectroscopy and *in vivo* imaging. These experimental results can be extended to the development of new techniques for early cancer diagnosis.

3:00 PM
Synthesis CuO Nanowire Array for Gas-Sensor Applications: *Kai Wang*[1]; Zhongming Zeng[1]; Weilie Zhou[1]; [1]University of New Orleans

CuO nanowires, a typical p-type oxide semiconducting nanostructures, can enhance the selectivity of gas sensor array using opposite resistance variation to n-type semiconductors when exposed to the gases. We present a synthesis of high density CuO nanowires and measurement of the electrical properties of a single nanowire. Large quantities of CuO nanowires have been synthesized by heating the copper foil in air. The as-synthesized nanowires are characterized by scanning electron microscopy (SEM) and transmission electron microscopy (TEM). The nanowires grow vertically on the foil and the diameter ranges from 50 nm to 120 nm with a length of tens micrometers. The nanowires were patterned by e-beam lithography. I-V characteristic of a single CuO nanowire indicates the resistance of CuO nanowire is in the order of 10^8ohm, which is a good for selective gas sensor fabrication. The nanowire array can be potentially used to build three-dimensional hybrid nanostructures for gas sensors.

3:15 PM
Electrospun Vanadium Oxide Fibers for Gas Sensor Applications: *Kevin Stokes*[1]; Chrisopher Lomatayo[2]; Jaijun Chen[1]; [1]University of New Orleans; [2]South Dakota School of Mines

We have fabricated vanadium oxide ultra-thin fibers from a simple organometallic vanadium precursor using electrospining. Fibers with diameters ranging from 700 nanometers to 3.0 microns were fabricated from a solution of vanadium oxytriisopropoxide (VOTIP), acetic acid and polyethylene oxide (less than 1% polymer by weight). As the clear precursor solution exits the spinneret, the VOTIP reacts with the moisture in the air resulting in a partially hydrolyzed orange fiber. The fibers are left overnight to completely hydrolyze, then collected and calcined at 400°C. The fiber morphology was characterized using field emission scanning electron microscopy (FESEM) before and after calcination. Electrical conductivity of collections of fibers deposited onto microelectrode arrays is also presented.

3:30 PM
GaN and ZnO-Based Nanowire Sensors for Bio and Chemical Detection: *Stephen Pearton*[1]; F. Ren[1]; B. Kang[1]; H. Wang[1]; B. Gila[1]; D. Norton[1]; L. Tien[1]; T. Chancellor[1]; T. Lele[1]; Y. Tseng[1]; J. Lin[1]; [1]University of Florida

In this talk we will give examples of using ZnO nanorods and nitride nanowires and High Electron Mobility Transistors (HEMTs) for pH sensing in the range of interest for human blood (7-8 pH), detection of DNA hybridization and detection of Hg. In all of these sensor systems, integrating the resulting sensors with modern GPS and wireless communication systems in a convenient module is important for ease of use and monitoring applications.

3:45 PM
SnO_2/GeO_2 Bicrystalline Nanowires: Synthesis, Characterization, Photoluminescence and Sensing Properties: *Ying Li*[1]; Jiajun Chen[1]; Weilie Zhou[1]; [1]University of New Orleans

Bicrystalline structure has unique optical and mechanical properties due to its grain boundary, which not only includes two combined single crystals in same materials, but also can be formed by different materials. We report a synthesis of SnO_2/GeO_2 bicrystalline nanowires by thermal evaporation with the mixture of metal Sn and Ge powders. The as-synthesized products have been characterized by scanning electron microscopy, energy-dispersive X-ray spectroscopy and selected-area electron diffraction. The diameters of the nanostructures range from 20 to 200 nm, and lengths are up to several hundreds of micrometers. Microstructure characterization indicates the orientation relationship between two crystals is [001]GeO_2// [001]SnO_2, (110)GeO_2// (110)SnO_2. The PL spectrum of the bicrystyalline nanowires shows some difference compared with pure SnO_2 and GeO_2 nanostructure which are associated with interface defects in SnO_2/

GeO_2 bicrystalline nanowires. In addition, the sensing properties of the SnO_2/GeO_2 bicrystalline nanowire to CO and H_2 will also be discussed.

4:00 PM Break

4:15 PM Invited

Atomic Layer Deposited Thin Films and Their Applications: *Hyeongtag Jeon*[1]; Seokhoon Kim[1]; [1]Hanyang University

Recently thin film deposition technology has been developed extensively due to the great needs in many application areas especially in the fields of semiconductor, nanomaterials and nanorelated technologies. There are many deposition methods introduced and actually applied in the real thin film processes. However, in these days thin films with nanoscale thickness are needed for research and development for many different areas. Therefore the deposition method to control nanoscale thin film is focused to develop and atomic layer deposition (ALD) technique is one of promising choices. ALD method provides to grow high quality thin film by a layer-by-layer fashion, and to deposit thin films with large area uniformity and low impurity content in nanoscale devices. There are many different ALD methods are already introduced such as thermal, plasma and other recactive ALDs. In this presentation, different types of ALD methods and application areas will be presented.

4:40 PM Invited

Nanoheteroepitaxy: An Approach toward a Monolithic Phosphor-Free White LED: *Timothy Sands*[1]; [1]Purdue University

The global energy challenge will be addressed in part by the development of more efficient energy conversion devices, from solid-state lighting to solid-state refrigerators and generators. Materials limit the performance of each of these devices. For example, the luminous efficiency of white LEDs is limited by the so-called "green gap" – i.e., the low internal quantum efficiency of LEDs that emit at wavelengths near 555 nm, the peak of the photopic vision sensitivity spectrum. In this talk, I will describe our approach to utilize nanostructured (In,Ga)N to bridge the green gap. The free surfaces of nanorod heterostructures allow elastic relaxation of lattice misfit strain, thereby altering the kinetics of InN incorporation. Thus, (In,Ga)N nanorods can incorporate higher InN mole fractions without the introduction of the dislocations that limit the internal quantum efficiency. Challenges remaining on the path toward a monolithic nanostructured phosphor-free white LED will be highlighted.

5:05 PM

Atomic-Scale Features of Dislocation Dynamics in Thin Films: *Yuri Osetsky*[1]; Roger Stoller[1]; Yoshitaka Matsukawa[1]; [1]Oak Ridge National Laboratory

Atomistic modelling has demonstrated that the dynamic interactions of dislocations in thin films have a number of remarkable features. A particular example is the interaction between a screw dislocation and a stacking fault tetrahedron (SFT) in Cu which can be directly compared with in situ observations of quenched or irradiated fcc metals. If the specimen is thin, the dislocation is slow and the temperature is high enough, a segment of the original SFT can be transported towards the surface via a double cross-slip mechanism and fast glide of an edge dislocation segment formed during the interaction. The particular mechanism depends on the stress distribution in the film for it affects the screw dislocation dissociation and reactions with an SFT. The mechanisms observed in the simulations provide an explanation for the results of in situ straining experiments and the differences between bulk and thin film experiments.

5:20 PM

Structure and Properties of Al/TiN Nanoscale Multilayers: *Dhriti Bhattacharyya*[1]; Nathan Mara[1]; Patricia Dickerson[1]; Richard Hoagland[1]; Amit Misra[1]; [1]Los Alamos National Laboratory

Nano-scale multilayers of Al/TiN have been deposited with Al:TiN ratio equal to 9:1 and 1:1, using reactive sputter deposition, with TiN layer thickness varying from 50 nm to 1 nm. The structure of these nano-scale multilayers has been studied using Transmission Electron Microscopy (TEM), high resolution TEM, and X-Ray diffraction. Nano-indentation experiments have been performed on these multilayered thin films to measure their hardness. This work clearly demonstrates that these multilayers are definitely stronger (hardness ~ 4 GPa) than a simple rule of mixtures would suggest (hardness ~ 1 GPa). It is shown that the hardness varies with bilayer thickness λ with a Hall-Petch behavior to a λ value of 20 nm, below which the hardness value drops below that predicted by the Hall-Petch equation. The effect of volume fraction of the two components is also demonstrated in terms of variations in hardness.

5:35 PM

Fabrication and Characterization of Single Stand-Alone TiO_2 Nanotube Devices: *Dongkyu Cha*[1]; Kyungmin Lee[1]; Bongki Lee[1]; M. J. Kim[1]; Hyunjung Shin[2]; Jaegap Lee[2]; Jiyoung Kim[1]; [1]University of Texas at Dallas; [2]Kookmin University

TiO_2 nanotubes have great potential to enhance performance for sensor applications and dye sensitized solar cell applications, primarily due to increased surface area to volume ratio. However, the nanotubes are very fragile, so it is still challenging to fabricate single stand-alone nanotube devices. We successfully fabricate devices with single stand-alone TiO_2 nanotubes using a process which combines Focused Ion Beam with photolithography. This process provides several advantages over previously published methods, including freedom of structural geometry, shorter fabrication time, and higher throughput. This rapid prototyping method enables the direct measurement of single nanotubes under ambient conditions. In this study, we will present the electrical characteristics and potential gas sensor applications of single TiO_2 nanotubes. This research was supported by a grant (code #: M105KO010026-05K1501-02611) from 'Center for Nanostructured Materials Technology' under '21st Century Frontier R&D Programs' of the Ministry of Science and Technology, Korea.

5:50 PM

Low Temperature Growth of ZnO Nanorods and Nanotubes by Atomic Layer Deposition for the Application of Field Emission: *Yung-Huang Chang*[1]; Chih Chen[1]; [1]National Chiao Tung University

Self-organized ZnO nanorods and nanotubes are grown on Si substrates by using AAO as a template and ALD to deposit ZnO. With the aid of the ALD, the deposition temperature can be lowered down to as low as room temperature, and no any metal catalysts or seed layers are needed. Each individual nanorod or nanotube is perpendicular to the Si substrate. We controlled the diameter and thickness of AAO template to modify the morphology of ZnO nanorod arrays. The screening effect and field enhancement were investigated to obtain the best parameters for the application of field emission. In addition, the nanorods and nanotubes were annealed at 700°C for one hour under oxygen ambient, and their average grain size grew up from 11 nm to 15 nm. The results of photoluminescence, TEM, and the performances of field emission for the ZnO nanorods and nanotubes arrays will be presented in the conference.

3-Dimensional Materials Science: Large Datasets and Microstructure Representation I

Sponsored by: The Minerals, Metals and Materials Society, TMS Structural Materials Division, TMS: Advanced Characterization, Testing, and Simulation Committee
Program Organizers: Michael Uchic, US Air Force; Eric Taleff, University of Texas; Alexis Lewis, Naval Research Laboratory; Jeff Simmons, US Air Force; Marc DeGraef, Carnegie Mellon University

Monday PM — Room: 286
March 10, 2008 — Location: Ernest Morial Convention Center

Session Chairs: Marc DeGraef, Carnegie Mellon University; Jeff Simmons, Air Force Research Laboratory

---

2:00 PM Invited

Towards the Incorporation of Realistic Microstructures in Computational Models: A Framework for Automated 3D Microstructure Analysis and Representation: *Michael Groeber*[1]; Michael Uchic[1]; Dennis Dimiduk[1]; Somnath Ghosh[2]; [1]Air Force Research Laboratory; [2]Ohio State University

Over the past five years there have been significant advances in developing serial-sectioning methods that provide quantitative data describing the structure and crystallography of grain-level microstructures in three dimensions (3D). Subsequent analysis and representation can provide modeling and simulation efforts with a highly-refined characterization of specific microstructural features. For example, the structure of an engineering alloy could be characterized and then translated directly into a 3D volume mesh for Finite Element (FE) analysis.

However, this approach requires a multitude of data sets in order to sample the heterogeneity observed in typical microstructures. One way to circumvent this issue is to develop computation tools that create synthetic microstructures that are statistically-equivalent to the measured structure. This presentation will discuss the development of software programs that perform a robust statistical analysis of a material's 3D microstructure as well as generate a host of synthetic structures which are analogous to the real material.

2:30 PM
Spectral Representation and Reconstruction of 3-D Materials: *David Fullwood*[1]; Steven Niezgoda[2]; Surya Kalidindi[2]; [1]Brigham Young University; [2]Drexel University

Representation of 3-D material data using correlation functions is a key statistical technique for material analysis. Reconstruction of large 3-D material realizations from such statistical data has historically been too computationally intensive to attempt with traditional reconstruction techniques (such as simulated annealing). We present a newly developed approach to reconstruction based upon phase retrieval methods from the signal processing industry. Rapid reconstruction of 3-D datasets from 2-point statistical data is demonstrated. We also investigate the space of 2-point statistics correlating to physically meaningful material realizations, and the issues of generating full sets of statistics from partial data.

2:50 PM
Moment Invariant Shape Descriptors for Microstructure Representation: *Jeremiah MacSleyne*[1]; Jeff Simmons[2]; Marc DeGraef[1]; [1]Carnegie Mellon University; [2]Wright Patterson Air Force Base

In this contribution we show how moment invariants (combinations of second order shape moments that are invariant w.r.t. affine or similarity transformations) can be used as sensitive shape discriminators in 2-D and 3-D. After defining the invariants, we introduce moment invariant space, and illustrate how all possible shapes reside within a finite region in this space. Then we provide applications of invariants, such as the quantitative representation of shapes and shape changes of precipitates that develop in real 3-D microstructure observations as well as in microstructure evolution simulations. Since particle shapes are characteristic of microstructures, this technique can be used to quantify the "closeness" of two microstructures by the statistics of their moment invariants. As an example of 3-D moment invariants, we show that the shapes of complex precipitates in a Rene-88DT alloy lie along a curved surface in moment invariant space.

3:10 PM Invited
Collecting, Segmenting and Analyzing Large Serial-Section Materials Data Sets: *David Rowenhorst*[1]; Alexis Lewis[1]; George Spanos[1]; [1]Naval Research Laboratory

As the field of 3-D Materials Science advances, the ability to collect large data sets has consistently grown, which has lead to new problems in the analysis, and representation of these data sets. We will present methods for collecting large serial sectioning data sets, addressing using image montaging, robust fiducial marks and image alignment. We will primarily as an example, a serial sectioning data set of β-Ti grains, containing 200 sections, and resulting in more than 1000 grains in the microstructure. We will also present how this data set is segmented using an adapted Watershed Algorithm. Finally will show different techniques for visualizing, analyzing and representing the data contained in such data sets.

3:40 PM Break

4:00 PM Invited
Statistical Methods for Segmentation of 3-D Microstructural Image Data with Minimal Supervision: *Mary Comer*[1]; Peter Chuang[1]; Jeff Simmons[1]; [1]Purdue University

3-D materials science is fueled simultaneously by the integration of computer controls with microscopes and by the increase in collection rates. Image data rates are expanding exponentially. To utilize all of this information, features must be extracted from images. Conventional image processing is currently used for this extraction, but is heavily labor intensive, often requiring manual segmentation of each frame. Developing minimally supervised algorithms for making these segmentations is the goal of this work. Segmentation seeks to classify pixels into regions, corresponding to Different objects or textures. We will describe a method we have developed for finding the segmentation that minimizes the expected number of misclassified pixels, with minimal supervision. Parameters of the statistical models used for the image data are automatically estimated during the segmentation procedure, reducing the amount of human interaction required. Preliminary results on serial section stacks of Ni-base alloys and carbon foam images will be presented.

4:30 PM
Applications of Active Contours in Microstructural Analysis: *Aleks Ontman*[1]; Gary Shiflet[1]; [1]University of Virginia

Edge detection is a widely used technique regularly employed as an intermediate step in microstructure analysis. Having an outline of region of interest enables the user to extract data about the region or use it in reconstruction of 3-D models. Since traditional edge detection relies on a user selected threshold value the results often are subjective. Furthermore, traditional edge detection frequently results in outlines that are incomplete, requiring additional processing steps, such as, edge linking and spur removal, and it is a very noise sensitive technique. Active contouring (AC) is an edge detection based technique that typically yields results superior to that of a traditional edge detector. High noise tolerance and built-in flexibilities of AC make the technique desirable to use across a broad range of applications with increasing automation. Several uses of AC are presented to demonstrate robustness and the range of applications that can employ AC.

4:50 PM
An Eigenvalue-Based Method for Characterizing Plastically Deformed Surfaces: *Mark Stoudt*[1]; Joseph Hubbard[1]; Lyle Levine[1]; [1]National Institute of Standards and Technology

Since real surfaces evolve and interact in three dimensions, it is essential that surface morphology be characterized in three dimensions with tools that maximize fidelity with the original surface. However, spatial analysis of plastically deformed polycrystalline surfaces in three-dimensions is problematic due to inadequate numerical tools. Moreover, mathematical artifacts such as boundary discontinuities or periodic extrapolations introduced by two-dimensional numeric parameters are exacerbated in three-dimensional analysis. We have developed a representation-independent, non-interpolated spatial analysis protocol that does not utilize conventional time series analysis methods. Because it exclusively examines the behavior of eigenvalue spectra calculated directly from a topographic image, this protocol eliminates the need for a priori assumptions about surface character. The eigenvalue spectra change systematically with plastic strain and correspond to correlations in the surface morphology at all length scales. The capabilities of this protocol and results of initial analyses shall be presented and discussed.

5:10 PM
Image Registration Using Neural Networks: *Aleks Ontman*[1]; Gary Shiflet[1]; [1]University of Virginia

Image Registration (IR) is a process of transforming images in a dataset into one common coordinate system. The original method, developed by Mangan and Shiflet, relied on hardness indentations to align serial images in the dataset. However, as the sample is continuously sectioned, the marks and the microstructure change and an appropriate 'hands-on' registration method is required to locate the marks for IR. Feature and area based algorithms fail to perform adequately when marks are scaled or rotated. A Neural Network can be trained to discriminate shapes of interest which can then be used to assist and automate the IR process. We will present a NN that can successfully isolate indentation squares that are rotated, scaled and located among other microstructural features and then use the information to automatically register a set of synthetic and optical microscope images.

9th Global Innovations Symposium: Trends in Integrated Computational Materials Engineering for Materials Processing and Manufacturing: Session I

Sponsored by: The Minerals, Metals and Materials Society, TMS Materials Processing and Manufacturing Division, TMS/ASM: Computational Materials Science and Engineering Committee, TMS: Global Innovations Committee, TMS: Nanomechanical Materials Behavior Committee, TMS/ASM: Phase Transformations Committee, TMS: Powder Materials Committee, TMS: Process Technology and Modeling Committee, TMS: Shaping and Forming Committee, TMS: Solidification Committee, TMS: Surface Engineering Committee
Program Organizers: Corbett Battaile, Sandia National Laboratories; Amit Misra, Los Alamos National Laboratory; Joy Hines, Ford Motor Company; James Sears, South Dakota School of Mines and Technology

Monday PM Room: 281
March 10, 2008 Location: Ernest Morial Convention Center

Session Chair: To Be Announced

2:00 PM Introductory Comments

2:05 PM Invited
CAE in Product Development and the Role of Computational Materials: *Gerould Young*[1]; [1]Boeing Phantom Works

CAE is an indispensable part of the product development cycle for Boeing. Computational fluid dynamics and computational structural analysis are used via general purpose tool sets to develop and certify products. As we look to further improve the performance of our products, we look to advanced alloys and composite materials, to speed the development of these new materials and associated manufacturing processes and to understand in service behavior. This leads us to look to the use computational materials run on high speed computing platforms. The challenge is to make these new tools systemic within a discipline which has traditionally not used the "perfect laboratory" offered by high speed computing, but instead relied on experiment and laboratory development. Furthermore, there's a challenge to develop general purpose tools for the materials engineer at each appropriate scale to simulate specific material behaviors and to link these tools across scales to other computational disciplines.

2:35 PM Invited
Application of ICME in the Air Force's Materials Research and Development Program: *Charles Ward*[1]; [1]US Air Force

Strides in the physical understanding of materials behavior coupled with advances in both modeling techniques and computing power are leading to the increasing application of integrated computational materials engineering to provide solutions to materials development, processing and life prediction problems. While the structural materials community is still quite some time off from having a truly integrated capability across all length and time scales, progress is clearly being made in linking descriptions of material behavior across several orders of magnitude in scale. This talk will present the current focus of the Air Force ICME efforts for propulsion materials, and will highlight several examples of ICME application.

3:05 PM Invited
An Automotive Perspective on Integrated Computational Materials Engineering: *Matthew Zaluzec*[1]; [1]Ford Motor Company

In the automotive industry, ICME has been a key enabler for "up-front" component and vehicle design and has provided savings in cost and timing in an era of increased competition and "just-in-time" manufacturing. Ford Motor Company's Research and Advanced Engineering Laboratory has been an innovator in the area of ICME for aluminum powertrain components for several years and has worked to expand that expertise into other areas of the vehicle requiring other materials and/or processing paths such as steel stampings, virtual paint and plastics processing used in the design and manufacturing of automotive components. This talk will focus on Ford's efforts in the area of ICME in a number of different applications as well as some of the collaborative efforts in ICME through its participation in the FreedomCAR/ USAMP programs.

3:35 PM Break

3:55 PM Invited
Structural Materials in Advanced Nuclear Energy Systems: The Need for Revolutionary Research: *Ronald Gibala*[1]; Steven Zinkle[2]; [1]University of Michigan; [2]Oak Ridge National Laboratory

We present a partial overview of key findings of the DOE-sponsored BES Workshop on *Basic Research Needs for Advanced Nuclear Energy Systems* held in August, 2006. The focus is on topics from our panel on structural materials and their performance under extreme environments. The recommendations and goals, although including dozens of specific questions to be answered, are generically three-fold: (1) discover mechanisms that render materials impervious to the interacting extreme conditions of irradiation, temperature, stress and environmental surroundings; (2) achieve seamless integration of novel experimental techniques with advances in the methodology of computational materials science; (3) bring fundamental design of materials to a new level of accomplishment that includes expanded development of functionalized interfaces for optimization of materials properties. We will also discuss related recommendations from other panels of the Workshop and give a brief 'scorecard' on how the Workshop recommendations have affected DOE program initiatives and funding.

4:25 PM Invited
Multiscale Modeling and Materials Design: *David Mcdowell*[1]; [1]Georgia Institute of Technology

Engineering design has historically been taught using the paradigm of selecting materials on the basis of tabulated databases of properties (mechanical, physical, electronic, etc.). Recent trends have moved towards concurrent design of material composition and microstructure together with the component/system level, moving through the process-structure-property-performance hierarchy. The goal is to tailor materials to meet specified ranges of performance requirements of the overall system, rectifying the aforementioned hierarchy of design with hierarchy of scales of structure that affect properties. Materials design falls under the general category of simulation-based design, in which computational materials science and multiscale modeling modeling play key roles in evaluating performance metrics necessary to support design decision-making. The interplay of hierarchical, multi-level systems-based design of materials with methodologies for multiscale modeling is core to materials design.

4:55 PM Panel Discussion

Advances in Semiconductor, Electro Optic and Radio Frequency Materials: Compound Semiconductors and Beyond

Sponsored by: The Minerals, Metals and Materials Society, TMS Electronic, Magnetic, and Photonic Materials Division, TMS: Thin Films and Interfaces Committee
Program Organizers: Nuggehalli Ravindra, New Jersey Institute of Technology; Narsingh Singh, Northrop Grumman Corporation ES; Choong-un Kim, University of Texas - Arlington; Yanfa Yan, National Renewable Energy Laboratory; Bhushan Sopori, National Renewable Energy Laboratory; Greg Krumdick, Argonne National Laboratory

Monday PM Room: 278
March 10, 2008 Location: Ernest Morial Convention Center

Session Chairs: Yanfa Yan, National Renewable Energy Laboratory; Greg Krumdick, Argonne National Laboratory

2:00 PM Introductory Comments

2:10 PM Invited
Effect of Growth Conditions on the Morphology of Nanodots: *Narsingh Singh*[1]; Sean Mclaughlin[1]; Anthony Margarella[1]; David Kahler[1]; David Knuteson[1]; Andre Berghmans[1]; Brian Wagner[1]; [1]Northrop Grumman Corporation

We have developed Germanium (Ge) nanodots and arrays of nanodots on Silicon (Si) wafers with etched trenches. We used Silicon trenches to study the effect of planar silicon with high energy interfaces. Several growth experiments were carried out and growth conditions were varied to study the nucleation and

growth of dots. The morphologies of the nanodots were very much dependent on the growth conditions. We observed that the germanium grew as nanodots in the field of edges and trenches. Larger Ge dots grew along high energy interfaces. We used diborane and arsine for doping. The growth rates for nanodots are slower for an arsine atmosphere in comparison to the case of diborane. Our experiments indicated that using oxides on Si wafers, growth of Ge nanodots can be grown on the desired area.

2:40 PM Invited

Medical Applications of Advanced Semiconductors: *Roger Narayan*[1]; Robin Brigmon[2]; Shaun Gittard[1]; Christopher Berry[2]; [1]University of North Carolina and North Carolina State University; [2]Savannah River National Laboratory

Medical device infection is associated with significant morbidity, mortality, and associated healthcare costs. Microorganisms colonize the medical device surface and form sessile communities known as a biofilms. These biofilms contain 5-50 micrometer thick glycoprotein matrices that protect the bacteria through a diffusion limitation process, and increase their resistance to antibodies, macrophages, and antibiotics. The sustained delivery of antimicrobial agents into the medical device microenvironment may prevent biofilm formation and avoid systemic side effects associated with oral or intravenous antimicrobial administration. For example, coating a medical device with a ceramic thin film may impart antimicrobial properties. Structural studies and microbial studies were performed on diamondlike carbon-silver nanocomposite films, diamondlike carbon-platinum nanocomposite films, diamondlike carbon-silver-platinum nanocomposite films, and zinc oxide thin films prepared using pulsed laser deposition. These materials may provide unique biological functionalities and improved lifetimes for next generation cardiovascular, orthopaedic, biosensor, and implantable microelectromechanical systems.

3:10 PM

Lithium Phthalocyanine: An Overview: *Sushil Sikha*[1]; Trishla Kanthala[2]; Raymonde Jean-Charles[3]; Shanakey Cupidon[3]; Nuggehalli Ravindra[1]; [1]New Jersey Institute of Technology; [2]New York Institute of Technology; [3]East Orange Campus High School

Lithium Phthalocyanine is a narrow bandgap semiconductor with an energy gap of 0.2 eV and a high frequency dielectric constant equal to 6. In recent years, this material has gained notoriety, both as bulk and in thin film form on various substrates, as an oxygen sensor for biological applications. An overview of the various electrical, optical, structural and magnetic properties of Lithium Phthalocyanine (LiPc) is presented in this study. The study concludes with the chemical and environmental stability of LiPc.

3:30 PM Break

3:40 PM Invited

Chemical-Mechanical Methods for Making Quality Compound Semiconductor Nanocrystals: *Nancy Michael*[1]; Choong-Un Kim[1]; [1]University of Texas

Synthesis of high quality compound semiconductor nanoparticles has been a topic of research interest as advances in nanoparticle manipulation and device structure have enabled many exciting applications. In order to achieve the needed high quality, most of these synthesis methods are bottom-up, that is, building the particles atom by atom, and involve expensive precursor chemicals and equipment. In this paper we present an inexpensive top-down method by which a larger particles are chemically/mechanically broken down to high quality nano-sized particles. This method is applicable to compound semiconductors as well as semiconductor alloys, enabling nanocrystals with tunable properties.

4:10 PM

Synthesis and Characterization of Ga and N Incorporated ZnO Films: *Sudhakar Shet*[1]; Kwang-Soon Ahn[1]; Yanfa Yan[1]; Todd Deutsch[1]; Muhammad Huda[1]; Nuggehalli Ravindra[2]; Mowafak Al-Jassim[1]; Johm Turner[1]; [1]National Renewable Energy Laboratory; [2]New Jersey Institute of Technology

Ga and N incorporated ZnO thin films (ZnO:N:Ga) were synthesized by reactive RF magnetron sputtering in N2/O2 gas ambient. All the films were deposited on F-doped tin oxide-coated glass. The gas ambient was mixed N2 and O2 gas with a gas ratio of O2/(N2+O2) = 5%. Structural properties, optical absorption and PEC responses for ZnO:N:Ga films were investigated. The influence of the varying Ga concentration in the ZnO:N:Ga films on the bandgap and resulting photoelectrochemical properties has been studied. The n-type conductivity in these films was confirmed by analysis of Mott-Schottky plots and current voltage characteristics under illumination.

4:30 PM

Novel Cu-Doped ZnO Diluted Magnetic Semiconductors for Spintronics Applications: *Deepayan Chakraborti*[1]; John Prater[2]; Jagdish Narayan[1]; [1]North Carolina State University; [2]Army Research Office

Recently transition metal doped ZnO based diluted magnetic semiconductors have drawn a lot of attention for use in spintronics applications where charge as well as spin of an electron can be utilized for device functionality. Here we present the systematic studies on epitaxial growth and properties of Cu-doped ZnO thin films grown on (0001)a-Al_2O_3 single crystals by PLD. The Cu-doped ZnO system has shown near 100% spin polarization making them an attractive candidate for efficient injection of spin polarized carriers in spin-based devices. The effect of free carriers and intrinsic point defects like oxygen vacancies on the long range ferromagnetic ordering of localized Cu^{2+} spins has been investigated to develop a clear understanding of the origin of ferromagnetism in ZnO based DMS systems. Finally we have fabricated a spin valve type device structures to study the injection of spin polarized carriers across a non-ferromagnetic layer sandwiched between two ferromagnetic layers.

4:55 PM

The Photocatalytic Oxidation of Water to O_2 over Vanadium-Dopant of Rutile TiO_2: *Daoxin Wu*[1]; Qiyuan Chen[1]; [1]Central South University

Vanadium doped rutile TiO_2 with different Vanadium doping concentration were prepared by low temperature hydrolysis using Tetrabutyl titanate. Powers were characterized by XRD,PL,DRS,BET. With Fe^{3+} as electron acceptor at pH=2.0 under UV irradiation and visible radiation. Results show that with appropriate concentration, Vanadium was doped into rutile TiO_2 lattice without causing any change in rutile TiO_2 crystal structure. Therefore, surface oxygen vacancies and the donor energy level near the bottom of the conduction band lead to easier departure of photoinduced electrons from holes to achieve stronger photocatalytic activity. The highest photocatalytic oxygen evolution and PL Spectra intensity were achieved with the O_2 evolution speed of 473umol.L^{-1}.h^{-1} and 88umol.L^{-1}.h^{-1} under UV irradiation and visible radiation when the Vanadium concentration was 1.0mol%, which demonstrated certain relationship between photoluminescence performance affected by Vanadium concentration and the photocatalytic activity. The best initial concentration of Fe^{3+} is 8.0mmol.L^{-1}.

5:15 PM Invited

New Phenomena in Luminescence of Gallium Phosphide: *Sergei Pyshkin*[1]; John Ballato[2]; Michael Bass[3]; Giorgio Turri[3]; [1]Academy of Sciences of Moldova; [2]Center for Optical Materials Science and Engineering Technologies, Clemson University; [3]University of Central Florida

We discuss the phenomena in luminescence of pure and doped GaP as the result of over 40 years ordering of impurity and host atoms. Data obtained between the last TMS conferences confirms the conclusions presented earlier on formation of a crystal lattice where periodically disposed impurities modify, improve and essentially change crystalline properties. The latter will be used as the basic element for new generation of optoelectronic devices. We demonstrate that spectra of bright "hot" luminescence in pure and N doped ordered GaP have deep analogy in origin, shape and position with those obtained in GaP nanocrystals. Unique ordered GaP:N:Sm at the uniformly intermixed impurities generates with high efficiency the luminescence, which depending on intensity of excitation is switched between green (N bound excitons) and yellow-red (Sm activators). These results well correlate with the data obtained from the same crystals in investigations on Raman light scattering and microhardness.

5:40 PM

Bandgap Narrowing of ZnO Films by Cu and In Incorporation: *Sudhakar Shet*[1]; Kwang-Soon Ahn[1]; Yanfa Yan[1]; Todd Deutsch[1]; Muhammad Huda[1]; Nuggehalli Ravindra,[2]; Mowafak Al-Jassim[1]; John Turner[1]; [1]National Renewable Energy Laboratory; [2]New Jersey Institute of Technology

ZnO thin films with significantly reduced bandgaps were synthesized by co-doping of Cu and Cu and In at room temperature and followed by post-deposition annealing at 500°C in air for 2 hours. All the films were synthesized by RF magnetron sputtering in O2 gas ambient on F-doped tin oxide-coated glass. Structural properties, optical absorption and PEC responses for ZnO:

Cu and ZnO:Cu:In films were investigated. ZnO:Cu and ZnO:Cu:In films with various bandgaps were realized by varying RF power and In concentration respectively. The band gap reduction and photoresponse with visible light for Cu and In incorporated ZnO thin films were investigated. The ZnO:Cu films exhibited higher total photocurrent when RF power was increased to 200 W. The n-type conductivity was confirmed for ZnO:Cu:In film by Mott-Schottky plots and illuminated I-V analysis.

Alumina and Bauxite: HSEC

Sponsored by: The Minerals, Metals and Materials Society, TMS Light Metals Division, TMS: Aluminum Committee
Program Organizers: Sringeri Chandrashekar, Rio Tinto Aluminium Limited; Peter McIntosh, Australus Management Services

Monday PM Room: 296
March 10, 2008 Location: Ernest Morial Convention Center

Session Chair: Benoit Cristol, Rusal Australia, United Company Rusal

2:00 PM Introductory Comments

2:05 PM
Alunorte Safety Performance: *Jorge Lima*[1]; [1]Alunorte

Alunorte have started-up the first two of its 5 production lines in July 1995, with a designed nominal capacity of 1.1 mi t/y. Considering that the project was in slow down for ten years, it was necessary to review and establish new policies and standards for operational training and others. Among those it was very much decisive the commitment with Safety. During the last eleven years the production has increased more than four times. Now Alunorte has five lines in full operation with a nominal capacity of 4,3 mi t/y and around 800 new employees, comprising around 160 operators with no former experience, hired through a CSR program. This paper aims to present the strategies implemented to reduce the Serious Accident Frequency Rate from 22,83, in the first year of operation 1995, down to 1,43 in the last year 2006, when the production reached 3,94 mi t/y.

2:30 PM
Sustainable Development of Chinese Alumina Industry: *Jibo Liu*[1]; Wangxing Li[1]; [1]Aluminum Corporation of China Limited

China has the second largest annual output of alumina in the world, however, the bauxite resources in china are relatively scarce with main content of diaspore which require higher energy consumption and more complex process in alumina production compared with other bauxite. How to produce alumina with low energy consumption and high efficiency resource utilization is an important issue for sustainable development of Chinese alumina industry. In this article, the latest features of bauxite resources and alumina production were introduced; the most important improvement of sustainable development including the aspects of bauxite resources utilization, energy consumption reduction, product quality improvement and environmental protection were illustrated, as well as the future strategy of sustainable development of alumina production in China was described.

2:55 PM
Tailings Impoundment Life Extension at Sherwin Alumina Company: Success Breeds Its Own Challenges: Thomas Ballou[1]; *Ed Peterson*[1]; [1]Sherwin Alumina, L.P.

In the mid-1990s, Sherwin Alumina, realizing that traditional dilute slurry storage of their 3300mt/day of Bauxite residue solids could not be sustained. Sherwin explored dense slurry "stacking" as the apparent least cost/most feasible life extension alternative. Laboratory testing of the residue showed that significant gains were feasible to achieve both objectives, minimal cost and life extension. Initially, stack slope results appeared disappointing; however core analysis of the highly plastic material demonstrated the stacking was achieving consolidation of not only the newly deposited material, but also of the underburden, well in excess of the expected values. As stacking proceeded, new issues arose with stormwater management, internal dike stability, leachate recovery and episodic fugitive dust. Ultimately, stack stability analysis and surface tilling, has allowed Sherwin to manage both placement and crust conditions for optimum life with minimum fugitive dust. The consolidated material exhibits permeability in the 10-8cm/sec range and when treated with simple amendments such as treated effluent it can be directly vegetated.

3:20 PM
Proposed Mechanism for the Formation of Dust Horizons on Bauxite Residue Disposal Areas: *Craig Klauber*[1]; Nicole Harwood[1]; Renee Hockridge[1]; Campbell Middleton[2]; [1]CSIRO Minerals; [2]Billiton Aluminium Australia Pty Ltd

Without some form of mitigation control bauxite residue disposal areas in Mediterranean climates can be subject to large-scale dust lift-off events during summer, with significant environmental impact. Intuitively dust formation relates simply to the process of drying. However, whilst wet solids will not produce dust, the converse is not always true. Both the rate of drying and the composition of the bauxite residue are critical factors in determining whether a potential dust horizon will form. In this work a dust formation mechanism is proposed in which caustic salts transport and effloresce along with a changing phase composition in the brine solids from sodium bicarbonate through to trona and then to carbonate monohydrate. The efflorescence leads to a white dust event, but the carbonate phase change and the associated reduction in sodium molar volume critically breaks inter-particulate bonding between the residue particles leading to a more severe red dust event.

3:45 PM Break

4:00 PM
Waste into Wealth: *Balasubramaniam Subbaian*[1]; Vasanthakumar Rangasamy[1]; [1]Madras Aluminium Company

Red mud generated from Bayer's Process for Alumina production is a high volume solid waste with 60 to 70% solids, doesn't have any wide industrial application. Though valuable elements like Alumina and Silica are available in Red Mud, presence of soda makes it a waste. But presence of Alumina, Silica and Iron Oxide in Red mud compensates for the deficiency of the same components in Limestone which is the primary raw material for Cement production. What makes Red Mud special in cement manufacturing is the presence of soda which neutralizes the sulfur content in pet coke that is used for burning clinker enroute cement production and adds to the cement's setting characteristics. This paper details MALCO's efforts in turning Red Mud considered a Waste into Wealth which otherwise would be lying in the back yards of Alumina Plant requiring special care and attention in storing and handling it.

4:25 PM
Short- and Long-Range Order in Smelter Grade Alumina – Development of Nano- and Microstructure during the Calcination of Bayer Gibbsite: *Linus Perander*[1]; Zoran Zujovic[2]; Margaret Hyland[1]; Mark Smith[3]; Luke O'Dell[3]; James Metson[1]; [1]Light Metals Research Centre; [2]University of Auckland, Department of Chemistry; [3]University of Warwick, Department of Physics

The development of structural features during the calcination of Bayer Gibbsite to produce Smelter Grade Alumina (SGA) is a complex process that involves both a dehydroxylation reaction and a rearrangement of the crystal lattice. The disorder and the co-existence of the transition alumina phases complicate structural and quantitative analysis. In order to evaluate a wider range of structural ordering both XRD and high-field solid-state MAS-NMR were applied on a variety of industrial and laboratory prepared alumina samples. Quantitative information was obtained by simulating the NMR spectra and assigning the peaks to various alumina phases and by Rietveld analysis of the XRD data. Although the thermodynamically stable alpha alumina content can be accurately monitored, the results clearly demonstrate some of the limitations of XRD, especially for quantifying the transition aluminas. An amorphous component, with aluminium in pentahedral coordination, detectable by NMR but not XRD, accounts for part of the observed differences.

4:50 PM
Start-up of the Lines 4 and 5 at Alunorte: Pre-Operational Strategy, Commissioning and Ramp-up: *Anderson Amaral*[1]; Jorge Lima[1]; Joaquim Filho[1]; [1]Alunorte

Alunorte began its operation in 1995 with two production lines and a designed nominal capacity of 1.1 mi t/y. Trough process improvements and minor investment this capacity was increased up to 1.6 mi t/y in 2000. In 2003 the third line was started-up increasing this capacity to 2.5 mi t/y. In 2006 the capacity of 4.3 mi t/y was reached, after the start-up of the lines 4 and 5. This paper aims to present the strategies implemented for the pre-operational, commissioning and ramp-up stages for the lines 4 and 5, allowing Alunorte to achieve the nominal daily production capacity in only 20 and 12 days respectively, emphasizing that this excellent result was achieved with the low index of 1.43 for Serious Accident Frequency Rate and that 50% of the operators were hired with no previous experience.

Aluminum Alloys: Fabrication, Characterization and Applications: Processing and Properties

Sponsored by: The Minerals, Metals and Materials Society, TMS Light Metals Division, TMS: Aluminum Committee
Program Organizers: Subodh Das, Secat Inc; Weimin Yin, Secat Inc

Monday PM Room: 293
March 10, 2008 Location: Ernest Morial Convention Center

Session Chairs: Subodh Das, Secat Inc; Weimin Yin, Secat Inc; Gyan Jha, ARCO Aluminum Inc

2:00 PM
Press Formability of Twin Roll Cast Aluminum Alloys for Automotive Applications: *Sooho Kim*[1]; Anil Sachdev[1]; [1]General Motors Research and Development Center

This study characterizes the material properties of low-cost twin roll cast (TRC) aluminum alloys, AA3005, AA5052 and AA5754. Tensile properties and forming limit curves of TRC AA5754 are comparable to those of AA5052, due to its lower limit of Mg content (2.6%), coarser grain structure and higher degree of centerline segregation with Fe-rich intermetallic particles. The grain size of TRC AA3005 is much larger than those of the other TRC 5xxx materials, but its plane strain limit is higher than the others, indicating its higher formability. The press formability tryout of all three TRC materials in actual stampings will be demonstrated.

2:20 PM
Forging of Long Flat Pieces of Aluminium with a Precise Mass Distribution Operation: *Malte Stonis*[1]; [1]Institute of Integrated Production Hannover

In the automotive forging industry parts made of aluminum alloys are used more often due to the favorable strength to mass relationship and their high ductility. A possibility for preform processes for long flat pieces is a multi-directional forging operation in partly closed dies. In a current project a multidirectional forming operation with three main axial directions is analyzed using FEM simulations. During the forging process, every two of three directions are combined with the third forming direction inactivated. The simulations are evaluated and analyzied regarding the form filling, the formation of flash and the development of temperature and fiber orientation. It was shown that with some combinations it is possible to realize a succesful forming operation with the advantage of decreasing the quota of flash in comparison to conventional preforming processes. The detected optimal combination will be verified in a real forging process.

2:40 PM
Hemispherical Bubbles Growth on Electrochemically Charged Aluminum with Hydrogen: *Paul Rozenak*[1]; [1]Hydrogen Energy Batteries Company

The formation of surface bubbles (blisters) in aluminum during electrochemical charging by hydrogen was studied. The experiments reveal that, in aluminum samples, a wide distribution of hydrogen bubbles on the surface (blisters) were produced during electrochemical charging. A wide variety in density, distribution and geometrical shape of the surface bubbles was obtained, with sizes ranging from large (tens of micrometers in the diameter) to very small (nanometers in the diameter). Bubble growth in a various shapes is controlled by hydrogen diffusion to the surface layer of the aluminum, from the defects region below it together with separation of cohesive atomic bonds between the hydroxide layer and the aluminum matrix. In such electrochemically charged aluminum the various hydrogen bubble structures formed during the growth process in the hydroxide layer, can be developed mathematically by the principles used in obtaining the shapes of the grains-boundaries in the polycrystalline microstructures of material.

3:00 PM
Mechanical Properties of Various Aluminum Alloys by Powder Metallurgy: *Antonyraj Arockiasamy*[1]; Seong Park[1]; Randall German[1]; [1]Mississippi State University

Complex aluminum alloy components economically fabricated by powder metallurgy (P/M) offer high strength-to-weight ratio, which meets the demands of the automotive sector. This paper describes die compaction and sintering behavior as well as mechanical properties of various aluminum alloy powders, containing Mg, Cu, Ti, Si and SiC, produced by conventional mixing based on a rapidly solidified 6061 alloy matrix. Three-point bending test, hardness test, dilatometer, TGA/DSC, and SEM/EDS were extensively employed for this study. Comparisons are based on density, flexural strength, and hardness, complimented by microstructure analysis. The overall consolidation is modeled using 3D finite element simulation for optimization of process conditions.

3:20 PM
Formability of Work Hardenable and Heat Treatable Aluminum Alloy Periodic Cellular Metals: *Eral Bele*[1]; Lily Cheng[1]; Brandon Bouwhuis[1]; Glenn Hibbard[1]; [1]University of Toronto

Periodic Cellular Metals (PCMs) are open cellular lattices which have a greater structural efficiency than conventional metallic foams. They can be fabricated using perforation stretching methods, in which the nodes of a perforated starting sheet are displaced above and below the plane to form three-dimensional architectures. This approach offers the advantage of being able to tailor the properties of the cellular core by a combination of architectural design, material selection and thermo-mechanical treatments. The focus of this study is the perforation stretching formability of aluminum alloy PCMs. A finite element model is used to investigate the mechanisms that control the load-displacement forming curves of pyramidal cores fabricated from both work-hardenable (AA3003) and heat treatable (AA6061) aluminum alloys.

3:35 PM
The Welding Behaviours of Hot and Cold Rolled AL 5754 Alloys and Residual Stress Analysis: *Firat Esit*[1]; Özgül Keles[1]; I. Yilmaz Taptik[1]; [1]Istanbul Technical University

Comparison to steels, aluminum is one over three times lighter on the contrary some aluminum alloys have the strength as high as steels. Furthermore, some of these aluminum alloys have application areas in automobile, shipbuilding, food processing and aviation industries because of their good corrosion resistance. Especially, Al 5000 (Al-Mg-Mn) alloys became the most popular metal in shipbuilding, food and chemical processing areas to meet the need of developing technology. Joint by welding has lots of defects which cause many serious damages in weldments in service conditions. Particularly, loss of strength and residual stress after welding are common problems in aluminum welding. In this work, welding behaviors of hot and cold rolled Al 5754 alloys are worked out. The aim of the study is analyzing the weldability features between two different alloys depend on the manufacturing methods, and the relations between welding parameters and weldability.

3:50 PM Break

4:00 PM
The Ablation Casting Process: John Grassi[1]; *John Campbell*[1]; [1]Alotech Limited

A new casting process is described, based on a precision aggregate mold, bonded with a water-soluble binder. For the first time the functions of the mold (i) defining shape and (ii) providing cooling have been successfully separated. Thus thin-walled castings can be filled without the loss of significant temperature,

allowing the production of extensive thin castings. Because solidification is separately controlled by the application of water a number of advantages follow immediately. The mold is ablated (i.e. eroded) away by the water without fume or dust, and the 'air gap' is eliminated by direct water contact with the cooling casting enhancing the rate of solidification to levels normally unattainable, resulting in significantly enhanced properties. The process is currently proving itself in commercial operation, having the additional advantages of modest costs of capital equipment and low piece part costs because of the use of low cost and recycling of consumables.

4:20 PM

Study of the Effects of Heating Rate on 7000 Series Aluminum Alloys: Courtney Nowill[1]; *Mohammed Maniruzzaman*[1]; Satya Shivkumar[1]; Richard Sisson[1]; [1]Worcester Polytechnic Institute

The quench sensitivity of various alloys has been studied with the use of the Jominy end quench test. Some studies have shown that heating rates also have an effect on mechanical properties, but data is scarce in the literature. A methodology has been developed in order to study the effects of heating rates. The apparatus designed is for a type of "reverse" Jominy test and results in one dimensional heating throughout the specimen, and therefore, a distribution of heating rates. Two 7000 series alloys, AA7075 and AA7136, were heated using this method to study the effects of heating rate on both solution and aging heat treatments. The effects of a rapid heat up by immersion in a salt bath were also studied versus the effects of a slow air furnace heat up. This study provides a better understanding of the effects of heating rate on 7000 series aluminum alloys.

4:40 PM

Strength-Toughness Optimization Scenarios through Interrupted Ageing in AA6061 and AA2024: *Doty Risanti*[1]; Pedro Rivera Diaz del Castillo[2]; Sybrand van der Zwaag[2]; [1]Netherlands Institute for Metals Research; [2]Delft Technical University

Aimed at maximisation of strength-toughness relationships in aluminium alloys, interrupted ageing has been proposed as a means to combine these properties. Such processing schedule initiates with a T6 short underageing (177°C for up to 1 hour) followed by a dwell period at a lower temperature for periods up to two weeks and re-aged to the T6 temperature. By combining DSC with hardness, tensile and Kahn-tear testing in studied alloys, the present work studies several heat treatment scenarios and their impact in strength-toughness improvements. Dwell temperatures above 65°C result in a hardness increase whereas those below 45°C decrease it in comparison to the standard T6. DSC scans of AA6061 reveal that dwell temperatures above 65°C lead to an increase in the dissolution of clusters which cannot evolve into GP-zones and β"-precipitate, while in AA2024 it leads to the formation of GPB2-zones. Toughness behaviour for different heat treatment scenarios is presented.

5:00 PM

The Evolution of Microstructure in Rapidly Solidified Al-Si Powders: *Eren Kalay*[1]; Scott Chumbley[1]; Iver Anderson[1]; [1]Ames Laboratory/Iowa State University

Increasing demand for lightweight materials has helped Al-Si alloy to become a key alloy systems in many industrial applications. In this study, the as-quenched microstructures of Al-Si produced by high pressure gas atomization at eutectic (12.6 wt% Si) and a hypereutectic composition (18 wt% Si) were investigated using scanning electron microscopy (SEM) and transmission electron microscopy (TEM) with respect to particle size. The interface growth velocities and undercooling values were estimated from Jackson-Hunt (JH) and Trivedi-Magnin-Kurz (TMK) solidification models. TEM studies showed that the particle size at which JH and TMK predicts a divergence is consistent with the appearance of microcellular growth morphology. High amount of solute trapping was observed with the evolution to microcellular microstructure. Enhanced solute trapping was determined using energy dispersive spectroscopy and x-ray diffractometry and it was compared with the results obtained from Cu block melt spinning experiments at similar compositions.

5:15 PM

Preparation of Al-Sr Alloys with High Concentration by Molten Salt Electrolysis: *Jidong Li*[1]; Mingjie Zhang[1]; Tingan Zhang[1]; Dan Li[1]; [1]Northeastern University

Al-Sr alloy was prepared by molten salt electrolysis in electrolyte system of SrCl¬2-SrF2-BaF2. Back electromotive force was measured by continuous pulse-computer and the influencing factors for back electromotive force and current efficiency were studied in detail. The result is as follows: the back electromotive force increases with the cathodic current density increasing; when the electrode distance raising, the back electromotive force also increases in a little; with the increase of electrolysis duration, the back electromotive force increases gradually whereas the current efficiency decreases gradually after reaching 73.2%; as the increase of electrolysis duration, the current intensity increasing and the amount of aluminium master alloy decreasing, a high strontium content of 34.8%(mass fraction) in Al-Sr alloy can be obtained.

5:35 PM

Preparation of Al-Li Alloy by Molten Salt Electrolysis: *Jidong Li*[1]; Mingjie Zhang[1]; Tingan Zhang[1]; Zhuo Zhang[1]; Dan Li[1]; [1]Northeastern University

Al-Li alloy was prepared with Li2CO3 as raw material by using liquid aluminium cathode and a mixture of LiF-KF-BaF2 as the molten salt electrolysis in a laboratory electrolyte cell. The back electromotive force was measured by the monitoring apparatus of molten salt electrolysis. The factors effecting on back electromotive force, current efficiency, period of feeding and lithium content of Al-Li alloy were studied in detail. Finally, at 770°C, the lithium content of 9.6%(mass fraction) in Al-Li alloy can be obtained by electrolyzing for 5h in the cathodic current density of 0.5A/cm2, which the current efficiency can reach 74%. It is affirmed by SEM that the distribution is uniform.

5:55 PM

The Preparation of Al-Sc Alloy by Molten Salt Electrolysis: *XiuJing Zhai*[1]; Yan Fu[1]; Junfu Li[1]; Mingjie Zhang[1]; [1]Northeastern University

The paper was studied on the preparation of Al-Sc alloy by molten salt electrolysis with LiF-ScF3-ScCl3 as the electrolyte. ScCl3 and Sc2O3 were used as raw material. And the processing condition of the preparation of Al-Sc alloy which include the influence of current density,the composition of the electrolyte and the electrolysis time were carefully studied respectively. As electrolysis time prolonged, the current efficiency increases gradually and can reach to 73% as the maximum. The content of Sc in alloy can reach to 5.86%. In this experiment condition, the period of adding material is 1g /20 min. It was proved that the current from 2A to 4A and temperature of 850°C is feasible.

Aluminum Reduction Technology: Sustainability and Environment

Sponsored by: The Minerals, Metals and Materials Society, TMS Light Metals Division, TMS: Aluminum Committee
Program Organizers: Martin Iffert, Trimet Aluminium AG; Geoffrey Bearne, Rio Tinto Aluminium Tech

Monday PM — Room: 298
March 10, 2008 — Location: Ernest Morial Convention Center

Session Chair: Nancy Jorunn Holt, Hydro Aluminium AS

2:00 PM

Innovative Solutions to Sustainability in Hydro: *Hans Petter Lange*[1]; Lene Solli[1]; Nancy Jorunn Holt[1]; Hogne Linga[1]; [1]Hydro

Sustainability represents challenges for the Aluminium industry but also opportunities. Innovation is essential in meeting these challenges. By being innovative and by having a sustainable approach to the whole value chain, there are large potential for improvements both environmentally as well as financially. Hydro have an innovative approach looking at the value chain from power production to the end user of aluminium products which is improving Hydro's environmental footprint as well as it is generating value for Hydro. The two main challenges the industry is facing today is climate change and energy consumption. In this paper we will show how Hydro systematically have worked

to reduce energy consumption as well as share with you what Hydro is working on for future improvements. Main focus on GHG was AE reduction. Today we are talking about CO2 capture on the energy production side as well as from the reduction process itself.

2:20 PM Invited
Smelters in the EU and the Challenge of the Emission Trading Scheme: *Heinrich Kruse*[1]; [1]Corus Aluminium Voerde GmbH

The majority of scientists believe that the increasing amounts of CO2 emitted into the atmosphere by mankind will have severe impacts on the world's climate. The Kyoto protocol was one of the first attempts to reduce CO2 emissions all over the world significantly. To enforce the protocol's intention within the EU, the commission had introduced the so called "Emission Trading Scheme" (ETS). This brought the EU into a leading position regarding the reduction of CO2 emissions. For those parties, who are already affected by the ETS, the emission of CO2 is no longer free of charge. Although the aluminium smelting industry in the EU is exempted from the ETS, it is indirectly – but significantly – affected due to the increasing prices for electrical energy. This paper will give a brief overview about the impacts of ETS and of the national schemes for the competitiveness of the EU aluminium smelters.

2:40 PM
Wireless Measurement of Duct Temperatures on Aluminum Smelting Pots: Correlation to Roofline HF Concentration: Daniel Steingart[1]; *James Evans*[2]; Andrew Redfern[1]; Paul Wright[2]; Neal Dando[3]; Weizong Xu[3]; Michael Gershenzon[3]; Henk Van der Meyden[3]; [1]Wireless Industrial Technologies; [2]University of California; [3]Alcoa Inc

Previous papers described wireless devices (motes) for measuring the temperature of the gas in ventilation ducts from smelting pots, and the heat flux through the pot shells. This paper describes more extensive, longer measurements of duct temperature carried out on ten pots at a smelter in 2006. Measurements were carried out for 43 days and 1.3 million temperatures were recorded, along with simultaneous real-time measurements of roofline HF concentration. The duct motes were self-powered using thermoelectric generators operating off temperature differences between the duct gasses and the surrounding air. Temperatures measured by the motes reflected all pot-work such as removal of cover panels or opening of end doors. Temperature measurements showed a good correlation with roofline measurements of HF above the pots. Even after elimination of temperatures when the pot were clearly being worked, significant variations in duct temperature were observed, both from pot-to-pot and from day-to-day on individual pots.

3:00 PM
Hard Gray Build-Up: Neal Dando[1]; *Stephen Lindsay*[1]; [1]Alcoa Inc

The dry scrubbing and secondary alumina handling systems for pre-bake cell technologies are hampered by accumulations of hard gray build-up, or HGB. These mineral-like deposits are dependant upon a number of factors that control the rate of scale formation. If not systematically addressed with cleaning and maintenance procedures HGB can: greatly reduce the removal efficiency of gaseous fluoride in dry scrubbers, reduce the capability to convey alumina in sufficient quantities, reduce filter life and alter the concentration of fluoride on secondary alumina. This paper will define the chemical structure of HGB, propose a mechanism for HGB formation, identify the key areas of concern in a smelter and discuss practical alternatives to control the rate of formation.

3:20 PM Break

3:30 PM
Comparison of PFC Emission Rates for Operating and Newly Started Pots at a Horizontal Stud Soderberg Smelter: *Neal Dando*[1]; Weizong Xu[1]; Steven Rusche[1]; [1]Alcoa Inc

Anode effect durations are commonly described as "total time above 8 volts," wherein the total pot operating time above 8 volts is integrated and used to estimate perfluorocarbon (PFC) emissions. Soderberg smelting pots are known to exhibit sustained periods of time where operating voltage may exceed 8 volts (commonly 8-10 volts), however the pots do not exhibit ore starvation, nor do they exhibit "typical" anode effect behavior (i.e. rapid voltage spikes to 20-50 volts). This behavior is observed during pot startups, as well as during "normal" pot operations. Continuous PFC monitoring studies of individual horizontal stud Soderberg pots were performed during startup and during normal operation to show that Soderberg pots exhibiting sustained elevated operating voltages (8-10V) in the absence of ore starvation do not generate PFC emissions. These observations suggest that an anode effect (AE) definition of "time > 8 volts" would overestimate true AE durations at Soderburg smelters.

3:50 PM
Reduced Emissions from the Elkem Aluminium Lista Søderberg Smelter: *Tor Pedersen*[1]; Marianne Jensen[1]; Kjell Kalgraf[1]; Willi Larsen[1]; Arnt Olsen[1]; [1]Elkem Aluminium ANS

Elkem Aluminium Lista has worked on developing its Søderberg Technology for many years. Dry paste was introduced in the early eighties. In 1986 Elkem Aluminium decided to develop a closed point feeding technology and improve the pot gas collection system. It was also decided to develop a technology to collect and clean the fumes from the Søderberg anode tops. These technologies are now developed and installed at the smelter. The point feeding technology comprises a complex of elements such as feeding locations, pot signal filtering, alumina feed algorithm, design of the point feeding system, equipment and not at least the standard operating practices. The technology has resulted in a substantial drop in the anode effect frequency, giving an according reduction in the emission of climate gases. The technology has also led to big reductions in fluoride, particulate and PAH emissions. Low emissions can be obtained even with an increased production.

4:10 PM
Comparison of PFC Emission Coefficients for Operating and Startup Pots at a Side Work Prebake Smelter: *Weizong Xu*[1]; Neal Dando[1]; David Sedlacek[1]; [1]Alcoa Inc

Tier 3b perfluorocarbon (PFC) emission coefficients are determined by performing ventilation duct PFC measurements under normal potline operation and used to estimate plant-specific PFC emissions based upon integrated anode effect duration. To-date, little information exists regarding the PFC emission of newly started pots relative to those under normal operation. In addition, the practice of including or excluding anode effect data from newly started pots is not uniform between aluminum smelters. Two PFC monitoring campaigns were performed during a side work prebake (SWPB) potline restart at an Alcoa smelter in 2007. The measured PFC slope terms agreed well (< 10%) from these two tests, and were also consistent with 2006 benchmarked data, suggesting that no significant difference exists between new and "old" pot PFC emission coefficients. This data also suggests that anode effect data from newly started prebake pots should be included in the plant's PFC reporting inventory.

4:30 PM
Study on the Anode Effect Reduction at Zhengzhou Research Institute of CHALCO: *Wangxing Li*[1]; Qingyun Zhao[1]; Shilin Qiu[1]; Hengwei Yan[1]; [1]Zhengzhou Research Institute of CHALCO

In order to cope with environment limits, many aluminum smelters are being forced to adapt their operations to reduce the emission of greenhouse gas. The anode effect plays an important role in PFC emission. So reducing the anode effect is an emergency task for primary aluminum smelters. Zhengzhou Research Institute of CHALCO (ZRIC) has achieved a substantial improvement on anode effect rate reduction in the prebaked cells with point-feeders. Those achievements mainly based on some initiatives in cell control and management. As a result of industrial experiment on somes real life pots, the anode effect rate has dropped from 0.35 to 0.03 anode effects per cell day (AE/C/D), which is an excellent result. This paper mainly presents the basic research on AE and some experiences on AE reduction, as well as the implementation of AE quenching techniques.

Biological Materials Science: Implant Biomaterials I

Sponsored by: The Minerals, Metals and Materials Society, TMS Structural Materials Division, TMS: Biomaterials Committee, TMS/ASM: Mechanical Behavior of Materials Committee
Program Organizers: Ryan Roeder, University of Notre Dame; Robert Ritchie, University of California; Mehmet Sarikaya, University of Washington; Lim Chwee Teck, National University of Singapore; Eduard Arzt, Max Planck Institute; Marc Meyers, University of California, San Diego

Monday PM Room: 390
March 10, 2008 Location: Ernest Morial Convention Center

Session Chairs: Ryan Roeder, University of Notre Dame; Albert Lin, University of California, San Diego

2:00 PM Invited
Phase-Separated Hydrogels Comprised of Both Hydrophilic and Hydrophobic Segments: *James Mason*[1]; Brian Thomas[1]; Mike Wallick[1]; Don Yakimicki[1]; [1]Zimmer Inc.

Typical hydrophilic hydrogels lack the required mechanical properties to be useful as articulating and weight bearing mediums. Therefore, hydrogels were developed which incorporated both a hydrophilic and a hydrophobic segment. These new hydrogels behave like semi-crystalline polymers utilizing both crystalline regions and amorphous regions. The hydrophilic segments (amorphous regions) provide the water absorption, fluid flow, and lubricious properties. The hydrophobic segments (crystalline regions) provide the strength, tear, shear and creep resistance. The initial focus of the work presented here was to provide a material with higher strength, ease of processing, and better shear resistance that can be injection molded. Therefore, efforts focused on utilizing polymer blends and reactive compounding. When tested, the new hydrogels show improved mechanical properties without loss of lubricity.

2:30 PM
Evaluation of a Synthetic Vertebral Body Augmentation Model for Rapid and Reliable Cyclic Compression Testing of Materials for Balloon Kyphoplasty: *Gladius Lewis*[1]; Jeffrey Schwardt[2]; Thomas Slater[2]; [1]University of Memphis; [2]Kyphon, Inc.

A validated synthetic vertebral body augmentation model — a cube (26 mm sides) of low-density polyurethane foam with a centrally-located through-thickness cylindrical hole completely filled with a bolus of augmentation material — was used to compare two balloon kyphoplasty (BKP) augmentation materials with very different chemistries (a high-viscosity acrylic bone cement (PMMA) and a calcium phosphate bone substitute (CP)) in cyclic compression tests. The model was immersed in PBS, at 37°C; the frequency was 3 Hz; and the maximum load was either 1150 N or 2300 N. Clear demarcation was seen in the qualitative results (fracture patterns) and the quantitative results (Kaplan-Meier survival analysis of the number of cycles to failure) obtained with the two materials tested. Thus, the use of this model for rapid and reliable ex vivo screening of BKP augmentation materials was considered both valid and appropriate (that is, clinically relevant to BKP).

2:50 PM
Rapid Prototyping of Biological Materials: Aleksandr Ovsianikov[1]; Boris Chichkov[1]; Anand Doraiswamy[2]; *Roger Narayan*[2]; [1]Laser Zentrum Hannover; [2]University of North Carolina and North Carolina State University

Recent studies have shown that rapid prototyping techniques may be used to create patient-specific medical devices and artificial tissues. In this presentation, recent advances in the use of laser direct writing and two-photon polymerization to fabricate microstructured medical devices and scaffolds for tissue engineering will be discussed. For example, we have used two-photon polymerization for rapid prototyping of microneedles and middle-ear bone replacement prostheses. In addition, we have developed differentially adherent surfaces using laser direct writing process. In this work, 60-400 micrometer-wide diameter channels were micromachined onto agarose surfaces using an ArF excimer laser and filled with extracellular matrix solution. Muscle-like and nerve-like cells were then allowed to proliferate on the surfaces of these micromachined channels. Our results demonstrate that laser-based rapid prototyping techniques may be used to fabricate medical devices with a larger range of sizes, shapes and materials than conventional microfabrication techniques.

3:10 PM
Microstructures and Mechanical Properties of Electron Beam – Rapid Manufactured Ti-6Al-4V Biomedical Prototypes Compared to Wrought Ti-6Al-4V: *L. Murr*[1]; E. Esquivel[1]; S. Quinones[1]; S. Gaytan[1]; M. Lopez[1]; E. Martinez[1]; D. Hernandez[1]; E. Martinez[1]; J. Martinez[1]; T. Hoppe[2]; W. Meyers[2]; S. Stafford[1]; R. Wicker[1]; F. Medina[1]; U. Lindhe[3]; [1]University of Texas; [2]Stratasys; [3]Arcam AB

This study represents an exploratory characterization and comparison of electron-beam manufactured (EBM) or rapid-prototype (RP) manufacturing of Ti-6Al-4V components (from nominal 30 μm diameter powder) with wrought products. Acicular α and β microstructures observed by optical metallography and electron microscopy (SEM and TEM) are compared along with corresponding tensile test and hardness data; including the initial powder particles where the Vickers microindentation hardness averaged 5.0 GPa in comparison with the fully dense, EB manufactured product with an average microindentation hardness ranging from 3.6 to 3.9 GPa. This compares with wrought products where the Vickers microindentation hardness varied from 3.4 to 5.4 GPa. Biomaterials/biomedical applications of EBM prototypes in direct prosthesis or implant manufacturing from CT or MRI data are reviewed in the context of this work, especially prospects for the tailoring of properties through EB control to achieve customized implant and prosthetic products direct from CT-scans.

3:30 PM Break

3:40 PM Short Oral Presentations for the Student Poster Contest

Bulk Metallic Glasses V: Structures and Mechanical Properties II

Sponsored by: The Minerals, Metals and Materials Society, TMS Structural Materials Division, TMS/ASM: Mechanical Behavior of Materials Committee
Program Organizers: Peter K. Liaw, University of Tennessee; Wenhui Jiang, University of Tennessee; Guojiang Fan, University of Tennessee; Hahn Choo, University of Tennessee; Yanfei Gao, University of Tennessee

Monday PM Room: 393
March 10, 2008 Location: Ernest Morial Convention Center

Session Chairs: A. L. Greer, University of Cambridge; Jurgen Eckert, IFW Dresden

2:00 PM Keynote
Effects of Shear Banding on the Structure and Properties of Metallic Glasses: *A. L. Greer*[1]; [1]University of Cambridge

It is well known that under ambient conditions, metallic glasses show plasticity in the form of shear bands. The localization of deformation in bands as little as 10 nm thick implies extreme conditions of high shear rate, high shear, high heating rate and cooling rate. The consequences of these conditions for the structure of the glass after shear will be reviewed, taking account of recent structural and calorimetric studies. The possibilities for using shear banding to tailor properties will be considered.

2:30 PM Invited
How to Improve the Deformability of Bulk Metallic Glasses: *Jurgen Eckert*[1]; [1]IFW Dresden

Metallic glasses have mechanical properties that make them attractive candidates for a variety of structural and functional applications. One drawback still limiting such applications is their tendency for shear localization upon deformation. To circumvent such limitations, concepts of creating heterogeneous materials with different type and length-scale of phases have been followed to control the mechanical properties by proper alloy and microstructure design. The recent developments along this line will be summarized and new results for different types of bulk metallic glasses and composites will be presented

to illustrate how the mechanical properties can be tuned by appropriate phase and microstructure control. In all these cases the details of the metastable phase formation are closely linked with optimized processing conditions required to form the desired microstructure. The possible mechanisms that govern the deformation behavior will be discussed and linked with the overall plastic deformability and the fracture of the material.

2:50 PM Invited
Size Effect in the Deformation and Failure of Metallic Glasses: *Ju Li*[1]; [1]Ohio State University

Recent experimental and theoretical work have suggested possible size effect in the plasticity and failure resistance of metallic glasses. While bulk metallic glasses manifest negligible tensile ductility, nanoscale metallic glasses show significant ductility under tension (PNAS 104, 11155). Nanopillar compression experiments also show intriguing behavioral differences sensitive to pillar size. Multiple reasons could contribute to this size dependence: (a) proliferation of amorphous-crystal interfaces or surfaces that directly mediate plasticity, as well as indirectly alter the glass structure, (b) Weibull-like statistics for the nucleation of a runaway flow defect from the condensation of shear transformation zones in a finite volume, and (c) intrinsic thermomechanical lengthscales, such as the glue zone width in the aged-rejuvenation-glue-liquid model of a runaway shear band (Acta Mater. 54, 4293). A "Hall-Petch" like relationship may exist with respect to the metallic glass sizescale, but for the useful ductility (tensile and compressive) instead of strength.

3:10 PM Invited
Size Dependence of Compressive Strength of a Zr-Based BMG: W.F. Wu[1]; *Yi Li*[1]; [1]National University of Singapore

A sample size dependence of the compressive strength has been established for a Zr-based bulk metallic glass (BMG) with a statistical method. Two competing factors, namely, free volume effect and flaw-sensitivity effect were found to affect the apparent strength of BMGs with different specimen sizes. As a result, there was a critical size with which the strength of BMG reached a maximum. In addition, a size dependence of Weibull modules was observed which is attributed to the fact that the resulted BMG samples possessed various structural configurations due to the different size dependence cooling rate. The decrease in Weibull modulus as the sample size increases indicates a deterioration of mechanical reliability for larger-sized BMG component.

3:30 PM Invited
Studies of Shear Band Propagation Using Spatially and Temporally Resolved Measurements of Strain During Compression of a Bulk Metallic Glass: *Wendelin Wright*[1]; Jeffrey Florando[2]; Mary LeBlanc[2]; Todd Hufnagel[3]; [1]Santa Clara University; [2]Lawrence Livermore National Laboratory, Engineering Technologies Division; [3]Johns Hopkins University

As a shear band rapidly deforms during constant displacement rate compression testing of bulk metallic glasses, the displacement rate of the material in the band exceeds the displacement rate imposed on the sample. Consequently, the load drops, and the load train and the bulk of the sample elastically recover. Previous work has recorded some features of these serrations, but typically only the sample average displacement is measured. Strain gages were applied to each side face of rectangular parallelpiped specimens which were then subjected to quasi-static uniaxial compression. The data indicate the existence of a latent period between the onset of strain events as recorded on opposing faces of the sample. The results also show that strain gages on opposing sides of the sample record strain events of opposite sign (tensile vs. compressive). The implications of this data for shear band initiation and propagation in bulk metallic glasses will be discussed.

3:50 PM Break

3:55 PM Invited
The Amorphous to Crystalline Massive Transformation in Al-10 at%Sm: Jason Hadorn[1]; *Gary Shiflet*[1]; [1]University of Virginia

Melt-spun amorphous Al90Sm10 ribbon has been previously documented to crystallize via massive transformation. In this study, the crystallization of this material was studied and analyzed using XRD, TEM, and EDS in order to determine whether or not this phase transformation met the requirements for a massive transformation. Crystallization was observed to be a single-phase to single-phase phenomenon and to occur without any chemical partitioning, both requirements for such a transformation. Additionally, the growth of the crystallized product phase was observed to be linear, a property also characteristic of a massive transformation. From analysis of the growth rate, an activation energy for growth of a precipitate was calculated. In addition to crystallization, subsequent phase transformations were observed en route to the equilibrium state. These other transformations were analyzed via similar methods, and an isothermal TTT curve was consequently constructed.

4:15 PM Invited
Mechanical Properties and Fracture Behaviors of Bulk Amorphous Alloys: *Jun Shen*[1]; [1]Harbin Institute of Technology

In this presentation, we will report on the observation of elastic-wave patterns on nano-scale that form in the compressive fracture process of a Ni-based amorphous alloy. The formation of nano-waves is evidenced via the creation of microbranching instability as well as the interaction of a crack front with the material inhomogeneities, i.e., micro-cracks. We will also report on the dramatic effect of sample size on the plastic deformation capability of a Ti-based bulk metallic glass. Compared with the larger one, the smaller size glassy alloy with the same chemical composition exhibits significantly enhanced plasticity, suggesting a "smaller is softer" trend of metallic glasses. The phenomenon is attributed to the fact that the smaller size alloy, which experienced a faster cooling rate during solidification, contains a larger number of soft regions - free volume sites, favoring the preferential nucleation of shear bands and thus allowing enhanced plasticity upon compressive loading.

4:35 PM
Effect of Temperatures on Plastic Flow and Shear Bands in a Zr-Based Bulk-Metallic Glass: *Wenhui Jiang*[1]; Fengxiao Liu[1]; Peter K. Liaw[1]; Hahn Choo[1]; Ran Li[2]; Tao Zhang[2]; [1]University of Tennessee; [2]Beijing University of Aeronautics and Astronautics

The recent development of bulk-metallic glasses (BMGs) makes the applications of metallic glasses as structural materials become reality. However, the poor ductility and subsequent premature fracture, which are imputed to the highly-localized inhomogeneous deformation, still limit their applications. In spite of intensive studies on the inhomogeneous deformation of metallic glasses, there are still inconsistent understandings on inhomogeneous-deformation behavior. It is known that strain rate and temperature are two important external factors affecting deformation behavior of BMGs. While some research focuses on effect of strain rate, little work has been done on effect of temperature. In this talk, we will present our recent work on the inhomogeneous deformation of a Zr-based BMG at various temperatures and strain rates. Based on the shear-banding spatiotemporality that we observed, we can explain strain-rate- and temperature-dependences of shear-banding operations and serrated plastic flows. The work provides new insights into the inhomogeneous-deformation behavior of bulk-metallic glasses.

4:50 PM
Rate Dependence of Shear Banding in a Mg-Based Bulk Metallic Glass Characterized by Nanoindentation: *Shuangxi Song*[1]; J.S.C. Jang[2]; T.G. Nieh[1]; [1]University of Tennessee; [2]I-Shou University

Nanoindentation behavior of Mg57Cu31Y6.6Nd5.4 bulk metallic glass was characterized at different loading rates. The load-displacement curves exhibit significant displacement serrations, apparently associated with discrete shear-band emission, at low loading rates but disappear at high rates. Analyses based on displacement serration, strain rate oscillation and hardness serration were carried out to determine the critical strain rate at which the transition from inhomogeneous to homogeneous deformation takes place. It was concluded that hardness serration analysis probably provides the most reasonable result as the other two were limited by the instrument noises. From a shear band nucleation model the critical nucleus size was also estimated to be a sphere of about 25 nm in diameter.

5:05 PM
Rate- and Temperature-Dependent Shear Band Initiation and Implications on Ductile to Brittle Transition: *Yanfei Gao*[1]; T. Nieh[1]; Takeshi Egami[1]; [1]University of Tennessee and Oak Ridge National Laboratory

Shear banding behavior in amorphous alloys is very sensitive to the environmental temperature, the applied strain rate, and the geometric constraints. The competition between cleavage fracture and crack tip blunting

in the amorphous alloy is studied by numerically determining the responses of a crack subjected to a history of applied stress intensity factor. The brittle fracture is modeled by a traction-separation law in the crack plane. The amorphous alloy is modeled by a viscoplastic constitutive law in which the viscosity depends on the free volume, while the free volume evolution equation is driven either by shear or by hydrostatic tension. Because of the strain softening and strain rate hardening behavior, it is found that at low loading rate, the initiation of shear bands will reduce the stress concentration, while the fracture behavior is brittle at high loading rate. A preliminary assessment of ductile fracture is also presented.

5:20 PM

Ductilization of Brittle Bulk Metallic Glass by Deformation at Room Temperature: *Min Ha Lee*[1]; Kwang Seok Lee[1]; Jayanta Das[1]; Uta Kühn[1]; Jürgen Eckert[1]; [1]IFW Dresden

Metallic glasses, especially bulk metallic glasses (BMGs) are well-known interesting for their exceptional properties, including high strength, relatively low Young's modulus, and perfect elastic behavior. However, in the case of typical glassy metallic alloys, there are no well-defined atomic planes or slip systems, and it is well established that at temperatures below the glass transition temperature (Tg), inhomogeneous plastic deformation occurs, during which localized narrow shear bands are formed and plastic flow is confined to these shear bands resulting in catastrophic failure. As a result BMGs show little macroscopic room temperature plasticity. To understand the plasticity in BMGs based on a comparative study between as-quenched state and the severely deformed state in typical brittle monolithic BMG, in the current study, we compare the physical and thermo-mechanical properties between the as-quenched state and the severely deformed state (structurally relaxed state) of typical monolithic BMG.

5:35 PM

Comparison of Formability between Zr-Based Monolithic Bulk Metallic Glass and Bulk Metallic Glass Composite in Supercooled Liquid Region: *Hyun-Joon Jun*[1]; Kwang Seok Lee[2]; Young Won Chang[1]; [1]POSTECH; [2]IKM

The deformation behaviors of a monolithic Cu47.5Zr47.5Al5 (at. %) bulk metallic glass (BMG) and Zr76.11Ti4.20Cu4.51Ni3.16Be1.49Nb10.53 (at. %) bulk metallic glass composite were studied through a series of compression tests in supercooled liquid region (SLR). In the homogeneous flow regime, a transition from the Newtonian to non-Newtonian flow was observed to take place depending upon both the strain rate and temperature. These two flow modes were then described by applying the Newtonian viscous flow theory and the transition state theory, respectively. On the basis of a dynamic materials model, a processing map could successfully be constructed to estimate the feasible forming conditions for these monolithic BMG and BMG composite alloys. Formability of the alloys through a processing map was compared with extrusion simulation results, and BMG composite was harder to deform compared to a monolithic BMG due to the hindrance of dendrite requiring strength for a viscous flow in the SLR.

5:50 PM

Relationship between the Viscous Deformation of Bulk Metallic Glasses and the Diffusional Creep of Polycrystalline Materials: *Young-Sang Na*[1]; Jong-Hoon Lee[1]; [1]Korea Institute of Materials Science, Korea Institute of Machinery and Materials

Viscous deformation of bulk metallic glass around glass transition temperature was analyzed based on the diffusional creep model. Viscous flow behaviors of 2 Zr-based BMG alloys and 1 Fe-based BMG alloy were employed. Viscous flow behaviors of the selected alloys in the supercooled-liquid state were obtained both from the literature and from a series of isothermal compression tests. Amorphous matrix of bulk metallic glasses was assumed to behave similar to the grain boundary in polycrystalline metals to approximate the diffusivity of major constituent elements. In spite of rough approximation of the parameters in Nabarro-Herring creep equation, the reasonable value of the diffusion path could be obtained from the experimentally-obtained metal flow data. By comparing the calculated average diffusion path with the shear bands observed, new viscous deformation model based on the atomic diffusional motion via free volume or nano-voids will be proposed.

6:05 PM

Effects of High Pressure Treatment on the Structural Relaxation and the Deformation of a La-Base Bulk Metallic Glass: *Jianguo Lin*[1]; Fenghua Wang[2]; Haowen Xie[1]; Cui'e Wen[1]; Peter Hodgson[1]; [1]Deakin University; [2]Xiangtan University

In the present study, a La-based, La62.0Al15.7 (Cu, Ni) 22.3, BMG was annealed at room temperature under the high pressure up to 5 GPa, and the structures of the samples treated at the different pressures were characterized by X-ray diffraction(XRD) and differential scanning calorimetry (DSC). It was found that the structural relaxation occurred in the BMG during HP treatment, and the extent was strongly dependent on the applied pressure. The glass transition temperature (Tg) and the onset temperature of the first crystallization (Tx1) of the BMG display a nonmonotonic increasing function of pressure. The effects of HP treatment on the mechanical properties and deformation of the BMG were also investigated by using indentation and compression tests.

Cast Shop Technology: Sustainability in the Casthouse

Sponsored by: The Minerals, Metals and Materials Society, TMS Light Metals Division, TMS: Aluminum Committee
Program Organizers: Hussain AlAli, GM Casthouse and Engineering Services, Aluminium Bahrain Company (ALBA); David DeYoung, Alcoa Inc

Monday PM
March 10, 2008

Room: 295
Location: Ernest Morial Convention Center

Session Chair: Subodh Das, Secat Inc

2:00 PM Keynote

Melting Furnaces, Technical Developments Reviewed and Thoughts for the Future: *Barry Houghton*[1]; [1]Solios Thermal

Over the last 20 years or so, melting furnace technology, has seen a few significant developments affecting efficiency, melt rate and reliability. The basic heat transfer technology is well understood, and small improvements to performance are now generally through incremental changes and optimisation. Compared to some other technologies however, there is still much scope for further development outside of the basic performance criteria. This paper looks at many of the improvements to date but then goes on to compare it to where other technologies are now positioning themselves. Are they relevant to the casthouse situation and can we learn from them? We believe so and this will be discussed in relation to environmental impact, safety, automation, service intervals and of course value for money. This is the big challenge, we all expect much more for our money than previously, can we achieve it?

2:20 PM

Metal Treatment Update: Bruno Maltais[1]; Dominique Privé[1]; *Martin Taylor*[1]; Marc-André Thibault[1]; [1]STAS

There have been significant improvements in the last few years to operating procedures and equipment in treating molten aluminium. It is now recognised that reducing bath from pot room crucibles with siphoning and/or skimming can reduce contaminants in cast house furnaces. The TAC (Treatment of Aluminium in a Crucible) is a well-known equipment to reduce sodium but there have been significant improvements in design. Furnace treatment in the cast house using an RFI (Rotary Flux Injector) to both efficiently stir the metal and remove alkalines and inclusions, can contribute to a chlorine free environment. In-line treatment with degassers can remove hydrogen, alkalines and inclusions. There have been significant advances to the operating procedures for the use of chlorine gas in degassers to enable cleaner metal, attaining high levels of cleanliness. Salt additions into the degassers have also been shown to significantly reduce inclusions, even with a chlorine free degasser.

2:40 PM
Highest Efficiency and Economic Burner Concepts: *Michael Potesser*[1]; Burkhardt Holleis[2]; Davor Spoljaric[3]; Helmut Antrekowitsch[1]; Adrianus Hengelmolen[4]; [1]University of Leoben; [2]Messer Austria GmbH; [3]LLC Elme Messer Gaas; [4]Hengelmolen Furnace Systems

The efficiency of industrial combustion processes can be raised in two ways, either by preheating the fuel and combustion air or by adding oxygen. The most important issue of the usage of oxygen burners is the substantially increasing melting rate by lowering the specific production costs because of the higher combustion efficiency and lower investment costs. The diluted or flameless combustion (internal offgas recirculation) and the external offgas recirculation solves the problem with the high flame temperature and leads to cold combustion and lower dross formation. The Oxipyr®-Air combines the technology of diluted combustion during air and oxygen usage decreasing the emission of pollutants. Constitutive of the Oxipyr®-Air development a fuel-oxygen-burner, Oxipyr®-Flex, was designed for a maximum of flexibility for the customer. The Oxipyr®-Air and Oxipyr®-Flex have been developed for the specific needs of melting and recycling companies for all non ferrous metals.

3:00 PM
Increase of the Productivity in an Aluminum Slug Plant Using Porous Plugs: *Klaus Gamweger*[1]; [1]RHI

Gas purging systems are well established in the non ferrous metallurgy at multiple steps in the metal production, including melting, converting, alloying and cleaning. The kinetics of all of these process steps are influenced positively by using gas purging systems. In the aluminum industry, inert or reaction gases are blown into the melt using porous plugs to achieve improved metal qualities and a higher productivity. To enable the best possible efficiency of the applied process gases a complete package was developed that includes porous plugs, refractory expertise, gas supply technology and gas control equipment. This paper discusses the technological and economical advantages of this system. The benefits in fuel reduction, gas consumption, service live, maintenance and most notably the potential time savings were shown on the basis of an aluminum slug plant in Austria.

3:20 PM
Minimizing Potroom Bath Transfer to the Casthouse: *Edward Williams*[1]; David DeYoung[1]; Robert Levesque[1]; [1]Alcoa, Inc

Transfer of electrolytic bath from potroom smelting cells to casthouse furnaces causes many problems in casting facilities. Bath that gets transferred collects in casthouse furnaces, reducing furnace capacity and refractory life. Bath transferred can also react in the furnace to release alkalis to the melt, which must be removed, typically by fluxing with some form of chlorine. These fluxing requirements lead to significant cost, cycle time and EHS issues. Measurement of the actual amount of bath transferred from the smelter has been difficult in the past. A method for evaluating the amount of bath transferred into an ingot has been developed. This method has been used to show a reduction in bath transfer by holding crucibles to a temperature where any bath present is solidified and is less likely to be transferred into the furnace.

3:40 PM Break

3:50 PM
Understanding of the Mechanisms of Bath Carryover with Molten Aluminium in Smelters: *Vincent Goutière*[1]; Claude Dupuis[1]; [1]Alcan International Limited, Arvida Research and Development Centre

Tapping of Hall-Héroult cells has always been associated with the simultaneous uncontrolled aspiration of a significant amount of electrolytic bath with the molten aluminium. The bath carried over with the molten metal has numerous negative impacts on tapping tube blockage, crucible cleaning and on downstream metal processing steps such as metal pre-treatment and furnace operations and costs. Over the years, few research works to understand the mechanisms responsible for bath aspiration during tapping were published. This paper presents the experimental work done at the Arvida Research and Development Centre. Physical modelling was used to develop an understanding of the key parameters and the mechanisms responsible for bath aspiration. The importance of integrating metal circulation patterns in the cell will be exemplified. The effect of the key operating parameters such as the tapping flowrate and tapping tube positioning will be presented and the correlation with industrial results will also be discussed.

4:10 PM
Furnace Energy Saving Myths: *David White*[1]; [1]Schaefer Group, Inc.

This will be a presentation on the true ROI for some of the more popular energy saving ideas out there. For example: (1) Recuperation, (2) Regenerative Burners, (3) Fixed Heat Loss (refractory construction), (4) Pre-heating, (5) Circulation, (6) Doors, (7) Thermocouple placement. Discussion about the best way to save money with each of these items. To do's and not to do's when trying to save energy.

4:30 PM
Salt Injection to Replace Chlorine in A622 In-Line Degassers: *Corleen Chesonis*[1]; David DeYoung[1]; [1]Alcoa Inc

Rotating impeller degassers like the Alcoa A622 typically inject a mixture of argon and chlorine to treat the metal as it flows from the furnace to the casting pit. The use of gaseous chlorine represents a significant environmental and industrial hygiene issue. Storage, piping, safety, and training requirements can be stringent. Eliminating the use of chlorine requires the development of alternative methods to remove alkali and alkaline earth impurities and to maintain metal cleanliness. Static and dynamic tests were conducted to evaluate the feasibility of using solid salts containing MgCl2 to replace chlorine in an A622 degasser. This paper will present comparisons between chlorine injection and salt injection for Na, Ca, and hydrogen removal, utilization efficiency of the injected reactant, metal cleanliness measured by LiMCA and PoDFA, and emissions of particulate, chlorine, and HCl. The effects of salt chemistry, particle size, and feed rate will also be discussed.

4:50 PM Panel Discussion

Characterization of Minerals, Metals, and Materials: Characterization of Extraction and Processing

Sponsored by: The Minerals, Metals and Materials Society, TMS Extraction and Processing Division, TMS: Materials Characterization Committee
Program Organizers: Jian Li, Natural Resources Canada; Toru Okabe, University of Tokyo; Ann Hagni, Intellection Corporation

Monday PM — Room: 284
March 10, 2008 — Location: Ernest Morial Convention Center

Session Chairs: Tzong Chen, CANMET-MMSL; Junji Shibata, Kansai University

2:00 PM
In-Situ Monitoring and Validation of a Uranium Mill Tailings Management Facility Design Using X-Ray Absorption Near-Edge Structure (XANES) Spectroscopy: *Jeff Warner*[1]; John Rowson Rowson[2]; [1]Canadian Light Source Inc.; [2]Areva Resources Canada Inc.

Uranium ore containing elevated concentrations of arsenic (up to 2 wt %) are processed at the McClean Lake Operation in the Athabasca Basin of northern Saskatchewan. This region of northern Saskatchewan is responsible for 33% of the world production of uranium. A major concern of AREVA Resources Canada Inc. (AREVA) as well as provincial and federal regulators is the potential long term risk that significant amounts of arsenic may pose to surrounding lakes and waters after their disposal in the JEB Tailings Management Facility (TMF). This article is concerned primarily with the geochemical monitoring of arsenic in sediments obtained from bore holes in the JEB TMF. Sample depth in the TMF corresponded to the time of disposal and the age of the sediments in the TMF. The evolution of arsenic oxidation states was investigated by X-ray Absorption Near-Edge Structure (XANES) spectroscopy.

2:20 PM
Characterization of Gold in a Conventional Copper Refinery Anode Slimes Treatment Circuit: *Tzong Chen*[1]; John Dutrizac[1]; [1]CANMET-MMSL

During the electrorefining of copper anodes, gold shows a strong affinity for selenium. In the raw anode slimes, gold occurs mainly as tiny metallic gold

particles which show a strong affinity for the selenide phases. Decopperizing of the anode slimes generates mostly metallic gold, but also promotes the incorporation of Au in silver selenide. A greater fraction of the gold is converted to $(Ag,Au)_2Se$ or Ag_3AuSe_2 when high-Se and high-Ag anode slimes are decopperized at elevated temperatures and pressures. After pelletization and roasting of the slimes, the gold is converted to a (Ag,Au)-alloy and Ag_3AuSe_2. Smelting of the roasted products eliminates the selenium and converts the gold to an Ag-rich (Ag,Au,Pd)-alloy in the Dore metal. In the subsequent silver refining process, gold collects as a gold-rich (Au,Ag,Pd)-alloy in the gold mud.

2:40 PM

Copper Release Velocity from Copper Vermiculite in Aquatic Environment: Bowen Li[1]; *Jiann-Yang Hwang*[1]; [1]Michigan Technological University

The lifespan of antimicrobial materials is an important factor for applications. Copper vermiculite is a new material with excellent antimicrobial ability. In this study, the antibacterial durability of copper vermiculite in static and shocked aquatic environments has been investigated. The release velocity of copper ions from copper vermiculite grains is demonstrated. The diffusion mechanism of copper from vermiculite structure and the testing method for discharge of metallic ions are also discussed.

3:00 PM

Characterization of Wastes from Water Treatment Plant: *Carlos Maurício Vieira*[1]; Jhonatas Vitorino[1]; Rubén Sánchez[1]; Sergio Monteiro[1]; [1]State University of the Northern Fluminense

This work has for objective the characterization by XRD, XRF, DTA/TG, SEM and sedimentation techniques of three types of waste from water treatment plant for incorporation into clayey ceramics for civil construction. The plasticity of the waste was evaluated by the Atterberg limits. The wastes were collected at different points: the sand collector, the decantation stage and the filter stage in the water treatment plant of the county of Campos dos Goytacazes, Rio de Janeiro State, Brazil. The results indicated that the sludges from decantation and filter stages are mainly formed by clay mineral. The waste from sand collector is basically quartz sand material. Both types of wastes can be used into clayey ceramic according to the characteristics of the clays used in the body formulation.

3:20 PM Break

3:40 PM

Measurement of Leaching Rate of Heavy Metals from Copper Tailing: Bowen Li[1]; *Jiann-Yang Hwang*[1]; Rick Nye[2]; Domenic Popko[2]; Peter O'Dovero[3]; [1]Michigan Technological University; [2]Lesktech Ltd.; [3]Westwood Lands, Inc.

The copper tailing piles in the Western Upper Peninsula of Michigan State is a significant concern for environment protection both for local land and Lake Superior. This study investigated the measurement of leaching rates of heavy metals including copper, arsenic, chromium, cobalt, barium, iron, titanium, and zinc from copper tailings piled on Lake Superior shore. The characteristics and compositions of copper tailing, and leaching mechanism are also discussed.

4:00 PM

Field-Emission Properties of Sulfide Minerals under High-Power Nanosecond Electromagnetic Pulses: *Igor Bunin*[1]; Valentin Chanturiya[1]; [1]Russian Academy of Sciences

The mechanism of absorption of the energy of high-power electromagnetic nanosecond pulses (HPEMP) due to the field emission from the surface of natural semiconductors is considered. The limitations and possibilities of implementing this mechanism in sulphide minerals (pyrite and arsenopyrite) are demonstrated. The effect of HPEMP on the physicochemical properties and surface state of sulphide minerals, as well as on the technological properties of resistant gold-(PGM)-containing ores and beneficiation products was investigated. The results of the SEM/EDX (LEO 1420VP scanning electron microscope equipped with an Oxford INCA Energy EDX detector) investigations of a pyrite and a pyrrhotite samples testify that the irradiation with a series of nanosecond HPEMP produced prebreakdown state of the mineral surfaces, with numerous microcracks and neoformations. The influence of HPEMP irradiation on composition change and oxidization process of a mineral surface, together with sorption and flotation activity of sulphide minerals was studied.

4:20 PM

Characterizations of Halloysite Clay as Functions of Temperature: *Dan Rutman*[1]; Joe Hutchins[1]; Eric Peterson[1]; Morgan Reed[1]; Donald Mencer[2]; Gary Beall[3]; Jewel Gomes[1]; David Cocke[1]; [1]Lamar University; [2]Wilkes University; [3]Texas State University

Halloysite, a natural kaolinitic clay mineral, has hollow nanotubular structure with diameters typically smaller than 100 nanometers and lengths ranging from about 500 nanometers to 5 microns. This unusual structure is spurring interesting modifications for novel applications. This warrants a thorough chemical and physical examination as a function of temperature since thermal treatments are requisite for future applications. The Halloysite was examined over the range from room temperature to 1000C by FTIR, XRD, DSC, TGA, and SEM. Particular attention was given to chemical changes that have been correlated with structural and physical alterations in properties associated with these clays to be used as a possible catalyst. Analytical SEM with EDAX provided detailed morphological information that has been correlated with size and structural data provided by XRD. Insights into the best approaches to perform ASEM have been gleaned from these comparative characterization methodologies which are outlined in this work.

4:40 PM

Study of the Leaching Kinetic of Low Grade Zinc Oxide Ores: *Feng Linyong*[1]; [1]Kunming University of Science and Technology

Low grade powdery zinc oxide ores (5.17% Zn, < 2 mm) are mixed with cement 5% (wt), pelletized and solidified. The diameters of the pellets obtained are between 5 mm to 8 mm. When the pellet solidification periods are 3 days, 10 days and 45 days respectively, the alkaline leaching rates of zinc in the pellets are up to 92.2%, 87.3% and 72.9% respectively. Decreasing the solidification time can reduce reaction time, increase dissolution of zinc in pellets and lower the effect of initial zinc concentration on leaching rate. The experiment results show that the minimum solidification time is three days, and the kinetic study indicates that alkaline leaching of the low grade zinc oxide pellets is controlled by the diffusion of the leach liquor through the gangue layer in the whole leach process, and the apparent rate constants are 3.51×10-2 day-1, 8.09×10-3 day-1, 4.74×10-3 day-1 respectively.

Complex Oxide Materials - Synthesis, Properties and Applications: Novel Functionality from Complex Oxide Heterointerfaces

Sponsored by: The Minerals, Metals and Materials Society, TMS Electronic, Magnetic, and Photonic Materials Division
Program Organizers: Zhiming Wang, University of Arkansas; Ho Nyung Lee, Oak Ridge National Laboratory

Monday PM Room: 277
March 10, 2008 Location: Ernest Morial Convention Center

Session Chair: To Be Announced

2:00 PM Invited

Dielectric and Magnetic Anomalies at Oxide Interfaces: *Harold Hwang*[1]; [1]University of Tokyo

The electrostatic, magnetic, and physical boundary conditions at oxide interfaces can lead to unusual non-bulk-like interface states, which have been the subject of much recent interest. We present investigations of rectifying Schottky junctions, which we have used as a probe of the near interface electronic structure. Using $Nb:SrTiO_3$ as an n-type semiconductor, the strong internal electric field across the junction induces significant dielectric nonlinearities, giving rise to a strongly temperature and bias dependent depletion barrier profile. Junctions formed by using manganites as the Schottky metal exhibit a magnetic field dependent shift of the current-voltage characteristics, resulting in an exponentially-enhanced differential magnetoresistance and junction magnetocapacitance. These features arise from a magnetic field dependent Schottky barrier height and depletion width, reflecting the large charge-spin coupling arising from the double-exchange mechanism at the interface.

2:30 PM Invited
Novel Physical Phenomena in $LaTiO_3/SrTiO_3$ and $LaTiO_3/LaAlO_3$ Oxide Superlattices Investigated by Optical Spectroscopy: *Tae Noh*[1]; [1]Seoul National University, ReCOE, Department of Physics and Astronomy

Recent advances in atomic-scale control and fabrication techniques of oxide multilayers have triggered extensive investigations on artificial oxide superlattices. $LaTiO_3$ is a well known d1 Mott-insulator, where correlation plays important roles. We fabricated $LaTiO_3/SrTiO_3$ and $LaTiO_3/LaAlO_3$ superlattices, both of which are composed of the d1 Mott-insulator and a band insulator. In $LaTiO_3/SrTiO_3$ superlattices, we found novel metallic behaviours at the interface due to electron spill-over effects. We carefully excluded the possibility of oxygen vacancy as a cause for the conducting interface. On the other hand, in $LaTiO_3/LaAlO_3$ superlattices, we obtained experimental evidences for strong confinement of the Ti 3d electronic states at the TiO_2 sheet, suggesting a sharp 2D Mott insulating state. In this talk, we will present some intriguing optical spectroscopy results in combination with the first-principle calculation results. We will also address why transport properties of the similar material systems (with $LaTiO_3$ layers) behave so differently.

3:00 PM Invited
Magnetic Effects at the Interface between Non-Magnetic Oxides: *Guus Rijnders*[1]; [1]University of Twente/ MESA+ Institute for Nanotechnology

The discovery of conduction caused by electronic reconstruction at oxide interfaces has attracted a lot of interest. A heterointerface between perovskites (ABO3) introduces polarity discontinuities when both elements A and B on either side of the interface have different valence states. Recently, a different electronic behavior for thin $LaAlO_3$ films on either SrO- or TiO_3-terminated $SrTiO_3$ substrates was found, the former interface being insulating and the latter interface being an n-type conductor. Here we show how, in analogy to this remarkable interface-induced conductivity, magnetism can be induced at the interface between the otherwise non-magnetic insulating perovskites $SrTiO_3$ and $LaAlO_3$. A large negative magnetoresistance of the interface is found, together with a logarithmic temperature dependence of the sheet resistance. At low temperatures, the sheet resistance reveals magnetic hysteresis. The conducting oxide interface now provides a versatile system to induce and manipulate magnetic moments in otherwise non-magnetic materials.

3:30 PM Invited
Engineering High-Mobility in $SrTiO_3$-Based Structures: *Gervasi Herranz*[1]; Mario Basletic[2]; Olivier Copie[1]; Manuel Bibes[3]; Cécile Carrétéro[1]; Emil Tafra[2]; Eric Jacquet[1]; Karim Bouzehouane[1]; Cyrile Deranlot[1]; Amir Hamzic[2]; Agnès Barthélémy[1]; Albert Fert[1]; [1]Unité Mixte de Physique CNRS/Thales; [2]University of Zagreb, Department of Physics, Faculty of Science; [3]Centre National de la Recherche Scientifique Université Paris-Sud, Institut d'Electronique Fondamentale

The development of electronic devices based on oxide requires materials with high carrier mobility. In this regard, $SrTiO_3$ (STO) is intensively investigated due to the dramatic sensitivity of its electronic properties to extrinsic impurity doping. Stoichiometric STO is a band insulator, but an insulator-to-metal transition is induced when STO is doped with extrinsic impurities. We have demonstrated that this doping is achieved by oxide thin film deposition on STO substrates,[1] providing promising ways to generate controlled high-mobility conduction. We have analyzed the mechanisms of oxygen vacancy formation and diffusion in STO to provide accurate protocols to control the electronic properties. We have also explored alternative methods for the generation of high-mobility carriers in STO, with the objective of achieving two-dimensional conduction. We discuss the relevance of these results for all-oxide electronic devices. [1]G. Herranz et al., Phys. Rev. B 73, 064403 (2006); Phys. Rev. Lett. 98, 216803 (2007).

4:00 PM Break

4:30 PM Invited
Interface Electronic and Magnetic States in Nanoscale $CaRuO_3/CaMnO_3$ Superlattices: *John Freeland*[1]; Jerald Kavich[1]; Jacques Chakhalian[2]; A. Boris[3]; P. Yordanov[3]; B. Keimer[3]; H. Lee[4]; [1]Argonne National Laboratory; [2]University of Arkansas; [3]Max Planck Institute for Solid State Physics; [4]Oak Ridge National Laboratory

By creating an atomically abrupt boundary between two different complex oxide systems, one can explore how strong electron correlations are modified in proximity to the interface. Here we present results on the mixing of a G type anti-ferromagnetic insulator ($CaMnO_3$) and a paramagnetic metal ($CaRuO_3$). Using pulsed laser deposition, high-quality (100) oriented ultra-thin superlattices were grown with the structure [$CaRuO_3$(N u.c)/$CaMnO_3$(10 u.c.)]x6 on $LaAlO_3$. Our results show the formation of a canted anti-ferromagnetic state at the interface, which is attributed to weakening of the antiferromagnetic interactions by leakage of the metallic state into the insulating $CaMnO_3$ layer. This strong interface magnetism gives rise to a large magneto-resistance resulting from interface spin scattering of carriers in the metallic $CaRuO_3$ layers. Work at Argonne is supported by the U.S. Department of Energy, Office of Science, under Contract No. DE-AC02-06CH11357. JC is funded by U.S. DOD-ARO under Contract No. 0402-17291.

5:00 PM Invited
Recent Theoretical Progress on Correlated-Electron Interface: *Satoshi Okamoto*[1]; [1]Oak Ridge National Laboratory

Correlated-electron systems have been providing a variety of functionalities including high-TC superconductivity in cuprates and colossal-magnetoresistance in manganites. Therefore, studies of interfaces involving such materials are indispensable for realizing electronic devices utilizing novel properties of these materials. Further, interfaces involving these systems may become an alternative route to explore further interesting phenomena because one can control carrier concentration and lattice parameters of constituent materials without introducing chemical disorder. In this talk, I will describe recent theoretical progress on correlated-electron interface problem along with these issues including (1) transport and optical properties of a metal/Mott insulator/metal junction, (2) possible carrier injection and superconductivity at a cuprate/manganite interface, (3) novel quantum phases at correlated interfaces. This work is supported by the Division of Materials Sciences and Engineering, Office of Basic Energy Sciences, U.S. Department of Energy, under contract DE-AC05-00OR22725 with Oak Ridge National Laboratory, managed and operated by UT-Battelle, LLC.

5:30 PM Invited
Material Design and Application Based on Magnetic Oxide Interfaces: *Hiroyuki Yamada*[1]; [1]National Institute of Advanced Industrial Science and Technology

Extensive studies of magnetic oxide superstructures have revealed the crucial roles of interface effects, such as spin exchange, charge transfer or orbital degree of freedom [H. Yamada, et al., APL 81, 4793 (2002), APL 89, 052506 (2006)]. Atomic scale control and observation of interfaces actually lead to some interesting discoveries. For example, (La,Sr)MnO_3-based junction with engineered interfaces shows huge tunneling magnetoresistance (TMR) [H. Yamada et al., Science 305, 646 (2004)]. Or we have found enhanced nonreciprocal directional birefringence (optical magneto-electric effect) originating from polar and ferromagnetic interfaces, which were realized in a form of 'tricolor' superlattice composed of $LaMnO_3$, $SrMnO_3$, and $LaAlO_3$. Those novel functionalites, from TMR to multiferroics, demonstrate the potential of the correlated electron magnetic interfaces for future devices. This work was done in collaboration with Tokura multiferroics and spin superstructure projects, ERATO, Japan Science and Technology Corporation (JST), and partly conducted in CREST, JST.

Computational Thermodynamics and Kinetics: Defect Structure II

Sponsored by: The Minerals, Metals and Materials Society, TMS Electronic, Magnetic, and Photonic Materials Division, TMS Materials Processing and Manufacturing Division, ASM Materials Science Critical Technology Sector, TMS: Chemistry and Physics of Materials Committee, TMS/ASM: Computational Materials Science and Engineering Committee, TMS/ASM: Phase Transformations Committee
Program Organizers: Yunzhi Wang, Ohio State University; Long-Qing Chen, Pennsylvania State University; Jeffrey Hoyt, McMaster University; Yu Wang, Virginia Tech

Monday PM Room: 288
March 10, 2008 Location: Ernest Morial Convention Center

Session Chairs: Yu Wang, Virginia Tech; William Curtin, Brown University

2:00 PM Invited
Modeling of Dynamic Strain Aging in Solid Solutions: Part I: Single Strengthening Mechanism: *William Curtin*[1]; Monica Soare[1]; [1]Brown University

The aim of this work is to propose a robust, physically-based constitutive model for aging mechanisms in various technologically important metal alloys. The study is motivated by the need to explain quantitatively the stress-strain rate-temperature regime of material instabilities that often arise in material processing. The first part of the study describes the general framework of the rate dependent theory and addresses a single rate-dependent mechanism: solute strengthening by dislocation pinning at favorable random static solute configurations followed by solute diffusion toward temporarily-arrested mobile dislocations. The analysis shows that such a single mechanism cannot produce a regime of negative strain rate sensitivity but it reduces this parameter (SRS). The model predicts the transient stress behavior occurring upon imposition of an instantaneous change in strain rate, qualitatively consistent with the ad-hoc model of McCormick. Multiple competing strengthening mechanisms necessary for negative SRS are considered in the second part of our study.

2:25 PM
Dislocation Pinning by Impurities and Obstacles: A Level-Set Simulation Study: Zi Chen[1]; Kevin Chu[1]; *Mikko Haataja*[1]; Jeffrey Rickman[2]; David Srolovitz[3]; [1]Princeton University; [2]Lehigh University; [3]Yeshiva University

A basic understanding of the mechanical behavior of advanced metallic systems utilized in the aerospace community is essential for the design of robust structures to ensure their performance under a variety of loads and under extreme thermal environments. In particular, in systems that are solution and/or precipitation hardened, such as γ-TiAl and Al-Mg-Cu alloys and reinforced $MoSi_2$, interactions among defects lead to a complex plastic response that is difficult to capture in empirical constitutive relations. Here, we employ a parallel three-dimensional level-set code to simulate the complex motion of dislocation lines and loops in an obstacle-rich environment. Specifically, we have extracted the effective dislocation mobility as a function of solute concentration and mobility, spatial obstacle distribution, misfit strain, and external stress. These studies will guide the development of coarse-grained dislocation dynamics models which have the capability to provide a better microstructurally-informed description of the continuum mechanics of plastically deformed metals.

2:40 PM
Interaction Energy between Carbon Solutes and Dislocation in BCC Iron: *Y. Hanlumyuang*[1]; P. Gordon[2]; N. Thirumalai[2]; D. Chrzan[1]; [1]University of California, Berkeley; [2]ExxonMobil Research and Engineering

The interaction energy between a carbon atom and an edge dislocation in BCC iron is computed using three approaches: (1) an anisotropic elastic model wherein the chemical contribution is ignored, (2) an open-system thermodynamics model with both anisotropic elastic and chemical contributions incorporated, and (3) an *ab initio* electronic structure based total energy method. In the ab initio approach, the segregation energy is computed within a local strain approximation that neglects strain gradients. The results of the three methods are compared, and the importance of electronic and magnetic effects assessed. This research is supported by ExxonMobil Research and Engineering.

2:55 PM
Computing Solute Drag Stresses in Al-Mg: *Fan Zhang*[1]; William Curtin[1]; [1]Brown University

In solute-strengthened alloys, dynamic strain aging could be associated with solute drag caused by diffusion of solute atoms around moving dislocations. Drag stresses predicted by classical theories using a singular core are much larger than experiments. Here, the drag stress is computed numerically, as in Yoshinaga et al. (Phil. Mag. 23, 1367 (1971)), but using a more-realistic dislocation core structure and literature atomistic data on energy barriers for Mg diffusion in Al. In the 700K-750K range typical of Al processing, the maximum drag stress is much smaller than analytic estimates (43 MPa vs. 3.4 GPa). Using the Orowan relationship, the predictions for drag stress versus strain rate are in the range of experimental data. But, a power-law behavior emerges with in contrast to data suggesting, which is accounted for by considering the stress dependence of the mobile dislocation density.

3:10 PM
Interface Properties from Their Equilibrium Fluctuations: *Moneesh Upmanyu*[1]; Zachary Trautt[1]; Branden Kappes[1]; Alain Karma[1]; [1]Colorado School of Mines

The thermodynamic and kinetic properties of interfaces play a central role in the interplay between growth and form of interfacial microstructures. Due to the limitations associated with accessible spatio-temporal scales in experiments and in atomic-scale simulations, extracting these properties has been challenging. In this talk, I will present our recent work on theoretical frameworks and associated computational techniques aimed at extracting equilibrium interface properties from their fluctuations. The main focus is on grain boundaries; the capillarity fluctuation method allows us to extract grain boundary stiffness, which the random walk of the mean interface position directly yields its absolute mobility. Comparisons with previous studies on driven grain boundaries will also be made. The misorientation dependence of these grain boundary properties in pure aluminum show that these properties are structurally coupled. Finally, I will also discuss extensions of this methodology to alloy systems, in particular on quantifying the solute drag effect.

3:25 PM
Toward Predicting the Properties of All Grain Boundaries in a Material: *David Olmsted*[1]; Stephen Foiles[1]; Elizabeth Holm[1]; [1]Sandia National Laboratories

Microstructural evolution depends on both the energy and mobility of the constituent grain boundaries. Because grain size and texture are key microstructural parameters that contribute to material properties, mesoscopic simulations of grain evolution that provided accurate predictions for specific materials would be of great value. Such simulations require detailed properties, including energy and mobility, for individual grain boundaries. The large crystallographic space of grain boundaries, with five macroscopic degrees of freedom, has always posed a challenge for general analysis of these properties. The focus on this work is on studying the properties of a large and general set of fcc grain boundaries. Our ultimate goal is to verify existing models, or develop novel models, which provide reasonably simply ways to predict these properties. We report on our studies of the zero-temperature energy and the finite temperature mobility of several hundred non-equivalent fcc grain boundaries in nickel and aluminum.

3:40 PM Break

4:00 PM Invited
Grain Growth of Metallic Nanocrystals: Insights from Molecular Dynamics: *Stephen Foiles*[1]; Elizabeth Holm[1]; David Olmsted[1]; [1]Sandia National Laboratories

Understanding the structural evolution of nanograin metals is important for both the processing of these materials and to ensure their stability during use. In this talk, the evolution of the grain structure of nanograined Ni will be studied using molecular dynamics simulations of both model grain structures and random grain structures. The results will be compared to predictions based on models of grain growth developed for conventional polycrystalline materials. The goal of these comparisons will be to determine how grain growth in nanocrystalline metals differs from grain growth in more conventional polycrystalline metals. Sandia is a multi-program laboratory operated by Sandia Corporation, a Lockheed Martin

Company, for the United States Department of Energy's National Nuclear Security Administration under contract DE-AC0494AL85000.

4:25 PM

Quantitative Phase Field Simulations of Anisotropic Grain Growth in Columnar Thin Films with a Fiber Texture: *Nele Moelans*[1]; Frans Spaepen[2]; Bart Blanpain[1]; Patrick Wollants[1]; [1]Katholieke Universiteit Leuven; [2]Harvard University

Many thin films have a columnar grain structure in which all crystals have nearly identical orientation in the axial direction or the direction perpendicular to the film, but nearly random radial or planar orientation. We simulated the evolution of the grain structure of such films with a generalized phase field model. The model allows quantitative specification of the grain boundary energy and mobility for each interface individually. A Read-Shockley orientation dependence of the grain boundary energy was assumed. The dependence on the boundary inclination was assumed negligible. The presence of special high-angle misorientations with lower energy was considered as well. In this presentation we will discuss how the fraction of low-angle and low-energy grain boundaries evolves in time and how the misorientation-dependence of the grain boundary energy affects the grain growth exponent. Our findings will be compared with those from mean field theories and previous mesoscale simulation studies.

4:40 PM

Phase Field Models of Grain Growth in Cubic Crystalline Materials: *Mogadalai Gururajan*[1]; Ian McKenna[1]; Peter Voorhees[1]; [1]Northwest University

We present a phase field model for grain growth based on quaternions; we show that by a proper ordering of the quaternion components, the grain orientations related by cubic point group operations can easily be identified, and the grain boundary energy can be made to depend only on the smallest angle (consistent with cubic symmetry) that is needed to rotate one grain to orient it with the neighbouring grain. Further, we also indicate how the anisotropic grain boundary energies due to the cubic symmetry of the underlying lattice can be incorporated into the phase field models by including a higher order fourth rank gradient energy coefficient tensor. Finally, we also discuss a multiple order parameter grain growth models implemented using a sparse matrix algorithm, and compare it with the quaternion based model in terms of computational efficiency.

4:55 PM

Multi-Phase Field Study of Grain Boundary/Particle/Solute Interaction: *Seth Wilson*[1]; J. Gruber[1]; A.D. Rollett[1]; [1]Carnegie Mellon University

We utilize a multi-phase field model to study the interaction between grain boundaries, solute, and second-phase particles. We first verify via simulation that our model correctly incorporates each pair of interactions (boundary-particle, solute-particle, and solute-boundary) in the absense of the third. We then study shape and volume change during boundary traversal as a function of global solute concentration and local misorientation-dependant boundary-solute interaction strength. The effect on particle drag is discussed.

5:10 PM

Simulation and Theory of Interface Texture Development: *Jason Gruber*[1]; Herbert Miller[1]; Anthony Rollett[1]; Gregory Rohrer[1]; [1]Carnegie Mellon University

The distribution of internal interface types in a polycrystal is often non-random. We discuss results from several computational models that show how interface texture results from grain growth with anisotropic interface properties. A quantitative theory that agrees with our simulated results is presented. We demonstrate that the qualitative features of our simulations and theory closely match a number of real materials.

5:25 PM

The Effect of Nb and Austenite Grain Size on γ/α Transformation in Nb Added Steels: *Jong Min Choi*[1]; Jong Hun Kim[1]; Kyung Sub Lee[1]; Kyung Jong Lee[1]; [1]Hanyang University

It was generally accepted that γ/α transformation in Nb added steels was strongly retarded by solute drag effect when most of Nb were not precipitated. When they were precipitated, the transformation was much faster than they were soluble since the pinning effect of coarse precipitates on γ/α transformation was negligible. However, when the prior austenite grain was smaller, this solute drag effect nearly disappeared. In this study, the combined effect of prior austenite grain size and solute drag effect on γ/α transformation was studied. The classical nucleation and growth theory was adopted considering solute drag effect. The results including CCT diagram were compared with the observed.

Deformation Twinning: Formation Mechanisms and Effects on Material Plasticity: Experiments and Modeling: Twin Effects on Material Deformation I

Sponsored by: The Minerals, Metals and Materials Society, TMS Structural Materials Division, TMS/ASM: Mechanical Behavior of Materials Committee
Program Organizers: George Gray, Los Alamos National Laboratory; Subhash Mahajan, Arizona State University; Ellen Cerreta, Los Alamos National Laboratory

Monday PM — Room: 383
March 10, 2008 — Location: Ernest Morial Convention Center

Session Chairs: Rodney McCabe, Los Alamos National Laboratory; Ian Robertson, University of Illinois

2:00 PM Invited

Texture, Twinning and Hardening Evolution during Deformation of Hexagonal Zr and Mg: *Carlos Tome*[1]; [1]Los Alamos National Laboratory

Hexagonal materials deform plastically activating diverse slip and twinning modes. The relative contribution to deformation of such modes depends on their critical stresses and the orientation of the crystals with respect to the loading direction. For a constitutive description of these materials to be reliable, it has to account for the dislocation-twin interaction and for twin creation and reorientation. This talk discusses the connection between twinning and the mechanical response of two HCP metals - Zr and Mg – and presents a model for their mechanical response based on the active crystallographic mechanisms. Information from TEM, OIM, neutron diffraction, and mechanical testing is used for developing a model of the grain which is, in turn, incorporated into our Visco-Plastic Self-Consistent (VPSC) polycrystal plasticity code. We apply this model to the challenging problem of reproducing the results of strain-path-change tests done in pure Zr and AZ31 Mg.

2:30 PM

Temperature and Rate Effects in the Deformation of Pure Zirconium: *Irene Beyerlein*[1]; Carlos Tome[1]; Gwenaelle Proust[1]; George Kaschner[1]; [1]Los Alamos National Laboratory

In this work, we develop a dislocation density-based constitutive law for slip and twinning in hcp materials that accounts for temperature and rate effects within the thermal activation regime. The evolution law for slip covers Stages II through IV, by including temperature-dependent terms for recovery and debris formation. The hardening law for twin propagation accounts for temperature effects through interactions with slip dislocations. In turn, slip dislocations interact with twin boundaries through a Hall-Petch relationship, including a temperature-dependent coefficient. When implemented in a VPSC model which contains a micromechanical model for twin reorientation, the constitutive law effectively predicts the plastic anisotropy of ultra-pure polycrystalline Zr over a wide range of temperatures, 76K to 450K, and strain rates, 10-3 1/s and 103 1/s. The model considers the four deformation modes observed previously via microscopy analyses in this Zr: prismatic slip, pyramidal <c+a> slip, tensile twinning {10-12}(10-1-1), and compressive twinning {11-22}(11-2-3).

2:50 PM

Effect of Twining on Deformation Behavior of Zirconium Alloys: *Young Suk Kim*[1]; Tae Ook Oh[1]; Yong Moo Cheong[1]; [1]Korea Atomic Energy Research Institute

Tensile tests were conducted from RT to 400°C on the tensile specimens taken from the tangential direction (TD) and the longitudinal direction (LD) of a Zr-2.5Nb tube with a strong tangential texture. When the tensile stresses were applied to the TD with the tensile axis normal to the basal plane, the {10 2} twining was activated. With the tensile stress applied to the LD with the tensile axis parallel to the {10 0} plane, however, slip only was activated. The

operation of the twining caused the tensile properties of the Zr-2.5Nb tube to be anisotropic, leading to higher yield strengths and lower tensile elongations in the TD when compared to those in the LD. Furthermore, it promoted necking soon after yielding only in the TD while slip on the prism plane facilitated strain hardening after yielding. The role of twining in tensile properties of the Zr-2.5Nb tube is discussed.

3:10 PM
Hardening from Plastically Deformable Twins in a CPFEM Framework: *Luc Hantcherli*[1]; Philip Eisenlohr[1]; Franz Roters[1]; Dierk Raabe[1]; [1]Max-Planck-Institut für Eisenforschung

A statistical model of mechanical twinning in fcc metals is formulated for inclusion in a CPFEM framework. Growth rate of the twin volume fraction is phenomenologically linked to the resolved shear stress on each twin system by a power law. Twins are first considered to be impenetrable to matrix dislocations. The resulting contributions of hardening due to increasing volume fraction of plastically non-deformable twins and due to extra storage of dislocations largely exceed experimental reference. We present a feasible way of how to account for the thus required — end experimentally confirmed — dislocation penetration through twins.

3:30 PM
Internal Stress Development Due to Deformation Twinning: *Bjorn Clausen*[1]; Carlos Tome[1]; Donald Brown[1]; Sean Agnew[2]; [1]Los Alamos National Laboratory; [2]University of Virginia

Most metals with hexagonal crystal structure exhibit deformation twinning due to the limited number of available slip systems. In the case of magnesium, tensile twinning is easily activated, and depending on the initial texture and the loading path it can be a primary mode of plastic deformation. In the present work we have focused on the development of the local stress state in grains that twin. In-situ bulk diffraction measurements have been employed to determine the development of elastic lattice strains and crystallographic texture during compressive loading of extruded magnesium and during unloading after various levels of applied plastic strain. De-twinning is observed during unloading following a few percent of plastic deformation consistent with the development of strong internal stresses in twinned grains. Correlating the measured data with predictions of the elastic-plastic self-consistent polycrystal deformation model shows that the developed stress state is consistent with an initial twinning overshoot.

3:50 PM
Interfacial Plasticity Governs Strain Rate Sensitivity and Ductility in Nano-Twinned Metals: *Ting Zhu*[1]; Ju Li[2]; Amit Samanta[2]; Hyoung Gyu Kim[2]; Subra Suresh[3]; [1]Georgia Institute of Technology; [2]Ohio State University; [3]Massachusetts Institute of Technology

Nano-twinned copper exhibits an unusual combination of ultrahigh strength and high ductility, along with increased strain-rate sensitivity. We develop a mechanistic framework for predicting the rate sensitivity and elucidating the origin of ductility in terms of the interactions of dislocations with twin boundaries. Using atomistic reaction pathway calculations, we show that slip transfer reactions mediated by twin boundary are the rate-controlling mechanisms of plastic flow. We attribute the relatively high ductility of nano-twinned copper to the hardening of twin boundaries as they gradually lose coherency during plastic deformation. These findings provide new insights into possible means of optimizing strength and ductility through interfacial engineering.

4:10 PM Break

4:30 PM Invited
Deformation Twinning and Transformation Plasticity in Rare Earth Orthophosphates: *Randall Hay*[1]; Pavel Mogilevsky[2]; Emmanuel Boakye[2]; [1]Air Force Research Laboratory; [2]UES Inc.

Rare earth orthophosphates are refractory materials that are thermochemically stable in a wide range of environments and are relatively soft. Their mechanical and physical properties make them attractive for use as oxidation resistant fiber-matrix interfaces in ceramic composites. They are also of interest as phosphors and as nuclear waste hosts. Deformation twinning modes in monazite (monoclinic) and xenotime (tetragonal) rare earth orthophosphates ($ABPO_4$) are identified from TEM of indented polycrystalline and single crystal samples. Five modes are active in monazite, and one in xenotime. These modes all have very small shuffles for the rare earth cation and the PO_4 group. Methods for predicting twin modes in complex oxides, and their relative abundance, based on analysis of atom shuffles and other considerations are discussed. Indentation of some xenotimes can cause transformation to monazite and softening by transformation plasticity. Conditions under which this occurs are described, and possible applications are discussed.

5:00 PM
On the Role of Deformation Twinning in Work Hardening Behavior of FCC Polycrystals: *Farzad Hamdi*[1]; Sirous Asgari[1]; [1]Sharif University of Technology

Results of an investigation on the evolution of microstructure during simple compression testing of some FCC polycrystals are reported. It is found that, in contrast to the current belief, deformation twinning may not be the sole cause of linear hardening in low SFE FCC polycrystals. It is suggested that, due to the requirement of slip system change prior to twinning, only FCC crystals with sufficiently low twinning stress are expected to form mechanical twins. In other FCC polycrystals that show linear hardening behavior, competitive mechanisms such as formation of dislocation locks may be dominant hardening mechanism. The effectiveness of these slip barriers is expected to increase with the tendency of the material to slip planarity. Therefore, parameters such as SFE, temperature, Peierls stress and short range ordering are expected to have a contribution to the linear hardening response of FCC polycrystals.

5:20 PM
Kinematic Hardening Arising from Grain Size and Twinning in TWIP Steels: Olivier Bouaziz[1]; Colin Scott[1]; Sebastien Allain[1]; *Chad Sinclair*[2]; [1]Arcelor Research; [2]University of British Columbia

While the role of deformation twinning in modifying the work hardening rate of TWIP steels is well appreciated, less well appreciated is the fact that this is accompanied by significant kinematic hardening. In this talk, experimental results from two different austenitic TWIP steels will be presented that reveal a large Bauschinger effect developed during straining. These results will be discussed in light of a new physically based model that is capable of capturing both isotropic and kinematic components of the work hardening rate.

5:40 PM
Mechanical Response of High Purity Alpha Titanium Orthotropic Plate: Role of Deformation Twinning on Anisotropy and Its Evolution with Deformation: *M.E. Nixon*[1]; R.A. Lebensohn[2]; Oana Cazacu[3]; M.L. Lovato[2]; G. Proust[2]; C. Liu[2]; C.N. Tome[2]; [1]Air Force Research Laboratory and University of Florida; [2]Los Alamos National Laboratory; [3]University of Florida/REEF

An experimental investigation on high-purity, polycrystalline alpha-titanium plate was performed. Quasi-static tests at room temperature were conducted in monotonic tension and compression. The response is orthotropic and highly dependent on the orientation of the loading direction with respect to the predominant orientation of the <c> axis of the grains. Furthermore, four-point bending tests were performed on beams cut from the same plate, along different in-plane directions, for two mutually perpendicular bending planes. A digital image correlation technique was used to analyze the distribution of deformation. Due to the plate anisotropy and directionality of twinning qualitative differences in response were observed between the response of the upper and lower fibers of the different bent beams. The results indicate the need to use a constitutive description that accounts for the interplay between slip and twinning and its effects on texture evolution and hardening response when simulating the inhomogeneous deformation of Ti.

Electrode Technology Symposium (formerly Carbon Technology): Carbon Sustainability and Environment Aspects

Sponsored by: The Minerals, Metals and Materials Society, TMS Light Metals Division, TMS: Aluminum Committee
Program Organizers: Carlos Zangiacomi, Alcoa Aluminum Inc; John Johnson, RUSAL Engineering and Technological Center LLC

Monday PM Room: 299
March 10, 2008 Location: Ernest Morial Convention Center

Session Chairs: Trygve Foosnas, Norwegian University of Science and Technology; Neal Dando, Alcoa Inc

2:00 PM
Triple Low–Triple High, Concepts for the Anode Plant of the Future: Wolfgang Leisenberg[1]; Dragan Dojc[2]; *Detlef Maiwald*[1]; [1]Innovatherm; [2]Anotec

For the next generation of anode plants six main goals should be achieved. Three of them, summarized in Triple Low, represent the targets of the process technology: Low Energy, Low Emissions, Low investment and running Costs. The three others, summarized as Triple High, stand for the product: High Quality, High Quality Consistency and High Density. And this should be governed under the umbrella of maximum operational safety and efficiency. Different concepts of anode plants are on the market, which only cover parts of the defined goals. This paper deals with technologies to achieve all of these partly contradicting goals which are available today or in the near future. Especially technologies with environmental impact like minimization of energy consumption and emissions will be spotlighted.

2:20 PM
New Environmental Approach at Baking Furnace: *Felippe Navarro*[1]; Francisco Figueiredo[1]; Helio Truci[1]; Hézio Oliveira[1]; Raimundo Reis[1]; Fabiano Mendes[1]; Marcos Silva[1]; [1]Alumar

Consorcio de Aluminio do Maranhao is one of the largest aluminium smelters of Latin America producing 450'000 tons of primary metal. The plant has three baking furnaces with capacity to produce 700 anodes/day. The furnaces are operated with diesel oil due to the lack of natural gas distribution in the Northeast of Brazil. Alcoa Inc. started in 2006 an effort to reduce the green house gases emission worldwide, increasing the sustainability of their business and allowing Alcoa to apply for carbon credits. Alumar's Baking Furnace started using in September a mix of light oil and biodiesel as standard fuel. The development presented in this paper presents a new environmental approach where the main targets have been: 1)Reduce CO_2 generation with lower cost impact; 2)Implement an environmental fuel in the baking furnace with no impacts in anode quality, fuel efficiency and baking furnace operations.

2:40 PM
Pneumatic Transfer of Fine Carbon Residues at Albras – A Case Study at the Carbon Plant: *Paulo Douglas Vasconcelos*[1]; André Mesquita[2]; [1]Albras Alumínio Brasileiro S.A; [2]Federal University of Pará

Albras Alumínio Brasileiro S.A has upgraded the carbon plant to capture and transport the fugitive dust emissions from the operations of butt cleaning, crushing and grinding of butts and reject anodes, and the anode baking furnace tending cranes to elevate environmental pollution in the work place and to the environment. Originally, the residual dusts, mostly carbon were conveyed by a screw conveyor for loading into a bulk solids truck for subsequent disposal. The rest of the paper describes the development, design, and implementation of a pneumatic conveying system developed at past of a Masters dissertations to resolve the environmental issues, eliminating the coke contamination from the residual dusts while reducing annual maintenance and labour expenditures.

3:00 PM Break

3:10 PM
Towards Fully Automated Cast-Iron Sealing of Anode Rods: *Barry Woodrow*[1]; [1]Stimir hf.

Cast-iron sealing of anode rods is one of the few areas in the rodding shop which remains to be fully automated. Today's semi-automatic casting machines are a considerable improvement on manually poured ladles but still require the operator to engage in accurate and repetitive work in a potentially unhealthy and dangerous environment. This paper examines recent developments and the application of automation technologies to the anode rod sealing process. Automation of repetitive tasks is examined. Health and safety considerations - hot metal, fumes, operator posture, eyestrain - are addressed. Remote sensing devices are proposed to enable relocation of the operator away from the danger area. In conclusion, a fully automatic anode rod casting machine is described.

3:30 PM
Development In Situ of a Semi-Automated System in the Casting Station: A Case Study at Albras: Emerson Santos[1]; Dourivaldo Dias[1]; Antônio Ivan Arruda[1]; Marco Antônio Reis[1]; *Luis Carlos Carvalho Costa*[1]; [1]Albras

The work in the Casting Station is very risky, because the flying sparks of molten cast iron are a safety hazard for operators. The objective of this work is present an automation project of the casting station developed by Albras team. The Semi-automated System it consists of: The static cabins with air-conditioner control and a large open view, for maximum operator comfort; automation metal emptying device operation with electronic-hydraulics drive, using Control Proportional Valves, controlled by electronics joysticks. Finally, the gains of productivity, casting quality, ergonomics and safety obtained by the project are showed.

3:50 PM
Chemical Stability of Fluorides Related with Spent Potlining: *Xiping Chen*[1]; Wangxing Li[2]; [1]Zhengzhou Research Institute of Chalco; [2]Chalco

Chemical stability of fluorides related with spent potlining was studied. Experiments were carried out under conditions of exposure to air and exposure to active calcium oxide or limestone. Results from exposure to air at high temperature of 700~950°C showed that most of aluminum fluoride changed into Al_2O_3 or volatilized when the temperature was over 800°C and the weight loss of aluminum fluoride surpassed 60%, sodium fluoride did not volatilize or alter when heated up, Na_3AlF_6 and Al_2O_3 generated when the mixture of aluminum fluoride and sodium fluoride was heated up, $NaAl_{11}O_{17}$ formed when cryolite and sodium fluoride were heated up together. When foregoing fluorides were heated up exposure to active calcium oxide or limestone, CaF_2 formed easily.

Emerging Interconnect and Packaging Technologies: Pb-Free and Sn-Pb Solders: Electromigration

Sponsored by: The Minerals, Metals and Materials Society, TMS Electronic, Magnetic, and Photonic Materials Division, TMS: Electronic Packaging and Interconnection Materials Committee
Program Organizers: Carol Handwerker, Purdue University; Srinivas Chada, Medtronic; Fay Hua, Intel Corporation; Kejun Zeng, Texas Instruments, Inc.

Monday PM Room: 275
March 10, 2008 Location: Ernest Morial Convention Center

Session Chairs: John Osenbach, Agere Systems Inc; K. Subramanian, Michigan State University

2:00 PM Invited
Effect of Current Crowding on Electromigration Induced Damage in Flip Chip Solder Joints: *King-Ning Tu*[1]; [1]University of California at Los Angeles

Owing to the line-to-bump configuration in flip chip solder joints, current crowding occurs when electric current enters into or exits from the solder bump. At the cathode contact where electrons enter into the bump, current crowding induced pancake-type void formation has now been recognized widely to be the unique mode of electromigraion failure. On the other hand, at the anode contact, the effect of current crowding induce electromgiration failure has rarely been studies. We report here that hillock and whisker formation occurs respectively

in eutectic SnPb and SnAgCu as the mode of electromigration failure at the anode. The effect of current crowding induced stress concentration at the anode on whisker and hillock growth will be analyzed.

2:30 PM

Basic Studies on Electromigration in Electronic Solders: *K. Subramanian*[1]; Andre Lee[1]; Cheng-En Ho[1]; [1]Michigan State University

Electromigration studies on electronic solders, present in a joint configuration with minimal current crowding, were carried out with a current density. These studies were aimed at identifying the migration of individual atomic species, evolution of microstructure, interface intermetallics layer stability, extents of surface undulations etc. Effects of joint thickness, temperature were also evaluated. These studies provided a possible scenario for hillock formation in the anode region of muti-phase solder alloy joints. Synergistic influences of temperature and electrical stressing were evaluated by comparing the microstructure development with and without current stressing under isothermal condition. To gain a better understanding the roles of alloying and presence of multiple phases on the electromigration behavior, results obtained with eutectic Sn-Pb solder joints are compared to the electromigration induced changes in a solder joint made with pure tin.

2:45 PM

Failure of SnAgCu Solder Joints Under Current and Mechanical Load: *Christopher Kinney*[1]; Tae-Kyu Lee[1]; J.W. Morris[1]; [1]University of California, Berkeley

The work reported here investigated the failure of Pb-free SnAgCu solder joints under the simultaneous action of electrical current and mechanical load. The solder joints were made in a simple planar configuration with Cu on both sides. They were tested to failure in an apparatus that permitted the application of creep loads to samples that were subjected to known electrical current at controlled temperature. The results show a strong symbiotic effect between load and current density. The samples failed much more quickly under both stress and current than under either alone. The evolution of microstructure was monitored and the temperature profile was measured for various operating conditions to help clarify this behavior.

3:00 PM

Electromigration Failure Mechanism in SnAg Flip-Chip Solder Joints during Lateral Current Stressing: *Ming-Hui Chu*[1]; Chih Chen[1]; Yung-Ching Hsu[1]; [1]National Chiao Tung University

Many studies have been performed on how the current crowding has affected the electromigration failure in flip-chip solder bumps. But the effect the lateral current stressing has not been studied. In this study, electromigration of Sn3.5Ag solder bumps with 5-μm-thick Cu UBM is investigated when the solder joints were stressed by a lateral current of 0.9 A at 100°C, that is, the current was applied through two Al traces on the chip end. The microstructure analysis and the measurement of the resistance reveal that the occurrence of electromigration failure occurs during the lateral current stressing, and the failure mode is quite different from that stressed through the chip and the substrate ends. Kelvin probes were employed to monitor the resistance change due to electromigration damage. The consumption of UBM and void formation occurred in solder bumps, and the resistance of bumps may increase to 50% of its original values.

3:15 PM Break

3:30 PM

Design Limitations Related to Conductive Anodic Filament (CAF) Formation in a Micro-World: *Laura Turbini*[1]; Antonio Caputo[2]; [1]Research In Motion; [2]University of Toronto

The drive toward more compact, highly functional and portable electronic devices has forced a reduction in conductor spacing. A direct reliability concern of reduced pitch designs is an electrochemical failure mode in printed wiring boards known as conductive anodic filament (CAF) formation. CAF test coupon designs must take into account a number of factors in the board manufacturing process which will affect the reproducibility of the coupons. These include glass fiber style, resin type and content, as well as the drilling parameters such as drill bit wear, speed, diameter, and drilling sequence. Cracking between barrels can occur during the drilling process, especially for more brittle laminate materials. During the plating process, residues can accumulate in the cracks. Subsequent testing under humidity and bias conditions will lead to shorts which can be mistaken for CAF. This paper will identify the limitations in designing a PWB for CAF reliability testing.

3:45 PM

Effect of Al Trace Width on Electromigration Failure Time of Flip-Chip Solder Joints: *Shih-Wei Liang*[1]; Chih Chen[1]; [1]National Chiao Tung University

The effect of Al-trace width on electromigration of flip-chip solder joints was investigated in this study. Two thicknesses of Al trace adopted for lead-free SnAg solder with 5-μm Cu under bump metallization (UBM) were 40μm and 100μm. For the same stressing condition, 0.5 A on a 165°C hotplate, the solder joints with larger width has longer electromigration lifetime. As predicted by Black equation, the two factors, current density and temperature, will affect the lifetime of the solder joint. A higher current crowding effect occurs in the solder joints with a 40-μm Al trace than that with a 100-μm Al trace. Also, large resistance of 40-μm Al trace caused more serious Joule heating effect to increase the temperature in the solder bump. By these two reasons, the solder joint with a 100-μm Al trace have 2.6 times of failure time than the solder joint with 40-μm Al trace.

4:00 PM

Effects of Bump Height on Electromigration Failure Time and Failure Modes of Pb-Free Solder Joints: *Min-Feng Ku*[1]; Chih Chen[1]; [1]National Chiao Tung University

Effects of bump height on electromigration failure time and failure modes have not been studied for Pb-free SnAg solder joints. In this study, we fabricated two kinds of solder joints with different bump heights: the low bump height (LBH) of 25 μm, and the high bump height (HBH) of 75μm. Both sets of solder joints were subjected by electromigration tests by 0.9A at 150°C. We measured the changes of bump resistance with Kelvin bump probes. It is found that when the bump resistance increased to 20% of its initial value, the failure time of LBH solder joints was about 80 hours and the HBH solder joints was about 300 hours. According to Joule heating results measured by infrared microscope, we found the different temperature increase in the two solder joints, which may be responsible for the difference in failure time. The failure mechanism will be presented in the conference.

4:15 PM

Electromigration Induced Microstructure and Morphological Changes in Eutectic SnPb Solder Joints: *Andre Lee*[1]; Cheng-En Ho[1]; K. Subramanian[1]; [1]Michigan State University

Simultaneous direct current stressing with thermal aging accelerates the migration of conducting species resulting in significant microstructural coarsening. Due to the synergistic influences of these fields such coarsening begins from the anode and propagates towards cathode. Prolonged current stressing with 10^4 A/cm^2 at 150C causes the inter-lamellar SnPb eutectic morphology to become a two-layer structure, with Pb-rich layer adjacent to the anode and Sn-rich layer adjacent to the cathode. This mass movement causes hillock/valley formation and the extents of such surface undulations increase with increases in the time duration of current stressing as well as with the joint thickness. In thinner solder joints these events occur sooner, although the extents of surface undulations depend on the thickness of joints. In addition Cu present in the substrate and in the intermetallic layer at the cathode migrates to form Cu_6Sn_5 within the Sn-rich layer, in a region close to the Pb-rich layer.

4:30 PM

Current Density Effect on the Interfacial SnAg/Cu Reaction: *Yeh Yu-Ting*[1]; Liu Cheng-Yi[1]; [1]National Central University

Current density effects on the interfacial reaction between Sn_5Ag solder and Cu were investigated. Firstly, we found that IMC formation and Cu pad consumption highly depends on the current density under EM test. A critical current density was determined to define the growth behavior of interfacial IMC. Above the critical current density, IMC thickness increases with EM time. On the contrary, below the critical current density, IMC remains constant thickness with time. We also examine how does 5% Ag content response with EM. It seems that Ag_3Sn IMC formation at the Sn_5Ag/Cu interface will also depend on the current density. Depending on the values of current density, different interfacial Ag_3Sn IMC formations were observed: (1) mixed CuSn and SnAg compounds or (2) distinguish CuSn and SnAg compound layers at Sn_5Ag/Cu interface.

4:45 PM
Electrothermal Effect on the Impression Creep of a Pb40Sn60 Alloy: *Rong Chen*[1]; Fuqian Yang[1]; [1]University of Kentucky

Solder joints provide electrical and mechanical interconnections in microelectronic circuits and devices. The mechanical behavior of the solder joints plays an important role in determining the reliability and lifetime of microelectronic devices. In this work, we studied the electrothermal effect on the creep behavior of a Pb40Sn60 alloy using the impression technique in the temperature range of 50 to 130°C and under the punching stress of 6.9 to 110 MPa. During the test, a constant DC electric current passed through the sample, which introduced electrothermal interaction through Joule heating. It was observed that there exists a stage of steady state creep when subjected to electrothermal interaction. The steady state impression velocity increased with the increase in electric current; and the stress dependence of the impression velocity followed the Eyring hyperbolic relation.

5:00 PM
Diffusion Mechanisms of Electromigration in Eutectic Solder Reaction Couples: Guangchen Xu[1]; Hongwen He[1]; *Fu Guo*[1]; [1]Beijing University of Technology

Electromigration is a well known threat to the reliability of flip chip solder joint in recent years. The formation of hillocks and valleys were regarded as diffusion of atoms/ions propelled by electron wind. Temperature is a key factor to influence the diffusion mechanics of electromigration in eutectic binary solder alloy. Few researchers provided the discussions on diffusion mechanisms of electromigration in eutectic solder materials both at room temperature (<30°C) and high temperatures (>90°C) in one study. In this study, a newly designed solder reaction couple which could effectively minimize current crowding effect and remove the influence of thermomigration was introduced to electromigration experiment. Through in-situ observation, the material migration of alpha-rich and beta-rich phases present in the inter-lamellar morphology will produce purer phases with less solute contents under different temperature, which could provide the explanations of diffusion mechanisms in eutectic solder alloy under high current densities.

Emerging Methods to Understand Mechanical Behavior: Digital Image Correlation

Sponsored by: The Minerals, Metals and Materials Society, TMS Structural Materials Division, TMS Materials Processing and Manufacturing Division, TMS: Advanced Characterization, Testing, and Simulation Committee, TMS/ASM: Mechanical Behavior of Materials Committee, TMS: Nanomechanical Materials Behavior Committee
Program Organizers: Brad Boyce, Sandia National Laboratories; Mark Bourke, Los Alamos National Laboratory; Xiaodong Li, University of South Carolina; Erica Lilleodden, Forschungszentrum

Monday PM Room: 285
March 10, 2008 Location: Ernest Morial Convention Center

Session Chair: To Be Announced

2:00 PM Invited
On the Digital Image Correlation (DIC) Technique and Its Applications: *Cheng Liu*[1]; [1]Los Alamos National Laboratory

Different techniques for determining various components of surface displacement field have been developed in the past, techniques like geometric moire, holography, moire interferometry, speckle shearing interferometry, to just name few. All these techniques involve either delicate sample surface preparation or complicated optical instrumentation. Also the outcome of these techniques is some kind of fringe patterns and their interpretation is sometimes tedious and difficult. The digital image correlation (DIC) technique has gained popularity for deformation measurement applications recently due to the advances of personal computer and software engineering. In this talk, I will present some of our recent applications of the DIC technique to different materials and specimen designs. The materials and specimen designs can be categorized as unconventional so that the conventional deformation measurement techniques are difficult to apply. The applications include polymeric foams, syntactic foam, high explosives and their mocks, and large deformation of some metallic materials.

2:30 PM Invited
Micro-Bending Experiments to Characterize the Elastic Properties and Interfacial Toughness of Yttria Stabilized Zirconia Thermal Barrier Coatings: Christoph Eberl[1]; Daniel Gianola[1]; Ming He[2]; Anthony Evans[2]; *Kevin Hemker*[3]; [1]Forschungszentrum Karlsruhe; [2]University of California Santa Barbara; [3]Johns Hopkins University

Multilayered thermal barrier systems offer tremendous technological advantages but must remain attached to the substrate to be effective. Important phenomena that affect delamination occur in each layer and at the interfaces between the different materials. This talk will detail the development and use of micro-bending experiments undertaken to measure the elastic modulus of physical vapor-deposited (PVD) 7-YSZ thermal barrier coatings. Digital image correlation (DIC) used to measure the spatial displacement fields associated with the application of point loads will be coupled with a detailed finite element (FE) model of the micro-bending specimen and used to deduce the strain dependence of the in-plane modulus. DIC also allows for observation of crack nucleation and propagation and determination of the crack tip for different applied loads. Comparisons with FE simulations allow for determination of the inter-columnar YSZ fracture strength and the interfacial toughness between the YSZ and the underlying thermally-grown oxide.

3:00 PM
Digital Image Correlation – Strain Evaluation Made Easy: *Carl Cady*[1]; Cheng Liu[1]; Billy Taylor[1]; [1]Los Alamos National Laboratory

Digital image correlation (DIC) technique was used in conjunction with standard loading techniques. The deformation on the surface of the samples was obtained using a series of random speckle images acquired during the loading and unloading of a sample. The strength of the DIC technique for measuring strains in samples that have unusual geometries, joints, and/or size limitations will be demonstrated in this presentation. The unique adaptability of this technique to measure overall strain as a standard extensometer can, or to measure local strains like a strain gage gives this technique the unique ability to re-evaluate a test multiple times. This ability to re-evaluate tests can bring insight into the failure process of different classes of materials. One strength of this technique is the ability to analyzing the deformation characteristics of welded materials. Evaluation of sub-sized samples, welded materials and constrained two phase materials will be discussed in this presentation.

3:20 PM
Digital Image Correlation in Materials Deformation Studies: From Fuel Cell Membranes to Advanced High Strength Steels: *Louis Hector, Jr.*[1]; [1]General Motors R&D Center

We present a survey of recent applications of digital image correlation (DIC) to deformation measurement in automotive materials. We begin our survey with a look at measurement of drying-induced strain fields in perfluorosulfonic acid membrane and membrane electrode assembly materials in fuel cells. We continue with a discussion of the measurement of strain fields in Portevin-LeChatelier (PLC) bands during deformation of an Al-Mg alloy with high speed digital photography. Next, we examine deformation and fracture of spot welds in a dual-phase steel and lap welds in Al alloys generated with a high power CW Nd:YAG laser. We complete our survey with plastic deformation behavior of press hardened boron steel and two grades of martensite steel. These materials belong to a new class of ultra-high strength steels that holds great promise for automotive applications. We conclude with a summary of potential future applications for DIC.

3:40 PM
Drift and Spatial Distortion Elimination in Atomic Force Microscopy Images by Digital Image Correlation Technique: Zhi-Hui Xu[1]; *Xiaodong Li*[1]; Michael Sutton[1]; Ning Li[1]; [1]University of South Carolina

The characterization of nanomaterials and nanostructures at the nanoscale has been a tremendous challenge to many existing testing and measurement techniques. With the rapid development of micro/nanofabrication technologies, the development of appropriate and accurate tools for nanometrology and nanomechanical testing is greatly needed. In this study, a recently developed methodology for scanning electron microscopy (SEM) image correction has been

successfully adapted to correct the drift and spatial distortions of atomic force microscopy (AFM) images. The errors in AFM images have been significantly reduced down to 0.015% with a standard deviation of 0.13% for an AFM sample stage and 0.02-0.03% with a standard deviation of 0.1% for a close loop sample stage.

4:00 PM Break

4:15 PM Invited

Strain Fields in Thin Metal Films for MEMS Subjected to Various Strain Rates: *Ioannis Chasiotis*[1]; Krishna Jonnalagadda[1]; John Lambros[1]; Jeff Pulskamp[2]; Ron Polcawich[2]; Madan Dubey[2]; [1]University of Illinois at Urbana-Champaign; [2]Army Research Laboratory

An optical method to obtain local deformations in rate sensitive films for MEMS was developed. A speckle pattern is generated with silicon nanoparticles on freestanding films. Digital Image Correlation (DIC) is used to resolve elastic/plastic deformations from high magnification optical images. In the reported study, the average gauge size of the test samples was 1x100x1000 microns, while the strain rates were 10-6 to 10-1 s-1. The strain resolution was 0.01%, which is equivalent to 1/10 of the pixel size. Two materials were investigated. The first were 0.4-micron Pt films, and the second were 2.0-micron Au films. The former showed significant strain rate sensitivity in terms of proportional limit (600-1000 MPa) and ultimate strain (3% - 4.3%) but their elastic modulus (175 GPa) and strength (1.8-2.0 GPa) were rate independent. On the other hand, Au films showed significant sensitivity in their strength and ductility especially at rates faster than 10-3 s-1.

4:45 PM

Strain Mapping of Al-Mg Alloy with Multi-Scale Grain Structure Using Digital Image Correlation Method: *Byungmin Ahn*[1]; Steven Nutt[1]; [1]University of Southern California

Al-Mg alloy powder was mechanically milled in liquid N2 (cryomilling) to produce thermally stable powder with nanocrystalline microstructure for the manufacture of high-strength alloys. A multi-scale microstructure was achieved by blending unmilled coarse-grained powder with the cryomilled powder and subsequently consolidating. The final bulk alloy was comprised of nanocrystalline regions separated coarse-grained bands. In-situ observations of tensile deformation of the alloy were made using a micro-straining stage attached to a light microscope. Interactions between ductile coarse-grain bands and nanocrystalline regions were investigated. Special emphasis was given to the distinct displacements between adjoining regions during the deformation, and these displacements were measured by digital image correlation (DIC).

5:05 PM

Full Field Strain Measurement of Resistant Spot Welds Using 3D Image Correlation Systems: *Hong Tae Kang*[1]; German Reyes-Villanueva[1]; Zhenzhen Lei[1]; Ilaria Accorsi[2]; [1]University of Michigan-Dearborn; [2]DaimlerChrysler

This paper describes the local strain measurement of resistant spot welds for three sheet stack-ups of DP600 and Mild steel under quasi-static and fatigue loading. The experiments were designed to investigate the effects of electrode tip types, surface indentation levels, and base metal strengths on local strain distributions at vicinity of spot welds. The used electrode tip types were B-nose and E-nose for DP600 and surface indentation levels were 10%, 30% and 50% of the sheet thickness. To obtain the goal, geometric factors were precisely controlled, especially the diameters of spot welds. Welding schedules varied to obtain a proper surface indentation levels while keeping the same weld sizes for the different materials and electrode tip types. Local strains at critical locations in resistant spot welds were measured using 3D image correlation systems (ARAMIS) during quasi-static and fatigue testing. The measured local strains were also compared with finite element analysis results.

5:25 PM

Using 3-Dimensional Digital Image Correlation to Map Deformation Fields in Bovine Cornea: *Brad Boyce*[1]; J. Mark Grazier[1]; Thao Nguyen[1]; Reese Jones[1]; [1]Sandia National Laboratories

Understanding the mechanical behavior of cornea tissue has implications to several ocular diseases and to corrective procedures such as LASIK. As a physiologically-relevant alternative to tensile-strip testing, intact ocular globes have been pressurized to observe the pressure-dependent response of cornea tissue. In our approach, the corneo-scleral junction is constrained as a fixed boundary condition, so all deformation occurs solely in the cornea. Digital image correlation analysis of the anterior cornea is enabled by imaging graphite speckles with transmission-illumination to prevent glare. A two-camera arrangement permits dynamic 3-dimensional mapping of the deformation field during pressure- or volume-controlled inflation and subsequent time-dependent creep/relaxation. To interpret observed displacement fields, we have developed a microstructurally-based viscoelastic fiber-composite model of the cornea accounting for multiple viscous-relaxation modes and an inhomogenous, anisotropic collagen fibril distribution. Discussion will focus on the observed viscoelastic properties of the cornea as well as the capabilities and limitations of the technique.

5:45 PM

New Techniques for the Characterization of Expansion in Thermal Barrier Coating Bond Coat Alloys: *Robert Thompson*[1]; Ji-Cheng Zhao[2]; Kevin Hemker[1]; [1]Johns Hopkins University; [2]General Electric Company

Thermal barrier coatings (TBCs), commonly used in modern gas turbines and jet engines, are dynamic multi-layered structures. Understanding the disparate thermal expansion behavior of the coating is essential to improving the overall performance of the system. Various components of the TBC, however, are incapable of actuating pushrods that commercial dilatometers use to determine the coefficient of thermal expansion (CTE). This paper outlines a non-contact digital image correlation technique for measuring the thermal strain and CTE of various bond coat and superalloy materials from room temperature to 1100°C. Results from well-characterized superalloys are used to validate the experimental and data processing methodologies. Temperature-dependent CTE results for 50 to 100 µm thick (Ni,Pt)Al and NiCoCrAlY coatings will be presented as well. The influence of other important properties, such as elevated temperature strength, creep, and phase transformations will also be discussed with regards to the system-level mechanical behavior of the TBC.

Enhancing Materials Durability via Surface Engineering: Steel and Other Alloys Surface Durability

Sponsored by: The Minerals, Metals and Materials Society, TMS Structural Materials Division, TMS/ASM: Corrosion and Environmental Effects Committee, TMS: High Temperature Alloys Committee

Program Organizers: David Mourer, GE Aircraft Engines; Andrew Rosenberger, US Air Force; Michael Shepard, Air Force Resaearch Laboratory/MLLMN; Bruce Pint, Oak Ridge National Laboratory; Brian Gleeson, Iowa State University

Monday PM — Room: 388
March 10, 2008 — Location: Ernest Morial Convention Center

Session Chair: Bruce Pint, Oak Ridge National Laboratory

2:00 PM Introductory Comments

2:05 PM

Low-Temperature Aluminide Coating Synthesized via Pack Cementation on Ferritic/Martensitic Alloys: *Brian Bates*[1]; Ying Zhang[1]; Yongqing Wang[1]; Bruce Pint[2]; [1]Tennessee Technological University; [2]Oak Ridge National Laboratory

Aluminide coatings synthesized at elevated temperatures showed good long-term oxidation protection in the water vapor environment. To prevent potential damage to the mechanical properties of the ferritic/martensitic alloys and also make the coating process more compatible with the heat treatment cycle of these alloys, efforts were made to fabricate coatings at lower aluminizing temperatures (~700ºC). Thermodynamic calculations carried out for packs containing NH_4Cl activator and binary Al-Cr masteralloys indicate that the partial pressure of metal halide vapors depends on both the pack composition and aluminizing temperature. Binary Cr-Al masteralloys containing 15 and 25 wt.% Al were used to lower the Al activity in the aluminization and therefore to reduce the tendency to form brittle Al-rich phases (e.g. Fe_2Al_5) in the coating.

2:25 PM

Evolution of Steel Surface Compositions with Heating in Vacuum and Air: *Colin Doyle*[1]; Bryony James[1]; [1]University of Auckland

The surface composition of mild steel and 304 and 316 austenitic stainless steels have been monitored using X-Ray photoelectron spectroscopy (XPS) whilst the steels were heated to 600°C. The bulk elemental compositions determined by OES are compared with the XPS data. The heating experiments were conducted under ultrahigh vacuum (UHV) and oxidizing conditions (6×10^{-6} Torr air). Before heating, the major elements at the steel surfaces were iron, oxygen, carbon, and manganese, along with chromium and nickel for the two stainless steel samples. The iron present at the surface was predominantly iron(III), with a small amount of zero-valent iron. UHV heated steel surfaces all showed zero-valent iron at temperatures greater than 450°C. Both stainless steels showed progressively decreasing iron content, with the surfaces becoming enriched with chromium oxides. Under oxidizing conditions the iron at the surface is converted to a mixture of Fe(II) and Fe(III).

2:45 PM

The Performance of Al-Rich Oxidation Resistant Coatings for Fe-Base Alloys: *Bruce Pint*[1]; Ying Zhang[2]; Sebastien Dryepondt[3]; [1]Oak Ridge National Laboratory; [2]Tennessee Technological University; [3]University of California at Santa Barbara

Oxidation resistant Al-rich coatings are being investigated for applications such as ultra-supercritical fossil-fuel plants. The presence of water vapor accelerates the environmental degradation of chromia-forming ferritic and austenitic steels but has little effect on coatings able to form an Al-rich surface oxide. Long-term (=10,000h) diffusion and oxidation experiments are being conducted to determine the rate of Al loss from the coating by oxidation and interdiffusion. Based on these data, a coating lifetime model is being developed. Creep experiments were conducted to assess the effect of the coating on substrate mechanical properties.

3:05 PM

Surface Treatment of Metals by Electro Plasma Technology: *Pratheesh George*[1]; Greg Tenhundfeld[1]; Edward Daigle[1]; Danila Ryabkov[1]; [1]CAP Technologies LLC

Electroplasma technology is a patented surface engineering technology developed by CAP Technologies LLC. The application of this technology includes surface cleaning, modification, alloying and coating of metal surfaces for corrosion resistance and wear resistance applications. The main advantages of this process are the environmentally friendly technology, cost effectiveness, unique surface profile for better coating adhesion and a fast deposition of nano-crsytalline coatings with deposition rates as high as 1µm per second with excellent corrosion resistance. The mechanism behind the electroplasma technology and its main characteristics will be presented. Different coatings such as Zn-Ni, Zn-Ni-Mo and Zn-Ni-P have been applied and are being considered as an alternative for the hazardous cadmium and chromium plating, especially in the aerospace industry. The processing and properties of these coatings will be also presented. The effect of this process on the fatigue and hydrogen embrittlement properties of the substrate materials will be discussed.

3:25 PM

A Functionally Graded Design Study for Boron Carbide and Boron Carbonitride Thin Films Deposited by Plasma Enhanced DC Magnetron Sputtering: *Tolga Tavsanoglu*[1]; Michel Jeandin[2]; Okan Addemir[1]; [1]Istanbul Technical University; [2]Ecole des Mines de Paris

The B–C–N system is characterized by short bond lengths and includes the hardest known materials, c-BN and boron carbide (B_4C), as well as other materials with remarkable tribological properties such as h-BN. Despite these good properties, adhesion problems were observed for B_4C and boron carbonitride (BCN) thin films on steel and Si substrates when the film thickness exceeds 500 nm. To enhance the adhesion, three functionally graded designs; surface boronizing of the steel substrate before deposition (B/B_4C), $Ti/TiC/B_4C$ and Ti/TiN/BCN structures were discussed. Cross-sectional FE–SEM examinations and elemental depth profiling by Secondary ion mass spectrometry were revealed the graded structure of the films. The elemental film composition was measured by EPMA. The mechanical properties were determined by nanoindentation and the tribological properties by pin-on disc measurements. The results demonstrated the possibility of growing well adherent boron carbide and boron carbonitride films with thicknesses in the µm range.

3:45 PM Break

3:55 PM

Enhancing Adhesive Fatigue Life of Wear Resistant HVOF Coating: *Ashwin Hattiangadi*[1]; Ram Krishnamurthy[1]; Jibin Han[1]; [1]Caterpillar Inc.

HVOF coatings consisting of ceramic carbides in metallic matrix are increasingly considered for use as wear resistant coatings, in machine applications such as tractor undercarriage sealing joints. Coating delamination, cracking and failure are critical considerations for their use and can limit overall benefits of wear life increase. Here, we examine post-processing heat-treatments that promote coating adhesion. Adhesion depends upon the post processing temperature, and adhered coatings develop a periodic array of through-thickness cracks or not depending upon the prescribed heat-treatment. The appearance of the periodic array of cracks and crack spacing conforms to elastic fracture analysis. FEM simulation with cohesive zone capability was developed to help predict fatigue life performance and S-N curve. It was calibrated with simple experiments to estimate the coating, interface energies and their dependence on the post processing method. Our findings have interesting implications for the production of crack-free bonded wear-resistant HVOF coatings.

4:15 PM Invited

High Performance Wear Materials for Earthmoving Applications: *M. Beardsley*[1]; Jason Sebright[1]; [1]Caterpillar Inc.

Sacrificial wear materials applied to buckets, blades and ground engagement tools represent a high maintenance cost of operation of earthmoving equipment. Improved wear materials can result in lower operating costs by reducing replacement intervals. New materials and processes to improve the surface durability of components have been developed and are currently under evaluation to demonstrate two times the wear life of standard heat treated steels.

4:35 PM

Pulsed Laser Treatment of 4Cr/2Mn/0.25C Steel: *Greg Kusinski*[1]; Jan Kusinski[2]; [1]Clemson University, School of Materials Science and Engineering; [2]AGH University of Science and Technology

The aim of this research was to experimentally verify the possibility of improvement of wear properties of 4Cr/2Mn/0.25C steel, used in automotive engine parts, by laser hardening and laser re-melting. A high power CO2 pulsed laser treatment was applied and the microstructure-property-relationship was studied as a function of both laser power and pulse duration. Advanced analytical techniques (SEM and TEM microscopy, and EDS microanalysis) were used to study structural details in the laser hardened layer, as well as to show fine differences in comparison with conventionally hardened steel. It was shown, that high wear resistance of the laser hardened layer (microHV65 > 2000) was due not only to the grain refinement caused by rapid laser heating but also to the high stresses induced during rapid cooling of the surface layer, both creating essentially fine, highly dislocated and internally twinned martensite with some amount of stable, interlath retained austenite.

4:55 PM

Reduced Wear and Friction Losses by DLC Coating of Piston Pins: Roman Morgenstern[1]; Frank Dörnenburg[1]; Wolfgang Kiessling[1]; *Simon Reichstein*[1]; [1]Federal-Mogul Nürnberg GmbH

Diamond like carbon coatings are well known to offer superiour friction and wear behaviour. To evaluate the potential of DLC coatings applied to piston pins in internal combustion engines, linearly reciprocating sliding wear examinations have been performed on uncoated and DLC coated piston pin segments versus different counter part materials. The tests have been investigated with respect to friction and wear performance of typical pin - piston material combinations. The analysis of the results show the enormous potential of DLC coatings to reduce wear and friction for each of the different counter part materials. Examined engine tests confirm the results of the non-engine wear test rig, showing that the specific engine output increases and the fuel consumption decreases if DLC coatings are applied to the piston pin.

5:15 PM
Re-Melt – Improved Durability for Aluminum Diesel Pistons by Local Surface Microstructure Modification: *Simon Reichstein*[1]; Scott Kenningley[1]; Peter Konrad[1]; Frank Dörnenburg[1]; [1]Federal Mogul

Driven by the customers request for increasing fuel efficiency and reduced CO2 emission solutions, pressure and temperature in internal combustion Diesel engines has rapidly increased during the last 15 years. Operated at maximum temperatures of up to 420°C in series production engines (which is equivalent to a homologous temperature of 0.92!) at complex thermo-mechanical loading conditions, Diesel pistons in modern passenger vehicles are probably today's most challenging Aluminium high temperature application. To meet these requirements, Federal Mogul has developed the process of local remelting for critical piston regions. In this paper a microstructure based model is discussed, showing how the modified (Re-melted) local microstructure can be directly attributed to an improvement in piston durability. The model is derived from surface crack initiation observations and quantified by microstructure modeling FE analysis. For validation the models predictions are compared to results from superimposed TMF-HCF rig testing and to engine testing results.

5:35 PM
Effect of Hot-Dip 55%Al-Zn Alloy Coating on Properties of Un-Hardened and Tempered N80 Steel: *Ming Jiang*[1]; Guoxi Li[1]; Changsheng Liu[1]; Yiran Zheng[1]; [1]Northeastern University

In this paper, the hot-dip 55%Al-Zn alloy coating was performed on the un-hardened and tempered N80 steel by two-step flux method, to prevent severe corrosion in oil field. The microstructure of hot-dip 55%Al-Zn alloy coating was analyzed by metalloscope, SEM, X-ray diffraction instrument and EDS. The corrosion resistance of the alloy-coated steels in NaCl solution was studied by means of laboratory immersion testing and EIS. And the comparison of the mechanical properties of N80 steel before-and-after coating was carried out, using tension machine and shock test machine. The results showed that the microstructure of 55%Al-Zn coating was composed of two layers: an Al-Zn alloy overlay and an intermetallic compound layer between overlay and substrate. Hot-dip 55%Al-Zn coating could improve the corrosion resistance of un-hardened and tempered N80 steel obviously in NaCl solution. After hot dipping 55%Al-Zn alloy, the strength and plasticity of the alloy-coated steels could also been greatly improved.

General Abstracts: Extraction and Processing: Session II

Sponsored by: The Minerals, Metals and Materials Society, TMS Extraction and Processing Division, TMS: Aqueous Processing Committee, TMS: Materials Characterization Committee, TMS: Process Technology and Modeling Committee, TMS: Pyrometallurgy Committee, TMS: Recycling and Environmental Technologies Committee
Program Organizers: Boyd Davis, Queens University; Michael Free, University of Utah

Monday PM Room: 272
March 10, 2008 Location: Ernest Morial Convention Center

Session Chair: Joe Ferron, VP Metallurgical Technology for Recapture Metals

2:00 PM
Electrochemical Reduction of Beryllium Oxide from CaCl2 Melts Saturated with CaO: *Joel Katz*[1]; [1]Los Alamos National Laboratory

Work to electrochemically reduce beryllium oxide to beryllium using the FFC Process will be reported on. Several samples underwent reduction for periods of up to two weeks in calcium chloride melts, which were held between 930 and 950°C. Experiments were performed using a graphite crucible and anode. Calcium oxide additions to the calcium chloride melt varied from a few percent to saturation. Cells were maintained between 2.6 and 3.2 V, which is sufficient to allow the electrolysis of calcium oxide to occur as follows. CaO = Ca2+ + O2- Calcium ions are thought to be responsible for the actual reduction. The overall reduction reaction is thought to be: BeO +Ca = Be + CaO Experimental evidence of reaction layers and intermediate reaction products will be discussed.

2:25 PM
Solid Oxide Membrane Process for Calcium Production Directly from Its Oxide: *Soobhankar Pati*[1]; Marko Suput[1]; Rachel Delucas[1]; Uday Pal[1]; [1]Boston University

Solid oxide membrane (SOM) technology has been successfully employed for the production of high energy metals such as magnesium, titanium and tantalum by directly reducing their oxides. This paper reports on the recent investigation for calcium production from CaO dissolved in fluoride and chloride based fluxes by the SOM process. This process employs an inert oxygen-ion-conducting stabilized zirconia membrane to separate the cathode in the flux from the anode. When the applied electrical potential between the electrodes exceeds the dissociation potential of CaO, oxygen ions are driven out of the melt and through the zirconia membrane to the anode where they are oxidized. Reduced calcium metal deposits or evolves at the cathode depending on the operating temperature. The SOM cell has been electrochemically characterized. Key concepts related to CaO dissociation, solubility of calcium in the flux and hygroscopic nature of the flux relevant to the SOM process has been explained.

2:50 PM
Studies on Coal in Pressure Leaching of Marmatite Concentrates: *Zhifeng Xu*[1]; Dingfan Qiu[2]; Haibei Wang[2]; [1]Jiangxi University of Science and Technology; [2]Beijing General Research Institute of Mining and Metallurgy

Pressure leaching of a Yunnan marmatite concentrates with adding coal as the elemental sulfur disperser was investigated. The experimental results showed that the coal with carbon content higher than 70% was incapable of dispersing the elemental sulfur from mineral and could not improve the leaching of zinc. The coal with low carbon content (lignite coal) could act as excellent sulfur-disperser in the pressure leaching at 423 K. The mechanism of the lignite coal as the sulfur-disperser was further discussed by ultraviolet, infra-red spectrum and mass spectrum.

3:15 PM Break

3:35 PM
Sulfurization Behavior of Cerium Doped Uranium Oxide by CS2: *Nobuaki Sato*[1]; Motohiro Komura[1]; Shintaro Kato[1]; Akira Kirishima[1]; Osamu Tochiyama[1]; [1]Tohoku University

A new recycle process of uranium from spent fuel by sulfide reprocessing process, which consists of voloxidation for decladding and sulfurization for FP separation, has been developed. During the voloxidation procedure, it was found that cerium doped UO2 solid solution as well as th U3O8 phase was formed by the reaction of U3O8 and cerium dioxide at 1000°C in air. Then the sulfurization of the cerium doped uranium oxide was examined at temperatures lower than 500°C, and found that U3O8 was reduced to form UO2. However, sulfurization of the cerium containing UO2 solid solution phase was surpressed compared with those for pure UO2 and CeO2 cases. The conditions for selective sulfurization were also discussed.

4:00 PM
Titanium Dioxide Potential of the Montecristi Region, Dominican Republic (Hispaniola Island): *Francisco Longo*[1]; [1]Xstrata

Titanium dioxide (ferrotitaniferous) sands deposits have been discovered and are presented as widely spread as beach sands along the Northwest coast of the Dominican Republic, close to actual shoreline, located on the Montecristi region, Dominican Republic (Hispaniola Island). Potential for these resources are now object of this study, taking in account the potential of the area, strategic location (close to a major Marine Port and on an inhabited area) and on a region declared by the DR State as of free taxes to promote and to incentivate investments.

General Abstracts: Light Metals Division: Session I

Sponsored by: The Minerals, Metals and Materials Society, TMS Light Metals Division, TMS: Aluminum Committee, TMS: Reactive Metals Committee, TMS: Recycling and Environmental Technologies Committee
Program Organizers: Neale Neelameggham, US Magnesium LLC; Anne Kvithyld, Norwegian University of Science and Technology

Monday PM Room: 297
March 10, 2008 Location: Ernest Morial Convention Center

Session Chairs: Anne Kvithyld, Norwegian University of Science and Technology; Mike Powers, Agilent Technologies Inc

2:00 PM
Possibilities of Aluminium Dross Treatment and Application of Dross Residue: *Helmut Antrekowitsch*[1]; Bernd Prillhofer[1]; [1]University of Leoben

Concerning the different European and world wide ecological regulations, as well as economic reasons the necessity of dross treatment will increase in future. Due to the processes of the secondary aluminium metallurgy the amount of impurities, the metallic aluminium and the chlorine content of the produced dross vary in a wide range. In the most cases landfilling of the treated dross or even of the whole dross is usual. A defined treatment as a function of the process and the composition leads to different applications without disposal. Furthermore old waste sites can also be treated. This paper characterises the dross in dependence on the processes and the parameters for the treatment and usage in the industry are discussed.

2:20 PM
An Optimization Study for Efficient Hydrogen Removal during Twin Roll Casting: *Aziz Dursun*[1]; Beril Corlu[1]; Murat Dundar[1]; Rasim Erdogan[1]; [1]Assan Aluminium

The efficiency of hydrogen gas removal from liquid metal depends mainly on operational parameters. Inert gas flow rate and rotational speed of the rotor are among those for the systems employing injection and shearing of the gas bubbles for gas removal mechanism. In this study we aimed at determining the optimum argon flow rate and rotor speed for the SNIF system which will result in the most efficient hydrogen removal rate within the liquid metal. The measurements were conducted during 1050 and 3003 aluminium alloy castings. Nine different gas flow rate-rotor speed combinations determined from Design of Experiments(DOE), were applied during castings. A mathematical equation estimating the hydrogen content as a function of flow rate and rotor speed has been developed using a statistical software. The optimum flow rate/rotor speed combinations were determined for the most effective hydrogen gas removal and implemented in real scale production.

2:40 PM
Methods of Aluminium Alloying and Their Impact on Melt Quality: *Volker Ohm*[1]; Reiner Bauer[1]; [1]HOESCH Metallurgie GmbH

Various alloying additions are used in primary or secondary smelters to adjust the chemical composition of aluminium based alloys of all kinds. Due to cost reasons those alloying additions are used as pure metals,where applicable. However, there are close limits for a series of metals used as alloying components. Metals like Mn are thus added either in form of cast low concentrated master alloys, as high concentrated powder metallurgically produced compacts and some are available as high concentrated cast master alloys. This article sets a special focus on the melt quality affected by application of the different products. Laboratory scale trials were carried out to determine the effects under reproducible and controlled conditions. The melt quality was monitored applying AlScan and Prefil. The resulting alloy composition was checked chemically by spectrometer and/or by ICP-OES.

3:00 PM
Manufacture and Characterization of Al-3Mg-Nb: *Noe Lopez P.*[1]; Xochitl Rodriguez G.[1]; Sandra Domínguez M.[1]; Lucio Vazquez B.[1]; V. J. Cortés S.[1]; Marco Domínguez[2]; Gabriel Lara[3]; Manuel Vite[4]; Joel Aguilar[4]; Silvia Buenavista[5]; [1]Universidad Autónoma Metropolitana; [2]Instituto Mexicano del Petroleo; [3]Universidad Nacional Autonoma de Mexico, Instituto de Investigación en Materiales; [4]Unidad Adolfo López Mateos, Sección de Posgrado en Ingeniería, ESIME; [5]Unidad Adolfo López Mateos, ESIQIE

Ingots of Al-3Mg-Nb alloys, were prepared in an electrical induction furnace using a 1/100 Torr vacuum, they were homogenized for 14 h in a box furnace in an argon atmosphere to avoid oxidation. The ingots were preheated and rolled to a final 20 mm thickness. The plates were annealed and samples were machined for tensile, wearing and corrosion tests and for metallography, as well. Yield stress, tensile stress, fracture stress, wearing resistance and corrosion resistance increased with niobium content. Crystalline subgrain size decreases as niobium increases. Results are presented by using graphs.

3:20 PM
An Investigation of Hexavalent-Free Chromate Conversion Coatings for Test and Measurement Instrumentation: *Mike Powers*[1]; [1]Agilent Technologies Inc

Test and Measurement (T&M) products represent a very high performance subset of the monitoring and control product category. These products are characterized by highly sensitive electrical systems that must perform at levels well beyond the conventional products they test. This is an investigation to define and develop a cost effective production process for application of a trivalent (Cr3+) chromate conversion coating (CCC) to replace the hexavalent (Cr6+) CCC that has been employed for aluminum alloy shields, waveguides and other aluminum components used in high frequency T&M instruments. Testing and characterization included surface contact resistivity, corrosion resistance and paint adhesion. It was found that several trivalent chromate conversion coating products demonstrate electrical performance and corrosion resistance that is essentially equivalent to the traditional Cr6+ CCC, while mitigating the toxicological and environmental concerns associated with the use of hexavalent chromium.

3:40 PM Break

3:50 PM
Cryomilled SiC Reinforced Aluminum Nanocomposites: *Timothy Lin*[1]; Fei Zhou[1]; Quan Yan[1]; Chufu Tan[1]; Bob Liu[1]; Adolphus McDonald[2]; [1]Aegis Technology Inc.; [2]U.S. Army Aviation and Missile Command

At present, metal matrix composites (MMCs) typically based on Al alloys are the materials of choice for many lightweight structural applications. Recent development in nanostructured material provides a new opportunity for the substantial strength enhancement of materials (e.g. over 50% improvement) unattainable with conventional approaches, leading to significant weight reduction in structures. In this paper, Aegis will present the development of lightweight, high strength, and impact shielding SiC reinforced Al-based NMMCs (Nanostructured Metal Matrix Composites), with a focus on microstructure design, processing repeatability/consistency, as well as preliminary impact and high-temperature performance. Aegis will also demonstrate the production of large-dimension NMMCs billets and plates by using a cost-effective synthesis and consolidation process that can be scaled up for the mass production.

4:10 PM
Comparative Analysis of the Influence of Inhibitor Concentrations on the Corrosion Susceptibility of Al - 1.0%Zn Alloy in Acidified Vernonia Amegdalina, Pipernigrum and Telferia Occidentalis: Ndubuisi Idenyi[1]; *Chinedu Ekuma*[1]; Simeon Neife[2]; [1]Ebonyi State University; [2]Enugu State University of Science and Technology

The influence of varying concentrations of extracts of vernonia amegdalina, pipernigrum and telferia occidentalis on the corrosion behaviour of Al - 1.0%Zn alloy in varying molarities of HCl has been investigated. Pre-weighed samples of the alloy were subjected to 0.5M and 1.0M HCl,each containing 50 cm^3 and 100 cm^3 of the extracts separately. The set-ups were allowed to stand for 28 days with a set of samples withdrawn weekly for corrosion rate characterization. The results obtained showed the usual corrosion behaviour of initial steep increase in corrosion rate followed by a gradual decline over exposure time, characteristic

of most passivating metals. Expectedly, the vegetable extracts showed inhibition traits with pronounced effects at lower acid molarities with higher extract concentrations. When compared, telferia occidentalis showed the best manifestations, vernonia amegdalina the worst and pipernigrum in-between.

4:30 PM

The Impact of Corrosion on the Deformation Behaviour of Al-Zn Alloys in 0.1M HCl and Seawater: Ndubuisi Idenyi[1]; *Israel Owate*[2]; Cajethan Okeke[3]; Simeon Neife[4]; [1]Ebonyi State University; [2]University of Port Harcourt; [3]University of Nigeria; [4]Enugu State University of Science and Technology

An investigation into the deformation characteristics of Al-Zn alloys exposed to corrosion environments has been carried out. Tensile specimen samples of four (4) different grades of aluminium alloys with varying percentages of zinc were prepared and immersed in baths containing 0.1M HCl and seawater separately and allowed to stand for 30 days. At expiration of the exposure time, the samples were withdrawn and rinsed with distilled water and acetone before being subjected to tensile loading until fracture occurred. The results showed that all the samples obeyed the stress-strain relationship for a relatively ductile material with those exposed to acid showing more brittle fracture than those exposed to seawater, a behaviour that is possibly attributable to hydrogen embrittlement necessitated by the diffusion of hydrogen into the alloy samples from the acidic media.

4:50 PM

Nitrocarburization of Tool Steels for High Temperature Aluminum Forming: *M. David Hanna*[1]; James G. Schroth[1]; [1]General Motors

Forming of aluminum at elevated temperatures requires wear-resistant tool surfaces. The effects of nitrocarburizing temperature and time on the compound layers developed on different low and medium carbon tool steels for use in high temperature forming processes were investigated. The surface layers were analyzed by optical and scanning electron microscopy, microhardness measurements, and X-ray techniques. AISI P20 tool steel was found to be suitable for nitrocaruburization and for use as an elevated temperature tool material due to its relative stability and durability, its availability in large block sizes, and also its functional properties in the forming environment. A non destructive method of relating the hardness of the nitrocarburized AISI P20 steel tool surface with the depth of the compound layer was used to evaluate tool durability with time to provide a means to monitor and estimate the compound layer thickness in the plant environment.

5:10 PM

Development of Ductility-Limited Local Yield Strength Model for High Pressure Die Cast A380 Alloy: *Mei Li*[1]; Jake Zindel[1]; John Allison[1]; Larry Godlewski[1]; [1]Ford Motor Company

In recent years there has been an increasing need for robust simulation methods and tools to accelerate the optimization of process and product design of cast aluminum components in automotive industry. High pressure die casting process provides tremendous cost saving opportunities in manufacturing cast components. Development of Virtual Casting tools for HPDC aluminum will lead to fast prototyping and tooling, thus fast final products with reduced cost. This work describes the development of yield strength model for HPDC A380 alloy. It was found that the yield strength of HPDC aluminum alloy depends not only on the amount of eutectic and precipitation phases, but alos strongly on the porosity level present in the casting. High level porosity reduces the ductility property which results in lower yield strength. The prediction can be used to design and optimize casting component and process.

5:30 PM

Effects of Different Annealing Processes on Microstructural Features of Twin Roll Cast 3003 Aluminum Alloy: *Beril Corlu*[1]; Aziz Dursun[1]; Murat Dündar[1]; Canan Inel[1]; [1]ASSAN Aluminium

Twin roll casting (TRC) can be used to produce aluminum sheets by direct solidification from the melt. Rapidly solidified (upto 800 0C/sec) outer skin has a supersaturated microstructure with very fine grains. Application of prescribed processing routes of TRC cast material, like soft annealing to produce H1X tempers, to the TRC 3003 and 8006 alloys, results in the formation of very large surface grains after recrystallization which causes unwanted surface features called “orange peel” after bending or deep drawing processes. In the present work, annealing processes were carried out in a salt bath in order to see the effect of high heating rate on recrystallized grain size. In addition, the effect of high temperature rapid annealing process prior to the rolling operation on microstructural features were also demonstrated. Surfaces and through thickness microstructures of the specimens were investigated under optical microscope and the mechanical properties have been discussed accordingly.

General Abstracts: Materials Processing and Manufacturing Division: Composition Structure Property Relationships I

Sponsored by: The Minerals, Metals and Materials Society, TMS Materials Processing and Manufacturing Division, TMS/ASM: Computational Materials Science and Engineering Committee, TMS: Global Innovations Committee, TMS: Nanomechanical Materials Behavior Committee, TMS/ASM: Phase Transformations Committee, TMS: Powder Materials Committee, TMS: Process Technology and Modeling Committee, TMS: Shaping and Forming Committee, TMS: Solidification Committee, TMS: Surface Engineering Committee

Program Organizers: Ralph Napolitano, Iowa State University; Neville Moody, Sandia National Laboratories

Monday PM — Room: 282
March 10, 2008 — Location: Ernest Morial Convention Center

Session Chairs: Michael Miles, Brigham Young University; Mohammed Maniruzzaman, Worcester Polytechnic Institute

2:00 PM

Acoustic Cavitation Assisted Improvement of Solidified Structure: *Mamoru Kuwabara*[1]; [1]Nagoya University

Ultrasound is applied before or during solidification of metals. SEM observations show improved refinement of crystal structure and/or entrapment of micro-voids in the matrices of the solidified materials. The results is attributed to micro-multibubble emerged during acoustic cavitation. Not only by vigorous agitation of melt due to micro-jets during solidification but also by a great many nano-bubbles entrapped in the melt before solidification may both contribute to the improved crystal structures. Cold model experiments using water and low melting point metals have been carried out. High speed photography of acoustic multibubble in water and SEM images of many indentations on aluminum foils dipped into the melts with ultrasound verifies the proposed mechanism. The effects of various operating parameters on the solidified structures of metals are discussed based on the experimental results. Many micro-voids acoustically entrapped in the materials are attractive to produce innovative foamed materials with different physical properties.

2:20 PM

Grain Refinement and Grain Boundary Character Distribution of Commercially Pure Molybdenum Produced by Equal Channel Angular Pressing (ECAP): Seng-Ho Yu[1]; Dong Hyuk Shin[2]; *Sun-Keun Hwang*[1]; [1]Inha University; [2]Hanyang University

Commercially pure Mo was grain-refined by ECAP at 500°C. A total of 8 passes of ECAP was conducted and the resulting microstructure and texture were studied. In the as-deformed state, the development of the microstructure and texture was influenced by the strain paths during repetitive ECAP. With four passes of ECAP, lamellar grains of 300 nm in thickness and equiaxed grains of 500 nm were obtained via route A and C, respectively. The grain refinement achieved by the ECAP was attributed to the evolution of low angle boundaries into high angle boundaries with increase in the number of pressing. Like other bcc metals, a strong fiber texture consisting of $<111>_{\theta}$ and $\{110\}_{\theta}$ components was generated in Mo by ECAP. The characteristics of the texture strongly implied that the {110}<111> slip systems were in operation, which is thought to be the main mode of deformation during the severe plastic deformation.

2:40 PM

Effect of Sn Content on the Magnetic Properties and Recrystallization Behaviors of Grain-Oriented Electrical Steels: *Chun-Chih Liao*[1]; Chun-Kan Hou[1]; [1]National Yunlin University of Science and Technology

Fe-3% Si with a sharp Goss orientation has a good magnetic property suitable for the core material of transformers. In order for secondary recrystallization to occur, the growth of other primary grain must be restrained. Sn is easy to segregates at grain boundary and on the surface that pinning the grain boundary mobile. This study was changing the Sn content range from 0 to 0.31wt%, and investigating the effects of SRT (secondary recrystallization annealing temperature) on the recrystallization behaviors and magnetic properties of oriented electrical steel sheets. It was found that the pinning effect of Sn was very strong as the SRT below to 900 degree. The specimens containing 0wt% and 0.05wt% Sn reached secondary recrystallization completing at 900 and 1100 degree, respectively. As Sn content was higher than 0.5wt%, the specimen has pool secondary recrystallization. Specimen containing 0.05wt% Sn has maximum flux density and minimum iron loss.

3:00 PM

Effects of Alloying Elements on the Properties of Mechanical Alloying Processed Cu-Cr Alloys: *Seung Hoon Yu*[1]; Kwang Seon Shin[1]; [1]Seoul National University

The mechanical alloying process has been widely used to refine the microstructure and obtain homogeneous distribution of second phases for the high strength and high conductivity Cu alloys. In powder metallurgy, contamination from the milling media, chamber and process control agent is unavoidable in the process. The electrical conductivity of Cu can be seriously affected by these contaminants, particularly by Fe and O. In this study, minor alloying elements were added to the initial charges of the Cu-Cr powders to form stable second phases. After mechanical alloying, the consolidated products were fabricated by canning, degassing and hot extrusion. The mechanical properties and electrical conductivity were evaluated. It was found that the addition of minor alloying elements improved the mechanical properties and conductivity of the Cu-Cr alloys. They are thought to have had scavenging effects on the contaminants and formed stable second particles which increased the strength of the Cu-Cr alloys.

3:20 PM

Microstructural Effects on Corrosion Behavior of ZnAl Alloy at Different Ag Addition: *S. Valdez*[1]; M. Flores[2]; Said R. Casolco[3]; [1]Universidad Nacional Autóoma de México, Instituto de Ciencias Físicas; [2]Universidad de Guadalajara, Departamento de Ingeniería de Proyectos, CUCEI; [3]University of California, Riverside, Department of Mechanical Engineering

The effect of electrochemical corrosion behavior and microstructure of ZnAl alloy with Ag addition has been investigated using Scanning electron microscopy (SEM), X-ray diffraction (XRD), EDX, Cyclic voltammetry and Corrosion potential measurements in 3.5 wt% NaCl. Surface examination and analytical studies showed that the corrosion behavior of α-Al, η-Zn and ε phases was significantly influenced by Ag additions. ZnAl-0.5 wt.% Ag alloyed exhibited a high corrosion resistance than the 4, 2, 1 wt. % Ag alloyed. Potentiodynamic polarization measurements showed higher icorr values of ZnAl-4 wt.% Ag alloyed. Experimental results revealed that precipitation of ε as a result of reaction between ZnAl alloy and Ag has a beneficial effect on corrosion resistance due to interruption of the continuity of the matrix.

3:40 PM Break

3:50 PM

Mechanical Properties and Microstructure of Friction Stir Welded High-Strength Automotive Steel: *Michael Miles*[1]; Eric Olsen[1]; Tracy Nelson[1]; Matthew Gallagher[2]; [1]Brigham Young University; [2]Mittal Steel

Friction stir welding (FSW) was used to weld high strength automotive steels, including TRIP 590 and DP 590, 780, and 980. Various processing conditions were used to weld these alloys, resulting in different levels of formability, weld hardness, and various weld microstructures. The relationship between welding conditions and resulting properties and weld microstructures will be discussed and compared to laser welded blanks.

4:10 PM

Prediction of Mechanical Strength Evolution during Aging Heat Treatment of Al-Si-Mg-Cu Based Cast Aluminum Alloy: *Mohammed Maniruzzaman*[1]; Boquan Li[1]; Richard Sisson[1]; [1]Worcester Polytechnic Institute

Age hardening of aluminum alloys is done to improve the alloy strength and other mechanical properties of interest. To optimize the properties, the aging schedule, i.e. aging time and temperature, is often chosen empirically. A more efficient way for optimizing the properties would be a model capable of predicting the microstructure and the properties as a function of aging schedule and the alloy compositions. A micromechanical model has been developed to predict the yield strength evolution of Al-Si-Mg-Cu based cast aluminum alloy as a function of time and temperature during aging heat treatment process. The model also predicts the size and volume fraction of the plate-shaped precipitates and incorporates various strengthening mechanisms describing the interaction between precipitates and the motion of dislocation as well as solid-solution strengthening and intrinsic strength of matrix. A set of experiments has been performed to verify the model predictions.

4:30 PM

Integrated Fabrication of Functionally Graded Ti_3SiC_2-TiC Binary Phase Rod by Traveling Zone Sintering Method: *Shuji Tada*[1]; Keizo Kobayashi[1]; [1]National Institute of Advanced Industrial Science and Technology

Ti_3SiC_2-TiC binary phase material was synthesized from raw powder compound of Ti, Si and TiC at molar ratios of 1:1:x (x = 1.8-7.0) with the aim of developing a new hard product. The product obtained by the sintering of the above compound was single phase Ti_3SiC_2 when x was 2.0 or less, while a Ti_3SiC_2-TiC binary phase structure was synthesized from the powder compound with larger x and the mass fraction of TiC in this structure increased with increasing x. Ti_3SiC_2 single phase structure was well densified at up to 1673 K, whereas higher temperature was required to dinsify the binary phase structure. Functionally graded Ti_3SiC_2-TiC binary phase rod was produced by the traveling zone sintering method which enabled integrated sintering of materials at variable temperatures. The synthesized structure was successfully graded and TiC mass fraction in the product varied from 0 to 50%.

4:50 PM

Influence of Small Amounts of Zn, Ni, Fe, Cr and Ti as Quaternary Additions on Shape Memory Characteristics of Cu-Al-Mn Shape Memory Alloys: *U.S. Mallik*[1]; Sampath Vedamanickam[2]; [1]Siddaganga Institute of Technology; [2]Indian Institute of Technology Madras

Quaternary alloying elements Zn, Ni, Fe, Cr and Ti were added to ternary Cu-Al-Mn shape memory alloy in quantities of 1to3 wt.% each. The Cu-12.5 wt.% Al-5 wt.% Mn- wt.% Quaternary element, alloys were prepared by melting pure metals in an induction furnace under an argon atmosphere. The Al and Mn concentrations were maintained constant and amount of quaternary element was varied. Ingots were then homogenized and step quenched to obtain martensitic structure. The alloys were characterized using XRD, DSC and microstructural examination. The shape memory effect and superelasticity were determined by bend and tensile tests. Quaternary elements Zn and Ni are completely soluble, forming solid solution, whereas quaternary elements Fe, Cr and Ti have low solubility and form precipitates. Addition of Zn and Ni increases transformation temperatures, whereas Fe, Cr and Ti decrease. Addition of these quaternary elements increases shape memory effect by 4%, whereas decreases superelasticity by 2%.

5:10 PM

Study on Deformation of Large-Scale Hydraulic Turbine Blade during the Casting Process: *Jiafeng Zhang*[1]; Jinwu Kang[1]; Baicheng Liu[1]; [1]Tsinghua University

Deformation is one of the most common defects during the casting process of large-scale hydraulic turbine blade because of the complex curved 3-D surface geometry. To finally obtain the exact surface contour, anti-deformation is given to wooden pattern in many factories. Numerical simulation is carried out to calculate the deformation of a blade casting used for Three Gorges Power Station. And the calculation is iterated by adjusting the anti-deformation values to finally realize even and appropriate machining allowance. By using ECDS (Electronic Coordinate Determination System), the surface of the casting is measured and machining allowance of each measurement point is given. The calculated results and the measured are in good agreement.

5:30 PM

A Research Study on the High Strength API Steel Production for Sour Gas Pipelines: *Shahrokh Pourmostadam*[1]; [1]Mobarakeh Steel Company

With regard to the achievement of the latest global Technologies for Pipe transportation of natural gas, containing substantial amounts of H2S (sour gas) is becoming increasingly common. Transportation of sour gas through HSLA pipelines can lead to failure from two mechanisms, hydrogen induced cracking (HIC) and sulfide stress corrosion cracking (SSCC). Over the years, suitable measures in alloy design, steelmaking technology and downstream processing has resulted in sour gas resistant linepipe steels. In line with these efforts MSCO, with the utilization of the latest technologies in production trends and suitable design has initiated the trial production of API steels. In this study, efforts are made to present the chemical analysis and mechanical properties of the coils produced in the trial running in addition to the characteristics of API steels for sour gas services.

General Abstracts: Structural Materials Division: Mechanical Behavior of Materials

Sponsored by: The Minerals, Metals and Materials Society, TMS Structural Materials Division, TMS: Advanced Characterization, Testing, and Simulation Committee, TMS: Alloy Phases Committee, TMS: Biomaterials Committee, TMS: Chemistry and Physics of Materials Committee, TMS/ASM: Composite Materials Committee, TMS/ASM: Corrosion and Environmental Effects Committee, TMS: High Temperature Alloys Committee, TMS/ASM: Mechanical Behavior of Materials Committee, TMS/ASM: Nuclear Materials Committee, TMS: Product Metallurgy and Applications Committee, TMS: Refractory Metals Committee, TMS: Superconducting and Magnetic Materials Committee, TMS: Titanium Committee
Program Organizer: Ellen Cerreta, Los Alamos National Laboratory

Monday PM Room: 387
March 10, 2008 Location: Ernest Morial Convention Center

Session Chairs: Rajan Vaidyanathan, University of Central Florida; Veronica Livescu, Los Alamos National Laboratory

2:00 PM

Investigation of the Oxidation Behavior of High Strength NiAl Alloys: *Arthur Brown*[1]; Michael Bestor[1]; Mark Weaver[1]; [1]University of Alabama

Cast model alloys were prepared to investigate the effects of combinations of alloying elements on the oxidation behavior of prospective high strength overlay bond coatings for Ni-base superalloys. Additions of Ti, a potent solid solution strengthener, were studied along with additions of Hf, a Heusler forming element, and Cr. For the investigated compositions, NiAl-1.0 at.% Ti was found to be single phase whereas those containing either higher Ti concentrations, i.e., 5 or 10 at.% Ti, or multiple alloying additions were found contain Heusler-phase and/or alpha Cr precipitates. Single and multi-phase alloys were examined following isothermal and cyclic exposures at 1100°C to determine the influence on the oxide growth rate and the propensity for scale spallation. Alloys containing multiple alloying elements were generally found to oxidize more rapidly and to form thicker oxide scales than single phase alloys. The results are discussed relative to those for binary and microalloyed NiAl.

2:20 PM

Oxidation Behavior of Mo-Si-B Alloys Produced by Reaction Synthesis: *Michael Middlemas*[1]; Joe Cochran[1]; [1]Georgia Institute of Technology

The oxidation behavior of Mo-Si-B alloys produced from the reaction of molybdenum, Si_3N_4 and BN powders was investigated. This powder metallurgy processing method yields finer grained microstructures than is achieved from melt processing. Specimens of composition 97Mo-3Si-1B (wt%), which lie in the phase field consisting of bcc-Mo and the intermetallics Mo_3Si and Mo_5SiB_2, were studied. During oxidation Mo-Si-B alloys undergo an initial period of high weight loss due to evaporation of MoO_3, followed by parabolic oxidation kinetics due to the formation of a protective borosilicate layer. The formation of borosilicate glass layers was examined under reduced P_O2. Oxidation resistance in air was examined between 700°C and 1300°C. The small spacing of the intermetallic phases significantly reduces the transient weight loss during the initial stages of oxidation. Using powder metallurgy processing allows the addition of aluminum to the alloy. The effect of aluminum additions on oxidation resistance was also examined.

2:40 PM

Martensitic Transformation Paths of NiTi: Nicholas Hatcher[1]; *Oleg Kontsevoi*[1]; Arthur Freeman[1]; [1]Northwestern University

Despite intensive investigations of NiTi shape memory alloy, the detailed microscopic mechanisms governing its structural evolution during the martensitic transformation is not fully understood. Using first-principles DFT calculations with the highly precise FLAPW method, we have studied the transition paths between the B2, R, B19, and B19' phases of NiTi to identifythe governing processes of the transformation by means of calculations of total energies, electronic and band structures, elastic moduli, and shear and generalized stacking fault energetics. We also investigated a new transition path between the B2 and B19' phases via a transformation that involves shuffles of atomic layers followed by a monoclinic angle relaxation. We show the role of electronic topological transitions, Fermi surface nesting and band structure evolution in the stability of the corresponding phases, and the effect of the doping on the electronic structure and transformation paths. Supported by the AFOSR (grant No. FA9550-07-1-0013).

3:00 PM

Mechanical Behavior of Electrodeposited Nanocrystalline Nickel: *Hsiao-Wei Yang*[1]; [1]University of California

In the present investigation, the mechanical behavior of bulk electrodeposited (ED) nanocrystalline nc-Ni having average grain size of 100 nm was investigated at temperatures, T, lower than 445 K (T < 0.25 Tm, where Tm is the melting point of the material) where there is limited grain growth and as a function of varying strain rate. The results show that for constant strain rate, the ductility of nc-Ni increases with increasing temperature, but the opposite is true for the ultimate tensile strength; and that for constant temperature, ductility decreases with increasing strain rate. The results are discussed with reference to findings recently reported for nc-materials.

3:20 PM

Pile-up/Sink-in in Nanoindentation Rate Sensitive Creeping Solids: *A. Elmustafa*[1]; [1]Old Dominion University

We use FEM to simulate materials of variable hardness, work hardening exponent, χ of 0.1-0.3 and a strain rate sensitivity of von Mises stress, υ_σ of 0.08-0.16 to estimate pile-ups and sink-ins during indentation creep. We report that materials pile-up for $\upsilon_H/\upsilon_\sigma \geq 1.0$ and sink-in for $\upsilon_H/\upsilon_\sigma \leq 1.0$, υ_H, is the strain rate sensitivity of the hardness. This is consistent with the fact that $\upsilon_H/\upsilon_\sigma$ approaches 1 for small H/E*, i.e., soft materials and deformation is intimately dominated by pile-up. On the other hand when $\upsilon_H/\upsilon_\sigma$ approaches 0 for high H/E* it corresponds to purely elastic deformation and is apparently dominated by sink-in in a manner prescribed by Herizian contact mechanics.

3:40 PM

Irradiated Mechanical and Microstructural Properties of a Nano-Structured Ferritic Alloy for Nuclear Applications: *David McClintock*[1]; David Hoelzer[2]; Mikhail Sokolov[2]; Randy Nanstad[2]; [1]University of Texas/Oak Ridge National Laboratory; [2]Oak Ridge National Laboratory

Advanced nano-structured ferritic alloys (NFAs) containing a high density of ultra-fine (2-5 nm) nanoclusters enriched in Y, Ti, and O are considered promising candidates for structural components in future nuclear systems. The microstructure of a NFA is composed of nanometer sized regions rich in Y-Ti-O uniformly distributed in a ferritic matrix. The high number density of nanoclusters in NFAs are responsible for their superior tensile strengths compared to conventional ODS ferritic alloys and may provide effective trapping centers for point defects and transmutation products produced during neutron irradiation. This paper summarizes the mechanical and microstructural properties of an advanced NFA, designated 14YWT, currently being developed at Oak Ridge National Laboratory. An identical alloy to 14YWT, designated 14WT, was produced without nanocluster dispersions in order to quantify the effect of the nanoclusters on mechanical properties. Microstructural characterization, tensile, and fracture toughness data for the irradiated and unirradiated condition will be presented.

4:00 PM Break

4:20 PM
Modeling of Hollow Particle Filled Functionally Graded Composites: Maurizio Porfiri[1]; *Nikhil Gupta*[1]; [1]Polytechnic University

Functionally graded composites are generally made by creating a particle volume fraction gradient along the material thickness. However, such composites have several inherent limitations, e.g. non-uniform coefficient of thermal expansion. A composite is analyzed in this work, which is based on creating a gradient of wall thickness of hollow particles in the material microstructure rather than the volume fraction gradient. A differential scheme is applied to estimate effective elastic modulus of such composites containing high volume fraction of particles. The modeling scheme extends the existing mathematical models applicable for dilute suspension of particles in a matrix material to account for the particle-particle interaction. The model can be used to prepare materials selection charts given the properties of the constituent materials and their volume fractions in the composite material.

4:40 PM
Modeling of Viscoelastic Properties of Syntactic Foams: Gabriele Tagliavia[1]; Maurizio Porfiri[1]; *Nikhil Gupta*[1]; [1]Polytechnic University

Glass hollow particle filled polymeric composites, called syntactic foams, are widely used in marine applications. The damping capabilities of syntactic foams are of major interest in marine structural applications. The objective of this analysis is to develop relations between the viscoelastic properties of syntactic foams in terms of the properties and the volume fractions of their constituents. Therefore, a new model for the complex dynamic Young's modulus is developed. The elastic-viscoelastic correspondence principle is applied to obtain the viscoelastic relation for an infinitely dilute dispersion of hollow particles. The differential effective medium approach (DEMA) is then used to extrapolate the solution for a concentrated dispersion. The developed model is validated with the data obtained with an in-house experimental setup.

5:00 PM
On Equations of Fatigue Crack Propagation (or FCG) of Materials: *Ngo Van Quyet*[1]; [1]Hanoi LeQuyDon University of Technology

After presenting overview on Equations of Fatigue Crack Propagation, the new equation of Fatigue Crack Propagation with load frequency and based on theory on analysis misuse of Sedov L.I. and experimental data of some the other researchers has been being suggestion by author. That new non-measure equation had been testing and its application in the practice (reinforced Frame of meter-gauged locomomotive of type D19E.

5:20 PM
Bending Analysis of Functionally Graded Hollow Particle Filled Composites: *Nikhil Gupta*[1]; Maurizio Porfiri[1]; [1]Polytechnic University

Particle reinforced functionally graded composites (FGCs) are analyzed for bending properties. The FGCs are based on filling hollow particles in a matrix material. Hollow particle filled composites are used in marine and aerospace structural applications. Hollow particle filled FGCs have potential to be used in a variety of additional applications. The bending performance is compared for FGCs having gradient of wall thickness and volume fractions. The tensile and compressive moduli values of hollow particle filled composites are different. Hence, the neutral axis of the composite is determined and then appropriate tensile or compressive modulus values are applied for the analysis. Results show that the variation in wall thickness provides better opportunities for tailoring the properties of such composites.

5:40 PM
Modeling Ductile Fracture Using the Discontinuous Velocity Domain Splitting Method: *Ioan Ionescu*[1]; [1]University Paris 13

We present a new method and its application to modeling ductile fracture of heterogeneous materials. This method considers a special class of velocities fields constructed as follows. The body is split into two subdomains: one subdomain is at rest and on the other the velocity corresponds to a rigid motion. Thus, the discontinuous velocity field is determined only by the shape of one subdomain and by a rigid motion. The deformation is localized at the boundary of this subdomain. The problem is thus reduced to the minimization of a mesh free plastic dissipation functional depending on shapes. For discretization we make use of the Bezier interpolation and genetic algorithms are used to minimize the plastic energy. Computational tests, performed for benchmarks related to the in-plane flow of a Von-Mises material, gives excellent results at a very low computational cost. Other examples involving plastic yield surfaces characterizing geo-materials are also presented.

Hael Mughrabi Honorary Symposium: Plasticity, Failure and Fatigue in Structural Materials - from Macro to Nano: High-Temperature Mechanical Properties: Creep, Fatigue and Thermomechanical Fatigue

Sponsored by: The Minerals, Metals and Materials Society, TMS Structural Materials Division, TMS Materials Processing and Manufacturing Division, TMS: High Temperature Alloys Committee, TMS/ASM: Mechanical Behavior of Materials Committee, TMS: Nanomechanical Materials Behavior Committee
Program Organizers: K. Jimmy Hsia, University of Illinois, Urbana-Champaign; Mathias Göken, Universitaet Erlangen-Nuernberg; Tresa Pollock, University of Michigan - Ann Arbor; Pedro Dolabella Portella, Federal Institute for Materials Research and Testing; Neville Moody, Sandia National Laboratories

Monday PM — Room: 386
March 10, 2008 — Location: Ernest Morial Convention Center

Session Chairs: Tresa Pollock, University of Michigan; Hans-Juergen Christ, University of Siegen

---

2:00 PM Keynote
Fatigue of Austenitic Stainless Steel under Isothermal and Thermomechanical Conditions: *Hans Christ*[1]; Valerij Bauer[1]; [1]University of Siegen

One of the first studies in the newly formed research group of Hael Mughrabi in Erlangen dealt with thermomechanical fatigue (TMF) behavior of an austenitic stainless steel. The results obtained at that time were broadly supplemented in the present work by means of isothermal and thermomechanical fatigue tests carried out at temperatures ranging from room temperature to 800°C. The tests were conducted both in air and vacuum applying plastic-strain control at constant plastic strain rate and amplitude. The test results in combination with microstructural findings regarding dislocation arrangement and damage evolution were used for an advancement of life prediction models. Three models published in literature were selected, since they were found to be suitable for isothermal fatigue conditions. The models were extended to non-isothermal conditions and applied to TMF. By means of tests comprising dwell times within the loading cycle, the predictive capability of the models were analysed.

2:30 PM Invited
Extending the Flow Behavior in High-Temperature Creep to Materials with Ultrafine Grain Sizes: *Terence Langdon*[1]; [1]University of Southern California

The characteristics of creep in conventional materials are now understood reasonably well. However, a considerable interest has developed in the last decade in the processing of materials with submicrometer or nanometer grain sizes. Many of these materials are fabricated using various techniques based on the application of severe plastic deformation. This presentation describes the principles of these techniques and examines the significance of extending the conventional creep mechanisms to materials with exceptionally small grain sizes. Special emphasis is placed on the role and significance of superplasticity in deformation at elevated temperatures and the possibility of achieving grain boundary sliding at relatively low homologous temperatures.

2:50 PM
Formation of a Braid Structure during Cyclic Deformation a Heat-Treated PM Ti-48Al-2Cr-2Nb Alloy at 500°C: *Gilbert Henaff*[1]; Mustapaha Jouiad[1]; Marc Thomas[2]; Olivier Berteaux[2]; [1]Ecole Nationale Supérique De Mécanique Et D´Aérotechnique; [2]ONERA

The present paper addresses the relation between the stress-strain behaviour, cyclic deformation mechanisms and the microstructures produced by various heat treatments applied to hipped Ti-48Al-2Cr-2Nb powder compacts. More precisely, it is shown that, at room temperature, the cyclic strain hardening is

directly related to the rate of formation of a vein-like structure. The influence of microstructural of parameters such as grain size, volume fraction of different phases, lamellar spacing, etc. on this relation has been examined. At 500°C, a vein-like structure is also observed, even in microstructures that do not exhibit this type of substructure at room temperature. Furthermore the superior fatigue resistance and limited strain hardening exhibited by a fine fully lamellar microstructure at 20°C still holds at 500°C, where the vein-like structure is changed into a braid-like structure due to the longer fatigue life.

3:05 PM

Point-Defect Mediated Dislocation Nucleation in Nanoindentation: *Amit Samanta*[1]; Ju Li[1]; Ting Zhu[2]; [1]Ohio State University; [2]Georgia Institute of Technology

We examine the conditions for heterogeneous nucleation of dislocations beneath an indenter in copper, aided by vacancies and interstitials near the surface. Atomistic calculations are performed to assess the stress-dependent formation and migration energies of point defects in the bulk and near the surface, which are used to predict the realistic kinetics of point-defect motion under the indenter due to the large stress gradient. The reaction pathways and activation energy barriers for dislocation nucleation near these point defects are computed using a modified nudged elastic band method, and compared with those of homogeneous nucleations. The activation volumes of point-defect mediated dislocation nucleations are also compared with homogeneous nucleation. A deformation mechanism map is drawn as a function of temperature and indentation load. Our results indicate the presence of a diffusive regime for small indentation loads while for higher loads dislocation-nucleation and defect migration govern the kinetics of the process.

3:20 PM

Effect of Particle Strengthening on the Very High Cycle Fatigue Behavior of Two Nickel-Base Alloys: *Martina Zimmermann*[1]; Christian Stoecker[1]; Hans-Juergen Christ[1]; [1]University of Siegen

Fatigue behaviour in the VHCF regime is dominated by crack initiation rather than long crack propagation. Due to heterogeneously distributed plastic deformation the correlation between microstructure and damage mechanism is widely discussed. Fatigue tests were carried out on two nickel-base alloys (solid-solution hardened Nimonic 75 and precipitation hardened Nimonic 80A) in order to characterize the damage evolution in the VHCF range. Fatigue failure still occurred beyond 10^7 cycles. An adjustment of the microstructure for the precipitation-hardened alloy Nimonic 80A showed surprisingly for the fatigue life that the overaged condition behaves more beneficial as compared to the peak-aged condition in the VHCF range. This result could not be rationalized by means of fracture surface analysis and, hence, seems to be a result of slip homogeneity. Transmission electron microscopy was carried out, in order to characterize the influence of microstructure, the resulting dislocation slip behaviour and the relevant dislocation particle interaction mechanism.

3:35 PM Break

3:45 PM Invited

Interfacial Dislocations and Creep in Ru-Containing Superalloy Single Crystals: *Tresa Pollock*[1]; Laura Carroll[2]; Shuwei Ma[1]; [1]University of Michigan; [2]General Electric Aviation

Ruthenium additions to Ni-base single crystals permit new alloying domains to be explored within these superalloy systems. Creep deformation and the development of interfacial dislocation networks have been investigated in alloys with wide variations in Ru, Cr and Co. Additions of Ru and Cr strongly influence partitioning of elements between the matrix and precipitate phases and therefore strongly influence misfit and the development of interfacial dislocation networks. The spacing of dislocations in interfacial nets following high temperature aging and after creep deformation at 950°C has been characterized. Additionally, the density of dislocations within "rafted" precipitates has been measured. Creep rates do not directly scale with interfacial network spacing and the density of dislocations in excess of that needed to relax misfit varies with alloy composition. The implications for creep modeling and for alloying to increase creep resistance will be discussed.

4:05 PM Invited

Interfacial Structure and Mechanical Properties of Al_2O_3 Long Fiber Reinforced NiAl Composites: *Günter Gottstein*[1]; Weiping Hu[1]; Hao Chen[1]; Yunlong Zhong[1]; [1]RWTH Aachen University

The intermetallic compound NiAl has excellent potential for high temperature structural applications but suffers from low temperature brittleness and insufficient high temperature strength. One way to remove these deficiencies is the reinforcement by high strength ceramic fibers. Such intermetallic matrix composites can be conveniently fabricated by hot pressing of matrix coated fibers. Al_2O_3 single crystal fibers show excellent chemical stability with the NiAl matrix, but the residual thermal compressive stresses during cool down dramatically degrades the fiber strength and thus, renders the composite useless for structural applications. We report on an experimental and computational study to mitigate this problem and to fabricate Al_2O_3/NiAl composites with sufficient high temperature strength. Analytical TEM, mechanical testing and push-out tests were employed to characterize chemistry, microstructure and mechanical properties of the composites. It will be shown that a processing window exists that allows producing intermetallic matrix composites with promising mechanical properties.

4:25 PM

Mechanisms of Crack Propagation in TiAl-Alloys Observed by In-Situ Testing in the Atomic Force Microscope (AFM): *Florian Pyczak*[1]; Farasat Iqbal[1]; Mathias Göken[1]; [1]University Erlangen-Nuernberg, Institute General Materials Properties

TiAl-alloys, especially the variants with high niobium content, are attractive light weight high temperature materials. Nevertheless, a deeper understanding of crack nucleation and propagation in these materials is desirable. AFM is an interesting technique to study crack propagation in-situ in TiAl-alloys. AFM is not only able to picture the crack path itself but also elastic and plastic deformation in the vicinity of the crack. Here AFM was employed to investigate the crack tip and the elastic and plastic deformation zone near it. Many TiAl-alloys have a lamellar microstructure, where boundaries between the gamma-TiAl and alpha2-Ti_3Al lamellae act as favorable sites for crack propagation mixed with sections of the crack path running more or less perpendicular to the lamellar interfaces along twins or deformation bands. Nucleation of new cracks was often preceded by deformation in the respective area visible as significant local elevations and depressions of the surface in an AFM.

4:40 PM

Characterization of Crystallographic Crack Initiation Sites in Renè 88DT at 593°C: *J. Miao*[1]; T.M. Pollock[1]; J.Wayne Jones[1]; [1]University of Michigan, Ann Arbor

The very high cycle fatigue behavior of a polycrystalline nickel-base superalloy René 88 DT has been studied by using ultrasonic fatigue testing instrumentation at 593°C. All fatigue failures initiated internally. Nearly all initiation sites consist of large crystallographic facets. Crystallographic facets at crack initiation sites can be divided into two groups according to their 3D geometric shape: single plane facets or chevron-shaped facets. The microstructure associated with crystallographic crack initiation was examined by combining metallographic serial sectioning, EBSD and fractographic analysis. Facets at crack initiation sites were formed by fatigue crack initiation and crack growth in large grains. The crystallographic planes of these facets are of {111} type and oriented close to the orientation for maximum shear stress. Clusters of grains with similar orientations exist at crack initiation sites. The mechanisms of fatigue crack initiation and early small crack propagation in this alloy are described.

4:55 PM

Interaction of Fatigue Crack Propagation with Grain Boundary Networks: Yong Gao[1]; *Mukul Kumar*[2]; James Stolken[2]; Robert Ritchie[1]; [1]University of California; [2]Lawrence Livermore National Laboratory

Grain boundary engineering has lead to performance improvements where intergranular degradation is operative. Such processing to improve the HCF properties of a Ni-base superalloy through modification of the grain-boundary distribution is considered. Fatigue properties at ambient and elevated temperatures for microstructures with varying proportions of crystallographically "special" vs. "random" boundaries are considered. We shall also examine the interaction of propagating (~10–900 μm) surface cracks with grain boundaries (and their

networks) of known character, with respect both to deflections in crack trajectory and local changes in crack-growth rates that occur at or near the boundary . In addition, FEM calculations are performed to evaluate the effective driving force and plastic-zone profile for such small-crack propagation, incorporating information from both the local microstructure (from EBSD scans) and the surface crack-path profile. This work was performed under the auspices of the U.S. DOE by University of California, LLNL under contract No. W-7405-Eng-48.

5:10 PM
Plasticity Size-Effects and Dislocation Substructures in Two Titanium Alloys: *Dave Norfleet*[1]; Peter Anderson[1]; Dennis Dimiduk[2]; Michael Uchic[2]; Michael Mills[1]; [1]Ohio State University; [2]Air Force Research Laboratory

Using current micromechanical fabrication and testing methods, micron-sized compression samples (Ti-6Al and single colony Ti-6Al-2Sn-4Zr-2Mo-0.1Si) were tested at room temperature. The results of these experiments are compared to recent Ni and Au microcrystal experiments under the context of obstacle vs. kink-mode dislocation mechanisms. Nickel and gold, obstacle controlled materials, display strong size effects with a marked increase in strength as the sample volumes were reduced. In comparison, the titanium alloys, kink-mode materials, exhibit a much less dramatic strengthening effect. Subsequent FIB-based TEM foil preparation was performed on the titanium microcrystals, utilizing an in-situ micromanipulator. Foils were prepared along active slip bands to study the dislocation dynamics of the slip system. Using a variety of TEM imaging conditions, such as Bright Field STEM, dislocation analysis was performed on each of these materials to gain an understanding as to the micro-mechanisms that control plasticity at this size scale.

5:25 PM
3D Modeling of Size Scaling Aspects of Plastic Flow in Single Crystal Ni-Based Superalloys: Jaafar El-Awady[1]; Akiyuki Takahashi[2]; *Nasr Ghoniem*[1]; [1]University of California, Los Angeles; [2]Tokyo University of Science, Faculty of Science and Technology

Here we utilize large scale 3-dimensional Parametric Dislocation Dynamics (PDD) simulations coupled with the Boundary Element Method (BEM) to study the deformation behavior of cylindrical micron sized single crystal Ni-based superalloys. The BEM is used to calculate the image fields due to the interaction of dislocations with precipitates and the finite dimensions of the crystal. The solution is then superimposed on the elastic field resulting from dislocation ensembles in an infinite medium as calculated from the PDD. Statistical analysis are performed on cylindrical samples have diameters in the range 0.25 to 5 μm and the range of initial dislocation densities in the simulations are varied from 10^{11} m^{-2} to 10^{13} m^{-2}. The fundamental aspects of size scaling aspects of plastic flow in a precipitation-strengthened material are identified through the use of these simulations and the simulated results of dimensional scaling of the flow stress agree well with experimental findings.

5:40 PM
Microscopic Examination of Fatigue Behavior in a Monocrystalline Ni-Based Superalloy: *Clarissa Yablinsky*[1]; Katharine Flores[1]; Michael Mills[1]; James Williams[1]; [1]Ohio State University

Historically, the critical design parameter for Ni-based superalloy turbine blades has been creep resistance. Recently, because of modern airfoil designs, the focus has broadened to include fatigue resistance, resulting in the need to better understand fatigue behavior. In this study, compact tension specimens of monocrystalline Ni-based superalloy René N5 were tested under cyclic loading conditions. Test temperature, frequency (0.5 Hz/10 Hz), and environment (air/vacuum) were varied in order to examine the effects of recovery, plastic zone size, oxidation, etc. on crack growth. Fracture surfaces and microstructures were characterized using a scanning electron microscope in order to examine crack path selection and changes to the γ/γ' morphology within the crack wake and in the far-field. Dislocation arrangements were characterized via transmission electron microscopy using conventionally prepared and site-specific foils prepared by focused ion beam techniques in order to understand the damage mechanisms active during cyclic loading.

Hume-Rothery Symposium - Nanoscale Phases: Session II

Sponsored by: The Minerals, Metals and Materials Society, TMS Electronic, Magnetic, and Photonic Materials Division, TMS: Alloy Phases Committee
Program Organizers: Sinn-wen Chen, National Tsing Hua University; David Cockayne, University of Oxford; Seiji Isoda, Kyoto University; Robert Nemanich, Arizona State University; K.-N. Tu, University of California, Los Angeles

Monday PM Room: 276
March 10, 2008 Location: Ernest Morial Convention Center

Session Chairs: Robert Nemanich, Arizona State University; King-Ning Tu, University of California, Los Angeles

2:00 PM Invited
Controlling Metal/Compound Semiconductor Interfacial Phase Formation at the Nanometer Scale through the Interplay of Thermodynamics and Kinetics: *Chris Palmstrom*[1]; [1]University of California at Santa Barbara

Determination and understanding phase formation sequences and reaction kinetics is of utmost importance for controlling thin films and interfaces at the nanoscale. In-situ and ex-situ atomic scale structural and chemical characterization in combination with molecular beam epitaxial growth and post growth reaction studies have been used to make predictions of phase diagrams and reaction kinetics at the nanometer scale to form stable films and interfaces in these systems. This presentation will emphasize approaches for controlling the interfacial and bulk structural and electronic properties of epitaxial ferromagnetic metal/compound semiconductor heterostructures for Spintronic and shape memory applications. Material systems will include elemental transition metals, transition metal-group-III compounds, rare-earth-group-V compounds and Heusler alloys grown on III-V semiconductor surfaces.

2:25 PM Invited
Coaxial Metal-Oxide-Semiconductor(MOS) Au/Ga_2O_3/GaN Nanowires: *Li-Jen Chou*[1]; [1]National Tsing-Hua University

Coaxial metal-oxide-semiconductor (MOS) Au-Ga_2O_3-GaN heterostructure nanowires were successfully fabricated by in-situ two-step process. The Au-Ga_2O_3 core-shell nanowires were first synthesized by the reaction of Ga powder, mediated Au thin layer and SiO_2 substrate at 800°C. Subsequently, these core-shell nanowires were nitridized in ammonia ambient to form GaN coating layer at 600°C. An atomic flat interface between oxide and semiconductor which warrant the high quality of the MOS device is achieved. The crystal structure of the GaN was characterized by field-emission transmission electron microscope (FETEM) indicated the single crystalline nature. These novel 1-D nitride based MOS nanowires would not only enrich a well-established bank of nanostructure morphologies, but also may have a promise for the building block to the future vertical high power and high frequency logic nanoelectronics.

2:50 PM Invited
Fabrication of Hollow Nanostructures: *Ulrich Goesele*[1]; [1]Max Planck Institute of Microstructure Physics-Halle

Various approaches will be discussed to fabricate hollow nanostructures including those based on nanoporous templates and those based on the nanoscale Kirkendall effect. The presentation will concentrate on one-dimensional nano-structures but will also touch on zero-dimensional nanostructures. Experimental as well as theoretical aspects will be presented

3:15 PM Invited
Employment of Oriental Philosophy in the Establishment of Framework for Probing Nano-Scale Science and Technology: *Jeng-Gong Duh*[1]; [1]National Tsing Hua University

Nano technology is not only scale-down of feature size for things of interest, but also envisages it as functional set of conceptual and spiritual essence. This study is aimed to demonstrate striking identity between nano-world and oriental philosophy. The theory of Yin and Yang in Yi-Jing describe system of cosmology and philosophy on the ideas of dynamic balance, and evolution of events. Being and non-being are two special aspects of Taoism by Lao-Tzu and Chuang-Tzu.

The spirit of Zen in Buddhism and Confucianism reflect internal constancy and wisdom to identify order and inevitability of change. It will be revealed that development of nano-science and technology is indeed originated from Yi-Jing, Taoism, Buddhism and Confucianism. Take the diffusion process as an example, and "vacancy" and "matrix atom" in material can be considered as "non-being" and "being" in Taoism. Especially, phase transformation encountered in materials seems like chance events in Yin-Ching.

3:40 PM Break

4:00 PM Invited
Silicide Nanostructure Evolution during Coarsening Processes: *Robert Nemanich*[1]; Matthew Zeman[2]; Anderson Sunda-Meya[2]; [1]Arizona State University; [2]North Carolina State University

The real time coarsening phenomena involving rare earth (Dy, Er) and transition metal (Ti, Zr. Hf) silicide nanotructures is studied with UV-PEEM. The measurements are obtained with the samples at ~1100C, and that in both cases larger islands grow at the expense of smaller islands. The process is characteristic of surface diffusion driven ripening of 3d nanostrucures on a 2d surface. Inspection of individual islands shows significant differences between the two groups of materials. The transition metal silicides show unfacetted structures and smoothly curved edges, while the rare earth silicides show facetted island structures some of which are elongated into nano wires. During the process the transition metal silicides show significant displacement and often are seen to attractively migrate and coalesce, while the transition metal islands do not show significant displacement. These differences are discussed in terms of the attachment and detachment of silicide clusters near edges of the islands.

4:25 PM Invited
Interplay of Nanoscale Phases in Some Ferroelectric Oxides: *Haydn Chen*[1]; [1]Tunghai University

The ever growing micro-to-nano electroic industries called for investigation of materials system in many aspects, not limiting to the scaling down technologies of devices but also the unverstanding of nanoscale phases or domains or oter entities by which the system behaviors. In the past decades, our group has been engaged in a range of studies focusing on the interplay of structure and properties in dilectrics and ferroelectrics. Our works ecompassed ferroelectric, anti-ferroelectric as well as relaxor materials in many bulk and thin-film complex oxides. Further, we have pursued investigation into the nontraditional behaviors including nonlinear, temporal and coupled interactions. This paper highlights our recent research and presents a systematic view of the interpaly among dipoles in multi-phase systems.

4:50 PM Invited
Stabilization of Nanometer-Thick Subsolidus Quasi-Liquid Interfacial Films: *Jian Luo*[1]; Haijun Qian[1]; Xiaomeng Shi[1]; Vivek Gupta[1]; [1]Clemson University

Recent observations of two classes of impurity-based, nanometer-thick, quasi-liquid interfacial films are presented. First, vanadia-based, surficial amorphous films are stabilized on anatase (101) surfaces (APL 91, DOI: 10.1063/1.2768315 (2007)). Second, impurity-based disordered grain boundary films are stabilized in Ni-doped W and other refractory metals (APL 87, 231902 (2005); Acta Mater. 55, 3131(2007)). These films exhibit an "equilibrium" thickness, which corresponds to the Gibbsian excess of solutes/adsorbates and is a function of the equilibration temperature and chemical potential(s). Both classes of films are stabilized well below the bulk eutectic/solidus temperatures; yet they exhibit large structural disorder (being quasi-liquid) in HRTEM, where analogies to prewetting and premelting phenomena are made. They can be considered as free-surface and metallic counterparts to the well-known equilibrium-thickness intergranular films (IGFs) in ceramics, respectively. Unified thermodynamic models are envisioned (Crit. Rev. Solid State Mater. Sci. 32, 67 (2007)). Acknowledgements: NSF CAREER and AFOSR Young Investigator awards.

Magnesium Technology 2008: Primary Production

Sponsored by: The Minerals, Metals and Materials Society, TMS Light Metals Division, TMS: Magnesium Committee
Program Organizers: Mihriban Pekguleryuz, McGill University; Neale Neelameggham, US Magnesium LLC; Randy Beals, Chrysler LLC; Eric Nyberg, Pacific Northwest National Laboratory

Monday PM — Room: 292
March 10, 2008 — Location: Ernest Morial Convention Center

Session Chair: Neale Neelameggham, US Magnesium LLC

2:00 PM
Effects of KCl on Density and Liquidus of MgF_2-BaF_2-LiF Electrolyte: *Ying Nie*[1]; Shaohua Yang[1]; Zhaowen Wang[1]; Linzhi Ma[1]; Xingliang Zhao[1]; [1]Northeastern University

This paper studies on the preparation of Mg-Al alloys from MgO by molten salt electrolysis method. MgF_2-BaF_2-LiF is taken as electrolyte. The experimental results indicated that KCl as additive can obviously improve the physical and chemical properties of electrolyte. The research is focused on density and liquidus. The density and liquidus of the electrolyte are decreased with the increase of KCl content. The density of electrolyte reduces from 3.250g/cm3 to 2.793g/cm3 with the mass percentage of KCl from 0 to 11% under 850°C temperature, the difference is about 0.457g/cm3. The liquidus of electrolyte decreases gradually from 807°C to 790°C with the mass percentage of KCl from 0 to 11%, the decreased value is 17°C.

2:20 PM
Electrodeposition of Magnesium from BaF_2-LiF-MgF_2 Electrolyte: Shaohua Yang[1]; *Zhaowen Wang*[1]; Ying Nie[1]; Xingliang Zhao[1]; [1]Northeastern University

Electrodeposition of magnesium from molten salts was studied by electrochemical techniques. BaF_2-LiF-MgF_2 was electrolyte system with magnesium oxide as raw material. It was proved Mg2+ was deposited more prior than other ions during cyclic voltammetry and potential step measurement at 850°C. There is difference of deposited potential on different electrode, such as glassy carbon, platinum and graphite. The determined concentration of diffusing species, as well as the fact that Mg2+ are the only cation to deposit on electrode, indicate that the process in diffusion of dissolved metal from the electrode interface to the electrolyte.

2:40 PM
Preparation of Al-Mg Alloys from MgO through Molten Salt Electrolysis Method: Shaohua Yang[1]; *Zhaowen Wang*[1]; Ying Nie[1]; Jidong Li[1]; [1]Northeastern University

Aluminum-magnesium alloys were prepared from magnesium oxide through molten salt electrolysis method. MgF_2-BaF_2-LiF was taken as electrolysis, and its density is higher than aluminum liquid, so upload cathode, which was aluminum liquid, was carried through in test. Current efficiency is more than 80%, the maximum comes up to 87.7%. Some amount of MgO was flowed into electrolytic cell every some time. The content of Mg in alloys increases gradually and up to 18.6% with lengthening electrolyzing time. It was revealed that addition of KCl can improve the physical-chemical property of the electrolyte.

3:00 PM Break

3:20 PM
The Application of Pattern-Recognition and a Back Propagation Artificial Neural Network Model in Mg Electrolysis Current Efficiency: *Bing Li*[1]; Jiangning Liu[1]; Ze Sun[1]; Jianguo Yu[1]; [1]East China University of Science and Technology

The effects of current density, electrode distance and temperature on the current efficiency for magnesium electrolysis have been investigated in laboratory cell. Patter-recognition method was used to analyze current efficiency data of the industrial magnesium cell. The current efficiency sort plot in planar main component space has been obtained and data points of current efficiency more than 85% can be centralized and the distinct optimizing region was obtained. The relationship between current efficiency and multifactors presents non-linear,

a back propagation artificial neural network model(BPANN) has been applied for magnesium electrolysis. The results has indicated that BPANN is suitable for setting up model between non-linear relationship current efficiency and multifactors with higher imitation definition, and it can be served to conduct practical application in industry by accurately predicting the current efficiency.

3:40 PM

The Reverse Effects of MgO on Magnesium Electrolyte Properties and Measure to Improve MgO Solubility: *Bing Li*[1]; Jun Li[1]; Jian Guo Yu[1]; Jiangning Liu[1]; [1]East China University of Science and Technology

In this paper MgO as impurity was added to the traditional quadribasic magnesium electrolyte, namely MgCl2(12%)-CaCl2(18%)-NaCl(40%)-KCl(30%). The effects of MgO on electrolyte physicochemical properties such as conductivity, density and interface tension and the liquid Magnesium aggregation state on cathode during Magnesium electrolysis have been studied. LaCl3 was used as additives to the above electrolyte to improve MgO solubility and the electrolyte composition has been evaluated by current efficiency.

4:00 PM

Electrochemical Co-Deposition of Magnesium Based Alloy from Molten Salts: Ninglei Sun[1]; Jialin Ren[1]; *Hongmin Zhu*[1]; [1]Beijing University of Science and Technology

Magnesium based alloys with aluminum and zinc were obtained through electrochemical co-deposition from LiCl-NaCl-$MgCl_2$ melt. The possibility of electrochemical co-deposition was discussed in detail by electro-analytical methods. The co-deposition happens when the concentration of aluminum and zinc ions were kept at low value and the current density is high enough. The components of alloy elements can be controlled by fixing the components of the feeding salts with the expected component and consistent with the current. A laboratory test of the co-deposition was also performed and certain compositions of the Mg-Al, and Mg-Zn were obtained. The alloys obtained from the co-deposition show a typical microstructure.

4:20 PM

Magnesiothermic Reduction of TiO_2 for the Production of Titanium Metal Using the Solid Oxide Membrane Process: *Rachel De Lucas*[1]; Soobhankar Pati[1]; Uday Pal[1]; [1]Boston University

Solid Oxide Membrane (SOM) Electrolysis is a revolutionary environmentally-sound new process for synthesis of metals from their oxides, which can potentially produce titanium metal at a small fraction of its current cost. This multi-phase process uses electrical and optionally chemical energy to reduce titanium oxide dissolved in a molten salt, producing either powder metal or dense solid ingot or billet product at the cathode. Previous experiments have found that during electrolysis the presence of multi-valence oxides of titanium (Ti^{2+},Ti^{3+} and Ti^{4+}) in the flux imparts electronic conductivity, leading to lower current efficiency and SOM degradation. A novel metallothermic reduction process was investigated wherein the Mg(g) generated from the SOM electrolysis of magnesium oxide was employed to reduce the oxidation state of TiO_2. The resulting Ti_3O can be utilized in the Ti-SOM process to address the problem of the electronic conductivity resulting from the presence of multi-valence oxides of titanium.

Magnesium Technology 2008: Wrought Alloys I

Sponsored by: The Minerals, Metals and Materials Society, TMS Light Metals Division, TMS: Magnesium Committee

Program Organizers: Mihriban Pekguleryuz, McGill University; Neale Neelameggham, US Magnesium LLC; Randy Beals, Chrysler LLC; Eric Nyberg, Pacific Northwest National Laboratory

Monday PM — Room: 291
March 10, 2008 — Location: Ernest Morial Convention Center

Session Chair: To Be Announced

2:00 PM

Baseline Ballistic Performance of AZ31B-H24 for Armor Applications: *Tyrone Jones*[1]; Matthew Burkins[1]; William Gooch[1]; [1]US Army Research Laboratory

The Army Research Lab is developing a ballistic specification for the use of magnesium alloy AZ31B-H24 as armor on Army platforms. Data were generated for a range of thicknesses of magnesium, 0.25 to 4 inches, using five different projectiles. The magnesium performance is parametrically quantified on an equivalent areal density to 5083 Aluminum because it is a mature well quantified, low density metal with a baseline specification performance. The results show the performance of magnesium to be dependent on the diameter of the threat. This research sets a baseline ballistic performance for magnesium for quality control purposes and for use in developing and evaluating improved alloys.

2:20 PM

Deformation Mechanisms of AZ31 Magnesium Alloy: *Timo Ebeling*[1]; Torsten Laser[1]; Christian Hartig[1]; Rüdiger Bormann[1]; [1]Hamburg University of Technology

A detailed investigation of the deformation mechanisms plays an important role for a better understanding of texture evolution and anisotropic behaviour of magnesium wrought alloys. Therefore, room temperature deformation tests of AZ31 hot rolled sheets and extruded bars have been performed. The experimental tensile textures of the rolled sheets show a reorientation resulting in a {0001}<10-10> main component. The results were compared with simulations using a viscoplastic self-consistent model to gain further information about deformation mode activities, texture evolution and mechanical properties. Thereby three simulation sets were executed: The first set included the results of both the rolled sheets and the extruded bars, while the others considered the results separately. Based on the simulations, it will be demonstrated that the activity of the basal, prismatic, pyramidal slip and the twinning mode is required to achieve comprehensive results for the mechanical properties as well as for the texture evolution.

2:40 PM

Effect of Coiling on Hot Bulge Testing of AZ31 Magnesium Sheet: *Jon Carter*[1]; [1]General Motors Corporation

The effect of coiling of AZ31B magnesium alloy sheets on subsequent hot blow formability was studied on lab scale. This work was undertaken largely to increase the formability of the softer ("O" temper) sheet, which is less than that of the harder ("H24" temper) sheet. Coiling the softer sheet increased the maximum dome height by 14%, increased the forming rate by 55%, and greatly increased the surface smoothness. Coiling the harder sheet decreased the maximum dome height by 5%, increased the forming rate by 9%, and had no effect on surface finish, which was always smooth. Although coiling greatly improved the bulge behavior of the soft sheet, the results were still worse than those of the hard sheet. The poorer behavior of the soft sheet is explained by the very large grains which form on the surface during the bulge test.

3:00 PM

Effect of Pre-Ageing Treatment on Hot Compression Behavior of AZ31 Magnesium Alloy: *Lihong Shang*[1]; Stephen Yue[1]; Elhachmi Essadiqi[2]; Javid Amjad[2]; Verma Ravi[3]; [1]McGill University; [2]CANMET Materials Technology Laboratory; [3]General Motors Research and Development Center

The effect of second phase precipitates on the hot working behavior of cast AZ31 magnesium alloy was investigated. A series of cast AZ31 samples were solution treated at 450°C, quenched, and then aged at 150-350°C for one hour to produce precipitates with different amounts and size distributions. The aged samples were heated to the test temperature of 350°C at a heating rate of 1°C s-1, and compression tested at a true strain rate of 0.01 s-1, to a true strain of 0.6. The results show that the lower the aging temperature, the higher is the compression flow stress. This is explained in terms of the second phase characteristics observed in the aged samples.

3:20 PM

Finite Element Modeling of the Thermo-Mechanical Behavior of an AZ31 Magnesium Alloy during Hot Rolling: *Fady Elsayed*[1]; Hany Ahmed[2]; Mary Wells[3]; Gary Lockhart[3]; Daan Maijer[3]; [1]German University in Cairo; [2]Netherlands Institute of Metals Research (NIMR); [3]University of British Columbia

A finite element model was developed using the commercial software package ABAQUS to predict the thermo-mechanical behavior of AZ31 magnesium alloy during hot rolling. Specifically, a 2-D model was employed to predict the distribution of temperature, and strain through the thickness of the strip, as well as the rolling loads. The model predictions were validated for a wide range of hot rolling conditions by comparison to experimental data obtained on a pilot rolling facility located at the CANMET Materials Technology Laboratory in Canada. The model predictions are in reasonable agreement with the experimental values. A sensitivity analysis was performed to quantify the influence of changing the heat transfer coefficient and friction coefficient between the roll and the strip on the predicted results. A study was performed to examine the effect of changing various rolling parameters including the strip entry temperature, the strain and strain rate on the predicted rolling loads.

3:40 PM

Flow Stress Modelling of Magnesium AZ31 Alloy Based on High Strain Plane Strain Compression Data: *Rahul Bhattacharya*[1]; Brad Wynne[1]; Mark Rainforth[1]; Bruce Davis[2]; [1]University of Sheffield; [2]Magnesium Elektron

Plane strain compression testing of commercial magnesium alloy AZ31 under commercial deformation conditions to equivalent tensile strains of 0.7 has been undertaken. The temperature of deformation varied from 350°C to 450°C and the strain rates for all the tests were between 0.5-50s^{-1}. The stress-strain curves at all temperatures and strain rates showed the alloy follows dynamic recrystallization behaviour. Quantitative metallography revealed the microstructure shows a dependence on the Zener-Hollomon (Z) parameter and decreases as the Z increases which produces fine equiaxed grains (~7µm at highest Z; 2.42 x $10^{11}s^{-1}$). Equations correlating flow stress and Zener-Hollomon parameter (Z) at fixed strain levels are obtained and continuous flow stress curves with the effect of dynamic recrystallization are derived. These computed flow stress curves show good match with the experimental flow curves.

4:00 PM

Grain Structure and Its Effect on the Deformation Behavior of AZ31 Magnesium Alloy at Room Temperature: *Li Jin*[1]; W. Ding[1]; X. Zeng[1]; D. Lin[1]; [1]Shanghai Jiaotong University

This paper investigates the grain structure and its effect on the deformation behavior of AZ31 Magnesium alloy at room temperature. Experiments were conducted on conventionally extruded AZ31 rod with grain size of 20µm and typical extrusion texture of ND//(0001), and the AZ31 rod after Equal Channel Angular Extrusion (ECAE) with fine grain size of 2µm and texture of. The slip traces and the crystal orientation transformation during tensile deformation were characterized by in-situ Scanning Electron Microscopy (in-situ SEM) and in-situ Electron Back-Scattered Diffraction (in-situ EBSD), respectively. The results indicated that the deformation mechanisms of magnesium alloy were different with different grain size, texture and grain boundary structures in the alloy samples. The contribution of twinning would decrease and grain boundary sliding (GBS) would contribute more to the strain of magnesium alloy with the grain size decreased during deformation at room temperature.

4:20 PM

Investigating the Effect of Strain Rate and Temperature on the Deformability and Microstructure Evolution of AZ31 Magnesium Alloy: *Ismael Abdel Maksoud*[1]; Hany Ahmed[2]; Johannes Rödel[1]; [1]German University in Cairo; [2]NIMR, Delft University of Technology

Magnesium, being one of the lightest available structural materials, is one of the primary candidates in automotive industries; however, the difficulty of deforming magnesium is a limiting factor. This research work aims to investigate the deformability of AZ31 magnesium alloy under different deformation conditions. Tensile testing experiments were applied to determine the constitutive behavior of AZ31 magnesium alloys. The effect of changing the deformation conditions on the resulting microstructure is examined and quantified by measuring the volume fraction and size of the dynamically recrystallized grains, to account for the material softening during deformation. It was found that as the strain rate decreases by a factor of 10, the peak stress is reduced by 23% while an increase in deformation temperature by 50°C results in a change in the fraction of dynamic recrystallization by 30%. Further correlations were developed to optimize the deformation behavior.

4:40 PM

Mechanical Behavior of AZ31 Sheet Materials at Room and Elevated Temperature: *Jon Carter*[1]; Ravi Verma[1]; Paul Krajewski[1]; [1]General Motors Corporation

Magnesium sheet is increasingly being considered for light-weighting of automotive body structures. In this paper, AZ31 magnesium sheets produced by both the current industrial direct-chill (DC) casting process and the developmental twin-roll continuous casting (CC) process are compared for potential use in hot forming of automotive body panels. The paper compares microstructure, texture, tensile properties both at ambient and elevated temperatures, and biaxial bulge forming of two DC and two CC materials. They exhibit significant, but different, anisotropies in tensile properties in the sheet plane. Both types of material show high tensile elongation-to-failure (~ 300%) under typical QPF (quick-plastic forming) conditions, but the DC materials show more necking. Both can form tall domes in hot pneumatic bulge tests, but, for the same inflation rate, the CC material requires less gas pressure. Recrystallization is critical during hot-forming of magnesium sheet, as it can enhance or reduce formability.

5:00 PM

Microstructure Refinement of AZ31B Alloys Processed with an Electromagnetic Vibration Technique: *Kenji Miwa*[1]; Mingjun Li[1]; Takuya Tamura[1]; [1]National Institute of Advanced Industrial Science and Technology (AIST)

Electromagnetic vibrations, which are generated by simultaneous imposition of a static magnetic field and an alternating electric field, are considered to lead to the formation and collapse of cavities even in a molten metal, and then achieve the refinement of solidified structure. In order to refine the microstructure of AZ31B magnesium alloy, the electromagnetic vibration (EMV) process has been applied. Fine equiaxed grains can be obtained when AZ31B alloys are solidified at a frequency interval of ca. 500 up to 2000 Hz. The difference in electrical resistivity between the solid and liquid in mushy zone originates uncoupled motion, which breaks dendrite into fragments, destroys the crystallographic orientations, and yields deformation twins. Effective refinement occurs when the leading solid is driven to move out the operation scope of solute redistribution area where the solute cannot be piled up to generate a constitutionally undercooled region that always destabilizes.

Materials in Clean Power Systems III: Fuel Cells, Hydrogen-, and Clean Coal-Based Technologies: Gas Separation and CO_2 Capture

Sponsored by: The Minerals, Metals and Materials Society, TMS Structural Materials Division, TMS/ASM: Corrosion and Environmental Effects Committee
Program Organizers: Zhenguo "Gary" Yang, Pacific Northwest National Laboratory; Michael Brady, Oak Ridge National Laboratory; K. Scott Weil, Pacific Northwest National Laboratory; Xingbo Liu, West Virginia University; Ayyakkannu Manivannan, National Energy Technology Laboratory

Monday PM Room: 392
March 10, 2008 Location: Ernest Morial Convention Center

Session Chairs: Henk Verweij, Ohio State University; Wei Liu, Pacific Northwest National Laboratory

2:00 PM Invited
Critical Material and Process Issues for CO_2 Separation from Coal-Powered Plants: *Wei Liu*[1]; [1]Pacific Northwest National Laboratory

Coal is a viable alternative energy source to petroleum, since other renewable energies such as biomass and solar can only supply a fraction of energy consumption in US. However, coal is one major source of air pollutants, CO_2, SO_2, NOx, Hg, particulates. Among those pollutants, CO_2 capture costs the US power industry a few hundred billion dollars per year if the regulation is implemented. It is imperative to develop cost-effective CO_2 capture technologies and replace the oil import with indigenous coal reserve. Concentrating CO_2 from the dilute coal combustion or gasification gas stream to a level suitable for sequestration presents a very challenging separation problem in Chemical Engineering and Materials Science disciplines. This is largely due to huge gas volume, complex and dirty gas compositions, and low value of CO_2 credit. Major innovations in separation materials and processes are required. A critical review on different separation technologies, absorption, adsorption, membrane, distillation, will be presented for respective flue gas and gasification application. As a result, important material issues and their impacts to the process viability will be identified. Finally, the author will share the latest research results on zeolitic adsorbent and membrane materials as potential, step-out separation technologies.

2:30 PM
Oxygen Transport Membrane Materials Development for Oxyfuel Firing of Coal Power Plants with CO_2 Capture: *G.M. Christie*[1]; B. vanHassel[1]; J. R. Wilson[1]; [1]Praxair

Praxair, in cooperation with The United States Department of Energy is developing an oxygen transport membrane (OTM) based oxycombustion process for carbon dioxide (CO_2) capture from coal power plants. Oxycombustion, or burning fuel in oxygen to generate flue gas consisting of primarily CO_2 and H_2O, is established as a credible means to facilitate CO_2 capture from coal power plants. The economics of conventional oxycombustion processes are currently limited by the parasitic power that is required for cryogenic oxygen production in conventional air separation units (ASU). Praxair has developed novel OTM technology that when integrated directly in a coal fired boiler has the potential to reduce the parasitic power consumption required for oxygen production by 70-80% as compared to cryogenic ASU. This paper describes the materials requirements for oxygen transport membranes designed for integration in a coal fired power boiler. The Praxair OTM materials development strategy will be discussed along with recent results from the development program.

3:00 PM Invited
Oxygen Production Using Ion Transport Membranes: *Phillip Armstrong*[1]; Michael Carolan[1]; Alexander Makitka[1]; VanEric Stein[1]; Richard Underwood[1]; Lori Vratsanos[1]; Charles Lewinsohn[2]; [1]Air Products and Chemicals, Inc.; [2]Ceramatec Inc.

Air Products, in partnership with the U.S. Department of Energy, is leading a team to develop Ion Transport Membranes (ITM) to separate oxygen from air. When operated at elevated temperature, these dense, ceramic membranes selectively permeate oxygen from a pressurized air stream to produce a pure oxygen permeate. Integrating the high temperature and pressure non-permeate stream from the membrane with a gas turbine allows the co-production of oxygen, power and steam. Consequently, the ITM Oxygen technology is ideally suited to advanced power generation processes such as integrated coal gasification combined cycle (IGCC) that require oxygen as a feedstock. The project is currently in the third phase of a three-phase program. During the first and second phases, the ITM Oxygen team designed and fabricated planar membrane modules. These membranes were then used to demonstrate the feasibility of air separation using ceramic membranes. During the current Phase 3, a prototype facility capable of producing 5 tons-per-day of oxygen is operating. This paper will present an overview of some of the key features and advantages of the microchannel ceramic membranes used in this technology, along with economic benefits of using ITM Oxygen technology to produce oxygen. This abstract was written with support of the U.S. Department of Energy under Contract No. DE-FC26-98FT40343. The Government reserves for itself and others acting on its behalf a royalty-free, nonexclusive, irrevocable, worldwide license for Governmental purposes to publish, distribute, translate, duplicate, exhibit and perform this copyrighted paper.

3:30 PM
Effect of Pd Addition on Hydrogen Permeability and Microstructures of $Nb_{49}Zr_{15}Ni_{36}$ Alloy: *Huixiang Tang*[1]; Kazuhiro Ishikawa[1]; Kiyoshi Aoki[1]; [1]Kitami Institute of Techonology

Effect of Pd addition on hydrogen permeability and the microstructure of as-cast $Nb_{49}Zr_{15}Ni_{36}$ (mol%) alloy prepared by arc melting has been investigated. Hydrogen permeability of $Nb_{49}Zr_{15}Ni_{36}$ and $Nb_{49}Zr_{15}Ni_{30}Pd_6$ alloys at 673K is 3.79 and 6.58×10^{-8} [mol H_2 m^{-1} s^{-1} $Pa^{-0.5}$], respectively. The former consists of the primary body-centered-cubic (bcc), rod-like and eutectic phases. On the contrary, the latter is composed mainly of the primary (bcc), plate-like (bcc) and ZrNi phases and the primary phase is connected by the plate-like phase. Activation energy Ea for hydrogen permeation of the $Nb_{49}Zr_{15}Ni_{36}$ alloy deceases with 6 mol % Pd addition. The changes in the microstructure and activation energy because of Pd addition may be the main causes for increment of hydrogen permeability, which make hydrogen atoms diffuse more easily in this metal membrane. It is expected that a small amount of Pd addition is effective to tune Nb-Zr-Ni alloys properties.

3:55 PM
Optimization of Supported Membrane Structures for Energy Conversion Technology: William Chiu[1]; Matthew Mottern[1]; Melissa Schillo[1]; Krenar Shqau[1]; *Henk Verweij*[1]; [1]Ohio State University

Supported inorganic membranes consist of a thin film of permselective material on top of a graded support structure with increasing pore size in the direction away from the membrane. The requirements for the membrane materials, in brief, are that they are <1 μm thick with a molar permeance of $>10^{-6}$ mol/(m^2•s•Pa) for the permeable gas, or a mechanical permeance of $>10^{-12}$ m for the permeable liquid and a separation factor >50. These requirements make that the supporting structure must have a smooth, fine-porous deposition surface with a flexure strength >100 MPa and a permeance higher than the membrane permeance. The supported membrane structures are expected to allow for thousands of hours uninterrupted operation, and their manufacturing costs should stay well below $500/$m^2$ at a surface to volume ratio of >100 m. The presentation will discuss progress in the integrated approach to optimize practical supported membrane structures for energy conversion technology.

4:20 PM Break

4:30 PM Invited
Thermodynamic Properties of the Pd-H, Pd-D, and Pd-T Systems: *Ricardo Schwarz*[1]; Douglas Safarik[1]; Stephen Paglieri[1]; [1]Los Alamos National Laboratory

The pressure-composition isotherms of metal-hydrogen systems often show hysteresis. A recent model[1] attributes the hysteresis to the coherence elastic strains that must be overcome (by a macroscopic change in the hydrogen chemical potential) to nucleate the coherent hydride phase (on absorption) and the coherent hydrogen solid solution (on desorption). The model predicts the hysteresis decreases as 1/T and vanishes, by definition, at the crossing of the van't Hoff lines (log of chemical potential plotted vs. 1/T). This suggests that the crossing can be used to accurately measure the critical pressure and temperature

for the two phase decomposition. We have used this method to accurately measure the critical points for the Pd-hydrogen, Pd-deuterium and, for the first time, the Pd-tritium system. These measurements are used to derive the entropy and enthalpy of hydride, deuteride and tritide formation. [1]R. B. Schwarz and A. G. Khachaturyan, Acta Mater. 54 (2006) 313.

5:00 PM Invited
Palladium Based Membranes for Hydrogen Permeation – A First-Principles Modeling Study: *Ole Lovvik*[1]; Susanne Opalka[2]; [1]University of Oslo; [2]United Technologies Research Center

Dense, hydrogen permeable metal membranes may find future applications in membrane reactors for hydrogen production from hydrocarbons and in systems requiring hydrogen purification, for example hydrogen fuel cells. Among the most promising materials for such membranes are palladium based alloys, which exhibit both very high selectivity and high hydrogen permeability. This study focuses on fundamental properties of such alloys, including surface segregation, hydrogen diffusion, and adsorption of various gases. The principal tool is modeling based on density functional theory, but links are close to experimental studies.

5:30 PM Invited
Self-Supporting Pd-Cu Alloy Membranes for Production of Coal-Derived Hydrogen: *Kent Coulter*[1]; [1]Southwest Research Institute

Thin self-supported permeable membranes of palladium alloys such as $Pd_{60}Cu_{40}$ have many applications in which hydrogen separation is required. High permeability membranes have been fabricated by magnetron sputtering onto a pretreated silicon substrate followed by lift-off to form free standing high quality films of controllable alloy composition down to 3 microns in thickness. Using these methods, $Pd_{60}Cu_{40}$ membranes 12 inches in diameter have been made with thicknesses ranging from 2 to 15 microns. The highest flux recorded was 242 SCFH/ft2 with a 2 µm thick $Pd_{53}Cu_{47}$ at 400°C and 20 psig feed pressure which when extrapolated is over twice the 2010 Department of Energy pure H2 flux target. Several membranes have been made with the same permeability, but with different thicknesses and these membranes are highly selective. The fabrication process, hydrogen separation performance and physical property characteristics of these vacuum deposited palladium alloys for hydrogen separation will be discussed.

6:00 PM Invited
Modeling of B2 Phase PdCuTM Alloy Hydrogen Selective Membrane Performance: *Susanne Opalka*[1]; Thomas Vanderspurt[1]; Sean Emerson[1]; Weiming Huang[2]; Da Wang[3]; Ted Flanagan[3]; Ying She[1]; [1]United Technologies Research Center; [2]QuesTek Innovations, LLC; [3]University of Vermont

The production of fuel cell grade H2 and sequestration grade CO2 from coal or other resources will be facilitated by a high permeability, sulfur resistant, thermally stable hydrogen separation membrane. A Pd-Cu-TM B2 phase alloy with commercially attractive permeability and sufficient thermal and chemical stability for practical application to H2 production from an Advanced Water-Gas Shift Membrane Reactor (AWGSMR) has been identified through combined first principles atomic predictions, thermodynamic modeling, and H solubility measurements. AWGSMR operation at reduced steam to carbon ratios could lead to increased efficiency and decreased implementation costs. However, these conditions may induce metal-catalyzed carbon formation, which could compromise membrane integrity, H permeability, or active surface area. Atomic modeling of CO reactions on the new alloy surface was used to evaluate possible impact of C solubilization and coke and carbide formation on H permeation performance.

Materials Processing Fundamentals: Process Modeling

Sponsored by: The Minerals, Metals and Materials Society, TMS Extraction and Processing Division, TMS: Process Technology and Modeling Committee
Program Organizer: Prince Anyalebechi, Grand Valley State University

Monday PM — Room: 283
March 10, 2008 — Location: Ernest Morial Convention Center

Session Chair: Prince Anyalebechi, Grand Valley State University

2:00 PM
Use of SEM Fractography to Guide Thermo-Mechanical Process (TMP) Optimization for Cu-Ni-Si-Cr Alloys: *Mark Hashiguchi*[1]; John Kuli[1]; [1]Brush Wellman Inc.

Examination of tensile and charpy bar surfaces shortly after destructive testing was conducted to search for clues that would aid in optimization of mechanical properties, especially tensile strength, yield strength and elongation to fracture. Cu-Ni-Si-Cr alloy bars in the as-cast, forged, rolled and extruded conditions were examined. Low ductility bars (<4% Elongation) showed dramatically different features than the fracture surfaces of high strength -high ductility bars (7 to 10% Elongation). Analysis of the fracture surfaces at 10X to 1500X and use of Energy-Dispersive X-Ray Spectroscopy (EDS) identified Ni-Si and Ni-Si-Cr precipitates of varying sizes and morphologies. TMP techniques to control the size and distribution of these precipitates show promise in improving the properties and performance of this alloy system and appear to correlate with improvements in the fracture surface morphology.

2:20 PM
Microstructural Analysis of Sticking Phenomenon Occurring during Hot Rolling of Two 430J1L Ferritic Stainless Steels: *Daejin Ha*[1]; Chang-Young Son[1]; Joon Wook Park[2]; Jong Seog Lee[3]; Yong Deuk Lee[3]; Sunghak Lee[1]; [1]Pohang University of Science and Technology; [2]Hyundai Steel Company, Ltd.; [3]Pohang Iron and Steel Company

Sticking phenomenon occurring during hot rolling of two STS 430J1L ferritic stainless steels were analyzed in this study. Hot-rolling simulation tests were conducted by using a high-temperature wear tester. The modified 430J1L steel had a smaller number of sticking nucleation sites and slower growth rate than the conventional 430J1L steel because of higher high-temperature hardness, thereby leading to less serious sticking. When the simulation test was conducted at 1070°C, chromium oxides were formed on the surface of the rolled materials, and thus the sticking was drastically reduced because of the increased surface hardness of the rolled materials. According to these findings, in order to prevent or minimize the sticking, it was suggested to improve high-temperature properties of stainless steels in the case of hot rolling at 900°C~1000°C, and to promote the formation of oxides in the case of hot rolling at temperatures higher than 1000°C.

2:40 PM
Numerical and Experimental Study of Constrained Solidification through Parallel Planar Channels: *Rui Shao*[1]; Matthew Krane[1]; Kevin Trumble[1]; [1]Purdue University

To understand the development of microstructure and microsegregation in constrained solidification, growth of Al-4.5wt%Cu through parallel planar channels of different widths is simulated using a 2-D CA-FV model. Experiments of dendrites growing through channels are also conducted. As the channel width decreases below the primary dendrite spacing, lateral solute diffusion is constrained, and thus the secondary arms become shorter and even disappear as channel width decreases. When the channel width decreases further, the solute diffusion in front of the dendrite tip is also constrained and the growth of the dendrite tip is suppressed. As a result, the dendrites grow at lower undercoolings than in wider channels, leading to higher and more uniform solute concentration in the primary phase and lower eutectic fraction in the alloy. The change of dendrite morphology and eutectic fraction with channel width obtained through experiments matches the numerical results.

3:00 PM

Fluid Flow, Heat and Mass Transfer in the Molten Pool of LENS® Processes: *Hebi Yin*[1]; Sergio Felicelli[1]; Liang Wang[1]; [1]Mississippi State University

A two-dimensional finite element solidification model was developed to simulate the transport phenomena occurring during laser deposition of AISI 410 stainless steel during the Laser Engineered Net Shaping (LENS®) process. The molten pool geometry and the distribution of temperature, solute concentration and velocity were calculated during deposition of a thin wall plate. An analysis revealed the importance of heat transfer by both conduction and convection as well as the roles of the driving forces for convection in the molten pool. The heat transfer and the flow pattern in the molten pool are considerably dependent on the travel speed of the laser beam. For the alloy and process parameters in the simulations, no significant macrosegregation was observed. The temperature-dependent properties and thermodynamic variables involved in solidification modeling were calculated using Thermo-Calc software. The simulation results contribute to the current understanding of transport phenomena in the molten pool of laser deposition processes.

3:20 PM

Effect of Boundary Heat Flux Transients on the Solidification Behavior and Microstructure of Al-Cu Alloys: *K.V. Sreenivas Rao*[1]; G. Phanikumar[1]; T.S. Prasanna Kumar[1]; [1]Indian Institute of Technology

A serial solution of the inverse heat conduction problem (IHCP) is extended for determining multiple heat fluxes at the metal mould interface during casting of Al-Cu alloys in permanent molds. The temperature history of the casting and the mold during solidification is recorded using mineral insulated K- type thermocouples. Computer interfaced data logger is used for temperature data acquisition. The measured temperatures are used as input to the IHCP algorithm for simulating multiple heat fluxes at the boundary. The obtained heat fluxes are used as boundary conditions for the casting simulation. It is observed that the measured heat flux is a function of alloy composition and thermo-physical properties of the mold material. The effect of heat diffusivity of the mold on interfacial heat flux and cooling rate is analyzed. The cooling rate decreases with increase in interfacial thermal resistance at the metal/mold interface and affects macrosegregation and microstructure formation.

3:40 PM Break

3:50 PM

Modeling and Simulation of a Large Composite Casting: *Autumn Fjeld*[1]; Andreas Ludwig[1]; [1]University of Leoben

The filling and solidification of an industrial scale composite casting has been simulated to investigate the remelting of the outer shell material of the casting. A composite casting requires a multi-step casting process which, in this investigation, includes casting of a high alloy cast iron outer material and subsequent conventional ingot casting of a nodular steel core material into the mold assembly. During casting of the nodular-steel, a thin layer of the high alloy material re-melts and mixes with the core material producing a bonding layer of intermediate composition. The present numerical model employs the volume of fluid method and an enthalpy-porosity technique to couple the filling of the core material and re-melting of the shell material. The interface between the solid and liquid phases is tracked and can be used as a guide to examine the extent of remelting and, to some degree, mixing of the two fluids and species diffusion.

4:10 PM

Model Studies on Slag Droplet Generation in Gas-Stirred Ladles: *Krishnakumar Krishnapisharody*[1]; Gordon Irons[1]; [1]McMaster University, Steel Research Centre

The phenomenon of slag droplet formation under the action of gas-stirring in steel ladles has been analyzed with the help of experiments conducted in a thin-slice room- temperature model using water and mineral oils as the working fluids. Visual and video investigations have been performed on the interface behaviour along with measurements of liquid velocities in both phases, using the Particle Image Velocimetry (PIV) technique. The measured velocity data and observations on the interface break-up establish that the droplet formation results primarily from an instability mechanism at the interface.

4:30 PM

Numerical Evaluation of the Performance of a BOF Steelmaking Lance: *Miguel Barron*[1]; Cesar Lopez[1]; Isaias Hilerio[1]; [1]Universidad Autonoma Metropolitana

Recently, a new lance design for BOF steelmaking has been proposed by Sambasivam et. al. (2007). This lance, in addition to six peripheral inclined supersonic nozzles, contains a vertical centered nozzle whose oxygen flow is independent from the main oxygen supply. The above authors affirm that their lance maximizes the droplet generation without causing spitting. In this work, the performance of a lance with four peripheral nozzles and one vertical centered nozzle is numerically modeled by means of Computational Fluid Dynamics (CFD) software. Transient 2D CFD computer simulations were carried out considering two phases, namely molten steel and gaseous oxygen. Numerical results confirm that bath agitation and droplet generation are enhanced as a result of the vertical centered nozzle; however a proper performance of this lance, related to a conventional one, strongly depends on lance height and Mach number of the oxygen jets.

4:50 PM

Numerical Simulation of Droplet Generation of the Buoyant Phase in Two-Phase Liquid Baths: *Krishnakumar Krishnapisharody*[1]; Gordon Irons[1]; [1]McMaster University, Steel Research Centre

A mathematical model has been developed to predict the interface dynamics and droplet generation of the buoyant phase in a two-fluid system. The model employs the well-known SIMPLE algorithm for obtaining flow fields and the Volume of Fluid (VOF) method, for interface tracking. The implementation of the model in water-oil systems, where the oil layer is placed above a recirculating water bath, is discussed. It is demonstrated that the evolution of the water-oil interface leading to the formation of oil droplets is predicted realistically. The model can be extended to include a third phase (gas) to simulate the generation of slag droplets in a gas-stirred ladle.

5:10 PM

CFD Simulation of a Copper Converter with Bottom Air Injection: Jesus Gonzalez[1]; *Cesar Real*[1]; Manuel Palomar[1]; Luis Hoyos[1]; Marco Gutierrez[1]; [1]Universidad Autonoma, Metropolitana

Peirce-Smith converters (PSC) are long cylindrical chemical reactors where copper matte reacts with air. Traditionally, air is injected laterally through submerged tuyeres at different subsonic velocities. However, the accumulated experience in steelmaking, particularly in the basic oxygen furnace (BOF) process, shows that the gas bottom injection may improve the mixing efficiency of a liquid pool. The aim of bottom injection is to maximize the copper kinetic energy meanwhile avoiding excessive reactor splashing. When gas is injected from a single orifice at the bottom of a liquid pool, two main gas flow regimes can be identified, bubbling and jetting. In this work, a PSC with bottom air injection is studied by means of multiphase 3D CFD numerical simulations considering multiple air velocities. Special attention is paid to the bubbles and jet formation mechanism. The mixing efficiency is measured by calculating the turbulent kinetic energy of the copper matte.

Mechanical Behavior, Microstructure, and Modeling of Ti and Its Alloys: Phase Transformation and Microstructure Development I

Sponsored by: The Minerals, Metals and Materials Society, TMS Structural Materials Division, TMS: Titanium Committee
Program Organizers: Ellen Cerreta, Los Alamos National Laboratory; Vasisht Venkatesh, TIMET; Daniel Evans, US Air Force

Monday PM Room: 384
March 10, 2008 Location: Ernest Morial Convention Center

Session Chair: Daniel Evans, US Air Force

2:00 PM Invited
Application of Thermodynamic Modeling to Multicomponent Titanium Alloys: *Fan Zhang*[1]; Shuanglin Chen[1]; Weisheng Cao[1]; Kaisheng Wu[1]; Ying Yang[1]; Y. Chang[1]; [1]CompuTherm LLC

To achieve desired microstructures and mechanical properties, alloy chemistry and processing conditions need to be carefully selected and adjusted. Traditionally, these improvements have been made by a slow and labor-intensive series of experiments. Today, with the help of models and simulation tools, significant amount of experimental work can be reduced. These modeling tools will accelerate the development of new alloys and the improvement of the existing ones. In this presentation, we will discuss the thermodynamic modeling tool we have developed at CompuTherm LLC, and its application to multicomponent titanium alloys. With this modeling tool, beta transus temperatures, beta approach curves, phase compositions can be calculated for Ti64, Ti6242, Ti17 and so on, which are critically needed in the selection of processing parameters. Integration of thermodynamic calculations with phase field modeling for the simulation of microstructure evolution will be discussed via the concept of pseudo-ternary system.

2:30 PM
Deoxidization Mechanism of In-Situ Electro-Deoxidization of TiO_2 to Titanium: *XiuJing Zhai*[1]; Zhuo Zhang[1]; Jidong Li[1]; Mingjie Zhang[1]; [1]Northeastern University

Molten salt electrolysis monitoring and controlling instrument (DD-A) had been used in this research. Electrolysis process of in-situ electro-deoxidization of Ti02 to titanium was measured. The change trend of back electromotive force indicated that the decomposition reaction of $CaCl_2$ was first happened during normal decomposition, then Ti02 was deoxidized to titanium by calcium which was from the decomposition reaction, the reaction equation is $2Ca2{+}{+}TiO_2{=}Ti{+}2CaO$.

2:50 PM
Investigating Macrozones in Titanium Billet using Electron Backscattered Diffraction: *Bradley Wynne*[1]; Peter Davies[1]; Mark Rainforth[1]; [1]University of Sheffield

The use of orientation image maps (OIMs) obtained from electron backscattered diffraction has led to significant improvement in our knowledge of titanium billet microstructure. Most significantly, OIM studies have shown that on a global scale the crystallographic texture is relatively weak but on the meso-scale can be composed of regions with strong local textures which are often referred to as macrozones. These strongly textured regions are inherited from the ingot forging process and are at least an order of magnitude greater than the apparent grain size. Most work to date, however, has investigated relatively small areas of billet, making it difficult to determine the average size and size and shape distribution of the macrozones. In this work we report on a large scale investigation of a slice of 200mm diameter Timetal®834 billet with the aim being to determine what amount of material is required for a statistical confident analysis.

3:10 PM
Kinetics of Elevated Temperature Phase Transformations in TIMETAL LCB: Henry Rack[1]; *Basak Yazgan Kokuoz*[1]; [1]Clemson University

This investigation has examined the phase transformations occurring during isothermal aging of TIMETAL LCB. Three differing alpha phase morphologies were considered, i.e grain boundary alpha heterogeneously forming at prior beta grain boundaries, side-plate alpha growing and/or forming in the vicinity of the aforementioned grain boundary alpha and intragranular alpha precipitating within the matrix. The beta-to-alpha phase transformation kinetics were found to be controlled by the kinetics of grain boundary alpha formation at the early stages of reaction, irrespective of aging temperature. Increased transformation successively included formation of side-plate and intragranular alpha. The overall transformation kinetics can be explained by considering the individual effects of the different morphologies on the variation of the total alpha phase volume fraction, the overall kinetics approaching that for intragranular alpha at lower aging temperatures and that for grain boundary alpha at increased aging temperatures.

3:30 PM Break

3:50 PM Invited
Phase Field Modeling of Phase Transformation and Microstructure Development in Alpha/Beta Titanium Alloys: Ning Ma[1]; Chen Shen[1]; *Yunzhi Wang*[1]; [1]Ohio State University

Phase transformations in alpha/beta Ti-alloys are dominated by strong coupling among different extended defects and produce extremely complicated microstructures with strong spatial variation, correlation and anisotropy. The traditional constitutive models representing microstructural features by their average values may not be sufficient to quantitatively define the microstructure and allow for establishing a robust microstructure-property relationship. We discuss recent development and applications of the phase field method to quantitative modeling of microstructural evolution during solid state phase transformations in alpha/beta Ti-alloys. The model accounts explicitly for anisotropy in interfacial energy and mobility, orientation relationship and lattice- and modulus-misfit between the parent and product phases and misfit dislocation structures at the alpha/beta interfaces. Applications of the model to globular alpha growth, development of sideplates from grain boundary alpha and formation of basketweave structures in three-dimensions will be presented. Variant selection during nucleation and growth of the colony and basketweave structures will be addressed.

4:20 PM
Nano-Structured Ti-6Al-4V Alloy by Severe Deformation Processes and Rolling: Ike Su-Chi[1]; Xiang Li[1]; Rick Lee[1]; Yi Liu[1]; *Amit Ghosh*[1]; [1]University of Michigan

Severe deformation was imparted into Ti-6Al-4V alloy by compression and die pressing at around 400C under superposed hydrostatic pressure. Nanocrystalline microstructure has been obtained with grain size in the range of 100nm although a small fraction of beta phase exists as in the original microstructure before it was heat treated and transformed by quenching from the beta phase. TEM observations indicated that there exists a high density of dislocations in the severe deformed samples. Dislocation dipoles are frequently observed by HREM. Microhardness measurements indicated extremely high strength of the severely deformed sample. Texture evolution showed enhancement of basal texture. Low temperature processing to sheet by rolling of the fine grain material is possible by this approach, and small size nanograin titanium sheet was demonstrated to have highly superplastic properties at 600-700°C. (Work supported by US Air Force).

4:40 PM Invited
Recent Advances and Challenges in Solidification and Microstructure Modeling of Titanium Alloys: *Laurentiu Nastac*[1]; [1]Concurrent Technologies Corporation

Modeling and simulation of microstructure evolution requires complex multi-scale computations, from computational fluid dynamics (CFD) macroscopic modeling through mesoscopic to microscopic modeling, as well as strategies to link various length-scales emerged in modeling of microstructural evolution. The presentation will cover numerical approaches able to predict the solidification structure evolution in large and complex casting geometries as well as relevant examples of the microstructure modeling in commercial casting technologies

including investment casting and remelting processes. The presentation will also discuss relevant techniques for controlling the structure formation during the solidification processes of Ti alloys and to identify means to improve quality of the castings (e.g., improvement of mechanical properties through the microstructure development and control to eliminate the casting factor, in particular in aerospace applications). Recent developments on ultrasonic technology modeling and integration efforts at CTC for grain refinement/ modification for improved Ti ingot/casting quality will also be covered.

5:10 PM
Microstructural Development in near Beta Titanium Alloy Ti-5Al-5V-5Mo-3Cr: *Nicholas Jones*[1]; Martin Jackson[1]; David Dye[1]; Richard Dashwood[1]; [1]Imperial College London

The selection of the near beta alloy Ti-5Al-5V-5Mo-3Cr (Ti-5-5-5-3) for use in the latest landing gear assemblies has lead to an increase in interest in relevant processing parameters. Previous work has suggested that Ti-5-5-5-3 offers benefits over the more established Ti-10V-2Fe-3Al, through higher strength, a shallower β approach curve and less microstructural sensitivity to forging temperature. Through the use of in-situ x-ray synchrotron experiments and more traditional electron microscopy new insights into the behaviour and timescale of microstructural development in Ti-5-5-5-3 have been obtained; particularly with regards to flow softening during hot working, the α dissolution kinetics and the α to ω to α transformation. The effect on subsequent thermomechanical processing and final properties has also been considered.

5:30 PM
Research on Inclusion in High Titanium Ferroalloy: *Lina Jiao*[1]; Ting'an Zhang[1]; Jianming Yao[1]; Changce Xing[1]; [1]Northeastern University

Microstructure of inclusion and occurrence state of oxygen in high titanium ferroalloy was examined against the problem of large-mount inclusion and high-content oxygen in high titanium ferroalloy production by aluminothermy reduction process of rutile. And then formation mechanism of oxygen-containing phase was discussed. It was assumed that there were four phases in high titanium ferroalloy. XRD, SEM and EPMA results showed that the main forms of inclusion were Al_2O_3 and titanoxane solid solutions. It was thought that Al_2O_3 was formed by incomplete metal-slag separation and Ti_2O, Fe_2TiO_4, TiO_2 and titanoxane solid solutions were the incomplete products of reduction reaction.

Mechanics and Kinetics of Interfaces in Multi-Component Materials Systems: Nanoscale Structures and Simulations

Sponsored by: The Minerals, Metals and Materials Society, TMS Electronic, Magnetic, and Photonic Materials Division, TMS Structural Materials Division, TMS/ASM: Composite Materials Committee, TMS: Thin Films and Interfaces Committee
Program Organizers: Bhaskar Majumdar, New Mexico Tech; Rishi Raj, University of Colorado, Boulder; Indranath Dutta, US Naval Postgraduate School; Ravindra Nuggehalli, New Jersey Institute of Technology; Darrel Frear, Freescale Semiconductor

Monday PM — Room: 279
March 10, 2008 — Location: Ernest Morial Convention Center

Session Chairs: Rishi Raj, University of Colorado; Mingwei Chen, Tohuku University

2:00 PM Keynote
The Ultra-Hardness of Nano-Structured Composite Ceramic Coatings of nc-TiN/a-Si_3N_4: *Ali Argon*[1]; Stan Veprek[2]; Ruifeng Zhang[2]; [1]Massachusetts Institute of Technology; [2]Technical University of Munich

The superior hardness of nano-structured ceramic composite coatings of nc-TiN/a-Si_3N_4 with hardnesses in the range of 100 GPa, exceeding that of polycrystalline diamond, can now be fully explained thanks to very recent first principles computations of the plastic shear resistances of the amorphous Si_3N_4 layers of atomic thickness separating the non-deformable nano-sized grains of TiN. This, and appropriate spacial averaging of the effects of the latter, as well as accounting for their substantial strength differential effects has permitted bridging the gap between atomic level and macro properties.

2:40 PM Invited
Influence of Interfaces on the Deformation Behavior of Materials at Small Length Scales: *Gerhard Dehm*[1]; [1]Erich Schmid Institute for Materials Science

Interfaces and surfaces can impose mechanical size-effects on materials. The deformation mechanisms become constrained when microstructural and/or geometrical dimensions decrease. This effect can improve, e.g. the strength of a bulk lamellar material, but it may cause failure for a miniaturized material component due to high internal stresses. Several dislocation mechanisms causing size-dependent flow stresses are addressed and the current understanding of size-effects in miniaturized and bulk materials is reviewed.

3:10 PM Invited
Stress-Induced Grain Boundary Migration: "Cold" Grain Growth in Nanocrystalline Metals: *Mingwei Chen*[1]; [1]Tohoku University

Stability of nano-grains is of great importance in technological applications of nanocrystalline materials because coarsening of nano-grains results in the loss of the advanced properties solely owned by the nanostructures. In polycrystalline materials, the elimination of GBs via grain growth is a thermodynamically favorable process, but controlled by the kinetics of atomic mobility at GBs. Thus, grain coarsening generally takes place at high temperatures where GB atoms have enough thermal energy. Nevertheless, recent observations suggested that grain growth in nanocrystalline metals can occur at room temperature during plastic deformation. The "cold" nanograin growth reveals an interesting new phenomenon arising from nanosize effect. Our recent results demonstrated that the "cold" nanograin growth is rate-dependent and can be described by a power law equation. The measured activation volume for the nanograin growth is well consistent with MD predications, suggesting that the nanograin growth is motivated by the stress-enhanced mobility of GB atoms.

3:40 PM Break

3:50 PM Invited
First Principles Calculations of Interfacial Boundaries in Ni-Ni_3Al and Al-Al_3Sc: *Christopher Woodward*[1]; Axel Van De Walle[2]; Mark Asta[3]; [1]US Air Force Research Laboratory; [2]California Institute of Technology; [3]University of California, Davis

Solute and precipitation strengthening are often used to optimize the properties of structural materials used in aerospace applications. A great deal can be learned about these alloys by studying the model binary and ternary systems. Here Ni-Ni_3Al and Al-Al_3Sc are used as model systems for the Ni-based superalloys and Sc strengthened Al alloys in order to estimate interfacial boundaries (IFB) properties. The thermodynamic properties of these IFB's strongly influence growth and coarsening rates of precipitates and are used in models of precipitation strengthening and microstructural evolution. Cluster expansion methods and lattice gas methods are used to study composition profiles and free energies of IFB's in these materials. In Al- Al_3Sc a lattice gas model is used to predict Mg impurity segregation to the Al side of the (100) IFB. This result has recently been verified by atom probe tomography.

4:20 PM Invited
Arbitrary Sharp-Diffuse Interface Computational Modeling of Phase Evolution in Multi-Component Systems: *Ganesh Subbarayan*[1]; Kaushik Setty[1]; [1]Purdue University, School of Mechanical Engineering

In this paper, we describe a computational procedure for arbitrary sharp-diffuse interface modeling through either explicit (geometrical) or implicit (material) descriptions of interfaces. The approach is based on iso-parametric descriptions of geometrical, material and behavioral fields over primitive domains, which in turn are hierarchically composed to describe complex domains. The process is philosophically similar to the Constructive Solid Geometry procedure of CAD. The compositions are constructed so that the basis functions used to approximate the fields obey the mathematical notion of partitions of unity thereby ensuring convergence of the approximations over the complex domain. Such a scheme avoids the complexity of representing multiple phases in phase field models, and the mesh density required to adequately resolve interfaces in phase field simulations. We demonstrate the computational scheme through simulations of solidification in the presence of heterogeneities (holes, inclusions), and through simulations of secondary phase evolution in solder alloys.

4:50 PM

Searching for the Low Energy Interfaces in β-Mg_5Si_6/α-Al: *Yi Wang*[1]; Zi-Kui Liu[1]; Chris Wolverton[2]; Long-Qing Chen[1]; [1]Pennsylvania State University; [2]Northwestern University

The main objective of this work is to search for low energy interfaces between the β"-Mg_5Si_6 precipitate and the α-Al matrix from a first-principles approach. Extensive calculations were performed to examine the effects of interfacial termination, atomic alignment and intermixing, and interfacial orientations. We have calculated interfacial energies, strain energies, and lattice mismatches for the interfacial system β"-Mg_5Si_6/α-Al. Our study involved three types of interfacial orientations between β"-Mg_5Si_6 and α-Al, namely, $(130)_{Al}\|(100)_{\beta"}$, $(001)_{Al}\|(010)_{\beta"}$, and $(-320)_{Al}\|(001)_{\beta"}$. In each case, we find that the low-energy interfaces possess two key attributes in common: a large amount of Al-Si bonds, and an alignment across the interface with a pre-β"/fcc topology.

5:15 PM

Atomistic Simulation of Dislocation Nucleation from Homogeneous and Doped Copper Grain Boundaries: *Douglas Spearot*[1]; Rahul Rajgarhia[1]; Ashok Saxena[1]; [1]University of Arkansas

Recently published simulation results have indicated that high temperature grain growth in nanocrystalline copper can be prevented by introducing dopant atoms, which segregate to the grain boundaries. Unfortunately, the impact of grain boundary dopant atoms on inelastic deformation mechanisms, such as dislocation nucleation, is unclear. Thus, the objectives of this work are to use molecular dynamics simulations (i) to capture the influence of interface structure on the strength required to nucleate a dislocation from homogeneous copper grain boundaries and (ii) to study the role of antimony dopant atoms at the interface on dislocation emission. It is shown that homogeneous grain boundaries with certain structural features are particularly susceptible to dislocation activity at low applied tensile stresses. It is expected that dopant atoms will have an analogous affect on the dislocation nucleation stress, depending on their position within the grain boundary and the conformation of nearby structural units.

Micro-Engineered Particulate-Based Materials: Session II

Sponsored by: The Minerals, Metals and Materials Society, TMS Materials Processing and Manufacturing Division, TMS: Powder Materials Committee
Program Organizers: Khaled Morsi, San Diego State University; Iver Anderson, Iowa State University

Monday PM Room: 271
March 10, 2008 Location: Ernest Morial Convention Center

Session Chairs: Khaled Morsi, San Diego State University; Iver Anderson, Iowa State University

2:00 PM

Controlled Transformations in Laser Multi-Deposited Alloy Steel: Nathan Smelser[1]; *Haitham El Kadiri*[1]; John Berry[1]; [1]Mississippi State University, Center for Advanced Vehicular Systems

The Laser Engineering Net Shaping (LENS®) technology has not yet yielded suitable control of deposited steel microstructures. Rather, the constraints implied by the need for defect-free deposits impose a very specific material microstructure. To facilitate broadening LENS® microstructural capabilities, researchers contend to correlate the obtained microstructure to the imposed thermal history. In this study, we generate different microstructure gradients while varying cooling rates and minimal temperatures of the last melting cycle (CT cycle) associated with each layer. The cooling properties of the CT cycle are varied thru varying the geometry of coupons deposited in the form of single thin walls. The microstructure evolution in these steel deposits is examined with electron and optical microscopy, and the mechanical properties are appreciated thru multi-scale depth sensoring indentation and standard static tests. The thermal history associated with each condition is modeled using a user LENS® suitable subroutine for the process implemented in Sysweld.

2:25 PM

Corrosion Behavior of Hot-Pressed TiB_2 in Metallic Neodymium and Nd_2O_3-NdF_3-LiF System: *Xudong Luo*[1]; Zhaowen Wang[1]; Zhongning Shi[1]; Xianwei Hu[1]; Kaiyu Zhang[1]; Bingliang Gao[1]; Ganfeng Tu[1]; [1]Northeastern University

TiB_2-based composite ceramics were sintered by vacuum hot-pressing furnace. Matrix materials were titanium diboride. Molybdenum powder and nickel powder were used as sintering additives, respectively. Corrosion resistant properties of the cermet materials at high temperature were studied in this paper. The experiments were carried out in metallic neodymium and Nd_2O_3-NdF_3-LiF system. Corrosion temperature was 1150°C and the holding time was 24h. The cermet materials and corrosion products were characterized by XRD and SEM, respectively. Effect of the sintering additives on sintering process and mechanism of corrosion process were discussed in paper. The results showed that hot-pressing TiB_2 ceramics is a kind of promising material for neodymium electrolysis.

Minerals, Metals and Materials under Pressure: Shock-Induced Phase Transformations and Microstructure

Sponsored by: The Minerals, Metals and Materials Society, TMS Structural Materials Division, TMS: Chemistry and Physics of Materials Committee
Program Organizers: Richard Hennig, Cornell University; Dallas Trinkle, University of Illinois; Ellen Cerreta, Los Alamos National Laboratory

Monday PM Room: 385
March 10, 2008 Location: Ernest Morial Convention Center

Session Chairs: Eric Brown, Los Alamos National Laboratory; Ellen Cerreta, Los Alamos National Laboratory

2:00 PM Invited

The Role of Crystalline Instabilities in Shock-Induced Plasticity and Melting: *Ramon Ravelo*[1]; [1]University of Texas El Paso

Large-scale atomistic simulations of shock-wave propagation in single crystals exhibit large anisotropies in the elastic-plastic and solid-liquid transitions. Characteristic of this type of simulations are the large strains at which the crystal yields plastically, regardless of crystal orientation. At these large strains, uniaxial deformations, such as those produced in planar shock loading can generate dynamical instabilities, which compete with defect nucleation mechanisms. At larger compressions near the melt transition, shear instabilities at the shock front enhance lattice amorphization and melting. We will review the criteria, which explain how these instabilities develop and discuss recent large-scale atomistic simulations of plastic deformation and melting in Cu and Al single crystals.

2:30 PM

Microstructural Modifications after Small Charge Explosions in Aluminum and Copper Targets: *Donato Firrao*[1]; Paolo Matteis[1]; Chiara Pozzi[1]; Giorgio Scavino[1]; Graziano Ubertalli[1]; Maria Rosa Pinasco[2]; Maria Giuseppina Ienco[2]; Paolo Piccardo[2]; Gabriella Pellati[2]; Girolamo Costanza[3]; Roberto Montanari[3]; Maria Elisa Tata[3]; Giovanni Brandimarte[4]; Santo Petralia[4]; [1]Politecnico Di Torino; [2]Università di Genova; [3]Università di Roma Tor Vergata; [4]Marina Militare Italiana

Metals exposed to explosions undergo several macro and micro changes. At the microstructural level slip bands or mechanical twins, caused by the pressure and temperature wave, can be detected. Twinning or slip occurs depending on the metal stacking fault energy, the blast wave pressure and the deformation rate. An experimental campaign was performed on different FCC metals. Results concerning OFHC copper and AA 2014 aluminum alloy are presented herein and compared with previous results concerning AISI 304Cu stainless steel and a 18 carat gold alloy. Specimens exposed to small charge explosion (50 or 100 g of plastic explosive) were analyzed by optical microscopy and by X-ray diffraction. Microstructural plastic deformation marks were detected and their possible attribution either to mechanical twinning or to cross slip is discussed on the basis of the X-ray diffraction patterns. The detectability target-to-charge distance limit, and hence the critical stress for microstructural changes, are evaluated.

2:50 PM Break

3:05 PM Invited
Direct Shock-Density Measurements Using Plate Impact and Proton Radiography: *Paulo Rigg*[1]; Cynthia Scwartz[1]; Robert Hixson[1]; Alexander Saunders[1]; Frank Merrill[1]; Chris Morris[1]; [1]Los Alamos National Laboratory

Proton radiography (pRad) is a powerful new diagnostic with the potential of producing accurate (1%) direct density measurements from dynamically loaded materials. Experiments have been performed to investigate the feasibility of using proton radiography (pRad) to obtain dynamic radiographs of shock-compressed materials during plate impact experiments. This work has involved the design, manufacturing, and testing of a new 40mm single-stage, powder driven gun, the development of methods to synchronize the shock event generated with the gun to proton output, and initial proof-of-principle experiments in Area C at the Los Alamos Neutron Science Center (LANSCE). The method used to attain synchronization of the shock event to proton beam output will be discussed and the results of our initial experiments will be presented.

3:35 PM
Plastic Deformation and Phase Transformations in Cyclotrimethylene Trinitramine (RDX) under Shock Loading: Theory and Experiment: *Marc Cawkwell*[1]; Tommy Sewell[1]; Von Whitley[1]; Kyle Ramos[1]; Dan Hooks[1]; [1]Los Alamos National Laboratory

The response of the secondary explosive RDX, and organic molecular crystals in general, to shock loading involves mechanisms that cannot reliably be extrapolated or inferred from those seen under quasi-static conditions. We employed non-equilibrium molecular dynamics simulations (NEMD), first-principles calculations and laser and flyer-plate generated shock waves in the study of (111) and (010) oriented single crystals. Shock waves propagating normal to (111) above a threshold particle velocity result in the homogeneous nucleation of partial dislocation loops on (001). The stacking faults generated by these dislocations are obstacles for the glide of perfect dislocations and hence give rise to an anomalous hardening. NEMD simulations of (010) oriented crystals predict that a phase transformation takes place for particle velocities > 750 m/s. Experimental validation of this result can be obtained from measurements of the Hugoniot locus and refractive index during flyer-plate and laser-driven shocks compared with NEMD and first-principles calculations.

3:55 PM Break

4:10 PM
Shock Damage Quantification and Modeling: *Veronica Livescu*[1]; John Bingert[1]; Scott Dillard[2]; Daniel Worthington[2]; Davis Tonks[1]; [1]Los Alamos National Laboratory; [2]University of California, Davis, Materials Design Institute

The characterization and quantification of damage in polycrystalline materials is an important component toward understanding mechanisms controlling failure processes. The effect of microstructural variables is of particular interest. This work is concerned with damage processes resulting from shock impact events. Incipient damage quantification in specimens from plate impact experiments was performed using a three-dimensional characterization technique. Important damage statistics needed for the validation of damage models were obtained from the three-dimensional reconstruction of the true shock-induced damage field. Reconstruction of grain vertices, edges and facets, and crystallographic orientation information from integrated optical and electron backscattered diffraction data provided quantitative information on the damage nucleation process. This characterization reveals the effect of high-pressure, high-rate loading on microstructural evolution, and the interplay between microstructure and damage processes. Results are applied to the development and validation of a mesoscale micromechanical damage model to reproduce the development and evolution of damage in shocked materials.

4:30 PM
Shock Induced Polycrystallization and Residual Tension in Tantalum Single Crystals: *Jikou Zhou*[1]; Luke Hsiung[1]; Ricky Chau[1]; Cheng Saw[1]; [1]Lawrence Livermore National Laboratory

In this presentation, we report shock-induced lattice orientation changes and residual lattice tension in tantalum single crystals. The single crystals with orientations in [001], [011], [111], and [123] directions are shock loaded at ~ 55 GPa in gas gun under the almost identical conditions. The crystal orientation changes at macroscale and microscale are revealed by a combination of x-ray diffraction analysis and microscopic examination. Rather than lattice compression that is frequently probed by in situ x-ray diffraction technique, we find significant residual lattice tension in the recovered tantalum crystals. Such residual lattice tension is attributed to the dislocation cells and their deformation. The dislocation cells are accordingly estimated to be greater than 100 nm from broadening of x-ray diffraction peak.

4:50 PM
Microstructural Investigation of Very High Strain Rate Deformation of DP 600: *Brian Hamburg*[1]; Judy Schneider[1]; [1]Mississippi State University

High gasoline prices and increasing safety regulations have forced the automotive industry to look beyond conventional steels to advanced high strength steels such as dual phase (DP) steels. Previous researchers have tested DP 600 up to strain rates order of 10^3 1/s and have found some very interesting properties which have been further investigated in this study. The object of this study is to gain an understanding of the microstructural changes occurring in DP 600 at very high strain rates. The method selected to produce the very high strain rates was normal impact of a hardened steel penetrator into a piece of DP 600 steel. The average strain rates produced from this method with the test set-up used are on the order of 10^5 1/s. The micro-structure has been observed with several different methods to study the micro-structural changes of DP 600 under high strain rate deformation.

Neutron and X-Ray Studies for Probing Materials Behavior: Diffraction at Small Dimensions

Sponsored by: National Science Foundation, The Minerals, Metals and Materials Society, TMS Structural Materials Division, TMS: Advanced Characterization, Testing, and Simulation Committee
Program Organizers: Rozaliya Barabash, Oak Ridge National Laboratory; Yandong Wang, Northeastern University; Peter K. Liaw, University of Tennessee

Monday PM — Room: 391
March 10, 2008 — Location: Ernest Morial Convention Center

Session Chairs: Vaclav Holy, Charles University; Sunil Sinha, University of California, San Diego

---

2:00 PM Invited
Studies of Structure and Dynamics of Surfaces and Interfaces with X-Rays and Neutrons: *Sunil Sinha*[1]; [1]University of California San Diego

In the last decade or so there has been increased attention paid to diffuse and off-specular scattering at grazing incidence from surfaces and interfaces, as a means of obtaining in-plane structural information about properties such as roughness, wetting phenomena, film growth morphologies, in-plane ordering and phase transitions, nanoparticle assemblies, mineral surfaces, dynamical surface fluctuations, thin film magnetism, domain morphology and dynamics, etc. Modern synchrotron and neutron sources have developed beamlines specially equipped for such studies. We shall discuss the development of the technique and the methods for analyzing such scattering, and illustrate with some examples of recent studies, including the extension to slow dynamics of films near the glass transition.

2:25 PM Invited
X-Ray Scattering Studies of Inhomogeneous Length Scales in Correlated Electron Systems: The Case of High-Tc Cuprates: *Zahirul Islam*[1]; [1]Argonne National Laboratory

High-temperature superconductors are electronically "inhomogeneous" on various length scales, which may be due to distortions modulating both pair potential and exchange interactions. X-ray scattering studies of cuprates reveal lattice modulations and superstructures on various length scales comparable to superconducting coherence lengths. These modulations can be one, two, or three dimensional in nature. In YBCO, modulations characterized by q=(qx, 0, 0) correspond to correlated atomic displacements due to relaxation effects caused by O-vacancy ordered "nanopatches". These nanopatches form well above room temperature and persist well into the superconducting state. Furthermore,

"bowtie"-shape Huang scattering in YBCO and LSCO indicates characteristic long-range strain, which makes the lattice intrinsically inhomogeneous at all doping levels. Structural modulations are also present in BSCCO and HBCO. An inter-play between electronic inhomogeneities and lattice modulations seems inevitable in cuprate superconductors. [APS is supported by the DOE, Office of Science, under Contract No. DE-AC02-06CH11357.]

2:50 PM

X-Ray Microscopic Studies on Electromigration in Electronics Solder Joints: *Andre Lee*[1]; K. Subramanian[1]; Cheng-En Ho[1]; Wenjun Liu[2]; [1]Michigan State University; [2]Argonne National Laboratory

Synchrotron X-ray investigations on a two-phase Sn-Pb alloy solder joint subjected to current stressing have provided significant insight on the events that take place under electromigration in a multi-phase alloy. X-ray fluorescence studies indicated that different conducting species move at different rates during electromigration. X-ray micro-diffraction, with sub-micrometer spatial resolution, facilitated the characterization of 2- and 3-dimensional crystallographic orientations and strain fields at different regions of the joint with respect to the direction of electron flow as a function of time. In the joint configuration, the continuous build-up of slow moving dominating species just behind the fast moving species causes significant compressive deformation in the anode region to push out the fast moving species towards the free surface to form the hillock. The non-destructive micro-beam X-ray techniques employed provided an effective means for the continuous monitoring of the microstructural evolution and development of surface features resulting from current stressing.

3:10 PM Invited

X-Ray Investigation of the Structure of Magnetic Semiconductor Epitaxial Layers: *Vaclav Holy*[1]; Vit Novak[2]; Tomas Jungwirth[2]; Guenther Bauer[3]; Rainer Lechner[3]; [1]Charles University; [2]Institute of Physics; [3]Kepler University

The main goal of the structural studies of magnetic semiconductor epitaxial layers such as GaMnAs or GeMn is to determine the lattice positions of the magnetic ions, since only substitutional positions of the ions give rise to a ferromagnetic ordering of their magnetic moments. Several x-ray methods are used for this task. X-ray diffraction precisely determines the lattice parameter of a magnetic semiconductor layer, however its connection with the density of the magnetic ions in substitutional and interstitial positions is not completely understood yet. A direct information on the positions of the magnetic ions in the lattice can be obtained by x-ray standing wave method or x-ray fluorescence holography; using these techniques the densities of the ions in different lattice positions were studied in non-annealed and annealed magnetic layers.

3:35 PM

Structural Characterization of $SrTiO_3$ Thin Films on Sr Terminated (100) Si Substrates by X-Ray Measurements: *Hong Ji*[1]; Xiaoyuan Zhou[2]; [1]University of Electronic Science and Technology of China; [2]Hong Kong Polytechnic University

X-ray diffraction is a very powerful tool for the structural characterization of thin films and heterostructures. In this work, a detailed structure analysis on the heterostructure of $SrTiO_3$(STO)/Sr using a variety of X-ray scattering techniques ($2\theta/\omega$, ω scan, ϕ-scan, pole figure and XRR) is demonstrated. The sample was prepared by laser molecular beam epitaxy under optimized conditions of substrate temperature and oxygen pressure. Symmetrical $2\theta/\omega$ scan indicates a high crystallization quality and epitaxial grown of STO. ϕ-scans over STO (101) and Si (202) reflections have further revealed the in-plane orientation relationship between STO and Si. The α- and c-lattice parameters of the STO thin film were found to be 0.3898, and 0.3901 nm, respectively, suggesting a slight lattice distortion. To better understand the role of the buried interface, further characterizations by pole figure and XRR have been carried out and will be reported in the conference presentation.

3:55 PM Break

4:05 PM Invited

Complex X-Ray Characterization of Magnetron Deposited TiO_2 Thin Films - Growth, Crystallization and Thermal Stability: *Radomir Kuzel*[1]; Lea Nichtova[1]; Zdenek Matej[1]; Jan Sicha[2]; Jindrich Musil[2]; [1]Charles University, Faculty of Mathematics and Physics; [2]University of West Bohemia, Faculty of Applied Sciences

Sets of amorphous and nanocrystalline titanium dioxide thin films with different thickness were studied after deposition, after annealing and also by in-situ measurements during the heating. Phase analysis and X-ray line broadening were studied by PXRD in parallel beam optics; the residual stresses and textures were measured with the Eulerian cradle and evolution of the surface roughness determined by X-ray reflectivity measurement. Microstructure parameters were extracted by peak profile fitting and by whole powder pattern modelling. Crystallization temperature of about 250°C for thicker films was found for amorphous films. The crystallite size immediately after crystallization was larger than 100 nm. Thin nanocrystalline films consisted mainly of about 7 nm rutile crystallites while thicker films (> 500 nm) were composed of mainly anatase crystallites of similar size. Depth profiling measurements indicated transformation of the rutile phase into anatase with increasing distance from the substrate.

4:30 PM Invited

Adaptive Diffraction Phenomenon of Nanodomained Materials: *Yu Wang*[1]; [1]Virginia Tech

A nanodomain diffraction theory is developed. It reveals drastically different diffraction phenomenon in nanodomained materials from that in coarse-domained materials, and a conventional interpretation of the diffraction data leads to identification of erroneous phases. Since the nanodomain sizes are significantly smaller than the coherence length of diffraction radiation, e.g., X-ray and neutron, the scattered waves from individual nanodomains coherently superimpose in diffraction, which produces significant interference effects and must be taken into account. Our analysis reveals an adaptive diffraction phenomenon peculiar to nanodomained materials, where fundamental Bragg peaks disappear while new reflection peaks appear, whose positions are determined by a lever rule according to twin domain volume fractions. The criterion for transition between adaptive diffraction and conventional diffraction is derived. Brillouin zone-dependent diffraction behaviors are discussed. Experimental confirmation of the adaptive nanodomain diffraction phenomenon is presented.

4:55 PM

Monitoring the Deformation Mechanism Evolution over a Large Range of Grain Sizes by In-Situ Diffraction: Xun-Li Wang[1]; *Alexandru Stoica*[1]; Sheng Cheng[2]; Jon Almer[3]; Yang Ren[3]; Don Brown[4]; [1]Oak Ridge National Laboratory; [2]University of Tennessee; [3]Argonne National Laboratory; [4]Los Alamos National Laboratory

The in-situ high-energy X-ray and neutron diffraction techniques were used to study the deformation of nickel under monotonic and cyclic tensile loading. The diffraction data evidenced a dramatic change in the deformation mechanisms as the grain size is reduced from microns to nanometers range. The classical dislocation-mediated plasticity induces in the coarse-grained nickel characteristic grain orientation dependent residual strains (intergranular strains), which are also visible in the ultafine-grained material. However, the evolution of the preferential grain orientation relative to the loading direction indicates that the deformation mechanism for the grain sizes ranging from 100 to 1000 nm includes the twining as an essential component. Under further grain refinement, down to the grain size of 20 nm, no intergranular strains develop during the plastic deformation and the texture remains unchanged. This behavior leads to the conclusion that the grain boundaries control the plastic deformation of nano-grained nickel.

5:15 PM

Wear Properties and Strain Distribution Analysis of Ti-Based Biomedical Alloy with Different Types of Microstructure: *Eri Fujiwara*[1]; Eliot Specht[2]; Gene Ice[2]; Kunihiro Hisatsune[1]; [1]Nagasaki University; [2]Oak Ridge National Laboratory

Effect of heat treatment on wear and frictional properties in Ti-6Al-7Nb was investigated by powder diffraction method. The frictional test between Ti and Ti-alloy was carried out using a pin-on-disk type method in artificial saliva at

310 K. Surface deformation and stress distribution were determined for the wear surface of a fine-grained a + ß phase Ti-6Al-7Nb biomedical alloy with lamellar or lamellar + equiaxed a structures from peak broadening observed in powder diffraction with a scanning X-ray microbeam probe. Broadening of powder diffraction peaks was observed, especially for the ß phase. Integrated diffraction spectrum suggested that crystalline orientation of the a phase occurred, and besides, the lattice parameter of the ß phase increased. A peak broadening analysis revealed that broadening was caused by deformation or faulting, and that higher strain was induced in the ß phase than in the a phase.

5:35 PM

Plasticity in Nanoscale Metallic Multilayers with In-Situ Synchrotron X-Ray Diffraction: *Cahit Aydiner*[1]; Don Brown[1]; Amit Misra[1]; Jon Almer[1]; Nathan Mara[1]; [1]Los Alamos National Laboratory

Free-standing Cu-Nb multilayer thin films (nominally 20 micrometers thick) have been tensile loaded as elastic strain tensors in both phases are determined in-situ by high-energy synchrotron X-ray diffraction (SXRD). This immiscible system with incoherent, weak interfaces has been studied heavily to investigate size effects in plasticity as the layer thicknesses are reduced to the nanometer scale. Typically, at tens of nanometers, single dislocation glide substitutes the dislocation pile-up at the interfaces, signifying a fundamental change in plasticity mechanism. We use in-situ SXRD to further our understanding of these mechanisms, by quantifying the load sharing between the two phases, texture, residual stress and unloading behavior. Samples of 5, 27, 40 and 100 nanometers layer thicknesses have been used to span the length scales of interest. The experimental data is interpreted by an adaptation of elasto-plastic self-consistent model that reflects dislocation mechanisms at the nanoscale.

Particle Beam-Induced Radiation Effects in Materials: Metals II

Sponsored by: The Minerals, Metals and Materials Society, American Nuclear Society, TMS Structural Materials Division, TMS/ASM: Nuclear Materials Committee
Program Organizers: Gary Was, University of Michigan; Stuart Maloy, Los Alamos National Laboratory; Christina Trautmann, Gesellschaft fur Schwerionenforschung; Maximo Victoria, Lawrence Livermore National Laboratory

Monday PM Room: 389
March 10, 2008 Location: Ernest Morial Convention Center

Session Chairs: Yong Dai, Paul Scherrer Institut; Maximo Victoria, Paul Scherrer Institut

2:00 PM

Dynamic Observations of Microstructural Evolution in Fe and Fe-Cr Alloys under Heavy-Ion Irradiation: *Michael Jenkins*[1]; Zhongwen Yao[1]; Mercedes Hernandez-Majoral[2]; Mark Kirk[3]; [1]University of Oxford; [2]Centro de Investigaciones Energeticas, Medioambientales y Tecnologicas; [3]Argonne National Laboratory

Thin foils of Fe-0-11%Cr alloys were irradiated with 100-150 keV Fe+ and Xe+ ions at 20C and 300C. Dynamic TEM observations followed the evolution of damage over doses 0-1dpa. Small 2-4nm dislocation loops with <100> and ½ <111> Burgers vectors first appeared at about 0.001-0.01dpa. Loop motion and loss of loops to the surface was induced by the electron beam. In iron the number of loops retained was strongly dependent on the foil orientation; less loop loss occurred in FeCr alloys. At doses >0.1dpa complex microstructures developed in thicker regions of foils, involving cooperative alignment and interaction of smaller loops. In UHP Fe irradiated at 300C the damage took the form of interstitial loops with b = ½<111>. Large finger-shaped loops developed by the growth and coalescence of smaller loops. Similar damage structures developed in UHP Fe at 20C and in Fe8%Cr at both 20C and 300C.

2:40 PM

The Effect of Cr and Ni Content on the Irradiated Microstructure of High Purity Austenitic Alloys: *Zhijie Jiao*[1]; Gary Was[1]; [1]University of Michigan

The mechanical properties of irradiated materials heavily depend on irradiation-induced microstructures. The effect of Cr and Ni content on the irradiated microstructure in iron-based austenitic alloys has been widely discussed but rarely studied in a systematic way. To isolate the effect of Cr and Ni from possible impurities, six high purity austenitic alloys with Cr and Ni content ranging from 13-22% and 12-32%, respectively, were selected and irradiated to 1 and 5 dpa at 360°C using 3.2 MeV protons. Irradiated microstructure consisting of dislocation loops and voids was characterized by transmission electron microscopy. The dependence of microstructure on Cr and Ni content by proton irradiations was compared to available data from neutron irradiations at similar doses and temperatures. The similarity and discrepancy between these two types of irradiations will be discussed.

3:00 PM

Self-Organization Processes in Metals by Low-Energy Ion Irradiation: I. Tereshko[1]; *V. Abidzina*[1]; I. Elkin[2]; V. Glushchenko[1]; A. Tereshko[1]; [1]Belarusian-Russian University; [2]"NANTES - Systemy Nanotechnologii" Plc.

The goal of this paper is to study self-organization processes that cause nanostructural evolution in nonlinear crystal media. The computer simulation was used to investigate the interaction between low-energy ions and nonlinear crystal lattices. A molecular dynamics method has been applied for calculating the evolution of atom ensembles in lattices of different dimensions using the equations of classical dynamics. The subjects of investigation were nonlinear homogeneous and heterogeneous (with embedded clusters) atoms chains.We showed that nonlinear oscillations become excited in the chains after low-energy ions irradiation and as a result of them the whole atoms become stabilized in new positions, which results in the formation and development of new metastable atomic groups (nanoclusters). We showed that in homogeneous atom chains critical energy needed for self-organization processes development is less than for nonlinear atom chain with embedded clusters. In this case nanocluster becomes active zone that determine further self-organization processes.

3:20 PM

Mechanical Properties of Ferritic/Martensitic Steels Irradiated in Spallation Target Environments: *Yong Dai*[1]; Bin Long[1]; Zhenfeng Tong[1]; [1]Paul Scherrer Institut

Comparing to neutron irradiation, irradiation of high energy protons can produce not only displacement damage, but also helium and hydrogen at high rate, which may result in severe embrittlement in FM steels. For developing advanced spallation targets, it is essential to understand the behaviors of FM steels under such an irradiation condition. For this reason, thousands of specimens of FM steels have been irradiated in the SINQ (the Swiss Spallation Neutron Source) target irradiation program (STIP). Since 1998 five large irradiation experiments have been carried out and samples of different FM steels such as T91, EM10, F82H, Optifer, Eurofer 97 have been irradiated up to 20 dpa in a wide temperature range. In this presentation, an overview will show the main interesting results obtained from mechanical testing on the FM steels irradiated in STIP with a comparison to results published in the literature after neutron irradiation.

3:40 PM Break

4:00 PM

Microstructural and Mechanical Effects of He Ion Implantation on Ultra Fine Grain Steel: *David Foley*[1]; K. Hartwig[1]; Engang Fu[1]; Stuart Maloy[2]; Peter Hoseman[2]; Ning Li[2]; Xinghang Zhang[1]; [1]Texas A&M University; [2]Los Alamos National Laboratory

The commercial viability of advanced nuclear reactor designs is currently limited by the radiation damage tolerance of structural steel components. Recent works have demonstrated that increasing the layer interface density of multilayer films can lead to an improvement in radiation damage tolerance. Several levels of microstructural refinement have been achieved in ferritic-martenistic steel via severe plastic deformation (SPD) using equal channel angular extrusion by varying processing temperature and plastic strain level. Room temperature helium ion implantation was carried out on the as-received and processed materials. Microstructural and mechanical properties of these materials were studied via transmission electron microscopy, x-ray diffraction and microhardness. The affects of SPD on the microstructure and resulting post-implantation properties will be discussed.

4:20 PM
Heavy-Ion Irradiation Damage in Bulk Fe-Cr Alloys: *Michael Jenkins*[1]; Sen Xu[1]; Zhongwen Yao[1]; [1]University of Oxford

Bulk Fe-0-12%Cr alloys have been irradiated with 1.5 MeV Fe+ ions at a temperature of 300C. The irradiation produces buried damage with the peak damage region at a depth of about 400 nm. A TEM specimen preparation technique has been developed to access this damage peak. Preliminary TEM experiments have been carried out on pure Fe, Fe-8%Cr and Fe-11%Cr. In all materials the damage took the form of interstitial dislocation loops with sizes ranging up to a few tens of nanometres. Loops with Burgers vectors b = <100> and b = ½<111> were both present with the majority of the loops having b = <100>. A full analysis is now underway. Loop Burgers vectors, nature, size distributions and number densities will be determined as a function of the Cr content of the alloys. Comparisons will also be made with in-situ experiments in which ion irradiations are performed on thin foils.

4:40 PM
Influence of Ion Irradiation Dose Rates on the Mechanical Properties in HT-9: *Richard Greco*[1]; Peter Hosemann[1]; Yongqiang Wang[1]; Stuart Maloy[1]; Marcus Cappiello[1]; John Swadener[1]; [1]Los Alamos National Laboratory

Materials irradiation experiments in nuclear reactors or spallation sources are essential for understanding the change of the materials properties due to irradiation. In a thermal reactor only ~12 dpa per year is possible and the specimen can become radioactive, making testing difficult. In order to save time a faster way to study the property changes in materials due to irradiation needs to be established. Particle accelerators using energetic particles can cause much higher radiation damage in a shorter time. A few studies performed previously have shown that these types of experiments produce comparable results to reactor irradiations. In this study HT-9, a candidate material for nuclear reactors, was irradiated to 7 dpa using He+ particles at three different dose rates. After irradiation, the samples were tested using nano-indentation to investigate the changes in mechanical properties. The data was compared to experiments from the literature and to the Dispersed Hardening Model.

5:00 PM
Irradiation-Induced Precipitation Modelling of Ferritic Steels: *Roy Faulkner*[1]; Zheng Lu[1]; [1]Loughborough University

Ferritic steels are the leading structural materials for nuclear reactor applications due to their excellent swelling resistance. Previously, phase-transformations under irradiation had only been treated in a semi-quantitative fashion (Nolfi1983). Until this current work was undertaken, no attempts had been made to accurately alter the thermodynamics of phases present as a function of neutron irradiation effects. In principle this should be straightforward, so long as the additional energy input to the system coming from the neutron irradiation is known. It is shown in this paper that this accommodation of the additional energy can be introduced to the model and that the model output reflects well the real situation for phase-transitions and second-phase particles in irradiated steels. The model considers formation of irradiation-induced inter-and intra-granular carbide-precipitation in reactor-pressure-vessel steels (C-Mn/MnMoNi). Predicted differences in carbide-distribution as a function of Ni/Cu ratio and absolute Ni-concentration will be highlighted and confirmed well experimental data.

5:20 PM
Nanoscale Mechanical Testing on Ion Irradiated Steels: *Peter Hosemann*[1]; Christiane Vieh[1]; Stuart Maloy[1]; Richard Greco[1]; [1]Los Alamos National Laboratory

Radiation induced mechanical property changes are a major difficulties in designing systems operating in a radiation environment. Testing various materials in an irradiation environment is a costly and time consuming activity. Ion beam accelerator experiments have the advantage of allowing relatively fast and inexpensive materials irradiations without activating the sample but do in general not allow large beam penetration depth. In this study, many different ferritic/martensitic steels (e.g. T91 and HT-9) were exposed in an ion beam and tested after irradiation using micro pillar testing and nano indentation in combination with a focused ion beam (FIB) instrument to investigate the changes on mechanical properties. Microstructural changes were evaluated using TEM. The results show good agreement with similar testing after irradiation in a fast neutron flux.

Recent Developments in Rare Earth Science and Technology - Acta Materialia Gold Medal Symposium: Session II

Sponsored by: The Minerals, Metals and Materials Society, TMS Electronic, Magnetic, and Photonic Materials Division, TMS: Superconducting and Magnetic Materials Committee
Program Organizers: Vitalij Pecharsky, Iowa State University; Ashutosh Tiwari, University of Utah; James Morris, Oak Ridge National Laboratory

Monday PM — Room: 280
March 10, 2008 — Location: Ernest Morial Convention Center

Session Chairs: James Morris, Oak Ridge National Laboratory; Ashutosh Tiwari, University of Utah

2:00 PM Invited
Cage Compounds of the Rare-Earth Metals: Interplay of Chemistry and Physics: *Grin Yuri*[1]; [1]Max-Planck-Institut fuer Chemische Physik Fester Stoffe

Intermetallic clathrates (e.g. $Eu_8Ga_{16-x}Ge_{30+x}$), clathrate-like compounds (like $EuSi_6$) and skutterudites (like $RE_xTM_4E15_{12}$, TM - transition metal, E15 - element of the group 15 of the Periodic Chart), with rare-earth (RE) cations attracted the worldwide attention, e.g., as promising thermoelectric materials. For the case of the covalent intra-network bonding with RE cations as bonding-balance medium in sense of the Zintl concept, a low charge carrier concentration should be expected. Application of the real space bonding analysis showed indeed the covalent 2*c*-2*e* interactions within the network and the charge transfer from the cations to the network. Deviations form the Zintl-like electronic balance or the *d* states of the TM participating in the bonding lead to the low-charge-carrier behaviour, favourable, e.g., for the thermoelectric applications. The question, how far the picture of the chemical bonding may be used for development of the new cage compounds, is still open.

2:30 PM Invited
Rare Earth Zintl Phases: From Power Generation to the Anomalous Hall Effect: *Brian Sales*[1]; [1]Oak Ridge National Laboratory

Zintl phases contain both ionic and covalent bonds, tend to be narrow gap semiconductors or low carrier concentration metals, and often have open crystal structures. In rare earth Zintl phases, the strongly electropositive rare earth atoms donate electrons to other atoms in the structure to form covalent bonds. Examples of rare earth Zintl phases are the filled skutterudites (e.g. CeFe4Sb12), Eu clathrates (e.g. Eu8Ga16Ge30) as well as more complex phases such as Yb14MnSb11. As will be discussed, many of these phases are good thermoelectric materials and can be used in devices to directly convert heat into electricity. In addition, the magnetic properties of the rare earth ions, coupled with the diversity in bonding inherent in Zintl compounds, often leads to unusual ground states and new physics. Two examples of unusual ground states will be discussed. A ferromagnetic compound where the Eu atoms tunnel among four equivalent sites at a frequency of -500 Mhz, and an underscreened ferromagnetic Kondo compound that exhibits a highly anisotropic anomalous Hall effect. Research at Oak Ridge was sponsored by the Division of Materials Sciences and Engineering, Office of Basic Energy Sciences, U.S. Department of Energy, under contract with Oak Ridge National Laboratory, managed and operated by UT-Battelle, LLC.

3:00 PM Invited
Recent Developments in Geometrically Frustrated Magnetic Materials: Rare Earth Pyrochlore Oxides: *John Greedan*[1]; A. Diego Lozano[1]; Shahab Derahkshan[1]; Delphine Gout[2]; Thomas Proffen[2]; [1]McMaster University; [2]Los Alamos National Laboratory

Rare earth oxides with the pyrochlore structure, Ln2M2O7, where M is a tetravalent element and Ln is a trivalent lanthanide have played a major role in research on geometrically frustrated magnetic materials. This arises from the topology of both the Ln3+ and M4+ sublattices which consist of three dimensional arrays of corner-sharing tetrahedra and the local, strongly axial, symmetry of the rare earth site. The role of the rare earth in determining the ground magnetic state will be reviewed. As well, the long standing puzzle of the

spin glass behavior of Y2Mo2O7 will be addressed using results from neutron diffraction and neutron pair distribution function analysis. These show the absence of evidence for a phase transition driven by frustration and a disorder model is proposed involving one of the oxygen positions. Earlier results from EXAFS and Y nmr are discussed in light of these new findings.

3:30 PM

Structure-Property Correlations in Rare Earth Based Manganites: *Nori Sudhakar*[1]; G. Trichy[1]; J. Narayan[1]; [1]North Carolina State University

The important physical phenomena exhibited by manganites, namely, metal-insulator transition (MIT), colossal magnetoresistance (CMR) and para to ferromagnetic phase transition are highly sensitive to the growth conditions. For lattice relaxation in thin films dislocations mostly nucleate at the film surface and propagate to the interface. Due to the difficulty in nucleation and propagation of dislocations in LCMO or oxides in general, only a small fraction of strain is reduced in low misfit systems and the remaining strain builds up with the thickness of the film. However, under a large misfit such as in LCMO on MgO, most dislocations nucleate at the steps and get set at the interface, so that the rest of the film can give relatively strain free with properties similar to bulk crystals. The structural and physical properties of the thin films are correlated and interpreted within the theoretical framework of the domain matching epitaxy. The field and temperature dependent magnetization data in the critical region is probed with the aid of Arrott analysis.

3:45 PM

Thermodynamic and Elastic Properties of La(TM)$_5$ Hydrides (TM = Fe, Co, Ni) from First Principles Density Functional Theory: *Louis Hector, Jr.*[1]; Jan Herbst[1]; [1]General Motors Research and Development Center

Thermodynamic and elastic properties computed with state-of-the-art density functional theory are presented for La(TM)$_5$H$_n$ materials with TM one of the magnetic transition metals Fe, Co, or Ni. We specifically focus on calculating 0K and 298 K formation enthalpies, ΔH, for all compounds. Room temperature ΔH values are obtained from phonon calculations based upon the direct method. Our phonon calculations for $LaCo_5$ and $LaCo_5H_4$ yield new information on their crystal structures. While no La-Fe compounds exist, we find $\Delta H(LaFe_5) > 0$, and hence its formation under experimentally attainable pressures may be possible. $LaFe_5$ hydrides are predicted to form for several prototype crystal structures. Some issues that arise between experiment and theory will be addressed.

4:00 PM Break

4:15 PM Invited

Synthesis and High-Temperature Thermoelectric Properties of the Rare Earth Containing Compounds of the $Ca_{14}AlSb_{11}$ Structure Type: Shawna Brown[1]; Catherine Cox[1]; *Susan Kauzlarich*[1]; Franck Gascoin[2]; Teruyuki Ikeda[3]; Eric Tobler[3]; G. Snyder[3]; [1]University of California; [2]Jet Propulsion Laboratory, California Technical Institute; [3]California Institute of Technology

Thermoelectric devices are becoming increasingly useful in a wide range of applications. Increasing the efficiency of these devices would boost the development of clean energy technologies; however, over the last two decades, even with new materials development, there has been a lack of high-temperature, high-efficiency materials, thus limiting the attainable effectiveness of thermoelectric devices. Existing thermoelectric data on Yb14MnSb11 show an improved figure of merit of at least 67% over the current material, SiGe. Our aim is to further improve this value and further increase device efficiency by optimizing the electronic and thermal parameters of the materials. Here, we present the synthesis and high-temperature thermoelectric properties of the Yb14Mn1-xZnxSb11 solid-solution (with x = 0.00, 0.17, 0.33, 0.50, 0.67, 0.83, and 1.0). Single crystal diffraction, microprobe analysis, differential scanning calorimetry, thermogravimetry, resistivity, Seebeck coefficient, and thermal conductivity results will be presented.

4:45 PM Invited

Structures and Physical Properties of Ternary Rare-Earth Intermetallic Phases in the RE–M–Ge and RE–M–Sb Systems: Haiying Bie[1]; Andriy Tkachuk[1]; Oksana Zelinska[1]; *Arthur Mar*[1]; [1]University of Alberta

The wide variety of magnetic properties displayed by intermetallic compounds containing rare-earth (RE) and transition metals (M) arises from differing interactions between the localized f-electrons of the RE atoms, through the possible intermediary of the d-electrons of the M atoms. Because Ge and Sb have similar electronegativities and atomic radii, we have been interested in extending our longstanding work on ternary rare-earth antimonides to germanides. New phases have been identified in these systems containing an early transition metal: $RECr_{1-x}Ge_2$, $REMGe_3$ (M = V, Cr), $RE_2Ti_7Sb_{12}$, and $RE_2Ti_9Sb_{15}$. In the Cr-containing phases, strong magnetic exchange interactions between the f and d electrons lead to relatively high ferromagnetic ordering temperatures (e.g. T_c = 155 K for $SmCrGe_3$) that coincide with prominent transitions in the electrical resistivity. Band structure calculations have been performed to draw insight into the bonding and properties of these compounds.

5:15 PM Invited

The Role of Rare-Earth Atoms in Polar Intermetallic Compounds: *Gordon Miller*[1]; [1]Department of Chemistry, Iowa State University

Polar intermetallic compounds involve combinations of electropositive, active metals and electronegative, late- or post-transition metals. Their structures are typically governed by optimized orbital interactions within the network of electronegative metals with an electron count achieved by formally donating the valence electrons of the active metals to the electronegative components. When rare-earth metals serve in place of the active metals, potentially interesting chemistry and physics can arise, phenomena that are related to the combination of valence 5*d* orbitals for chemical bonding and 4*f* orbitals with localized electron character at the rare-earth metals. This seminar will summarize these characteristics in polar intermetallics ranging from heavy fermion-like Ce-Ni-Al phases to the magnetic refrigerants $(Gd_{1-x}Y_x)_5Ge_4$ and $(Gd_{1-x}Y_x)_5Si_4$.

5:45 PM

Effect of Fluoride Coating on Mechanical Properties of Polymer-Bonded Rare Earth Magnets: *Nathaniel Oster*[1]; Peter Sokolowski[1]; Iver Anderson[2]; Wei Tang[2]; Y. Wu[2]; Kevin Dennis[2]; Matthew Kramer[2]; R. McCallum[2]; [1]Iowa State University; [2]Ames Laboratory (US Department of Energy)

Mixed rare earth (MRE) magnetic alloy particulate of the MRE2Fe14B type readily form a brittle, non-protective oxide layer. Efforts have been made to passivate MRE magnet alloy powders through the creation of a fluoride surface layer. This study is an investigation of the effect of a fluoride coating on the mechanical properties of polymer-bonded magnets made from MRE magnetic particulate. Surface chemistry, particle geometry, and mixing ratios were among the factors considered in this study. High-pressure gas atomized MRE2Fe14B spherical powder and crushed MRE2Fe14B melt spun ribbon were used in the study. Nitrogen trifluoride was used at elevated temperatures to passivate the powders. The powders were mixed with polyphenylene sulfide and compression molded at elevated temperature to form the bonded magnets. Mechanical strength was measured with a four point bend test and the findings will be reported. Support from DOE-EERE-FCVT Office through Ames Lab contract DE-AC02-07CH11358.

Recent Industrial Applications of Solid-State Phase Transformations: Alloy Design, Microstructure Prediction and Control

Sponsored by: The Minerals, Metals and Materials Society, TMS Materials Processing and Manufacturing Division, TMS/ASM: Phase Transformations Committee
Program Organizer: Milo Kral, University of Canterbury

Monday PM — Room: 287
March 10, 2008 — Location: Ernest Morial Convention Center

Session Chair: Milo Kral, University of Canterbury

2:00 PM Introductory Comments

2:05 PM Invited

Design Applications of Transformation Theory: *Gregory Olson*[1]; [1]Northwestern University and QuesTek Innovations LLC

The new industry of Computational Materials Scieneering is built on a foundation of predictive phase transformation theory. In the parametric design of new alloys, the Langer-Schwarz framework for precipitation at high

supersaturations allows control of length and time scales through transformation driving forces and coarsening rate constants employing the ThermoCalc/DICTRA multicomponent thermokinetic system, with unstable equilibrium trajectory models giving accurate control of peak hardness, dispersed phase transformation toughening, and Zener-Smith grain refinement. Accelerated process optimization at the component/device level and prediction of property variation in multistage manufacturing under the DARPA-AIM methodology employs explicit simulation of multimodal precipitation with the PrecipiCalc software. Under the ONR/DARPA "D3D" Digital Structure initiative, a company-led university consortium addresses integration of multiscale tomographic characterization with high fidelity simulation of the spatial distribution of precipitate dispersions in processing and service for the accurate design and AIM qualification of high performance steels combining strength, toughness and fatigue resistance.

2:30 PM
Phase Transformation Theory, a Powerful Tool for the Design of Advanced Steels: From Macro to Nano: *Francisca Caballero*[1]; Michael Miller[2]; Carlos Garcia-Mateo[1]; Carlos Capdevila[1]; Carlos Garcia de Andrés[1]; [1]CENIM-CSIC; [2]Oak Ridge National Laboratory (ORNL)

An innovative design procedure based on phase transformation theory alone has been successfully applied to design steels with a microstructure consisting of a mixture of bainitic ferrite, retained austenite and some martensite. An increase in the amount of bainitic ferrite is needed in order to avoid the presence of large regions of untransformed austenite, which under stress, decompose to brittle martensite. Therefore, the maximum amount of bainite that can be obtained at any temperature is limited by the T'o curve. The design procedure addresses this difficulty by adjusting the T'o curve to greater carbon concentrations using substitutional solutes such as Mn and Cr. With this design procedure, bainitic microstructures with strengths in the range of 1600-1700 MPa and toughness values of 130 MPa m^1/2 were obtained. The concepts of bainite transformation theory can be exploited even further to design steels with a strength in excess of 2.5 GPa and considerable toughness (30 MPa m^1/2). Research at the Oak Ridge National Laboratory SHaRE User Facility was sponsored by Basic Energy Sciences, U.S. Department of Energy.

2:55 PM
Microstructure Prediction of Hot-Rolled Sheet during Continuous Cooling Using Phase Field Method: *Katsumi Nakajima*[1]; Yasushi Tanaka[1]; Yoshihiro Hosoya[1]; Markus Apel[2]; Ingo Steinbach[2]; [1]JFE Steel Corporation; [2]RWTH-Aachen

A precise prediction of microstructure during continuous cooling after hot-rolling is very important for steel engineers. Each sheet product has each controlled cooling history in order to get an ideal microstructure. Phase field simulation has proved to be a useful tool for not only solidification, but also solid-state transformation. In this paper, we applied phase field method to gamma-alpha transformation of low carbon steel which has various kinds of continuous cooling histories and compared them to experimental data. At first, we tried simulations without strain energy effect during transformation in the case of constant continuous cooling rate and also in the case of a few types of commercial cooling. In the presentation, a simulation with strain energy effect will be discussed.

3:20 PM Invited
Design and Development of Mg-Gd-Zn Based Alloys for Elevated Temperature Applications: *Jian-Feng Nie*[1]; Xiang Gao[1]; Laure Bourgeois[1]; Keiichiro Oishi[2]; Kazuhiro Hono[2]; [1]Monash University, ARC Centre of Excellence for Design in Light Metals; [2]National Institute for Materials Science

Lightweight magnesium alloys have attracted increasing interest in recent years for potential applications in the automotive and aircraft industries. One important group of magnesium alloys is those strengthened by precipitation hardening. Unfortunately, the age hardening response achievable in these magnesium alloys is substantially lower than that obtained in aluminium alloys. Further improvement in strength of magnesium alloys requires better understanding of precipitate microstructures and microstructural factors that are important in controlling the strength of the alloys. This presentation will show recent results on the design and development of Mg-Gd based alloys for elevated temperature applications. It shows that Zn additions to dilute Mg-Gd alloys result in a substantial enhancement in precipitation hardening and creep resistance. The strengthening precipitates in these Mg-Gd-Zn alloys are characterised using TEM and 3D atom probe, and results will be discussed in the context of previous work on other Mg-RE-Zn alloys of similar compositions.

3:45 PM Break

3:55 PM Invited
Phase Transformations during Friction Stir Welding: *Richard Fonda*[1]; Keith Knipling[1]; [1]Naval Research Laboratory

Friction stir welding has become an established and commercially-viable joining technique for aluminum alloys. This welding technique is a solid-state joining process which uses a rotating tool to heat the surrounding material such that it can be "stirred" and then consolidated in the wake of the tool. This presentation discusses the phase transformations that occur during the friction stir welding process and relates those phase transformations to the thermal and deformation history of different regions within the weld. The presentation will focus primarily on aluminum alloys, although friction stir welding of higher-strength alloys such as titanium and steel, both of which undergo a high temperature allotropic phase transformation, are also discussed. This presentation also examines the benefits, and limitations, of using friction stir welding in an industrial environment.

4:20 PM Invited
Controlling the Microstructure of CF8C-Plus and CF8C-Plus+Cu/W Alloys to Improve High Temperature Strength and Creep Properties: *Neal Evans*[1]; Philip Maziasz[1]; John Shingledecker[1]; Michael Pollard[2]; [1]Oak Ridge National Laboratory; [2]Caterpillar Inc.

CF8C-Plus cast austenitic stainless steel (Fe-19Cr-12Ni-0.07C-0.7Nb-0.4Si-4Mn-0.25N; Wt%) is a new cost-effective material upgrade for improved performance, durability, and temperature capability relative to current heavy-duty diesel engine exhaust components made from SiMo ductile cast iron and other creep resistant stainless steels. The improved tensile and creep properties observed in both centrifugally cast and thin-section castings of CF8C-Plus and CF8C–Plus+Cu/W alloys will be discussed in terms of the scientifically designed microstructures, which have been revealed by electron microscopy, that develop during high-temperature exposure or creep-rupture testing. These include the formation of nano-scale dispersion-strengthening precipitates of MX and a Cu-rich precipitate phase, and interdendritic regions that are stabilized with $M_{23}C_6$ carbides.

4:45 PM Invited
Mechanical Design with Low Temperature Carburization: *Sunniva Collins*[1]; P. Williams[1]; [1]Swagelok Technology Services Company

Fluid systems in a variety of industries use tube fittings to readily install leak free connections. Robust tube fitting performance depends on both an adequate differential hardness gripping element to tube, and a guided plastic deformation of the tube gripping components. Low-temperature carburization technology hardens the surface of austenitic stainless steel. For many years, this treatment has been applied to the ferrules of the Swagelok tube fitting, ensuring tube grip, gas-tight seal, and vibration resistance in hundreds of millions of fluid system connections around the world. The process involves activation of the surface followed by a gas phase treatment, performed at temperatures low enough to avoid the formation of carbides, for a sufficient time to allow carbon diffusion to occur. The result is a hardened conformal case on the treated parts, without distortion or change to dimension. The treated case remains austenite (with verified carbon concentrations over 12 atomic percent at the surface) and retains its ductility. This presentation will discuss the design features and performance characteristics of tube fittings enabled by low temperature carburization. Examples of other mechanical designs in wear, fatigue, and corrosive applications will also be given.

5:10 PM
Alloying Effects on Precipitation and Microstructural Evolution in Self-Shielded Ferritic Weld Metal: *Badri Narayanan*[1]; Peter Sarosi[2]; Marie Quintana[1]; Michael Mills[2]; [1]Lincoln Electric Company; [2]Ohio State University

The effect of alloying additions on the morphology and composition of nitride/oxide precipitates and subsequent effect on the austenite to ferrite phase transformation has been studied in a high strength ferritic weld metal deposited with a self-shielded arc welding process. Aluminum, titanium and zirconium

are intentional additions to protect the weld metal during solidification. The complex precipitates and coarse ferritic microstructures resulting from the unique alloying additions, prevents achieving acceptable strength and toughness of the weld. The precipitates are characterized in the TEM using energy dispersive spectroscopy and electron energy loss spectroscopy techniques to differentiate the effect of titanium and zirconium on the morphology of the complex precipitates. Orientation microscopy utilizing electron backscattered diffraction has been used to characterize the effect of alloying on the austenite-ferrite phase transformation. This work focuses on understanding the link between the microstructural features to strength and toughness of the weld metal.

5:35 PM Invited
Phase Transformation in Meteorites: The Effect of Cooling under 'Equilibrium' Conditions: *John Jonas*[1]; Youliang He[2]; [1]McGill University; [2]Cornell University

The microstructures of the Gibeon and other meteorites were examined by means of optical microscopy and EBSD techniques. The orientations of the bcc lamellae formed from a single prior-austenite grain were determined and found to lie between the Kurdjumov-Sachs (K-S) and Nishiyama-Wassermann (N-W) correspondence relations. These can all be characterized as 'co-planar' variants. Measurements carried out in the plessite regions indicated that the variants were continuously distributed around the Bain circles and included both the co-planar and 'co-directional' variants. Thus the crystallographic data support the view that somewhat different mechanisms are involved in the formation of the Widmanstatten and plessitic structures in meteorites. The above observations obtained from materials cooled at such low ('equilibrium') rates are compared with those pertaining to steels cooled in industrial rolling mills to indicate that the very much higher industrial rates do not influence the orientations of the transformation products in a significant way.

Sloan Industry Centers Forum: Techno-Management Issues Related to Materials-Centric Industries: Session I

Sponsored by: The Minerals, Metals and Materials Society
Program Organizers: Subodh Das, Secat Inc; Diran Apelian, Worcester Polytechnic Institute

Monday PM Room: 397
March 10, 2008 Location: Ernest Morial Convention Center

Session Chair: Diran Apelian, Worcester Polytechnic Institute

2:00 PM Introductory Comments by Diran Apelian and Subodh Das

2:10 PM Invited
Overview of Sloan Industry Studies: *Gail Pesyna*[1]; [1]Alfred P. Sloan Foundation

Sloan's Industry Studies program was founded in 1990 on the belief that industries are sufficiently different from one another that they individually deserve rigorous and deep academic study grounded in direct observation. Industry studies research requires close cooperation between academics and industry, and supports the integration of observation-based research with appropriate theory and analysis. There are 26 Industry Centers at U.S. universities, consisting of groups of faculty and students who study a specific industry, plus nearly 1,000 affiliated researchers working in many other university and scholarly settings around the world. Opportunities for participation in this unique program will be described.

2:30 PM Invited
Robustness of Materials Selection Decisions Using Various Life-Cycle Assessment Methods: *A. Allen*[1]; Subodh Das[2]; F. Field[1]; Jeremy Gregory[3]; Randolph Kirchain[4]; [1]Massachusetts Institute of Technology, Materials Systems Laboratory; [2]Secat Inc.; [3]Massachusetts Institute of Technology, Materials Systems Laboratory, Laboratory for Energy and the Environment; [4]Massachusetts Institute of Technology, Materials Systems Laboratory, Department of Material Science and Engineering, Engineering Systems Division

The use of alternative materials to reduce vehicle mass is a tactic often promoted as improving the fuel efficiency and environmental performance of vehicles. However, a growing array of materials candidates confronts today's designer. While life-cycle assessment methods are available to provide quantitative input into this selection decision, their implementations are evolving and distinct. This paper explores the robustness of materials selection decisions when using different LCA methods. Specifically, this paper surveys the major analytical variations of LCA implementations and explores the implications of several of these variants when applied to an automotive materials selection case study. This case study examines analytical variations in: valuation method, secondary weight savings, and treatment of recycling. Preliminary results indicate that, although the choice of analytical method can have real impacts on individual metrics, there are sets of analytical variation over which strategic results are not strongly affected.

2:50 PM Invited
Material Change in Automotive: Enablers and Obstacles: *Glenn Mercer*[1]; [1]International Motor Vehicle Program

The amount of steel, aluminum, and polymer in a modern car is only exceeded by the weight of the engineering studies published by advocates of one or the other material as to their relative merits. Despite all the solid scientific work, material choices in cars remain mystifyingly capricious to the outside observer. This talk will cover some of the real-world enablers of and obstacles to changes in automotive materials, with a focus on the nuances that tilt the balance, as in: "not just price... but price volatility over time", "not just weight... but weight class", and "not just performance... but performance in context". This paper will draw upon two decades of field experience in OEMs and suppliers sectors of the automotive material selection business. Further more, recommendations will be made on how material suppliers can advance their own practical solutions more efficiently and effectively.

3:10 PM Break

3:20 PM Invited
Identification, Development and Commercialization of Recycling – Friendly Aluminum Alloys: *Subodh Das*[1]; John Kaufman[1]; John Green[2]; Frank Field[3]; Randolph Kirchain[3]; [1]Secat Inc; [2]JASG Consulting; [3]Massachusetts Institute of Technology

Today's commercial aluminum alloys have largely been designed for production from primary aluminum with pure alloying elements added. However, the changing aluminum supply situation, in which the US has become primarily a fabricator of aluminum products comprising imported primary aluminum and domestically recycled secondary aluminum, means that new, recycle-friendly aluminum alloys must be identified, developed and commercialized to sustain the industry's economic and environmental strengths. In addition to suggesting several recycling friendly compositions, this paper examines the issues associated with rapid commercialization of aluminum alloys, and suggests several strategies and paths forward that may expedite early adoption. Furthermore, this paper also discusses several mathematical modeling techniques and methodologies, such as chance constraint modeling, that can be used to refine the composition of starting and finished products to maximize benefits over the entire supply chain.

3:40 PM Invited
An Overview of Global Aluminum Industry: Challenges and Opportunities: *Ed Hoag*[1]; [1]Aleris International

World aluminum industry has experienced steady growth and significant structural changes in the past years aligning with booming global economy. Fueled by globalization and consolidation in the world materials industry, the aluminum industry is going through a period of hyper changes in mergers and acquisition. Great efforts have been made to develop novel process and product to maintain and enhance the sustainability of the aluminum industry. The understanding, development and implementation of recycling friendly-industry is a key component to sustain the aluminum industry. This paper will overview the trends of aluminum industry and examines the complex forces in leading to these changes. Additionally, this paper will also discuss lessons learned including an attempt to suggest some paths forward.

4:00 PM Invited
Wood Products - What Does the Consumer Want?: *Al Landers*[1]; [1]Huber Engineered Woods LLC

Driven primarily by the domestic residential housing market, the annual value of wood products manufactured in the US is nearly $165 billion. The wood products industry has evolved into a highly fragmented supply chain that has been designed and continues to operate using the mass production model that is most efficient at moving high volumes of only a limited few commodities or standard products. However, on the consumer side of the wood supply chain, this business model is no longer sufficient to address the emerging needs of customers. In addition to new product designs, new capabilities are also needed to install, maintain, interface, integrate, service, and recycle these wood products in ever more diverse ways. This presentation describes the emerging needs of the consumer and opportunities for restructuring the wood products supply chain that can better match and balance material needs and production capability with demand.

4:20 PM Invited
Demand Driven Materials Management: From the "Woods" to the Consumer: *Earl Kline*[1]; [1]Virginia Tech

The wood products supply chain, with many independently operating segments, has become very "detached" from the final customer. To compensate for this detachment the supply chain relies on traditional strategies such as demand forecasting and holding excessive inventories "just-in-case". Today, these strategies are creating costly "feast or famine" variations in wood materials and their associated products. Dealing with such supply variations has led to monumental infrastructures, policies, and regulations that are negatively impacting supply chain effectiveness and competitiveness. This presentation presents a "forest to consumer" benchmarking study that maps the flow of wood materials with respect to final consumer demand. Key metrics benchmarked are those related to inventory levels, product quality, demand amplification, transportation, lead times, and information availability/quality. Systems modeling analyses results are presented to identify and prioritize potential areas for improved material and product flow through the supply chain.

Structural Aluminides for Elevated Temperature Applications: Mechanical Behavior

Sponsored by: The Minerals, Metals and Materials Society, TMS Structural Materials Division, TMS: High Temperature Alloys Committee, TMS/ASM: Mechanical Behavior of Materials Committee
Program Organizers: Young-Won Kim, UES Inc; David Morris, Centro Nacional de Investigaciones Metalurgicas, CSIC; Rui Yang, Chinese Academy of Sciences; Christoph Leyens, Technical University of Brandenburg at Cottbus

Monday PM Room: 394
March 10, 2008 Location: Ernest Morial Convention Center

Session Chairs: Thomas Bieler, Michigan State University; Antonin Dlouhy, Academy of Sciences

2:00 PM Invited
Durability Assessment of TiAl Alloys: *Susan Draper*[1]; Bradley Lerch[1]; Young-Won Kim[2]; [1]NASA; [2]UES Inc

This paper will present a summary of durability issues for TiAl alloys, particularly impact and environmental resistance. Various gamma alloys, including a TNB alloy (Ti-45Al-5Nb-B-C) and a new beta-gamma TiAl alloy (Ti-44Al-4Nb-2Cr-2V-B-C), along with some more traditional TiAl alloys were ballistically impacted. Variables such as impact energy, projectile hardness and impact location were related to the resulting damage. The goal was to produce damage that was similar to the domestic object damage found in low pressure turbine blades. Damaged samples were subsequently tested under high cycle fatigue loading using the step-test method. The fatigue strength of each alloy was characterized as a function of initial crack size and modeled using a threshold-based fracture mechanics approach. Differences among the various alloys will be discussed, particularly with respect to their microstructure, manufacturing process, and tensile properties. The effect of environmental exposure on impact resistance and resulting fatigue strength will be discussed.

2:30 PM
Influence of Impact on the Mechanical Behaviour of a Cast and a Forged Gamma Based TiAl Alloy: *Susanne Gebhard*[1]; Piet Peters[1]; Dan Roth-Fagaraseanu[2]; Heinz Voggenreiter[1]; [1]German Aerospace Center; [2]Rolls-Royce Deutschland

One of the main problems representing a barrier for TiAl gas turbine applications is its low resistance against impact. For this reason, the influence of high-speed impact on the mechanical behaviour of a cast TiAl alloy and a more ductile, forged alloy has been investigated. Impact tests are performed and the caused damage has been evaluated as a function of the impact speed, the particle weight (the impact energy) in relation to the specimen thickness and location of the impact. Impact near the specimen edge produces a severer damage than an impact in the centre. This is shown with the aid of residual strength and fatigue experiments. The residual strength could be described on the basis of a linear elastic fracture mechanics analysis and a fracture toughness of 15 to 17MPa(m)$^{1/2}$. Fatigue experiments were performed to determine the threshold for crack growth as a function of the impact damage size.

2:50 PM
Effect of Heat Treatment on Microstructures and Properties of Y-Bearing TiAl Alloy: *Yuyong Chen*[1]; Baohui Li[2]; Fei Yang[1]; Fantao Kong[1]; Shulong Xiao[1]; Zhiguang Liu[1]; [1]Harbin Institute of Technology; [2]Harbin Institute of Technology, Institute of SAST

In this article, the microstructure controls and properties for various microstructures of Ti-45Al-5Nb-0.3Y have been studied using relatively large forged pancake. The canned forging pancake was successfully gained. The effect of processing and heat treatment on microstructure and properties was studied using X-ray diffraction, optical microscopy, scanning electron microscopy (SEM) and transmission electron microscopy (TEM). Results showed that the microstructure of forged pancake consisted of major curved lamellar, broken lamellar and minor dynamic recrystallized grains (DRX) with the size of about 1-2μm and the YAl2 phase at grain boundaries. Three different microstructures, duplex, nearly lamellar and fully lamellar, have been obtained through heat treatment, respectively. And the microstructure evolution was also analyzed. The alloy with duplex microstructure owed the best ductility, the elongation reached 1.9%, and which with fully lamellar microstructure took on better strength, yield strength and fracture strength were 557.1MPa and 715MPa, at room temperature, respectively.

3:10 PM
Effect of Surface Condition and Thermal Exposure on the Fracture Mechanisms on a Gamma-TiAl Alloy: *Maria Perez-Bravo*[1]; Iñaki Madariaga[1]; Koldo Ostolaza[1]; [1]Industria de Turbo Propulsores

The use of gamma-TiAl alloys in the aeronautical market has been a long during wish. Developments carried out up to now are close to allow their exploitation. Although several processing routes have been considered for manufacturing turbine components, casting would be the preferred one. Current casting technology might require going through various machining stages up to the final shape. Hence, it is relevant to consider the effect of the resulting surface condition of a cast gamma-TiAl alloy after different machining routes as ECM and grinding. The nature of this condition will be assessed through metallurgical and fractographic analysis on specimens tested under various LCF and HCF test conditions. This research will focus on identifying the acting fracture mechanisms and their contribution to the macroscopic mechanical behaviour. Specimens will be investigated in the as-machined and in the as-exposed condition, aiming at capturing temperatures and exposure times representative of engine working conditions.

3:30 PM
Predicting Microcrack Nucleation Due to Slip-Twin Interactions at Grain Boundaries in Duplex Near Gamma-TiAl: *Thomas Bieler*[1]; Philip Eisenlohr[2]; Deepak Kumar[1]; Martin Crimp[1]; Franz Roters[2]; Dierk Raabe[2]; [1]Michigan State University; [2]Max-Planck-Institut für Eisenforschung

A fracture initiation parameter (fip) based upon the geometry of the Burgers vector interactions as they are related to slip transfer across the grain boundary is described. The fip is expressed as a probability statement consisting of factors,

which when multiplied together, allow weak boundaries to be identified in the context of a state of stress. In addition to Burgers vectors, the misorientation between slip planes in the grain boundary and differences in elastic properties in adjoining grains are considered. Boundaries are characterized to identify tilt and twist character and whether they are low SIGMA value boundaries. There is no definite preference for crack initiation based on SIGMA values or tilt and twist character of the boundary, implying that these are not critical parameters affecting crack nucleation at the grain boundary in duplex near-γ TiAl. Incorporation of this parameter in finite-element crystal plasticity simulations for predicting optimal microstructures is discussed.

3:50 PM Break

4:00 PM

Heat Treatment Response of Forged Powdered Metal 03k near Gamma Titanium Aluminide Disks of Nominal Composition Ti-45.5Al-1.0Cr-3.0Nb-0.2W-0.2B-0.2Si-0.4C (at%): *Ray Simpkins*[1]; [1]Williams International

The attractive density corrected strength of gamma titanium aluminides for use in aerospace applications has led to extensive alloy and process development over the few past decades. This research has led to the development of a powdered metal (PM) processing technique that yields repeatable chemistries and avenues to forgable pre-forms. A PM TiAl alloy with a nominal composition of Ti-45.5Al-1.0Cr-3.0Nb-0.2W-0.2B-0.2Si-0.4C (at%) was evaluated as a compressor rotor material. The PM preforms were varied in size to scale up the fabrication process to replicate component size forgings. Mechanical testing was performed to measure the response to heat treatment of the PM forgings. These results were compared to a cast/HIP + forged version of a similar chemistry. Forging defects were detected during post PM forging ultrasonic inspection. Microscopic analysis of the defects was also performed. The resultant mechanical properties and microstructural relationships will be presented along with forging defect analysis.

4:20 PM

Effect of Al Content on Microstructure/Phase Distribution and Strength/Ductility in a PM Gamma Alloy: Young-Won Kim[1]; *Stephan Russ*[2]; Christopher Woodward[2]; Charles Yolton[3]; [1]UES Inc; [2]US Air Force; [3]Crucible Materials Corporation

The dependency of strength and ductility of TiAl alloys to microstructure and variations in chemistry are quite complicated, and possible interaction effects exist. For example, Al is known to affect strength and the volume fraction of gamma and alpha-2 phases have been credited with the effect. However, the impact of chemistry versus phase has not been satisfactorily quantified. In an effort to understand such effects, four billets of gamma alloy 03K, nominal composition of Ti-45.5Al-3Nb-1Cr-0.2W-0.2B-0.4C-0.2Si (at%), were produced from gas atomized powder. The realized Al content varied between 44.8 and 47.4 at%. The forgings were heat treated to develop three microstructure variants: fully lamellar, nearly lamellar and duplex. The microstructure and Rockwell hardness were analyzed on all samples, and room temperature tensile testing was conducted on the fully lamellar materials. The resulting strength and ductility as a function of Al content and microstructure will be discussed.

4:40 PM

Determination of the Creep Rate in Gamma Titanium Aluminide by Stress Relaxation Tests: *Jonathan Paul*[1]; Roland Hoppe[1]; Michael Oehring[1]; Fritz Appel[1]; [1]GKSS Research Centre

In high temperature applications the creep behaviour of TiAl components can be an important issue. In this respect alloy composition and processing are important factors which need to be optimised so that a proper balance of mechanical properties can be obtained. To obtain a large creep property database requires many tests to be performed at different stress levels and temperatures which of coarse is both time consuming and expensive. To overcome this requirement during alloy and processing development, a method of obtaining the minimum creep rate at a single temperature but at a series of stress levels from a single short term tensile test including repeated stress relaxations has been developed. The experimentally measured minimum creep rates are in quite good agreement with those predicted from the stress relaxation tests.

5:00 PM

Axial-Torsional Thermo-Mechanical Fatigue Behavior of Ti-45Al-5Nb-0.2B-0.2C: Stephen Brookes[1]; Hans- Kühn[1]; *Birgit Skrotzki*[1]; Hellmuth Klingelhöffer[1]; Rainer Sievert[1]; Janine Pfetzing[2]; Gunther Eggeler[2]; [1]BAM; [2]Ruhr-University Bochum

Structural components in aeronautical gas turbine engines typically experience large variations in temperatures and multiaxial states of stress under non-isothermal conditions. Therefore, the uniaxial, torsional and axial-torsional thermo-mechanical fatigue (TMF) behavior was studied. TMF tests were performed at 400-800°C and with mechanical strain amplitudes from 0.15%-0.7%. The tests were conducted axially thermo-mechanically in-phase (IP) and out-of-phase (OP). For the same lifetimes, IP tests required the highest strain amplitudes, while OP test conditions were most damaging and needed the lowest strain amplitudes. The Mises equivalent mechanical strain amplitudes of pure torsional tests are found in between uniaxial IP and OP tests for the same lifetimes. As a result, for the same equivalent mechanical strain amplitude uniaxial IP tests showed also significantly longer lifetimes than pure torsional TMF tests. The non-proportional multiaxial OP test showed the lowest lifetime at the same equivalent mechanical strain amplitude compared to the other types of tests.

5:20 PM

Tensile Impact Behavior of Duplex Ti-46.5Al-2Nb-2Cr at Elevated Temperatures: Xiang Zan[1]; *Yang Wang*[1]; Yuehui He[1]; Yuanming Xia[1]; [1]University of Science and Technology of China

The tensile behavior of Duplex Ti-46.5Al-2Nb-2Cr intermetallics (DP TiAl) is studied at strain rates ranging from 0.001 to 1350 s-1 and temperatures from room temperature to 840°C, in which tensile impact tests are conducted on a self-designed rotating disk indirect bar-bar tensile impact apparatus at University of Science and Technology of China(BTIA at USTC). Results show obvious effects of temperature and strain rate. The strength under dynamic loading is higher that that under quasi-static loading. The Brittle-to-Ductile Transition Temperature (BDTT) rises with elevated strain rates. The fractographic analysis show that below BDTT the fracture mode changes from planar cleavage fracture to intergranular fracture with increased test temperatures and voids are found on the colony boundaries at elevated temperature.

Ultrafine-Grained Materials: Fifth International Symposium: Processing and Materials

Sponsored by: The Minerals, Metals and Materials Society, TMS Structural Materials Division, TMS Materials Processing and Manufacturing Division, TMS: Shaping and Forming Committee, TMS: Nanomechanical Materials Behavior Committee
Program Organizers: Yuri Estrin, Monash University and CSIRO Melbourne; Terence Langdon, University of Southern California; Terry Lowe, Los Alamos National Laboratory; Xiaozhou Liao, University of Sydney; Zhiwei Shan, Hysitron Inc; Ruslan Valiev, UFA State Aviation Technical University; Yuntian Zhu, North Carolina State University

Monday PM — Room: 273
March 10, 2008 — Location: Ernest Morial Convention Center

Session Chairs: Ruslan Valiev, UFA State Aviation Technical University; David Alexander, Los Alamos National Laboratory; Cheng Xu, University of Southern California; Laszlo Kecskes, US Army Research Laboratory

2:00 PM Invited

Experimental Attempts to Manage Both High Strength and Adequate Ductility in Ultrafine Grained Metals: *Nobuhiro Tsuji*[1]; [1]Osaka University

It has been recognized that the ultrafine grained metals usually perform very high strength but limited ductility. However, there are several ways to overcome this trade-off relationship through microstructure control: for example, bimodal nanostructures, ultrafine grained dual phase, ultrafine grains including fine dispersoids, transformation induced plasticity, etc., are expected to result in managing strength and ductility. In this presentation, results of several experimental attempts to manage both high strength and adequate ductility in ultrafine grained metals, which have been carried out in the author's group

by using severe plastic deformation processes and other thermomechanical processing techniques, will be introduced.

2:20 PM
Role of Strain Reversal in Grain Refinement by Severe Plastic Deformation: *Dmitry Orlov*[1]; Yoshikazu Todaka[2]; Minoru Umemoto[2]; Nobuhiro Tsuji[1]; [1]Osaka University; [2]Toyohashi University of Technology

Most of severe plastic deformation processes involve strain reversal. Till now quite big number of researches has been done on indirect study of its role, which discusses the effect of loading path in ultra-fine grained structure formation. The present work was aimed to study directly the role of the strain reversal in grain refinement by severe plastic deformation. A 99.99% purity aluminum was processed by High Pressure Torsion up to 96° rotation (average equivalent strain e ≈ 4) with two deformation modes: monotonic and reversal deformation with a step of 12° rotation (average equivalent strain e ≈ 0.5). It was shown that strain reversal retards the grain refinement in comparison with (quasi)monotonic deformation. This explains less effectiveness of SPD schemes that involve full strain reversal after each consequent processing step.

2:35 PM Invited
Application of ECAP in Tailoring the Mechanical Property of Magnesium Alloys: *Jingtao Wang*[1]; Jinqiang Liu[1]; Jun Tao[1]; Ping Huang[1]; Deliang Yin[1]; [1]Nanjing University of Science and Technology

An approach of combination of processing by grain refinement via equal channel angular pressing, conventional extrusion and/or age hardening was applied to a new Mg-12Gd-3Y-0.5Zr aging hardening alloy and an AZ31 alloy respectively. Four passes of ECAP of the alloy at elevated temperature effectively refined their grains effectively, and improved ductility significantly in both alloy. Additional conventional extrusion with an extrusion ratio of 9 after 4 passes of ECAP improved obviously their strength, especially yield strength, without obvious lose of ductility. Subsequent ageing of the aging hardening alloy Mg-12Gd-3Y-0.5Zr significantly increased its yield and tensile strength further, nevertheless, its ductility was substantially decreased. These results indicate the effectiveness of the influences of these processing, individually or in combination on the mechanical properties of the experimental magnesium alloy. And good combination of strength and ductility could be obtained by optimizing the processing parameter of this approach.

2:55 PM
Effect of Shear Strain in an Al-6061 Alloy Processed by HPT: *Cheng Xu*[1]; Terence Langdon[1]; [1]University of Southern California

It has been established that High Pressure Torsion (HPT) is capable of producing exceptional grain refinement, often even to the nanometer level for some materials. This is attributed to the large shear strain which is introduced during the torsional straining. This paper examines the effect of shear strain using an Al-6061 alloy subjected to HPT for 1 and 5 turns under a pressure of 4 GPa and with the alloy pressed under the same pressure for the same time spans as 1 and 5 turns. The Vickers microhardness was recorded on the surface of the as-processed disks and plotted in contour form to give microhardness distributions on the samples.

3:10 PM Invited
Property Optimization of Nanostructured Metals by Post-Process Deformation: *Xiaoxu Huang*[1]; Naoya Kamikawa[1]; Niels Hansen[1]; [1]Riso National Laboratory

Nanostructured metals produced by high strain deformation typically have high strength and low elongation when deformed in tension. In a recent study it has however been found for nanostructured aluminum processed by accumulative roll bonding (ARB) that a slight post-process deformation may have a beneficial effect on the elongation followed by a slight decrease in strength (X. Huang, N. Hansen and N. Tsuji, Science, 312 (2006) 249). This effect has been explored for aluminum and IF steel representing fcc and bcc metals, respectively. These metals have been produced by ARB to an ultrahigh strain and afterwards cold rolled to thickness reductions from 5 to 50%. For both metals it has been found that only a small strain is required to obtain the beneficial effect of post-process deformation. This finding is underpinned by a structural characterization carried out by transmission electron microscopy.

3:30 PM Invited
Mechanical Properties and Microstructure Evolutions of ECAPed Ultrafine Grained Al during Low Temperature Annealing: *Yonghao Zhao*[1]; Andrea Dangelewicz[2]; Peiling Sun[2]; Xiaozhou Liao[3]; Yuntian Zhu[2]; Yizhang Zhou[1]; Enrique J. Lavernia[1]; [1]University of California at Davis; [2]Los Alamos National Laboratory; [3]University of Sydney

Ultrafine grained (UFG) metals processed by severe plastic deformation usually exhibit strain softening in tensile testing. To overcome the strain softening, the easiest way is to introduce recovery or recrystallization/grain growth by annealing. Usually annealing elevates ductility by lowering strength. We will report results obtained with UFG Al by equal-channel angular pressing (ECAP) with routes A, Bc and C. It was found that the strength of the UFG Al by all routes increases first and then decreases with isothermal annealing. With increasing annealing time, the ductility increases first and then is unchanged for UFG Al by route A, and decreases first and then increases for UFG Al by route Bc, while remaining unchanged for UFG Al by route C. The different mechanical responses versus isothermal annealing of the UFG Al by different ECAP routes will be explained by their different microstructural evolutions during annealing.

3:50 PM Break

4:05 PM Invited
Dynamic Plastic Deformation: A Novel Approach for Processing Bulk Nanostructured Metals: *K. Lu*[1]; N. R. Tao[1]; [1]Chinese Academy of Sciences, Institute of Metal Research

The minimum grain sizes obtained in metals and alloys subjected to severe quasi-static plastic deformation at ambient temperature are usually in the submicrometer regime. In this talk, we will present a novel approach to further refine grains of bulk metals into the nanometer regime. The process, referred to as Dynamic Plastic Deformation (DPD), is to deform bulk metals dynamically at high strain rates and/or at cryogenic temperatures. During dynamic deformation, the recovery or recrystallization kinetics (of dislocation structures) is suppressed and meanwhile twinning tendency is enhanced. Combination of the two effects leads to a substantial change in grain refinement mechanism. We will demonstrate a twinning-dominated grain refinement mechanism in the nanometer regime. For DPD-Cu, the average grain size is reduced down to about 50 nm and the tensile strength is elevated above 620 MPa. Perspectives on development of DPD processes and their applications in other engineering alloys will be addressed.

4:25 PM
Application of ECAP for Ferritic Stainless Steel Sheets to Control Texture and Alleviate Ridging: *Hiroyuki Miyamoto*[1]; Masaharu Hatano[2]; Takuro Mimaki[1]; [1]Doshisha University; [2]Nippon Steel and Sumikin Stainless Steel Corporation

Equal-channel angular pressing (ECAP) has been applied to ferritic stainless steel sheets with 17wt%Crominum in oder to control texutre and alleviate ridging. The hot rolled and annealed sheets of 4 mm thickness were ECA-pressed only for one pass, followed by cold rolling and final annealing. Microstructures were fragmented by heterogenous plastic deformation such as shear bands during ECAP, and they appear to remain after cold rolling. When the final sheets were strained by 20%, they exhibited alleviated ridging as compared with the counterpart fabricated by conventional process. Local orientational change due to shear bands formation during ECAP may disconnect colonies of grains with similar orientations such as {001}<110> texture, which are otherwise hard to be recrystallized and frequently regarded as the cause of the ridging.

4:40 PM Invited
Ultrafine-Grained Ni and Ti with High Ductility: Yonghao Zhao[1]; *Enrique J. Lavernia*[1]; [1]University of California at Davis

The limited ductility of nanocrystalline/ultrafine-grained materials has emerged as a singular issue in the study and application of this novel class of materials. Numerous investigators have addressed this issue, with varying degrees of success, via a variety of approaches, most of which can be grouped into two general categories: microstructural design and introduction of alternative deformation mechanisms. In this talk, we will report results obtained with ultrafine-grained Ni prepared by cryo-milling and subsequent forging. The consolidated Ni has a yield strength of 480 MPa, and a ductility of 40%. Similarly, an ultrafine-grained (UFG) Ti was prepared by equal-channel angular

(ECAP) and subsequent rolling. Following annealing the UFG-Ti at 350°C for 6 h, the ductility increased from 5% to 10%, the ultimate strength increased from about 1100 MPa to 1400 MPa. The microstructural origins for such combinations of good strength and high ductility are discussed in the present paper.

5:00 PM

Processing of Copper by Flat Plate Equal Channel Angular Extrusion: *David Alexander*[1]; [1]Los Alamos National Laboratory

Flat plate samples of copper have been processed by equal channel angular extrusion (ECAE). Processing was performed at room temperature, for die angles of both 120 and 90°, for up to 4 passes, by route C. The mechanical properties have been measured in both tension and compression, in 3 orthogonal directions. The processed material showed mechanical anisotropy, depending on testing orientation, and also showed a tension/compression asymmetry. The tooling for flat plate ECAE will be described, and the problems associated with scaling up to larger sizes will be considered.

5:15 PM

Consolidation of Cu and Al Nanoparticles via Equal Channel Angular Extrusion (ECAE) and the Effect of Post-ECAE: *Mohammed Haouaoui*[1]; Cathleen Hutchins[1]; Ibrahim Karaman[1]; Hans Maier[2]; Enrique Lavernia[3]; [1]Texas A&M University; [2]University of Paderborn, Lehrstuhl f. Werkstoffkunde; [3]University of California, Davis

Ultrafine grained (UFG) and nanocrystalline (NC) materials are of interest due to their high strength, compared with coarse grained counterparts. In the present work, Equal Channel Angular Extrusion (ECAE) is used to consolidate microcrystalline and nanocrystalline Cu and Al particles into bulk samples with relatively large dimensions (all dimensions in cm range). The effects of ECAE route, extrusion temperature, and post-ECAE processing such as swaging and wire drawing on microstructure and mechanical behavior are investigated. The main objective of the study is to determine the optimum processing parameters to increase the ductility of the consolidates, while maintaining relatively high strength. The preliminary results showed UTS levels as high as 800 MPa with fracture strains up to 10% for consolidated Cu nanoparticles. The ability of ECAE for the consolidation of cryomilled Al-10.5Mg microparticles and pure Al nanoparticles are demonstrated. The effect of post-ECAE processing on the consolidate will be presented.

5:30 PM

Hall-Petch and Recrystallization Behavior of Heavily Worked Tungsten: *Suveen Mathaudhu*[1]; Armand deRosset[1]; Qiuming Wei[2]; Laszlo Kecskes[1]; Ted Hartwig[3]; [1]US Army Research Laboratory; [2]University of North Carolina-Charlotte; [3]Texas A&M University

We investigated the recrystallization behavior and Hall-Petch relationship of large-grained, commercial purity tungsten (W) processed by ECAE to obtain UFG microstructures. Extrusions were performed to strains of ~4.6 with a 90 degree tool, up to 1200C. Subsequent 60 min annealing up to 1600C of the worked W allowed to determine the recrystallization temperature. Light, scanning electron, and transmission electron microscopy, Vickers microhardness, and quasi-static (~10-3 s-1) uniaxial compression testing were used to examine the properties of the W extrudates. The ECAE-processed W showed 100-300 nm grainsize in the fully worked state, ~10 µm equiaxed grains in the recrystallized state, and grains >500 µm after the onset of grain growth. The range of grain size was used to determine the Hall-Petch relationship for W. The recrystallization behavior, along with the interdependence between quasi-static yield strength, microhardness, and grain size and are to be discussed.

5:45 PM

Plane-Strain Machining for Studying Severe Plastic Deformation in Metals and Alloys: Srinivasan Swaminathan[1]; M. Ravi Shankar[1]; W. Dale Compton[1]; Alex King[1]; Srinivasan Chandrasekar[1]; *Kevin Trumble*[1]; [1]Purdue University

Large plastic strains up to ~15 can be imposed by plane-strain machining of metals and alloys. In addition to achieving a wide range of well-defined strains in a single-pass, continuous process, the strain rate and temperature also can be controlled over large ranges. The deformation field in plane-strain machining is compared with other methods of severe plastic deformation (SPD) such as equal channel angular extrusion. The paper focuses on the application of machining to study microstructure refinement by SPD in a wide range of metals and alloys, including copper and its solid solution alloys, CP titanium, precipitation-hardenable aluminum alloys, and a nickel-based superalloy. The capabilities and limitations of developing bulk structural materials through machining are also discussed.

A

Aalund, R 283
Abakumov, A 326
Abbott, T 289, 337
Abdel Maksoud, I 134
Abdelmalek, F 219
Abe, H 342
Abedrabbo, S 63
Abeykoon, A 197
Abidzina, V 143
Abinandanan, T 43, 276
Abot, J 59
Abromeit, C 71, 94
Abu Leil, T 336
Accorsi, I 122
Achurra, G 330
Adams, J 88
Adams, K 338
Addemir, O 123, 233
Adedokun, S 65
Adelakin, T 321
Adharapurapu, R 182
Afanasjev, V 168
Aga, R 275, 319
Agaliotis, E 362
Agarwal, A 60
Agarwal, R 74
Ager, J 66, 308, 324
Agnew, S 95, 118, 189, 241, 278, 286, 297
Aguiar, M 213
Aguilar, J 125
Ahart, M 92
Ahluwalia, R 224
Ahmed, H 65, 134
Ahn, B 51, 52, 122
Ahn, K 105
Ahn, S 48
Ahuja, R 293
Ahuwan, A 346
Aichun, D 78, 302
Aidhy, D 252
Ajayan, P 59
Akbari Mousavi, S 53, 54
Akin, I 358
Akinc, M 364
Akray, S 332
Akuzawa, N 227
Al-Fadhalah, K 82
Al-Jallaf, M 325
Al-Jassim, M 105
Al-Khalifa, J 351
Al-Maharbi, M 52, 334
Al-Sharab, J 41
AlAli, H 112, 164, 220, 271, 319, 361
Alam, M 338, 339
Albe, K 99
Albert, C 287
Alekseeva, N 326
Alexander, D 149, 151, 170, 230, 260
Alexandrov, I 51, 306
Alfarsi, Y 266
Alge, D 216
Ali, M 315
Alisch, G 57
Alkorta, J 225
Allain, S 118
Allen, A 64, 147
Allen, T 198, 199, 252, 299
Allison, J 49, 80, 85, 86, 126, 367
Alloyeau, D 308
Allred, L 194
Alman, D 189
Al Marzouqi, A 226
Almer, J 142, 143, 328
Alterach, M 181
Alurralde, M 299, 300
Alves, E 252
Al Zarouni, A 357
Amaral, A 107, 356
Amberger, D 307
Amin, S 260
Amini, S 40
Amirouche, L 324
Amjad, J 134
An, H 80
An-Ping, L 327
Anand, K 234
Andermann, L 211
Anderoglu, O 174
Andersen, P 229
Anderson, I 90, 108, 140, 145, 200, 254, 318, 327, 351
Anderson, K 340
Anderson, M 319, 320
Anderson, P 39, 131
Andersson, J 87
Ando, D 241
Ando, T 177
Andrievskaya, N 57
Angulo, R 192
Aning, A 361
Ankem, S 73, 246
Anopuo, O 186
Antipov, E 326
Antônio Reis, M 119
Antony, J 325
Antrekowitsch, H 113, 125, 165, 202, 220, 302
Anumalasetty, V 100
Anyalebechi, P 86, 87, 136, 192, 245
Aoki, K 45, 47, 48, 135
Aourag, H 293
Aoyagi, T 245
Apel, M 146
Apelian, D 147, 202, 351
Apisarov, A 314
Appel, F 74, 149, 304, 347, 348, 349, 350
Appel, J 64
Aquino, R 221
Arabaci, A 79
Arai, K 254
Arai, M 193
Arapan, S 293
Arce-Estrada, E 260, 322
Ares, A 87, 181, 272, 362
Arfaei, B 277
Argon, A 139, 182
Arjunan, S 51
Armstrong, P 135
Arockiasamy, A 107
Arora, V 213
Arruda, A 119
Arseneault, A 361
Arsenlis, T 72
Arzt, E 66, 110, 160, 215, 267, 316, 358
Asa, Y 193
Asadi, M 87
Asami, C 344
Asgari, S 118
Ashcroft, N 196
Ashida, D 306
Asif, S 76
Askin, J 39
Asokamani, R 51
Asokan, K 271
Aspen, E 164
Asta, M 72, 78, 139, 191, 224, 276, 364
Aswath, P 215, 358
Atamanenko, T 272
Athman, M 363
Athreya, B 169
Atmeh, M 40
Atsumi, T 300
Atzmon, M 67
Aubain, M 278
Aude, M 260
Aujla, D 260
Auld, J 187
Avasthi, D 343
Averback, R 71
Avraham, S 187
Awakura, Y 272, 321
Aydin, S 79, 302
Aydiner, C 143, 306, 329
Azevedo, M 321
Azhazha, V 57

B

Baars, D 303
Bache, M 235
Bacon, D 73, 169
Bade, K 309
Badillo, A 71
Badowski, M 320
Bae, C 152
Bae, D 39, 47, 309
Bae, G 292
Bae, I 299
Bae, J 292, 365
Bagheri, S 277
Bagheri, Z 277
Bagley, S 268
Bahadur, H 71
Bahr, D 174, 195, 316
Bai, C 219, 256
Bai, H 86
Bai, J 268
Bajenaru, O 180
Baker, I 204, 351
Baker, K 216
Baker, S 278
Bakke, P 337
Balaban, N 295
Balachandran, S 370
Balani, K 60
Balasubramanian, J 39
Ballard, D 70
Ballato, J 105
Ballentine, F 264
Ballou, T 106

Balogh, A. 342
Balogh, L. 307, 341
Bamberger, M. 187, 188, 290
Ban, Y. 191, 314, 326
Bandaru, P. 59, 60
Banerjee, R. 166, 181, 193, 194, 275, 340
Bang, W. 48
Banhart, J. 178
Banik, K. 293
Banister, G. 271
Bankson, J. 267
Banovic, S. 211
Bao, Y. 239, 336
Baoyan, Z. 178
Barabash, O. 221
Barabash, R. 92, 93, 141, 197, 221, 250, 297, 341
Barbee, T. 218, 236
Barber, R. 370
Barbi, N. 349
Barbosa, E. 210
Barboza, M. 358
Barker, E. 170
Barnard, B. 359
Barnes, S. 248
Barnett, M. 100
Barney, M. 328
Baron, J. 172
Barrallier, L. 298
Barron, M. 137, 166, 273
Barsoum, M. 40
Bartels, A. 256, 304, 305, 347, 348, 349
Barthélémy, A. 115
Bartolo, L. 339
Bartsch, M. 340
Barzola-Quiquia, J. 299
Basletic, M. 115
Basquin, J. 357
Bass, M. 105
Bassler, K. 197
Basson, F. 320
Basu, J. 76
Batane, N. 236
Bates, B. 122
Batey, J. 190
Batista, E. 213
Batista, J. 263
Battaile, C. 104, 155, 247, 248, 278
Battiste, R. 233
Bauer, G. 142
Bauer, R. 125
Bauer, V. 129
Baxi, J. 181
Baydogan, M. 295, 332
Bayha, T. 294
Bayles, B. 234
Bayles, R. 294
Bazan, G. 91
Beall, G. 114
Beals, R. 85, 86, 132, 133, 186, 188, 238, 240, 288, 289, 335, 336
Beardsley, M. 123
Bearne, G. 108, 159, 213, 266, 313, 315, 357
Beaudoin, A. 287
Beck, T. 50, 286
Becker, A. 95
Becker, C. 276
Becker, R. 72
Beckmann, F. 335
Beercheck, D. 346
Behrens, B. 282
Bei, H. 360
Belak, J. 169, 175
Belasco, J. 328
Bele, E. 107, 234
Belin-Ferré, E. 184, 309
Bellon, P. 49, 71
Belous, A. 322
Belova, I. 44
Belt, C. 279, 280, 329
Bender, M. 310
Bengus, V. 57
Benhaddad, S. 243
Benkahla, B. 357
Bennet, J. 360
Benoit, G. 204
Benson, D. 334
Benson, M. 197
Bentancur, M. 229
Bentley, J. 90
Benzerga, A. 45, 179, 184, 282, 340, 355
Berghmans, A. 104
Bergmann, S. 282
Berkley, M. 164
Bernabai, U. 231
Bernier, J. 329
Berramdane, N. 204
Berry, C. 105
Berry, J. 140, 298
Berteaux, O. 129
Berzansky, J. 164
Bessa, E. 213
Bessada, C. 227
Besser, M. 90
Bestor, M. 128, 175
Bettles, C. 294
Bewlay, B. 325
Beyerlein, I. 100, 117, 229, 257, 279
Bhadeshia, H. 297
Bhadrachalam, P. 153
Bharadwaj, M. 289, 336
Bharathula, A. 163
Bhattacharjee, A. 247
Bhattacharya, P. 176
Bhattacharya, R. 134
Bhattacharyya, D. 102, 171, 230
Bian, X. 269
Bibee, M. 328
Bibes, M. 115
Bicalho, L. 358
Bichler, L. 289
Bie, H. 145
Bieler, T. 90, 148, 170, 228, 229, 277, 303, 347
Biermann, D. 282
Biermann, H. 236
Bilani, O. 168
Binbrek, A. 171, 266
Bindl, D. 212
Biner, S. 95
Bing, L. 313
Bingert, J. 141, 209, 249
Birat, J. 219
Biswas, A. 284
Biswas, P. 154, 158
Bjelkengren, C. 65
Bjørneklett, B. 158
Blacket, S. 336
Blaine, J. 288
Blanpain, B. 117, 301
Blau, P. 89, 233
Blicharski, M. 80
Blobaum, K. 249
Blochwitz, C. 183
Blue, C. 295
Blum, W. 285
Boakye, E. 118
Bobadilla, J. 330
Bobrovnitchii, G. 222, 321
Bock, U. 79
Bodde, S. 67
Bodepalli, S. 42
Boehlert, C. 90, 194, 195, 246, 288
Boettger, B. 325
Boettinger, W. 72, 169, 276
Bogdanov, Y. 315
Bohn, T. 206
Bohner, H. 213
Bojarevics, V. 315
Bolcavage, A. 78
Bonarski, B. 52, 353
Bonfrisco, L. 176
Bonnett, J. 338
Booty, M. 296
Borbely, A. 84
Border, K. 64
Borges, A. 311
Borgesen, P. 277
Boris, A. 115
Borisenko, K. 184
Bormann, R. 133, 186, 241, 256
Bosch, M. 320
Bosse, M. 336
Botelho, J. 171
Bott, R. 156, 157, 263
Böttcher, H. 165, 220
Bouaziz, O. 118
Bourgeois, L. 146
Bourke, M. 75, 121, 173, 229, 278, 328
Bourne, G. 69
Bourne, N. 249
Bouville, M. 224
Bouwhuis, B. 107
Bouzehouane, K. 115
Bower, A. 46, 157, 228
Bowers, R. 157, 171, 172
Boyce, B. 75, 121, 122, 173, 229, 278, 328
Boyce, D. 153
Boyle, K. 85
Boysen, K. 244
Braccini, M. 363
Bradley, J. 157, 293
Brady, M. 86, 135, 189, 190, 243, 292, 338, 368
Bramhoff, D. 165
Brandimarte, G. 140
Brandt, M. 336
Brant, D. 161
Braun, P. 260
Braun, R. 349, 370, 371
Brederholm, A. 87
Brenner, R. 279
Brewer, L. 278
Brewster, A. 165

Bridi, R 220
Brigmon, R 105
Bringa, E 169, 334
Bringas, Jr., P 160
Brinkmeyer, B 277
Brittes, G 210
Brockdorf, K 310
Brockenbrough, J 49
Brockman, R 78
Broderick, S 293
Brodie, G 356
Bronfenbrenner, D 328
Bronfin, B 337
Brookes, S 149
Brooks, J 193, 256
Brooks, R 247
Brown, A 128, 175
Brown, D 93, 118, 142, 143, 166, 170, 197, 198, 230, 251, 279, 297, 306, 329, 342
Brown, E 91, 140, 198, 249, 335
Brown, L 183, 338
Brown, S 145
Browning, N 355
Bruder, E 206
Brueck, S 298
Bruggeman, J 313
Brunner, R 317
Bsesnbruch, G 338
Buchanan, D 78
Buchholz, A 362
Buchholz, D 185
Buchovecky, E 228
Budai, J 93
Budak, S 41, 208, 327
Buenavista, S 125
Buergi, H 342
Bugge, M 159
Bulanova, M 181
Bulatov, V 72
Bunin, I 114
Bunzel, P 364
Burjak, V 325
Burkatsky, O 160
Burkins, M 133
Burleigh, T 233
Busby, J 199, 284
Busch, R 318
Buslaps, T 256, 304
Bustamante, O 323
Buttard, P 366
Butz, T 299
Buzunov, V 160, 313
Byler, D 92
Bystrov, V 268
Bystrova, N 268

C

Caballero, F 146
Cabrera, J 56
Caceres, C 290
Caceres-Valencia, P 244
Cady, C 121, 170
Cai, J 55
Cai, M 69, 272, 329, 362
Cai, W 49, 282
Cai, Z 292
Calderón, H 47
Calin, M 56
Calonne, O 203
Calvert, P 267
Camara, J 213
Camili, R 213
Campbell, A 177, 232
Campbell, B 342
Campbell, C 97
Campbell, J 107
Campillo, B 45
Cañas, R 356
Candic, M 273
Cannova, F 171, 172
Canutas De Wit, C 315
Cao, B 334
Cao, F 81, 304
Cao, G 239, 288, 289, 368
Cao, H 187
Cao, W 138, 294
Cao, X 78, 177, 314, 326, 366
Cao, Y 174
Cao, Z 312
Capdevila, C 146
Capdevila-Montes, C 54
Cappiello, M 144
Caputo, A 120
Caratini, Y 357
Carden, Z 165
Caricato, A 252
Carlton, C 76
Carolan, M 135
Caron, A 269, 360
Caron, P 82
Carpenter, J 69
Carpenter, T 317
Carradó, A 298
Carreño, F 353
Carrétéro, C 115
Carroll, L 130
Carroll, M 94
Carsley, J 282
Carter, C 76, 363
Carter, J 133, 134, 199
Carter, M 208
Carvalho Costa, L 119
Casem, D 295
Casolco, S 127
Castellero, A 68
Castelnau, O 279
Castillo, D 245
Castro, D 323
Castro-Colin, M 197
Catalano, J 295
Caton, M 50
Catoor, D 81, 82
Causey, S 347, 370
Cavins, M 87
Cawkwell, M 141, 174
Caya, C 157
Cazacu, O 81, 118, 180
Ceder, G 293
Celik, O 284
Cerreta, E 73, 74, 81, 88, 91, 117, 128, 138, 140, 169, 171, 180, 193, 196, 225, 234, 246, 249, 283, 294, 304, 332, 340
Ceylan, U 358
Cha, D 102
Cha, S 39, 59
Chada, S 74, 119, 172, 199, 228, 253, 277, 300, 326, 343
Chai, L 255, 346
Chakhalian, J 115
Chakkingal, U 51
Chakraborti, D 105
Chakraborty, P 61
Chamberlain, O 156
Champion, Y 100
Chan, K 346
Chan, L 264
Chan, P 169
Chancellor, T 101
Chandra, D 368
Chandra, S 71
Chandrasekar, S 55, 57, 151
Chandrashekar, S 106, 156, 210, 263, 311, 356
Chang, C 75, 300
Chang, H 318
Chang, J 200, 355
Chang, L 262
Chang, R 185
Chang, S 283, 284, 332
Chang, W 331
Chang, Y 96, 102, 112, 138, 158, 184, 187, 294
Chan Gyung, P 310
Chanturiya, V 114
Chao, J 54
Chapuis, A 350
Charles, N 331
Charlier, P 320
Chasiotis, I 122
Chason, E 228
Chatterjee, A 185, 340
Chatterjee, U 65
Chau, R 141
Chaubal, M 311
Chawla, N 74, 210, 248, 263, 277, 317
Chbihi, A 354
Chembarisova, R 306
Chen, B 98, 231, 298
Chen, C 75, 91, 102, 120, 153, 173, 199, 253, 254, 300, 301, 343
Chen, D 319
Chen, G 42, 60, 270, 292, 356, 370
Chen, H 130, 132, 188, 243, 244, 253, 263
Chen, J 41, 80, 101, 213, 230, 251
Chen, L 42, 71, 72, 84, 92, 116, 140, 168, 200, 222, 223, 224, 274, 275, 280, 298, 323, 331, 364
Chen, M 139, 218, 250, 300
Chen, P 66, 317, 344
Chen, Q 95, 105, 322, 330, 356
Chen, R 121, 289
Chen, S 75, 84, 131, 138, 174, 184, 199, 237, 238, 240, 253, 294, 300, 324, 325, 343, 344
Chen, T 113
Chen, W 243, 245, 246, 300
Chen, X 62, 64, 119, 249, 285, 311
Chen, Y 72, 148, 169, 184, 200, 248, 295, 339, 360
Chen, Z 116, 253, 266, 365
Cheng, L 107
Cheng, S 142, 198
Cheng, Y 218

Cheng-Yi, L. 120
Chengyi 344
Chengjun, L. 44, 345
Chengyi, L. 327
Cheong, S. 93, 264, 287
Cheong, Y. 117
Chernova, L. 340
Cherukuri, B. 295
Cheruvathur, S. 363
Chesonis, C. 113, 164
Chesonis, D. 362
Chhay, B. 70, 299
Chhowalla, M. 41, 60
Chiang, H. 201
Chiang, K. 246, 340
Chiang, T. 341
Chiarbonello, M. 237, 321
Chichkov, B. 110
Chien, W. 368
Chirranjeevi, B. 276
Chisholm, M. 274
Chiu, W. 135, 189
Chladil, H. 347, 348, 349
Cho, H. 59
Cho, J. 47, 88, 188, 195, 365
Cho, K. 284
Cho, M. 254
Cho, S. 248
Choate, W. 280
Choi, B. 174, 218
Choi, H. 39, 288, 289, 309
Choi, I. 174
Choi, J. 117, 190, 240, 292
Choi, S. 237, 277
Choi, W. 39, 42, 59, 101, 152, 207, 260, 308
Choo, H. 67, 69, 93, 110, 111, 161, 197, 198, 216, 251, 268, 298, 317, 352, 359
Chou, C. 344
Chou, K. 42
Chou, L. 131
Chou, Y. 85
Choudhury, S. 224, 274, 275
Chrisey, D. 208
Christ, H. 129, 130, 349
Christen, H. 222
Christie, G. 135
Christodoulou, J. 60
Chrzan, D. 66, 76, 116, 308, 324
Chu, J. 200, 217, 300, 331, 360
Chu, K. 116
Chu, M. 120
Chu, P. 42, 238
Chu, T. 216
Chuang, C. 218, 361
Chuang, H. 300
Chuang, P. 103
Chukwuocha, E. 265
Chumbley, L. 95
Chumbley, S. 108, 318
Chung, J. 93
Chwee Teck, L. 66, 110, 160, 215, 267, 316, 358
Cieslar, M. 258
Cimenoglu, H. 284, 295, 332
Cingi, M. 295
Cipoletti, D. 46
Ciulik, J. 303, 346, 369
Clarke, A. 166, 170, 230
Clarke, J. 84
Clarke, R. 251
Clarry, D. 164
Clausen, B. 93, 118, 198, 279, 297, 329
Clemens, H. 256, 304, 305, 347, 348, 349, 371
Clement, P. 264
Clifton, R. 91
Cloutier, B. 357
Cluasen, B. 298
Cochran, J. 128
Cockayne, D. 84, 131, 184, 237
Cocke, D. 114, 214
Cockeram, B. 303, 346, 369
Coimbra, A. 213
Colas, D. 203, 350
Cole, A. 261
Collins, P. 61, 88, 166, 209, 230, 246, 340
Collins, S. 146
Colombo, G. 89
Comer, M. 103
Compton, B. 68
Compton, C. 303, 347
Compton, W. 55, 57, 151
Condore, F. 330
Cong, Z. 298
Conner, B. 161
Conner, R. 68
Connors, D. 338
Converse, G. 215
Cooksey, M. 330
Cooley, J. 206
Cooper, P. 272
Copie, O. 115
Coratolo, A. 243
Cordill, M. 173
Corinne, G. 260
Corlu, B. 125, 126
Corr, D. 208
Correa, L. 356
Cortés S., V. 125
Costa, J. 159
Costanza, G. 140
Cotts, E. 277, 327
Coughlin, J. 248
Coulter, K. 136
Counter, J. 263
Couper, M. 220
Courtenay, J. 220, 362
Coury, A. 352
Cowen, C. 189
Cox, C. 145
Cox, W. 169
Crawford, G. 317
Crawford, P. 155
Crimp, M. 148, 170
Cristol, B. 106
Crooks, R. 278
Cross, C. 243
Cruse, T. 292
Cruz Rivera, J. 322
Cui, H. 351
Cui, J. 78
Cui, Y. 98, 256, 350
Cuong, N. 240
Cupid, D. 44, 324, 365
Cupidon, S. 105
Currat, R. 342
Currie, K. 239
Curtin, W. 43, 116
Cutler, E. 46

D

D'Abreu, J. 79
D'Alessandro, F. 331
D'Amours, G. 325
D'Armas, H. 92
da Costa, L. 167, 363
Daehn, G. 67, 175, 264, 293, 360
Dahle, A. 75, 265, 272, 326, 327
Dahlman, J. 162, 270
Dahotre, N. 47, 60, 80, 359, 361
Dai, K. 367
Dai, Q. 156, 264
Dai, Y. 94, 143
Daigle, E. 123
Dailey, N. 46
Dalla Torre, F. 68, 99, 217, 257
Daly, S. 328
Dandekar, D. 295
Dando, N. 109, 119
Dangelewicz, A. 150
Daniil, M. 261
Dantzig, J. 169
Dao, M. 82, 307
Darell, O. 227
Darling, K. 205
Darsell, J. 292
Das, J. 112
Das, K. 65
Das, M. 235
Das, S. 64, 107, 112, 147, 157, 202, 211, 242, 264, 279, 291, 303, 312
Dash, P. 180
Dashwood, R. 139, 247, 282
Dassylva-Raymond, V. 315
Dattelbaum, D. 92, 198, 249
Dauskardt, R. 89
David, S. 221, 233
Davidson, D. 83
Davies, P. 138
Davis, A. 252
Davis, B. 78, 124, 134, 301
Davis, J. 320
Davy, C. 260
Dawson, P. 153, 328
Dayananda, M. 364
Daylami, M. 266
Daymond, M. 197, 328
Dayong, Z. 323
de Boissieu, M. 342
Decamps, B. 203
de Carvalho, E. 70
Deck, C. 60
Decker, R. 188
De Cooman, B. 283
Dedyukhin, A. 314
DeGraef, M. 60, 102, 103, 153, 154, 209, 262, 309, 355
Dehm, G. 139
Deibert, M. 243, 244
Deisenroth, J. 79
Deiters, C. 165
Deka, S. 280

Dekhtayr, Y 268
De Klerk, R 214
Delaire, O 43
Delimova, L 168
Delplanque, J 179
De Lucas, R 133, 177
Delucas, R 124
Demetriou, M 67, 68, 319, 359
Demirkiran, H 358
Demkowicz, M 199
De Moares, J 210
Demopoulos, G 214
den Bakker, A 189
Deng, J 251
Deng, S 268
Dennis, K 145
Depinoy, M 266
Deppisch, C 74
Depres, C 83
Derahkshan, S 144
Deranlot, C 115
Derguti, F 282
Derin, B 192
Derosa, P 331
deRosset, A 151
Deryugin, Y 158
Desai, T 99, 252
Despinasse, S 159
Desrosiers, P 159
Deutsch, T 105
Devanathan, R 299
Devincre, B 72, 83
Devine, T 333
DeWald, A 77
DeYoung, D 112, 113, 164, 220, 271, 319, 361
Dhiman, M 265
Dias, D 119
Diaz De La Rubia, T 351
Dickerson, C 299
Dickerson, P 102, 209, 230
Dickerson, R 92
Dickinson, J 69
Didier, R 260
Didier, T 260
Dieringa, H 335, 336
DiGiacomo, S 92
Dilanian, R 309
Dillard, S 141, 209
Dimiduk, D 72, 97, 101, 102, 104, 114, 131, 154, 183, 209, 348, 350
Ding, F 311
Ding, W 134, 188, 239, 240, 290
Dinh, L 205
Diniz, R 263
Dinkel, M 56
Dinu, C 208
Diologent, F 82, 349
Dion, M 79
Dittmann, R 274
Dixit, V 340
Djambazov, G 98, 177
Dlouhy, A 97, 148
Dlouhy, I 97
Dmowski, W 197, 218, 269
Dobatkin, S 257, 258
Dobbins, T 46, 47, 48, 341
Dobra, G 319
Docekalova, K 97
Dogan, O 346, 347, 370
Doheim, M 315
Dohi, M 358
Dojc, D 119
Domack, M 278
Domínguez, M 125
Domínguez M., S 125
Donchev, A 371
Dong, J 290
Dong, L 53
Dong, Z 60, 101
Donner, W 197
Doraiswamy, A 110
Dorantes Rosales, H 260
Dörnenburg, F 123, 124
Dorr, K 168
Dorr, M 169
dos Santos, C 358
dos Santos, L 221
Dotson, K 233
Dotson, T 233
Dougherty, L 180, 209, 332
Downey, J 62
Downs, J 369
Doyle, C 123
Drabble, D 278
Drache, M 200
Drapala, J 343
Draper, S 148
Dressler, J 165
Drevermann, A 98, 256
Dreyer, C 189
Dring, K 329
Driver, J 84
Droste, W 320
Druschitz, E 87
Dryepondt, S 123
Du, D 217
Du, L 240
Du, N 157
Du, P 81
Du, Q 72
Du, X 68
Du, Z 55
Duan, G 319
Duan, H 309
Dubach, A 217
Dube, G 164
Dube, J 361
Dubey, M 122
Dubois, J 184, 309
Duchesne, C 159, 213
Dudek, M 74
Dudnik, E 181
Dufour, G 159, 213, 225
Duh, J 131, 301
Dulikravich, G 191
Dunand, D 247, 328
Dundar, M 125
Dündar, M 126
Dunlop, G 290
Dunne, R 229
Dupas, N 226
Dupon, E 79
Dupuis, C 113, 320
Dupuis, M 315
Durandet, Y 336
Durst, K 174
Dursun, A 125, 126
Duszczyk, J 65
Dutrizac, J 113
Dutta, I 89, 139, 194, 228, 229, 247, 296
Dutta, T 45
Duz, V 88
Dwivedi, D 265
Dye, D 139, 247
Dymek, S 80

E

Easton, M 289, 290, 336, 337
Ebeling, T 133, 241
Eberl, C 121
Ebrahimi, F 256, 260, 324, 365
Echlin, M 355
Eckert, J 39, 56, 59, 110, 112
Eden, T 64
Edwards, L 171
Efe, M 57
Effgen, M 304, 347
Egami, T 111, 161, 167, 197, 269, 318, 319
Eggeler, G 149, 222, 223, 224, 236
Egorov, I 191
Eh.Hovsepian, P 371
Ehiasarian, A 349, 371
Eifler, D 285
Eiken, J 239, 256
Eisenlohr, P 118, 148, 170
Eivani, A 65
Ekuma, C 125
El-Awady, J 131
El-Bealy, M 320
El-Desouky, A 192
El-Kersh, A 315
Elangovan, S 271
El Bekkali, A 227
Elder, K 168, 169
Elias, C 358, 359
El Kadiri, H 140, 155, 295
Elkholy, A 49
Elkin, I 143
Ellis, D 168, 222, 223
El Mehtedi, M 188
Elmustafa, A 128, 278
Elsamadicy, A 327
Elsayed, F 134
Emamian, A 39
Emerson, S 136
Engberding, N 98
Enomoto, M 247
Enright, P 165
Eom, C 222
Erb, A 53, 221
Erdogan, R 125
Eremets, M 196
Eres, G 274
Ergin, L 346
Ernst, F 233, 234
Ersundu, E 79, 302
Es-Said, O 65
Escobedo, J 249
Escuadro, A 236
Esit, F 107

Eskin, D.....209, 220, 272, 362
Esquinazi, P.....299
Esquivel, E.....110
Essadiqi, E.....134
Estrin, Y.....50, 99, 100, 149, 205, 257, 258, 306, 334, 352, 359
Etienne, A.....198, 354
Etzion, R.....227
Evangelista, E.....188
Evans, A.....121, 175, 176
Evans, D.....88, 99, 138, 193, 246, 294, 340
Evans, J.....109, 213, 219, 362
Evans, N.....146
Evans, P.....274
Ewing, R.....59, 101
Ezekoye, O.....338

F

Fabbreschi, M.....321
Fabre, A.....298
Fabrichnaya, O.....44, 365
Facsko, S.....343
Fafard, M.....325
Falah, A.....49
Faleschini, M.....369
Falk, M.....162
Fan, D.....311
Fan, G.....67, 110, 161, 216, 268, 317, 352, 359
Fan, X.....62
Fan, Y.....255
Fanchini, G.....41
Fang, J.....200
Fang, Z.....193, 261, 326
Fangbin, C.....78, 302
Farber, D.....249
Farias, S.....67
Farrell, J.....304, 347
Farrer, J.....363
Fashanu, A.....65
Fathi, E.....271
Fattebert, J.....169
Faulhaber, S.....176
Faulkner, R.....144
Favilla, P.....181
Faza, S.....291
Fecht, H.....51, 247, 269, 306, 360
Feldman, J.....219
Felicelli, S.....137, 155, 298
Fell, B.....179
Felli, F.....47, 231
Feng, C.....178
Feng, J.....196, 294
Feng, N.....345
Feng, S.....343
Feng, W.....72
Feng, Y.....177
Feng, Z.....198, 221, 233, 298
Fengchun, J.....66
Fennie, C.....167
Fenton, G.....175
Feret, F.....214
Fergus, J.....243
Fernandez, J.....46, 299
Fernandez-Gil Bando, R.....302
Ferreira, A.....362
Ferreira, H.....213
Ferreira, P.....76, 332
Ferrell, S.....233
Ferrer, D.....184
Ferris, K.....294
Ferron, C.....214
Ferron, J.....124
Fert, A.....115
Fertig, R.....278
Fetcu, D.....280
Fevre, M.....42
Field, D.....158, 249
Field, F.....64, 147
Field, R.....166, 170, 230
Fielden, D.....297
Figueiredo, F.....119
Figueiredo, R.....52
Filevich, A.....300
Filho, J.....107, 356
Filius, J.....62
Fillit, R.....84
Findley, K.....94
Fine, M.....96, 191, 364
Finel, A.....42, 224, 275
Finsterbusch, M.....243
Finstrom, N.....274
Fiory, A.....63, 296, 297
Firrao, D.....69, 140, 237, 321
Fischer, C.....293
Fischer, J.....236
Fisher, W.....46
Fivel, M.....83
Fjær, H.....158, 361
Fjeld, A.....137, 362
Flanagan, T.....136
Flandorfer, H.....199, 253, 300, 343
Flicker, J.....296
Florando, J.....91, 111
Flores, K.....67, 131, 163, 317, 359, 360
Flores, M.....127
Flowers, J.....60
Fnu, S.....296
Foecke, T.....211
Foiles, S.....116, 170
Foley, D.....143
Follstaedt, D.....307
Fonda, R.....146
Fong, H.....66
Foosnæs, T.....226, 227, 326
Foosnas, T.....119
Fortenberry, N.....185
Fraczkiewicz, A.....203, 350
Francis, J.....297
Francoual, S.....342
Frank, S.....267
Franz, C.....156
Frary, M.....46, 176, 182, 229
Fraser, H.....61, 88, 166, 181, 194, 209, 230, 246, 275, 340
Frear, D.....74, 89, 139, 172, 194, 228, 247, 296
Frederick, A.....338
Frederick, D.....233
Fredrickson, G.....62
Free, M.....78, 124, 214
Freeland, J.....115
Freels, M.....217, 361
Freeman, A.....128, 234
Freibert, F.....155
Freitas, M.....80
Frerichs, A.....95
Fridy, J.....49
Friedland, E.....253
Friedman, L.....207
Friedrich, B.....98
Fries, S.....181
Froehlich, M.....371
Fröhlich, M.....371
Frost, L.....271
Frosta, O.....226
Fu, C.....249
Fu, E.....143, 199
Fu, H.....359
Fu, R.....238
Fu, Y.....108
Fuchs, G.....46, 363
Fugetsu, B.....288
Fujii, T.....184
Fujimatsu, T.....283
Fujino, S.....223
Fujiwara, E.....142
Fujiyoshi, M.....194
Fukuda, H.....288
Fukumoto, S.....283
Fullwood, D.....103
Fultz, B.....43
Funakubo, H.....223
Funkhouser, C.....316
Furrer, D.....340
Furu, T.....212
Furuhara, T.....193
Furusawa, T.....367
Furuya, K.....208, 245
Futter, K.....357

G

Gaal, S.....201
Gabay, S.....233
Gabb, T.....176
Gabrielyan, T.....311
Gabrisch, H.....322
Gagne, J.....225
Gagnidze, T.....202
Gaies, J.....347, 370
Galarraga, R.....356
Gallagher, M.....127
Galli, G.....78
Galstyan, E.....323
Gama, S.....197
Gamweger, K.....113
Gan, J.....251, 299
Ganapathysubramanian, B.....154, 155, 364
Gandhi, R.....210
Ganesan, Y.....76
Ganeshan, S.....186
Gang, S.....88
Gangloff, R.....278, 286
Gangopadhyay, A.....162
Gannon, P.....232, 243, 244
Ganuza, A.....67
Gao, B.....140
Gao, F.....299
Gao, M.....43, 44, 98, 347
Gao, X.....146

Gao, Y ..... 67, 110, 111, 130, 161, 180, ... 216, 217, 268, 317, 319, 359
Gapud, A 339
Garay, J 192
Garcia, E 190
García, N 299
Garcia, R 224
García-Hinojosa, A 211
Garcia-Mateo, C 146
Garcia-Moreno, F 178
Garcia de Andrés, C 146
Garcia de la Infanta Belio, J 353
García H., A 45
Gardner, T 164
Garimella, N 190, 351
Garkida, A 346
Garlea, E 251
Garrido, F 251
Garza, K 369
Garzon, F 338
Gascoin, F 145
Gassa, L 272
Gaubert, A 275
Gaudreault, B 159
Gaustad, G 155
Gauthier, C 159, 213, 225, 226
Gavrielatos, I 190
Gaytan, S 110, 281
Gazonas, G 341
Ge, Y 233
Geantil, P 83, 183, 250, 329
Gebhard, S 148, 371
Gehring, G 276
Geifman, I 322
Geltmacher, A 209, 210
Gemmen, R 243
Gemming, T 39, 59
Genc, A 166, 194, 275, 340
Gendron, M 171, 225
Geng, H 72
George, E 198
George, P 123
Gerberich, W 76, 173
Gerling, R 256, 305, 349
German, R 107, 155, 283, 295
Gerold, B 336
Gerosa, R 237, 321
Gershenzon, M 109
Gervasio, D 338
Ghaderi Namin, A 288
Gharghouri, M 337
Ghiban, B 180
Ghidini, A 237, 321
Ghomashchi, R 272
Ghoniem, N 94, 131, 182
Ghosh, A 138, 188, 288
Ghosh, G 191, 364
Ghosh, K 65
Ghosh, S 61, 102, 154, 247, 283, 284, 334
Gianola, D 121, 229
Gibala, R 104
Gibson, M 290, 337
Gierlotka, W 344
Gil-Sevillano, J 183, 225
Gila, B 101
Gill, A 221
Gilman, J 73, 183
Gimazov, A 52, 353
Ginzbursky, L 299
Girard, Y 204
Giribaskar, S 53
Gittard, S 105
Giummarra, C 287
Glaessgen, E 99
Glavatskikh, M 348, 350, 371
Glavicic, M 88, 250, 340
Gleeson, B 77, 122, 175, 231
Glicksman, M 262, 276
Gludovatz, B 369
Glushchenko, V 143
Godet, S 97
Godlewski, L 126
Goebel, W 216
Goel, M 219
Goesele, U 131
Goettert, J 268
Göken, M ..... 49, 56, 82, 129, 130, 174, ... 182, 236, 285, 307, 333, 367
Gokhale, A 262, 272
Goldenfeld, N 169
Golestanifard, F 323
Golladay, T 280
Goller, G 358
Golovina, I 322
Golowin, S 293
Golubov, S 343
Gomathi, G 271
Gomes, J 114, 214
Gong, H 364
González, B 50
Gonzalez, J 137
Gonzalez-Carrasco, J 54
Gonzalez-Reyes, L 260, 322
Gonzalez De Moricca, M 370
Gooch, W 133
Goodall, R 349
Goranson, G 283
Gordon, J 164
Gordon, P 116
Gornostyrev, Y 234
Gorny, A 290
Gorokhovsky, V 243
Gosslar, D 256
Goswami, R 309
Gottstein, G 130, 205, 206, 207
Goud, P 80, 281
Goundla, P 46
Gourlay, C 326, 327
Gout, D 144
Gouthama 53
Goutière, V 113
Gower, L 160
Goyel, S 256
Gräb, H 165
Graham, G 338
Grandfield, J 271
Grassi, J 107
Grater, J 204
Gray, G ..... 73, 74, 117, 169, 170, ... 174, 225, 249, 304, 332
Grazier, J 122
Greco, R 95, 144
Greedan, J 144
Green, J 147, 303
Greenberg, B 81
Greene, R 196
Greer, A 110, 199, 253, 300, 343
Greer, L 162
Gregory, J 64, 147
Grekhov, I 168
Griffin, R 370
Grimm, T 303, 347
Groeber, M 102, 154, 209, 262
Groebner, J 337
Groeschel, F 94
Gronbech-Jensen, N 224
Gronsky, R 328
Groza, J 179, 223, 358
Gruber, J 117, 154
Gruber, P 172
Gruen, G 362
Grunschel, S 91
Grunspan, J 178, 179
Gschneidner, K 95, 279
Gu, S 210, 263
Guan, S 288, 335
Guangchun, Y 60
Guanghui, L 283
Gudbrandsen, H 227
Guebels, C 179
Gueijman, S 87
Guenther, R 256
Guether, V 347, 348
Guimarães, M 159, 214
Guimarâes, O 210
Gulsoy, E 209
Gunda, V 268
Gunderov, D 354
Guner, S 41, 208
Gungor, M 194
Günther, R 186
Gunyuz, M 295
Guo, A 291
Guo, F 121, 277
Guo, X 42, 246, 339, 345
Guo, Y 59, 101, 251, 260, 261
Guo, Z 232, 312, 313, 341
Guofeng, C 48
Gupta, A 240
Gupta, N 129
Gupta, R 308
Gupta, S 291
Gupta, V 41, 132, 278
Guruprasad, P 45, 184
Gururajan, M 43, 61, 117, 276
Gusberti, V 315
Güther, V 348
Guthrie, R 320
Gutierrez, G 321
Gutiérrez, I 183
Gutierrez, M 137
Gutierrez-Urrutia, I 203, 353
Guyer, J 72
Guzman, J 324

H

Ha, D 136
Ha, S 253
Haase, R 231
Haataja, M 116, 169, 296

Habchi, R 281
Hackenberg, R 166, 230
Hackett, M 199
Haddad, A 63
Hadorn, J 111
Haeckel, T 349
Hafok, M 57, 334
Hagelstein, K 46
Hagiwara, M 227
Hagni, A 69, 113, 166, 221, 272, 321, 362
Hahn, H 342
Hahn, J 156, 157, 263
Haines-Butterick, L 161
Haley, B 224
Hall, N 319
Halle, T 57
Haller, E 308, 324
Ham, H 277
Hamann, B 209
Hamburg, B 141
Hamdan, A 195
Hamdi, F 118
Hamer, S 165
Hamilton, B 79, 80
Hamilton, C 277
Hamilton, J 238
Hammers, T 368
Hammi, Y 295
Hamza, A 218
Hamzic, A 115
Han, B 98
Han, E 289
Han, H 277
Han, J 123, 286
Han, K 260
Han, L 290
Han, M 267
Han, Q 187, 239
Han, S 53, 153, 331
Han, T 328
Han, W 192
Han, X 75
Han, Z 40
Handa, T 201
Handwerker, C 74, 119, 172, 228, 277, 326
Hanlumyuang, Y 116
Hanna, M 126
Hänninen, H 87
Hansen, N 52, 150, 206
Hantcherli, L 118
Hänzi, A 257, 336
Hao, L 313
Haouaoui, M 52, 151, 257, 334
Haque, A 312
Harder, D 317
Harding, R 98
Hardy, J 292
Harel, G 188
Harimkar, S 60
Hark, R 64
Harlow, D 217
Harmon, B 96
Haro Rodriguez, S 265
Harrell, J 207, 261
Harringa, J 200, 254, 327
Harris, P 356
Hartig, C 133, 186, 241, 256
Hartvigsen, J 271
Hartwig, K 58, 143, 206, 257, 370
Hartwig, T 151
Harvey, É 157
Harwood, N 106
Hasan, M 80, 281
Haseeb, A 309
Hashemian, S 92
Hashiguchi, M 136
Hashimoto, K 283
Hashimoto, S 258
Hass, D 176
Hassan, H 90
Hassan Ali, M 279
Hata, S 71, 355
Hatano, M 150
Hatcher, N 128
Hatkevich, S 293
Hattiangadi, A 123
Haugh, M 215
Haupt, T 339
Hautier, G 293
Haxhimali, T 276
Hay, R 118
Hayashi, T 56
Hayden, D 282
Haynes, A 231
Hazel, B 176, 231
He, H 121
He, L 371
He, M 121
He, T 250
He, X 291, 349
He, Y 74, 97, 147, 149
Heard, R 176
Hebert, R 68, 235
Hecht, U 256
Hector, Jr., L 85, 121, 145, 157
Hector, L 282
Hefferan, C 310, 328
Heggset, B 164
Heifets, E 222
Heil, T 261
Heilmaier, M 55, 98, 334
Heinze, J 46
Heller, R 343
Hemburrow, P 159
Hemker, K 121, 122, 195, 229
Hemley, R 92
Henaff, G 129, 204
Hengelmolen, A 113
Henkel, S 236
Hennig, R 91, 140, 196, 249
Henriksen, B 361
Henry, P 214
Her, E 46
Herbst, J 145
Herklotz, A 168
Hernandez, D 110
Hernandez-Garcia, A 211
Hernandez-Majoral, M 143
Hernández-Pérez, I 260, 322
Herranz, G 115
Herrera, M 355
Herring, J 271
Herzog, R 50, 286
Hess, W 69
Heuer, A 233, 234
Heying, M 244
Hibbard, G 107, 234, 289
Hibbins, S 239
Hidetoshi, S 291
Hierro de Bengoa, M 350, 371
Higashi, K 239
Hilck, A 156
Hilerio, I 137, 166, 273
Hilgraf, P 156
Hill, M 77
Hill, T 87
Hiltunen, P 156
Hines, J 86, 104, 155
Hirata, T 239
Hirsch, J 287
Hisatsune, K 142
Hixson, R 74, 141
Ho, C 120, 142, 248
Ho, S 289
Ho, W 86
Hoag, E 147
Hoagland, R 39, 102, 174, 199, 230
Hoc, T 83
Hockauf, M 57
Hockridge, R 106
Hodge, A 236
Hodgson, P 69, 100, 112, 216
Hoelzer, D 90, 128
Hoffelner, W 230
Hoffmann, A 369
Hoffmann, C 342
Hoffmann, R 196
Hofmeister, W 207
Hohenwarter, A 285
Hohl, B 325
Hojo, H 367
Holby, E 72
Holden, I 226
Hollang, L 225
Holleis, B 113, 302
Holm, E 116
Holt, N 108
Holy, V 141, 142, 342
Hommes, G 72
Hong, K 248
Hong, S 39, 59, 190, 292
Honghui, T 40
Hongqiang, R 43
Honma, T 241
Hono, K 55, 146, 187, 241
Hooks, D 141, 174
Hoppe, R 149
Hoppe, T 110
Höppel, H 56, 236, 307
Horita, Z 257, 306
Horky, J 367
Horstemeyer, M 77, 155, 158, 339
Hort, N 186, 239, 335, 336
Hoseman, P 143
Hosemann, P 95, 144
Hosokawa, K 321
Hosoya, Y 146
Hostetter, G 194
Hou, C 127
Hou, H 291
Houda, H 100

Houghton, B 112
Hourlier, D 199
Houston, J 317
Houston, K 53
Hovsepian, P 349
Howard, B 331
Howe, J 89
Hoyos, L 137
Hoyt, J ..... 42, 71, 116, 168, ... 223, 275, 276, 323, 364
Hryn, J 270
Hsia, K 49, 82, 129, 182, 236, 285, 333, 367
Hsiao, H 173
Hsieh, K 68, 217
Hsiung, L 141
Hsu, C 45, 318
Hsu, E 241
Hsu, T 301
Hsu, Y 120
Hu, D 178, 194, 305
Hu, H 290, 337
Hu, J 42
Hu, S 72, 275
Hu, W 130, 244
Hu, X 78, 140, 314, 366
Hu, Z 208, 268, 269
Hua, F 74, 119, 172, 173, 228, 277, 326
Hua, Y 281
Huang, C 300
Huang, E 93
Huang, H 208
Huang, J 59, 68, 217, 218, 253, 360
Huang, L 366
Huang, P 150
Huang, S 191, 255, 364
Huang, W 136
Huang, X 52, 150, 206, 273, 346
Huang, Y 223, 238, 306, 331, 344, 353
Huang, Z 169, 344
Hubbard, C 298
Hubbard, J 103
Huber, D 230
Huda, M 105
Hudson, J 194
Hufnagel, T 111
Hughes, D 298
Huh, J 248, 292
Hui, X 270
Hulbert, D 48
Hull, L 74
Hundley, M 174
Husseini, N 251
Hutchins, C 151
Hutchins, J 114
Hutchinson, N 360
Hvidsten, R 213
Hwang, C 74
Hwang, H 114
Hwang, J 64, 114, 193, 221, 240, 268, 273, 346
Hwang, K 193
Hwang, S 126
Hwang, T 202
Hwu, Y 342
Hyers, R 70, 162, 244
Hyland, M 106, 233, 313

I

Iadicola, M 211
Iannacchione, G 309
Ibarra, L 246
Ice, G 92, 93, 142, 341
Idenyi, N 125, 126, 265
Ienco, M 140, 321
Iffert, M 108, 159, 213, 266, 313, 315, 357
Iijima, T 223
Ikeda, M 351
Ikeda, T 145
Ikuno, H 367
Ila, D 41, 70, 208, 299, 327, 342, 343, 359
Ilavsky, J 175, 341
Iliev, M 197
Im, J 58
Imagawa, H 227
Imai, H 288
Imam, M 294
Imanaka, N 96
Imayev, R 205, 347, 348
Imayev, V 347, 348
Inaba, Y 207
Inami, T 245
Inel, C 126
Ingram, B 292
Inoue, A 163, 217, 268, 269, 360
Instone, S 362
Inui, H 203, 204
Inzunza, E 171
Ionescu, I 129
Ipser, H 229, 343, 344
Iqbal, F 130
Irons, G 137
Irsen, S 98
Isac, M 320
Isanaka, S 87
Ishida, K 254, 300
Ishida, M 360
Ishikawa, K 45, 47, 48, 135
Ishimasa, T 342
Islam, Z 141
Islamgaliev, R 54
Isoda, S 84, 131, 184, 237, 238, 240
Itsumi, Y 193
Ivanisenko, Y 51, 306, 333
Ivanov, M 81
Ivanov, V 326
Ivanushkin, N 311
Ivey, D 243, 292
Iwasawa, M 72
Iwata, S 293, 339
Izmailova, N 205

J

Jablonski, P 189, 292
Jackson, M 139, 235, 247
Jacob, T 222
Jacobs, M 271
Jacobson, A 197
Jacot, A 305
Jacques, P 97
Jacquet, D 315
Jacquet, E 115
Jadhav, N 228
Jagielski, J 251
Jahed, H 77
Jain, A 297
Jain, J 189
Jain, P 81
Jain, V 174
Jakobsen, B 93, 328
James, B 123, 179, 233
Jang, D 67
Jang, H 178
Jang, J 68, 111, 174, 217, 218
Jang, S 360
Jang, Y 47, 212
Jannasch, E 287
Janz, A 337
Jaquinde, W 316
Jarmakani, H 169
Jasinski, J 191, 245, 317
Jayaraman, N 77
Je, J 342
Jean, Y 67
Jean-Charles, R 105
Jeandin, M 123, 233
Jee, S 160
Jenabali Jahromi, S 288
Jenkins, D 94
Jenkins, M 143, 144
Jenkins, R 347, 370
Jensen, D 250
Jensen, M 109
Jeon, H 39, 102
Jeon, M 39
Jeong, C 365
Jeong, H 45, 309
Jeong, I 171
Jeong, J 202
Jeong, Y 59, 212
Jha, A 235
Jha, G 107
Jha, M 163, 202
Jha, S 50, 78, 237
Jhon, M 66
Ji, H 142
Ji, V 298
Jia, C 274
Jia, N 297, 298, 352
Jia, Q 98
Jia, S 335
Jia Ming, Z 160
Jiang, C 204, 349
Jiang, D 48, 285
Jiang, F 69
Jiang, H 194, 215, 305, 347
Jiang, J 335
Jiang, L 240
Jiang, M 124, 255
Jiang, Q 250
Jiang, R 246
Jiang, T 62
Jiang, W ..... 67, 68, 110, 111, 161, 216, ... 217, 268, 269, 299, 317, 359
Jiang, X 215, 245
Jiang, Y 239, 244, 336
Jiao, J 195
Jiao, L 89, 139
Jiao, T 91
Jiao, Z 143, 252

Jiawei, W. 314
Jie, L. 314, 330
Jimbo, I. 193
Jin, L. 134, 188, 240
Jin, M. 76
Jin, S. 85, 96, 101, 152, 267
Jin, X. 42, 60
Jin, Y. 223, 331
Jin, Z. 301
Jinhong, L. 214
Johansson, B. 96
John, R. 78
John, V. 200, 300, 331, 360
Johnson, C. 243, 244
Johnson, I. 280
Johnson, J. 119, 171, 175, 225, 226, 283, 325, 365
Johnson, R. 195
Johnson, S. 351
Johnson, W. 67, 68, 319, 359
Jolly, B. 233
Jolly, M. 79
Jonas, J. 97, 147, 240
Jones, D. 294
Jones, H. 294
Jones, J. 49, 130, 172, 182, 187, 237, 251, 367
Jones, N. 139, 247
Jones, R. 122
Jones, T. 133
Jong, J. 248
Jong Gu, B. 310
Jonnalagadda, K. 122
Joseph, D. 61
Joshi, S. 100
Jou, J. 360
Jouiad, M. 129
Joung, J. 171
Ju, J. 240
Juhas, M. 246
Jun, H. 112
Jun, J. 292
Jun, Y. 335
Jun, Z. 314
Jung, J. 174
Jung, S. 201, 253, 261, 345
Jung, Y. 45
Jungwirth, T. 142
Junior, C. 356
Juretzko, F. 312
Jyoth, S. 281

K

K., A. 176
Kabir, M. 340
Kabirian, F. 337
Kabra, S. 198, 279
Kachler, W. 348
Kad, B. 257
Kadiri, H. 298
Kadkhodabeigi, M. 316
Kaftelen, H. 40
Kahl, A. 319
Kahler, D. 104
Kahn, H. 233, 234
Kai, H. 42
Kai, W. 359, 361
Kain, V. 283, 284
Kainer, K. 335, 336
Kainuma, R. 254
Kaiyu, Z. 191
Kajinic, A. 305
Kajiwara, Y. 185
Kakkar, B. 357
Kalay, E. 108, 318
Kalban, A. 266
Kale, P. 200
Kalemba, I. 80
Kalgraf, K. 109
Kalidindi, S. 103
Kalinin, S. 274
Kalkan, K. 207
Kaltenboeck, G. 319
Kalu, P. 53, 221, 241, 260, 362
Kamado, S. 241
Kamal, M. 194, 246
Kamegawa, A. 237
Kamikawa, N. 52, 150
Kamikihara, D. 361
Kan, H. 314, 326
Kaneta, Y. 72, 339
Kang, B. 101, 153, 163
Kang, C. 365
Kang, F. 51
Kang, H. 122
Kang, I. 292
Kang, J. 127
Kang, S. 39, 59, 101, 152, 172, 188, 207, 254, 260, 280, 308, 327, 331
Kang, Y. 292
Kannan, R. 216
Kanthala, T. 105
Kao, C. 75, 238, 253, 300, 326, 327
Kao, P. 91
Kappes, B. 43, 116
Kar, A. 233
Kar, S. 325, 364, 365
Kar, Y. 181
Karabelchtchikova, O. 234
Karabin, M. 287
Karaman, I. 52, 151, 236, 257, 334
Karhausen, K. 287
Karjalainen, P. 332, 354
Karma, A. 116, 168, 276
Karnesky, R. 247
Karumuri, S. 207
Kaschner, G. 117, 229, 279
Kashimoto, S. 342
Kasisomayajula, V. 296
Kasouf, C. 203
Kassner, M. 83, 182, 183, 206, 250, 329
Katgerman, L. 209, 220, 272, 362
Kato, A. 189
Kato, M. 184
Kato, S. 124
Kato, T. 45
Katoda, T. 223
Katsman, A. 187, 290
Katz, J. 124
Kaufman, J. 147, 242, 303
Kaufman, M. 64, 193, 363
Kauzlarich, S. 145
Kavanagh, L. 219
Kavich, J. 115
Kawalla, R. 240
Kawamura, Y. 241
Kawasaki, M. 71, 258
Kayal, S. 267
Kayali, E. 284, 295, 332
Kazimirov, A. 93, 262
Kazyhanov, V. 54
Keblinski, P. 308
Keck, A. 210, 237, 247
Kecskes, L. 149, 151, 204, 206
Keimer, B. 115
Keles, Ö. 107
Keller, C. 279
Kelly, T. 97
Kelm, K. 98
Kelton, K. 162, 269
Kempkes, M. 226
Keniry, J. 160, 266
Kennedy, M. 81, 195
Kenningley, S. 124, 248
Kent, M. 195
Keppens, V. 318
Keralavarma, S. 282, 340
Kern, K. 60
Kesavan, M. 178
Kesler, M. 256
Ketabchi, M. 52
Key, C. 243
Khaleel, M. 298
Khalifa, H. 268
Khan, A. 338, 339
Khan, S. 239
Khasanova, N. 326
Khater, H. 73
Khatibi, G. 367
Khismatullin, T. 348
Kholkin, A. 268
Khoroshilov, D. 181
Khraisheh, M. 279
Khramov, A. 314
Kiessling, W. 123
Kiggans, J. 295
Kildea, J. 263
Kilmametov, A. 54, 342
Kim, B. 55, 202
Kim, C. 47, 63, 104, 105
Kim, D. 39, 44, 45, 47, 173, 240, 254, 262, 290, 292, 318, 337
Kim, H. 57, 118, 188
Kim, J. 102, 117, 166, 201, 253, 292, 320, 333, 338
Kim, K. 39, 59, 173, 200, 228
Kim, M. 98, 102, 158, 202
Kim, N. 269
Kim, S. 39, 45, 74, 102, 107, 152, 154, 155, 173, 200, 212, 228, 260, 261, 277, 284, 289, 292, 331, 348, 365
Kim, T. 44, 45
Kim, W. 44, 45, 47, 240, 290, 318, 337
Kim, Y. 48, 55, 97, 98, 117, 148, 149, 203, 238, 255, 277, 304, 305, 347, 348, 349, 350, 370
Kimura, H. 70, 192, 202
Kimura, K. 355
Kimura, M. 201
Kimura, T. 245
Kimura, Y. 344, 350
King, A. 151

King, P 280, 347
Kinney, C 120
Kinney, J 175
Kinoshita, M 72
Kirchain, R 64, 65, 147, 155
Kirishima, A 124
Kirk, M 143
Kishida, K 204
Kiss, L 234, 315
Kissell, J 242
Kita, K 48
Kitade, S 79
Kitiyanant, Y 216
Klarstrom, D 197, 367
Klauber, C 106
Klaumünzer, S 94
Kleber, S 56
Klemmer, T 261
Klett, C 156
Kline, E 148
Klingelhöffer, H 149
Klose, J 348
Kluge, T 176
Kluk, D 346
Klut, P 79
Knaak, U 287
Knapp, J 307
Knepper, R 278
Knipling, K 146
Knizhnik, A 315
Knuteson, D 104
Ko, C 358
Ko, Y 55, 307, 345
Kobayashi, K 127
Kobayashi, S 351
Kobe, P 264
Koch, C 205, 308
Koch, H 165, 320
Kodash, V 223
Kodentsov, A 300, 344
Koduri, S 340
Koester, K 66
Koh, P 177
Koh, S 39, 59, 101, 152,
153, 207, 208, 260, 308
Kohno, T 254
Koike, J 241
Kojima, Y 306
Kolitsch, A 371
Kolli, R 310
Komova, O 369
Komura, M 124
Kondoh, K 288
Konetschnik, S 202
Kong, C 293
Kong, F 148
Kongoli, F 330
Koniar, M 159
Konishi, H 288, 289
Konrad, P 124
Kontsevoi, O 128, 234
Koo, J 201
Koo, Y 80, 171, 284
Kopczyk, M 243
Kopecek, J 350
Kopka, L 86
Korzekwa, D 155
Korzhenevskii, A 197
Kostorz, G 341, 342
Kotb, N 315
Kotomin, E 222, 223
Kottada, R 333
Kou, S 239
Kouchmeshky, B 156, 225
Kouznetsov, D 263
Kovarik, L 73
Kovarik, T 258
Kovrov, V 314
Kowandy, C 51
Kozar, R 340
Kozeschnik, E 349
Krachler, R 365
Kraft, O 174, 286, 317, 333
Krajewski, P 46, 64, 134, 157, 355
Kral, K 153
Kral, M 96, 145, 278
Kramer, M 90, 145, 162, 318, 364
Krane, M 136
Krasilnikov, N 54
Krasovitsky, A 160
Kraus,, L 258
Krein, R 204
Kremmer, S 347, 348, 349
Krempaszky, C 50
Krenn, H 56
Kresch, M 43
Krimm, R 282
Kripesh, V 253
Krishnamoorthy, S 178
Krishnamurthy, R 123, 296
Krishnapisharody, K 137
Kroupa, A 343
Kruesi, P 280
Krüger, L 57
Krumdick, G 63, 104, 201, 255, 302, 345
Kruml, T 183
Krumpelt, M 292
Kruse, H 109
Krystian, M 257
Kryukovsky, V 314
Kryvasheyeu, Y 275
Ku, M 120
Kubin, L 83, 182
Kuester, F 67
Kugler, G 87
Kühn, H 149
Kühn, U 112
Kulcinski, G 94
Kuli, J 136
Kulin, R 66
Kulkarni, K 364
Kulkarni, N 324, 327
Kulkarni, S 188
Kulovits, A 55, 308
Kumah, D 251
Kumar, A 191, 234, 240, 253, 280, 357
Kumar, B 354
Kumar, D 82, 148, 170, 182
Kumar, K 228
Kumar, M 130, 175, 278
Kumar, P 228, 296
Kumar, S 81, 82, 228
Kumar Mehta, V 291
Kunz, L 236
Kuo, R 218
Kuramoto, S 76
Kurata, H 238
Kurmanaeva, L 51
Kurtoglu, K 192
Kurzydlowski, K 57, 206
Kusakov, A 315
Kusinski, G 123, 291, 333
Kusinski, J 123
Küstner, V 347
Kutkova, N 211
Kuvyrkina, A 263
Kuwabara, M 126
Kuzel, R 142
Kuznetsova, N 263
Kvande, H 99, 266
Kvello, J 227
Kvithyld, A 125, 178, 201
Kwak, C 331
Kweon, S 287
Kwon, S 333
Kwon, Y 188, 212, 263, 283
Kyeong, J 47
Kyrolainen, A 332

L

Laabs, F 327
Labidi, O 200
Lahiri, A 235
Lai, R 301
Lai, Y 201, 316, 326, 366
Lamb, J 368
Lambert, E 357
Lambros, J 122
Lamperti, A 252
Lampke, T 57
Lan, Y 356
Lander, G 96
Landers, A 148
Landoulsi, J 51
Lane, G 177
Lang, G 226
Lang, K 285, 368
Langdon, T 50, 52, 99, 129, 149, 150,
205, 257, 258, 306, 352, 353
Lange, H 108
Langeloh, T 156, 157, 263
Langlois, C 308
Lanyon, M 314, 330
Lao, J 50, 100
Lapin, A 263, 311
Lapovok, R 258, 334
Lara, G 125
Larouche, D 320, 361
Larsen, J 50, 78, 237
Larsen, W 109
Larson, B 83, 92, 93, 183, 250, 309, 329
Larson, D 162
Larsson, H 324
Laser, T 133, 241
Lasko, G 158
Lass, E 319
Lassila, D 91, 249
Last, J 316
Latysh, V 258
Laucouret, R 227

Laughlin, D 365
Launois, S 204
Laurent, V 227, 366
Lauridsen, E 61, 251
Lavernia, E 51, 52, 53, 150, 151, 306
Lawson, D 211
Leal, J 350
Leau, W 300
Lebeau, J 262
LeBeau, S 188
Lebensohn, R 81, 118, 170, 210, 279
LeBlanc, M 111
Le Bouar, Y 42, 275, 308
Le Brun, P 220
Lechner, R 142
Leckie, R 175
LeDonne, J 49, 368
Lee, A 120, 142, 248
Lee, B 48, 102
Lee, C 48, 55, 301, 307
Lee, D 277
Lee, E 65
Lee, G 212
Lee, H 70, 114, 115, 167, 222, 254, 274, 322, 327
Lee, I 91
Lee, J 71, 102, 112, 136, 188, 199, 201, 202, 212, 240, 247, 253, 290, 300, 337, 343, 344, 345, 361
Lee, K 45, 78, 102, 112, 117, 152, 173, 212, 261, 269
Lee, M 112
Lee, N 260, 261
Lee, P 45, 46, 318
Lee, R 138, 288
Lee, S 46, 53, 55, 71, 91, 93, 136, 154, 209, 212, 269, 283, 344, 352
Lee, T 65, 74, 84, 120, 284
Lee, Y 136, 188, 201, 223, 331
Lefebvre-Legry, P 199
Lefrançois, L 159
Lehmann, D 310
Lei, Y 160
Lei, Z 122
Leisenberg, W 119
Leite, P 213
Leitner, H 221
Lejava, T 202
Lejcek, P 350
Lekakh, S 219, 302
Lele, T 101
Lemieux, T 234
Lena, C 177
Lenosky, T 169
Léonard, F 170
Leonhardt, T 303, 346, 347, 369
Lepselter, M 63
Lerch, B 148
LeSar, R 293
Lesuer, D 258, 332
Letzig, D 241
Leu, M 87
Levashov, V 319
Levesque, R 113
Levi, C 175
Leviatan, T 187
Levine, L 83, 103, 175, 183, 250, 329
Lewandowska, M 57
Lewandowski, J 89, 90
Lewellyn, M 156, 264
Lewinsohn, C 135
Lewis, A 60, 61, 102, 103, 153, 209, 210, 262, 309, 355
Lewis, D 253
Lewis, G 110
Leyens, C 97, 148, 203, 255, 304, 347, 348, 349, 350, 370, 371
Li, B 100, 114, 127, 132, 133, 148, 170, 268, 273, 312, 326, 346, 353
Li, C 64, 89
Li, D 108, 317, 320, 322, 330
Li, F 310
Li, G 62, 124, 184
Li, H 87, 312, 313
Li, J 62, 69, 91, 108, 111, 113, 118, 130, 132, 133, 138, 166, 169, 180, 185, 187, 218, 221, 225, 272, 311, 316, 321, 326, 330, 362, 364, 366
Li, K 182
Li, L 352
Li, M 80, 126, 134, 287, 361
Li, N 121, 143, 199
Li, Q 50, 82, 214, 269, 303, 326, 346
Li, R 111, 218
Li, S 190, 208, 260, 276, 316
Li, W 106, 109, 119, 214, 262, 290, 311
Li, X 41, 75, 91, 121, 138, 173, 207, 229, 243, 278, 288, 289, 306, 328
Li, Y 69, 98, 101, 111, 212, 216, 224, 231, 275, 285, 312, 369
Li, Z 64, 157, 242, 282, 305
Lian, J 59, 101
Liang, C 335
Liang, H 181
Liang, J 81, 309
Liang, L 270
Liang, S 120, 289
Liang, Y 43
Liang, Z 43
Liang-xing, J 330
Liao, C 127, 308, 324
Liao, X 50, 99, 149, 150, 205, 257, 306, 352
Liao, Y 204, 351
Liaw, P 67, 68, 69, 92, 93, 110, 111, 141, 161, 163, 191, 197, 198, 216, 217, 218, 250, 251, 268, 297, 298, 317, 319, 341, 352, 359, 361, 364, 367
Lie, J 62
Lienert, U 93, 310, 328, 329, 342
Lill, J 43, 324, 325
Lilleodden, E 75, 121, 173, 229, 278, 328
Lim, C 53, 222
Lim, G 233
Lim, H 47, 240, 290, 337
Lim, K 44, 45
Lim, S 223
Lima, A 166
Lima, J 106, 107, 210, 263, 311, 356
Lin, A 110, 317
Lin, C 200, 331
Lin, D 134
Lin, J 69, 101, 112, 153, 216, 370
Lin, K 301
Lin, M 230
Lin, P 176
Lin, S 344
Lin, T 51, 58, 125, 360
Lin, Y 301
Lindemann, J 348, 350, 371
Lindhe, U 110
Lindley, T 235
Lindsay, S 109
Linga, H 108
Lin Peng, R 251
Linyong, F 114
Liou, W 301
Liping, N 234
Lipkin, D 365
Lipko, S 39
Liss, K 256, 304
Litvinov, D 262
Liu, B 51, 58, 85, 125, 127
Liu, C 118, 121, 124, 153, 191, 230, 318
Liu, D 62, 238, 256, 311, 330
Liu, F 111, 172, 217
Liu, G 101
Liu, H 265, 301
Liu, J 50, 106, 132, 133, 150, 175, 263, 287, 356
Liu, K 98
Liu, L 81, 182, 238, 251, 367
Liu, M 62, 283
Liu, P 254
Liu, Q 326
Liu, R 226
Liu, T 177, 201
Liu, W 61, 83, 92, 93, 135, 142, 193, 248, 250, 298, 316
Liu, X 86, 135, 189, 193, 216, 232, 243, 244, 292, 338, 344, 368
Liu, Y 64, 138, 157, 172, 197, 198, 220, 231, 250, 264, 312, 313, 366
Liu, Z 72, 92, 140, 148, 186, 187, 311, 323
Livescu, V 128, 141, 209, 249
Llorca, N 56
Lochbichler, C 98
Lockhart, G 134
Lodzik, J 159
Loehe, D 285, 368
Loffler, J 68
Löffler, J 217, 257, 336
Loh, J 356
Loiseau, A 308
Lomatayo, C 101
Lombard, D 227
Long, B 143
Long, G 250
Long, H 62
Long, Z 157
Longanbach, S 90, 288
Longo, F 124
Longstreth-Spoor, L 269
Loomis, E 92
Lopes, F 362, 363
Lopez, C 137
Lopez, M 110, 281, 332
Lopez P., N 125
Lorentsen, O 325, 365
Loretto, M 88, 178, 194, 304, 305
Lossius, L 171
Lou, J 76

Louchet, F 203
Lourie, O 76
Louzguine, D 268
Lovato, M 118, 229
Lovrenich, R 281
Lovvik, O 136
Lowe, C 339
Lowe, T 50, 54, 99, 149, 205, 257, 258, 306, 334, 352
Lowengrub, J 208, 276, 316
Lozano, A 144
Lu, C 85
Lu, G 78
Lu, H 41, 63, 245, 247, 314
Lu, K 85, 150, 200, 285, 354
Lu, L 285, 307
Lu, N 40
Lu, W 371
Lu, X 190
Lü, X 326
Lu, Y 43, 76, 174, 266, 365
Lu, Z 144, 360
Luan, B 216
Lubas, M 317
Lucadamo, G 238
Lucas, J 243
Lucas, M 43
Ludwig, A 137, 244
Ludwig, W 251
Lugo, M 77
Lugo, N 56
Lui, L 231
Lukas, P 236
Luo, A 85, 188, 240
Luo, H 220
Luo, J 132
Luo, Q 335
Luo, S 92
Luo, T 207, 358
Luo, W 160, 163
Luo, X 140
Lushchik, A 299
Luss, D 262, 323
Lv, M 40, 235
Lykotrafitis, G 316

M

M'Hamdi, M 361
Ma, D 318
Ma, E 76, 100, 170, 216, 218, 353
Ma, F 42
Ma, G 269
Ma, J 180, 314
Ma, K 78
Ma, L 132, 349
Ma, N 96, 138, 163, 169, 294, 345
Ma, R 266
Ma, S 42, 130
Ma, X 181
Ma, Y 98, 289
Ma, Z 255
Macdonald, W 239
Macht, M 94
MacSleyne, J 103
Madariaga, I 148
Madhavan, R 202
Madhavan, V 180
Madison, J 355
Maeda, M 70, 192, 202
Mahajan, S 73, 117, 169, 225
Mahammed, Q 63
Mahapatra, R 53, 204
Maheraeen, S 355
Mahmoud, M 315, 326
Mahmudi, R 337
Maier, H 151, 236, 257, 334
Maijer, D 134
Maiti, S 69
Maiwald, D 119
Majaniemi, S 168
Majumdar, B 89, 139, 194, 195, 247, 248, 296
Makaraci, M 181
Makitka, A 135
Malard, T 266
Malherbe, J 253
Maliha, S 357
Malkinski, L 331
Mallik, U 127
Maloy, S 94, 95, 143, 144, 198, 199, 251, 299, 342
Maltais, B 112
Malysheva, S 205
Mamforia, M 202
Man, J 183
Mancio, M 333
Mandal, M 308
Mani, V 336
Maniruzzaman, M 108, 126, 127, 234
Manivannan, A 86, 135, 189, 243, 292, 338, 368
Manivasagam, G 51
Manjarres, M 367
Manley, M 224
Mann, J 55
Mann, V 160
Manna, I 269
Mannava, S 77, 221
Manohar, P 232
Mansoor, B 188
Mansour, B 188
Manuel, M 283
Mao, S 307, 308
Mao, X 89
Maofa, J 44, 323
Maoz, Y 187
Maple, M 95
Mar, A 145
Mara, N 102, 143, 230
Marathe, G 235
Mardare, C 244
Margarella, A 104
Margaritondo, G 342
Margem, F 166
Markmaitree, T 368
Markmann, J 51, 99, 333
Marques, C 252
Marquis, E 170
Martens, R 175, 261
Martin, F 234
Martin, J 291
Martin, M 199, 257
Martin, O 159
Martin, P 70, 100, 246
Martinez, E 110, 265, 281
Martinez, J 110, 297
Martínez, L 45
Martins, J 159, 214
Martirosyan, K 262, 267, 323
Marton, Z 167
Maruyama, K 255, 304
Marx, M 367
Mason, J 110
Massalski, T 95
Mastuura, H 345
Masuda, C 88, 178
Mataya, M 93
Matej, Z 142
Mathaudhu, S 99, 151, 206
Mathur, A 171
Mato, S 350
Mato Díaz, S 371
Matos, J 50
Matsukawa, Y 102
Matsumoto, K 193
Matsumura, S 71, 355
Matsushita, T 247
Matsuyama, K 355
Matteis, P 140, 237, 321
Mauirce, C 84
Mauro, N 269
Maveety, J 74
May, G 192
May, J 307
Mayrhofer, P 370, 371
Maziasz, P 146
McBow, I 330
McCabe, R 117, 170, 171, 230
McCallum, R 145
McClain, D 195
McClellan, K 92, 179, 195, 263
McClimon, C 263
McClintock, D 128
McCormick, H 277
McCune, R 86
McDeavitt, S 252
McDonald, A 51, 58, 125
McDowell, D 49, 83, 170, 334
Mcdowell, D 104
McEvily, A 237
McFadden, G 72
McHargue, C 252
McHugh, L 329
McIntosh, P 106, 156, 210, 263, 311, 356
McKenna, I 61, 117
McKenzie, P 334
McKenzie, W 357
McKinney, S 172
McKittrick, J 66
Mclaughlin, S 104
McNabb, P 195
McNelley, T 52, 53, 352, 353
McNutt, J 203
Mechler, S 94
Meco, H 244
Medina, F 110
Medlin, D 170, 238
Medvedev, S 196
Meghlaoui, A 266
Mehta, A 328
Mehta, V 63
Mei, J 194, 235

Meier, M....225
Meier, W....226
Mejia, S....184
Mellenthin, J....168
Mencer, D....114
Mendelev, M....162
Mendes, F....119
Mendez, J....84
Mendez, P....191, 320
Mendis, C....187, 241
Mendoza, R....262
Menéndez, O....47
Meng, F....245
Menon, S....296
Mercer, G....147
Merrill, F....141
Merrill, J....152
Meskers, C....201, 255, 302, 345
Mesquita, A....119
Messner, T....202
Metson, J....106, 227
Meuffels, P....274
Meydanoglu, O....295
Meyer, H....338
Meyer, L....57
Meyer, M....79
Meyers, M....66, 67, 110, 160, 169, 215, 257, 267, 316, 317, 333, 334, 358
Meyers, W....110
Mezin, H....357
Mhaisalkar, S....253
Mi, S....274
Mialhe, P....281
Miao, H....365
Miao, J....130, 367
Michael, J....248
Michael, N....105
Michal, G....233, 234
Michal, S....191, 245, 317
Michler, J....230
Middlemas, M....128
Middleton, C....106
Migchielsen, J....165
Mihalkovic, M....44
Mikulowski, B....52, 353
Miles, M....126, 127, 270
Miller, B....225
Miller, G....145
Miller, H....117, 176
Miller, J....163, 340
Miller, M....54, 93, 146, 162, 166, 262, 310, 318, 328
Miller, S....41
Miller, W....86
Millett, P....99, 252
Mills, M....56, 73, 131, 146, 183, 193, 225, 247, 264, 294, 340
Mimaki, T....150
Min, S....47
Min, Y....356
Minh, N....86
Minich, R....278
Minor, A....76, 307
Miodownik, P....232, 341
Miracle, D....162, 246, 317
Mironov, S....54
Miryala, M....214
Mishima, Y....350
Mishin, Y....276
Mishra, A....257
Mishra, B....242, 291
Mishra, C....211
Mishra, R....154, 157, 158, 188, 240, 307
Mishra, S....203
Misra, A....102, 104, 143, 155, 171, 174, 199, 230
Misra, D....216, 267, 354
Misra, M....333
Missalla, M....156
Missori, S....321
Mitchell, D....303
Mitchell, M....328
Mitsche, S....221, 273
Mitsuishi, K....208
Mitsuoka, N....245
Miwa, K....134, 361
Miyake, M....70, 192, 202
Miyamoto, G....193
Miyamoto, H....150
Mizusawa, A....254
Moats, M....163
Moavenzadeh, J....352
Modinaro, D....190
Moeck, P....40
Moelans, N....43, 117, 301
Moenig, R....229
Moffatt, S....264
Mogilevsky, P....118
Mohamed, A....325
Mohamed, F....205, 335
Mohamed, W....153
Mohandas, A....358
Mohri, T....169
Moitra, A....155
Moldovan, D....50, 100
Moldovan, P....180, 319
Molina, J....225
Moll, A....46
Moll, S....251
Molodova, X....206
Moloney, M....232
Mondal, K....219, 271
Montanari, R....140, 321
Monteiro, A....222
Monteiro, S....70, 114, 166, 167, 221, 222, 273, 321, 346, 362, 363
Moody, N....49, 79, 82, 126, 129, 173, 179, 182, 233, 236, 282, 285, 287, 288, 289, 333, 367
Mook, W....76
Moon, H....47
Moon, J....88
Moon, K....192
Mooney, A....211
Moore, K....47, 249
Moore, R....310
Moosbrugger, J....236
Moraes, J....263
Moran, B....61
Moreno, H....214
Moreno, J....302
Moreno Exebio, J....320
Morgan, D....72, 199, 223, 355
Morgenstern, R....123
Moriarty, J....91
Morin, P....363
Morisaku, K....48
Morishige, T....239
Morral, J....364
Morrell, R....303
Morris, C....141
Morris, D....97, 148, 203, 255, 304, 347, 349, 352, 353, 370
Morris, J....69, 76, 84, 95, 120, 144, 162, 173, 275, 319
Morris, R....207
Morrison, D....236
Morrissey, R....182
Morrow, B....340
Morsi, K....90, 140, 192
Mortarino, G....237, 321
Mortensen, A....349
Mortensen, D....361
Moscoso, W....57
Moscovitch, N....337
Mosengue, N....361
Moser, M....370, 371
Moss, S....197
Mottern, M....135
Mourao, M....301
Mourer, D....77, 122, 175, 176, 231
Moxson, V....88
Mozolic, J....329
Mrozinski, T....245
Mubarok, A....68
Muddle, B....196, 275, 294, 309
Mueller, J....333
Mueller, S....282
Mukai, T....100, 189, 291
Mukherjee, A....48, 285
Mukherjee, M....178
Mukherjee, R....43
Mukherjee, S....288
Mulder, A....213
Müller, C....206
Mulyadi, M....193
Mulyukov, R....205
Munoz, J....43
Muñoz, V....281
Muñoz-Morris, M....203, 353
Münstermann, R....274
Muntele, C....41, 94, 152, 208, 235, 299, 327, 359
Murakami, H....351
Murakami, M....223
Muraleedharan, V....363
Muransky, O....250
Murase, K....272
Murayama, N....208
Murch, G....44
Murdoch, D....159
Murphy, C....316
Murphy, K....175
Murr, L....110, 281, 369
Murray, C....328
Murray, M....290
Murty, B....334
Murty, K....153
Murzinova, M....54
Musil, J....142
Müßener, D....349, 370
Muthubandara, N....44

N

Na, M 61
Na, Y 112, 361
Nachimuthu, P 243, 299
Nadano, T 48
Nafisi, S 272
Nag, S 166, 181, 194, 275, 340
Naga, S 261
Nagai, T 70
Nagaraj, B 231
Nagasawa, K 94
Nagasekhar, A 290
Nagem, N 213
Nahar, M 221
Naidenkin, E 258
Naik, S 354
Nair, A 215
Nair, M 211
Najjar, S 350
Nakagawa, I 300
Nakai, Y 217
Nakajima, K 146
Nakamura, T 186
Nakao, H 342
Nalagatla, D 75
Namilae, S 327
Nan, H 295
Nanninga, N 212
Nanstad, R 128, 284
Napolitano, R 79, 86, 126, 179, 233, 282
Narayan, J 45, 105, 145, 261
Narayan, R 105, 110, 215
Narayana, C 196
Narayanan, B 146
Narendra Kumar, G 159
Narita, H 48
Narvekar, R 171
Nascimento, D 221
Nasipuri, T 213
Nastac, L 138
Nastasi, M 71
Natesan, K 292
Natishan, P 234
Navarra, P 234
Navarro, F 119
Nawaz, A 182
Nayak, S 180
Nazarov, A 205
Needleman, A 230
Needs, R 196
Neelakantan, S 88
Neelameggham, N 85, 125, 132, 133, 163, 178, 186, 188, 219, 238, 240, 270, 288, 289, 335, 336
Neife, S 125, 126, 265
Neil, C 189
Neira, A 193
Nelson, S 242
Nelson, T 127
Nemanich, R 84, 131, 132, 184, 237
Nemir, D 281
Neophytides, S 190
Nesbitt, C 333
Netskina, O 369
Nettles, K 327
Neumann, P 83
Neumann, S 287
Newbauer, T 234
Newbery, A 51
Newman, J 77
Newman, K 293
Ng, H 294
Nghiem, N 202
Nguyen, K 358
Nguyen, T 122
Nguyen, V 271
Ni, C 60
Nicholson, D 162, 327, 342
Nichtova, L 142
Nickel, D 57
Nickens, A 271
Nicola, L 230
Nicolaou, P 88
Nie, J 146, 289, 337
Nie, Y 132, 366
Nie, Z 190, 198
Niederstrasser, J 320
Nieh, T 111, 216
Niehoff, T 280
Niendorf, T 236
Nieto, J 350
Nieto Hierro, J 371
Niezgoda, S 103
Nikles, D 308
Nikulin, A 309
Ningileri, S 64, 157, 171, 172, 279, 312
Nishida, K 223
Nishimiya, Y 178
Nishimura, T 75, 327
Nishiyama, N 163, 360
Niu, X 67
Nixon, M 81, 118
Niyomwas, S 192
Nobuhiro, I 245
Noda, T 98
Nogita, K 75, 265, 326, 327
Nogueira, T 359
Noh, B 345
Noh, J 283
Noh, S 98
Noh, T 115
Noldin, J 79
Noll, H 153
Noor, A 271
Norfleet, D 131, 183
Noro, J 204
Northwood, D 290
Norton, D 101, 153
Nose, Y 272, 321
Novak, V 142
Nowak, J 76
Nowell, M 69
Nowill, C 108
Noyan, I 328
Nuggehalli, R 89, 139, 194, 247, 296
Nurislamova, G 54
Nürnberg, M 241
Nutt, S 52, 122
Nyberg, E 85, 132, 133, 186, 188, 238, 240, 288, 289, 335, 336
Nychka, J 68, 316, 317
Nye, R 114

O

O'Brien, E 330
O'Brien, F 215
O'Brien, J 271
O'Brien, K 263
O'Dell, L 106
O'Dovero, P 114
O'Keefe, M 277
Oberson, P 73, 246
Ode, M 351
Odessky, P 258
Oechsner, A 44
Oehring, M 149, 347, 350
Oguma, N 367
Ogunmola, B 65
Ogura, K 271
Oh, C 74, 284
Oh, H 260, 261
Oh, K 46, 88
Oh, T 117
Oh-ishi, K 55, 187, 241
Ohashi, T 92, 204
Ohba, Y 79
Ohm, V 125
Ohno, M 169
Ohnuma, I 254, 300
Ohnuma, T 72
Ohriner, E 346
Ohtomo, A 71
Oi, T 273
Oikawa, T 308
Oishi, K 146
Okabe, S 186
Okabe, T 69, 113, 166, 221, 272, 273, 321, 362
Okada, M 237
Okada, N 193
Okada, O 254
Okamoto, S 115, 223
Okeke, C 126, 265
Oki, S 239
Okino, H 223
Okitsu, Y 258, 307
Okuofu, C 346
Okura, T 186
Olaya-Luengas, L 48
Oleneva, T 348
Oliana, R 79
Oliveira, A 210, 263
Oliveira, H 119
Oliver, E 250
Olmsted, D 116
Olsen, A 109
Olsen, E 127
Olson, D 291
Olson, G 61, 145, 188, 234, 310
Omran, A 39
Omura, N 361
Onaka, S 184
Onck, P 316
Ontman, A 103
Opalka, S 136
Opeka, M 347, 370
Oportus, J 288, 289
Orlikowski, D 72
Orlov, D 150
Orlovskaya, N 243

Orsborn, J 88
Ortalan, V 355
Ortiz, A 367
Ortiz, C 302
Ortiz, U 184
Osborn, W 368
Osenbach, J 119, 121, 173, 228
Osetskiy, Y 73
Osetsky, Y 102
Ossi, P 252
Oster, N 145
Ostolaza, K 148
Oswald, M 240
Ota, N 47
Oteri, E 48, 341
Otsuka, K 306
Ott, R 162, 261
Otto, A 347, 348
Ou, S 229
Ouimet, L 86
Ouyang, F 228, 253
Ovcharenko, A 343
Öveçoglu, M 40, 91
Ovsianikov, A 110
Owate, I 126, 265
Oye, H 226
Øye, H 226, 326
Ozaki, C 227
Özgün, E 91
Ozolins, V 245

P

Packard, C 68
Padilla, R 245
Padron, I 297
Paglieri, S 135
Paidar, V 350
Paik, C 338
Paine, M 160
Paisley, D 92
Paital, S 47, 359, 361
Pal, U 124, 133, 177
Palanisamy, B 234
Palau, P 366
Palkowski, H 87, 298
Palm, M 98, 204
Palmlund, D 172
Palmstrom, C 131
Palomar, M 137
Palosz, B 269
Pan, T 338
Pan, X 338, 364
Pan, Z 71, 206
Pandey, R 200
Pang, J 92, 228
Pang, L 63
Paninski, M 98
Panov, A 211, 263, 311
Pantke, K 336
Pantleon, W 83, 93, 328, 342
Pao, P 294
Paquin, D 320
Paramonova, E 268
Pareige, P 198, 354
Park, C 296
Park, E 318
Park, H 97, 283, 332
Park, J 44, 45, 93, 136, 251, 262, 284, 328
Park, K 361
Park, S 48, 107, 155, 195, 238, 263, 283, 295, 331
Paromova, I 211, 311
Parra, M 247
Parra Garcia, M 195, 263
Parry, S 156
Parthasarathy, T 72, 183
Parvin, N 52
Paster, F 178
Patel, K 233
Patel, V 192
Pati, S 124, 133
Patrick, B 279
Paturaud, F 56
Paul, J 149, 347
Pawlek, R 365
Payton, E 294
Pearton, S 101, 153
Peaslee, K 219
Pecharsky, V 95, 144
Peck, A 319
Pedersen, T 109
Peiyang, S 323
Pekguleryuz, M 85, 132, 133, 186, 188, 238, 240, 288, 289, 335, 336
Pellati, G 140
Pelton, A 328
Peng, B 255
Peng, K 205
Peng, L 239, 240, 275, 335
Peng, R 297
Peng, T 303
Peng, Y 51
Pennycook, S 274
Peralta, P 92, 179, 195, 237, 247, 263
Perander, L 106
Pereira, C 213
Perepezko, J 304
Perez, R 45
Perez-Bravo, M 148, 349
Perez-Tijerina, E 184
Perez-Trujillo, F 350, 371
Periaswamy, P 200
Pericleous, K 98, 177, 315
Perrot, P 199
Pesyna, G 147
Pétein, A 97
Peter, W 295
Peters, H 266
Peters, P 148
Peterson, B 230, 246
Peterson, E 106, 114, 214
Peterson, R 155, 163, 280
Petralia, S 140
Petrov, A 168
Pettersen, T 212
Pfetzing, J 149
Phanikumar, G 137
Phelan, D 304
Phillips, D 99
Phillips, E 210
Phillpot, S 252
Picard, D 325
Piccardo, P 140
Pickard, C 196
Pickens, J 194
Pihl, J 338
Pilchak, A 246
Pillai, S 177
Pilone, D 47, 231
Pimentel, N 79
Pinasco, M 140, 321
Piñero, N 356
Pint, B 77, 122, 123, 175, 231
Pinto, E 315
Pippan, R 56, 57, 285, 334, 369
Pirhoseinloo, H 158
Pirling, T 298
Pirouz, P 73
Piskunov, S 222, 223
Pisutha-Arnond, N 72
Plapp, M 168, 324
Pletcher, B 262
Plumtree, A 367
Pochan, D 161
Pocock, L 297
Podolskiy, A 57
Poirier, J 227
Polat, A 181
Polcawich, R 122
Polesak III, J 189
Pollard, M 146
Pollock, T 49, 82, 129, 130, 182, 187, 236, 251, 285, 333, 351, 355, 367
Pomykala, J 345
Ponnusamy, M 160
Poole, W 53, 189
Poon, J 319
Poon, S 68, 319
Poorganji, B 193
Popa-Simil, L 94, 152, 235
Popescu, C 180
Popescu, G 180
Popko, D 114
Popov, M 258
Popova, L 181
Porfiri, M 129
Portella, P 49, 82, 129, 182, 236, 285, 333, 367
Porter, W 182
Potesser, M 113, 301, 302
Potirniche, G 155
Potocnik, V 315
Pouchon, M 230
Poudel, B 59
Poulain, X 179
Poulsen, H 76, 93, 251, 328, 342
Pourboghrat, F 277, 347
Pourmostadam, S 128
Powell, A 177, 186, 232
Powell, B 86
Powell, J 174
Power, G 356
Powers, M 125
Pownceby, M 330
Pozzi, C 140
Pradeilles, N 181
Pradhan, D 178
Pradhan, N 309
Prangnell, P 306, 353
Prasad, S 89, 90, 173, 248
Prasad, V 336

Prasanna Kumar, T 137
Prater, J 105
Pratt, P 298
Prebble, J 220
Prepeneit, J 357
Preuss, M 178
Prevey, P 77
Prillhofer, B 125, 165, 202, 220
Prime, M 298
Pritantha, W 244
Privé, D 112
Priyantha, W 243
Proffen, T 144
Proshkin, A 226
Proulx, J 320
Proust, G 117, 118, 229, 279
Provatas, N 168
Provenzano, V 176
Przybyla, C 49
Pshenichnuk, A 54
Pucci, A 157
Pugazhenthy, L 242
Pulskamp, J 122
Purcek, G 52
Purushotham, S 267
Puthicode, A 363
Puthucode, A 193, 194
Puxley, D 157
Pyczak, F 56, 130
Pyshkin, S 105

Q

Qazi, J 194
Qi, Y 46
Qian, H 132
Qian, K 205, 226
Qidwai, M 209, 210
Qin, H 322
Qin, W 244
Qingxiu, J 312, 313
Qiu, D 124
Qiu, K 269
Qiu, S 109, 214
Qiu, X 204
Qu, J 89, 233
Quach, D 223
Quan, Q 325
Quast, J 195
Quelennec, X 354
Querin, J 212
Quinones, S 110
Quintana, M 146
Quintino, L 80

R

Raab, G 54
Raabe, D 118, 148, 170
Rabba, S 226
Rack, H 138, 194
Rack, P 217, 251
Radhakrishnan, B 327
Radiguet, B 198, 354
Rae, A 172
Rae, P 174, 198, 249
Raeisinia, B 53
Rafea, M 165
Raffaelle, R 152
Raghavan, P 264, 311
Raghavan, R 158
Raghunathan, S 247
Rahbar, N 67
Rahman, M 333
Rahman Rashid, R 46, 80, 281
Rainforth, M 134, 138
Rainforth, W 371
Raj, R 89, 139, 194, 247, 296
Raja, K 333
Rajagopalan, J 286
Rajagopalan, S 181, 340
Rajamoorthy, S 178
Rajan, K 191, 244, 293, 339
Rajasekhara, S 332
Rajgarhia, R 140
Rajkiran 281
Rajkiran, G 46, 80
Rajulapati, K 67
Rakowski, J 189, 190, 338
Ram-Mohan, L 364
Ramanath, G 39, 59, 101, 152, 207, 260, 308
Ramanujan, R 261, 267
Ramaswamy, J 159
Ramesh, K 100, 170, 334
Ramesh, R 167
Ramirez, J 265
Ramos, A 204
Ramos, K 141, 174
Randall, N 174
Randow, C 341
Ranganathan, S 186
Rangasamy, V 106, 160
Rao, A 59
Rao, B 55
Rao, K 330, 336
Rao, P 240
Rao, S 72, 183
Rao, W 224
Rashmi 71
Rata, D 168
Ratvik, A 227
Ravelo, R 140
Ravi, V 134
Ravindra,, N 105
Ravindra, N 63, 64, 104, 105, 247, 296, 297
Ravindran, C 289
Ravindranath, R 77
Ravishankar, N 308, 363
Rawlins, C 219
Ray, K 283, 284
Ray, P 364
Ray, V 153, 208
Raymond, G 363
Read, C 171
Read, J 327
Ready, J 296
Real, C 137
Reddy, R 163, 178, 219, 270, 271
Reddy, S 46, 80
Redfern, A 109
Redkin, A 179, 314
Reed, B 169, 278
Reed, M 114
Reed, R 276, 324
Reedy, E 195
Reek, T 357
Rehbein, D 162, 200, 254
Reichstein, S 123, 124
Reilly, C 79
Reinbold, L 228
Reinhard, C 349, 371
Reis, J 214
Reis, L 80
Reis, R 119
Reitan, B 99
Reiten, E 99
Reiter, G 197
Reitz, J 98
Ren, F 101, 153
Ren, I 359, 361
Ren, J 133
Ren, R 367
Ren, Y 69, 93, 142, 197, 250, 251, 269, 352
Ren, Z 59
Renaudier, S 357
Renavikar, M 228
Rencis, J 333
Repetto, E 263
Restrepo, O 323
Retford, C 224, 364
Rettenmayr, M 40
Reusch, F 220
Reuther, K 225
Révész, Á 353
Reyes-Villanueva, G 122
Reynante, B 60
Rezaie, H 41
Rezvanian, O 184
Rhee, M 72
Richard, C 51, 159
Richard, D 315
Richards, C 195
Richards, D 169
Richards, R 195
Richards, V 87, 219
Richardson, J 198, 318
Ricketts, M 338
Rickman, J 116
Ricolleau, C 308
Ried, P 86
Rieken, J 90
Riesterer, J 363
Rigg, P 141
Rijkeboer, A 211
Rijnders, G 115
Rimoshevsky, S 302
Rinderer, B 164
Ringnalda, J 317
Rioja, R 287
Rios, O 256, 324, 365
Rios, P 262
Risanti, D 108
Rist, M 193
Ritchie, R 66, 110, 130, 160, 215, 267, 316, 358
Ritter, C 159
Ritter, Y 99
Rivas, C 245
Rivera, R 316
Rivera Diaz del Castillo, P 108
Rivero, R 64, 296
Riveros, R 330

Rivolta, B 237, 321
Rizzi, N 255
Ro, Y 286
Robbins, D 249
Roberts, C 179, 180
Robertson, C 83
Robertson, D 302
Robertson, I 117, 225
Robinson, A 64
Robles Hernandez, F 260, 322
Rödel, J 134
Rodrigo, R 213
Rodriguez, M 189
Rodriguez G., X 125
Roeder, R 66, 110, 160, 161, 215, 267, 316, 358
Rogers, J 70, 162, 244
Roh, J 212
Rohan, P 271
Rohrer, G 117, 209, 264
Rokhlin, S 247
Rollett, A 43, 45, 49, 100, 117, 153, 154, 180, 209, 210, 212, 222, 264, 368
Romansky, M 277
Rong, Y 155, 156
Ronning, F 174
Roos, A 72
Rosefort, M 320
Rosen, G 188
Rosenberger, A 77, 122, 175, 231, 246
Rosenberger, M 181, 362
Ross, F 84
Ross, I 371
Rostamian, A 305
Roters, F 118, 148, 170
Roth, J 260
Roth, R 65
Roth-Fagaraseanu, D 148, 348, 371
Rothe, C 348
Rothermel, M 299
Roussel, P 200
Rovere, F 370, 371
Rowenhorst, D 61, 103, 153, 210, 355
Rowson, J 113
Roy, A 338
Roy, I 205, 335
Roy, S 295
Royva, T 202
Rozenak, P 107
Ruano, O 353
Rudd, R 278
Rui, G 41
Ruiz, G 165
Ruiz, M 245
Rumpf, K 56
Rundell, S 258
Ruoff, A 196
Rupert, T 229
Rusche, S 109
Russ, S 149
Russell, A 95, 279
Russell, K 94, 166
Russo Spena, P 237, 321
Rutledge, S 213
Rutman, D 114, 214
Ruvalcaba-Jimenez, D 209
Ryabkov, D 123
Rye, K 213, 325
Ryu, T 193

S

Saage, H 98, 194, 305, 334
Sabirov, I 100
Sachdev, A 107, 154, 188, 240
Sadayappan, K 85
Sadhukhan, P 310
Sadoway, D 270
Sadrabadi, P 174
Saeed, U 229, 343
Saegusa, T 254
Saether, E 99
Safarik, D 135, 369
Sahin, F 192
Sahu, T 226
Saif, T 286
Saito, K 223
Saitoh, H 342
Sakai, J 223
Sakai, T 202, 367
Sakamoto, D 48
Saket Kashani, M 180
Sakidja, R 304
Salam, B 301
Salamanca-Riba, L 223
Salame, C 281
Salazar-Villalpando, M 164
Saldana, C 55
Saleh, T 155
Salehpour, B 158
Salem, A 88
Sales, B 144
Salick, D 161
Salimgareeva, G 258
Salishchev, G 54, 205
Salman, U 224
Salvador, P 292
Samant, A 80
Samanta, A 118, 130, 364
Samaras, M 230
Sanchez, R 167
Sánchez, R 114
Sandhanam, A 271
Sandhu, P 232
Sands, T 102
Sangiorgi Cellini, G 272
Sano, T 295
Santafé, H 167
Santella, M 338
Santerre, R 159
Santos, E 119
Santos, H 210
Santos, L 166, 356
Santos, T 80
Saotome, Y 163, 360
Saphin, E 205
Sargent, G 250, 257
Sarihan, V 228, 296
Sarikaya, M 66, 110, 160, 161, 215, 267, 316, 358
Sarma, D 93
Sarma, V 55, 334
Sarosi, P 56, 73, 146
Sarvinis, J 164
Sasaki, H 202
Sastry, S 53, 89
Satapathy, R 269
Sato, H 181
Sato, N 124
Sato, Y 201, 227
Saunders, A 141
Saunders, N 232, 341
Sauvage, X 354
Savage, G 289
Savan, A 244
Saw, C 141
Saxena, A 140
Saylor, D 72
Scattergood, R 205
Scavino, G 140
Schaedler, T 175
Schaef, W 367
Schafler, E 52, 353
Schalk, T 285
Scharf, T 90
Scherer, D 331
Scheriau, S 56
Schille, J 232, 341
Schilling, J 196
Schillo, M 135
Schimansky, F 256, 305
Schlegel, S 182
Schmauder, S 158, 237, 239
Schmetterer, C 343, 344
Schmid-Fetzer, R 186, 337
Schmidt, C 240
Schmidt, H 156
Schmidt, S 251, 348
Schmidt, T 165
Schmitz, G 98
Schneibel, J 56, 332
Schneider, A 315
Schneider, J 53, 141, 161, 212
Schoning, C 227
Schramm, J 319
Schroers, J 359
Schroth, J 126
Schuetze, M 349
Schuh, C 68, 248, 286
Schultz, R 287
Schumacher, G 94
Schütze, M 371
Schvezov, C 87, 181, 272, 362
Schwaiger, R 174, 317, 333
Schwam, D 288
Schwardt, J 110
Schwartz, A 249
Schwarz, M 177
Schwarz, R 135, 260, 369
Scott, B 331
Scott, C 118
Scott, M 70
Scwartz, C 141
Sears, J 104, 155, 208, 303
Sebright, J 123
Sediako, D 232, 239, 337
Sediako, O 232
Sedlacek, D 109
Seelaboyina, R 42
Seelam, U 270
Seetharaman, S 247

Seidman, D.....61, 247, 310
Seifert, H.....44, 256, 324, 365
Seki, Y.....48, 67
Sekulic, D.....75
Seman, T.....296
Semenova, I.....258
Semenova, O.....365
Semiatin, L.....54
Semiatin, S.....88, 180, 250, 257, 340
Semones, J.....205
Senft, D.....39, 59, 101, 152, 207, 260, 308
Seniw, M.....236
Senkov, O.....65, 317
Senkova, S.....65
Senn, J.....189
Seo, D.....174
Seo, J.....333
Seo, S.....327, 331
Seppala, E.....278
Serbruyns, A.....301
Sereni, S.....188
Serra, A.....73
Setty, K.....139
Severo, D.....315
Sewell, T.....141, 174
Sha, Y.....251
Shaarbaf, M.....57
Shackelford, J.....358
Shagalina, S.....258
Shaghiev, M.....65
Shahab, A.....53, 54
Shahbazian Yassar, R.....158, 241
Shaidulin, E.....160
Shaigan, N.....243
Shalini, T.....176
Shamsuzzoha, M.....200, 308, 312
Shan, Z.....50, 76, 99, 149, 205, 257, 306, 307, 352
Shang, C.....291
Shang, L.....134
Shang, S.....186
Shankar, M.....55, 151
Shanmugasundaram, T.....334
Shao, L.....199, 252
Shao, R.....136
Shao-Horn, Y.....72
Sharafat, S.....94
Sharafutdinov, A.....54
Sharma, A.....70
Sharon, J.....229
Sharp, I.....308, 324
Sharp, J.....58
Sharpe, W.....64
Shaw, L.....205, 218, 367, 368
She, Y.....136
Shechtman, D.....90
Shelton, E.....256
Shen, C.....73, 138, 224, 225, 275
Shen, H.....265
Shen, J.....111, 319
Shen, T.....260, 306, 342, 343
Shen, X.....313
Shen, Y.....251, 360
Sheng, H.....218
Sheng, W.....72
Shenoy, G.....93
Shepard, M.....77, 122, 175, 231
Shepelev, D.....290
Sherby, O.....258, 332
Sherman, D.....310
Shet, S.....105, 296
Sheu, S.....287
Shi, D.....59, 101
Shi, J.....184
Shi, L.....349
Shi, W.....85
Shi, X.....132
Shi, Z.....78, 140, 314, 326, 366
Shibata, J.....113, 208
Shields, J.....346
Shifflet, D.....228
Shiflet, G.....44, 68, 103, 111, 319
Shih, D.....172, 327
Shih, T.....301
Shim, S.....332
Shimizu, Y.....360
Shin, B.....47
Shin, C.....83
Shin, D.....48, 55, 126, 307
Shin, H.....102, 152
Shin, J.....47, 309
Shin, K.....127, 187, 240
Shin, S.....324
Shingledecker, J.....146, 221
Shinozaki, D.....174
Shipova, O.....211
Shiu, K.....230
Shivkumar, S.....108
Shiwen, B.....178
Shoji, T.....177, 189
Shqau, K.....135
Shuey, S.....201, 280
Shui-ping, Z.....330
Shuiping, Z.....214
Shull, R.....185
Shunwen, W.....91
Shurov, N.....314
Shurygin, A.....179
Shutthanandan, V.....94, 243
Sibila, A.....357
Sicha, J.....142
Sickafus, K.....251, 252, 343
Siddiq, A.....237
Sievert, R.....149
Sigworth, G.....164
Sikha, S.....105
Sillekens, W.....189
Silva, G.....237, 321
Silva, H.....210
Silva, M.....119
Simagina, V.....369
Simakov, D.....326
Simmons, J.....43, 60, 102, 103, 153, 154, 209, 262, 309, 323, 324, 325, 355
Simões, T.....159, 214
Simpkins, R.....149
Sinclair, C.....53, 118, 189
Sinclair, R.....84
Singh, A.....87, 189, 199, 290, 291
Singh, G.....156
Singh, J.....49
Singh, N.....63, 104, 365
Singh, P.....86, 190
Singh, R.....308
Singh, V.....268
Singheiser, L.....50, 286
Sinha, S.....141, 342
Sinha, V.....70
Sinitsa, N.....181
Sintay, S.....49, 154, 368
Sisneros, T.....279
Sisson, R.....108, 127, 234
Sitaula, S.....338, 339
Sitdikov, V.....306
Sittner, P.....250
Sjöberg, G.....87
Skladan, K.....159
Skrotzki, B.....149, 255
Skrotzki, W.....183, 225
Skury, A.....222, 273, 321
Skybakmoen, E.....227
Slater, T.....110
Sloan, T.....233
Smarsly, W.....97, 101, 104, 114, 348
Smelser, N.....140
Smetniansky-De Grande, N.....299
Smirnov, S.....57
Smith, C.....47, 225
Smith, M.....106
Smith, P.....311
Smith, R.....189, 243, 244, 303
Smyslov, A.....205
Snead, L.....303
Snead, M.....160
Snugovsky, P.....277
Snyder, G.....145
Soare, M.....43, 116
Soboyejo, W.....67
Soffa, W.....365
Sohn, H.....193
Sohn, S.....44, 45
Sohn, Y.....175, 190, 324, 351
Sokolov, M.....128, 284
Sokolowski, P.....145
Solak, N.....302
Solheim, A.....227
Solis, F.....316
Solli, L.....108
Somani, M.....354
Somekawa, H.....189
Somerman, M.....66
Sommer, K.....57
Sommitsch, C.....221, 273
Son, C.....136
Son, J.....274
Son, S.....361
Song, C.....81
Song, G.....359
Song, H.....221
Song, J.....300
Song, M.....208
Song, S.....111, 216
Song, W.....336
Song, X.....40, 193, 324
Song, Y.....59
Sopori, B.....63, 64, 104, 296
Sordelet, D.....162
Sorlie, M.....325
Soto, K.....369
Souza, F.....359
Souza, R.....358
Spaepen, F.....43, 117

Spain, J.....347
Spaldin, N.....167
Spanos, G.....61, 103, 210
Spearot, D.....140
Specht, E.....142
Speck, T.....317
Spemann, D.....299
Spence, K.....269
Spencer, D.....352
Spiegel, M.....244
Spitzer, D.....156
Spohr, E.....222
Spoljaric, D.....113
Spowart, J.....355
Spranklin, J.....220
Sreenivas Rao, K.....137
Sreeranganathan, A.....262
Srinivasan, R.....294, 295
Srivastava, A.....71
Srivastava, C.....39, 200, 261
Srolovitz, D.....116
Stach, E.....307
Stacy, J.....231
Stafford, R.....267
Stafford, S.....110
Stam, M.....213
Stanescu, C.....319
Stanica, C.....319
Stanzl-Tschegg, S.....367
Stark, A.....256, 304, 305
Starostenkov, M.....181
Stas, M.....159
Stein, F.....98
Stein, V.....135
Steinbach, I.....146, 239, 256, 324
Steinberg, M.....163
Steinbrech, R.....50, 286
Steinbrecher, T.....317
Steingart, D.....109, 213
Stelzer, N.....153
Stemmer, S.....274
Stephenson, K.....94
Stevens, A.....203
Stevens, R.....43
Stevenson, J.....190
Stewart, I.....234
Stewart, J.....180, 305
Stockinger, M.....221
Stodolnik, B.....317
Stoecker, C.....130
Stoica, A.....142, 318
Stoica, G.....297
Stokes, A.....66
Stokes, K.....101, 192, 331
Stolken, J.....130
Stoller, R.....102, 343
Stone, D.....365
Stone, H.....297
Stonis, M.....107
Stoots, C.....271
Støre, A.....227
Störmer, M.....335
Storozhenko, P.....369
Stotter, C.....221
Stoudt, M.....103
Stoughton, T.....282
Stout, M.....229
Strachan, A.....91
Streitz, F.....169
Struhr, U.....298
Stuart, P.....203
Stukowski, A.....99
Stukowski, M.....244
Su, J.....53
Su-Chi, I.....138
Suarez, M.....48
Suarez, O.....321
Suárez, O.....47
Subbaian, B.....106
Subbarayan, G.....139
Subhash, G.....69
Subra, S.....307
Subramanian, K.....119, 120, 121, 142, 248, 271
Subramanian, R.....153
Sudhakar, N.....145
Suenaga, S.....75, 327
Suganuma, K.....173, 199, 200, 228, 253, 300, 343
Sugimoto, J.....74
Suh, C.....293
Suh, D.....74
Sukumaran, C.....159
Sun, F.....81
Sun, G.....298
Sun, H.....42, 359
Sun, J.....319
Sun, K.....357
Sun, N.....133
Sun, P.....150, 206, 352
Sun, W.....256
Sun, X.....198, 298
Sun, Y.....56, 93
Sun, Z.....132
Sunda-Meya, A.....132
Sundararajan, A.....362
Sundarraj, S.....232, 289
Sung, S.....98
Suñol, J.....56
Suput, M.....124
Suresh, S.....82, 118, 316
Suryanarayana, C.....270
Suss, A.....211, 263, 311
Suter, R.....310, 328
Sutton, M.....121
Suwas, S.....51, 295
Suzuki, M.....48, 163, 219, 270
Svoboda, M.....236
Swadener, J.....144, 230
Swaminathan, S.....52, 53, 151, 353
Swamy, V.....196
Swamydhas, V.....154
Swart, D.....192
Sweatman, K.....75
Sweeney, D.....294
Syed, B.....82
Syed Asif, S.....307
Sylvester, K.....347, 370
Syn, C.....258, 332
Szczepanski, C.....237, 367
Szot, K.....274
Szpunar, J.....241

T

Tabachnikova, E.....57
Tack, W.....194
Tada, S.....127
Tafra, E.....115
Tagliavia, G.....129
Taheri Hashjin, M.....158
Tajik, A.....77
Takahashi, A.....94, 131
Takahashi, T.....71, 306
Takai, K.....182
Takai, O.....161
Takaku, Y.....254, 300
Takano, C.....301
Takasu, I.....79
Takasugi, T.....351
Takata, N.....258, 307
Takechi, H.....97
Takeda, H.....360
Takeda, O.....201
Takeguchi, M.....208
Takeuchi, I.....223
Takeyama, M.....305
Takizawa, R.....367
Talavera, M.....210
Taleff, E.....60, 102, 153, 157, 209, 262, 309, 355, 369
Talke, F.....317
Talling, R.....247
Tamerler, C.....161
Tamerler Behar, C.....358
Tamimi, S.....52
Tamirisa, S.....246
Tamirisakandala, S.....295
Tamura, K.....48
Tamura, T.....134, 361
Tan, C.....51, 58, 125
Tan, P.....246
Tan, S.....63, 344
Tanaka, H.....184
Tanaka, K.....204
Tanaka, M.....48, 208, 254
Tanaka, T.....193
Tanaka, Y.....146
Tang, H.....135
Tang, L.....215, 226
Tang, M.....71, 72, 343
Tang, W.....145
Tang, X.....41, 356
Tanner, C.....200
Tanniru, M.....260
Tao, D.....42
Tao, J.....50, 62, 150, 283
Tao, N.....150, 354
Tao, W.....337
Taptik, I.....107
Tarcy, G.....213, 357
Tata, M.....140, 321
Tatenuma, K.....164
Tateyama, M.....208
Tatiparti, S.....260
Tatsumi, K.....254
Tauson, V.....39
Tavsanoglu, T.....123, 233
Taylor, B.....121
Taylor, M.....112, 213
Taylor, P.....201, 280
Tayon, W.....278
Tchakhalian, J.....167

Teale, R 237, 247
Tedenac, J 181, 260
Telang, A 277
Telesman, J 176
Templeton, J 190
Teng, Z 191
Tenhundfeld, G 123
Terada, D 100
Terashima, S 254
TerBush, J 187
Terdalkar, S 333
Tereshko, A 143
Tereshko, I 143
Terrones, L 166, 363
Tessier, J 159, 213
Teter, D 166
Tewari, A 154
Thadhani, N 257
Thein-Han, W 216
Thibault, M 112, 225
Thirumalai, N 116
Thoma, D 166, 209, 230, 351
Thomas, B 110, 362
Thomas, M 129, 255
Thomé, L 251
Thompson, G 39, 207, 261
Thompson, J 261
Thompson, R 42, 122
Thonstad, J 365
Thornton, K 72, 169, 235, 262, 263, 316
Threadgill, P 178
Tian, B 273
Tian, J 218, 367
Tian, Q 42, 246, 339
Tian, Z 326, 366
Tianzu, Y 78, 302
Tiearney, T 365
Tieman, B 310
Tien, L 101, 153
Tierney, C 215
Tikhonovsky, M 57
Tilak, R 165
Tiley, J 191, 198, 309, 355
Tilghman, D 296
Timokhina, I 100
Ting-an, Z 234
Tirschler, W 183
Tischler, J 83, 92, 93, 183, 250, 329
Tiwari, A 95, 144
Tiwari, S 289, 334, 336
Tkacheva, O 179, 314
Tkachuk, A 145
Tobler, E 145
Tochiyama, O 124
Todaka, Y 56, 150
Todd, P 324
Togashi, N 163, 360
Tokita, M 283
Tomasino, T 159, 315
Tome, C 117, 118, 170, 171, 225, 229, 257, 279, 329
Tomesani, L 272
Tomsett, A 225
Tomsia, A 215
Tomus, D 334
Tong, C 44, 230, 296
Tong, L 157, 255
Tong, Z 143
Tonks, D 141, 209, 249
Topic, I 56
Topping, T 51
Torabi, S 276
Torbet, C 182, 251
Toribio, J 50
Toroghinejad, M 57
Torres, K 261
Tortorelli, P 338
Tosta, R 171
Totemeier, A 252
Toyoda, Y 306
Traiviratana, S 334
Tran, T 179, 358
Trau, M 101
Trautmann, C 94, 143, 198, 251, 252, 299, 342
Trautt, Z 116
Trelewicz, J 286
Tremblay, S 361
Trenkler, J 197
Triantafylopoulos, N 190
Tribyshevsky, L 302
Tribyshevsky, V 302
Trichy, G 45, 145, 261
Trinkle, D 91, 140, 196, 224, 249
Trojan, I 196
Truci, H 119
Trujillo, C 174, 332
Trumble, K 55, 57, 136, 151
Trunova, O 50, 286
Tsai, A 87, 199
Tsai, C 244
Tschofen, J 255
Tschopp, M 49, 83, 170, 334
Tseng, C 360
Tseng, H 327
Tseng, Y 101
Tsipas, S 350
Tsirlina, G 326
Tsuchimoto, K 272
Tsuji, N 56, 100, 149, 150, 258, 307
Tsujikawa, M 239
Tsujimoto, M 228
Tsukazaki, A 71
Tsukihashi, F 345
Tsurkan, V 223
Tu, G 140
Tu, K 84, 85, 119, 131, 184, 194, 200, 228, 229, 237, 245, 253, 254
Tubman, N 168
Tucker, G 49
Tucker, J 199
Tulenko, J 252
Tumne, P 277
Turbini, L 120, 277
Turchi, P 169
Turchin, A 220, 362
Turco, T 79
Turner, C 39
Turner, J 105, 338
Turri, G 105
Tursunov, P 326
Tyagi, V 290

U

Ubertalli, G 140
Uche, O 238
Uchic, M 60, 72, 102, 131, 153, 154, 183, 209, 262, 309, 355
Ucisik, A 181
Ucok, I 194
Uda, T 221, 272, 321
Uddin, S 80
Ueno, H 344
Ueshima, M 74
Uesugi, K 326
Uggowitzer, P 257, 336
Uhlenhaut, D 68
Uihlein, A 368
Uju, S 184
Ulfig, R 162
Ullmann, M 240
Umemoto, M 56, 150
Umstead, W 304
Underwood, R 135
Ungar, T 83, 236, 307, 329, 341
Ungár, T 83
Unocic, K 264
Unocic, R 73
Unuvar, C 358
Uotani, Y 350
Upadhyaya, A 180, 234
Upmanyu, M 40, 43, 100, 116
Urbanek, F 320
Usta, M 181
Uttarwar, M 215
Utyashev, F 54
Uyar, F 154

V

Vaagland, J 164
Vaidyanathan, R 128
Vainik, R 220
Valanoor, N 223
Valdez, J 343
Valdez, S 45, 127
Valiev, R 50, 51, 54, 99, 149, 205, 257, 258, 306, 342, 352, 353, 354
van Dalen, M 247
van der Berg, N 253
Van der Giessen, E 230, 316
van der Linden, D 189
Vandermeer, R 206
Van der Meyden, H 109
Vanderspurt, T 136
van der Winden, M 158
van der Zwaag, S 88, 108
Van De Walle, A 139
vanHassel, B 135
Van Hauwermeiren, M 159
Van Quyet, N 129
Van Tyne, C 186
Vanzetti, L 252
Varatharajan, A 223
Varela del Arco, M 274
Varma, S 370
Vasconcelos, P 119
Vásquez, F 323
Vassiliev, S 326

Vasudevan, V 77, 221, 347
Vattre, A 72
Vaughan, G 54
Vazquez B., L 125
Vecchio, K 60, 66, 268
Vedamanickam, S 127
Vehoff, H 367
Vékony, K 315
Velasco, E 165
Velikodniy, A 57
Venkatasubramanian, R 267
Venkatesh, V 88, 138, 193, 194, 246, 294, 340
Venuturumilli, R 234, 280
Veprek, S 139
Verbrugge, M 85
Vergazova, G 227
Verlinden, B 57
Verma, R 64, 134, 157, 241
Verma, V 39
Vernon, C 356
Verweij, H 135
Veselkov, V 315
Veyssiere, P 93, 183
Veyssière, P 73
Vichikganina, L 51
Victoria, M 94, 143, 198, 251, 299, 342
Vidal, E 279, 280, 329
Vidal, V 57
Vieh, C 144
Viehweger, B 348, 349
Vieira, C 114, 273, 346
Vieira, T 204
Vilaça, P 80
Villechaise, P 84
Villegas, J 367
Vinogradov, A 258
Virieux, F 266
Viswanathan, A 51
Viswanathan, G 181, 275, 340
Vitchus, B 171, 172
Vite, M 125
Vitek, J 338
Vitorino, J 114, 346
Vizdal, J 344
Vogel, S 198
Voggenreiter, H 148
Vogt, H 240
Voice, W 235
Volkert, C 229, 285, 286, 287, 288, 289
Voller, V 232
Volpi, F 363
Volz, H 166
Voorhees, P 61, 117, 169, 262, 263
Vratsanos, L 135
Vrestal, J 343
Vurpillot, F 354

W

Wadsworth, J 332
Wagner, B 104
Wagner, J 221, 278
Wagner, M 224
Wagner, V 285
Wagner, W 94
Wahba, J 357
Wain, N 194
Wakabayashi, T 254
Walczak, G 191
Walker, D 327
Walker, L 89, 90
Wall, J 198
Wall, M 249
Walleser, J 254, 327
Wallgram, W 347, 348
Wallick, M 110
Walter, G 234
Walther, F 285
Wan, X 368
Wanderka, N 94
Wang, A 194
Wang, B 43, 44, 96, 221, 324
Wang, C 75, 344
Wang, D 42, 136, 215, 286
Wang, F 112, 277, 369
Wang, G 68, 156, 163, 187, 191, 197, 198, 217, 250, 251, 294, 319, 361
Wang, H 73, 98, 101, 124, 153, 174, 199, 215, 245, 247, 261, 338, 339, 350, 359
Wang, J 50, 51, 52, 55, 56, 150, 204, 216, 241, 366
Wang, K 101, 193
Wang, L 81, 87, 89, 101, 137, 155, 252, 298, 314
Wang, M 41, 193
Wang, N 313
Wang, P 155
Wang, Q 55, 156, 303, 346
Wang, S 56, 59, 212, 214, 292, 298, 331, 335, 337
Wang, T 293
Wang, W 41, 98, 101, 360, 370
Wang, X 66, 142, 162, 198, 318
Wang, Y 42, 43, 61, 69, 71, 73, 75, 92, 93, 96, 116, 122, 138, 140, 141, 142, 144, 149, 168, 169, 186, 188, 197, 198, 205, 207, 217, 218, 223, 224, 225, 250, 251, 266, 275, 279, 294, 297, 298, 323, 324, 336, 341, 343, 352, 360, 364, 365
Wang, Z 70, 75, 78, 114, 132, 140, 152, 167, 185, 191, 215, 222, 245, 274, 286, 306, 314, 322, 326, 366
Wan Tang Kuan, S 315
Ward, C 104, 246
Warner, J 113
Warnken, N 276, 324
Warren, J 72, 169
Warren, O 76, 307
Waryoba, D 53, 221, 362
Was, G 82, 94, 143, 182, 198, 199, 251, 252, 299, 342
Waser, R 274
Wasson, A 46
Wastavino, G 302
Watanabe, C 184
Watanabe, T 252
Watling, K 75
Weaver, M 128, 175
Webb-Robertson, B 294
Weber, W 252, 299
Weder, M 336
Weertman, J 236
Wei, C 254
Wei, H 301
Wei, L 231, 312
Wei, Q 151, 205, 206, 207
Wei, W 243
Weidner, A 183
Weifeng, L 78, 302
Weil, K 86, 135, 189, 190, 243, 292, 338, 368
Weiland, H 49, 264
Weimer, M 97
Weimin, L 272
Weismüller, J 51, 333
Weiss, B 229, 367
Weiss, I 160
Weissmüller, J 99, 364
Wejdemann, C 93
Wejrzanowski, T 57
Welberry, T 341, 342
Welch, B 313
Wells, D 168
Wells, M 134
Wen, C 69, 112, 216, 335
Wen, L 219
Wen, W 351
Wen, X 157, 211
Wen, Y 43, 324, 325
Wenyuan, W 345
Werner, E 50
West, J 208
Westerlund, K 79
Weston, M 210
Wheeler, D 169
Wheeler, K 179, 195, 263
Whelan, S 171
Whetten, J 64
White, C 212
White, D 113
White, P 243
White, S 160
Whitehorn, R 295
Whitfield, R 256
Whitley, V 141, 174
Wicker, R 110
Wickett, M 169
Wickins, M 98
Widom, M 44, 347
Wielage, B 57
Wierzbicka, A 173
Wiest, A 68, 319
Wiest, J 39
Wiest, L 319
Wiezorek, J 55, 307, 308
Wignacourt, J 200
Wilde, G 364
Wildey, B 219
Wilkosz, D 338
Willard, M 261, 309
Williams, C 178
Williams, E 113, 164
Williams, J 131, 246, 247, 248, 263
Williams, P 146
Williams, R 61, 209, 246
Williams, S 95, 279
Wilson, B 363
Wilson, J 135
Wilson, M 338
Wilson, S 45, 117, 154
Wilson, T 268
Wimmer, M 287
Windl, W 163

Wingate, C 311
Winter, S 348
Wiredu, L 220
Wisbey, A 256
Wise, S 208, 276
Withers, P 178, 297, 342
Withey, E 76
Witte, F 335
Witusiewicz, V 256
Wögerer, C 153
Wojewoda, J 173
Wolcott, J 277
Wolf, A 156
Wolf, D 99, 252
Wolfson, N 68
Wollants, P 117, 301
Wollmershauser, J 95
Wolverton, C 140, 323
Wombles, R 172
Wong, B 338
Wong, C 158, 253, 264
Wong, H 81
Woo, C 71
Woo, K 39
Woo, W 298
Wood, A 243
Wood, J 187, 347, 370
Woodrow, B 119
Woods, J 277, 327
Woodward, C 72, 139, 149, 224, 348, 350
Worthington, D 141, 191, 209, 364
Wright, P 109, 213
Wright, S 69
Wright, W 111
Wu, A 300
Wu, C 331, 360
Wu, D 105, 330
Wu, E 298
Wu, H 41, 200
Wu, J 243, 244
Wu, K 96, 138, 169, 238, 294
Wu, L 297
Wu, Q 221
Wu, R 275
Wu, W 111, 200
Wu, X 178, 235, 256, 282, 303, 305, 353, 354
Wu, Y 145
Wunderlich, R 247, 269, 360
Wuttig, M 223
Wynne, B 134, 138, 178

X

Xia, F 219
Xia, G 190
Xia, K 256
Xia, S 51
Xia, Y 149
Xia, Z 277
Xiangfa, L 65
Xiangxin, X 43
Xiao, B 156
Xiao, S 148
Xiao, Z 70, 330
Xiaodong, H 313
Xiao Dong, Y 160
Xie, H 69, 112
Xie, S 95
Xie, X 41
Xing, C 139
Xing, D 319
Xing, Q 322
Xing, Y 327
Xiquan, Q 214
Xu, B 311
Xu, C 149, 150, 257
Xu, D 73, 245, 350
Xu, G 121
Xu, H 233
Xu, J 304, 347, 366, 369
Xu, K 42
Xu, L 41, 228, 245, 254, 256
Xu, Q 308
Xu, S 144
Xu, T 260
Xu, W 109, 256
Xu, X 194, 276
Xu, Y 194, 229, 316
Xu, Z 121, 124
Xue, B 345
Xue, J 215, 245, 314, 326
Xue, L 80, 335
Xue, P 246
Xue, W 251, 360
Xue, Y 77, 323

Y

Yablinsky, C 131
Yacaman, M 184
Ya Feng, L 160
Yagi, Y 300
Yajima, K 345
Yakimicki, D 110
Yamada, H 115
Yamada, Y 300
Yamaguchi, M 193
Yamaguchi, S 186, 202
Yamakov, V 99
Yamamoto, A 283
Yamamoto, K 190
Yamamoto, T 223
Yamamoto, Y 326
Yamasaki, T 163
Yamashita, D 208
Yan, H 109
Yan, Q 51, 58, 125
Yan, S 41
Yan, X 314, 330
Yan, Y 41, 63, 104, 105
Yan-qing, L 330
Yanada, I 228
Yang, B 72
Yang, F 44, 68, 121, 148, 217, 317
Yang, H 42, 128, 205, 215, 255
Yang, L 72, 273
Yang, M 40, 235
Yang, Q 288
Yang, R 73, 97, 98, 148, 203, 218, 255, 256, 304, 347, 349, 350, 370
Yang, S 132, 265, 290, 314, 326, 327
Yang, W 265
Yang, X 235
Yang, Y 138, 239, 251, 294, 299, 325, 352
Yang, Z 86, 135, 189, 190, 242, 243, 255, 292, 338, 368
Yankov, R 371
Yanli, J 43
Yanqing, L 314
Yao, G 231, 265, 312, 313, 335
Yao, J 89, 139
Yao, S 265, 290
Yao, Z 143, 144
Yapici, G 257
Yashin, A 181
Yasuda, H 265, 326
Yavari, A 54
Yavari, R 162
Yazgan Kokuoz, B 138
Yazici, H 358
Ye, B 89
Ye, F 197
Ye, J 76
Yeager, J 195
Yeh, Y 360
Yen, Y 300, 301
Yeoh, L 256, 304
Yeon, D 169
Yexiang, L 314, 330
Yi, D 265, 290
Yi, G 70
Yi, T 322
Yim, C 238
Yin, D 50, 150
Yin, H 137
Yin, W 64, 107, 157, 211, 264, 312
Yin, Z 311, 322, 330, 356
Yinglu, Z 312
Yip, T 100
Yokka, Y 201
Yokoyama, S 223
Yokoyama, Y 163, 216, 217, 218, 269
Yolton, C 149, 305
Yong, L 78, 302
Yong, W 313
Yong, Z 318
Yoo, B 174, 218
Yoo, C 249
Yoo, H 152
Yoo, J 202
Yoo, K 202
Yoon, C 260
Yoon, M 274
Yoon, S 292, 333
Yoon, Y 289
Yordanov, P 115
Yo Sep, Y 310
Yoshihara, M 370
Yoshiya, M 265
You, B 238
You, J 248
Youguo, H 314
Young, D 231
Young, G 104
Young, M 328
Yount, H 252
Yu, F 337
Yu, G 218
Yu, H 48, 231
Yu, J 132, 133, 255, 313
Yu, L 42

Yu, M.....331
Yu, P.....72
Yu, S.....126, 127, 335
Yu, W.....228
Yu, Y.....366
Yu-Ting, Y.....120
Yuan, C.....251, 308, 324, 356
Yuan, Q.....216, 267
Yuan, X.....269
Yucel, O.....192
Yue, L.....178
Yue, S.....134, 241
Yuferev, V.....168
Yun, Y.....261
Yunusova, N.....54
Yuqing, W.....322
Yuri, G.....144

Z

Zabaras, N.....154, 155, 156, 225, 262, 364
Zaefferer, S.....278, 351
Zaikov, Y.....314
Zaluzec, M.....104
Zambrano, A.....301
Zamiri, A.....277, 347
Zan, X.....149
Zangiacomi, C.....119, 171, 225, 226, 325, 365
Zarandi, F.....241
Zargar, H.....41, 323
Zatsepin, N.....309
Zbib, A.....195
Zehetbauer, M.....52, 353, 367
Zelberg, B.....39, 315
Zelinska, O.....145
Zeman, M.....132
Zemcik, L.....97
Zeng, K.....74, 119, 172, 199, 228, 229, 253, 277, 300, 326, 343
Zeng, Q.....211
Zeng, X.....134, 188, 290
Zeng, Z.....101, 292
Zenobia, S.....94
Zestrea, V.....223
Zhai, Q.....81, 87, 180
Zhai, T.....157, 211, 304, 347
Zhai, X.....108, 138
Zhan, S.....281
Zhang, C.....187
Zhang, D.....251, 312
Zhang, F.....96, 116, 138, 157, 251, 294, 324
Zhang, H.....62, 69, 186, 268, 335, 351
Zhang, J.....40, 44, 127, 193, 221, 231, 274, 275, 298, 347, 348, 349
Zhang, K.....140, 361
Zhang, L.....56, 155, 156, 201, 220, 302
Zhang, M.....108, 138, 185, 271, 288, 330
Zhang, N.....370
Zhang, R.....80, 139, 276, 277
Zhang, S.....60, 187, 188, 276, 333
Zhang, T.....69, 89, 108, 111, 139, 177, 218, 238, 330, 366
Zhang, W.....50, 217, 269, 312
Zhang, X.....41, 143, 174, 185, 199, 205, 231, 241, 327, 370
Zhang, Y.....52, 56, 122, 123, 162, 205, 231, 252, 255, 299, 360
Zhang, Z.....53, 57, 75, 108, 138, 180, 240, 318, 330, 334
Zhao, H.....75, 314
Zhao, J.....122
Zhao, L.....370
Zhao, Q.....109, 177, 214
Zhao, S.....193
Zhao, X.....78, 132, 366
Zhao, Y.....77, 150, 206, 257, 306
Zheng, B.....70
Zheng, G.....59
Zheng, H.....321
Zheng, K.....290
Zheng, L.....322
Zheng, S.....87
Zheng, Y.....124
Zherebtsov, S.....54, 205
Zhihe, D.....234
Zhihui, X.....178
Zhilyaev, A.....52, 353
Zhong, Y.....130, 349
Zhongliang, T.....314
Zhou, F.....51, 58, 125
Zhou, J.....65, 141
Zhou, N.....224
Zhou, R.....252
Zhou, W.....41, 60, 101
Zhou, X.....44, 142
Zhou, Y.....53, 150
Zhu, A.....319
Zhu, C.....215
Zhu, H.....40, 133, 235, 304
Zhu, J.....187, 190
Zhu, M.....89
Zhu, S.....288, 337
Zhu, T.....118, 130, 364
Zhu, W.....255
Zhu, X.....49, 367
Zhu, Y.....50, 54, 99, 149, 150, 205, 206, 207, 257, 286, 306, 352
Zhuang, L.....158
Zhukovskii, Y.....223
Zi, A.....344
Zieba, P.....173
Ziegler, D.....213
Zigoneanu, L.....100
Zikry, M.....184
Zimmerman, R.....343, 359
Zimmermann, M.....130
Zimprich, P.....229
Zina, B.....363
Zindel, J.....126
Zinkle, S.....104, 343
Zlatko, C.....357
Zmierczak, W.....163
Zolotoyabko, E.....93, 341, 342
Zou, J.....350
Zou, Z.....311
Zrnik, J.....250, 258
Zschack, P.....92
Zschau, H.....349
Zu, G.....312, 313
Zuberova, Z.....359
Zujovic, Z.....106
Zuo, L.....197, 198, 250, 251
Zuo, X.....201, 302
Zuo-kun, C.....313